

**COAL MINE VENTILATION - A STUDY OF THE USE OF VENTILATION IN
THE PRODUCTION ZONE**

Tariq Feroze

A thesis submitted to the Faculty of Engineering and the Built Environment, University of the Witwatersrand, Johannesburg, in fulfilment of the requirements for the degree of
Doctor of Philosophy.

Johannesburg, 2016

DECLARATION

I declare that this thesis is my own, unaided work. Where use has been made of the work of others, it has been duly acknowledged. It is being submitted for the Degree of Doctor of Philosophy in the University of the Witwatersrand, Johannesburg. It has not been submitted before in any form for any degree or examination in any other University.

Signed:

Tariq Feroze

This _____ day of _____ 2016

ABSTRACT

The blind headings created in room and pillar mining are known to be the high risk areas of the coal mine, since this is where the coal production is actually taking place and hence the liberation of maximum quantity of methane. The ventilation of this region called the localized ventilation is carried out using auxiliary ventilation devices. This ventilation may be planned and be the subject of mine standards, but it is not very well understood and implementation on a day to day basis is usually left to the first level of supervisory staff. Majority of the methane explosions have been found to occur in these working areas and blind headings. The correct use of auxiliary ventilation devices can only be carried out once the effect of the system variables associated with each device is very well understood and can be calculated mathematically. Presently, no mathematical models or empirical formulas exist to estimate the effect of the associated system variables on the flow rates close to the face of the heading. The extent of ventilation of a heading ventilated without the use of any auxiliary device is not clear. Furthermore, to design additional engineering solutions, the flow patterns inside these heading ventilated with the auxiliary ventilation devices needs to be understood.

The study of the face ventilation systems and the effect of the system variables associated system with each auxiliary ventilation device can be carried out experimentally, but doing a large number of experiments underground is very difficult as it disturbs the mine production cycles. Furthermore, studying the flow patterns experimentally is even more cumbersome, and can only be done to some extent using smoke or tracer gas. Therefore, Computational Fluid Dynamic's (CFD) advanced numerical code ANSYS Fluent was used to study the effect of a number of system variables associated with the face ventilation systems used in blind headings.

As part of the procedure, the CFD model used was validated using four validation studies, in which the numerical results were compared with the actual experimental results. The numerical results differed to a maximum of 10% for all the experimental results. The system variables associated with ventilation of a heading, without the use of any auxiliary device, with the use of Line Brattice (LB) and fan with duct were selected. A range of values was chosen for each variable, and scenarios were created

using every possible combination of these variables. All the scenarios were simulated in Ansys Fluent, the air flow rates, air velocities, velocity vectors, and velocity contours were calculated and drawn at different locations inside the heading. The effect of each system variable was found using a comparative analysis. The results were represented in simple user-friendly form and can be used to estimate the air flows at the exit of the LB and face of the heading for various settings of the LB and fan and duct face ventilation systems.

The analysis of the ventilation of a heading without the use of LB shows that a maximum penetration depth is found with the Last Through Road (LTR) velocity of 1.35m/s. The flow rates and the maximum axial velocities increase with the increase in the LTR velocity up to a depth of 10m (maximum air flowing into a heading of 1.26m³/s and 1.58m³/s is found for the 3m and 4m high heading using 2m/s LTR velocity).

For the LB ventilation system the LTR velocities, heading height, length of the LB in the LTR and heading, angle of the LB in LTR, and distance of the LB to the wall of the heading (side wall) were varied to identify clearly the effect of these control variables, on the flow rate at the exit of the LB, and close to the face of the heading. The flow rate at the exit of the LB is found to be proportional to the product of the distance of the LB to the wall in the LTR and heading. The flow rate at the exit of the LB, face of the heading, and inside the heading is found proportional to the LTR velocity and height of the heading. It is found that a minimum length of LB is associated with each distance of the LB to the wall in the heading, to maximize the delivery of air close to the face of the heading. This length is found to be equal to 15m for 1m LB to wall distance, and 10m for 0.5m LB to wall distance. Mathematical models were developed to estimate the effect of each studied system variables on the flow rates at the exit of the LB and close to face of the heading.

For the fan and duct systems the length, diameter, and the fan design flow rates were varied. It is found that for a force fan duct system only a maximum of 50% of the total air that reaches the face is fresh and the remaining 50% is recirculated air. The flow rate with the exhaust fan system is found to be much lower than the force fan duct system. It increases with the reduction in duct mouth to heading face distance, and increase in duct

diameter. Mathematical models are developed to calculate the flow rates at the face of the heading using the effect of each studied system variable.

The research reveals that the ANSYS numerical code is an appropriate tool to evaluate the face ventilation of a heading in a three dimensional environment using full scale models. The South African coal mining industry can benefit from the outcomes of this study, specially the mathematical models, in a number of ways. Ventilation engineers can now estimate the flow rates close to the face of the heading for different practical mining scenarios and ensure sufficient ventilation by using the appropriate auxiliary ventilation settings. The results can easily be developed into training aids using easy to use excel spread sheets to ensure that mineworkers at the coal face have a better understanding of the working of the auxiliary ventilation devices. It can also serve Academia as part of the curriculum to teach the future mining engineers how the different variables associated with the auxiliary ventilation system affect the ventilation in a heading. The research therefore, has the potential to provide a significant step toward, understanding airflow rates delivered by the auxiliary devices close to the face of the heading and the air flow patterns inside the heading as a basis for improving the working environment for underground mineworkers.

LIST OF PUBLICATIONS

The publications listed below have emanated from this research work so far:

1. **Feroze, T.**, and Phillips, H. W. (2015). An Initial Investigation of Room and Pillar Ventilation Using CFD to Investigate the Effects of Last Through Road Velocity. *24th International Mining Congress and Exhibition of Turkey (IMCET 15)*. Antalya, Turkey, 14-17 April. pp. 970-977.
2. **Feroze, T.**, and Genc, B. (2016). Estimating effects of line brattice ventilation system variables using CFD in the empty heading in room and pillar mining. Accepted for publication in the *Journal of The Southern African Institute of Mining and Metallurgy*.
3. **Feroze, T.**, and Genc, B. (2016). Evaluation of line brattice length in an empty heading to improve air flow rate at the face using CFD. Accepted for publication in the *International Journal of Mining Science and Technology*.
4. **Feroze, T.**, and Genc, B. (2016). Analysis of ducted fan system variables on ventilation in an empty heading using CFD. Accepted for publication in the *Journal of The Southern African Institute of Mining and Metallurgy*.
5. **Feroze, T.**, and Genc, B. (2016). A CFD model to evaluate variables of the line brattice ventilation system in an empty heading. Submitted to the *Journal of The Southern African Institute of Mining and Metallurgy*, March, 2016.
6. **Feroze, T.**, and Genc, B. (2016). Ventilation of underground coal mines - A Computational Fluid Dynamics study. Submitted to the *Conference of MVSSA*, September, 2016.

The paper abstracts are included in Appendix X.

ACKNOWLEDGEMENTS

Immeasurable appreciation and sincere gratitude to the following persons for their guidance, help, and support in making this study possible.

- National University of Sciences and Technology (NUST) Pakistan, for sponsoring my studies.
- My Supervisors, Prof. Bekir Genc and Prof. Emeritus Huw Phillips, School of Mining Engineering, University of Witwatersrand, for their invaluable academic support, trust and patience throughout the research and writing of this thesis.
- Prof. F.T. Cawood, former head, School of Mining Engineering, University of Witwatersrand, for providing School's support to get a high performance computer and the license for ANSYS Fluent Software.
- Prof. C. Musingwini, Head, School of Mining Engineering, University of the Witwatersrand, for providing funding from the School to pay the ANSYS Annual Tech Support fee.
- Cor Meyer for sharing the results of his experimental study.
- Andrew Thompson from Anglo Thermal Coal, Eric Nkosi from Kriel Coal, Marco Biffi, Alan Cook, Rodiney Fourie, and Robyn Biffi for making the experimental testing possible.
- Dr. Danie de Kock from Qfinsoft (ANSYS License provider in South Africa) for his guidance on the use of ANSYS Fluent.
- Lindy, Mona, Anzolette, Sonja and Jacob, School of Mining Engineering, University of the Witwatersrand, for their moral support throughout the stay at the School.
- Dr Sarfraz Ali, Muhammad Arif, and Faiq Javaid for their prayers.

DEDICATION

To my loving wife, adorable daughter and son, caring parents, supportive siblings, maternal aunt and all the miners who lost their lives on duty.

| CONTENTS | Page |
|---|--------------|
| ABSTRACT..... | II |
| LIST OF PUBLICATIONS | V |
| ACKNOWLEDGEMENTS | VI |
| DEDICATION..... | VII |
| LIST OF FIGURES | XVI |
| LIST OF TABLES..... | XXIX |
| LIST OF IMPORTANT SYMBOLS USED IN THE THESIS..... | XXXIX |
| GLOSSARY OF IMPORTANT TERMS USED IN THE THESIS | XII |
| | |
| 1 INTRODUCTION AND BACKGROUND OF THE RESEARCH | 1 |
| 1.1 Background | 1 |
| 1.2 Problem statement..... | 4 |
| 1.3 Scope and Objectives of the Research | 5 |
| 1.4 Relevance of the Research and Research Questions..... | 6 |
| 1.5 Research Conceptual Framework and Methodology | 7 |
| 1.6 Thesis Structure | 10 |
| 1.6.1 Chapter 1- Introduction..... | 10 |
| 1.6.2 Chapter 2 - Literature review | 10 |
| 1.6.3 Chapter 3 - Methodology | 10 |
| 1.6.4 Chapter 4 - Validation - Case Studies..... | 10 |
| 1.6.5 Chapter 5 - Analysis and discussion - Ventilation of headings without the use of any auxiliary equipment | 11 |
| 1.6.6 Chapter 6 - Ventilation of headings with the use of line brattice | 11 |
| 1.6.7 Chapter 7 - Ventilation of headings with CM using line brattice | 11 |
| 1.6.8 Chapter 8 - Ventilation of a heading using fan with duct system | 11 |
| 1.6.9 Chapter 9 - Conclusion and Recommendations..... | 11 |
| 1.7 Significance of the Study | 12 |

| | | |
|----------|---|-----------|
| 1.8 | Conclusion | 12 |
| 2 | LITERATURE REVIEW | 13 |
| 2.1 | General | 13 |
| 2.2 | Coal Mine Hazards | 15 |
| 2.3 | Auxiliary ventilation | 18 |
| 2.3.1 | LB ventilation system | 19 |
| 2.3.2 | Fan with duct ventilation system | 21 |
| 2.3.3 | Stand - alone fans (Jet fans) | 24 |
| 2.4 | Computational Fluid Dynamics | 25 |
| 2.4.1 | Governing equations of fluid dynamics | 29 |
| 2.4.2 | Key steps of CFD | 32 |
| 2.4.3 | Discretization | 32 |
| 2.4.4 | Solution of algebraic equations | 35 |
| 2.5 | Solving CFD Problems Using Available Software | 38 |
| 2.5.1 | ANSYS Fluent | 39 |
| 2.5.2 | Turbulence | 41 |
| 2.5.2 | Turbulence models | 41 |
| 2.6 | Ventilation Network Design Software | 43 |
| 2.6.1 | Theory and principle | 43 |
| 2.7 | Conclusion | 45 |
| 3 | METHODOLOGY | 47 |
| 3.1 | General | 47 |
| 3.2 | Practical Site Considerations / Creation of Practical Scenarios | 50 |
| 3.3 | Case A - No Auxiliary Ventilation Equipment | 50 |
| 3.4 | Case B - Use of Scoop / LB | 52 |
| 3.5 | Case C - Ventilation of a Heading in the Presence of a Continuous Miner Using LB | 55 |
| 3.6 | Case D - Auxiliary Fan (Ducted) | 57 |
| 3.7 | Numerical Considerations for the Research | 60 |
| 3.7.1 | Modelling and meshing | 61 |
| 3.7.2 | Specification of boundary conditions | 61 |

| | | |
|----------|---|-----------|
| 3.7.3 | Selection of turbulence models..... | 62 |
| 3.7.4 | Solution..... | 68 |
| 3.7.5 | Post-processing - evaluation of results..... | 69 |
| 3.8 | Conclusion | 70 |
| 4 | NUMERICAL MODEL VALIDATION STUDIES | 71 |
| 4.1 | General | 71 |
| 4.2 | Validation Study One..... | 71 |
| 4.2.1 | Model geometry and meshing..... | 72 |
| 4.2.2 | Boundary conditions and numerical details | 73 |
| 4.2.3 | Results and discussion | 73 |
| 4.2.4 | Validation..... | 77 |
| 4.3 | Validation Study Two | 78 |
| 4.3.1 | Experimental setup and results | 81 |
| 4.3.2 | Numerical Calculations..... | 82 |
| 4.3.3 | Validation..... | 84 |
| 4.4 | Validation Study Three | 85 |
| 4.4.1 | Experimental setup and results | 85 |
| 4.4.2 | Numerical Calculations..... | 87 |
| 4.4.3 | Validation..... | 90 |
| 4.5 | Validation Study Four..... | 91 |
| 4.5.1 | Experimental setup and results | 91 |
| 4.5.2 | Numerical Calculations..... | 92 |
| 4.5.3 | Validation..... | 96 |
| 4.6 | Conclusion | 97 |
| 5 | ANALYSIS AND DISCUSSION - VENTILATION OF HEADINGS WITHOUT THE USE OF ANY AUXILIARY EQUIPMENT | 98 |
| 5.1 | General | 98 |
| 5.2 | Case A - No Auxiliary Ventilation Equipment..... | 99 |
| 5.2.1 | Penetration depth | 100 |
| 5.2.2 | Flow rate at specified depth planes..... | 104 |
| 5.3 | Conclusion | 106 |

| | | |
|----------|---|------------|
| 6 | ANALYSIS AND DISCUSSION - VENTILATION OF HEADINGS WITH THE USE OF LINE BRATTICE..... | 108 |
| 6.1 | General..... | 108 |
| 6.2 | Mathematical Model to Estimate Flow Rates at the Exit of the LB | 112 |
| 6.2.1 | Area Calculation at the Inlet of LB..... | 112 |
| 6.2.2 | Flow rates at exit of LB in the headings | 114 |
| 6.2.3 | Conclusion | 121 |
| 6.3 | Comparison of Air Flows, with the Change in LTR Velocity | 122 |
| 6.3.1 | Change of LTR velocity - 6.6 x 3 x 10m heading | 122 |
| 6.3.2 | Change of LTR velocity - 6.6 x 4 x 10m heading | 124 |
| 6.3.3 | Change of LTR velocity - 6.6 x 3 x 20m heading | 125 |
| 6.3.4 | Change of LTR velocity - 6.6 x 4 x 20m heading | 126 |
| 6.3.5 | Conclusion | 127 |
| 6.4 | Comparison of Air Flows with the Change in the Length of LB inside the Heading for Each LTR Velocity | 128 |
| 6.4.1 | Length of LB inside the heading - 6.6 x 3 x 10m heading..... | 128 |
| 6.4.2 | Length of LB inside the heading - 6.6 x 4 x 10m heading..... | 135 |
| 6.4.3 | Length of LB inside the heading - 6.6 x 3 x 20m heading..... | 135 |
| 6.4.4 | Length of LB inside the heading - 6.6 x 4 x 20m heading..... | 136 |
| 6.4.5 | Conclusion | 136 |
| 6.5 | Comparison of Air Flows, with the Change in Length of LB Inside the LTR for Each LTR Velocity..... | 138 |
| 6.5.1 | Length of LB inside the LTR - 6.6 x 3 x 10m heading..... | 138 |
| 6.5.2 | Length of LB inside the LTR - 6.6 x 4 x 10m heading..... | 142 |
| 6.5.3 | Length of LB inside the LTR- 6.6 x 3 x 20m heading..... | 143 |
| 6.5.4 | Length of LB inside the LTR - 6.6 x 4 x 20m heading..... | 144 |
| 6.5.5 | Conclusion | 144 |
| 6.6 | Comparison of Air Flows, with the Change in the Distance of LB from the Wall inside the Heading for Each LTR Velocity | 146 |
| 6.6.1 | Distance of LB from the wall inside the heading - 6.6 x 3 x 10m heading | 146 |
| 6.6.2 | Distance of LB from the wall inside the heading - 6.6 x 4 x 10m heading | 153 |
| 6.6.3 | Distance of LB from the wall inside the heading - 6.6 x 3 x 20m heading | 154 |

| | | |
|----------|--|------------|
| 6.6.4 | Distance of LB from the wall inside the heading - 6.6 x 4 x 20m heading | 154 |
| 6.6.5 | Conclusion | 154 |
| 6.7 | Comparison of Air Flows, with the Change in Angle of LB in the LTR for Each LTR Velocity | 156 |
| 6.7.1 | Angle of LB in the LTR - 6.6 x 3 x 10m heading..... | 156 |
| 6.7.2 | Angle of LB in the LTR - 6.6 x 4 x 10m heading..... | 161 |
| 6.7.3 | Angle of LB in the LTR - 6.6 x 3 x 20m heading..... | 161 |
| 6.7.4 | Angle of LB in the LTR - 6.6 x 4 x 20m heading..... | 161 |
| 6.7.5 | Conclusion | 161 |
| 6.8 | Flow Rate Estimation at the Face of the Heading..... | 163 |
| 6.8.1 | Effect of the change in velocity | 165 |
| 6.8.2 | Effect of the change in heading height | 166 |
| 6.8.3 | Effect of the length and angle of LB in the LTR | 167 |
| 6.8.4 | Effect of the length of LB in heading and distance from face | 167 |
| 6.8.5 | Summary of the rules to use equation 6.9 for any heading dimension | 177 |
| 6.8.6 | Generalised equation..... | 178 |
| 6.9 | Dead Zones/Low Flow Rate Regions | 180 |
| 6.10 | Conclusion | 186 |
| 7 | ANALYSIS AND DISCUSSION - VENTILATION OF HEADINGS WITH CONTINUOUS MINER USING LINE BRATTICE..... | 188 |
| 7.1 | General | 188 |
| 7.2 | CM in 6.6 x 3 x 20m Heading..... | 190 |
| 7.2.1 | Airflows on a horizontal plane and vertical plane constructed at a distance of 0.7m from right wall | 190 |
| 7.2.2 | Airflows on a horizontal plane constructed at a height of 2.9m and a vertical plane constructed at a distance of 0.7m from right wall | 192 |
| 7.2.3 | Airflows on a horizontal plane constructed at a height of 1.6m and vertical plane constructed at a distance of 0.7m from right wall | 194 |
| 7.3 | CM in 6.6 x 4 x 20m Heading..... | 197 |
| 7.4 | Conclusion | 198 |

| | | |
|----------|--|------------|
| 8 | VENTILATION OF A HEADING USING FAN AND DUCT SYSTEM.. | 199 |
| 8.1 | General | 199 |
| 8.2 | Force Fan Duct System | 200 |
| 8.2.1 | Flow rates | 200 |
| 8.2.2 | Mathematical formulation to estimate air flows for force fan duct system | 202 |
| 8.2.3 | Flow definition | 207 |
| 8.2.4 | Force fan duct system - Duct inlet at entrance of heading vs duct inlet 3m inside LTR | 211 |
| 8.2.5 | Conclusion | 212 |
| 8.3 | Exhaust Fan Duct System | 213 |
| 8.3.1 | Flow rates | 213 |
| 8.3.2 | Mathematical formulation to estimate air flows for exhaust duct system | 214 |
| 8.3.3 | Flow definition | 219 |
| 8.3.4 | Conclusion | 222 |
| 9 | CONCLUSIONS AND RECOMMENDATIONS..... | 223 |
| 9.1 | Introduction..... | 223 |
| 9.2 | Key Findings of the Research | 223 |
| 9.3 | Research Contribution | 230 |
| 9.4 | Research Limitations | 231 |
| 9.5 | Recommendations for the Future Research Work | 232 |
| | REFERENCES..... | 234 |
| | APPENDIX A COMPLETE AND NUMERICAL NAMES..... | 243 |
| | APPENDIX B FLOW RATES AT THE EXIT OF LB FOR EACH LTR VELOCITY | 245 |
| | APPENDIX C EFFECT OF LTR VELOCITY ON THE FLOW RATE AT EXIT OF LB..... | 247 |
| | APPENDIX D EFFECT OF HEADING HEIGHT ON AIR FLOW AT THE EXIT OF LB..... | 251 |
| | APPENDIX E EFFECT OF LTR VELOCITY ON FLOW RATES..... | 253 |

| | |
|--|------------|
| APPENDIX F EFFECT OF LTR VELOCITY ON FLOW RATE CLOSE TO FACE..... | 265 |
| APPENDIX G EFFECT OF LENGTH OF LB INSIDE HEADING ON FLOW RATES | 268 |
| APPENDIX H EFFECT OF LENGTH OF LB INSIDE HEADING ON FLOW RATE CLOSE TO FACE | 276 |
| APPENDIX I EFFECT OF LENGTH OF LB INSIDE HEADING ON FLOW RATE CLOSE TO FACE | 279 |
| APPENDIX J EFFECT OF LENGTH OF LB INSIDE HEADING ON FLOW RATES | 284 |
| APPENDIX K EFFECT OF LB LENGTH INSIDE HEADING FOR EACH WALL DISTANCE ON FLOW RATES CLOSE TO FACE..... | 289 |
| APPENDIX L EFFECT OF THE LENGTH OF LB INSIDE THE LTR ON FLOW RATES | 292 |
| APPENDIX M EFFECT OF LENGTH OF LB IN LTR ON FLOW RATES AT EXIT OF LB AND FACE OF HEADING | 300 |
| APPENDIX N EFFECT OF LB LENGTH IN LTR ON FLOW RATES CLOSE TO FACE | 303 |
| APPENDIX O EFFECT OF LB LENGTH IN LTR ON FLOW RATE AT ALL DEPTH PLANES..... | 308 |
| APPENDIX P EFFECT OF DISTANCE OF LB FROM WALL IN HEADING ON FLOW RATE | 313 |
| APPENDIX Q EFFECT OF DISTANCE OF LB FROM WALL IN HEADING ON FLOW RATE CLOSE TO THE FACE AND AT THE EXIT OF LB | 321 |
| APPENDIX R EFFECT OF LB DISTANCE FROM WALL IN HEADING ON FLOW RATE AT FACE..... | 324 |

| | |
|--|------------|
| APPENDIX S EFFECT OF LB DISTANCE FROM WALL IN HEADING ON FLOW RATE AT ALL DEPTH PLANES | 329 |
| APPENDIX T EFFECT OF CHANGE IN ANGLE OF LB IN LTR ON FLOW RATES AT ALL DEPTH PLANES INSIDE THE HEADING..... | 334 |
| APPENDIX U EFFECT OF CHANGE IN ANGLE OF LB IN LTR ON FLOW RATES CLOSE TO FACE AND EXIT OF LB | 338 |
| APPENDIX V EFFECT OF LB ANGLE IN LTR ON FLOW RATE CLOSE TO FACE..... | 341 |
| APPENDIX W EFFECT OF LB ANGLE IN LTR ON FLOW RATE..... | 346 |
| APPENDICES X SUMMARY OF PAPER ABSTRACT ON THE RESEARCH | 351 |
| Paper 1 | 351 |
| Paper 2 | 352 |
| Paper 3 | 353 |
| Paper 4 | 354 |
| Paper 5 | 355 |
| Paper 6 | 357 |

LIST OF FIGURES

| Figure | Page |
|--|-------------|
| Figure 1.1 Conceptual framework of the study | 8 |
| Figure 2.1 Distribution of methane explosions by place (Tkachuk et al., 1997) ... | 14 |
| Figure 2.2 Opencast strip mining in Witbank coal field, South Africa (Chabedi, 2015)..... | 16 |
| Figure 2.3 Longwall coal face (Chabedi, 2015) | 16 |
| Figure 2.4 Room and Pillar mine (Chabedi, 2015) | 16 |
| Figure 2.5 Coward diagram for methane in air (McPherson, 1993) | 17 |
| Figure 2.6 Air from LTR entering downstream in a development heading | 19 |
| Figure 2.7 Upstream LB | 20 |
| Figure 2.8 Downstream LB (Meyer, 1993)..... | 20 |
| Figure 2.9 Force fan duct ventilation system (Thorp, 1982)..... | 22 |
| Figure 2.10 Exhaust fan and duct ventilation system..... | 23 |
| Figure 2.11 Forcing overlap system (Zhang et al., 2011) | 24 |
| Figure 2.12 Exhaust overlap system (Thorp, 1982) | 24 |
| Figure 2.13 U Type flow pattern | 25 |
| Figure 2.14 Figure of Eight flow pattern (Meyer and Vanzyl, 1999) | 25 |
| Figure 2.15 Important aspects of CFD and numerical modeling (Anderson, 2015) | 28 |
| Figure 2.16 Divergence | 29 |
| Figure 2.17 Convergence | 29 |
| Figure 2.18 Divergence = 0..... | 29 |
| Figure 2.19 Grid points used for forward differencing, (Hoffmann and Chiang, 2000) | 33 |
| Figure 2.20 Grid points used for backward differencing, (Hoffmann and Chiang, 2000)..... | 33 |
| Figure 2.21 Grid points used for central differencing, (Hoffmann and Chiang, 2000) | 34 |
| Figure 2.22 Grid for FVM, (Hoffmann and Chiang, 2010) | 34 |
| Figure 3.1 Practical site characterization / considerations | 48 |
| Figure 3.2 Numerical model characterization / considerations | 49 |

| | | |
|-------------|--|----|
| Figure 3.3 | Geometric parameters for Case A..... | 52 |
| Figure 3.4 | Geometric parameters for Case B | 53 |
| Figure 3.5 | Schematic of the CM in the heading..... | 55 |
| Figure 3.6 | Geometric parameters for force fan duct Case..... | 59 |
| Figure 3.7 | Geometric parameters for exhaust fan duct Case..... | 60 |
| Figure 3.8 | Vertical plane to monitor the integral of velocity magnitude | 68 |
| Figure 4.1 | Three dimensional model..... | 72 |
| Figure 4.2 | Hexahedral mesh with boundary layers (Inset view of mesh boundary) | 73 |
| Figure 4.3 | Maximum axial velocities at specified planes | 74 |
| Figure 4.4 | Axial velocity contours at 15m plane in the heading for 0.78 m/s LTR velocity | 75 |
| Figure 4.5 | Axial velocity contours at 15m plane in the heading for 1 m/s LTR velocity..... | 75 |
| Figure 4.6 | Axial velocity contours at 15m plane in the heading for 1.35 m/s LTR velocity | 75 |
| Figure 4.7 | Axial velocity contours at 15m plane in the heading for 1.9 m/s LTR velocity | 75 |
| Figure 4.8 | Average positive flow in at specified planes | 76 |
| Figure 4.9 | Velocity vectors on 1.5 m high horizontal plane for 1m/s LTR velocity | 77 |
| Figure 4.10 | Velocity vectors on 1.5 m high horizontal plane for 1.9 m/s LTR | 77 |
| Figure 4.11 | Comparison of experimental and numerical results validation case study one | 78 |
| Figure 4.12 | School of Mining Engineering, University of the Witwatersrand, tunnel and fan with duct system..... | 79 |
| Figure 4.13 | Schematic diagram of the duct..... | 79 |
| Figure 4.14 | Outline of the Tunnel | 79 |
| Figure 4.15 | Dimension of the tunnel face and duct distances from the walls of tunnel..... | 80 |
| Figure 4.16 | Outline of the duct | 80 |
| Figure 4.17 | Measurement points at the face of the tunnel | 81 |

| | | |
|-------------|--|----|
| Figure 4.18 | Velocity vectors close to the face of the tunnel on vertical plane..... | 83 |
| Figure 4.19 | Velocity contours close to the face of the tunnel on vertical plane | 83 |
| Figure 4.20 | Comparison of experimental and numerical results validation study two..... | 84 |
| Figure 4.21 | Important dimensions of the heading and LTR | 85 |
| Figure 4.22 | Three dimensional model..... | 87 |
| Figure 4.23 | Air flow inside the heading using velocity vectors..... | 88 |
| Figure 4.24 | Velocity Contours on a plane parallel to face of heading passing through Point 1..... | 88 |
| Figure 4.25 | Velocity Contours on a plane parallel to face of heading passing through Point 2..... | 89 |
| Figure 4.26 | Velocity Contours on a plane parallel to face of heading passing through Point 3..... | 89 |
| Figure 4.27 | Velocity Contours on a plane parallel to face of heading passing through Point 4..... | 89 |
| Figure 4.28 | Velocity Contours on a plane parallel to face of heading passing through Point 5..... | 89 |
| Figure 4.29 | Comparison of the experimental and numerical results validation study three | 90 |
| Figure 4.30 | Important dimensions of the heading and LTR..... | 91 |
| Figure 4.31 | Air flow inside the heading using velocity vectors..... | 93 |
| Figure 4.32 | Velocity contours on a plane at the entrance of LB passing through point 1 | 94 |
| Figure 4.33 | Velocity contours on a plane at the entrance of LB passing through point 2 | 94 |
| Figure 4.34 | Velocity Contours on a plane parallel to face of heading passing through Point 3..... | 94 |
| Figure 4.35 | Velocity Contours on a plane parallel to face of heading passing through Point 4..... | 95 |
| Figure 4.36 | Velocity Contours on a plane parallel to face of heading passing through Point 5..... | 95 |

| | | |
|-------------|---|-----|
| Figure 4.37 | Velocity Contours on a plane parallel to face of heading passing through Point 6..... | 95 |
| Figure 4.38 | Velocity Contours on a plane parallel to face of heading passing through Point 7..... | 95 |
| Figure 4.39 | Velocity Contours on a plane parallel to face of heading passing through Point 8..... | 96 |
| Figure 4.40 | Comparison of the experimental and numerical results validation study four | 97 |
| Figure 5.1 | Air flow in a heading without the use of any auxiliary equipment..... | 99 |
| Figure 5.2 | Maximum axial velocities at specified planes for 6.6 x 10m heading with 3 and 4m height..... | 101 |
| Figure 5.3 | Maximum axial velocities at specified planes for 6.6 x 20m heading with 3 and 4m height..... | 101 |
| Figure 5.4 | Axial velocity contours on 9.5 m deep vertical plane in the 6.6 x 3 x 10 m heading..... | 102 |
| Figure 5.5 | Axial velocity contours on 9.5 m deep vertical plane in the 6.6 x 4 x 10 m heading..... | 102 |
| Figure 5.6 | Axial velocity contours on 15 m deep vertical plane in the 6.6 x 3 x 20 m heading..... | 103 |
| Figure 5.7 | Axial velocity contours on 15 m deep vertical plane in the 6.6 x 4 x 20 m heading..... | 103 |
| Figure 5.8 | Average positive flow rates at specified planes for 6.6 x 10m heading with 3 and 4m height | 105 |
| Figure 5.9 | Average positive flow rates at specified planes for 6.6 x 20m heading with 3 and 4m height | 105 |
| Figure 6.1 | Air flow inside a heading using LB | 108 |
| Figure 6.2 | Components of analysis for Case B - Ventilation of a heading using LB | 111 |
| Figure 6.3 | LB setting variables | 113 |
| Figure 6.4 | Trend line of flow rate at LB exit | 116 |
| Figure 6.5 | Percentage increase in flow rates at the 9.5m deep plane with the increase in LTR velocity for 6.6 x 3 x 10m heading..... | 124 |

| | | |
|-------------|--|-----|
| Figure 6.6 | Percentage increase in flow rates at the 9.5m deep plane with the increase in LTR velocity for 6.6 x 4 x 10m heading..... | 125 |
| Figure 6.7 | Percentage increase in flow rates at the 19.5m deep plane with the increase in LTR velocity for 6.6 x 3 x 20m heading..... | 126 |
| Figure 6.8 | Percentage increase in flow rates at the 19.5m deep plane with the increase in LTR velocity for 6.6 x 4 x 20m heading..... | 127 |
| Figure 6.9 | Flow rates at 9.5m deep planes using 5m and 7.5m LB inside the heading for LTR velocity of 1m/s..... | 130 |
| Figure 6.10 | Flow rates at 9.5m deep planes using 5m and 7.5m LB inside the heading for LTR velocity of 1.5m/s..... | 130 |
| Figure 6.11 | Flow rates at 9.5m deep planes using 5m and 7.5m LB inside the heading for LTR velocity of 2m/s..... | 131 |
| Figure 6.12 | Flow rates at specified planes using 5m and 7.5m LB inside the heading for LTR velocity of 1m/s..... | 132 |
| Figure 6.13 | Flow rates at specified planes using 5m and 7.5m LB inside the heading for LTR velocity of 1.5m/s..... | 132 |
| Figure 6.14 | Flow rates at specified planes using 5m and 7.5m LB inside the heading for LTR velocity of 2m/s..... | 133 |
| Figure 6.15 | Air pushed away from the wall towards LB due to centrifugal force. | 134 |
| Figure 6.16 | Flow rate variations at the exit of the LB for set of cases with 1m and 0.5m LB to wall distance (left to right)..... | 135 |
| Figure 6.17 | Flow rates at 9.5m deep planes using 3m and 6m LB inside the LTR for LTR velocity of 1m/s..... | 140 |
| Figure 6.18 | Flow rates at 9.5m deep planes using 3m and 6m LB inside the LTR for LTR velocity of 1.5m/s..... | 140 |
| Figure 6.19 | Flow rates at 9.5m deep planes using 3m and 6m LB inside the LTR for LTR velocity of 2m/s..... | 141 |
| Figure 6.20 | Flow rates at specified planes using 3m and 6m LB inside the LTR for LTR velocity of 1m/s | 141 |
| Figure 6.21 | Flow rates at specified planes using 3m and 6m LB inside the LTR for LTR velocity of 1.5m/s | 142 |

| | | |
|-------------|---|-----|
| Figure 6.22 | Flow rates at specified planes using 3m and 6m LB inside the LTR for LTR velocity of 2m/s | 142 |
| Figure 6.23 | Flow rates at 9.5m deep planes using 0.5m and 1m distance of LB from wall for LTR velocity of 1m/s..... | 147 |
| Figure 6.24 | Flow rates at 9.5m deep planes using 0.5m and 1m distance of LB from wall for LTR velocity of 1.5m/s..... | 148 |
| Figure 6.25 | Flow rates at 9.5m deep planes using 0.5m and 1m distance of LB from wall for LTR velocity of 2m/s..... | 148 |
| Figure 6.26 | Flow rates at specified planes using 5m and 7.5m LB inside the heading for LTR velocity of 1m/s..... | 149 |
| Figure 6.27 | Flow rates at specified planes using 5m and 7.5m LB inside the heading for LTR velocity of 1.5m/s..... | 149 |
| Figure 6.28 | Flow rates at specified planes using 5m and 7.5m LB inside the heading for LTR velocity of 2m/s..... | 150 |
| Figure 6.29 | Velocity vectors and velocity stream lines (left to right) - Case 1 for 1m/s LTR velocity (0.5m distance of LB from the wall in the heading)..... | 151 |
| Figure 6.30 | Velocity vectors and velocity stream lines (left to right) - Case 2 for 1m/s LTR velocity (1m distance of LB from the wall in the heading)..... | 152 |
| Figure 6.31 | Flow rates at 9.5m deep plane using 0°, 7.5° and 15° LB inside the LTR for LTR velocity of 1m/s..... | 158 |
| Figure 6.32 | Flow rates at 9.5m deep plane using 0°, 7.5° and 15° LB inside the LTR for LTR velocity of 1.5m/s..... | 158 |
| Figure 6.33 | Flow rates at 9.5m deep plane using 0°, 7.5° and 15° LB inside the LTR for LTR velocity of 2m/s..... | 159 |
| Figure 6.34 | Flow rates at specified planes using 0°, 7.5° and 15° LB inside the LTR for LTR velocity of 1m/s..... | 159 |
| Figure 6.35 | Flow rates at specified planes using 0°, 7.5° and 15° LB inside the LTR for LTR velocity of 1.5 m/s..... | 160 |
| Figure 6.36 | Flow rates at specified planes using 0°, 7.5° and 15° LB inside the LTR for LTR velocity of 2m/s..... | 160 |

| | | |
|-------------|--|-----|
| Figure 6.37 | Trend line of air flow rate at the face of the heading (0.5m distance from face)..... | 165 |
| Figure 6.38 | Percentage increase in flow rates close to the face for each LTR velocity with the increase in heading height from 3m to 4m - 6.6 x 3 x 10m vs 6.6 x 4 x 10m headings..... | 166 |
| Figure 6.39 | Percentage increase in flow rates close to the face for each LTR velocity with the increase in heading height from 3m to 4m - 6.6 x 3 x 20m vs 6.6 x 4 x 20m headings..... | 166 |
| Figure 6.40 | Axial velocity contours at 5 to 15m length of the LB for Case 38 (1 m LB wall distance)..... | 170 |
| Figure 6.41 | Axial velocity contours at 5 to 15m length of the LB for Case 37 (0.5m LB wall distance)..... | 171 |
| Figure 6.42 | Typical low flow rate and recirculation zones - Ventilation of a heading using LB | 180 |
| Figure 6.43 | Typical low flow rate zone 1 - Ventilation of a heading using LB..... | 181 |
| Figure 6.44 | 10m long headings using LB settings of; 0° angle, 5m length of LB in heading, 3m length in LTR, 0.5m and 1m distance from face (left to right)..... | 183 |
| Figure 6.45 | 10m long headings using LB settings of; 0° angle, 7.5m length of LB in heading, 3m length in LTR,0.5m and 1m distance from face (left to right)..... | 183 |
| Figure 6.46 | 10m long headings using LB settings of; 7.5° angle, 5m length of LB in heading, 3m length in LTR, 0.5m and 1m distance from face (left to right)..... | 183 |
| Figure 6.47 | 10m long headings using LB settings of; 7.5° angle, 5m length of LB in heading, 6m length in LTR, 0.5m and 1m distance from face (left to right)..... | 184 |
| Figure 6.48 | 10m long headings using LB settings of; 15° angle, 7.5m length of LB in heading, 6m length in LTR, 0.5m and 1m distance from face (left to right)..... | 184 |
| Figure 6.49 | Air flow vectors on a vertical plane drawn at a distance of 0.1m from the right wall for 10m long heading | 185 |

| | | |
|-------------|--|-----|
| Figure 6.50 | Air flow vectors on a vertical plane drawn at a distance of 0.1m and 0.4m from the right wall for 10m long heading using a 5m long LB having a wall distance of 0.5m | 185 |
| Figure 7.1 | Schematic of the CM in the heading..... | 189 |
| Figure 7.2 | Velocity vectors on the 0.5m high horizontal plane and vertical plane at 0.7m from the right wall of the heading..... | 191 |
| Figure 7.3 | Velocity vectors on the 0.5m high horizontal plane showing middle stream of air rising up | 191 |
| Figure 7.4 | Velocity vectors on the 2.9 m high horizontal plane and vertical plane at 0.7m from the right wall of the heading..... | 192 |
| Figure 7.5 | Three dimensional view of the velocity vectors on the 19.9 m deep vertical plane (perpendicular to the LB) | 193 |
| Figure 7.6 | Velocity vectors on the 2.9m high plane; slower air in region 4 | 193 |
| Figure 7.7 | Velocity vectors on the 2.9m high plane; curling down of outer air stream from the left side wall of the heading (region 5)..... | 194 |
| Figure 7.8 | Velocity vectors on the 1.6 m high horizontal plane and vertical plane at 0.7m from the right wall of the heading..... | 195 |
| Figure 7.9 | Velocity vectors on the 1.6m high horizontal plane | 196 |
| Figure 7.10 | Velocity vectors on the 1.6m high horizontal plane close to the face | 196 |
| Figure 7.11 | Velocity vectors on the 2m high horizontal plane close to the face for 4m high heading..... | 197 |
| Figure 8.1 | Flow rate close to the face of the heading vs Factors for force fan duct system..... | 203 |
| Figure 8.2 | Regions of air flow on a plane parallel to the face at 0.01m distance from the face | 208 |
| Figure 8.3 | Air flows on a plane parallel to the face at 0.01m distance from the face | 208 |
| Figure 8.4 | Air flows on a plane parallel to the left side wall of the heading at a distance of 0.6m from the left wall (showing the section after the duct exit) | 209 |
| Figure 8.5 | Airflows on horizontal planes constructed at height of 0.1m and 2.9m from the bottom of the heading..... | 210 |

| | | |
|-------------|--|-----|
| Figure 8.6 | Air flows on a plane parallel to the right face of the heading at a distance of 0.1m from the right face (showing the section after the duct exit) | 211 |
| Figure 8.7 | Airflows on horizontal planes constructed at a heights 2.9m from the floor of the heading | 212 |
| Figure 8.8 | Flow rate close to the face of the heading vs Factors for exhaust fan duct system..... | 215 |
| Figure 8.9 | Air flow path of exhaust duct ventilation system | 220 |
| Figure 8.10 | Air flows on a plane parallel to the left wall of the heading at a distance of 0.6m (air moving parallel to the duct), inset; air turning clock wise on reaching close to the face | 220 |
| Figure 8.11 | Air flow on a plane parallel to the face at 0.01m distance from the face..... | 221 |
| Figure 8.12 | Air flow on a horizontal plane, exhaust fan duct ventilation system.. | 221 |
| Figure I1 | Flow rates at 9.5m deep planes using 5m and 7.5m LB inside the heading for LTR velocity of 1m/s..... | 279 |
| Figure I2 | Flow rates at 9.5m deep planes using 5m and 7.5m LB inside the heading for LTR velocity of 1.5m/s..... | 279 |
| Figure I3 | Flow rates at 9.5m deep planes using 5m and 7.5m LB inside the heading for LTR velocity of 2m/s..... | 280 |
| Figure I4 | Flow rates at 19.5m deep planes using 10m and 15m LB inside the heading for LTR velocity of 1m/s..... | 280 |
| Figure I5 | Flow rates at 19.5m deep planes using 10m and 15m LB inside the heading for LTR velocity of 1.5m/s..... | 281 |
| Figure I6 | Flow rates at 19.5m deep planes using 10m and 15m LB inside the heading for LTR velocity of 2m/s..... | 281 |
| Figure I7 | Flow rates at 19.5m deep planes using 10m and 15m LB inside the heading for LTR velocity of 1m/s..... | 282 |
| Figure I8 | Flow rates at 19.5m deep planes using 10m and 15m LB inside the heading for LTR velocity of 1.5m/s..... | 282 |
| Figure I9 | Figure I9 Flow rates at 19.5m deep planes using 10m and 15m LB inside the heading for LTR velocity of 2m/s | 283 |

| | | |
|-----------|--|-----|
| Figure J1 | Flow rates at specified planes using 5m and 7.5m LB inside the heading for LTR velocity of 1m/s..... | 284 |
| Figure J2 | Flow rates at specified planes using 5m and 7.5m LB inside the heading for LTR velocity of 1.5m/s..... | 285 |
| Figure J3 | Flow rates at specified planes using 5m and 7.5m LB inside the heading for LTR velocity of 2m/s..... | 285 |
| Figure J4 | Flow rates at specified planes using 10m and 15m LB inside the heading for LTR velocity of 1m/s..... | 286 |
| Figure J5 | Flow rates at specified planes using 10m and 15m LB inside the heading for LTR velocity of 1.5m/s..... | 286 |
| Figure J6 | Flow rates at specified planes using 10m and 15m LB inside the heading for LTR velocity of 2m/s..... | 287 |
| Figure J7 | Flow rates at specified planes using 10m and 15m LB inside the heading for LTR velocity of 1m/s..... | 287 |
| Figure J8 | Flow rates at specified planes using 10m and 15m LB inside the heading for LTR velocity of 1.5m/s..... | 288 |
| Figure J9 | Flow rates at specified planes using 10m and 15m LB inside the heading for LTR velocity of 2m/s..... | 288 |
| Figure N1 | Flow rates at 9.5m deep planes using 3m and 6m LB inside the LTR for LTR velocity of 1m/s..... | 303 |
| Figure N2 | Flow rates at 9.5m deep planes using 3m and 6m LB inside the LTR for LTR velocity of 1.5m/s..... | 303 |
| Figure N3 | Flow rates at 9.5m deep planes using 3m and 6m LB inside the LTR for LTR velocity of 2m/s..... | 304 |
| Figure N4 | Flow rates at 19.5m deep planes using 3m and 6m LB inside the LTR for LTR velocity of 1m/s..... | 304 |
| Figure N5 | Flow rates at 19.5m deep planes using 3m and 6m LB inside the LTR for LTR velocity of 1.5m/s..... | 305 |
| Figure N6 | Flow rates at 19.5m deep planes using 3m and 6m LB inside the LTR for LTR velocity of 2m/s..... | 305 |
| Figure N7 | Flow rates at 19.5m deep planes using 3m and 6m LB inside the LTR for LTR velocity of 1m/s..... | 306 |

| | | |
|-----------|--|-----|
| Figure N8 | Flow rates at 19.5m deep planes using 3m and 6m LB inside the LTR for LTR velocity of 1.5m/s..... | 306 |
| Figure N9 | Flow rates at 19.5m deep planes using 3m and 6m LB inside the LTR for LTR velocity of 2m/s..... | 307 |
| Figure O1 | Flow rates at specified planes using 3m and 6m LB inside the LTR for LTR velocity of 1m/s | 308 |
| Figure O2 | Flow rates at specified planes using 3m and 6m LB inside the LTR for LTR velocity of 1.5m/s | 308 |
| Figure O3 | Flow rates at specified planes using 3m and 6m LB inside the LTR for LTR velocity of 2m/s | 309 |
| Figure O4 | Flow rates at specified planes using 3m and 6m LB inside the LTR for LTR velocity of 1m/s | 309 |
| Figure O5 | Flow rates at specified planes using 3m and 6m LB inside the LTR for LTR velocity of 1.5m/s | 310 |
| Figure O6 | Flow rates at specified planes using 3m and 6m LB inside the LTR for LTR velocity of 2m/s | 310 |
| Figure O7 | Flow rates at specified planes using 3m and 6m LB inside the LTR for LTR velocity of 1m/s | 311 |
| Figure O8 | Flow rates at specified planes using 3m and 6m LB inside the LTR for LTR velocity of 1.5m/s | 311 |
| Figure O9 | Flow rates at specified planes using 3m and 6m LB inside the LTR for LTR velocity of 2m/s | 312 |
| Figure R1 | Flow rates at 9.5m deep planes using 0.5m and 1m distance of LB from wall for LTR velocity of 1m/s..... | 324 |
| Figure R2 | Flow rates at 9.5m deep planes using 0.5m and 1m distance of LB from wall for LTR velocity of 1.5m/s..... | 324 |
| Figure R3 | Flow rates at 9.5m deep planes using 0.5m and 1m distance of LB from wall for LTR velocity of 2m/s..... | 325 |
| Figure R4 | Flow rates at 19.5m deep planes using 0.5m and 1m distance of LB from wall for LTR velocity of 1m/s..... | 325 |
| Figure R5 | Flow rates at 19.5m deep planes using 0.5m and 1m distance of LB from wall for LTR velocity of 1.5m/s..... | 326 |

| | | |
|-----------|--|-----|
| Figure R6 | Flow rates at 19.5m deep planes using 0.5m and 1m distance of LB from wall for LTR velocity of 2m/s..... | 326 |
| Figure R7 | Flow rates at 19.5m deep planes using 0.5m and 1m distance of LB from wall for LTR velocity of 1m/s..... | 327 |
| Figure R8 | Flow rates at 19.5m deep planes using 0.5m and 1m distance of LB from wall for LTR velocity of 1.5m/s..... | 327 |
| Figure R9 | Flow rates at 19.5m deep plane using 0.5m and 1m distance of LB from wall for LTR velocity of 2m/s..... | 328 |
| Figure S1 | Flow rates at specified planes using 5m and 7.5m LB inside the heading for LTR velocity of 1m/s..... | 329 |
| Figure S2 | Flow rates at specified planes using 5m and 7.5m LB inside the heading for LTR velocity of 1.5m/s..... | 329 |
| Figure S3 | Flow rates at specified planes using 5m and 7.5m LB inside the heading for LTR velocity of 2m/s..... | 330 |
| Figure S4 | Flow rates at specified planes using 10m and 15m LB inside the heading for LTR velocity of 1m/s..... | 330 |
| Figure S5 | Flow rates at specified planes using 10m and 15m LB inside the heading for LTR velocity of 1.5m/s..... | 331 |
| Figure S6 | Flow rates at specified planes using 10m and 15m LB inside the heading for LTR velocity of 2m/s..... | 331 |
| Figure S7 | Flow rates at specified planes using 10m and 15m LB inside the heading for LTR velocity of 1m/s..... | 332 |
| Figure S8 | Flow rates at specified planes using 10m and 15m LB inside the heading for LTR velocity of 1.5m/s..... | 332 |
| Figure S9 | Flow rates at specified planes using 10m and 15m LB inside the heading for LTR velocity of 2m/s..... | 333 |
| Figure V1 | Flow rates at 9.5m deep planes using 0°, 7.5° and 15° LB inside the LTR for LTR velocity of 1m/s..... | 341 |
| Figure V2 | Flow rates at 9.5m deep planes using 0°, 7.5° and 15° LB inside the LTR for LTR velocity of 1.5m/s..... | 341 |
| Figure V3 | Flow rates at 9.5m deep planes using 0°, 7.5° and 15° LB inside the LTR for LTR velocity of 2m/s..... | 342 |

| | | |
|-----------|--|-----|
| Figure V4 | Flow rates at 19.5m deep planes using 0°, 7.5° and 15° LB inside the LTR for LTR velocity of 1m/s..... | 342 |
| Figure V5 | Flow rates at 19.5m deep planes using 0°, 7.5° and 15° LB inside the LTR for LTR velocity of 1.5m/s..... | 343 |
| Figure V6 | Flow rates at 19.5m deep planes using 0°, 7.5° and 15° LB inside the LTR for LTR velocity of 2m/s..... | 343 |
| Figure V7 | Flow rates at 19.5m deep planes using 0°, 7.5° and 15° LB inside the LTR for LTR velocity of 1m/s..... | 344 |
| Figure V8 | Flow rates at 19.5m deep planes using 0°, 7.5° and 15° LB inside the LTR for LTR velocity of 1.5m/s..... | 344 |
| Figure V9 | Flow rates at 19.5m deep planes using 0°, 7.5° and 15° LB inside the LTR for LTR velocity of 2m/s..... | 345 |
| Figure W1 | Flow rates at specified planes using 0°, 7.5° and 15° LB inside the LTR for LTR velocity of 1m/s..... | 346 |
| Figure W2 | Flow rates at specified planes using 0°, 7.5° and 15° LB inside the LTR for LTR velocity of 1.5m/s..... | 346 |
| Figure W3 | Flow rates at specified planes using 0°, 7.5° and 15° LB inside the LTR for LTR velocity of 2m/s..... | 347 |
| Figure W4 | Flow rates at specified planes using 0°, 7.5° and 15° LB inside the LTR for LTR velocity of 1m/s..... | 347 |
| Figure W5 | Flow rates at specified planes using 0°, 7.5° and 15° LB inside the LTR for LTR velocity of 1.5m/s..... | 348 |
| Figure W6 | Flow rates at specified planes using 0°, 7.5° and 15° LB inside the LTR for LTR velocity of 2m/s..... | 348 |
| Figure W7 | Flow rates at specified planes using 0°, 7.5° and 15° LB inside the LTR for LTR velocity of 1m/s..... | 349 |
| Figure W8 | Flow rates at specified planes using 0°, 7.5° and 15° LB inside the LTR for LTR velocity of 1.5m/s..... | 349 |
| Figure W9 | Flow rates at specified planes using 0°, 7.5° and 15° LB inside the LTR for LTR velocity of 2m/s..... | 350 |

LIST OF TABLES

| Table | | Page |
|--------------|--|-------------|
| Table 2.1 | Major coal dust and methane explosions of the historical data (Holding, 1982)..... | 14 |
| Table 2.2 | Production of coal from underground coal mining methods (Dougall, 2010)..... | 16 |
| Table 2.3 | Major coal mine explosions incidents between 2005 and 2011 (Dubinski et al., 2011)..... | 18 |
| Table 2.4 | Sample of single-event, multi-fatality mine explosions in the English speaking world (Phillips, 2015)..... | 18 |
| Table 3.1 | Summary of variables used in the research..... | 50 |
| Table 3.2 | Details of the parameters varied for Case A..... | 51 |
| Table 3.3 | Research matrix for Case A..... | 51 |
| Table 3.4 | Details of the parameters varied for Case B..... | 53 |
| Table 3.5 | Research matrix for Case B..... | 54 |
| Table 3.6 | Details of parameters for Case C..... | 56 |
| Table 3.7 | Research matrix Case C..... | 56 |
| Table 3.8 | Details of the parameters varied for Case D (Force fan)..... | 57 |
| Table 3.9 | Details of the parameters varied for Case D (Exhaust fan)..... | 58 |
| Table 3.10 | Force fan duct system variables..... | 58 |
| Table 3.11 | Exhaust fan duct system variables..... | 59 |
| Table 3.12 | Summary of boundary conditions..... | 62 |
| Table 4.1 | Numerical results of maximum penetration depths for each LTR velocity..... | 74 |
| Table 4.2 | Average positive flow inwards at specified planes..... | 76 |
| Table 4.3 | Measured experimental results of maximum penetration depths for each LTR velocity, (Meyer, 1989)..... | 78 |
| Table 4.4 | Air velocities measured using hot wire anemometer..... | 81 |
| Table 4.5 | Numerically calculated values of air velocities..... | 83 |
| Table 4.6 | Air velocities measured using hot wire anemometer..... | 86 |

| | | |
|------------|--|-----|
| Table 4.7 | Numerically calculated values of air velocities | 90 |
| Table 4.8 | Air velocities measured using hot wire anemometer | 92 |
| Table 4.9 | Numerically calculated values of air velocities | 96 |
| Table 5.1 | Maximum axial velocity at specified planes for 6.6 x 3 x 10m and 6.6 x 4 x 10m headings | 100 |
| Table 5.2 | Maximum axial velocity at specified planes for 6.6 x 3 x 20m and 6.6 x 4 x 20m headings | 100 |
| Table 5.3 | Maximum flow rates at specified depth planes for 6.6 x 3 x 10m and 6.6 x 4 x 10m headings | 104 |
| Table 5.4 | Maximum flow rates at specified depth planes for 6.6 x 3 x 20m and 6.6 x 4 x 20m headings | 104 |
| Table 6.1 | Complete and numerical names for the cases of group 1 | 109 |
| Table 6.2 | Set of cases formed for Case B | 110 |
| Table 6.3 | LB inlet areas for all heading dimensions..... | 114 |
| Table 6.4 | Flow rates at LB exit vs product of LB entrance length and distance from wall..... | 115 |
| Table 6.5 | Percentage decrease in flow rate at the exit of LB for each LTR velocity with the increase in length of LB from 3 to 6m in the LTR for zero angled LB | 117 |
| Table 6.6 | Percentage decrease in flow rate at the exit of LB for each LTR velocity with the increase in length of LB from 5 to 7.5m for the 10m deep and 3m high heading | 118 |
| Table 6.7 | Percentage increase in flow rates at the 9.5m deep plane with the increase in LTR velocity | 123 |
| Table 6.8 | Percentage increase in flow rate for each LTR velocity with the increase in the length of LB in the heading from 5 to 7.5m | 129 |
| Table 6.9 | Percentage increase in flow rate for each LTR velocity with the increase the length of LB in the heading from 5 to 7.5m separately for 0.5m and 1m distance of LB from wall in the heading | 134 |
| Table 6.10 | Percentage change in flow rate at the 9.5m deep plane and exit of the LB for each LTR velocity with the change in length of LB in the LTR from 3 to 6m | 139 |

| | | |
|------------|--|-----|
| Table 6.11 | Percentage increase in flow rate at 9.5m deep plane for each LTR velocity with the increase in the distance of the LB from 0.5 to 1m from the wall in the heading | 147 |
| Table 6.12 | Percentage increase in flow rate at 9.5m deep plane and at the exit of the LB for each LTR velocity with the increase in the distance of the LB from 0.5 to 1m from the wall in the heading | 151 |
| Table 6.13 | Percentage increase in flow rate at 9.5m deep plane, for each set of cases, for each LTR velocity, with the increase in the distance of the LB from 0.5 to 1m from the wall in the heading, separately for cases using 5m long LB and 7.5m long LB | 153 |
| Table 6.14 | Difference of the percentage increase in flow rates for the set of cases with 1m and 0.5m distance from the wall in the heading, between the sets with long (7.5m) and short (5m) LB..... | 153 |
| Table 6.15 | Percentage increase in flow rates at the 9.5m deep plane with the increase in LB angle in the LTR from 0° to 7.5°, 0° to 15°, and 7.5° to 15° | 157 |
| Table 6.16 | Percentage increase in flow rates at the exit of LB with the increase in LB angle in the LTR from 0° to 7.5°, 0° to 15°, and 7.5° to 15°.... | 157 |
| Table 6.17 | Percentage difference in flow rate at the exit of the LB and close to the face of the heading | 164 |
| Table 6.18 | Flow rate at the face of the heading (0.5m from face) vs product of factor, X and b..... | 164 |
| Table 6.19 | Percentage decrease in flow rate close to face with the increase in length of LB from 3 to 6m in the LTR for zero angled LB | 167 |
| Table 6.20 | Difference of LB lengths and distances from the face for the 10m long heading with 5m LB and the 20m long heading | 168 |
| Table 6.21 | Comparison of the flow rate between two halves of the “LB-wall channel” in the heading - Case 38 with 1m/s LTR velocity | 169 |
| Table 6.22 | Comparison of the flow rate between two halves of the “LB - wall channel” in the heading - Case 37 with 1m/s LTR velocity | 170 |

| | | |
|------------|---|-----|
| Table 6.23 | Percentage difference in flow rate (0.5m from the face) 10m heading vs 20m heading with 5 and 15 m LB in heading, separately for LB wall distance of 0.5m and 1m - 1m/s LTR velocity..... | 172 |
| Table 6.24 | Incremental percentage increase in flow rate due to the increase in length of the LB from 5m (wall distance 1m)..... | 173 |
| Table 6.25 | Incremental percentage increase in flow rate due to the increase in length of the LB from 5m (wall distance 0.5m)..... | 174 |
| Table 6.26 | Incremental percentage increase /decrease in flow rate due to the difference in the length of the LB and LB exit distance from the face from the standard cases (1 st 12 cases) - 1m wall distance | 176 |
| Table 6.27 | Incremental percentage increase /decrease in flow rate due to the difference in the length of the LB and LB exit distance from the face from the standard cases (1 st 12 cases)- 0.5 wall distance | 176 |
| Table 8.1 | Details of force fan duct cases | 201 |
| Table 8.2 | Flow rates and percentage of fresh air flow rates on planes at specified distances from the face | 201 |
| Table 8.3 | Flow rate close to the face and different factors for force fan duct system | 203 |
| Table 8.4 | Percentage increase in flow rate at the face of the heading with the increase in fan design flow rate from 2.971-3.7125 m ³ /s | 204 |
| Table 8.5 | Percentage increase in flow rate at the face of the heading with the decrease in duct diameter from 0.76 - 0.57m..... | 205 |
| Table 8.6 | Percentage increase in flow rate at the face of the heading with the reduction in distance of the duct mouth to face of the heading from 10m - 8m | 206 |
| Table 8.7 | Percentage error of the mathematical model for force fan duct system | 207 |
| Table 8.8 | Details of Exhaust fan duct system cases..... | 213 |
| Table 8.9 | Flow rates at specified distances from the face of the heading for exhaust fan duct system | 214 |
| Table 8.10 | Flow rate close to the face and different factors for Exhaust fan duct system | 215 |

| | | |
|------------|--|-----|
| Table 8.11 | Percentage increase in flow rate at the face of the heading with the increase in fan design flow rate from 2.971-3.7125 m ³ /s | 216 |
| Table 8.12 | Percentage increase in flow rate at the face of the heading with the decrease in duct diameter from 0.76 - 0.57m..... | 217 |
| Table 8.13 | Percentage reduction in flow rate at the face of the heading with the increase in distance of the duct mouth to face of the heading from 2m - 4m | 218 |
| Table 8.14 | Percentage error of the mathematical model for exhaust fan duct system | 219 |
| Table A1 | Complete and numerical names of all the cases of Case B..... | 243 |
| Table B1 | Flow rates at the exit of the LB for all heading dimensions with each LTR velocity | 245 |
| Table C1 | Percentage increase in flow rates at the exit of the LB with the increase in LTR velocity - 6.6 x 3 x 10m heading | 247 |
| Table C2 | Percentage increase in flow rates at the exit of the LB with the increase in LTR velocity - 6.6 x 3 x 20m heading..... | 248 |
| Table C 3 | Percentage increase in flow rates at the exit of the LB with the increase in LTR velocity - 6.6 x 4 x 10m heading..... | 249 |
| Table C4 | Percentage increase in flow rates at the exit of the LB with the increase in LTR velocity - 6.6 x 4 x 20m heading..... | 250 |
| Table D1 | Percentage increase in flow rates at the exit of the LB for each LTR velocity with the increase in heading height; 6.6 x 3 x 10m vs 6.6 x 4 x 10m headings | 251 |
| Table D2 | Percentage increase in flow rates at the exit of the LB for each LTR velocity with the increase in heading height; 6.6 x 3 x 20m vs 6.6 x 4 x 20m headings | 252 |
| Table E1 | Percentage increase in flow rates at the specified planes with the increase in LTR velocity from 1-1.5, 1-2 and 1.5-2m/s - 6.6 x 3 x 10 m heading..... | 253 |
| Table E2 | Percentage increase in flow rates at the specified planes with the increase in LTR velocity from 1-1.5, 1-2 and 1.5-2m/s - 6.6 x 4 x 10 m heading..... | 256 |

| | | |
|----------|---|-----|
| Table E3 | Percentage increase in flow rates at the specified planes with the increase in LTR velocity from 1-1.5, 1-2 and 1.5-2m/s - 6.6 x 3 x 20 m heading..... | 259 |
| Table E4 | Percentage increase in flow rates at the specified planes with the increase in LTR velocity from 1-1.5, 1-2 and 1.5-2m/s - 6.6 x 4 x 20 m heading..... | 262 |
| Table F1 | Percentage increase in flow rates at the 9.5m deep plane with the increase in LTR velocity from 1 to 1.5, 1 to 2 and 1.5 to 2m/s - 6.6 x 4 x 10 m heading..... | 265 |
| Table F2 | Percentage increase in flow rates at the 19.5m deep plane with the increase in LTR velocity from 1 to 1.5, 1 to 2 and 1.5 to 2m/s - 6.6 x 3 x 20 m heading..... | 266 |
| Table F3 | Percentage increase in flow rates at the 19.5m deep plane with the increase in LTR velocity from 1 to 1.5, 1 to 2 and 1.5 to 2m/s - 6.6 x 4 x 20 m heading..... | 267 |
| Table G1 | Percentage change in flow rate for each LTR velocity with the change in the length of LB inside the heading from 5 to 7.5m (1/2 to 3/4 the length of the heading) - 6.6 x 3 x 10m heading | 268 |
| Table G2 | Percentage change in flow rate for each LTR velocity with the change in the length of LB in the heading from 5 to 7.5m (1/2 to 3/4 the length of the heading) - 6.6 x 4 x 10m heading | 270 |
| Table G3 | Percentage change in flow rate for each LTR velocity with the change in the length of LB in the heading from 10 to 15m (1/2 to 3/4 the length of the heading) - 6.6 x 3 x 20m heading | 272 |
| Table G4 | Percentage flow rate change for each LTR velocity with the change in the length of LB in the heading from 10 to 15m (1/2 to 3/4 the length of the heading) - 6.6 x 4 x 20m heading | 274 |
| Table H1 | Percentage increase in flow rate for each LTR velocity with the increase in the length of LB in the heading from 5 to 7.5m - 6.6 x 4 x 10m heading..... | 276 |

| | | |
|----------|--|-----|
| Table H2 | Percentage increase in flow rate for each LTR velocity with the increase in the length of LB in the heading from 10 to 15m - 6.6 x 3 x 20m heading..... | 277 |
| Table H3 | Percentage increase in flow rate for each LTR velocity with the increase in the length of LB in the heading from 10 to 15m - 6.6 x 4 x 20m heading..... | 278 |
| Table K1 | Percentage increase in flow rate for each LTR velocity with the increase in length of LB in the heading from 5 to 7.5m, separately for 0.5 and 1m distance of the LB from wall in the heading - 6.6 x 4 x 10m heading..... | 289 |
| Table K2 | Percentage increase in flow rate for each LTR velocity with the increase in length of LB in the heading from 10 to 15m, separately for 0.5 and 1m distance of the LB from wall in the heading - 6.6 x 3 x 20m heading..... | 290 |
| Table K3 | Percentage increase in flow rate for each LTR velocity with the increase in length of LB in the heading from 10 to 15m, separately for 0.5 and 1m distance of the LB from wall in the heading - 6.6 x 4 x 20m heading..... | 291 |
| Table L1 | Percentage change in flow rate for each LTR velocity with the change in the length of LB in the LTR from 3 to 6m - 6.6 x 3 x 10m heading..... | 292 |
| Table L2 | Percentage change in flow rate for each LTR velocity with the change in the length of LB in the LTR from 3 to 6m - 6.6 x 4 x 10m heading..... | 294 |
| Table L3 | Percentage change in flow rate for each LTR velocity with the change in the length of LB in the LTR from 3 to 6m - 6.6 x 3 x 20m heading..... | 296 |
| Table L4 | Percentage change in flow rate for each LTR velocity with the change in length of LB in the LTR from 3 to 6m - 6.6 x 4 x 20m heading..... | 298 |

| | | |
|----------|--|-----|
| Table M1 | Percentage change in flow rate at the 9.5m deep plane and exit of the LB for each LTR velocity with the increase in length of LB in the LTR from 3 to 6m - 6.6 x 4 x 10m heading | 300 |
| Table M2 | Percentage change in flow rate at the 19.5m deep plane and exit of the LB for each LTR velocity with the increase in the length of LB in the LTR from 3 to 6m - 6.6 x 3 x 20m heading | 301 |
| Table M3 | Percentage change in flow rate at the 19.5m deep plane and exit of the LB for each LTR velocity with the increase in length of LB in the LTR from 3 to 6m - 6.6 x 4 x 20m heading | 302 |
| Table P1 | Percentage increase in flow rate at specified planes for each LTR velocity with the increase in the distance of the LB from 0.5 to 1m from the wall in the heading - 6.6 x 3 x 10m heading | 313 |
| Table P2 | Percentage increase in flow rate at specified planes for each LTR velocity with the increase in the distance of the LB from 0.5 to 1m from the wall in the heading - 6.6 x 4 x 10m heading | 315 |
| Table P3 | Percentage increase in flow rate at specified planes for each LTR velocity with the increase in the distance of the LB from 0.5 to 1m from the wall in the heading - 6.6 x 3 x 20m heading | 317 |
| Table P4 | Percentage increase in flow rate at specified planes for each LTR velocity with the increase in the distance of the LB from 0.5 to 1m from the wall in the heading - 6.6 x 4 x 20m heading | 319 |
| Table Q1 | Percentage increase in flow rate at 9.5m deep plane and at the exit of the LB for each LTR velocity with the increase in the distance of the LB from 0.5 to 1m from the wall in the heading - 6.6 x 4 x 10m heading | 321 |
| Table Q2 | Percentage increase in flow rate at 19.5m deep plane and at the exit of the LB for each LTR velocity with the increase in the distance of the LB from 0.5 to 1m from the wall in the heading - 6.6 x 3 x 20m heading | 322 |
| Table Q3 | Percentage increase in flow rate at 19.5m deep plane and at the exit of the LB for each LTR velocity with the increase in the distance of | |

| | | |
|----------|--|-----|
| | the LB from 0.5 to 1m from the wall in the heading - 6.6 x 4 x 20m heading..... | 323 |
| Table T1 | Percentage increase in flow rates at the specified planes with the increase in angle (0°, 7.5° and 15°) of LB in the LTR – 6.6 x 3 x 10m heading..... | 334 |
| Table T2 | Percentage increase in flow rates at the specified planes with the increase in angle (0°, 7.5° and 15°) of LB in the LTR – 6.6 x 4 x 10m heading..... | 335 |
| Table T3 | Percentage increase in flow rates at the specified planes with the increase in angle (0°, 7.5° and 15°) of LB in the LTR - 6.6 x 3 x 20m heading..... | 336 |
| Table T4 | Percentage increase in flow rates at the specified planes with the increase in angle (0°, 7.5° and 15°) of LB in the LTR - 6.6 x 4 x 20m heading..... | 337 |
| Table U1 | Percentage increase in flow rates at the 9.5m deep plane with the increase in LB angle in the LTR from 0° to 7.5°, 0° to 15°, and 7.5° to 15°- 6.6 x 4 x 10m heading..... | 338 |
| Table U2 | Percentage increase in flow rates at the exit of the LB with the increase in LB angle in the LTR from 0° to 7.5°, 0° to 15°, and 7.5° to 15°- 6.6 x 4 x 10m heading..... | 338 |
| Table U3 | Percentage increase in flow rates at the 19.5m deep plane with the increase in LB angle in the LTR from 0° to 7.5°, 0° to 15°, and 7.5° to 15°- 6.6 x 3 x 20m heading..... | 339 |
| Table U4 | Percentage increase in flow rates at the exit of the LB with the increase in LB angle in the LTR from 0° to 7.5°, 0° to 15°, and 7.5° to 15°- 6.6 x 3 x 20m heading..... | 339 |
| Table U5 | Percentage increase in flow rates at the 19.5m deep plane with the increase in LB angle in the LTR from 0° to 7.5°, 0° to 15°, and 7.5° to 15°- 6.6 x 4 x 20m heading..... | 340 |

| | | |
|----------|--|-----|
| Table U6 | Percentage increase in flow rates at the exit of the LB with the increase in LB angle in the LTR from 0° to 7.5°, 0° to 15°, and 7.5° to 15°- 6.6 x 4 x 20m heading..... | 340 |
|----------|--|-----|

LIST OF IMPORTANT SYMBOLS USED IN THE THESIS

ρ = Density (kg/m^3)

u, v, w = Velocity components in the x, y, z direction respectively (m/s)

f_x, f_y, f_z = Forces in the x, y, z direction respectively (N)

P = Pressure (N/m^2 , Pa)

$\tau_{xx}, \tau_{yy}, \tau_{zz}$ = Normal stress in the x, y, z direction respectively (N/m^2 , Pa)

τ_{ij} = Shear stress in the j direction exerted on a plane perpendicular to the i axis (N/m^2 , Pa)

K = Atkinson Friction factor (kg/m^3)

L = Length (m)

L_e = Equivalent length to cater for the shock losses (m)

Per = Perimeter (m)

A = Cross sectional area (m^2)

Q = Volume Flow Rate (m^3/s)

R = Atkinson Resistance of the Airway (Kg/m^8)

P_f = Frictional pressure loss (N/m^2 , Pa)

NVP = Natural Ventilation Pressure (N/m^2 , Pa)

\bar{u} = Mean velocity (m/s)

\acute{u} = Fluctuating velocity (m/s)

k = Turbulence kinetic energy ($\text{J/Kg}, \text{m}^2/\text{s}^2$)

ε = Turbulence dissipation rate ($\text{J/Kg.s}, \text{m}^2/\text{s}^3$)

G_k = Generation of kinetic energy due to turbulence ($\text{J/Kg}, \text{m}^2/\text{s}^2$)

G_b = Generation of kinetic energy due to buoyancy ($\text{J/Kg}, \text{m}^2/\text{s}^2$)

μ = Dynamic viscosity (Pa.s)

D = Hydraulic diameter (m)

Re = Reynolds number

a = Speed of sound ($\text{m/s}, 343\text{m/s}$)

LB = Line Brattice

b = Distance of the LB from the wall in the heading (m)

c = Length of the LB in the LTR (m)

d = Length of the LB in the heading (m)

e = Effect of angle on the entrance length (m)
f = Distance of the LB to the face of the heading (m)
HH = Heading height (m)
HW = Heading width (m)
HD = Heading depth (m)
 θ_{LB} = Angle of LB in the LTR ($^{\circ}$)
X = Entrance length of the LB in the LTR (m)
 $FR_{E_{LB}}$ = Flow rate at the exit of LB (m^3/s)
 $FR_{F_{LB}}$ = Flow rate close to the face of the heading ventilated using LB (m^3/s)
 F_{LB} = Factor for LB ventilation system
 FL_{LB} = Factor for the length of LB in the heading
 RF_{LB} = Reduction factor for LB
 FR_{F_F} = Flow rate at the face of the heading for force fan duct system
 FFR_F = Factor flow rate for force fan duct system
 FD_F = Factor diameter for force fan duct system
 FF_F = Factor duct mouth to face distance for the force fan duct system
 FR_{F_E} = Flow rate at the face of the heading for exhaust fan duct system
 FFR_E = Factor flow rate for exhaust fan duct system
 FDE_E = Factor diameter for the exhaust fan fan system
 FF_E = Factor duct mouth to face distance for the exhaust fan duct system

GLOSSARY OF IMPORTANT TERMS USED IN THE THESIS

Anemometer: Instrument for measuring air velocity.

Auxiliary fan: A small fan installed underground for ventilating coal faces or headings that are not adequately ventilated by the air current produced by the main ventilation fan. An auxiliary fan is usually from 0.5 to 1.0 m in diameter. The auxiliary fan can be used to force or exhaust ventilate the workplace.

Auxiliary ventilation/localised ventilation: Portion of main ventilating current directed to face of dead end entry by means of line brattice, an auxiliary fan with duct or jet fan.

CFD: Computational fluid dynamics, usually abbreviated as CFD, is a branch of fluid mechanics that uses numerical analysis and algorithms to solve and analyse problems involving fluid flows.

Coal: A solid, brittle, stratified, combustible rock-like material formed by decomposition of plant vegetation that has been submitted to compaction and induration.

Colliery: A coal mine including surface, plant and underground workings.

Continuous miner: Continuous mining machine is used to cut or rip coal from the face and load it onto conveyors or into shuttle cars in a continuous mining operation.

Control volume: A term used in fluid mechanics and thermodynamics to describe a volume fixed in space or moving with constant velocity through which the fluid flows.

CWP: Coal workers' pneumoconiosis also known as black lung disease or black lung, is caused by long exposure to coal dust.

Density: The density of a substance is its mass per unit volume, measured in kilogram per meter cube (kg/m^3).

Drift: A horizontal passage underground.

Energy: It is the capacity for doing work, measured in Joules (J).

Explosive: Any rapidly combustive or expanding substance.

Face: The place where a miner works in excavating coal.

Fan: A machine used to force ventilation through a mine. It may be a blow or suction fan, located on the surface or underground.

Flow rate: The quantity of air passing through the cross sectional area in metre cube per second (m^3/s).

Force: Something that causes a change in the motion of an object, measured in Newton (N).

Gravitational force: The gravitational force is a force that attracts any object with mass, measured in Newton (N).

Line brattice: A cloth or plastic sheet attached to roof, and floor in underground coal mines to channel fresh air to operating faces.

Main fan: A mechanical ventilator installed at the surface; operates by either exhausting or blowing to induce airflow through the mine roadways and workings.

Mass: The property of matter that measures its resistance to acceleration, measured in Kilogram (Kg).

Methane: Methane is the principal component of natural gas, and is frequently encountered in underground coal mining operations. It is potentially explosive and formed naturally from the decay of vegetative matter.

Momentum: The quantity of motion of a moving body, measured as a product of its mass and velocity, measured in kilogram meter per second (Kg m/s).

Natural ventilation: Ventilation of a mine without the aid of fans or furnaces.

Newton's second law of motion: The acceleration of an object is directly proportional to the magnitude of the applied force, and inversely proportional to the mass of the object.

Normal stress: It is a stress state where the stress is normal/vertical to the surface, measured in Pascal (Pa).

Numerical analysis: The branch of mathematics that deals with the development and use of numerical methods for solving problems.

Pillar: An area of coal left to support the overlying strata in a mine; sometimes left permanently to support surface structures.

PMF: Progressive massive fibrosis is the most advanced and debilitating form of lung disease found among labourers in respirable dust industries.

Respirable dust: Dust particles 5 microns or less in size.

Room and Pillar mining: A system of mining in which the coal is mined in rooms separated by narrow ribs or pillars. This method is applicable to flat deposits, such as coal, that occur in bedded deposits.

Shear stress: It is a stress state where the stress is parallel to the surface of the material, measured in Pascal (Pa).

Silicosis: Lung fibrosis caused by the inhalation of dust containing silica.

Smoke tube: It is used to determine the presence of moving air, the direction of flow, and the approximate velocity of flow by creating smoke. The device consists of an aspirator bulb, which discharges air through a glass tube containing a smoke-generating reagent.

Stress: It is defined as the force per unit area and measured in Pascal (Pa).

Tracer gas: A substance used to tag volumes of air so as to be able to find its movement.

Vector: A quantity having direction as well as magnitude.

Velocity: Rate of airflow in metre per second.

Ventilation: The provision of fresh air along all underground roadways, traveling roads, workings, and service parts.

Working face: The exposed area of a coal bed from which coal is extracted during a mining cycle.

1 INTRODUCTION AND BACKGROUND OF THE RESEARCH

1.1 Background

The ventilation of underground mines is required to allow mine workers and machines to survive and work in an environment which can be hundreds of metres underground. A well designed ventilation system should be able to provide air of good quality, in adequate quantity, and with controlled temperature and humidity. This will ensure the presence of sufficient flow of air to dilute/remove dangerous gases like methane, oxides of nitrogen, sulphur dioxide, carbon monoxide and dust generated underground contributed by the equipment, mining activities and coal itself. A compromised ventilation system can result in accidents, such as methane explosions and coal dust explosions (Amyotte and Pegg, 1993 and McPherson, 1993).

Mine ventilation systems have been designed and installed almost since the beginning of mining, and ventilation is a well-studied subject with a number of books available on the subject. Computerised mine ventilation network analysis software is available since the 1990's which can estimate the fan power requirements, distribution of air flows (air quantities at every place in a network). Mandatory ventilation requirements are also in place and are regulated by the local legislation (for South Africa, Mine Health and Safety Act in 1996) (Mine Health and Safety Act No 29, 1996). Generally the outbye ventilation is well planned by competent and experienced ventilation personnel, often using simulation packages to meet the requirements set by legislation and Codes of Practice. This outbye area is also routinely monitored by production supervisors as well as ventilation officials and in most cases underground instrumentation reports to a surface control room.

Room and Pillar mining is based on creating blind headings until through ventilation is established by cutting through when the pillar is formed. Even when longwall mining is the preferred method, the access roadways (gate roads) are created by room and pillar mining. This all leads to the development of many blind headings which require ventilation both when being mined and when standing. These headings, where the coal production is actually taking place, are known to be the high risk areas of the mine,

since this is where the maximum quantity of methane is accumulated and the risk of incendive sparking from machine cutter picks is also present. Localized ventilation may be planned and be the subject of mine standards, but it is not very well understood and implementation on a day to day basis is usually left to the first level of supervisory staff. Usually common sense is used for the installation of control devices, but sometimes fans are placed where it is convenient rather than where it is best required, and this can go undetected because the fan is still running. There have been instances of very high recirculation because of poorly located auxiliary fans (AMC Consultants Pty Ltd, 2005). The result of this negligence sometimes leads to accidents.

Underground coal mines are always subject to the inherent risks of methane explosions, coal dust explosions and lung diseases if they are not properly ventilated. If methane explosions are analysed by their location then about 75% of explosions occurs immediately in the working areas and blind drifts (Tkachuk et al., 1997). These accidents can be/are avoided by providing sufficient/ controlled ventilation air through the use of control devices like, line brattices (LBs), fan with duct, and ductless air movers (jet fans) etc. (falling under Auxiliary Ventilation) and thus mitigating the amount of dangerous gases/dust that can accumulate.

The effect of the system variables such as LTR velocity, heading dimensions and settings of auxiliary devices, related to the ventilation of headings is not very clear. No mathematical models are available to estimate the air flow quantities inside the heading close to the face when changes take place in the dimensions of the heading and the settings of the auxiliary ventilation equipment. Therefore, reliance on the wits of an individual having years of work experience is a common practice, no matter even if the approach is incorrect. The mine standards in place only dictate the user to ensure a certain minimum quantity of flow rates inside the heading. The user has to decide upon the selection and installation settings of auxiliary equipment to ensure the supply of the required air flow rate. The length of the heading and the air flow rates available in the Last Through Road (LTR) are not the same throughout a mine. Therefore, the settings of the auxiliary equipment used at one place may not work at another place and the ventilation engineers/supervisory staff needs to use instructions based on scientific reasoning to change the settings to get the desired flow rates for each location. The

ventilation engineers planning the ventilation need to understand the air flow patterns, flow rates and the issues related with the type and orientation of the auxiliary equipment they order the shift staff to install at different locations and at each stage of the mining.

The ability of ventilation air, with the use of these control devices, to take away methane and dust in the development headings is in fact a complete subject. The efficiency of an auxiliary ventilation system is largely affected by the system variables (Suglo and Frimpong, 2002b). The effect of the system variables associated with the auxiliary ventilation devices like the dimensions of the headings, the dimension, orientation and capacity of the auxiliary equipment, and velocity of air in the LTR can be studied through rigorous experimentation. Even tracer gas can be used to estimate the effectiveness of auxiliary ventilation systems (Suglo and Frimpong, 2002a). But to carry out a large number of experiments may not be possible as it can very time consuming and disturb the production cycles. Nowadays, experimentation has often been overtaken by simulations using powerful computers, and well developed engineering software programs that provide extensive solutions to a ventilation problem.

The advanced numerical tools, and powerful computing machines should be used in the mining industry to determine correct, quick, easy to use, and energy efficient solutions to all the ventilation problems, without disturbing the production cycles. Keeping in mind the harsh underground conditions, the educational levels of the workers / supervisors, and the requirement to meet production goals, the solutions should be easily implementable for the decision makers. An in-depth study is required to establish and recommend guidelines using mathematical models (which can estimate the effect of various system variables) for the optimum use of these devices, through analysis of the air flow, in different mining scenarios, using mathematical fluid models and software programs specially designed to study fluid flows. The simulation results will potentially help mines to use auxiliary ventilation devices in a more effective and efficient way. The intentions of this research is to provide a significant step towards understanding airflow rates delivered by the auxiliary devices close to the face of the heading, and the air flow patterns inside the heading, as a basis for improving the working environment for underground miners.

1.2 Problem statement

Ventilation network design software may show the provision of sufficient air, and ventilation conditions within the legislative requirements for the ventilation circuit. But accidents are still taking place in the headings, where methane gas and dust accumulates in the cutting zone. The local ventilation of these headings is left as the responsibility of individuals, who make decisions about the installation of the auxiliary ventilation devices based on experience, since no mathematical models have been developed to estimate the outcome of these devices.

The ability of ventilation air, with the use of the auxiliary devices, to remove or dilute methane and dust in development headings is dependent on the amount of air entering the heading. The quantity of this air changes with the variation/settings of the system variables associated with the auxiliary ventilation devices, such as heading dimension, settings of the device, and velocity of air in the LTR. The length of the development headings and the air flow rates available in the LTR are not the same throughout a mine and change at each stage of the mining. Therefore, the settings of the auxiliary equipment, used at one place may not work at another place, and supervisors need to be guided by instructions based on scientific reasoning to change the settings in order to achieve the desired flow rates for each location. The correct/optimum use of the auxiliary ventilation devices at each location can only be determined, once, the effect of each associated system variable on the flow rate is known to the user. Otherwise, the ventilation will either be more than the requirement, adding to costs, or insufficient to ensure compliance with regulations and may result in accidents and loss of lives, due to the build-up of methane and dust.

Ventilation is concerned with the flow of air and falls under the topic of fluid dynamics. Computational fluid dynamics (CFD) has become a powerful tool in almost every branch of fluid dynamics and engineering (Ren and Balusu, 2010). Ventilation network design software cannot calculate the minute details of the air flow, and its primary task is to design the ventilation of the main circuit. CFD on the other hand is used where detailed analysis is required, and where it is difficult, dangerous or impossible to perform experiments. Therefore, as a research tool to study the ventilation of a heading

in a coal mine, CFD can provide new answers regarding the variables related to auxiliary ventilation.

Although, modelling of ventilation systems for room and pillar workings has been undertaken for many years, the need for the current study using CFD and the ANSYS software package was to look at the effects of the various system variables associated with the ventilation of development headings. Through this parametric study, effects of the system variables related to the ventilation of development heading, considering a range of practical configurations with/without the use of auxiliary ventilation devices on the flow rates were estimated. The effect of the studied system variables associated with the auxiliary devices were developed into mathematical equations, to estimate the flow rates at the exit of the LB, and close to the face of the heading, in headings ventilated with LB and fans with duct. The effect of the LTR velocity, on the ventilation and maximum penetration of air, inside the headings of different dimensions ventilated without any auxiliary devices was also analysed.

1.3 Scope and Objectives of the Research

The scope of the research was to evaluate the effect of LTR velocity and different configurations of the auxiliary ventilation devices (LB and Fans with duct) on the ventilation of a development heading in room and pillar mining using CFD. The objectives of the study included the following:

- To understand the capabilities and limitations of the network designs software.
- To develop proper fluid dynamic models in ANSYS Fluent for various layouts and operating conditions and demonstrate how it can be an attractive approach to evaluate face ventilation systems using auxiliary ventilation devices.
- Analyse the effect of LTR velocity on the air penetration depths inside the heading ventilated without any auxiliary ventilation devices.
- Analyse the influence of the system variables associated with LB i.e. heading dimensions, LB settings (length of LB inside the heading and LTR, LB distance from the wall in the heading and LTR etc.) and LTR velocity, on the air flow rates at the exit of the LB and close to the face of the heading.

- Analyse the air flow pattern in a heading ventilated with LB in the absence and presence of a Continuous Miner (CM).
- Analyse the influence of the various system variables related to both the force, and exhaust fan duct system, such as, distance between the duct and the face of the heading, the diameter of the duct, and fan design flow rates, on the flow rates close to the face of the heading.
- Analyse the air flow patterns in a heading, ventilated using a force fan duct ventilation system and an exhaust fan duct ventilation system.
- Develop mathematical models, to calculate the effect of the studied system variables, related to LB, and fans with duct, on the air flow rates in a heading ventilated with these devices.

1.4 Relevance of the Research and Research Questions

The research illustrates the capabilities of CFD numerical modelling techniques, used to study the ventilation of a heading connected to the LTR in a room and pillar coal mine. The research has presented user friendly solutions to the practical issues faced by the coal mining industry related to the effective use of the auxiliary ventilation systems. The research answered the following questions.

- What is the efficacy of the numerical tools like ANSYS for the evaluation of face ventilation systems?
- How air penetration depths vary, with the change in the LTR velocity, and the dimensions of the heading?
- Relation between the LTR air velocity, depth of the heading, and the requirement of LB to ventilate a heading.
- What is the effect of the change of the following parameters on air flow rates close to the face of the heading ventilated using a LB.
 - LTR velocity
 - Length and height of the heading
 - Length of the LB in the heading
 - Length of the LB in the LTR
 - Angle of the LB in the heading

- Distance of the LB from the wall in the LTR
- Distance of the LB from the wall in the heading
- How can we estimate / calculate the air flow rates at the exit of the LB and close to the face of the heading incorporating the parameters discussed above?
- How does the air flow inside a heading ventilated with LB, and what is the impact of the above mentioned parameters on the air flow patterns?
- How does the air flow inside a heading ventilated with the use LB in the presence of a CM?
- The location of the low air flow and recirculation zones inside a heading ventilated with the use of a LB.
- How does the air flow inside a heading ventilated using force fan duct ventilation or exhaust fan duct ventilation system?
- How can we estimate / calculate the effect of the distance between the duct mouth and the face of the heading, the diameter of the duct, and fan design flow rates on air flow rates close to the face of the heading ventilated using force, or exhaust fan duct ventilation system?

1.5 Research Conceptual Framework and Methodology

The conceptual framework of the study has two distinct components; practical site characterization / considerations and numerical characterization / considerations as shown in Figure 1.1. The methodology that was adopted for the study is given below:

- Detailed literature review pertaining to the scope and objectives of this research.
- Visit to underground coal mines to understand the ventilation practices followed and to identify the critical areas in heading ventilation systems and parameters. This also allowed the creation of practical scenarios for the research.

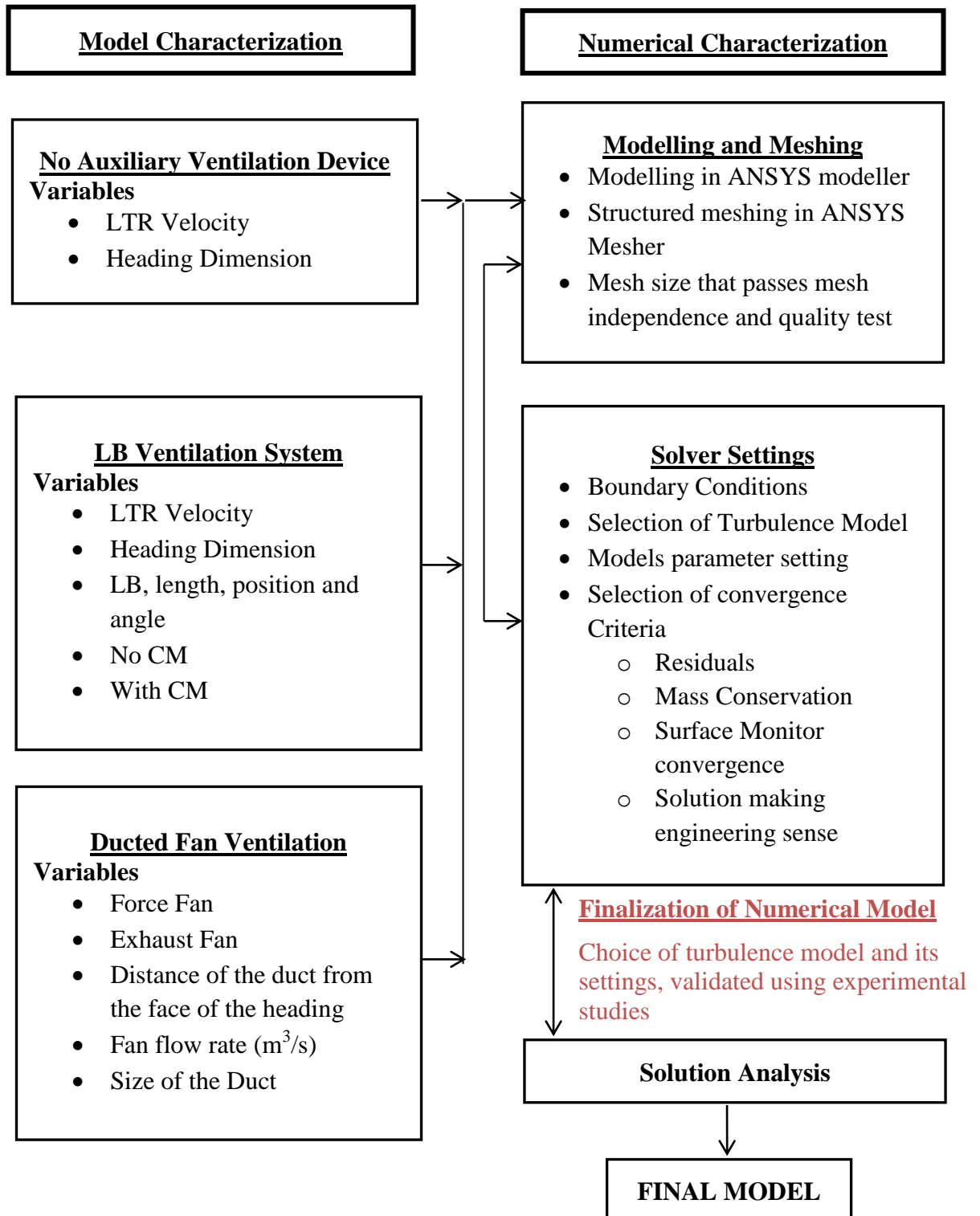


Figure 1.1 Conceptual framework of the study

- **Creation of the modelling framework**

The ultimate goal for this study was to use CFD models to simulate the effects of the system variables on the auxiliary ventilation for effective ventilation planning and miner training. The framework followed to carry out the simulations is given below:

- Geometric modelling
- Meshing of the geometry
- Governing equations
- Numerical model (for turbulence)

These items highlighted in the framework are all inter-related, and a technique used in one may affect the choices of the techniques in the other. The commercially available Fluent program was used to model airflows for this study. The first step to run a numerical simulation is the creation of the meshed model of the domain. To become familiar with numerical modelling, initially, the meshing and modelling was carried out using CFD pre-processor software, GAMBIT. Since, the service provider has stopped providing new licences for GAMBIT, the meshed models were also created in Fluent Modeller and Mesher.

Generally a structured and fine mesh with boundary (inflation) layers was used for all the cases. It was ensured the results are grid independent (that is, a more fine mesh did not affect the results). The latest k-e realizable turbulence model (explained in chapter 3) was used for this study. The model was finalized after conducting “Validation Studies” to ensure that the chosen numerical model, and its settings are the most suitable for the problem being simulated.

- The broad categories of scenarios (named as Cases followed by alphabetical name in this thesis, i.e. Case A, Case B, Case C, Case D) considered for this study are given below. The sub cases of each broad category are also named as Case, but followed with numerical numbering i.e. Case 1, Case 2 and so on:
 - Case A - Ventilation of headings without the use of any auxiliary equipment (varying heading depth and height and LTR velocity).

- Case B - Ventilation of the headings with the use of LB (varying depth and height of heading, LTR velocity and length and settings of the LB).
- Case C - Ventilation of the headings in the presence of a CM (varying the height of the heading, LTR velocity and settings of the LB).
- Case D - Ventilation of the headings using a force and exhaust fan duct system (varying the length and diameter of the duct and fan flow rates).

1.6 Thesis Structure

1.6.1 Chapter 1- Introduction

Chapter One covers the background and introduction to the problem. It also describes the problem statement, the scope of the research, objectives of the research, research questions, conceptual framework, methodology and organization of the thesis. The significance of the study is also briefly discussed in the chapter.

1.6.2 Chapter 2 - Literature review

Chapter Two covers the review of the auxiliary ventilation devices used in room and pillar coal mines. The various aspects of numerical modeling and the mathematics involved are discussed along with the methodology used by the ventilation network design software.

1.6.3 Chapter 3 - Methodology

The conceptual framework and methodology implemented for this research is presented in this chapter. The details of the components of the research related to the research matrix and the numerical modelling are discussed in detail.

1.6.4 Chapter 4 - Validation - Case Studies

This chapter gives an account of the studies carried out to validate the CFD model used in this study. A comparison of the experimental and numerical results is shown.

1.6.5 Chapter 5 - Analysis and discussion - Ventilation of headings without the use of any auxiliary equipment

The effect of the LTR air velocity on the penetration of air and flow rates inside an empty heading, ventilated without the use of any auxiliary ventilation devices is presented in this chapter.

1.6.6 Chapter 6 - Ventilation of headings with the use of line brattice

A comparative study based on the flow rates going into the heading at different depths inside the heading for each varied configuration parameter of LB, velocity of air in the LTR, and heading height and depth is presented in this chapter. Mathematical models to calculate the effect of these system variables, and estimate the flow rates at the exit of the LB and the face of the heading are also presented.

1.6.7 Chapter 7 - Ventilation of headings with CM using line brattice

The ventilation of a heading using LB, in the presence of a CM, making a straight cut, using LB ventilation is presented in this chapter to develop a better understanding of the face ventilation process.

1.6.8 Chapter 8 - Ventilation of a heading using fan with duct system

The ventilation of a heading using force and exhaust fan duct ventilation systems is presented in this chapter. The effect of some of the system variables related to these ducted systems, along with the mathematical models encompassing the effect of these system variables on the flow rates close to the face of the heading are presented.

1.6.9 Chapter 9 - Conclusion and Recommendations

This chapter highlights the findings of the study, conclusions drawn, limitations of the study and the recommendations.

1.7 Significance of the Study

This research will contribute towards enhancing the understanding of the ventilation of the development heading among Academia and mine ventilation engineers. Safety should be enhanced if ventilation engineers and the supervisory staff install the ventilation devices in an efficient and effective manner. It would be beneficial and may help to redefine the health and safety regulations as regards the installation of auxiliary ventilation devices in the coal mining industry. It would demonstrate how CFD can be an attractive tool to evaluate face ventilation systems and encourage the industry to use numerical modelling for the detailed analysis of other aspects of mine ventilation, which cannot be attained with network design software.

1.8 Conclusion

The existing limitations in the use of the auxiliary ventilation devices and the dangers of their incorrect use have been briefly discussed here. The need for the study along with the possible research questions to be answered and the methodology that was used to achieve the objectives of the study have also been explained.

2 LITERATURE REVIEW

2.1 General

The ventilation of underground coal mines is one of the most important aspects of mining. Coal mines have been using different techniques for centuries to provide sufficient air for breathing and to remove harmful contaminants from the air. Initially natural ventilation was used in which the air flow was created using the difference in temperature in the intake and return shafts and hence densities. These mines were abandoned once the natural ventilation became insufficient with the increase in the size of the mine. Ventilation continued to improve and steam driven fans were introduced starting the real regime of Mechanical Ventilation. Steam fans were followed by the presently used powerful electrically driven fans. Growing awareness of the requirements for worker health and safety resulted in the mining industry striving for better practices resulting in an early guideline for ventilation design in 1929 (Reed and Taylor, 2007).

The ventilation procedures and practices vary according to the type of mine, and the mining methods in use. Generally, the ventilation of shallow underground mines, irrespective of the type of mine and mining method, is divided into two broad branches, the primary ventilation and secondary or auxiliary ventilation systems. The primary ventilation is responsible for the total volume flow through the mine and is calculated based on the pressure, size, complexity, equipment used, production rate, etc. The auxiliary ventilation is responsible for the ventilation of the development ends, production zones and facilities disconnected from the main circuit, that is, where there is no through ventilation connections. The design and planning of primary ventilation can normally be done using ventilation network design software applications (simulators), but CFD analysis is used for the working face areas (Wu and Gillies, 2005).

The ventilation of underground coal mines is one of the most challenging amongst the mining commodities, because of the presence of methane and coal dust, which are explosive in nature and have been the cause of many major coal mine explosions. Over 330 explosions causing more than 1036 fatalities and 532 injuries have been recorded in South Africa since 1891 (Phillips and Brandt, 1995) with majority of the incidents

taking place in the production zones. The reason for these and other gas emission problems in South African coal mines is considered to arise mostly as a result of locally disrupted ventilation systems (Creedy, 1996). If methane explosions are analysed by their location then about 75% of explosions occur immediately in the working areas and in blind drifts as shown in Figure 2.1 (Tkachuk et al., 1997). The details of some of the major methane and coal dust explosions of the past are given in Table 2.1. The more recent accidents are covered in Tables 2.3 and 2.4. The gas accumulates in the production zone due to insufficient ventilation and this result in accidents. The effectiveness of the control devices used for face ventilation varies with the dimensions of the airways, the presence of equipment, placement, size, velocity of air and other factors.

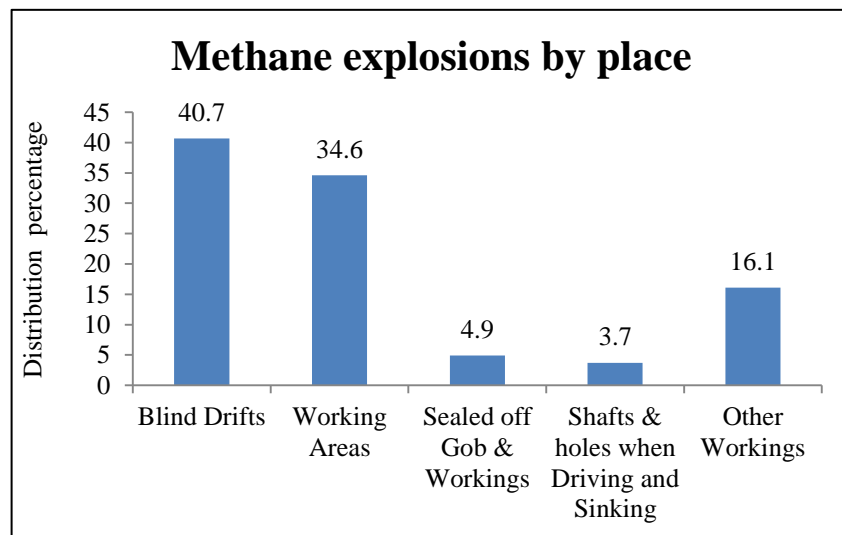


Figure 2.1 Distribution of methane explosions by place (Tkachuk et al., 1997)

Table 2.1 Major coal dust and methane explosions of the historical data (Holding, 1982)

| Major coal dust and methane explosions historical data | |
|--|------------|
| Place and year | Casualties |
| Courrieres, France, 1906 | 1100 |
| Honkeiko, Manchuria, 1942 | Over 1500 |
| Monopolgrimberg, Germany, 1946 | Over 400 |
| Luisenthal, Saar, 1962 | 299 |
| Mike, Japan, 1963 | 458 |
| Wankie Colliery, Zimbabwe, 1972 | 462 |

This chapter reviews, the coal mine hazards, types of auxiliary ventilation devices, the theory/background of CFD and the need for CFD software to solve complex fluid dynamics problems, alongside the research that has already been undertaken on the subject. The following are the components of this chapter which are explained with illustrations in the ensuing sections:

- Coal mine hazards
- Auxiliary ventilation
 - LB ventilation system
 - Fan and duct Systems
 - Ductless fans/Air movers
- Computational fluid dynamics (CFD)
- Solution methodology for CFD problems
 - Governing equations
 - Discretization techniques
 - Solution of algebraic equations
- Solving CFD problems using available software
 - Pre-processing
 - Solution
 - Post processing
 - Turbulence models
- Modeling and meshing technique/software
- Ventilation network design software

2.2 Coal Mine Hazards

The challenges for ventilation vary depending on the mining method used in the coal mines and the quality of coal. Coal in South Africa is generally shallow lying with depths of cover being less than 200m. Approximately 51% of the coal is obtained from underground mines and the remaining coal is obtained from opencast mines (Dougall, 2010). Open Cast, Longwall and Room and Pillar mining pictures are shown in Figures 2.2 through 2.4 respectively. A breakdown of the contribution to coal mining

productions made by each of the underground coal mining methods is given in Table 2.2. As shown around 90% of the coal is extracted using room and pillar mining.

Table 2.2 Production of coal from underground coal mining methods (Dougall, 2010)

| Longwall | Room and pillar | Pillar recovery (stooping) |
|----------|-----------------|----------------------------|
| 5% | 90% | 5% |



Figure 2.2 Opencast strip mining in Witbank coal field, South Africa (Chabedi, 2015)



Figure 2.3 Longwall coal face (Chabedi, 2015)

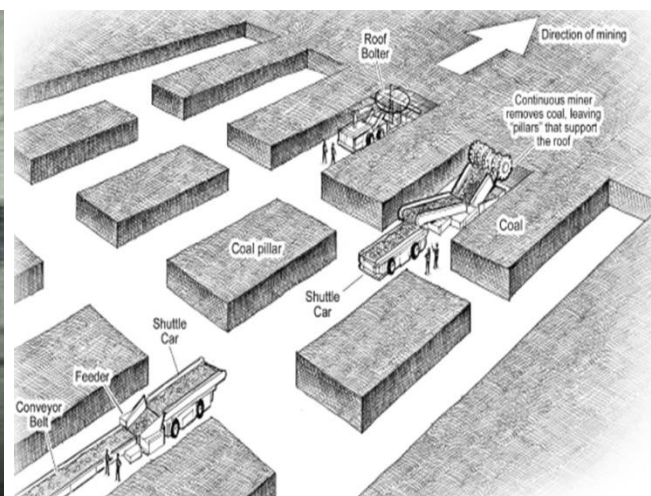


Figure 2.4 Room and Pillar mine (Chabedi, 2015)

The major hazards associated with room and pillar mining is the emission and accumulation of methane and coal dust. Methane is one of the most common strata gases and is dangerous because of its explosive nature. The ventilation air exiting the mine ventilation systems are considered to be the largest source of methane emissions from underground coal mines (US underground coal mine ventilation air methane exhausts characterization, 2010). The explosive range for methane in air is 5% to 15% as shown in Figure 2.5, beyond which methane burns, but do not explode because of the shortage of oxygen (Peng and Chiang, 1984 and McPherson, 1993). Coal mine gas explosions are generally followed by coal mine dust explosions, that take place by the ignition of a large quantity of fine coal dust, which is raised in the air (Holding, 1982). Besides explosion, coal mine dust causes lung diseases to the workers such as simple coal workers' pneumoconiosis (CWP), silicosis, progressive massive fibrosis (PMF), and other diseases collectively known as Chronic Obstructive Pulmonary (or Airway) Disease (COPD or COAD) (Stanton et al, 2006).

Coal mining history is full of coal mine explosion fatalities caused due to the disruption of the auxiliary ventilation systems, which is primarily responsible for the ventilation of the development headings. The major coal mine explosions from 2005 to 2011 are given in Table 2.3. Table 2.4 lists some of the major mine explosions (not all are in coal mines) that occurred in the English speaking world in the last 40 years.

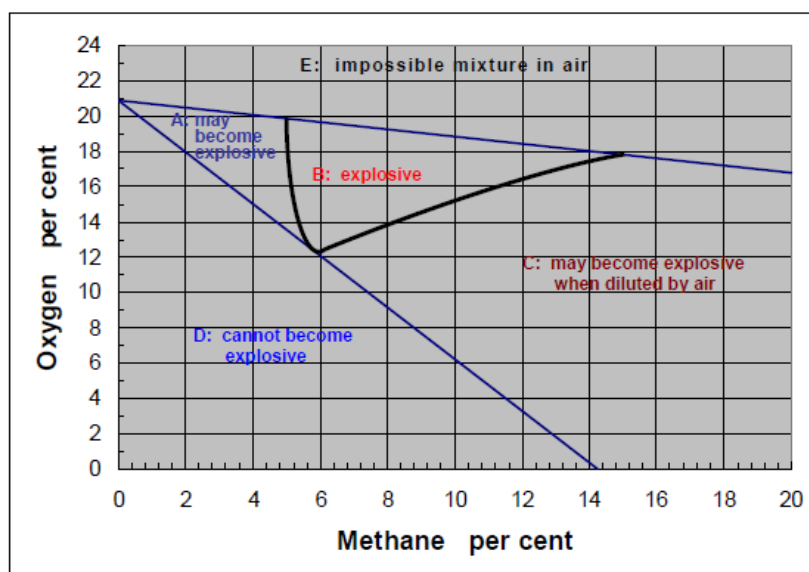


Figure 2.5 Coward diagram for methane in air (McPherson, 1993)

Table 2.3 Major coal mine explosions incidents between 2005 and 2011 (Dubinski et al., 2011)

| Major coal mine explosion incidents between 2005 and 2011 | | | |
|---|-----------|--|----------------------|
| Country | Date | Coal mine | Number of fatalities |
| China | 14-Feb-05 | Sunjiawan, Haizhou shaft, Fuxin | 214 |
| Kazakhstan | 20-Sep-06 | Lenina, Karaganda | 43 |
| USA | 2-Jun-06 | Sago, West Virginia | 12 |
| Russia | 19-Mar-07 | Ulyanovskaya, Kemerovo | 108 |
| Ukraine | 19-Nov-07 | Zasyadko, Donetsk | 80 |
| China | 21 Nov-09 | Heilongjiang | 104 |
| USA | 5-Apr-10 | Upper Big Branch, Montcoal, West Virginia | 38 |
| Russia | 8-May-10 | Raspadskaja, Mezhdurechensk | 66 |
| New Zealand | 19-Nov-10 | River Pike | 29 |
| Columbia | 26-Jan-11 | La Preciosa, Sardinata | 21 |
| Pakistan | 20-Mar-11 | Sorange district of Pakistan | 45 |
| Ukraine | 29-Jul-11 | Suhodolskaya - Vostochnaya coal mine | 19 |
| China | 29-Oct-11 | Xialiuchong mine in Hengyang of Hunan province | 29 |

Table 2.4 Sample of single-event, multi-fatality mine explosions in the English speaking world (Phillips, 2015)

| Country | Year | Fatalities |
|---------------|------|------------|
| United States | 1981 | 15 |
| United States | 2001 | 13 |
| United States | 2006 | 12 |
| United States | 2010 | 29 |
| Australia | 1975 | 13 |
| Australia | 1979 | 14 |
| Australia | 1986 | 12 |
| Australia | 1994 | 11 |
| South Africa | 1983 | 68 |
| South Africa | 1985 | 34 |
| South Africa | 1987 | 63 |
| South Africa | 1987 | 35 |
| South Africa | 1992 | 6 |
| South Africa | 1993 | 53 |
| New Zealand | 2010 | 29 |

2.3 Auxiliary ventilation

The ventilation of the development headings is carried out using the auxiliary ventilation system. These equipment are required to deliver $0.15/\text{m}^3/\text{s}/\text{m}^2$ at the face of

the coal mine as per the current regulations in South Africa. The auxiliary ventilation is usually classified into the three basic types as namely LB ventilation system, fan with ducted system and Jet fans (air movers) as discussed below:

2.3.1 LB ventilation system

A LB is a low cost, short term solution to direct air into the development heading without using any local power (McPherson, 1993). It is manufactured of plastic sheeting with or without fabric reinforcement (Hartman et al, 2012). It can be used to ventilate a development heading and increase the air penetration distance which varies with the air velocity in the LTR. If no LB is used in a development heading as shown in Figure 2.6, the air enters the development heading from the downstream side, ventilates the face, and returns to join the LTR air, but in these conditions air may not be ventilating beyond 10m in normal production conditions (Meyer, 1989 and Feroze and Phillips, 2015).

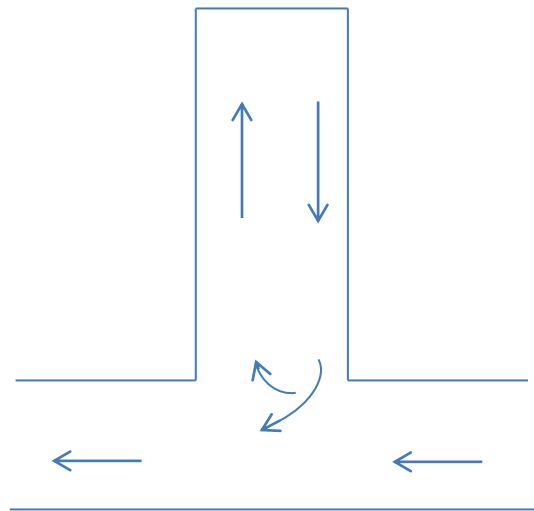


Figure 2.6 Air from LTR entering downstream in a development heading

However, the design and installation of a LB are still fundamental issues for ensuring sufficient air supply required for effective ventilation (Aminossadati and Hooman, 2008). LB ventilation systems have been studied for years. Luxner (1969) showed that in a LB ventilation system the airflow patterns were independent of the flow rate delivered by the LB system. Aminossadati and Hooman (2008) studied the effects of LB length on ventilation of the crosscut region using the 2D CFD model. Meyer (1993)

showed in the situations he studied that the recirculation with an upstream brattice (Figure 2.7) is 10% and 50% with the downstream brattice (Figure 2.8). Taylor et al. (2005), and Goodman and Pollock (2004) showed the effects of LB setback distance on return airway dust and gas levels. Meyer et al. (1991) have shown that the upstream scoops and downstream scoops increases penetration by 16% and 46% respectively and also the air velocities were more than without the use of LB. Tien (1988) revealed that a LB is essential to prevent recirculation and control respirable dust and methane in the face area. Thimons et al. (1999) studied the influence of LB setback distance on the airflow at the coal face in the presence of a continuous miner. Sasmito et al. (2013) examined the ventilation of the cross-cut region and found that a combination of brattice-exhausting system yields the best performance. Wang et al. (2011) numerically evaluated the usefulness of the air curtain to resolve the problem of dust-isolation at a fully mechanized working face. Candra et al. (2014) carried out the comparison of different auxiliary ventilation systems and concluded that the LB is the most suitable for application in underground mine. In another study Candra et al. (2015) proposed a hybrid brattice system to mitigate dust dispersion from the face to keep the working area safe for the miners.

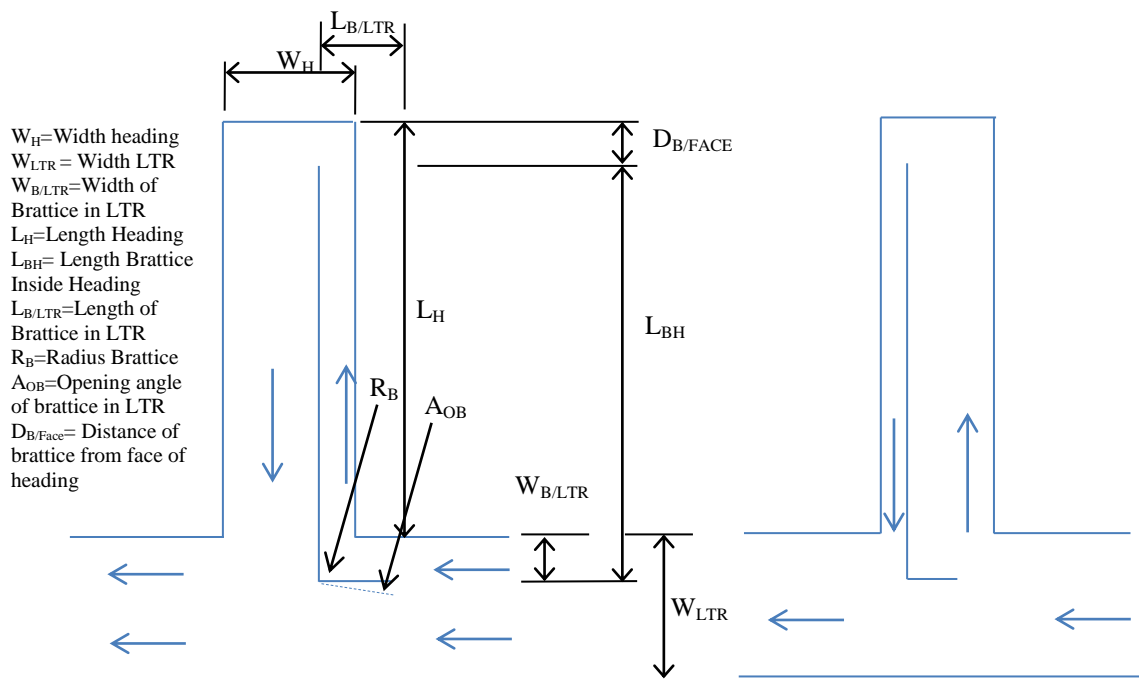


Figure 2.7 Upstream LB

Figure 2.8 Downstream LB (Meyer, 1993)

2.3.2 Fan with duct ventilation system

The increase in production rates and the use of high production machines resulted in increased dust and methane levels in the production zone. The lengths of the heading has increased to about 30 m and require higher pressure to mover the air through a longer distances to ventilate the headings. This has resulted in the introduction of fans with duct systems. There are three types of this system, namely, force, exhaust, and overlap system. The decision to select a particular type of system depends on the nature of the hazard (Pawinski and Roszkowski, 1985 and McPherson, 1993). These hazards can be:

- Methane
- Dust
- Heat
- Fire Hazards

The choice of the fan with duct system is generally considered to depend on the following factors:

- Length of duct/ducts inside the heading
- Distance of duct mouth from the face of the heading
- Length of duct in the LTR
- Air speed in the main air way
- Depth and height of the heading
- Location of equipment in the heading
- Water spray system and scrubbers mounted on a CM
- Overlap distance in overlap system

2.3.2.1 Force fan duct system

The force fan duct system consists of a line of ducting, to which a fan is connected to force air into the heading as shown in Figure 2.9. It is usually used in mines with high methane hazards, and can effectively remove the methane hazard through dilution (Taylor et al., 1997). Szlajak et al. (2003) have also shown that the methane concentration measured in headings is lower with the force system than with the exhaust

systems under the same ventilation and methane emission conditions. The high velocity of air helps in mixing the methane with air, which prevents it from settling on the roof and provides cooler air at the face (McPherson, 1993). Studies by Schultz (1993) and Kissell (2003) indicated that the proportion of fresh air reaching the face is 39.9% for the force system and 10 % for the exhaust system. Torano et al. (2009) found these proportions to be equal to 35% and 12%, respectively. The force system results in a positive gauge pressure so a cheaper and flexible duct can be used (AMC Consultants, 2005). When higher dust concentrations are encountered, the force system is generally not used because of the higher air velocity and also because the return air pollutes the main circuit air once it returns back from the heading.

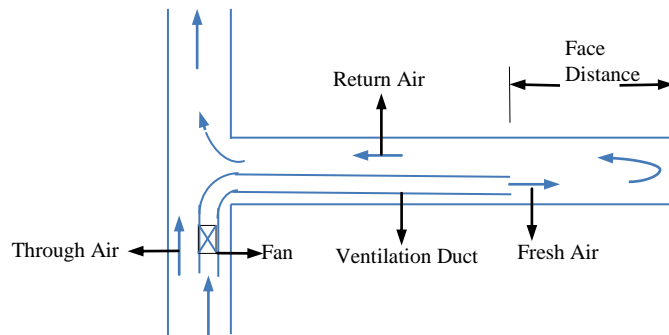


Figure 2.9 Force fan duct ventilation system (Thorp, 1982)

2.3.2.2 Exhaust fan duct ventilation system

The exhaust fan duct system consists of a duct line, to which a fan is connected, to spent air from the heading as shown in Figure 2.10 (expected to change with the positioning of the duct and LTR velocity). It is primarily used in mines with higher dust hazards since a force system with high velocity spreads the dust. Normally a dust collector / filter is used within the system. Rigid or spiral type flexible ducting is required to be used because of the negative pressure involved (AMC Consultants, 2005). This system is not suitable for long headings since the resistance of the duct becomes large warranting the use of multiple fans in series (McPherson, 1993). The danger of methane build-up and recirculation is a general concern with this system. In Polish coal

mines in the year 2002, the contribution of the force, exhaust and overlap auxiliary ventilation system was 16%, 43% and 41% respectively (Szlazak, 2003).

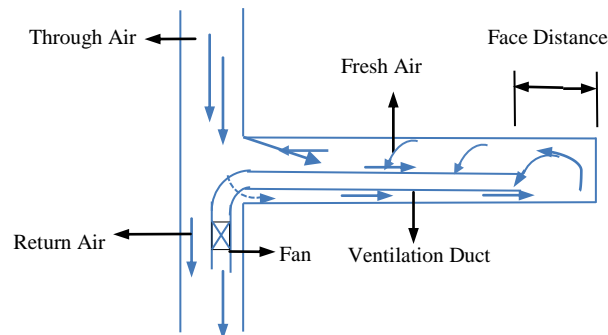


Figure 2.10 Exhaust fan and duct ventilation system

2.3.2.3 Overlap system

An overlap ventilation system is the combination of a primary and a secondary duct. The overlap of a primary force duct and a secondary exhaust overlap duct as shown in Figure 2.11 is called the force overlap. The overlap of a primary exhaust duct and a secondary force overlap duct as shown in Figure 2.12 is called the Exhaust overlap system. Overlap ventilation systems are generally used when the development end needs to advance more rapidly than normal in rock blasting scenarios. The force overlap is used when the CM is cutting in the heading, and an exhaust overlap is used when thermal, methane and dust hazards are encountered at the same time (Szlazak, 2003). The fans are electrically interlinked when using the overlap system as a safety measure, to avoid the operation of the overlap system when the fan of the primary duct is not on or vice versa. The overlap distance and the length of the auxiliary duct are of varying proportions in the literature. The overlap distance varies between 10m and 15m and the length of the auxiliary duct is controlled by the overlap distance and its distance from the face.

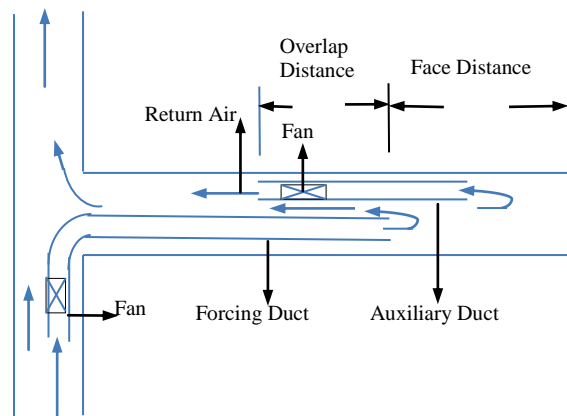


Figure 2.11 Forcing overlap system (Zhang et al., 2011)

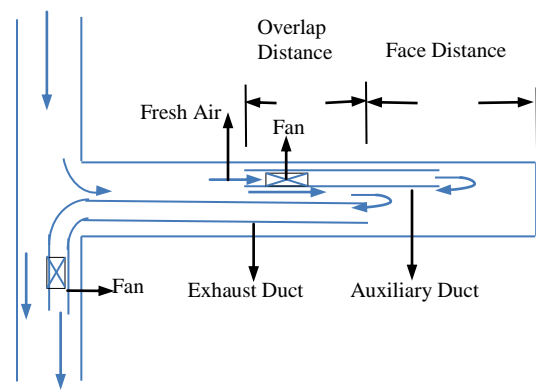


Figure 2.12 Exhaust overlap system (Thorp, 1982)

2.3.3 Stand - alone fans (Jet fans)

The jet fan is a free standing fan that produces a higher velocity stream of air in comparison to the ducted fans. It produces a narrow flow pattern that expands by pulling the air from its surroundings into the stream as shown in the Figure 2.13. It is used to ventilate very deep headings because it can move the air to longer distances.

The problems with a jet fan are that the return (contaminated) air can enter the intake of the fan causing recirculation and it is very noisy (Campbell, 1987). The jet fan may be feasible for ventilating cut depths greater than 12 m (40 ft) (Taylor et al., 1992). Meyer and Vanzyl (1999) have shown on the basis of tests conducted for SIMRAC that jet fans produce two types of flows in a heading, the “U” type or the “Figure of Eight” type as shown in Figure 2.13 and 2.14 respectively. The design parameters of a jet fan, controls the reach, air velocity and the type of flow it produces, but the U type of flow is preferred for better dust and methane control.

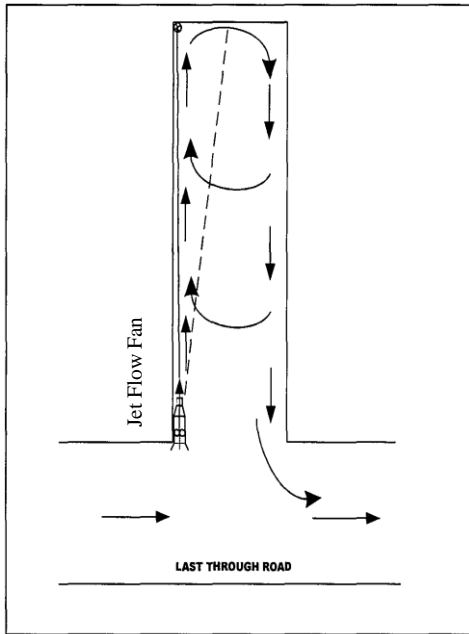


Figure 2.13 U Type flow pattern (Meyer and Vanzyl, 1999)

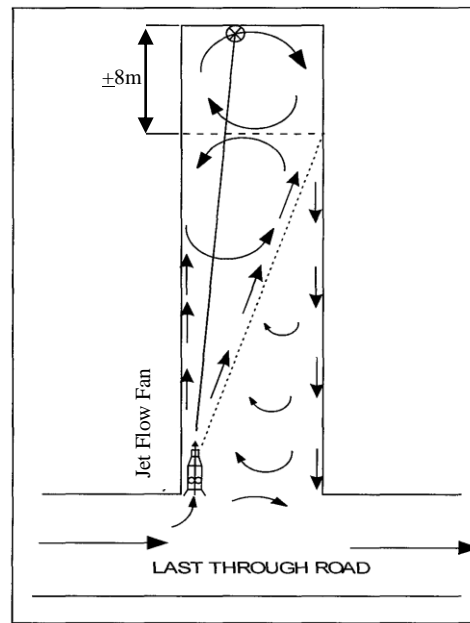


Figure 2.14 Figure of Eight flow pattern (Meyer and Vanzyl, 1999)

The literature review of the auxiliary ventilation systems shows that the ventilation of headings using these devices changes with the variation/settings of the associated system variables, such as heading dimension, settings of the auxiliary equipment, and velocity of air in the LTR. However, no mathematical models have been developed to estimate the outcome or comparison of results of the auxiliary ventilation systems. Therefore, an in depth study is required to investigate the ventilation of the development headings to develop mathematical models to estimate the ventilation.

2.4 Computational Fluid Dynamics

The study, planning and design of the primary ventilation are carried out using ventilation network design software, such as Vnet PC, VUMA, VentSim, Vent Graph etc. However, the auxiliary ventilation is generally studied and planned using experiments, experience and CFD analysis. CFD is one of the branches of fluid mechanics. It started in the early 1970's and employed physics, numerical mathematics and computer sciences to simulate fluid flows. CFD has been described (Anderson, 1995) as "the art of replacing the partial derivatives in the fluid motion equations with discretized algebraic form". The algebraic equations are solved to obtain flow field

values at discrete points in the time and or space, using numerical methods. CFD can be used to solve fluid dynamics problems in both two and three dimensions, producing illustrative results, which helps the user to have an increased understanding of the problem. It has become a powerful tool in almost every branch of fluid dynamics and engineering (Ren and Balusu, 2010).

CFD has been extensively used to simulate air flows in the mining industry. Siddique et al. (2005) used CFD to investigate flow patterns, water vapour and temperature in a mine situation. Conglu et al. (2012) used Ansys Fluent to study the local forced ventilation of the long headings. Van Heerden and Sullivan (1993) used CFD to simulate the continuous miner and road header working areas. Wala et al. has carried out simulations related to working face with a continuous miner (Wala et al., 2003), and the air requirement to ventilate methane during box cut and slab cut (Wala et al., 2007). Purushotham and Bandopadhyay (2010) simulated the shock-loss phenomenon of different configurations of air-crossings. Diego et al. (2011) simulated the air loss calculation all over the installation using CFD. Yuan and Smith (2008) simulated the spontaneous heating of coals in gob areas. Meyer and Vanzyle (1999) showed that the U type of flow produced by the jet fan is preferred for better dust and methane control. Zheng and Tien (2008) used CFD to simulate the diesel particulate exhaust from machines used in mining. Lihong et al. (2015) studied the effect of the LB distance from the face in the presence of a continuous miner using CFD and showed that the ventilation improves with the reduction in this distance.

The important aspects of CFD and the theory behind the CFD solvers is discussed in this section to understand why CFD software programs and powerful machines are required to solve the complex problems of fluid dynamics.

The CFD solvers are designed to solve a set of Partial Differential Equations (PDE's) defining the flow fields of the problem. These PDE's are derived from the following three fundamental principles of physics which rule all the aspects of fluid flows (Anderson, 1995).

- Conservation of Mass
- Newton's Second Law of Motion
- Conservation of Energy


The governing equations used to solve any physical problem in fluid dynamics are derived using these fundamental principles. The governing equations are coupled equations, which are nonlinear and are therefore, very difficult to solve analytically, necessitating the use of numerical methods. The system of equations is converted into algebraic equations which are subsequently solved numerically, using different explicit and implicit numerical techniques. The important aspects of CFD and numerical modelling are shown in Figure 2.15 and discussed in the ensuing paragraphs. A few important terminologies necessary to understand these aspects, as defined by Anderson (2005) are therefore given below first:

- **Substantial derivative**

Substantial or material derivative D/Dt is defined as the time rate of change of any physical quantity following a moving fluid element. It is used to describe a quantity in a velocity field and is equal to the sum of the time derivative and the dot product of velocity with space derivative of that quantity as shown in equation 2.1 and 2.2.

$$\boxed{\frac{D\rho}{Dt} = \frac{\partial\rho}{\partial t} + u\frac{\partial\rho}{\partial x} + v\frac{\partial\rho}{\partial y} + w\frac{\partial\rho}{\partial z}} \quad (2.1)$$

$$\Rightarrow \frac{D}{Dt} = \frac{\partial}{\partial t} + \underbrace{u\frac{\partial}{\partial x} + v\frac{\partial}{\partial y} + w\frac{\partial}{\partial z}}_{\text{Convective Derivative}} = \frac{\partial}{\partial t} + (\vec{v} \cdot \nabla) \quad (2.2)$$


Local Derivative
Convective Derivative

- **Local and convective derivative**

Local and convective derivatives are the time rate of change at a fixed point and the time rate of change because of the movement of a fluid element from one location to another in the flow field where the flow properties are spatially different.

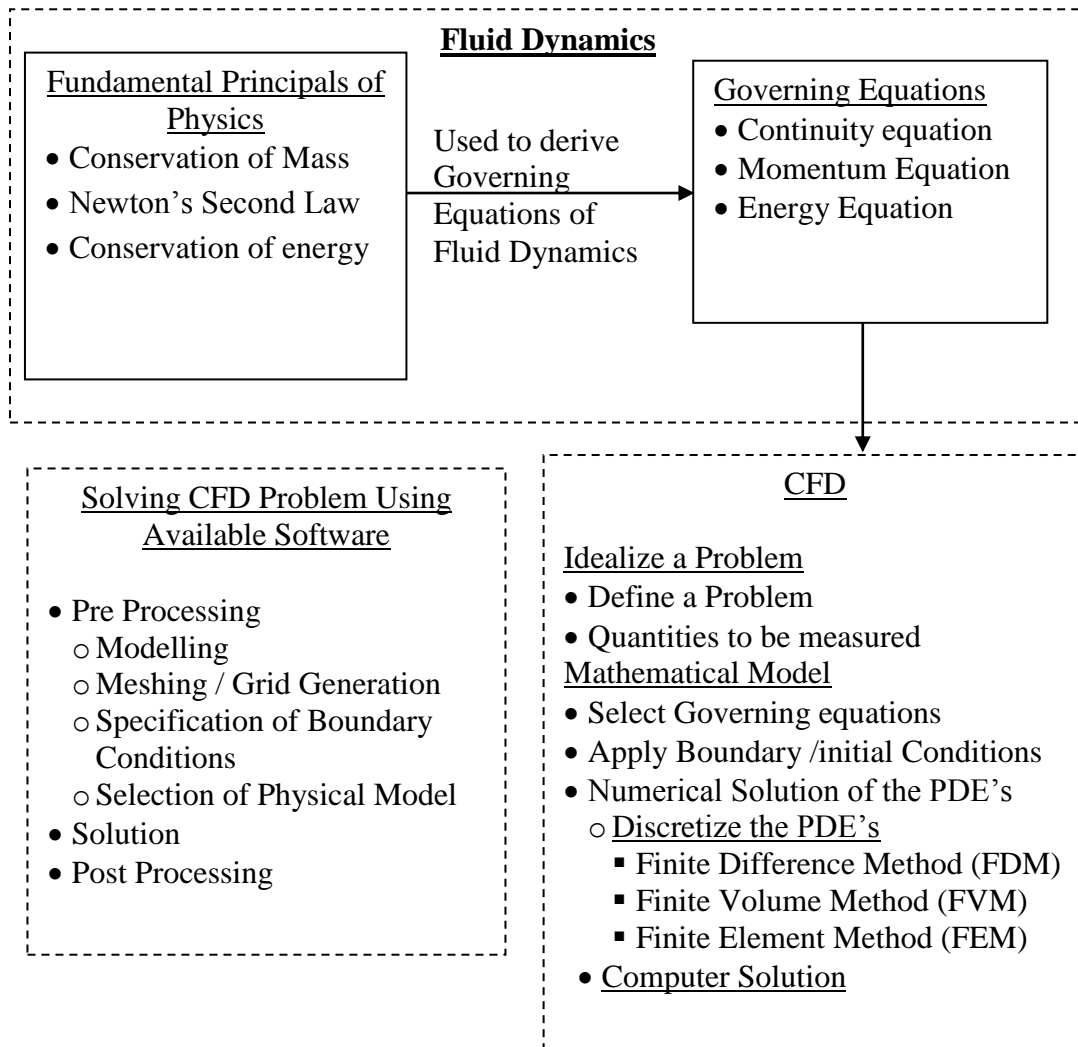


Figure 2.15 Important aspects of CFD and numerical modeling (Anderson, 2015)

- **Divergence of a vector**

The divergence of a vector field is defined as the dot product of “Del” with the vector $\nabla \cdot vector$. Where “Del” is defined as $\nabla \equiv i \frac{\partial}{\partial x} + j \frac{\partial}{\partial y} + k \frac{\partial}{\partial z}$, so for a vector with components (P,Q,R) the divergence is defined as:

$$\left(\frac{\partial}{\partial x} + \frac{\partial}{\partial y} + \frac{\partial}{\partial z}\right) \cdot (P, Q, R) = \frac{\partial P}{\partial x} + \frac{\partial Q}{\partial y} + \frac{\partial R}{\partial z} \quad (2.3)$$

The divergence, convergence, and zero divergence are shown in Figure 2.16 through 2.18 respectively. These figures are showing whether a vector flow into a body is more, less or equal to the out flow.

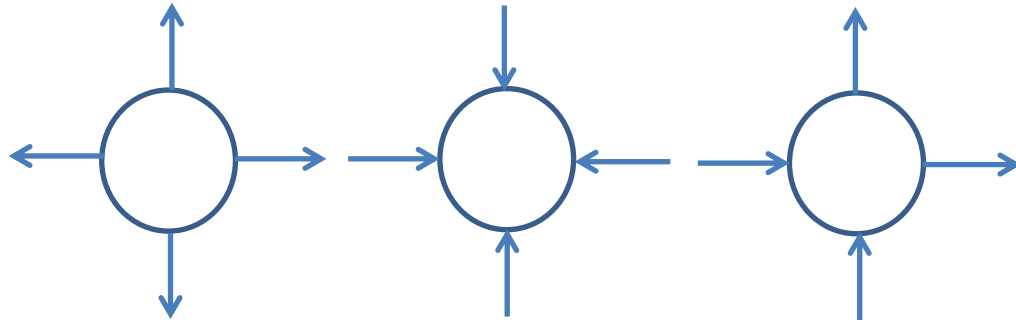


Figure 2.16 Divergence

Figure 2.17 Convergence

Figure 2.18 Divergence = 0

2.4.1 Governing equations of fluid dynamics

A brief account of the governing equations of fluid dynamics as discussed by Anderson (2005) is given below:

- **Continuity equation (Conservation of mass)**

The continuity equation is derived from the physical principal of mass conservation, i.e. net mass flow out of a control volume is equal to zero or is equal to the time rate of decrease of mass / density inside a volume as given in equation 2.4 and 2.5.

$$\left[\frac{\partial(\rho u)}{\partial x} + \frac{\partial(\rho v)}{\partial y} + \frac{\partial(\rho w)}{\partial z} \right] dx dy dz = - \frac{\partial \rho}{\partial t} (dx dy dz) \quad (2.4)$$

$$\nabla \cdot (\rho \vec{v}) = - \frac{\partial \rho}{\partial t} \quad (2.5)$$

where,

$\rho = \text{density}$, $v = \text{velocity}$

$$\nabla \equiv i \frac{\partial}{\partial x} + j \frac{\partial}{\partial y} + k \frac{\partial}{\partial z} \quad (2.6)$$

$$\nabla \cdot (\rho \vec{v}) \equiv \frac{\partial(\rho u)}{\partial x} + \frac{\partial(\rho v)}{\partial y} + \frac{\partial(\rho w)}{\partial z} \quad (2.7)$$

u, v, w are velocity components in x, y, z direction

When density is constant (steady flow) this expression reduces to $\nabla \cdot \vec{v} = 0$, which means that the divergence $\frac{\partial u}{\partial x} + \frac{\partial v}{\partial y} + \frac{\partial w}{\partial z} = 0$ of velocity vector field is zero.

- **Momentum equation (conservation of momentum)**

The momentum equations are derived from the application of Newton's Second law of motion to a fluid and are famously known as the Navier - Stokes equations. Any fluid element in equilibrium is acted upon by "body forces" and the "gravitational force". The body forces include, the pressure gradient on the fluid particle and the shear stresses arising due to the velocity gradient (difference in velocity of fluid on either side of the fluid particle) forces which can deform the particle. If these forces are not in equilibrium, the particle of fluid will not remain in equilibrium and accelerate (Dv/Dt). The momentum equation can then be written as:

Mass x Acceleration of fluid particle = pressure gradient +shear stress +body forces

$$\rho \frac{Du}{Dt} = \frac{\partial(\rho u)}{\partial t} + \nabla \cdot (\rho u \vec{v}) = -\frac{\partial p}{\partial x} + \frac{\partial \tau_{xx}}{\partial x} + \frac{\partial \tau_{yx}}{\partial y} + \frac{\partial \tau_{zx}}{\partial z} + \rho f_x \quad (2.8)$$

$$\rho \frac{Dv}{Dt} = \frac{\partial(\rho v)}{\partial t} + \nabla \cdot (\rho v \vec{v}) = -\frac{\partial p}{\partial y} + \frac{\partial \tau_{xy}}{\partial x} + \frac{\partial \tau_{yy}}{\partial y} + \frac{\partial \tau_{zy}}{\partial z} + \rho f_y \quad (2.9)$$

$$\rho \frac{Dw}{Dt} = \frac{\partial(\rho w)}{\partial t} + \nabla \cdot (\rho w \vec{v}) = -\frac{\partial p}{\partial z} + \frac{\partial \tau_{xz}}{\partial x} + \frac{\partial \tau_{yz}}{\partial y} + \frac{\partial \tau_{zz}}{\partial z} + \rho f_z \quad (2.10)$$

where,

$\frac{D}{Dt}$ = Substantial derivative

$\frac{\partial}{\partial t}$ = Local derivative

f_x, f_y, f_z are body forces in x, y, z directions respectively

P = Pressure

$\tau_{xx}, \tau_{yy}, \tau_{zz}$ = Normal Stress in x, y, z direction respectively,

τ_{ij} = Shear stress on j direction exerted on a plane perpendicular to the i axis

u, v, w are velocity components in x, y, z direction

- **Energy equation:** The energy equation is based on the physical principle of conservation of energy, which is defined by the 1st law of thermodynamics as: The rate of change in energy inside a fluid element (A) = Rate of work done due to the body forces on the element (B)+ Rate of work done due to surface forces on the element (C) + Net heat flow into the element (D) (Anderson, 1995).
- The total energy is the sum of the internal energy (due to random molecular motion), and the kinetic energy $V^2/2$. The time rate of change of total energy per unit mass is thus given by the substantial derivative as shown in equation 2.11.

$$\rho \frac{D}{Dt} \left(e + \frac{V^2}{2} \right) dx dy dz = \left[\frac{\partial}{\partial t} \left[\rho \left(e + \frac{V^2}{2} \right) \right] + \nabla \cdot \left[\rho \left(e + \frac{V^2}{2} \vec{V} \right) \right] \right] dx dy dz \quad (2.11)$$

- The rate of work is defined as force x velocity, so the rate of work done by the body force per unit mass is given by equation 2.12.

$$B = \rho f \cdot V dx dy dz \quad (2.12)$$

- The rate of work done by the surface force is due to the pressure, shear and normal stress calculated using force x velocity is given by the equation

$$C = \left[\begin{aligned} & - \left(\frac{\partial(up)}{\partial x} + \frac{\partial(vp)}{\partial y} + \frac{\partial(wp)}{\partial z} \right) + \frac{\partial(u\tau_{xx})}{\partial x} + \frac{\partial(u\tau_{yy})}{\partial y} + \frac{\partial(u\tau_{zz})}{\partial z} + \frac{\partial(v\tau_{xy})}{\partial x} \\ & + \frac{\partial(v\tau_{yx})}{\partial y} + \frac{\partial(v\tau_{zy})}{\partial z} + \frac{\partial(w\tau_{xz})}{\partial x} + \frac{\partial(w\tau_{yz})}{\partial y} + \frac{\partial(w\tau_{zx})}{\partial z} \end{aligned} \right] dx dy dz \quad (2.13)$$

- The sources of heat flux are, heating due to absorption or emission of radiation (volumetric heating), and the heating due to thermal conduction i.e. heat transfer due to temperature gradient. The volumetric heat addition is given by equation 2.14. Where rate of volumetric heat addition is given by \dot{q}

$$\text{Volumetric heating of element} = \rho \dot{q} dx dy dz \quad (2.14)$$

- The heat transferred by thermal conduction is given by equation 2.15, where k is the thermal conductivity.

$$\left[\frac{\partial}{\partial x} \left(k \frac{\partial T}{\partial x} \right) + \frac{\partial}{\partial y} \left(k \frac{\partial T}{\partial y} \right) + \frac{\partial}{\partial z} \left(k \frac{\partial T}{\partial z} \right) \right] dx dy dz \quad (2.15)$$

The energy equation 2.16 is a combination of the time rate of change of energy per unit mass, the work done by the body and surface forces, and the addition of heat flux due to volumetric and conductive heat addition.

$$\begin{aligned}
\frac{\partial}{\partial t} \left[\rho \left(e + \frac{V^2}{2} \right) \right] + \nabla \cdot \left[\rho \left(e + \frac{V^2}{2} \vec{V} \right) \right] &= \rho \dot{q} + \frac{\partial}{\partial x} \left(k \frac{\partial T}{\partial x} \right) \frac{\partial}{\partial y} \left(k \frac{\partial T}{\partial y} \right) + \frac{\partial}{\partial z} \left(k \frac{\partial T}{\partial z} \right) - \frac{\partial(u p)}{\partial x} \\
- \frac{\partial(v p)}{\partial y} - \frac{\partial(w p)}{\partial z} + \frac{\partial(u \tau_{xx})}{\partial x} + \frac{\partial(u \tau_{yx})}{\partial y} + \frac{\partial(u \tau_{zx})}{\partial z} + \frac{\partial(v \tau_{xy})}{\partial x} + \frac{\partial(v \tau_{yy})}{\partial y} + \frac{\partial(v \tau_{zy})}{\partial z} + \\
\frac{\partial(w \tau_{xz})}{\partial x} + \frac{\partial(w \tau_{yz})}{\partial y} + \frac{\partial(w \tau_{zz})}{\partial z} + \rho \vec{f} \cdot \vec{V} &
\end{aligned} \tag{2.16}$$

2.4.2 Key steps of CFD

CFD is used to discretize the fundamental partial differential equations into algebraic form which are solved to give results at discrete locations. The three steps to solve any fluid dynamics problem are (Anderson, 1995):

- Visualizing the problem and defining the quantities that are required to be measured.
- Designing a mathematical model includes the selection of the governing equation/equations, and the initial and boundary conditions.
- Use numerical techniques to solve the fluid problems, which involve discretization of the governing equations into algebraic forms to be solved at discrete locations.

2.4.3 Discretization

The fundamental idea behind numerical schemes is to approximate the partial derivatives by algebraic expressions. This process of approximation is called discretization. Physically, it is the division of a domain into a number of discrete sub-domains (elements, control volumes etc. depending on the method used) with each sub domain represented by a discrete set of points (grid points, nodes etc.). The governing differential equations are then converted into a system of algebraic equations valid at each of these discretized points. These algebraic equations are then solved using direct or indirect methods available for solving a set of algebraic equations. The three classical choices for approximation as discussed by Hoffmann and Chiang (2000) are briefly discussed below:

2.4.3.1 Finite difference method (FDM)

FDM is the oldest technique in which Taylor series expansion is used to discretize a differential equation. Forward, backward, and central difference approximations schemes, using grid points shown in Figure 2.19 through 2.21 respectively, and derived using Taylor series expansion are given below (Hoffmann and Chiang, 2000):

$$f(x + \Delta x) = f(x) + (\Delta x) \frac{\partial f}{\partial x} + \frac{(\Delta x)^2}{2!} \frac{\partial^2 f}{\partial x^2} + \frac{(\Delta x)^3}{3!} \frac{\partial^3 f}{\partial x^3} + \dots \quad \text{(Taylor Series)} \quad (2.17)$$

$$\left. \begin{aligned} \frac{\partial f}{\partial x} &= \frac{f(x + \Delta x) - f(x)}{\Delta x} - \frac{(\Delta x)}{2!} \frac{\partial^2 f}{\partial x^2} - \frac{(\Delta x)^2}{3!} \frac{\partial^3 f}{\partial x^3} + \dots \\ \frac{\partial f}{\partial x} &= \frac{f(x + \Delta x) - f(x)}{\Delta x} + O(\Delta x) \end{aligned} \right\} \quad \text{(Forward Difference)} \quad (2.18)$$

$$\frac{\partial f}{\partial x} = \frac{f(x) - f(x - \Delta x)}{\Delta x} + O(\Delta x) \quad \text{(Backward Difference)} \quad (2.19)$$

$$\frac{\partial f}{\partial x} = \frac{f(x + \Delta x) - f(x - \Delta x)}{2\Delta x} + O(\Delta x)^2 \quad \text{(Central Difference)} \quad (2.20)$$

Where x is a function of $f(x)$, Δx is the increment and $O(\Delta x)$ is the order of error

FDM is the easiest approach implement and is best suited to handle rectangular shapes and simple geometries. It is very hard and cumbersome to handle irregular shapes with this method, which requires the division of the shape into regular zones.

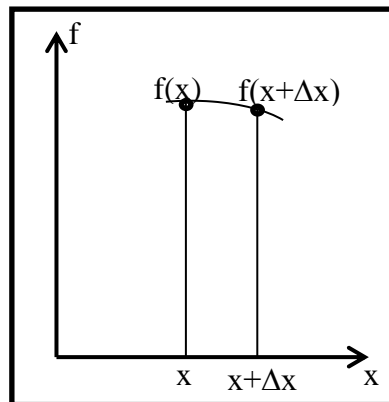


Figure 2.19 Grid points used for forward differencing, (Hoffmann and Chiang, 2000)

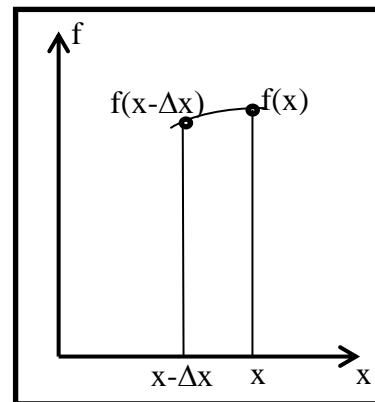


Figure 2.20 Grid points used for backward differencing, (Hoffmann and Chiang, 2000)

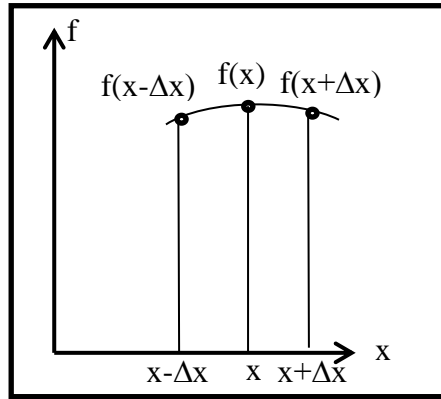


Figure 2.21 Grid points used for central differencing, (Hoffmann and Chiang, 2000)

2.4.3.2 Finite volume method (FVM)

The integration of the governing equations over a control volume is used for discretization, i.e. a control volume approach, which allows this method to solve complex geometries in multi-dimensional problems. The geometric difficulty is the concern of grid generation routines and not the FVM solver. The illustration of FVM is given below for the model equation 2.21.

$$\frac{\partial A}{\partial t} + \frac{\partial B}{\partial x} + \frac{\partial C}{\partial y} = 0 \quad (2.21)$$

The steps to solve equation 2.21 over the quadrilateral domain shown in Figure 2.22 are (Hoffmann and Chiang, 2000):

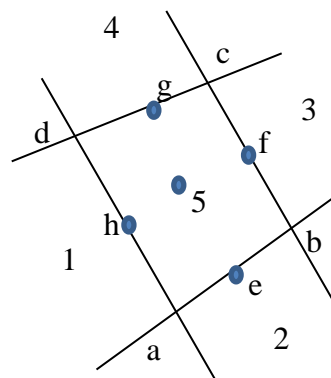


Figure 2.22 Grid for FVM, (Hoffmann and Chiang, 2010)

- Integrate the equation over the quadrilateral mesh element abcd.

$$\int_{abcd} \left(\frac{\partial A}{\partial t} \right) dx dy = - \int_{abcd} \left(\frac{\partial B}{\partial x} + \frac{\partial C}{\partial y} \right) dx dy = 0 \quad (2.22)$$

- Convert area integral to line integral using Green's Theorem (Calculus, G. Strang, 2009).

$$\int_{abcd} \left(\frac{\partial A}{\partial t} \right) dx dy = - \oint_{abcd} (B dy - C dx) \quad (2.23)$$

- Approximate the integral over the quadrilateral element to find the dependent variable A at point 5. The resultant Equation 2.24 is equivalent to a central difference scheme.

$$\left(\frac{A_5^{n+1} - A_5^n}{\Delta t} \right) A_{abcd} = - \left[B_e \Delta y_{ab} + B_f \Delta y_{bc} + B_g \Delta y_{cd} + B_h \Delta y_{da} \right] + \left[C_e \Delta x_{ab} + C_f \Delta x_{bc} + C_g \Delta x_{cd} + C_h \Delta x_{da} \right] \quad (2.24)$$

Where,

A_{abcd} = area of cell

efgh = mid points of ab, bc, cd, da

Pt₁, Pt₂, Pt₃, Pt₄, Pt₅ = control points of the five quadrilaterals

$B_e = 1/2(B_5^* + B_2^*)$ similarly others by averaging values from control points on either side

$C_e = 1/2(C_5^* + C_2^*)$ similarly others by averaging values from control points on either side

$\Delta x_{da} = x_a - x_d$ similarly others

2.4.3.3 Finite element method (FEM)

This method is generally used for structural mechanics analysis, like stress calculation, deformation calculation etc. and is not discussed here. Details can be found from Hoffmann and Chiang (2010).

2.4.4 Solution of algebraic equations

The resultant algebraic set of equations obtained from discretization can be written in the matrix equation form as $AX=B$, where A is the coefficient matrix, X is the solution vector, and B is the matrix of right side of the algebraic equations (Strang, 2009). These algebraic equations are solved using direct and indirect methods. These two methods as discussed by Strang (2009) and Collins II (2003) are briefly explained below:

$$\left. \begin{array}{l} a_{11}x_1 + a_{12}x_2 + \dots + a_{1n}x_n = b_1 \\ a_{21}x_1 + a_{22}x_2 + \dots + a_{2n}x_n = b_2 \\ \vdots \\ a_{m1}x_1 + a_{m2}x_2 + \dots + a_{mn}x_n = b_n \end{array} \right\} \text{(Set of Linear Equations)} \quad (2.25)$$

$$A = \begin{pmatrix} a_{11} & a_{12} & \cdot & a_{1n} \\ a_{21} & a_{22} & \cdot & a_{2n} \\ \cdot & \cdot & \cdot & \cdot \\ a_{m1} & a_{m2} & \cdot & a_{mu} \end{pmatrix} \quad (2.26) \quad X = \begin{pmatrix} x_1 \\ x_2 \\ \cdot \\ x_n \end{pmatrix} \quad (2.27)$$

$$B = \begin{pmatrix} b_1 \\ b_2 \\ \cdot \\ b_n \end{pmatrix} \quad (2.28) \quad \text{Augmented Matrix} = \begin{pmatrix} a_{11} & a_{12} & \cdot & a_{1n} & | & b_1 \\ a_{21} & a_{22} & \cdot & a_{2n} & | & b_2 \\ \cdot & \cdot & \cdot & \cdot & | & \cdot \\ a_{m1} & a_{m2} & \cdot & a_{mn} & | & b_n \end{pmatrix} \quad (2.29)$$

$$\text{Upper Triangular Matrix} = \begin{pmatrix} C_{11} & C_{12} & \cdot & C_{1n} & | & d_1 \\ 0 & C_{22} & \cdot & C_{2n} & | & d_2 \\ \cdot & \cdot & \cdot & \cdot & | & \cdot \\ 0 & 0 & \cdot & C_{mn} & | & d_n \end{pmatrix} \quad (2.30)$$

2.4.4.1 Direct methods

The direct methods are used when high precision is required and the augmented matrix is fully populated/dense or for tri-diagonal matrices. The general types of direct method given by (Strang, 2009) are discussed below:

- **Gauss elimination method** (Strang, 2009)

The gauss elimination method of solving a system of linear equations $AX=B$, is a method in which an augmented matrix (equation 2.29) is reduced to an upper triangular matrix (equation 2.30), through a sequence of elementary row operations. The upper triangular matrix is then solved by back substitution to get the solution vector. The row operations used to reduce the augmented matrix to an upper triangular matrix can be:

- Multiplication of a row by a non-zero real number.
- Swapping of two rows.
- Multiply a row a real number and add it to another row.
- **Cramer’s rule** (Strang, 2009)
 The solution of a system of “n” algebraic equations using Cramer’s rule is given by $x_1 = D_1/D$, $x_2 = D_2/D$, ………, $x_n = D_n/D$, Where D is the determinant of matrix A (equation 2.26) and D_k , ($K=1, 2, 3, \dots, n$) is the determinant of a matrix obtained from A by replacing the k^{th} column of B (B as given in equation 2.28).
- **Gauss - Jordan elimination** (Strang, 2009)
 The Gauss-Jordan elimination method is a forward elimination, backward substitution method in which an augmented matrix is reduced to a “Row Reduced Echelon Matrix” and the solution vector is obtained by back substitution. An augmented matrix is in “**reduced row echelon**” form when:
 - The leftmost or the first element in each row of the matrix is 1.
 - The column containing this 1 has all the other entries of 0.
 - If a row consists entirely of 0’s it should be placed below any row having at least one non zero element.

2.4.4.2 Indirect methods

The indirect methods are called the iterative methods, which provide an alternative to the direct method of solving a set of linear equations by elimination. It is preferred to a direct method when the latter requires comparatively more computer storage as, for example, for a system of equations with a sparse coefficient matrix (Jamil, 2012).

$$\begin{array}{l}
 a_{11}x_1 + a_{12}x_2 + a_{1k}x_k + \text{-----} + a_{1n}x_n = b_1 \\
 a_{21}x_1 + a_{22}x_2 + a_{2k}x_k + \text{-----} + a_{2n}x_n = b_2 \\
 \vdots \\
 a_{k1}x_1 + a_{k2}x_2 + a_{kk}x_k + \text{-----} + a_{kn}x_n = b_k \\
 \vdots \\
 a_{n1}x_1 + a_{n2}x_2 + a_{nk}x_k + \text{-----} + a_{nn}x_n = b_n
 \end{array}
 \quad \text{System of Algebraic Equations}$$

Solving for $x_k = \frac{1}{a_{kk}} \left[b_k - \sum_{i=1}^{k-1} a_{ki}x_i - \sum_{i=k+1}^n a_{ki}x_i \right], k = 1, 2, 3, \dots, n$ (2.31)

The basic concept of an iterative method is to select a trial solution, and using equation 2.31 for each unknown, compute a new solution. This solution, if not satisfactory, is taken as a new trial, and equation 2.31 is again used for each unknown, to compute another solution. This procedure is repeated, until it is observed that the difference between trial and computed solution are sufficiently small. The general types of direct methods explained by (Collins, 2003) are briefly given below:

- **Jacobi method** (Collins, 2003)

Express $r+1^{\text{th}}$ value in terms of r^{th} iterative values, beginning with an initial approximation x^1 , we compute each component of x^{r+1} using equation 2.31 for $k=1,2,3, \dots, n$ in the following form:

$$X_k^{r+1} = \frac{1}{a_{kk}} \left[b_k - \sum_{i=1}^{k-1} a_{ki} x_i - \sum_{i=k+1}^n a_{ki} x_i \right], k = 1, 2, 3, \dots, n \quad (2.32)$$

- **Gauss- Seidel method** (Collins II, 2003)

In the Jacobi method, the updated value of an iteration is not used, and the iterates converge to the exact solution rather slowly. In Gauss-Seidel method the $r+1^{\text{th}}$ iterative values are used as soon as they are available.

- **Successive Over Relaxation (SOR) method** (Collins II, 2003)

The convergence of Gauss Seidel iteration can be accelerated by SOR method, by rewriting the equation 2.32 and using a relaxation parameter ‘w’ as given in equation 2.33.

$$X_k^{r+1} = \frac{w}{a_{kk}} \left[b_k - \sum_{i=1}^{k-1} a_{ki} x_i^{r+1} - \sum_{i=k+1}^n a_{ki} x_i^r \right] - (w-1) x_i^r, k = 1, 2, 3, \dots, n \quad (2.33)$$

2.5 Solving CFD Problems Using Available Software

The complex physical problems of fluid dynamics involve solution of a system of intricate non-linear PDE’s. The system of equations becomes very complex with the increase in the size (or grid size) and thus the number of equations, making it impossible to solve it analytically. Numerical methods are considered to provide the best possible solution to these problems and have now been used for decades. The computer

programs/algorithms can help us get approximate solutions of a high/acceptable level of accuracy. Commercial software applications are available and user codes are seldom required for majority of the problems. These commercial software applications provide solution options for most classes of fluid dynamics problems.

2.5.1 ANSYS Fluent

A number of general purpose commercial CFD software, such as Ansys Fluent /CFX, Cradle CFD (scSTREAM, SC/Tetra), CD ADAPCO (STAR CCM+), etc. are available. Ansys fluent was chosen for this study, since it is considered as an extremely versatile code, which comes as a tightly integrated package that has probably been applied with success, to more classes of flow than any other (Haghgoo, 2013). It is the most widely used software when it comes to the study of underground mine ventilation. It has been found most suitable for complicated indoor fluid environments (Li, 2015). It is a high performance software, allows parallel processing, and is used to model turbulent, laminar, incompressible, compressible, transient and steady state flows. It is flexible enough to solve problems involving air flows, heat transfer, multiphase flow, reacting flow and acoustics.

The three key steps to solving problems with ANSYS Fluent computational modeling are problem definition, mathematical model, and computer simulation. These steps are discussed in Ansys Fluent Getting Started Guide (2015) and a brief account of these steps is given below:

2.5.1.1 Pre-processing

It involves the creation and discretization of the solution domain, the description of the properties of the domain being studied and, finally, the specification of the boundary conditions.

- **Modeling**

The problem domain and every component of it are required to be modeled. This can be done within Ansys or the modeling can be done in CAD software applications (AMD, Pro Engineer, CATIA, Solid works etc.) and the model files can be imported into Ansys (Ansys Design Modeler User's Guide and Ansys Fluent Meshing User's Guide, 2015).

- **Meshing / Grid generation**

The mesh defines the locations, at which the governing equations are solved for the given flow domain. The mesh resolution controls these locations, the accuracy of the calculation, and the solution time required by the computer. Software programs (Pointwise, GAMBIT etc.) have been specially developed for the purpose of mesh and grid generation. The common types of mesh elements used in CFD solvers are hexahedral, tetrahedral Prism and Wedge in 3D and quadrilaterals and triangles in 2D (GAMBIT User Manual, 2007). Both structured and non-structured meshes can be generated in ANSYS Fluent as well. The mesh types that are supported by ANSYS Fluent include triangular, quadrilateral, tetrahedral, hexahedral, pyramid, prism (wedge) and polyhedral (Ansys Fluent Meshing User's Guide, 2015).

- **Specification of boundary conditions**

The boundary conditions are specified after grid generation. These boundary conditions are applied at different locations of the problem domain i.e. for mine ventilation problems the inlet, walls, outlets etc., depending on the problem.

- **Selection of solution model**

A number of solution models (Turbulence models, radiation models, Large Eddy Simulation model etc.) generally called the physical models are available within the CFD software (Diego et al., 2011). These models are chosen depending on the nature of the problem, for example, a turbulence model is used to simulate turbulent flow. Turbulent flow shows rapid fluctuations of flow variables about a mean value which are very difficult to resolve and turbulent models are used to simulate these variables by solving additional equations.

2.5.1.2 Solution

Once the problem has been completely defined, it is ready for computation of a solution. Iterative strategy is used to solve the non-linear system of governing equations in order to calculate the solutions. A lot of patience is required in this step because a fluid flow problem can take a long time to converge.

2.5.1.3 Post-processing

The solution stage is followed by the results; the results are in the form of a huge number of flow field variables depending upon the size of the problem. These variables are represented in illustrative and meaningful ways using plots of contours and vectors, streamlines, data curve etc. which help the user, to have an increased understanding. Comparison of these results is done with the available physical experimentation results for verification, since incorrect input data, poor choice of simulation methods or incorrect interpretations of the outputs can mislead the researcher and result in incorrect conclusions.

2.5.2 Turbulence

When the Reynolds numbers are high the viscosity effects are too low to restrict / stop the amplification of disturbances and they grow and interact with the neighbouring disturbances. The flow become disordered and non-repeating and is called the turbulent flow (Launder, 1991). The problems and solution of Turbulence are:

- **Problem of Turbulence**
 - One of the characteristics of turbulent flow is the fluctuating velocity fields; causing the fluctuation of the transported quantities as well.
 - The calculation of these large numbers of small fluctuations of high frequency is computationally very expensive.
- **Solution**

The solution to this problem is that the exact governing equations be time averaged or ensemble averaged, resulting into a less computationally expensive set of equations. These equations though bring additional unknown variables with them which are determined using turbulence models.

2.5.2 Turbulence models

The selection of a particular turbulence model is one of the difficult parts of using Ansys Fluent, because it is not possible to strictly classify turbulence models and flow problems (Ansys Fluent Theory Guide, 2015). It depends on the type of the physical problem, the memory limitations/accuracy required and the normal practice that is

followed. ANSYS Fluent provides the following choices of turbulence models (Ansys Fluent Theory Guide, 2015). The turbulence models are discussed in more detail in chapter 3.

- Spalart - Allmaras model
- K- ϵ models
 - Standard k- ϵ model
 - Renormalization-group (RNG) K- ϵ model
 - Realizable K- ϵ model
- A k-w models
 - Standard K-w model
 - Shear stress transport (SST) K-w model
- Transition K-Kl-w model
- Transition SST model
- v^2 -f model (add-on)
- Reynolds stress models (RSM)
 - Linear pressure-strain RSM model
 - Quadratic pressure-strain RSM model
 - Low-Re stress-omega RSM model
- Detached eddy simulation (DES) model, it includes one of the following RANS models.
 - Spalart - Allmaras RANS model
 - Realizable k- ϵ RANS model
 - SST k-w RANS model
- Large eddy simulation (LES) model, it includes one of the following sub-scale models.
 - Smagorinsky - Lilly sub grid-scale model
 - WALE subgrid - scale model
 - Dynamic Smagorinsky model
 - Kinetic-energy transport subgrid - scale model

2.6 Ventilation Network Design Software

A number of commercially available Mine Ventilation Network Design Software applications (simulators) are available, which are based on the Hardy Cross method (McPherson, 1993). Nodes and branches are used to represent a mine (a branch represents an airway and a node is the point where airways meet). The simulator is used to determine the fan power, and air flow pressure distribution in the network based on the airway resistance (calculated using Atkinson's Equation) and can be used to meet fixed flow requirements for the given mine geometry. The ventilation network design models for analysis and the designing of mine ventilation systems are static models, which are less memory extensive than the dynamic CFD models (Wu and Gillies, 2005). The network design software are not designed to simulate the details of air flow (air flow patterns, flow rates at points and planes etc.) inside headings. A few of the commercially available software packages are:

- Vnet PC (US)
- VentSim (Australia)
- Vent Graph (Poland)
- Mivena (Japan)
- VUMA (South Africa)

2.6.1 Theory and principle

Air flow for ventilation of underground mines with depths less than 500m is generally accepted to be incompressible (Hartman et al., 2012 and McPherson, 1993). These ventilation facilities are treated by the air flow relation given by Atkinson, which is famously known as the Square Law.

$$P = k(L + L_e) \frac{Per}{A^3} Q^2 \quad (2.34)$$

$$P = RQ^2 \quad (2.35)$$

$$R = k(L + L_e) \frac{per}{A^3}, \left(\frac{Ns^2}{m^8} \right) \quad (2.36)$$

Where,

P = Pressure, pa

K = Atkinson Friction factor, kg/m³

L = Length, m

Le = Equivalent length to cater for the shock losses, m

Per = Perimeter, m

A = Cross sectional area, m²

Q = V x A = Volume Flow Rate = m³/s

V = Velocity = m/s

R = Atkinson Resistance of the Airway, Ns²/m⁸

Kirchhoff's laws are the basis for ventilation network design software applications. Similar to the Kirchhoff's first law instead of current (electrical circuit), sum of flow rate of air through a node (going in and coming out from a node) is considered as equal to zero and in the second law instead of voltage drop around any closed electrical circuit, the pressure change around any closed ventilation circuit is considered as equal to zero.

$$\text{First Law, } \sum Q = 0 \quad (2.37)$$

$$\text{Second Law, } \sum (P - P_f) - NVP = 0 \quad (2.38)$$

Where

Q = Volumetric flow rate, m³/s

P = Frictional pressure drop, Pa

P_f = Fan Pressure, Pa

NVP = Natural Ventilation Pressure, Pa

Furthermore, for the resistance in a ventilation network the formulas used for resistance in series and parallel circuits are given as:

$$\text{Series Resistance} \quad R_{ser} = \sum R \quad (2.39)$$

$$\text{Parallel Resistance} \quad \frac{1}{\sqrt{R_{par}}} = \sum \frac{1}{\sqrt{R}} \quad (2.40)$$

The analytical solution of a mine network can be done for very small networks, but as the size of the network grows the number of equations becomes large and using them

manually become almost impossible. The numerical technique used in the network analysis software is iterative in nature and is based on the Hardy Cross Method which utilizes the Square Law and Newton - Raphson technique (Chapra and Canale, 2010) of dividing a function by its first derivative, to estimate the correction factor (McPherson, 1993). The formula for the correction factor is:

$$\Delta Q_m = \frac{-\sum (RQ_a |Q_a| - P_f - nvp)}{\sum (2R |Q_a| + S_f + S_{nv})} \quad (2.41)$$

Where,

ΔQ_m = Correction factor

R = Frictional resistance

Q_a = Initial Guess of Air Flow

P_f = Fan Pressure

NVP = Natural ventilating pressure

S_f = Slope of fan P and Q curve

S_{nv} = Slope of natural ventilation P and Q curve (normally taken as zero)

2.7 Conclusion

This chapter reviewed the coal mine hazards, types of auxiliary ventilation devices, the theory/background of CFD and the need for CFD software to solve complex fluid dynamics problems, alongside the research that has already been undertaken on the subject. It was found that accidents are still taking place in the mining industry with a high percentage of accidents taking place due to methane explosion in working areas. The ventilation of the working area is carried out using auxiliary ventilation devices and the ventilation is dependent on the system variables of these auxiliary ventilation devices.

Network design software are not designed to study the ventilation in these working areas (production zones) and can only be studied through practical experimentation or CFD analysis. CFD studies involve the solution of the problem domain using complex fluid dynamics equations which cannot be solved analytically and require specially designed numerical codes. Commercially available numerical codes have been used in the past for the study of the ventilation of the production zone. However, an in depth study is

required to find the impact of various system drives associated with the use of the auxiliary ventilation devices in mathematical form. The mathematical models should be able to specify the impact of each system variable on the flow rates inside the production zone, which in return should help the supervisory staff to install these devices correctly knowing how it will impact the flow rates and the ventilation.

The next chapter explains the methodology adopted for the study. It covers the research matrix, and details of the numerical techniques used.

3 METHODOLOGY

3.1 General

Auxiliary ventilation is required to ventilate development headings which form part of the secondary circuit and are separate from the main air flows. The design, selection and installation of any auxiliary ventilation device requires an understanding of the capabilities of the equipment and the requirement in hand. This understanding may help in improving the guideline for the practitioner and ventilation planner. Ventilation managers and mine operators use these guidelines to develop their plans for managing the hazards presented by the mining operations and the environment.

In this research, initially, headings ventilated without the use of any auxiliary ventilation devices is studied to recognize the need for auxiliary ventilation, and then the response of auxiliary devices, Scoop/LB, and Fan with Duct (Force and Exhaust) involved in the ventilation of development headings is studied through the use of CFD. The system variables used for this research were adjusted and each possible combination of these variables was studied. This was done to find the effect of each system variable on the flow rates and air flow patterns inside a heading. As a result, a total of 339 scenarios were formed and considered for this research. The flow rates at different depths inside the heading on vertical planes were calculated and the air flow patterns were visualized on horizontal and vertical planes constructed inside the heading. Furthermore, this information was used to create mathematical models to estimate the flow rates close to the face of the heading with the use of these auxiliary ventilation devices and also at the exit of the LB.

The conceptual framework and methodology implemented for this research is divided into two distinct parts i.e. practical site characterization / considerations and numerical characterization / consideration as shown in Figures 3.1 and 3.2. Each component of the research methodology is illustrated and discussed here in detail.

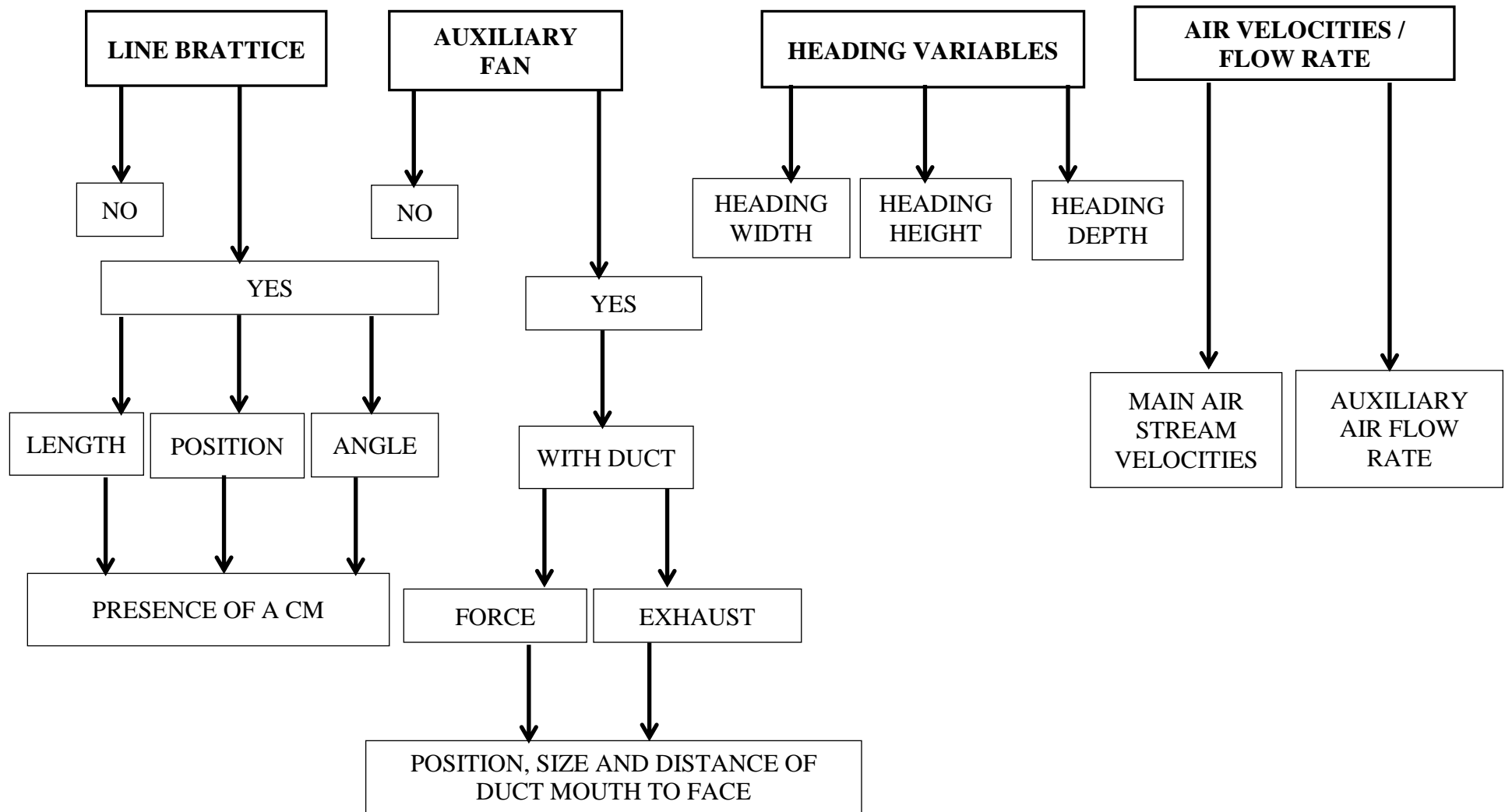


Figure 3.1 Practical site characterization / considerations

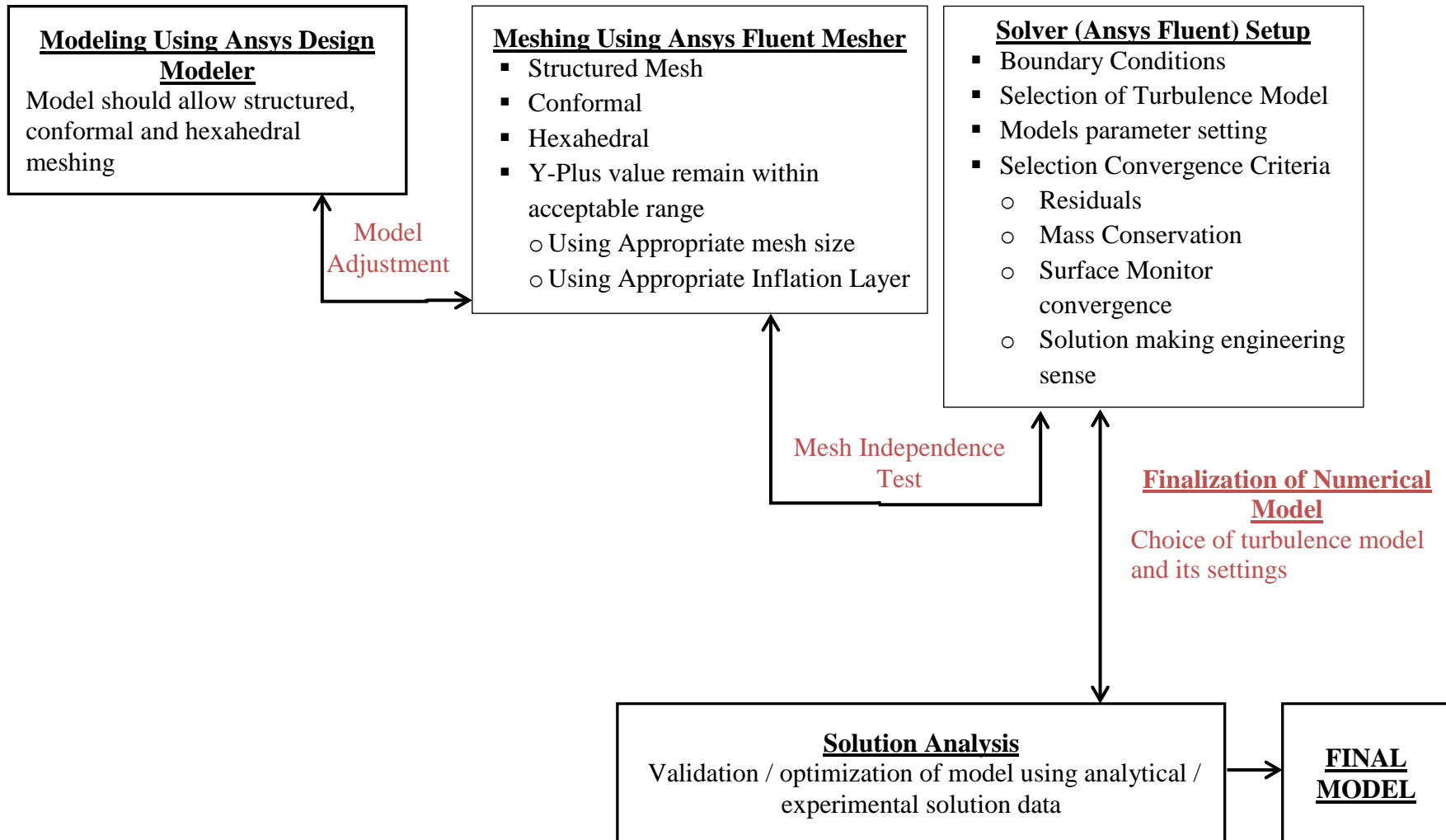


Figure 3.2 Numerical model characterization / considerations

3.2 Practical Site Considerations / Creation of Practical Scenarios

Coal mining conditions vary from one mine to another depending on its location, depth, seam height, dimensions of the mining area, mining methods used. The ventilation parameters / equipment used not only vary with these conditions but also vary within a mine depending on the ventilated area and hazards present. Creating practical ventilation scenarios applicable to development headings universally in any Room and Pillar mine, encompassing all ventilation parameters is not possible. Therefore, the most commonly encountered conditions were considered with a view to ensuring the trends were captured to predict the situations in missing scenarios. This was done by using the practical combination of local ventilation variables involved in Room and Pillar coal mines. The variables considered for this research as shown in Figure 3.1 are summarized in Table 3.1:

Table 3.1 Summary of variables used in the research

| Summary of variables used for this research | | | | | | | | |
|---|---------------------------------|--------------------|---------------------------|--------------------------------|--------------------------------|--|------------------------|-------|
| Parameters | No auxiliary ventilation device | LB | Air velocity in LTR (m/s) | Auxiliary fan (ducted) | | Auxiliary fan flow rates (m ³ /s) | Heading dimensions (m) | |
| | | | | Force | Exhaust | | Height | Depth |
| Value / variables | | Length | 1 | Position | Position | 2.97 | 4 | 10 |
| | | Position | 1.5 | Size | Size | 3.71 | 3 | 20 |
| | | Angle of LB in LTR | 2. | Distance of duct mouth to face | Distance of duct mouth to face | | | |
| | | Presence of CM | | Flow rate | Flow rate | | | |

3.3 Case A - No Auxiliary Ventilation Equipment

Room and Pillar mining is based on creating blind headings until through ventilation can be established. This leads to the development of many blind headings which require ventilation both when being mined and when not being mined. In the first studied case, mining scenarios/sub cases were created with the consideration that no auxiliary ventilation equipment was used to assist the ventilation of the development heading

connected to the LTR. The effects of the LTR velocity on the ventilation of the heading were studied. The details of the parameters that were varied for this Case A are given in Table 3.2. A total of 12 scenarios/sub cases were created /studied under Case A as shown in Table 3.3, the geometric parameters used are shown in Figure 3.3. Air flow and penetration depths were determined based on the maximum axial velocity and flow rates were calculated using absolute axial velocity at different depth planes. Four additional cases as discussed in Chapter 4 section 4.2 were simulated in the validation study carried out for this research.

Table 3.2 Details of the parameters varied for Case A

| No auxiliary equipment | Parameter | Heading height (m) | Heading depth (m) | Heading width (m) | LTR velocity (m/s) |
|------------------------|-----------|--------------------|-------------------|-------------------|--------------------|
| | Value | 3 | 10 | 6.6 | 1 |
| 4 | 20 | 1.5 | | | |
| | | 2 | | | |

Table 3.3 Research matrix for Case A

| Matrix for Case A | Seam Height (m) | | | | | | | | | | | | | |
|-------------------|-------------------|-----|---|---|-----|---|--|-------------------|-----|---|----|-----|----|--|
| | 4 | | | | | | | 3 | | | | | | |
| | Heading width 6.6 | | | | | | | Heading width 6.6 | | | | | | |
| | Depth heading (m) | | | | | | | | | | | | | |
| | 10 | | | | 20 | | | | 10 | | | | 20 | |
| | Velocity (m/s) | | | | | | | | | | | | | |
| | 1 | 1.5 | 2 | 1 | 1.5 | 2 | | 1 | 1.5 | 2 | 1 | 1.5 | 2 | |
| Number of Cases | 1 | 2 | 3 | 4 | 5 | 6 | | 7 | 8 | 9 | 10 | 11 | 12 | |

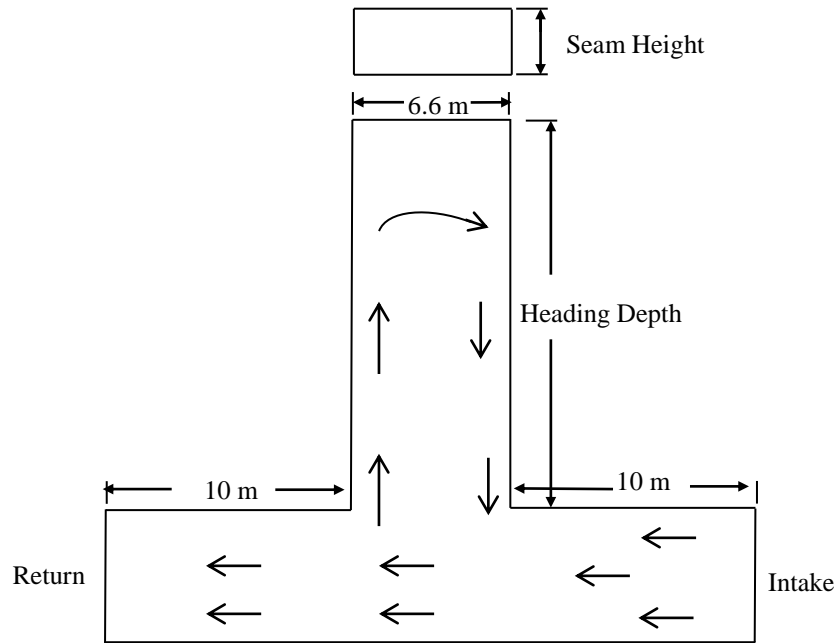


Figure 3.3 Geometric parameters for Case A

3.4 Case B - Use of Scoop / LB

A number of ventilation techniques are used to ventilate the face of the development headings, these techniques are used to increase the air flow rate in the development heading depending upon the extent of hazards and the method of mining. LB or scoop brattice is a thin plastic or fire proof fabric anchored at the roof and floor to channel the last through road air into the development heading without the use of any external force other than that created by the LTR airflow. In Case B of this research, the effects of LB on the ventilation of the development heading were studied. The geometric parameters used are shown in Figure 3.4. The details of the parameters that were varied for this Case are given in Table 3.4. A total of 288 scenarios as shown in Table 3.5 were created for this Case using combinations of these parameters.

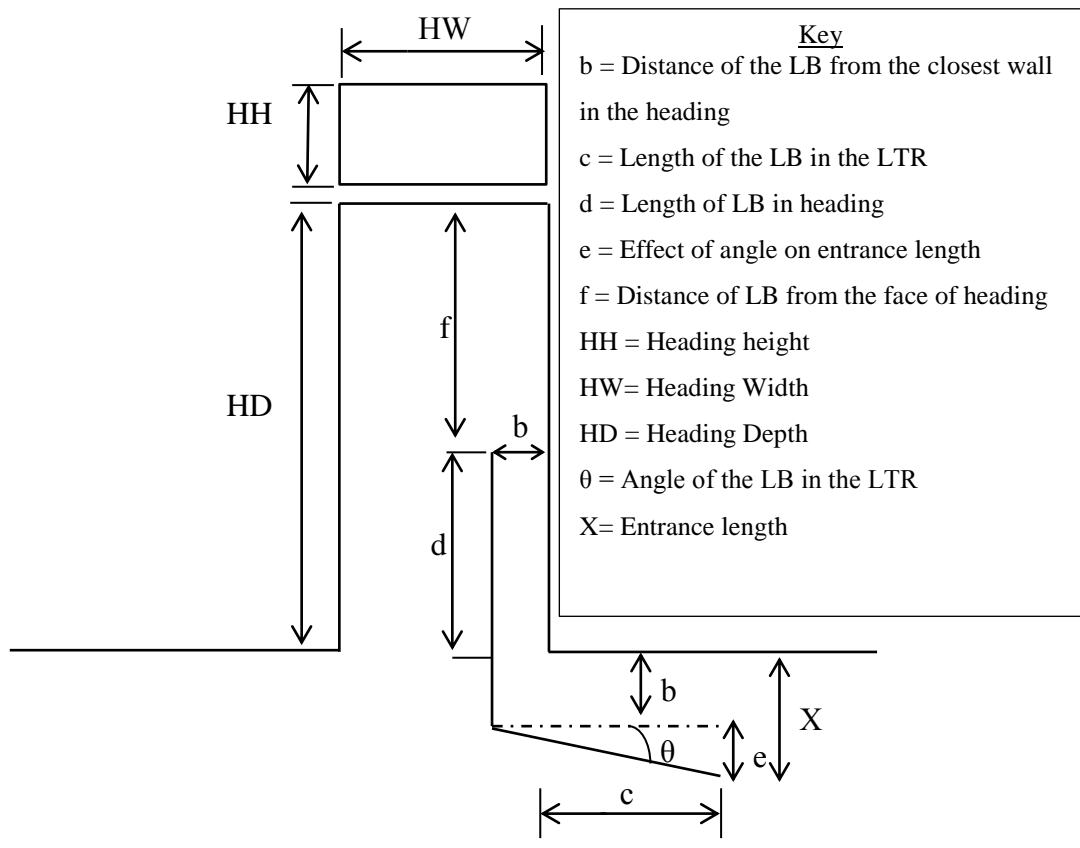


Figure 3.4 Geometric parameters for Case B

Table 3.4 Details of the parameters varied for Case B

| Use of LB- Case B | Seam height | Heading depth | Heading width | LTR velocity | Length of LB inside heading | Length of LB inside LTR | LB distance from the wall in LTR & heading | Angle of LB in LTR |
|-------------------|-------------|---------------|---------------|--------------|---------------------------------|-------------------------|--|--------------------|
| | (m) | (m) | (m) | (m/s) | (m) | (m) | (m) | (Degree) |
| | 3 | 10 | 6.6 | 1 | 1/2 of Heading depth (5 & 10) | 3 | 0.5 | 0 |
| | 4 | 20 | | 1.5 | 3/4 of Heading depth (7.5 & 15) | 6 | 1 | 7.5 |
| | | | | 2 | | | | 15 |

Table 3.5 Research matrix for Case B

| | | | | | | | | | | | | | | | |
|---|---|---|---|-----------------------|---|---|---|-----------------------|---|-------------------|---|-----------------------|---|-----|---|
| LB research matrix (For the three LTR velocities i.e. 1,1.5, and 2m/s and two seam sizes i.e. 6.6 m x 4 m and 6.6 m x 3m) | | | | | | | | | | | | | | | |
| Velocity (m/s) | | | | | | | | | | | | | | | |
| 1, 1.5, 2 | | | | | | | | | | | | | | | |
| Depth heading (m) | | | | | | | | | | | | | | | |
| 10 | | | | | | | | 20 | | | | | | | |
| Length of LB inside heading (m) | | | | | | | | | | | | | | | |
| 1/2 of heading length | | | | 3/4 of heading length | | | | 1/2 of heading length | | | | 3/4 of heading length | | | |
| LB length in LTR (m) | | | | | | | | | | | | | | | |
| 3 | | 6 | | 3 | | 6 | | 3 | | 6 | | 3 | | 6 | |
| LB distance from wall (m) | | | | | | | | | | | | | | | |
| 1/2 | 1 | ½ | 1 | ½ | 1 | ½ | 1 | 1/2 | 1 | ½ | 1 | 1/2 | 1 | 1/2 | 1 |
| Angles (degree) | | | | | | | | | | | | | | | |
| Using 0,7.5,15 degree angles for each case | | | | | | | | | | | | | | | |
| 1 | 2 | 3 | 4 | . | . | . | . | . | . | 48 cases in total | | | | | |
| <p>Note: A total of 48 cases for a single velocity, 48 x 3 = 144 for the three velocities, and cumulative total number of cases for 2 x seam heights is 288.</p> | | | | | | | | | | | | | | | |

3.5 Case C - Ventilation of a Heading in the Presence of a Continuous Miner Using LB

The ventilation of a heading in the presence of a CM making a straight cut ventilated using LB as shown in Figure 3.5 was carried out using a simplified model of the CM (3.3 x 1.5 x 10.5, W x H x L) without the drum and scrubber. This was done to study the effectiveness of the ventilation through the study of the air flow patterns and the identification of low velocity and recirculation zones. The most effective scenarios from Case B based on maximum flow rates (close to the face of the heading) for each LTR velocity were selected. Details of the parameters used for this Case are given in Table 3.6. A total of 18 scenarios/cases were created as shown in Table 3.7.

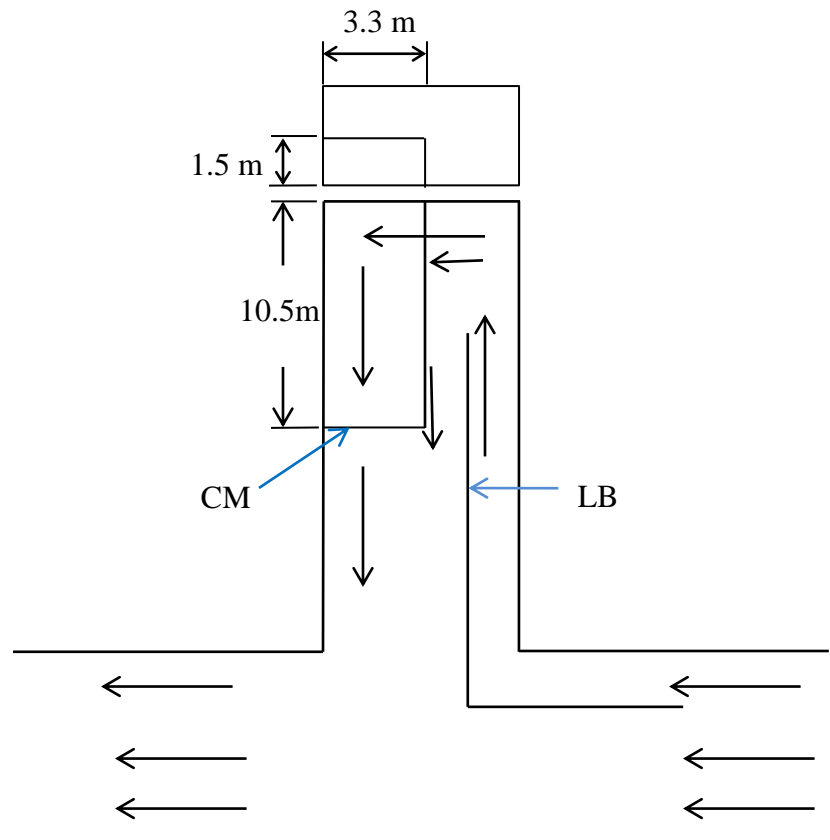


Figure 3.5 Schematic of the CM in the heading

Table 3.6 Details of parameters for Case C

| Details of parameters for Case C | | | | | | |
|----------------------------------|---------------|--------------|---------------------------------|-------------------------|--|--------------------|
| Heading height | Heading depth | LTR velocity | Length of LB inside the heading | Length of LB inside LTR | LB distance from the wall in the heading | Angle of LB in LTR |
| (m) | (m) | (m/s) | (m) | (m) | (m) | (Degree) |
| 3 | 20 | 1 | 15 | 6 | 0.5 | 0 |
| 4 | | 1.5 | | | 1 | 7.5 |
| | | 2 | | | | 15 |

Table 3.7 Research matrix Case C

| | | | | | | | | | |
|----------------|---|-----|---|-----|-----|---|----|-----|---|
| Matrix Case C | Ventilation of a heading in the presence of a CM using LB for heading height of 3m and 4m | | | | | | | | |
| | Heading width | | | | | | | | |
| | 6.6 | | | | | | | | |
| | Heading depth | | | | | | | | |
| | 20m | | | | | | | | |
| | Length of LB in LTR | | | | | | | | |
| | 6m | | | | | | | | |
| | Length of LB in heading | | | | | | | | |
| | 15m | | | | | | | | |
| | Distance of the LB from the wall in the heading | | | | | | | | |
| | 1m | | | | | | | | |
| | Angle of LB in LTR | | | | | | | | |
| | 0 | | | 7.5 | | | 15 | | |
| | LTR velocity | | | | | | | | |
| | 1 | 1.5 | 2 | 1 | 1.5 | 2 | 1 | 1.5 | 2 |
| Number of case | 1 | 2 | 3 | 4 | 5 | 6 | 7 | 8 | 9 |

3.6 Case D - Auxiliary Fan (Ducted)

Another conventional method employed to ventilate the face of a development heading is the use of fans with duct. A fan with duct is generally installed on the intake side in the force configuration and on the return side in the exhaust configuration (Reed and Taylor, 2007). The choice of system depends on the type of hazard, with a force system used where high velocity air is required to dilute the predominant methane hazard from the newly exposed surface and an exhaust system is used when dust is the main hazard. The velocity of air at the face of the heading for a force fan duct system is higher than for an exhaust fan duct system therefore; the distance of the mouth to face of the heading for a force fan duct system is kept larger than for an exhaust fan duct.

The details of the parameters that were varied for this Case are given in Table 3.8 and 3.9. A total of 16 scenarios as shown in Tables 3.10 and 3.11 were created. The geometric parameters used for these configurations are shown in Figure 3.6 and 3.7.

Table 3.8 Details of the parameters varied for Case D (Force fan)

| Force fan duct System- Case D | Parameter | Heading dimensions W x H x L (m) | Duct diameter (m) | Flow rate m^3/s | LTR velocity (m/s) | Distance of duct mouth to face (m) | Distance of duct from the side wall (m) | Distance of duct from roof (m) |
|-------------------------------|---|--|----------------------|----------------------|-----------------------|---------------------------------------|--|-----------------------------------|
| | Value | 6.6 x 3 x 20 | 0.57 | 2.97 | 2 | 8 | 1 | 0.5 |
| | | 0.76 | 3.713 | 10 | | | | |
| Remarks | Flow rates are chosen based on the generally used requirement of $0.15/m^3/s/m^2$ (generally used) and 25 % more than the requirement | | | | | | | |

Table 3.9 Details of the parameters varied for Case D (Exhaust fan)

| Exhaust Fan duct System Case D | Parameter | Heading dimensions | Duct diameter | Flow rate | LTR velocity | Distance of the duct mouth to face | Distance of duct from the side wall | Distance of duct from roof |
|---|-----------|--------------------|---------------|-------------------|--------------|------------------------------------|-------------------------------------|----------------------------|
| | Value | W x H x L (m) | (m) | m ³ /s | (m/s) | (m) | (m) | (m) |
| Remarks | Value | 6.6 x 3 x 20 | 0.57 | 2.97 | 2 | 2 | 1 | 0.5 |
| | | | 0.76 | 3.713 | | 4 | | |
| Flow rates are chosen based on the generally used requirement of 0.15/m ³ /s/m ² and 25 % more than the requirement | | | | | | | | |

Table 3.10 Force fan duct system variables

| Auxiliary force fan (Ducted) research matrix | | | | | | | |
|---|--------|------|--------|------|--------|------|--------|
| Heading width, heading height and depth (constant) | | | | | | | |
| 6.6 x 3 x 20 m (W x H x L) | | | | | | | |
| Duct distance from side wall and roof (constant) | | | | | | | |
| 1m and 0.5m respectively | | | | | | | |
| Distance of duct mouth to face of heading (m) | | | | | | | |
| 8 | | | | 10 | | | |
| Duct diameter (m) | | | | | | | |
| 0.57 | | 0.76 | | 0.57 | | 0.76 | |
| Quantity of air m ³ /s | | | | | | | |
| 2.97 | 3.7125 | 2.97 | 3.7125 | 2.97 | 3.7125 | 2.97 | 3.7125 |
| 1 | 2 | 3 | 4 | 5 | 6 | 7 | 8 |
| Note: total cases = 8, Plus an additional case with bended duct (Sec 8.2.4) | | | | | | | |

Table 3.11 Exhaust fan duct system variables

| Auxiliary exhaust fan (Ducted) research matrix | | | | | | | |
|---|--------|------|--------|------|--------|------|--------|
| Heading width, heading height and depth (constant) | | | | | | | |
| 6.6 x 3 x 20 m (W x H x L) | | | | | | | |
| Duct distance from side wall and roof | | | | | | | |
| 1m and 0.5m respectively | | | | | | | |
| Distance of duct mouth to face of heading (m) | | | | | | | |
| 2 | | | | 4 | | | |
| Duct diameter (m) | | | | | | | |
| 0.57 | | 0.76 | | 0.57 | | 0.76 | |
| Quantity of air m ³ /s | | | | | | | |
| 2.97 | 3.7125 | 2.97 | 3.7125 | 2.97 | 3.7125 | 2.97 | 3.7125 |
| 1 | 2 | 3 | 4 | 5 | 6 | 7 | 8 |
| Note: total cases = 8 | | | | | | | |

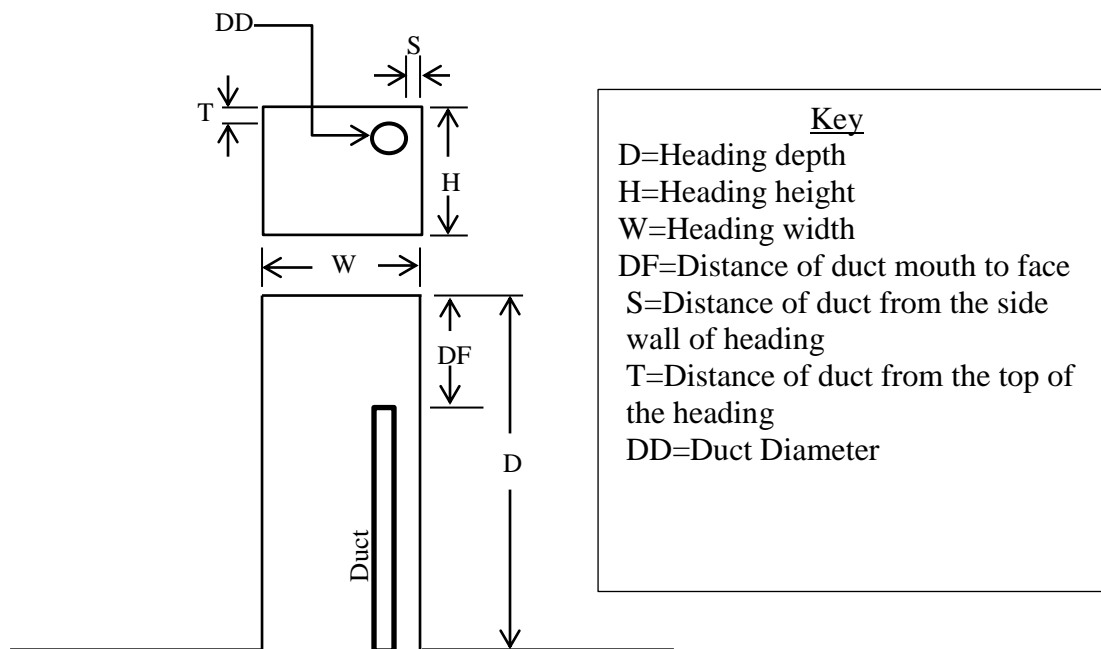


Figure 3.6 Geometric parameters for force fan duct Case

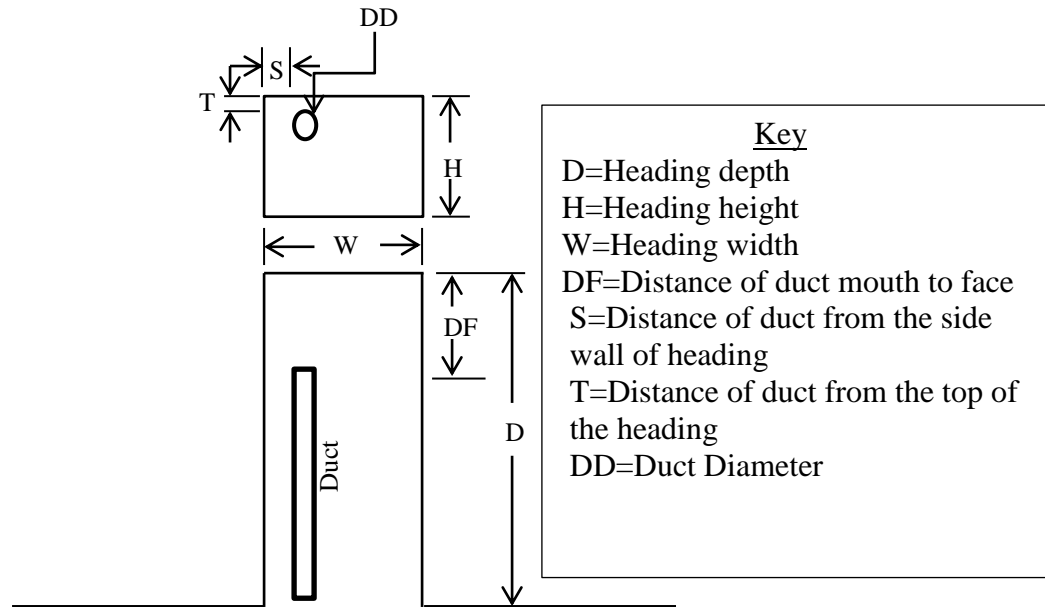


Figure 3.7 Geometric parameters for exhaust fan duct Case

3.7 Numerical Considerations for the Research

CFD software ANSYS Fluent 15.0 was used to iteratively solve the fluid flow scenarios for all the cases undertaken in this research. The software can only give correct or near correct results once the problem in hand is clearly understood and well defined. The definition of the problem includes correct modeling and meshing of the domain into fine cells, correct definition of the boundary conditions of the domain, and selection of appropriate physical models from the software. Once the definition of the problem (pre-processing) is complete, the problem is solved iteratively until the solution is fully converged and is independent of the mesh size (grid independent). The optimization/validation of the model is carried out to make sure the numerical model and its parameters are correct for solving the problem at hand. Four validation studies were carried out to validate the numerical model that was used for this research (covered in Chapter 4). The following numerical considerations were generally used for this research:

3.7.1 Modelling and meshing

ANSYS Design Modeller and Mesher were used in this research to model and mesh the geometries. As per the software and literature guidelines, following was achieved:

- Generally a structured (hexahedral) mesh aligned with the direction of flow was created for all the geometries to avoid false diffusion and reduce the number of nodes as compared to a tetrahedral mesh.
- Inflation layers, where required, were used at the boundaries (walls) of the geometries to allow smooth transition from the laminar flow near the wall to turbulent flow away from the walls.
- Sufficiently fine mesh of 0.04m was created for all the geometries to resolve the salient features of flow. A fine mesh also reduces the interpolation errors. The number of nodes used varied between 8.5 million and 25 million for this research.
- The final mesh size was selected after undertaking the Grid Independence test for all the category of cases. A mesh independence test was carried out using mesh sizes of 0.1m, 0.075m, 0.04m and 0.03m. A mesh size of 0.04m was found to be the most suitable which gave negligible deviation in results with further reduction in mesh size.

3.7.2 Specification of boundary conditions

The choice of the boundary conditions significantly impacts the accuracy of the solution in numerical analysis. Therefore, the boundary conditions were very carefully selected and finalized after going through, the Ansys Fluent theory guide and discussions with the software providers. The summary of the boundary conditions applied to the cases of this study are given below in Table 3.12.

Table 3.12 Summary of boundary conditions

| Case | Boundary condition | Location |
|-------------------------------------|--------------------|---|
| Case A- No Auxiliary equipment used | Velocity Inlet | Inlet of the LTR |
| | Outlet | Outlet of the LTR |
| | Wall | All the boundaries of the domain except for inlet and outlet |
| Case B-LB used | Velocity Inlet | Inlet of LTR |
| | Outlet | Outlet of the LTR |
| | Wall | Brattice and all the boundaries of the domain except for inlet and outlet of the LTR |
| Case C-LB (CM) | Velocity Inlet | Inlet of LTR |
| | Outlet | Outlet of the LTR |
| | Wall | Brattice and all the boundaries of the domain except for inlet and outlet of the LTR |
| Case D-Ducted fans | Velocity Inlet | Inlet of the LTR |
| | Outlet | Outlet of the LTR |
| | Fluid Fan | Force and Exhaust fan in the duct |
| | Wall | Duct boundary and all the boundaries of the domain except for inlet and outlet of the LTR |

3.7.3 Selection of turbulence models

Turbulent flows are characterized by fluctuating velocity fields, which are generally of small scale and high frequency. Mathematical equations and numerical procedures are available as discussed in the literature review (Chapter 2) to solve turbulent flows. However, as the fluctuations are very small they require a grid size even smaller making the numerical solution computationally too long, because of the increase in the number of calculation points. A turbulence model avoids the simulation of the details of

turbulence and allows us to capture the effects of turbulence on the averaged flow. This is done by time or ensemble averaging of the governing equations resulting in a modified set of equations (with additional unknowns) requiring turbulence models for their solution.

3.7.3.1 Reynolds averaging, Ansys Fluent theory guide (2015)

In Reynolds averaging the solution variables in the mathematical equation are written as the sum of a mean and a fluctuating component. For the velocity component u and any other quantity ϕ it can be written as:

$$u_i = \bar{u}_i + u'_i \quad (3.1)$$

Where \bar{u}_i and u'_i are the mean and fluctuating velocity components ($i = 1,2,3$)

$$\phi = \bar{\phi} + \phi' \quad (3.2)$$

Substituting expressions of this form for the flow variables into the (incompressible) instantaneous continuity and momentum equations and taking a time (or ensemble) average yields the ensemble-averaged momentum equations. They can be written in Cartesian tensor form as:

$$\frac{\partial \rho}{\partial t} + \frac{\partial \rho}{\partial x_i} (\rho u_i) = 0 \quad (3.3)$$

$$\frac{\partial}{\partial t} (\rho u_i) + \frac{\partial}{\partial x_j} (\rho u_i u_j) = -\frac{\partial p}{\partial x_i} + \frac{\partial}{\partial x_j} \left[\mu \left(\frac{\partial u}{\partial x_j} + \frac{\partial u_j}{\partial x_i} - \frac{2}{3} \delta_{ij} \frac{\partial u_l}{\partial x_l} \right) \right] + \frac{\partial}{\partial x_j} (-\rho \overline{u'_i u'_j}) = 0 \quad (3.4)$$

Equation 3.3 and 3.4 are known as the Reynolds-averaged Navier-Stokes equations.

The additional term $-\rho \overline{u'_i u'_j}$ is known as the Reynolds stresses and it must be modelled to close equation 3.4. The Boussinesq's hypothesis is commonly used to model the Reynolds stresses by relating it to the mean velocity gradients. For general flow situations, this hypothesis may be expressed as:

$$-\rho \overline{u'_i u'_j} = \mu_t \left(\frac{\partial u}{\partial x_j} + \frac{\partial u_j}{\partial x_i} \right) - \frac{2}{3} \left(\rho k + \mu_t \frac{\partial u k}{\partial x k} \right) \delta_{ij} = 0 \quad (3.5)$$

Where μ_t is the turbulent viscosity which is not a fluid property but a turbulence property, and k is the kinetic energy of the fluctuating motion. The turbulent viscosity is proportional to the average velocity and the mean free path of the molecules and the Prandtl equation is as follows:

$$\mu_t = \hat{V} L \quad (3.6)$$

Where \hat{V} is the velocity characterizing the fluctuating motion (called the velocity scale) and L is the length of this motion (mixing length or the length scale).

3.7.3.2 Choosing a turbulent model

ANSYS Fluent provides a number of turbulence models; they are generally differentiated on the basis of the number of transport equations each uses to solve for the velocity and the length scale. No model is universally accepted as being superior for all classes of problems. The choice depends upon:

- The physics encompassed in the flow
- Established practice for a specific class of problems
- The level of accuracy required
- Available computational resources
- The amount of time available for the simulation

A summarized account of the turbulence models provided in ANSYS Fluent Theory Guide, (2015) is given below:

- **Spalart - Allmaras model**

This is a one equation model. Only one additional transport equation is solved for the velocity scale and the length scale is assumed to be constant. It was specifically designed for aerospace applications.

- **K- ϵ models**

The K- ϵ model uses two transport equations to solve the velocity and the length scale. The turbulence kinetic energy, k , represents a velocity scale while turbulence dissipation rate, ϵ , represents the length scale. This is the widely used method for underground turbulent airflow analysis, even though it is computationally intensive (Silvester, 2002 and Xu et al., 2016).

Keeping in mind the successful use of the K- ϵ in the previous studies related to mine ventilation studies, consultation with the software provider validation studies were carried out using the K- ϵ realizable model. The validation studies given in Chapter 4 showed that this model is suitable to carry out studies related to the ventilation of empty headings using auxiliary ventilation devices. Therefore, **the realizable K- ϵ model was used for this study.**

- **Standard k- ε model**

The standard K-ε model is the simplest two equation model that is valid only for high Reynolds number fully turbulent flows. This model has been improved into the RNG and realizable models.

- **Renormalization-group (RNG) K-ε model**

This model is derived from the instantaneous Navier-Stokes equations, using a mathematical technique called “renormalization group” method.

- **Realizable K- ε model**

The realizable K- ε is the latest model of this series and is considered the best K- ε model for a wide range of problems.

The turbulence kinetic energy can be written as

$$\frac{\partial}{\partial t}(\rho k) + \frac{\partial}{\partial x_j}(\rho k u_j) = \frac{\partial}{\partial x_j} \left[\left(\mu + \frac{\mu_t}{\sigma_k} \right) \frac{\partial k}{\partial x_j} \right] + G_k + G_b - \rho \varepsilon - Y_M + S_k = 0 \quad (3.7)$$

and the turbulence dissipation rate can be written as

$$\frac{\partial}{\partial t}(\rho \varepsilon) + \frac{\partial}{\partial x_j}(\rho \varepsilon u_j) = \frac{\partial}{\partial x_j} \left[\left(\mu + \frac{\mu_t}{\sigma_\varepsilon} \right) \frac{\partial \varepsilon}{\partial x_j} \right] + \rho C_1 S \varepsilon - \rho C_2 \frac{c^2}{k + \sqrt{\nu \varepsilon}} + C_{1\varepsilon} \frac{c}{k} C_{3\varepsilon} G_b + S_\varepsilon \quad (3.8)$$

Turbulent / eddy viscosity is calculated using (Ansys Fluent Theory Guide, 2015):

$$\mu_t = \rho C_\mu \frac{k^2}{\varepsilon} \quad (3.9)$$

$$C_\mu = \frac{1}{A_0 + A_s \frac{k U^*}{\varepsilon}} \quad (3.10)$$

$$U^* = \sqrt{S_{ij} S_{ij} + \tilde{\Omega}_{ij} \tilde{\Omega}_{ij}} \quad (3.11)$$

$$\tilde{\Omega}_{ij} = \Omega_{ij} - 2\varepsilon_{ijk} \omega_k \quad (3.12)$$

where $\tilde{\Omega}_{ij}$ is the mean rate - of - rotation tensor viewed in a rotating reference frame with the angular velocity ω_k . The model constants $A_0 = 4.04$, $A_s = \sqrt{6} \cos\phi$

where

$$\phi = \frac{1}{3} \cos^{-1}(\sqrt{6} W) \quad (3.13)$$

$$W = \frac{S_{ij}S_{jk}S_{ki}}{\tilde{S}^3} \quad (3.14)$$

$$\tilde{S} = \sqrt{S_{ij}S_{ij}} \quad (3.15)$$

$$S_{ij} = \frac{1}{2} \left(\frac{\partial u_j}{\partial x_i} + \frac{\partial u_i}{\partial x_j} \right) \text{ (mean strain rate)} \quad (3.16)$$

G_k represents the generation of turbulence kinetic energy due to the mean velocity gradients and is calculated as:

$$G_k = -\rho \overline{u'_i u'_j} \frac{\partial u_j}{\partial x_i} \quad (3.17)$$

To evaluate it in a manner consistent with Boussinesq hypothesis

$$G_k = \mu_t S^2 \quad (3.18)$$

where S is the modulus of the mean rate of strain tensor, defined as

$$S \equiv \sqrt{2S_{ij}S_{ij}} \quad (3.19)$$

$$C_1 = \max \left[0.43, \frac{\eta}{\eta + 5} \right] \quad (3.20)$$

$$\text{where } \eta = S \frac{k}{\varepsilon} \quad (3.21)$$

$$C_{1\varepsilon} = 1.44, C_2 = 1.9, \sigma_k = 1.0, \sigma_\varepsilon = 1.2$$

S_k and S_ε are user defined source terms

G_b is the generation of turbulence kinetic energy due to buoyancy and is calculated as below:

$$G_b = \beta g_i \frac{\mu_t}{Pr_t} \frac{\partial T}{\partial x_i} \quad (3.22)$$

Where Pr_t is the Prandtl number = 0.85

g_i is the component of the gravitational vector in the i^{th} direction

β is the coefficient of thermal expansion and is defined as

$$\beta = -\frac{1}{\rho} \left(\frac{\partial \rho}{\partial T} \right)_p \quad (3.23)$$

Y_M is the dilation dissipation term which represents the compressibility effects of turbulence for high Mach number flows and is neglected for incompressible flows, it is represented as:

$$Y_M = 2\rho\varepsilon M_t^2 \quad (3.24)$$

where M_t is the turbulent Mach number defined as $= \sqrt{\frac{k}{a^2}}$ and a is the speed of sound

- **k-w models**

This model uses two transport equations to solve the velocity and the length scale. The turbulence kinetic energy, k , represents a velocity scale and specific dissipation rate, while w , represents the length scale. It is used for predicting free shear flows and has the following two variants.

- Standard K-w model
- Shear stress transport (SST) K-w model

- **Transition K-Kl-w model**

This model is used to predict boundary layer development and addresses the transition of the boundary layer from a laminar to a turbulent regime.

- **Transition SST model**

The transition SST model is based on the coupling of the SST k-w transport equations with two other transport equations, one for the intermittency and one for the transition onset criteria, in terms of the momentum-thickness Reynolds number.

- **Reynolds stress models (RSM)**

This model uses seven additional transport equations for 3D problems. It is used for complex flows to account for the effects of streamline curvature, swirl, rotation and rapid changes in strain rate. It has the following three variants:

- Linear pressure-strain RSM model
- Quadratic pressure-strain RSM model
- Low-Re stress-omega RSM model

- **Detached eddy simulation (DES) model**

These models have been specifically designed to address high Reynolds number wall bounded flows, where the cost of using a near wall resolving LES model would be prohibitive. The three variants of this model are given below:

- Spalart-Allmaras RANS model
- Realizable k- ϵ RANS model
- SST k-w RANS model

- **Large eddy simulation (LES) model**

This model is used to resolve large eddies directly and also for modeling the small eddies. It includes one of the following sub-scale models.

- Smagorinsky-Lilly subgrid-scale model
- WALE subgrid-scale model
- Dynamic Smagorinsky model
- Kinetic-energy transport subgrid-scale model

3.7.4 Solution

The solution was calculated using a second order scheme, which is computationally more expensive than the first order scheme but the error, is less (Bates et al., 2005). The iterative process for all the cases was stopped till the desired convergence was achieved, furthermore, the convergence in all the cases was judged by monitoring and ensuring the following:

- Overall mass conservation was satisfied at the inlet and outlet of the domain (property conservation).
- Residual decreased to 10^{-5} (discussed in more detail in section 3.7.4.1).
- The surface monitor of the integral of the velocity magnitude in a vertical plane as defined in the domain as shown in Figure 3.8 converged properly.

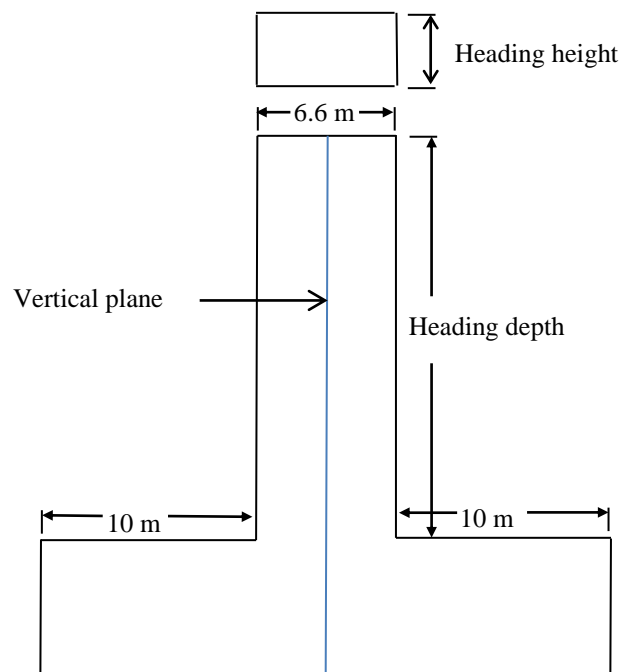


Figure 3.8 Vertical plane to monitor the integral of velocity magnitude

3.7.4.1 What is Residual?

The whole domain is divided into finite control volumes, and ANSYS Fluent solves the governing equations iteratively for each of the control volumes. Residual of a variable is the amount by which the finite volumes are out of balance (conservation of the variable). After discretization, the conservation equation for a general variable ϕ at a cell p can be written as (Ansys Fluent Theory Guide, 2015):

$$\alpha_p \phi_p = \sum_{nb} \alpha_{nb} \phi_{nb} + b \quad (3.25)$$

Where,

α_p is the centre coefficient = $\alpha_p = \sum_{nb} \alpha_{nb} - S_p$

ϕ_{nb} are the influence coefficients for the neighbouring cells

b is the contribution of the constant part of the source term S_c in $S = S_c + S_p \phi$ and of the boundary conditions.

The residual computed R^ϕ is the imbalance in equation 3.25 summed over all the computational cells P , which is written as:

$$R^\phi = \sum_{cellsp} \left| \sum_{nb} \alpha_{nb} \phi_{nb} + b - \alpha_p \phi_p \right| \quad (3.26)$$

3.7.5 Post-processing - evaluation of results

The results were in the form of flow field variables in huge numbers to represent them in any meaningful way, the techniques used for each case studied in this research are briefly given below:

- **Case A:** The penetration depths were assessed using the maximum axial velocities. Positive flow rates were calculated on vertical planes constructed at different depths inside the heading using absolute axial velocities. Velocity contours and velocity vectors were plotted on vertical and horizontal planes respectively to see the air flow patterns.
- **Case B:** The flow rates going into the heading were calculated at different depths on vertical planes constructed inside the heading, and at the exit of the LB, to compare the effect of each parameter and to develop mathematical models to estimate the air flow rates close to the face of the heading and at the

exit of the LB. The distinct air flow features were visualized by constructing velocity stream lines and velocity vectors on the horizontal and vertical planes.

- **Case C:** Air flow patterns were studied by constructing various horizontal and vertical planes inside the heading at different distances from the floor, face and walls of the heading.
- **Case D:** Air flow rates going into the heading were calculated on vertical planes constructed at a distance of 0.5m, 0.4m, and 0.3m from the face of the heading. Mathematical models to estimate the airflow rates close to the face of the heading were developed using this data. Air flow patterns were studied by constructing various horizontal and vertical planes inside the heading constructed at different distances from the floor, face and walls of the heading.

3.8 Conclusion

The conceptual framework and methodology implemented for this research was presented in this chapter. The components of this research that is the research matrix and the numerical considerations were discussed in detail.

The next chapter covers the various case studies undertaken to validate the results of the numerical model used for this research. A comparison of the results of experimental and numerical results for these studies is discussed in this chapter.

4 NUMERICAL MODEL VALIDATION STUDIES

4.1 General

Validation of a numerical model is required to demonstrate its accuracy in order to be used with confidence and that the results be considered reliable. The numerical model is optimized for the validation case until the results are comparable with actual physical process results (analytical results) or experimental results. The validated model can then be used for studies involving large number of situations in similar environments without doing further validations. This becomes an even bigger advantage when it comes to ventilation in the mining industry, where it is extremely difficult and at times even dangerous to perform experiments and take accurate measurements of the flow features. The validation of a numerical model is generally carried out using one of the three approaches, (a) comparison of simulated results with the laboratory results, (b) using experimental results from literature, and (c) comparison of simulated results with in-situ experimental results.

Laboratory studies usually involve the use of a scaled down model, and similarity parameters. In this research, the validation of the numerical model was carried out using the results from literature as well as doing in-situ experiments. The results showed that k-e realizable model is well suited for the studies related to the ventilation of the development heading. A brief account of the validation studies carried out for this research is given in this chapter.

4.2 Validation Study One

In the first study, a three dimensional analysis to find the depth of air flow in empty headings ventilated without any auxiliary devices was carried out. The model dimensions were kept constant and air penetration into the heading for four LTR velocities was compared. Determination of penetration of air was based on the maximum axial velocity, and flow rates were calculated using absolute axial velocity at different depth planes. The results were compared with experimental results from experimental work undertaken previously by the Chamber of Mines Research Organization (COMRO), (Meyer,1989). The validation showed good correlation with

the experimental results (Feroze and Phillips, 2015). The validation case and its results are given below:

4.2.1 Model geometry and meshing

The three dimensional model as shown in Figure 4.1 was generated in the Ansys Design Modeller software. The width chosen for the LTR and the heading was 6.6m, while both the heading and LTR were 3 m high. The length of the LTR modelled on both the upstream and downstream side of the heading was 10 m and the length of the heading itself was 20 m. A structured mesh with a size of 0.05 m was created using the Ansys Fluent Mesher. A finer mesh was created in the near wall region as shown in Figure 4.2. A total of 10 boundary layers were used in this fine mesh using a growth rate of 1.2 to accurately resolve the boundary layer and to allow a smooth transition between the boundary mesh and the main mesh.

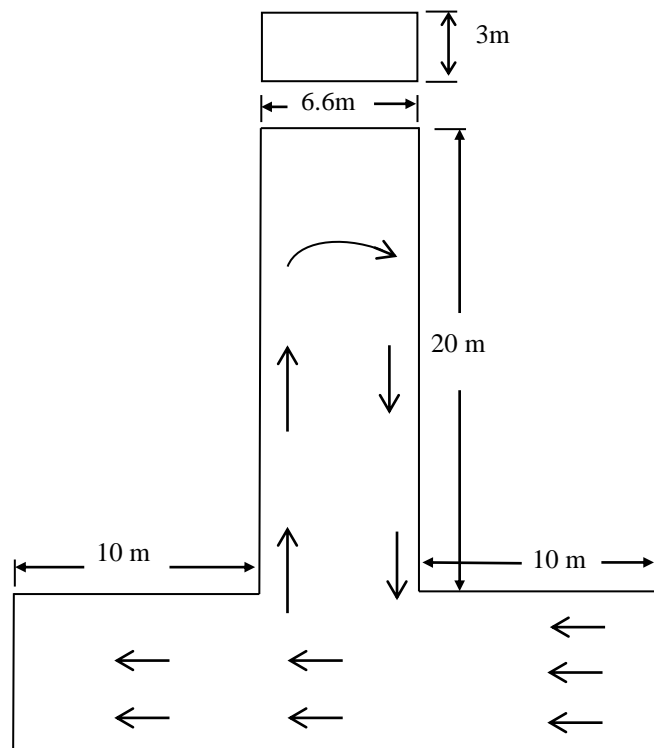


Figure 4.1 Three dimensional model

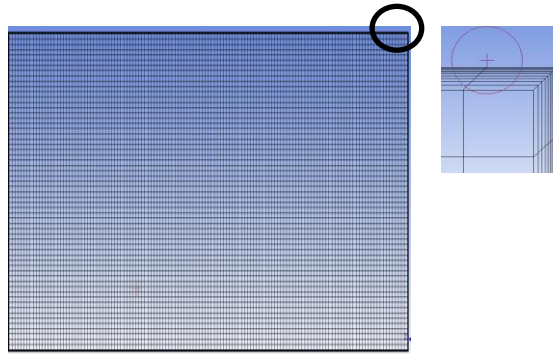


Figure 4.2 Hexahedral mesh with boundary layers (Inset view of mesh boundary)

4.2.2 Boundary conditions and numerical details

“Velocity Inlet” and “Outflow” boundary conditions were used at the inlet and outlet of the LTR. Since it was intended to validate the CFD results with experimental results obtained in a coal mine located near Johannesburg, the properties of air at 20°C were used. Reynolds numbers for the four LTR velocities (0.78m/s, 1m/s, 1.35m/s, 1.9m/s) were calculated to be 1.74×10^5 , 2.23×10^5 , 3.01×10^5 , 4.24×10^5 respectively. The Reynolds number was calculated using equation 4.1. These LTR velocities are the same as were used for the experimental study.

$$\text{Re} = \frac{\rho u D}{\mu} \quad (4.1)$$

where,

ρ = Density (Kg / m^3), μ = Viscosity (Pa.s)

D = Hydraluc Diameter (m), u = m/s

The two equation k-e realizable turbulent model was used for this study. The iterative process used for the calculation of results was set to run until five orders of residual reduction was achieved (convergence criteria of 10^{-5}) with second order accuracy. At the velocity inlet, turbulent intensity and hydraulic diameter were used as the turbulent quantities.

4.2.3 Results and discussion

Figure 4.3 shows the maximum axial velocities (velocity component along the direction of the heading) on planes inside the heading, located at depths of 1m, 5m, 12m, 15m, and 16m respectively. These velocities have been compiled for each LTR velocity used

for this validation study i.e. 0.78m/s, 1m/s, 1.35m/s, 1.9m/s respectively. Considering 0.05m/s as the minimum measurable limit of velocity, the air penetration depth with 1.35m/s and 1m/s LTR velocities were the maximum i.e. 15m as shown in Table 4.1.

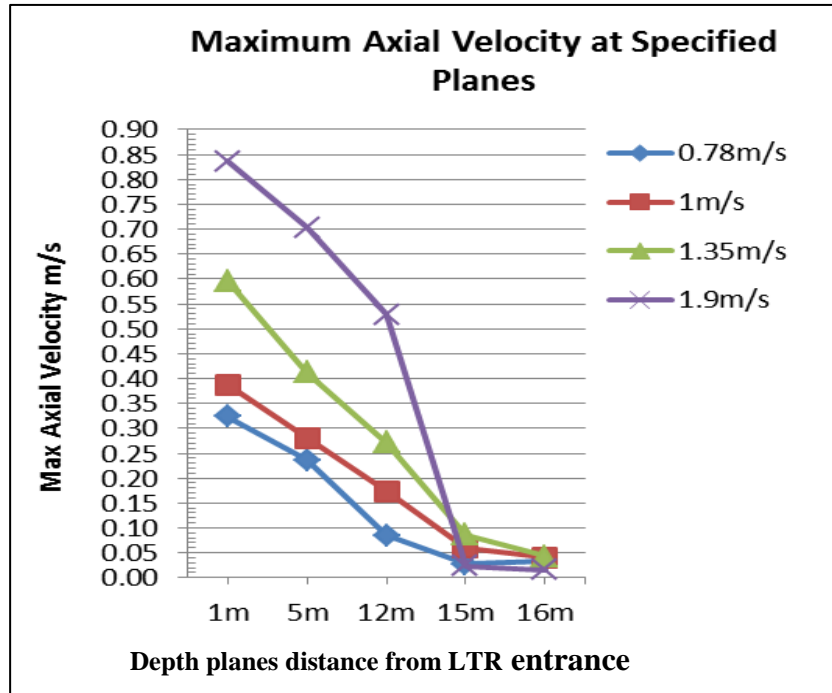


Figure 4.3 Maximum axial velocities at specified planes

Table 4.1 Numerical results of maximum penetration depths for each LTR velocity

| Numerical results | |
|----------------------|-------------------------|
| LTR velocity (m/s) | Penetration depth (m) |
| 0.78 | 12.3 |
| 1 | 15.2 |
| 1.35 | 15.9 |
| 1.9 | 12.7 |

Figures 4.4 through 4.7 shows the detailed variation of axial velocity contours on a plane located at 15m depth for each LTR velocity. The contours have been divided into five regions; showing different velocity ranges. The velocity ranges for these regions are shown with the contours. Positive velocities indicate inflows and the negative flows are the return air flows. The return axial velocity for the case of 1.35m/s LTR was again the maximum i.e. 0.04294 m/s. The highest inflows can be seen on the left half, with the minimum flow in the centre and the highest outflow on the right side.

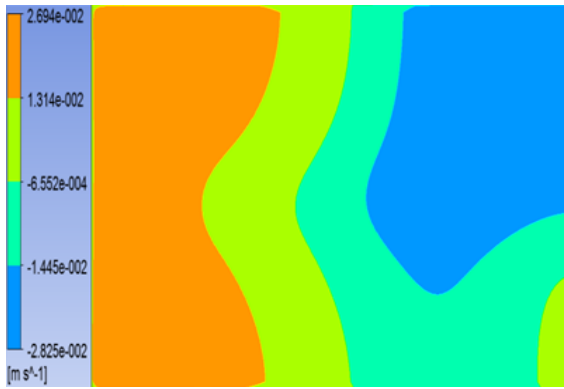


Figure 4.4 Axial velocity contours at 15m plane in the heading for 0.78 m/s LTR velocity

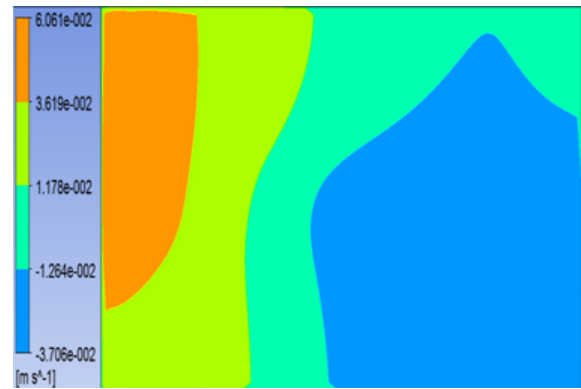


Figure 4.5 Axial velocity contours at 15m plane in the heading for 1 m/s LTR velocity

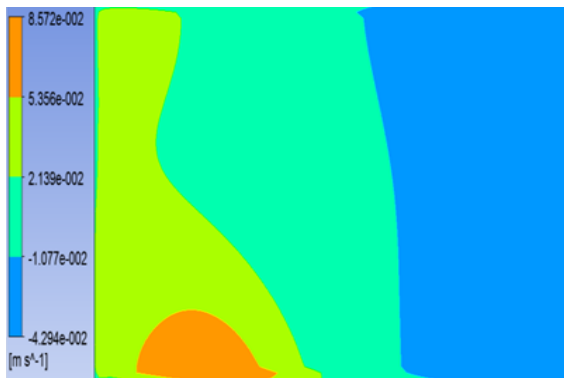


Figure 4.6 Axial velocity contours at 15m plane in the heading for 1.35 m/s LTR velocity

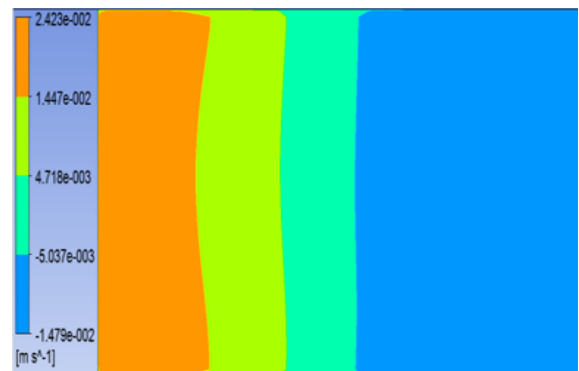


Figure 4.7 Axial velocity contours at 15m plane in the heading for 1.9 m/s LTR velocity

Table 4.2 and Figure 4.8 illustrate the average positive “flow in” of air through planes set at the specified depths of 1,5,12, and 15m respectively inside the heading. The air flow rates decreased considerably after the depth of 12 m for all the LTR velocities and became insufficient to ventilate the heading.

Table 4.2 Average positive flow inwards at specified planes

| Planes at depth (m) | LTR Velocities (m/s) | | | |
|---------------------|---|---------|---------|---------|
| | 0.78 | 1 | 1.35 | 1.9 |
| | Average positive flow inwards at specified planes (m ³ /s) | | | |
| 1 | 0.44641 | 0.52216 | 0.73248 | 1.09781 |
| 5 | 0.74364 | 0.87828 | 1.29108 | 2.88777 |
| 12 | 0.21092 | 0.43951 | 0.76674 | 0.21202 |
| 15 | 0.15206 | 0.23408 | 0.22431 | 0.11558 |

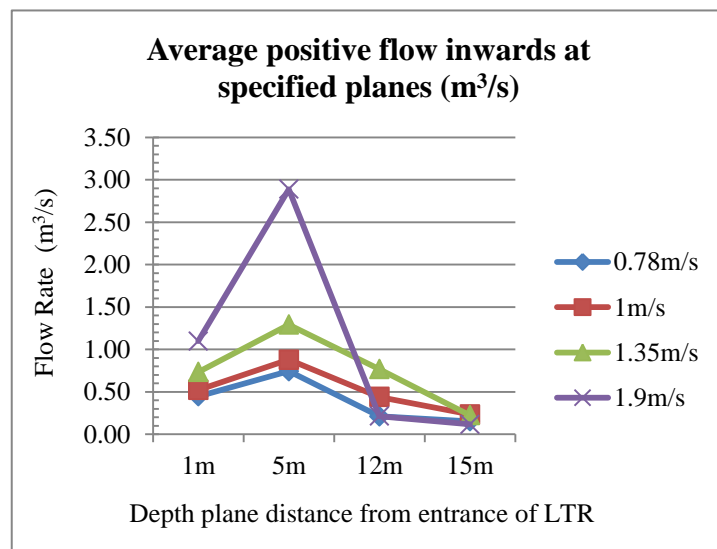


Figure 4.8 Average positive flow in at specified planes

Figures 4.9 and 4.10 show the velocity contours on a horizontal plane at a height of 1.5m. It can be seen from these contours that air entered from the downstream side and the flow rate decreased very considerably after the 12m depth. For low LTR velocity (1m/s) secondary flows are visible for higher velocity of 1.9m/s secondary air flows are not very prominent and most of the air did not go beyond the 12m depth.

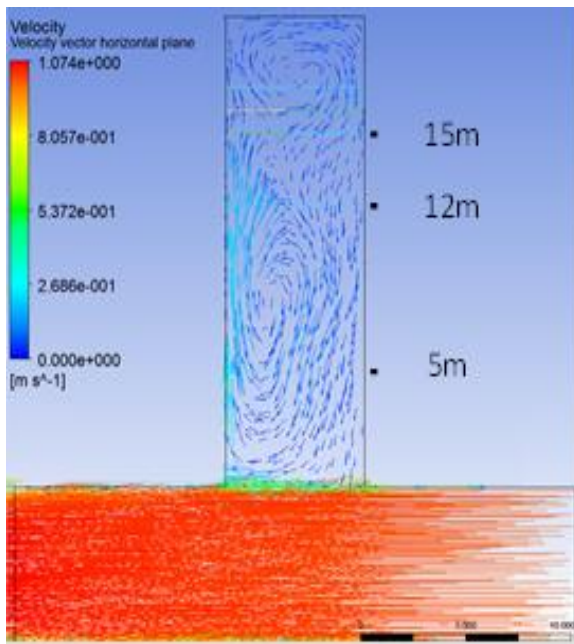


Figure 4.9 Velocity vectors on 1.5 m high horizontal plane for 1m/s LTR velocity

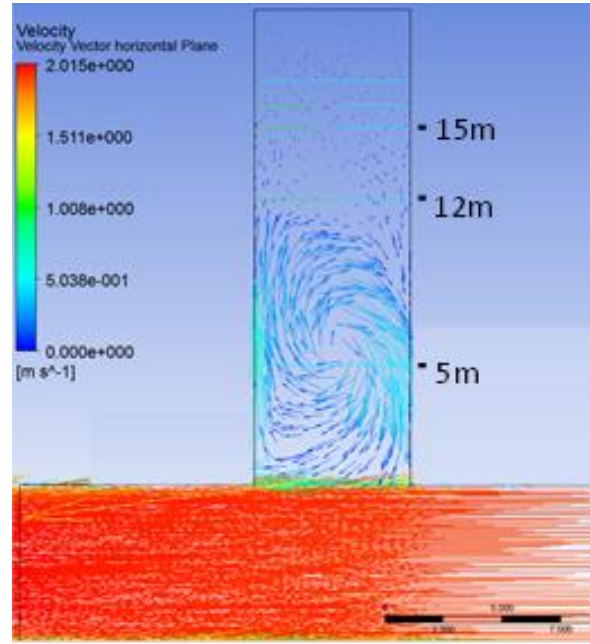


Figure 4.10 Velocity vectors on 1.5 m high horizontal plane for 1.9 m/s LTR velocity

4.2.4 Validation

Meyer (1989) conducted a study of the ventilation in Room and Pillar headings of a coal mine. He selected the headings which were not ventilated by any auxiliary means and, using regulators, varied the LTR velocity to see its effect on the airflow patterns and penetration distance inside the headings (Meyer, 1989). He used smoke generating chemical tubes to visualize the airflow patterns and to measure the penetration distances. Table 4.3 shows the results of his experiments in a heading with dimensions of 6.6 x 3 x 20m (the same size was also chosen for the numerical cases). The maximum air penetration depth for each LTR velocity was determined and the results of the field trial showed that the maximum air penetration depth was achieved with a LTR velocity of approximately 1.35m/s.

Table 4.3 Measured experimental results of maximum penetration depths for each LTR velocity, (Meyer, 1989)

| Experimental results | |
|-----------------------------|----------------------------|
| LTR velocity (m/s) | Penetration depth (m) |
| 0.78 | 12.2 |
| 1 | 15.8 |
| 1.35 | 16.8 |
| 1.9 | 12.4 |

A comparison of the present CFD simulation results, using ANSYS' k-e realizable model (Table 4.1), with those of Meyer (Table 4.3), is given in Figure 4.11 which showed that the numerical results followed the trend of the experimental results.

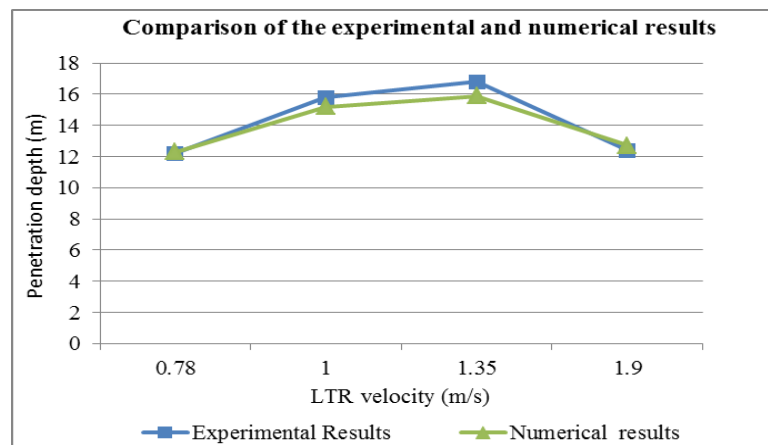


Figure 4.11 Comparison of experimental and numerical results validation case study one

4.3 Validation Study Two

The School of Mining Engineering, University of the Witwatersrand, has developed a 66.2m long mock tunnel. This is equipped with a fan and duct ventilation system as shown in Figure 4.12. The duct length is 55.2m and the diameter of the duct is 0.5m. The duct delivers a quantity of $1.98\text{m}^3/\text{s}$ and the average air velocity at the mouth of the duct is approximately 10.08m/s . The distance of the duct mouth from the face of the heading is 11m as shown in Figure 4.13.



a) Tunnel and fan duct

b) Fan and duct

Figure 4.12 School of Mining Engineering, University of the Witwatersrand, tunnel and fan with duct system

The tunnel is dome shaped at the entrance, but becomes rectangular near the face as shown in Figure 4.14. The height and width of the tunnel at the face are 2.4m and 2.6m respectively. The distance of the duct from the top and left wall of the tunnel is 0.07m and 0.57m respectively as shown in Figure 4.15. The shape of the duct all along its length is shown in Figure 4.16.

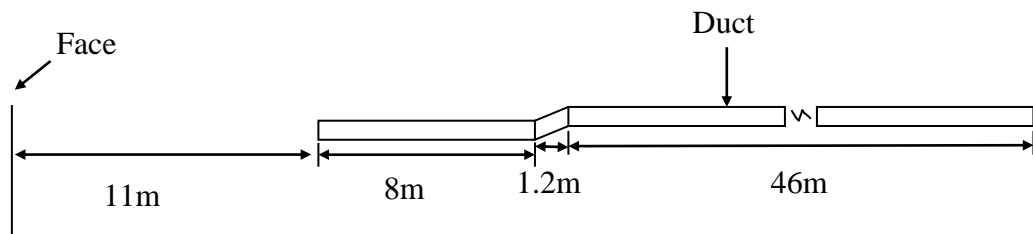


Figure 4.13 Schematic diagram of the duct

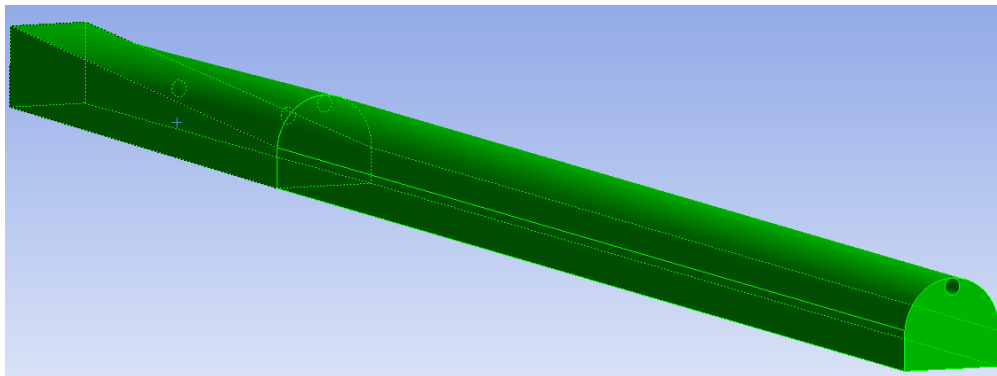


Figure 4.14 Outline of the Tunnel

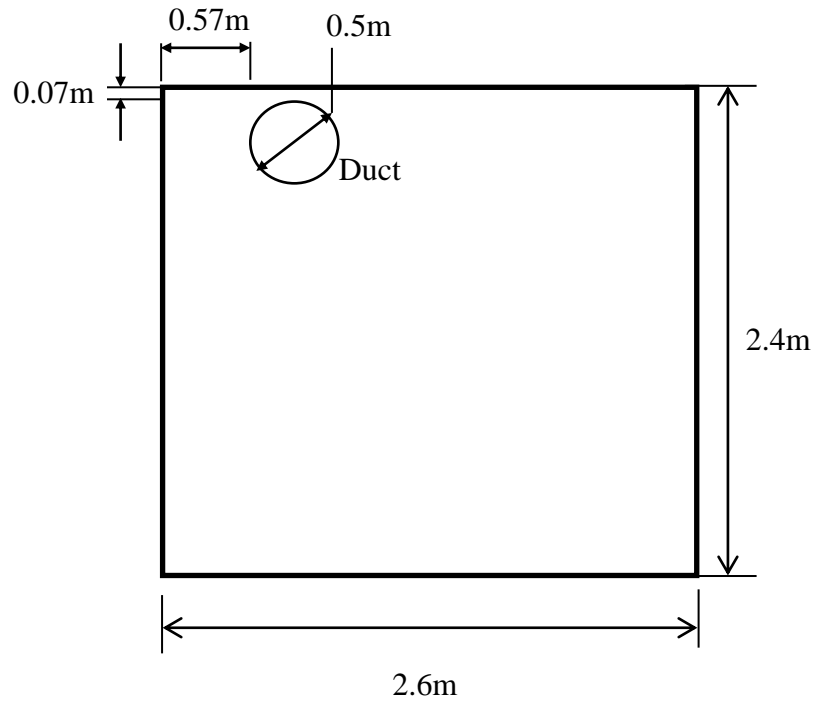


Figure 4.15 Dimension of the tunnel face and duct distances from the walls of tunnel

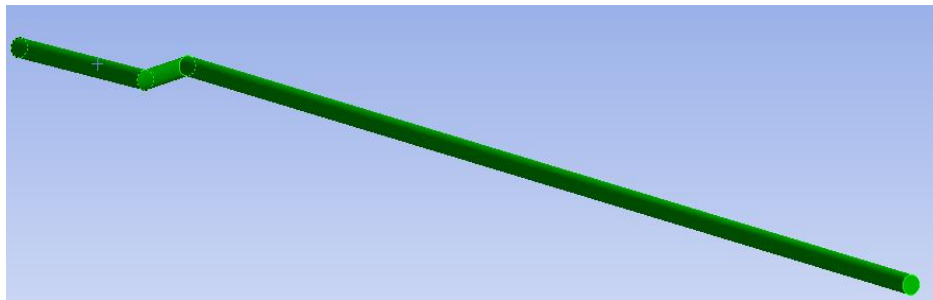


Figure 4.16 Outline of the duct

This study was also undertaken to validate the numerical model used for the research. The air velocities were determined at several points on a vertical plane at a distance of 0.5m from the face of the tunnel. This was carried out using both physical experiments and numerical solutions. A positive sign with velocity indicate the direction of air going into the heading and a negative sign is for the air moving in the opposite direction. A comparison of the results showed good correlation, and gave confidence to use the same numerical model for further simulations required for the research.

4.3.1 Experimental setup and results

The face of the heading was divided into five regions as shown in Figure 4.16. Velocity at the centre of each region was measured using both the hot wire and rotating vane anemometers (Airflow TA440, LCA 6000). The flow rate at the exit of the duct is equivalent to $1.98\text{m}^3/\text{s}$. This was confirmed using both the anemometer and digital pressure meter (GMH 3110). The same flow rate was used for the numerical model. The velocities of the air, going into or leaving the five locations as shown in Figure 4.17 were measured (+ve sign for air going into the heading and -ve for opposite direction), and the results are given in Table 4.4.

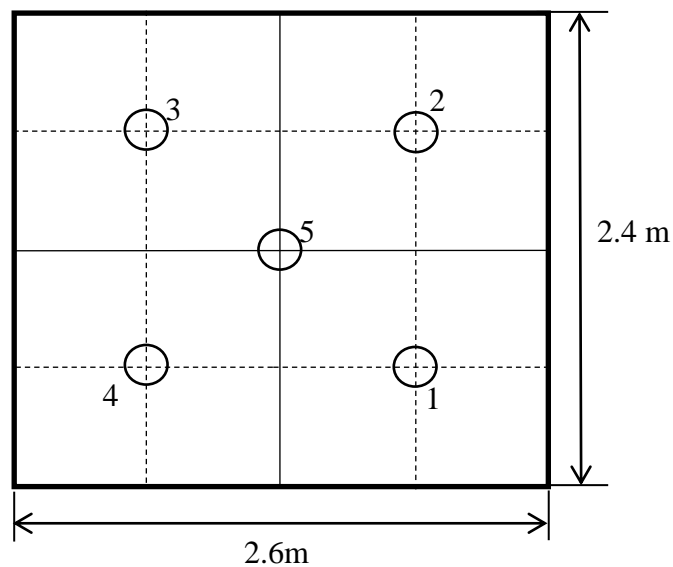


Figure 4.17 Measurement points at the face of the tunnel

Table 4.4 Air velocities measured using hot wire anemometer

| Experimental Results | |
|----------------------|----------------|
| Point | Velocity (m/s) |
| 1 | -0.84 |
| 2 | -0.11 |
| 3 | 2.35 |
| 4 | 0.30 |
| 5 | 0.75 |

4.3.2 Numerical Calculations

4.3.2.1 Model geometry and meshing

The three dimensional model as shown in Figure 4.14 was generated in the Ansys Design Modeler software. A fine mesh of size 0.04 m was created using the Ansys Fluent Mesher. A finer mesh was created on all the boundaries (walls) of the domain.

4.3.2.2 Boundary conditions and numerical details

“Velocity inlet” and “Outflow” boundary conditions were used for the fan and the outlet of the tunnel, respectively. “Wall boundary” condition was used at all the walls of the domain. The properties of air at 24°C (as calculated in the tunnel) were used for the calculation of the numerical solution. The two equation k-e realizable turbulent model was again used for this study. The iterative process used for the calculation of results was set to run until five orders of residual reduction was achieved (convergence criteria of 10^{-5}) with second order accuracy.

4.3.2.3 Numerical Results

The air velocity vectors on a vertical plane constructed at a distance of 0.5m from the face of the tunnel are shown Figure 4.18. Air can be seen moving from left to right of the face of the tunnel and returning. The contours of the axial velocity going through and coming out the plane is shown in Figure 4.19. The velocity of air at each location can be seen on these contours.

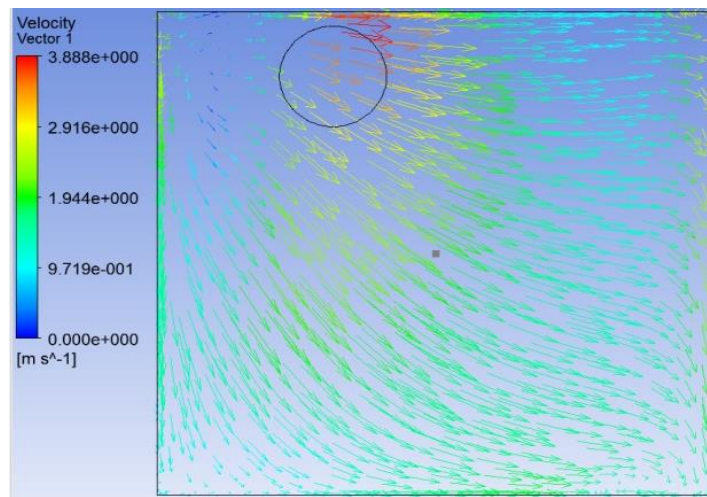


Figure 4.18 Velocity vectors close to the face of the tunnel on vertical plane

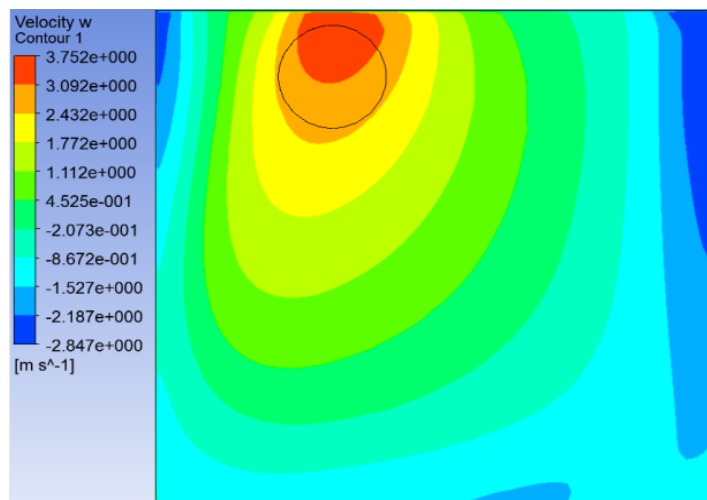


Figure 4.19 Velocity contours close to the face of the tunnel on vertical plane

The velocities of the air, going into or leaving the five locations selected for this validation study as determined numerically, are given in Table 4.5 and can be seen in Figure 4.19.

Table 4.5 Numerically calculated values of air velocities

| Numerical Results | |
|-------------------|----------------|
| Point | Velocity (m/s) |
| 1 | -0.871 |
| 2 | -0.104 |
| 3 | 2.437 |
| 4 | 0.311 |
| 5 | 0.784 |

4.3.3 Validation

A comparison of the numerical and experimental results is given in Figure 4.20, which shows that the numerical results are in line with the experimental results.

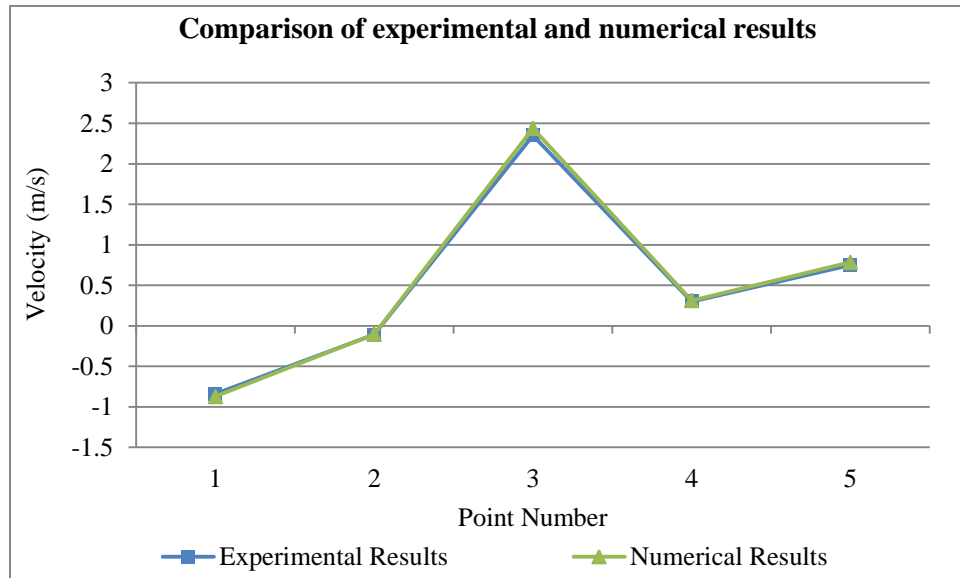


Figure 4.20 Comparison of experimental and numerical results validation study two

4.4 Validation Study Three

This validation study was also undertaken to validate the numerical model used for the research. In-situ measurements of the air velocities inside a long heading (41.1m) ventilated using a LB were taken in an actual mine (Mine A, no permission given to publish the name of the mine). A comparison of the results showed that the numerical results follow the trends of the experimental results. An account of this study is given in this section.

4.4.1 Experimental setup and results

The height of the heading was 1.8m. The dimensions of the LTR, heading and LB are given in Figure 4.21.

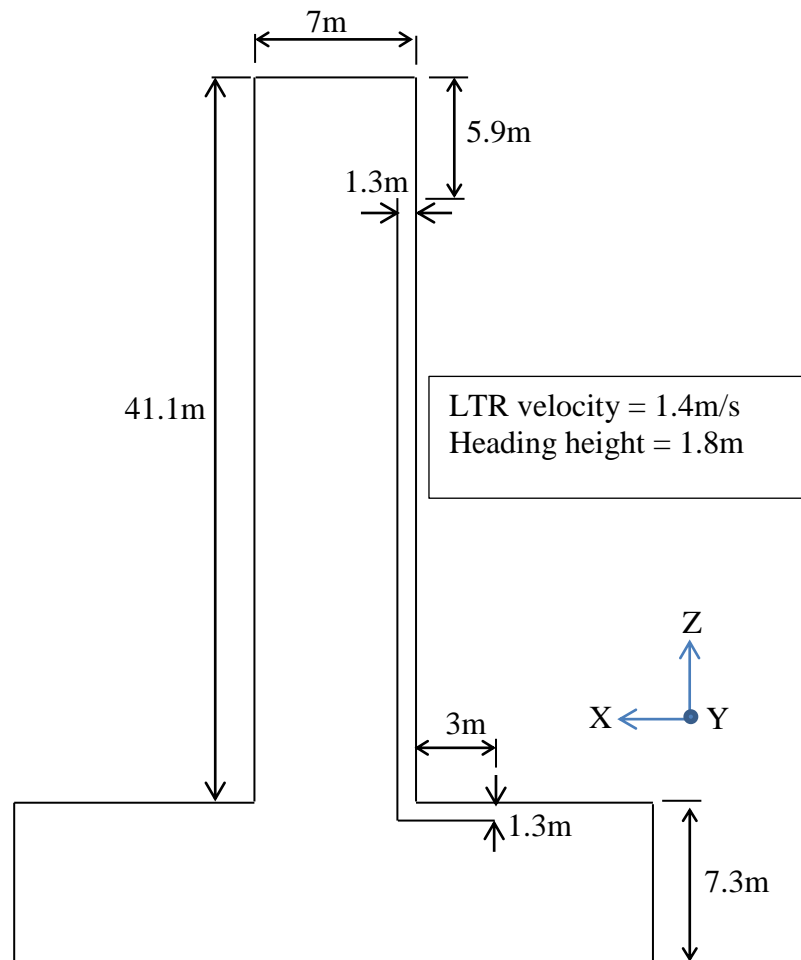


Figure 4.21 Important dimensions of the heading and LTR

The air velocities and direction of the air inside the heading at various points were recorded using the hot wire anemometer and smoke tube respectively. These air velocities are given in Table 4.6 along with the coordinates of these points. The coordinates of the bottom right corner of the LTR was considered as (0,0,0) and the other coordinates were worked out using this reference point. Positive and negative signs are indicating the direction of air movement (A positive sign indicated movement of air into the heading, and a negative for the opposite movement). The air flow rate at the exit of the LB was also measured. Access to area within 4m of the face was not allowed therefore, flow rates close to the face were not taken. The description of the chosen points is given below:

- 1) Point 1: 1.5m from the right wall of the heading, 3m from face, and 0.9m from the floor of the heading (11.5, 0.9, 45.4).
- 2) Point 2: At the centre of the LB and wall channel, 41m into the heading from the reference coordinates and 0.1m from the roof of the heading (10.65, 1.7, 42.5).
- 3) Point 3: 2m from the left wall of the heading, 17m from the face, and 0.1m from the floor of the heading (15, 0.1, 31.4).
- 4) Point 4: 3m from the left wall of the heading, 25.1m from the face (16m from the entrance of the heading) 0.1m from roof of heading (14, 1.7, 23.3).
- 5) Point 5: 1m from the left wall, 25.1m from the face (16m from the entrance of the heading) 0.1m from floor of heading (16, 0.1, 23.3).

Table 4.6 Air velocities measured using hot wire anemometer

| Experimental Results | |
|----------------------|----------------|
| Coordinate points | Velocity (m/s) |
| 11.5, 0.9, 45.4 | 1.13 |
| 10.65, 1.7, 42.5 | 0.98 |
| 15, 0.1, 31.4 | -0.4 |
| 14, 1.7, 23.3 | -0.15 |
| 16, 0.1, 23.3 | -0.62 |

The air flow rate at the exit of the LB was found using the average air velocity at the exit of the LB and the area of LB and wall channel and was found equal to $2.18\text{m}^3/\text{s}$.

4.4.2 Numerical Calculations

4.4.2.1 Model geometry and meshing

The three dimensional model as shown in Figure 4.22 was generated in the Ansys Design Modeler software. The length of the LTR on both the up and down stream side were kept constant equal to 10m for the numerical model. A mesh with a size of 0.04 m was created using the Ansys Fluent Mesher. A finer mesh was created on all the boundaries of the domain.

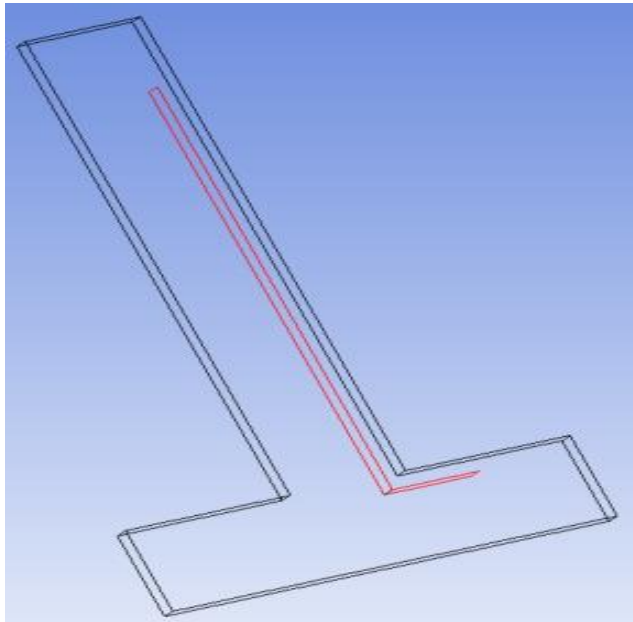


Figure 4.22 Three dimensional model

4.4.2.2 Boundary conditions and numerical details

“Velocity inlet” boundary condition was used at the inlet of the LTR and outflow boundary condition was used at the outlet of the LTR respectively. “Wall boundary” condition was used for the LB at all the walls of the domain. The properties of air at 19°C (as measured in the heading) were used for the calculation of the numerical solution. The other numerical considerations were kept same as discussed in section 4.3.2.2.

4.4.2.3 Numerical Results

The flow of air inside the heading is shown using velocity vectors in Figure 4.23. The air entered the LB - wall channel ventilated the heading and returned from the downstream side.

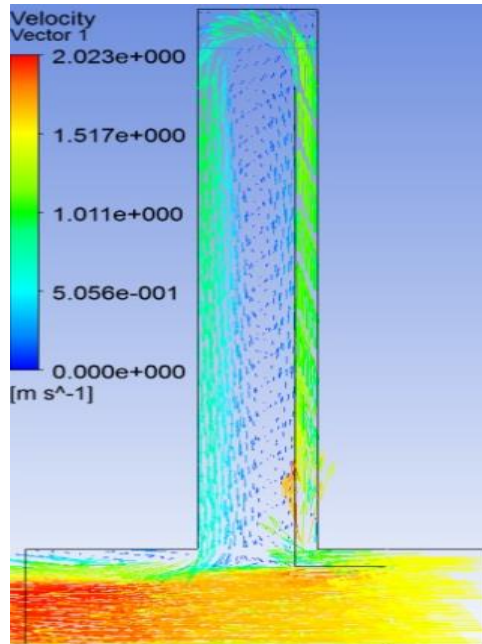


Figure 4.23 Air flow inside the heading using velocity vectors

The velocities of the air inside the heading at five points (same points as were chosen for the experiment) are shown in Figures 4.24 through 4.28 using the velocity contours and given in Table 4.7. The sign convention in the tabulated data is the same as was chosen for the experimental results, only positive signs are used in the Figures showing the velocity contours, indicating the magnitude of the velocities. The flow rate at the exit of the LB was found equal to $2.3376 \text{ m}^3/\text{s}$.

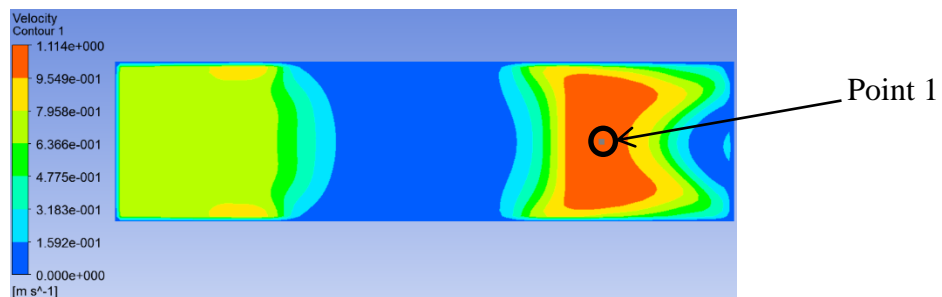


Figure 4.24 Velocity Contours on a plane parallel to face of heading passing through Point 1

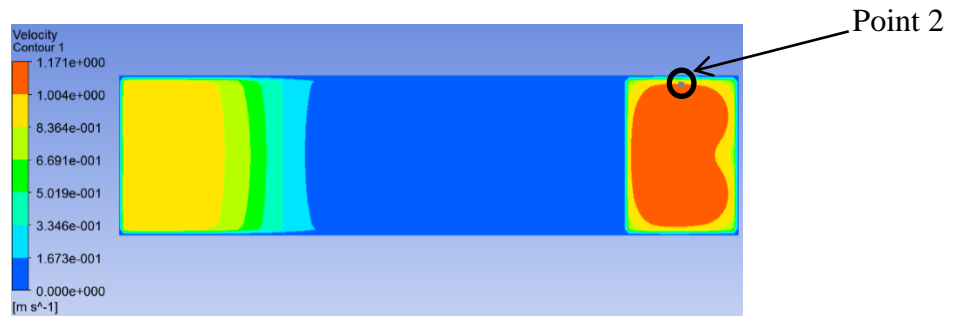


Figure 4.25 Velocity Contours on a plane parallel to face of heading passing through Point 2

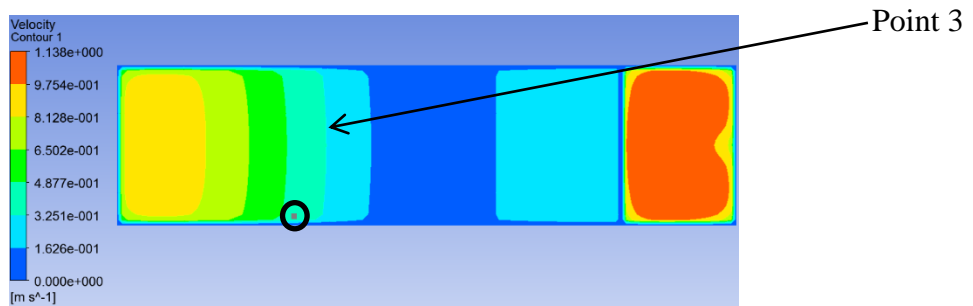


Figure 4.26 Velocity Contours on a plane parallel to face of heading passing through Point 3

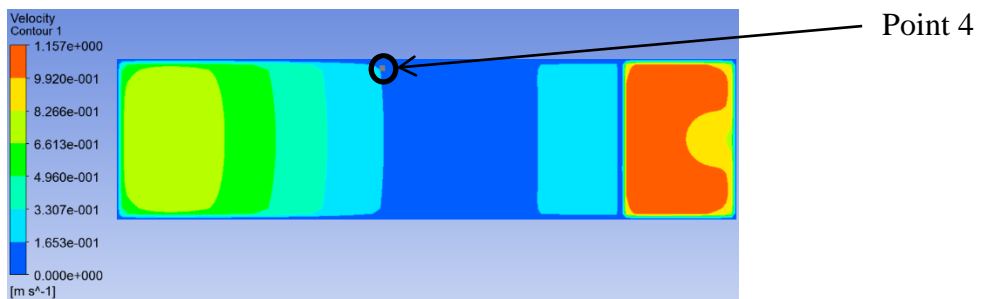


Figure 4.27 Velocity Contours on a plane parallel to face of heading passing through Point 4

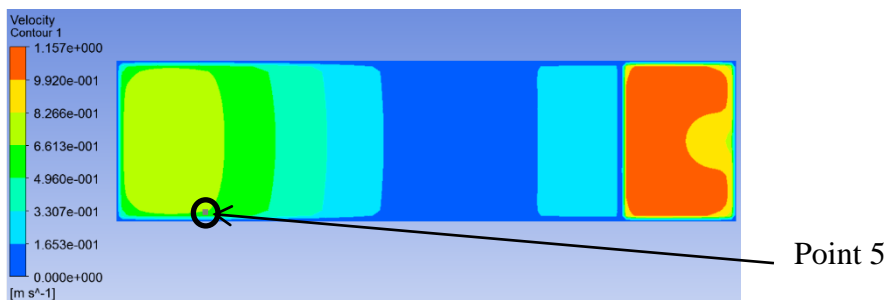


Figure 4.28 Velocity Contours on a plane parallel to face of heading passing through Point 5

Table 4.7 Numerically calculated values of air velocities

| Numerical Results | |
|----------------------|----------------|
| Coordinate point (m) | Velocity (m/s) |
| 11.5, 0.9, 45.4 | 1.0732 |
| 10.65, 1.7, 42.5 | 1.0226 |
| 15, 0.1314, | -0.4284 |
| 14, 1.7, 23.3 | -0.16 |
| 16, 0.1, 23.3 | -0.6484 |

4.4.3 Validation

A comparison of the numerical and experimental results is given in Figure 4.29 which shows that the numerical results are in line with the experimental results.

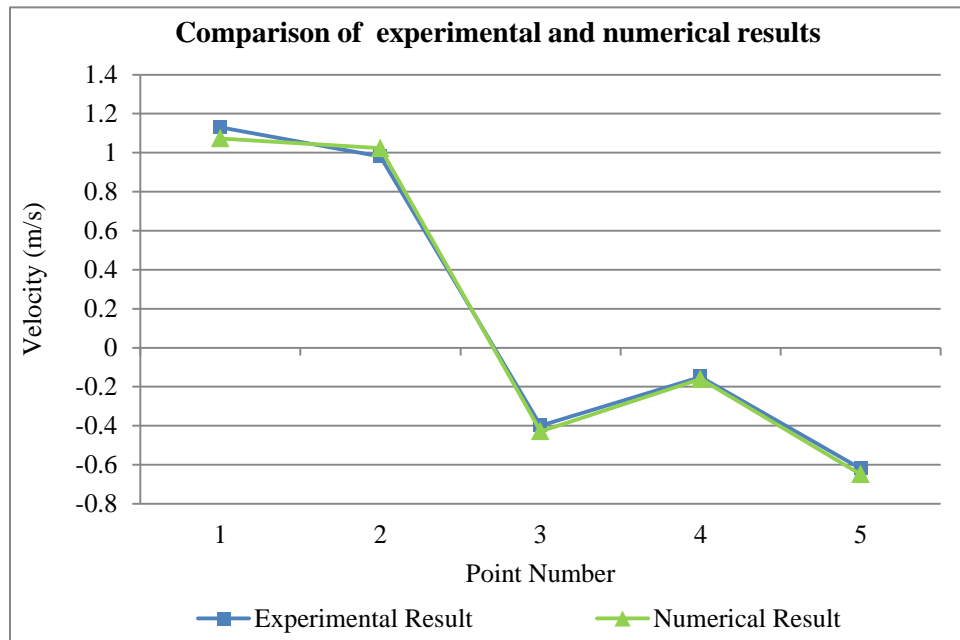


Figure 4.29 Comparison of the experimental and numerical results validation study three

4.5 Validation Study Four

In the fourth validation case study, in-situ measurements were taken in the Kriel Colliery, which is situated 120km east of Johannesburg and 50km south west of Witbank. These measurements were then compared with the numerical results, and found in-line with the experimental results. An account of this study is given in this section.

4.5.1 Experimental setup and results

The in situ measurements were taken in a heading ventilated using LB; the dimensions of the heading and LB are given in Figure 4.30. The velocity of air at several locations inside the heading along with the flow rate at the exits of the LB was measured. The air velocities and direction of the air inside the heading were recorded using the hot wire and rotating vane digital anemometers and smoke tube respectively. The air flow rate was calculated by using average velocity at the exit of the LB. Access to area within 4m of the face was not allowed therefore, flow rates close to the face were not taken.

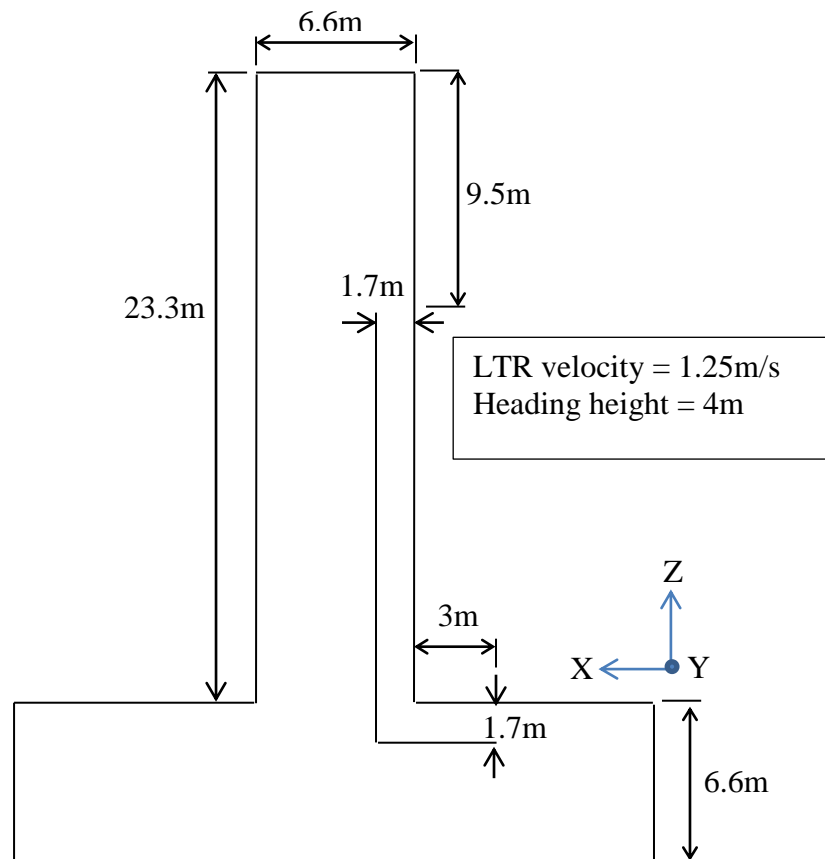


Figure 4.30 Important dimensions of the heading and LTR

The velocities of air measured inside the heading are given in Table 4.8 along with the coordinates of these points. The coordinates of the bottom right corner of the LTR was considered as (0,0,0) and the other coordinates were worked out using this reference point. Positive and negative signs are indicating the direction of air movement (positive sign indicated movement air into the heading, and negative for the opposite movement).

Table 4.8 Air velocities measured using hot wire anemometer

| Experimental Results | |
|---------------------------|-------------------|
| Coordinate point (m) | Velocity (m/s) |
| At the inlet of LB | |
| (7, 0.5, 5.75) | 0.96 |
| (7, 2, 5.75) | 0.96 |
| Inside the heading | |
| 12.64, 0.5, 9.92 | -0.11 |
| 12.64, 2, 9.92 | -0.13 |
| 15.28, 0.5, 9.92 | -0.51 |
| 15.28, 2, 9.92 | -0.48 |
| 15.28, 0.5, 14.92 | -0.55 |
| 15.28, 2, 14.92 | -0.60 |

Average velocity = 0.92m/s

Flow rate at the exit of the LB = $0.92 \times 1.7 \times 4 = 6.26\text{m}^3/\text{s}$

4.5.2 Numerical Calculations

4.5.2.1 Model geometry and meshing

The three dimensional model was generated in the Ansys Design Modeller software. The length of the LTR on both the up and down stream side were kept constant equal to 10m for the numerical model. A mesh with a size of 0.04 m was created using the Ansys Fluent Mesher. A finer mesh was created on all the boundaries of the domain.

4.5.2.2 Boundary conditions and numerical details

The boundary conditions and numerical details are the same as discussed in section 4.4.2.2. The only change is that the properties of air at 19.1°C (as measured in the heading) were used for the calculation of the numerical solution.

4.5.2.3 Numerical Results

The flow of air inside the heading is shown using velocity vectors in Figure 4.31. It can be seen that the air entered the LB - wall channel ventilated the heading and returned from the downstream side. As a result of a big (1.7m) distance of LB from the wall very less air exiting the LB actually reached the face of the heading, the reason for this is explained in more detail in Chapter 6.

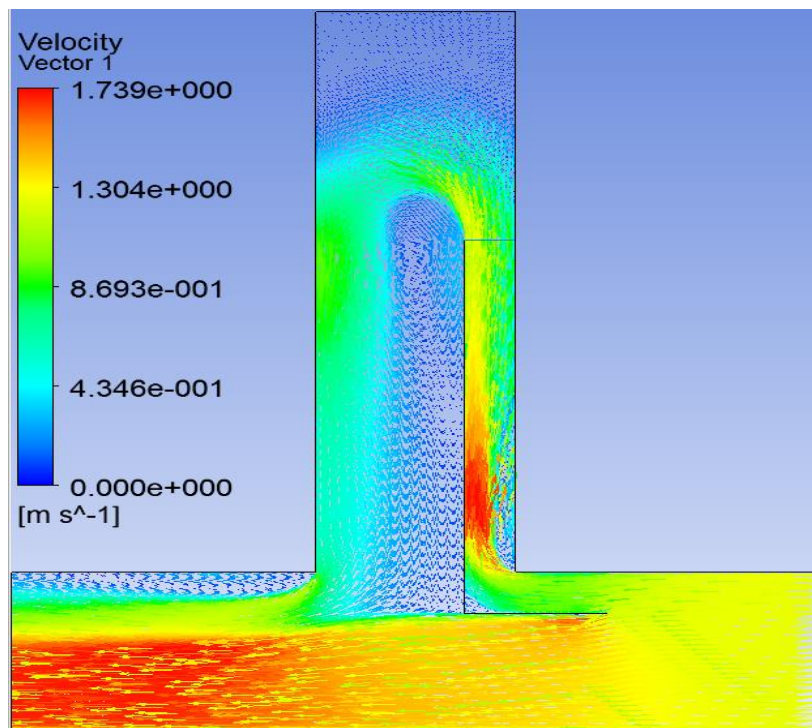


Figure 4.31 Air flow inside the heading using velocity vectors

The velocities of the air inside the heading at five points (same points as were chosen for the experiment) are shown in Figures 4.32 through 4.39 using the velocity contours and given in Table 4.9. The sign convention in the tabulated data is the same as was chosen for the experimental results, only positive signs are used in the Figures showing

the velocity contours, indicated the magnitude of the velocities. The flow rate at the exit of the LB was found equal to $6.566\text{m}^3/\text{s}$, which is low since the velocity of air in the LTR is low.

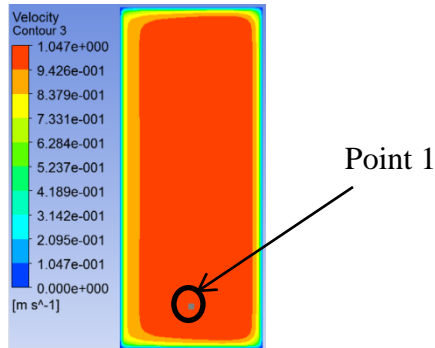


Figure 4.32 Velocity contours on a plane at the entrance of LB passing through point 1

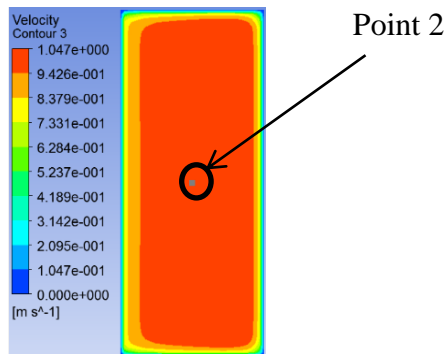


Figure 4.33 Velocity contours on a plane at the entrance of LB passing through point 2

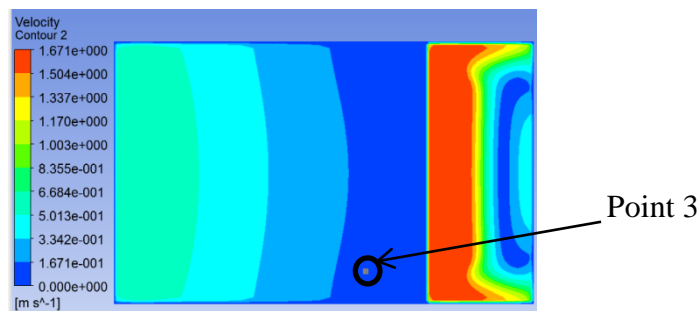


Figure 4.34 Velocity Contours on a plane parallel to face of heading passing through Point 3

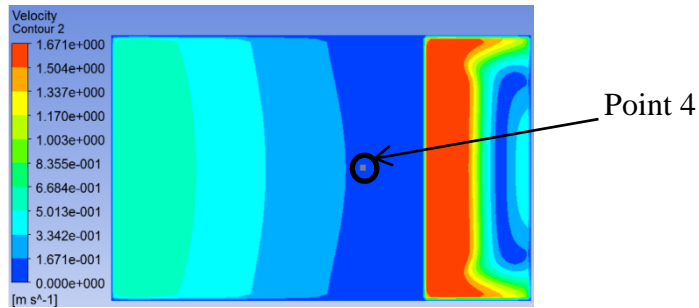


Figure 4.35 Velocity Contours on a plane parallel to face of heading passing through Point 4

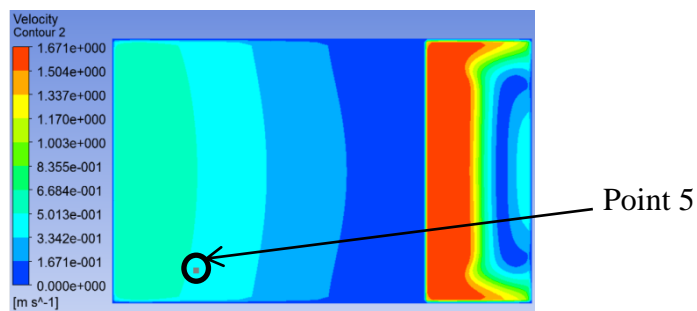


Figure 4.36 Velocity Contours on a plane parallel to face of heading passing through Point 5

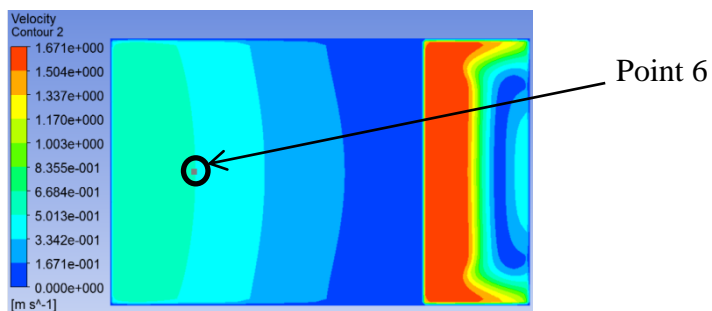


Figure 4.37 Velocity Contours on a plane parallel to face of heading passing through Point 6

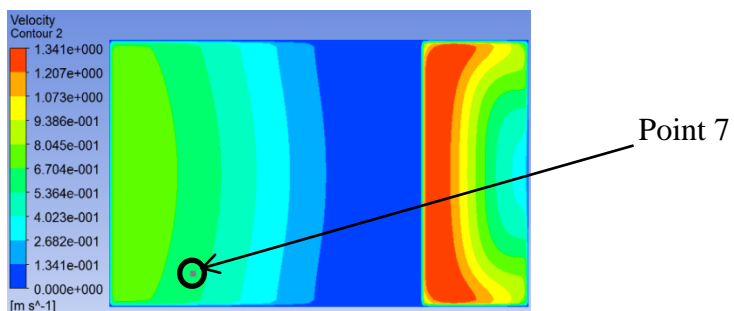


Figure 4.38 Velocity Contours on a plane parallel to face of heading passing through Point 7

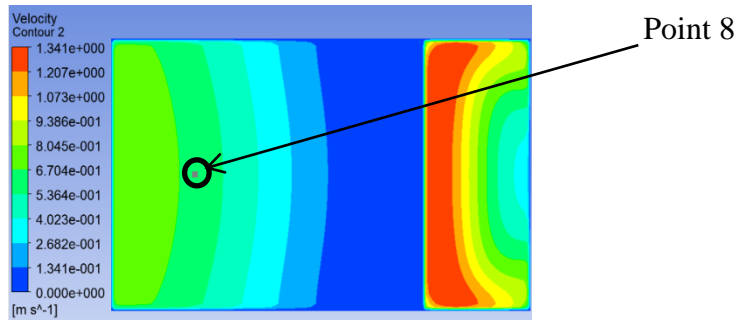


Figure 4.39 Velocity Contours on a plane parallel to face of heading passing through Point 8

Table 4.9 Numerically calculated values of air velocities

| Numerical Results | |
|---------------------------|----------------|
| Coordinate point (m) | Velocity (m/s) |
| At the inlet of LB | |
| (7, 0.5, 5.75) | 1.0304 |
| (7, 2, 5.75) | 1.0338 |
| Inside the heading | |
| 12.64, 0.5, 9.92 | -0.1207 |
| 12.64, 2, 9.92 | -0.14171 |
| 15.28, 0.5, 9.92 | -0.4818 |
| 15.28, 2, 9.92 | -0.504 |
| 15.28, 0.5, 14.92 | -0.5847 |
| 15.28, 2, 14.92 | -0.6278 |

4.5.3 Validation

A comparison of the numerical results, with the experimental results is given in Figure 4.40. It can be seen that the numerical results are in line with the experimental results.

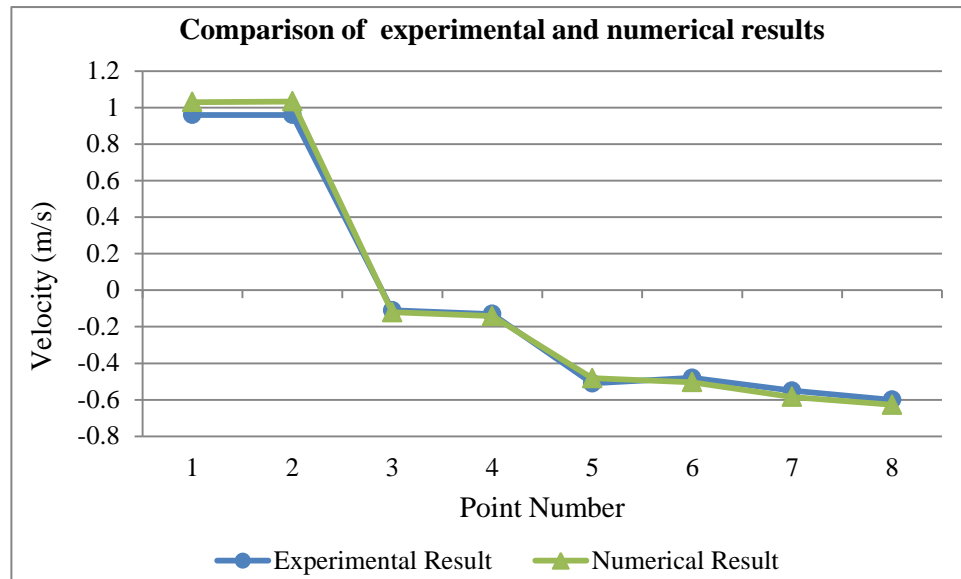


Figure 4.40 Comparison of the experimental and numerical results validation study four

4.6 Conclusion

The validation studies showed that the ANSYS Fluent k-e realizable model is suitable to study the ventilation of a heading connected to the LTR with reasonably acceptable accuracy. The same numerical model was therefore, chosen and used to carry out the remainder of this study.

The next chapter covers the results of the various scenarios used to study the effect of the LTR velocity on the penetration of air and the flow rates inside a heading ventilated without the use of any auxiliary ventilation device.

5 ANALYSIS AND DISCUSSION - VENTILATION OF HEADINGS WITHOUT THE USE OF ANY AUXILIARY EQUIPMENT

5.1 General

The ventilation of a heading connected to the last through road (LTR) in room and pillar coal mines, alters with the variation of the dimensions of the headings, the air flows in the LTR, the use and orientation of auxiliary equipment and the presence of equipment in the heading. In an actual mine, the condition of the heading varies and may face one or all of the following situations at different times. An effort was made to alter these factors in a systematic way to see the effect of each parameter on the air flows in the heading with specific emphasis on the axial flow rates close to the face of the heading. A total of 342 scenarios were created and simulated as discussed in Chapter 3 Methodology and Chapter 4 Validation studies. These scenarios were divided into four broad categories and named as Case A, Case B, Case C and Case D (see below). The simulation process took around two years to complete using two machines running day and night for millions of iterations, creating a huge volume of data. The part of the data related to the axial air flow rates at different depth planes in the heading and close to the face (generally 0.5m from the face) was gathered and discussed in the analysis using tables and graphs. Most of these tables and graphs have been placed in the appendices and a bare minimum has been kept in the main document to avoid distraction to the readers, without making it difficult to comprehend. The tables and graphs placed in the appendices have been named using alphabetic and Arabic numerals and referred to in the text by means of the table and figure numbers. Thus, an in-text reference Table E3 means the third table in Appendix E. Each Case has been discussed and analysed in separate chapters as given below:

- Chapter 5 - Analysis and discussion Case A - Ventilation of heading without the use of any auxiliary equipment.
- Chapter 6 - Analysis and discussion Case B - Ventilation of the heading with the use of LB.
- Chapter 7 - Analysis and discussion Case C - Ventilation of the heading with CM using LB.

- Chapter 8 - Analysis and discussion Case D - Ventilation of the heading using a ducted fan.

5.2 Case A - No Auxiliary Ventilation Equipment

Headings ventilated without the use of any auxiliary ventilation devices was studied to recognize the need for auxiliary ventilation and find out the effect of the change in LTR velocity on the penetration of air inside a heading. Four heading sizes and three LTR velocities (to cover a range of dimensions and LTR velocities) were used for the simulations as discussed in Chapter 3 - Methodology, Table 3.3. The air penetration depths were assessed using the maximum axial velocity. Maximum air penetration depths were identified for each heading dimension and LTR velocity using a threshold limit of 0.05m/s (considering 0.05 m/s as the minimum measurable limit of velocity). Positive flow rates (flow in) were calculated at different depth planes inside the heading using absolute axial velocities. The variation of the air penetration depths and flow rates with a change in the LTR velocity and the change in the dimension of the headings are discussed in the ensuing paragraphs.

The flow of air for all the cases followed a clockwise flow path as shown in Figure 5.1, which is conformal to the typical case of flow in a cavity. The air entered from the downstream side and joined the LTR air from the upstream side, and the overall flow rate was minimal as compared to the flow rate in the main stream.

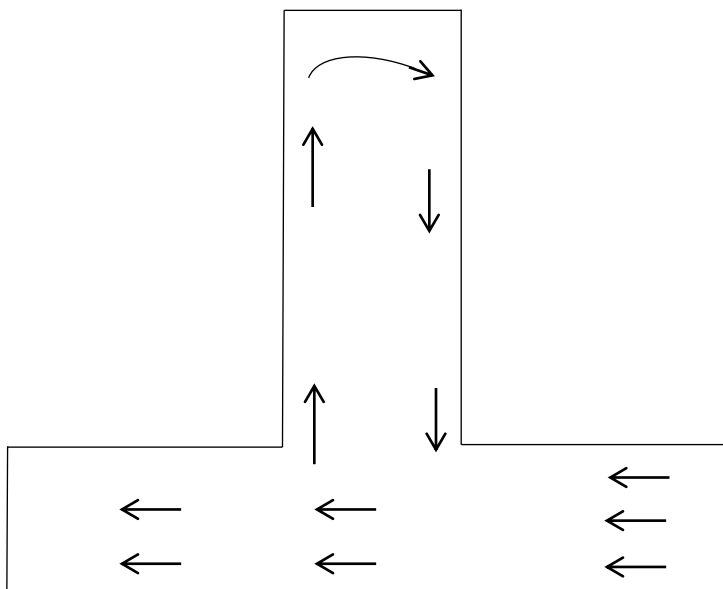


Figure 5.1 Air flow in a heading without the use of any auxiliary equipment

5.2.1 Penetration depth

Tables 5.1 and 5.2 shows the maximum axial velocities (velocity component along the direction of the heading) on planes inside the heading, located at depths of 1m, 5m, and 9.5m for the 10m deep heading and 1m, 5m, 12m, 15m for the 20m deep headings respectively. These velocities were compiled for each LTR velocity i.e. 1m/s, 1.5m/s, and 2m/s.

Table 5.1 Maximum axial velocity at specified planes for 6.6 x 3 x 10m and 6.6 x 4 x 10m headings

| Depth of Plane (m) | LTR velocities (m/s) | | | | | |
|--------------------|--|--------|--------|------------------------|--------|--------|
| | 1m/s | 1.5m/s | 2m/s | 1m/s | 1.5m/s | 2m/s |
| | 6.6 x 3 x 10m heading | | | 6.6 x 4 x 10 m heading | | |
| | Maximum axial velocity at specified planes (m/s) | | | | | |
| 1m | 0.4327 | 0.691 | 0.9321 | 0.4359 | 0.7304 | 0.9375 |
| 5m | 0.3153 | 0.4829 | 0.6871 | 0.3686 | 0.5383 | 0.7225 |
| 9.5m | 0.1288 | 0.1454 | 0.2778 | 0.156 | 0.1647 | 0.2829 |

Table 5.2 Maximum axial velocity at specified planes for 6.6 x 3 x 20m and 6.6 x 4 x 20m headings

| Depth of Plane (m) | LTR velocities (m/s) | | | | | |
|--------------------|--|--------|--------|-----------------------|---------|---------|
| | 1m/s | 1.5m/s | 2m/s | 1m/s | 1.5m/s | 2m/s |
| | 6.6 x 3 x 20m heading | | | 6.6 x 4 x 20m heading | | |
| | Maximum axial velocity at specified planes (m/s) | | | | | |
| 1m | 0.3873 | 0.6988 | 0.9575 | 0.4254 | 0.7181 | 0.9582 |
| 5m | 0.2811 | 0.4716 | 0.7515 | 0.3416 | 0.5193 | 0.7558 |
| 12m | 0.1734 | 0.232 | 0.1826 | 0.1862 | 0.2423 | 0.2022 |
| 15m | 0.06061 | 0.0709 | 0.0279 | 0.05757 | 0.06819 | 0.02273 |

The maximum axial velocities were found to be above the 0.05m/s limit right up till the face of the heading for all the LTR velocities. The maximum axial velocities on the depth planes increased with the increase in the LTR velocity and increased slightly with the increase in the height of the heading.

A similar trend was seen for the 20m depth headings up till the depth of 12m. However, the maximum penetration depth in the range of 15m was achieved and therefore, planes deeper than 15m were not included in Table 5.2. The maximum penetration velocity at

the 15m deep plane was achieved by the 1.5m/s LTR velocity. As seen in (Chapter 4), LTR velocity of 1.35m/s achieved the maximum penetration of 15m with a maximum axial velocity of 0.08572m/s. The penetration depth started decreasing when the LTR velocity of air decreased below 1.35m/s or increased above 1.35m/s.

The maximum axial velocities up till the 12m plane were slightly higher for the 4m high heading than for the 3m high heading similar to the 10m deep heading.

Figures 5.2 and 5.3, shows the variations in maximum axial velocities on the specified planes. The velocities decreased with the depth of the heading. The maximum decrease rate was found for 2 m/s LTR velocity for all the sub cases as shown in these figures.

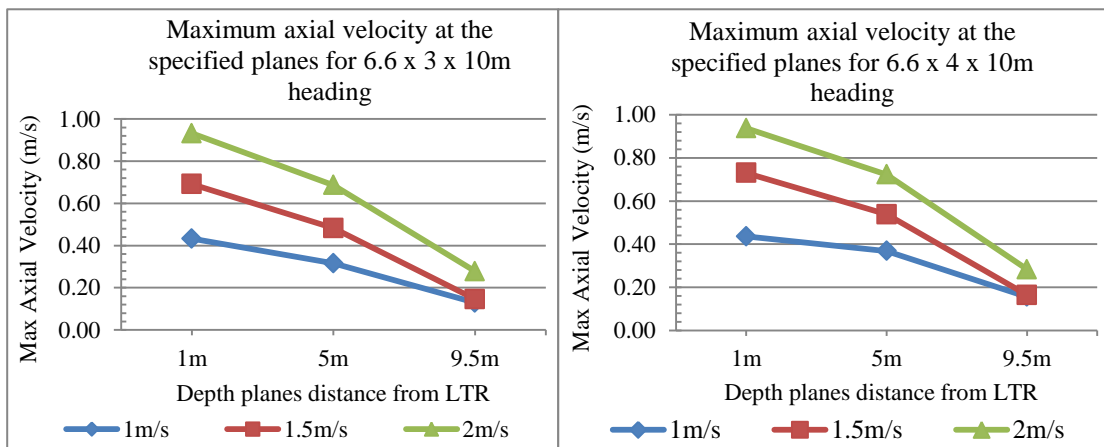


Figure 5.2 Maximum axial velocities at specified planes for 6.6 x 10m heading with 3 and 4m height

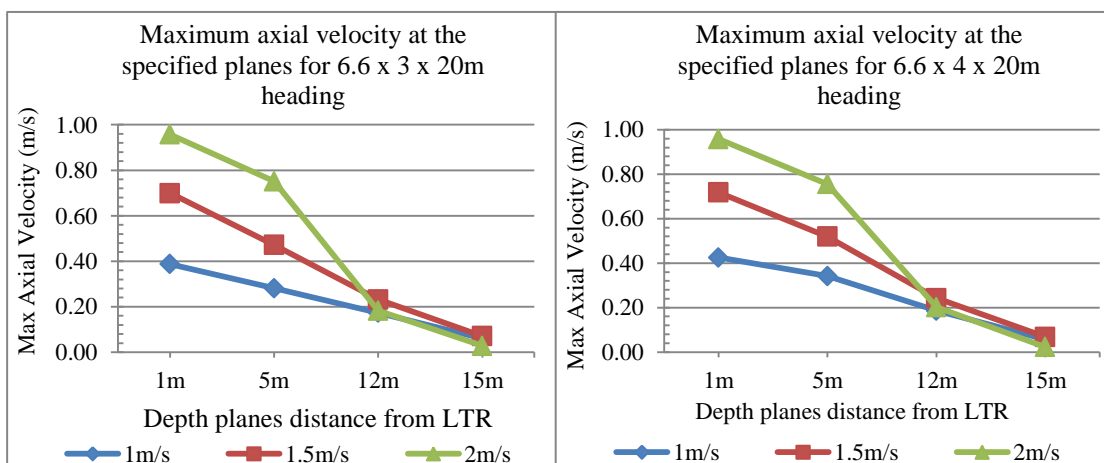


Figure 5.3 Maximum axial velocities at specified planes for 6.6 x 20m heading with 3 and 4m height

Figures 5.4 and 5.5 shows the detailed variation of axial velocity contours for the 10m deep headings on a plane located at the depth of 9.5m for each LTR velocity. Positive velocities indicate inflows and the negative flows are the return air flows. The maximum return axial velocities, like the maximum intake velocities, were also higher for higher LTR velocities. The maximum return airflow velocities like the maximum intake velocities for the 3m high heading were slightly less than the 4m high headings for all LTR velocities.

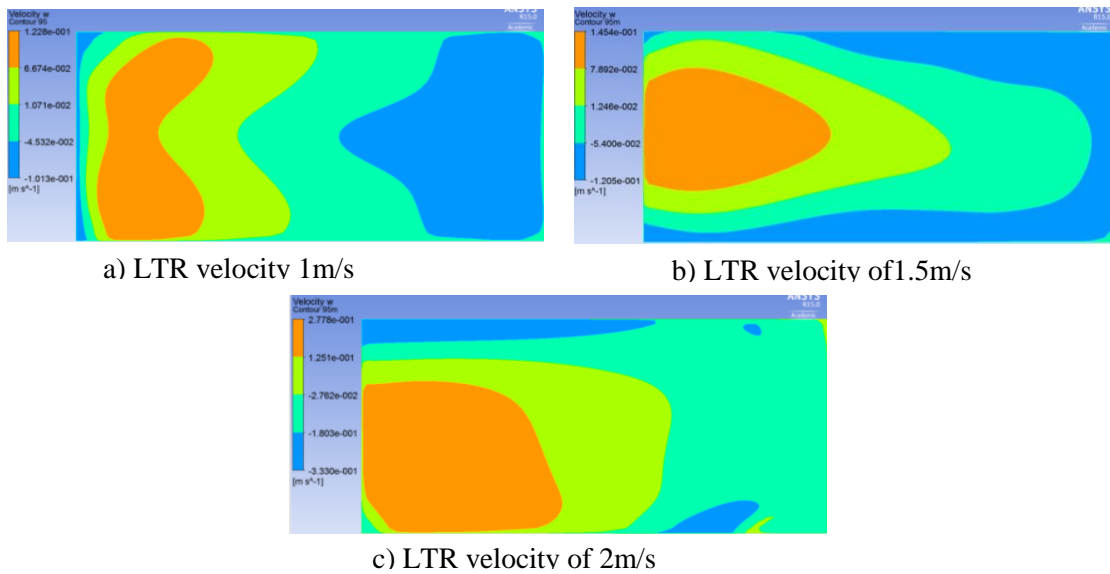


Figure 5.4 Axial velocity contours on 9.5 m deep vertical plane in the 6.6 x 3 x 10 m heading

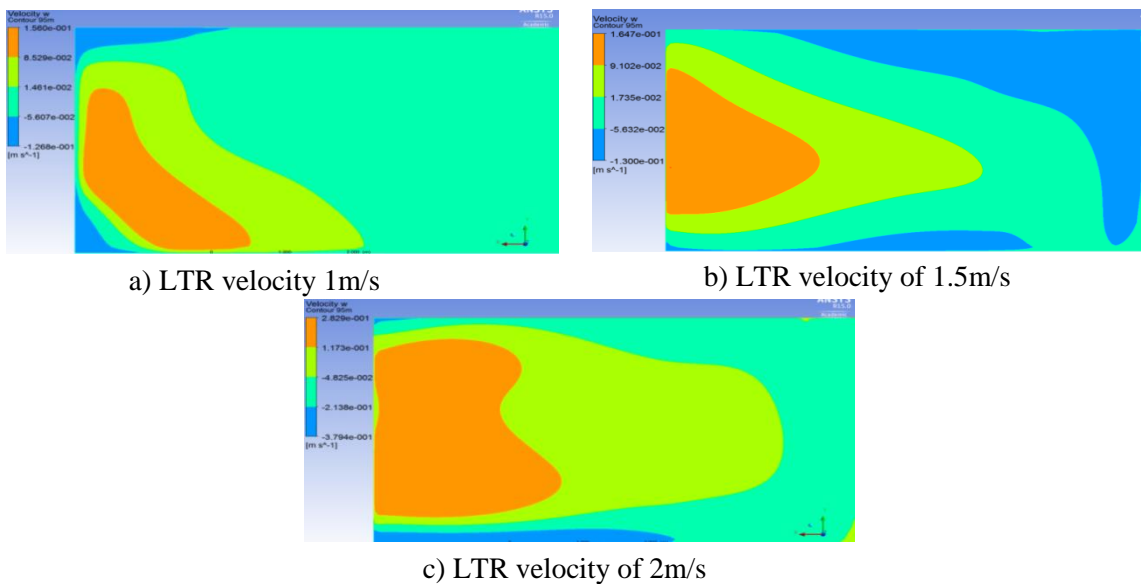


Figure 5.5 Axial velocity contours on 9.5 m deep vertical plane in the 6.6 x 4 x 10 m heading

Figures 5.6 and 5.7 show the detailed variation of axial velocity contours for the 20m deep headings on a plane located at the depth of 15m for each LTR velocity. The maximum return axial velocity for LTR velocity of 2m/s was less than those for 1 and 1.5 LTR velocity for both the 3m and 4m high headings. Therefore, depth had the same effect on the maximum return air velocities as it had on the maximum intake velocities.

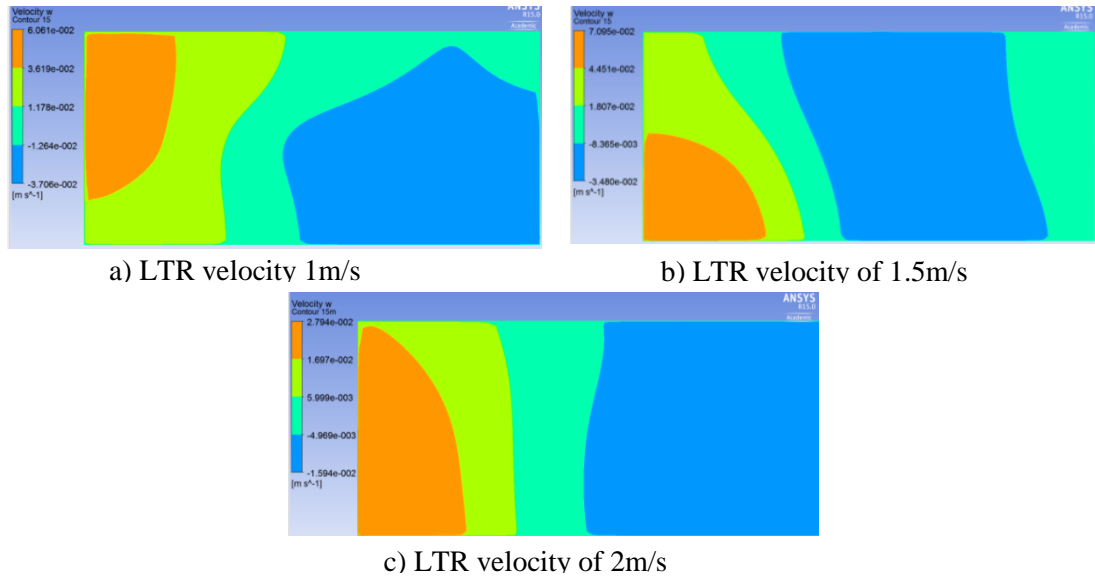


Figure 5.6 Axial velocity contours on 15 m deep vertical plane in the 6.6 x 3 x 20 m heading

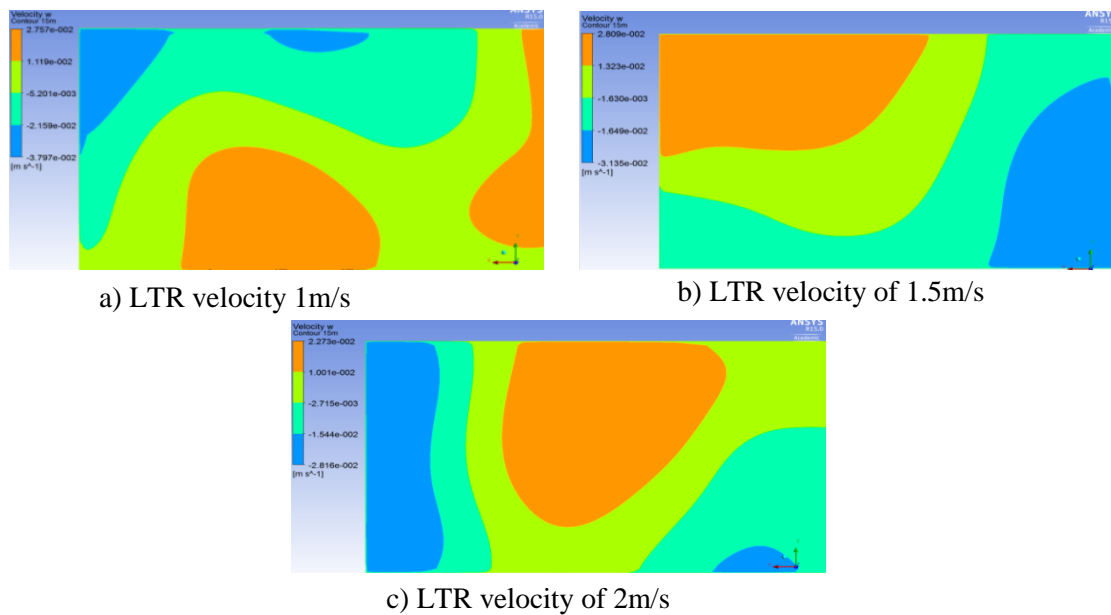


Figure 5.7 Axial velocity contours on 15 m deep vertical plane in the 6.6 x 4 x 20 m heading

5.2.2 Flow rate at specified depth planes

The flow rates at specified planes were calculated to find the effectiveness of the ventilation for each scenario. The average positive flow (flow in) at the specified planes for the 10m and 20m deep headings are given in Tables 5.3 and 5.4 respectively. Figure 5.8 illustrates these flow rates for the 6.6 x 3 x 10m and 6.6 x 4 x 10m headings and Figure 5.9 is showing the flow rates for the 6.6 x 3 x 20m and 6.6 4 x 20m headings.

Table 5.3 Maximum flow rates at specified depth planes for 6.6 x 3 x 10m and 6.6 x 4 x 10m headings

| Depth of plane (m) | LTR velocities (m/s) | | | | | |
|--------------------|---|--------|---------|-----------------------|---------|---------|
| | 1m/s | 1.5m/s | 2m/s | 1m/s | 1.5m/s | 2m/s |
| | 6.6 x 3 x 10m Heading | | | 6.6 x 4 x 10m Heading | | |
| | Maximum axial flow rate at specified depth planes (m ³ /s) | | | | | |
| 1m | 0.5745 | 0.8494 | 1.1298 | 0.87089 | 1.2018 | 1.59994 |
| 5m | 1.0196 | 1.5415 | 2.64569 | 1.52092 | 2.34202 | 3.78567 |
| 9.5m | 0.4572 | 0.6682 | 1.2559 | 0.58358 | 0.75374 | 1.57574 |

Table 5.4 Maximum flow rates at specified depth planes for 6.6 x 3 x 20m and 6.6 x 4 x 20m headings

| Depth of plane (m) | LTR Velocities (m/s) | | | | | |
|--------------------|---|---------|---------|-----------------------|---------|---------|
| | 1m/s | 1.5m/s | 2m/s | 1m/s | 1.5m/s | 2m/s |
| | 6.6 x 3 x 20m Heading | | | 6.6 x 4 x 20m Heading | | |
| | Maximum axial flow rate at specified depth planes (m ³ /s) | | | | | |
| 1m | 0.52216 | 0.91551 | 1.1603 | 0.87952 | 1.22804 | 1.63135 |
| 5m | 0.87828 | 1.55058 | 2.9005 | 1.3792 | 2.42371 | 4.04763 |
| 12m | 0.43951 | 0.63189 | 0.20139 | 0.57296 | 0.84851 | 0.32229 |
| 19.5m | 0.10429 | 0.02414 | 0.02025 | 0.1141 | 0.05506 | 0.04304 |

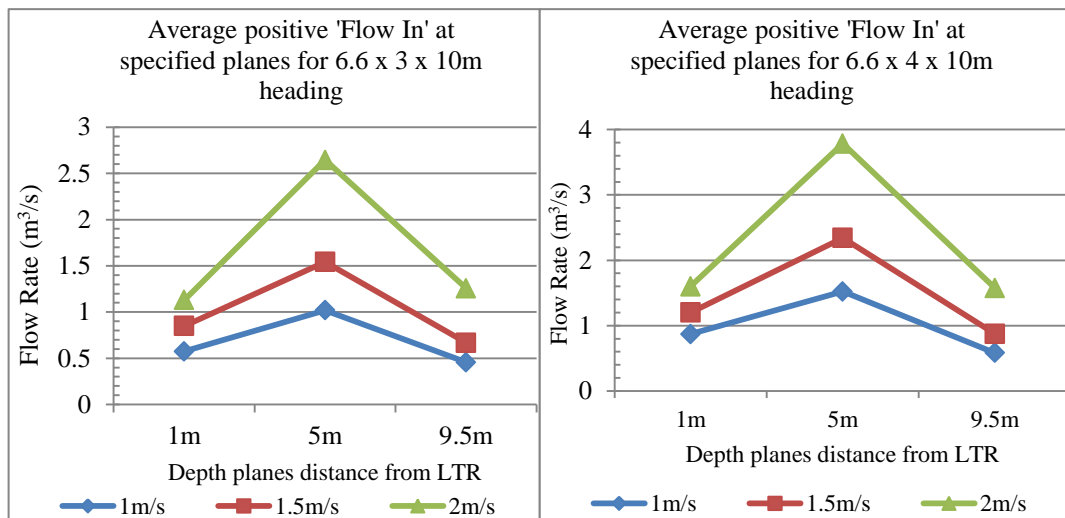


Figure 5.8 Average positive flow rates at specified planes for 6.6 x 10m heading with 3 and 4m height

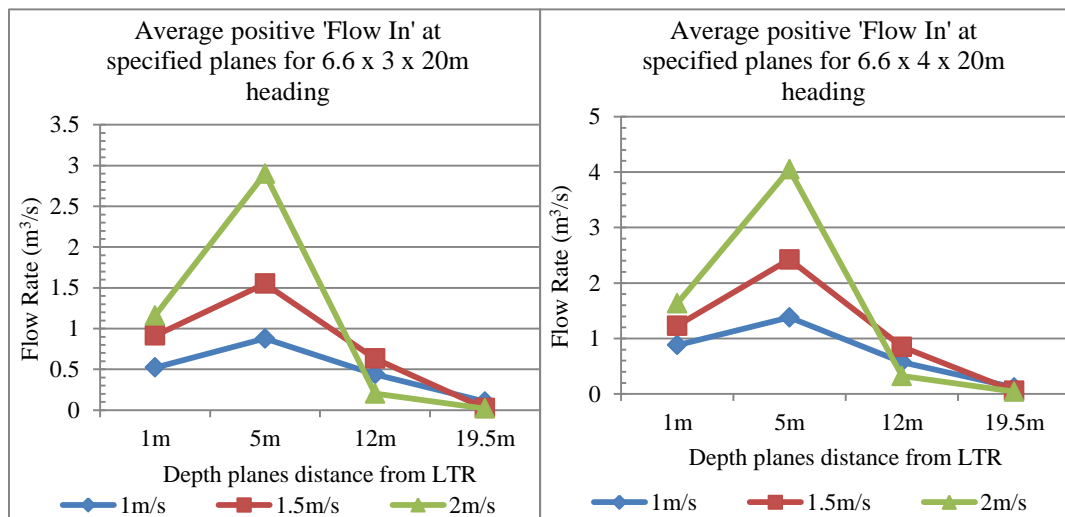


Figure 5.9 Average positive flow rates at specified planes for 6.6 x 20m heading with 3 and 4m height

The flow rates were very low as compared to the air flow in the LTR, and most of the air continued going straight in the LTR. The air flow rates for the 4m high headings were higher than the 3m headings, because the inlet areas were bigger. Maximum flow rates took place around the 5m depth where the recirculation was the highest, after which there was a sharp decrease in air flows.

In the 10m deep headings flow rates increased with the increase in the LTR velocity and higher flow rates were observed for the higher LTR velocities at each depth plane up till

the face of the heading. Once again maximum flow rates were observed for the 2m/s LTR velocity. The sharp decline after the 5m plane also increased with the increase in the LTR velocity and maximum decline was observed for the 2m/s LTR velocity, but the air flow near the face still stayed higher for the 2m/s LTR velocity. However, for the 20m deep headings the flow rate at the face of the heading with the 2m/s LTR velocity was less than the lower LTR velocities, because most of the air returned before reaching the 12m plane. The air flow after the depth of 12m, called the secondary flow was very negligible for all the cases and occurs only because of the local circulation of air. This was found to be the highest for the lowest LTR velocity of 1m/s between the 15m and the 19.5m plane, consequently the maximum flow rate (although negligible) was achieved with this velocity in that region. Considering the flow rates of $0.76674\text{m}^3/\text{s}$ for the LTR velocity of 1.35m/s given in Chapter 4, Table 4.2, at the 12m plane, it was concluded that flow rates at and after the 12m plane reduced with the increase or decrease in the LTR velocity from 1.35m/s similar to the experimental results (Meyer, 1989).

From the tabulated data for the 10m headings it was found that velocities and thus the airflows were higher for higher LTR velocities. The recirculation occurred between the 1m and 9.5m deep plane causing a rise in airflow through the 5m deep plane. For the 20m heading most of the air turned back from the 12m deep plane for all LTR velocities, the recirculation therefore, occurred between the 1m and the 12m plane causing a rise in airflow through the 5m deep plane.

5.3 Conclusion

The results for the 10m and 20m deep headings showed that the maximum axial velocities and flow rates increased with the increase in the LTR velocity up to the depth of 10m. Maximum flow rates were observed at the depth of 5m which identifies the occurrence of maximum recirculation. After which there was a sharp decline in the flow rates. At depths greater than 10m both the maximum axial velocities and the flow rates were very low, but they were the highest for the LTR velocity of 1.35m/s. Therefore, the highest penetration depth (based on the maximum axial velocity) was achieved by the 1.35m/s LTR velocity and the penetration decreased with the increase or decrease in

velocity from the 1.35m/s velocity (keeping in mind the results given in Chapter 4). Similar trends were followed by the flow rates as well, although they became too low to be meaningful as far as the ventilation of the heading is concerned after the 10m depth. Therefore, headings longer than 10m should never be ventilated without the use of auxiliary ventilation devices for any LTR velocity. Even the ventilation of a 10m long heading using a LTR velocity of 2m/s would give a maximum flow rate (air going into the heading) of around 1.2559 m³/s and 1.57574 m³/s for the 3 and 4m high headings respectively.

In the next chapter, the influence of the system variables associated with the LB ventilation system is discussed. Mathematical models to estimate the air flow rate at the exit of the LB and close to the face of the heading using comparative study, encompassing the effect

6 ANALYSIS AND DISCUSSION - VENTILATION OF HEADINGS WITH THE USE OF LINE BRATTICE

6.1 General

A total of 288 scenarios were simulated and studied in Case B as discussed in Chapter 3, Table 3.5, to visualize the effects of the change of LTR velocity, and the change of configuration of LB for different dimensions of the headings. A force ventilation system was studied with the LB used on the upstream side. The air therefore, followed a counter clockwise flow inside the heading, entering from the upstream side through the channel between the LB and the wall and joining the main stream at the downstream side as shown in Figure 6.1.

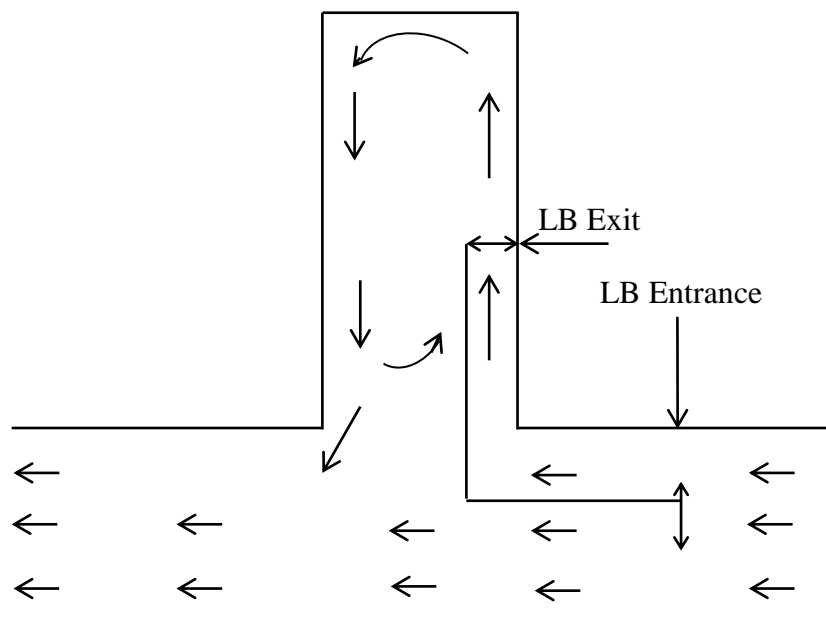


Figure 6.1 Air flow inside a heading using LB

The system variables used to study the LB ventilation system are the heading dimension, LB settings and the LTR velocity. Each possible combination of these variables were studied, resulting in a total of 96 cases for each LTR velocity (combined cases for all LTR velocities were 288). To carry out the analysis, these cases were organized in such a way that there are four groups based on the dimensions of the heading, and in each group there are a total of 24 base cases. These cases were named

using the syntax, case number - width of heading - height of heading - length of heading - length of LB inside the heading - length of LB in the LTR - distance of LB from wall in the heading - angle of LB in the LTR. So 1-6.6-3-10-Half-3-0.5-0, means case number 1, the dimensions of the heading are 6.6 x 3 x 10 (W x H x D), the length of the LB inside the heading is half the size of the heading, the length of the LB in the LTR is 3m, the distance of LB from the wall in the heading is 0.5m and the angle of the LB in the LTR is 0°. The system variables were changed within each group in the same sequence, the numerical and complete names of group 1 are given in Table 1 (The complete list is given in Table A1). Therefore, sets of cases became available within each group and amongst groups as well. In each set, except for one system variable, all the others are same for all the cases of a set. This helped in undertaking comparative analyses and calculating the exact effect of each system variable. The sets of cases formed in this study for each system variable are given in Table 6.2.

Table 6.1 Complete and numerical names for the cases of group 1

| Complete names | Numerical name | Complete names | Numerical name |
|---------------------------|----------------|-----------------------------------|----------------|
| 1-6.6-3-10-Half-3-0.5-0 | 1 | 13-6.6-3-10-threebyfour-3-0.5-0 | 13 |
| 2-6.6-3-10-Half-3-1-0 | 2 | 14-6.6-3-10-threebyfour-3-1-0 | 14 |
| 3-6.6-3-10-Half-6-0.5-0 | 3 | 15-6.6-3-10-threebyfour-6-0.5-0 | 15 |
| 4-6.6-3-10-Half-6-1-0 | 4 | 16-6.6-3-10-threebyfour-6-1-0 | 16 |
| 5-6.6-3-10-Half-3-0.5-7.5 | 5 | 17-6.6-3-10-threebyfour-3-0.5-7.5 | 17 |
| 6-6.6-3-10-Half-3-1-7.5 | 6 | 18-6.6-3-10-threebyfour-3-1-7.5 | 18 |
| 7-6.6-3-10-Half-6-0.5-7.5 | 7 | 19-6.6-3-10-threebyfour-6-0.5-7.5 | 19 |
| 8-6.6-3-10-Half-6-1-7.5 | 8 | 20-6.6-3-10-threebyfour-6-1-7.5 | 20 |
| 9-6.6-3-10-Half-3-0.5-15 | 9 | 21-6.6-3-10-threebyfour-3-0.5-15 | 21 |
| 10-6.6-3-10-Half-3-1-15 | 10 | 22-6.6-3-10-threebyfour-3-1-15 | 22 |
| 11-6.6-3-10-Half-6-0.5-15 | 11 | 23-6.6-3-10-threebyfour-6-0.5-15 | 23 |
| 12-6.6-3-10-Half-6-1-15 | 12 | 24-6.6-3-10-threebyfour-6-1-15 | 24 |

Table 6.2 Set of cases formed for Case B

| System variables | Set of cases | | | | System variable settings used |
|-----------------------------|--|--|--|--|--|
| | Group 1 6.6 x 3 x 10 | Group 2 6.6 x 3 x 20 | Group 3 6.6 x 4 x 10 | Group 4 6.6 x 4 x 20 | |
| Length of LB in the heading | 1 vs 3, 2 vs4,...12-24 | 25 vs 37, 26 vs38,36vs48 | 49 vs 61, 50 vs 62,...60 vs 72 | 73 vs 85, 74 vs 86,... 84 vs 96 | Length of LB in short heading = 5 and 7.5m and long heading 10 and 15m |
| Distance of LB from face | 1 vs 3, 2vs4,...12-24 | 25 vs 37, 26 vs38.... 36-48 | 49 vs 61, 50 vs 62,... 60 vs 72 | 73 vs 85, 74 vs 86,... 84 vs 96 | Distance of LB in short heading = 2.5 and 5m and in long heading 5 and 10m |
| LB distance from wall | 1 vs 2, 3 vs4,23 vs 24 | 25 vs 26, 27 vs28,.....35 vs 36 | 49 vs 50, 51 vs 52,.....71 vs 72 | 73 vs 74, 75 vs76,.....95 vs 96 | 0.5m and 1m distance used |
| Length of LB in LTR | 1 vs 3, 2vs 4,22 vs 24 | 25 vs 27, 26 vs28,34 vs 36 | 49 vs 51, 52 vs54,70 vs 72 | 73 vs 75, 74 vs76,94vs96 | 3m and 6m used |
| Angle of LB in LTR | 1 vs 5 vs 9, 2 vs 6 vs10,.....16 vs 20 vs 24 | 25 vs 29 vs 33, 26 vs 30 vs34,40 vs 44 vs 48 | 48 vs 53 vs 57, 49 vs 54 vs50,64 vs 68 vs 72 | 73 vs 77 vs 81, 74 vs 78 vs82,88 vs 92 vs 96 | 0°, 7.5°, and 15° |
| LTR air velocity | 1vs1, 2vs2,24vs24 | 25vs25, 26vs26,48vs48 | 49vs49, 50vs50,72vs72 | 73vs73, 74vs74,96vs96 | 1m/s, 1.5m/s and 2m/s (each case was run with 3 LTR velocities, creating 3 sets of 2 cases each) |
| Heading height | 1 vs 49, 2 vs 50...24 vs 48 and 25 vs 73, 26 vs 74,....48 vs 96, group 1 and group 2 were run with 3m high heading and group 3 and 4 were run with 4m high heading | | | | |

A comparative study, based on the air flow rates going into the heading at different depths inside the heading using depth planes, was carried out to find the effect of each system variable, related to the installation of LB, heading dimension, and the velocity of air in the LTR. The air flow rates at different depth planes were calculated using only the amount of air going into the heading (the total air going through a plane was divided by 2 assuming the amount of air going in is coming out as well). The air flow rate at the exit of the LB was calculated using the total amount of air moving through the plane at the exit of LB (channel between LB and wall of the heading). Mathematical models to estimate the effect of these system variables were created which could be used to calculate flow rates at the exit of the LB and at the face of the heading. The analysis has been divided into four major components; first component encompasses the mathematical model to estimate flow rates at the exit of the LB, second component dilates the comparison of flow rates inside the heading with the change in LB settings, third component highlights the mathematical model to estimate flow rates close to the face of the heading and the fourth component shows the distinct air flow features of LB ventilation system. The summary of the discussion following ahead is given in Figure 6.2.

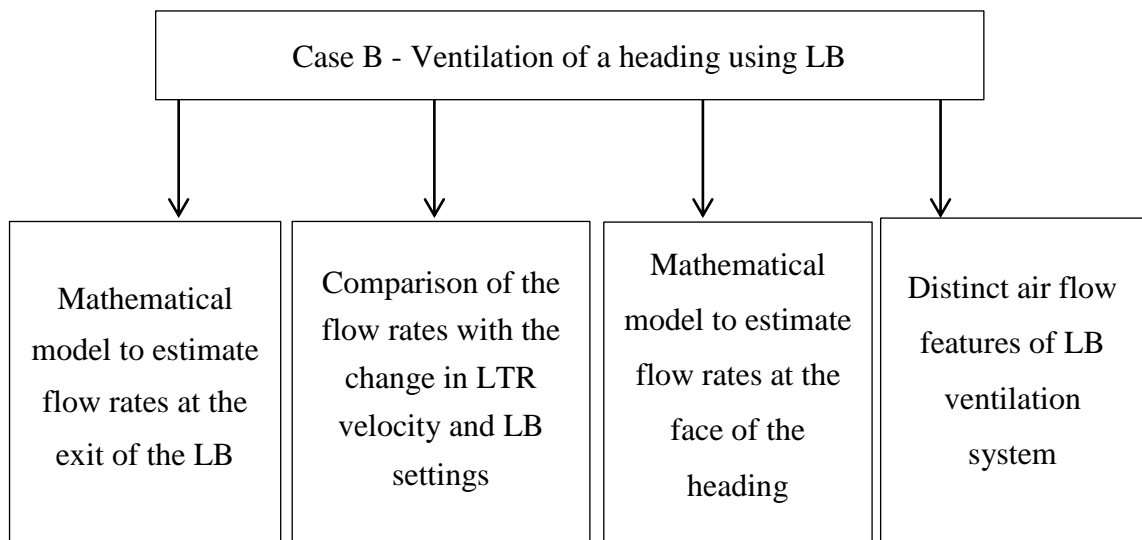


Figure 6.2 Components of analysis for Case B - Ventilation of a heading using LB

Components of the analysis for Case B - Ventilation of a heading using LB

- Mathematical models to calculate the effect of studied system variables on the flow rates at the exit of the LB.

- Area calculation at the inlet of the LB in the LTR.
- Flow rates at the exit of the LB in the heading.
- Mathematical conditions to use the model for all heading dimensions, LTR velocities and LB settings.
- General equation to estimate the flow rates at the exit of the LB.
- Comparison of air flows, with the change in LTR velocity and LB settings
 - Comparison of the “effects of change of LTR velocity”.
 - Comparison of the “effects of change of length of LB inside the heading”, for each LTR velocity.
 - Comparison of the “effects of change of length of LB inside the LTR”, for each LTR velocity.
 - Comparison of the “effects of change of the distance of LB from the wall in the heading”, for each LTR velocity.
 - Comparison of the “change of the angle of LB inside the LTR”, for each LTR velocity.
- Mathematical models to estimate the effect of studied system variables on the flow rates at the face of the heading (0.5m from face).
 - Flow rate estimation at the face of the heading.
 - Formulation of mathematical conditions to use the mathematical model for all heading dimensions, LTR velocities and LB settings.
- Distinct air flow features of LB ventilation system
 - Dead zones/low velocity regions

6.2 Mathematical Model to Estimate Flow Rates at the Exit of the LB

The air moving in the LTR was channelled into the heading using the LB. The quantity of the air exiting the LB besides other factors affected the ventilation of the heading, therefore, the first goal was to find out, how this flow rate changes, and how to estimate this flow rate incorporating all the factors?

6.2.1 Area Calculation at the Inlet of LB

The system variables associated with the installation of the LB are shown in Figure 6.3. It can be seen that, the distance of the LB from the wall in the heading, the length of the

LB in the LTR, and the angle of the LB in the LTR, changed the overall distance of the LB from the wall inside the LTR (called the entrance length). The change of the entrance length changed the inlet area at the entrance of the LB in the LTR. This change in the entrance length and area affected the quantity of air exiting the LB into the heading. The entrance lengths and entrance areas for each configuration of the LB, calculated using equations 6.1 and 6.2 are given in Table 6.3.

$$e = (\tan \theta) \times (c+b) \quad (\text{note: 'e' remains same for 3m and 4m high heading}) \quad (6.1)$$

$$\text{LB Inlet Area} = X \times \text{HH} \quad (6.2)$$

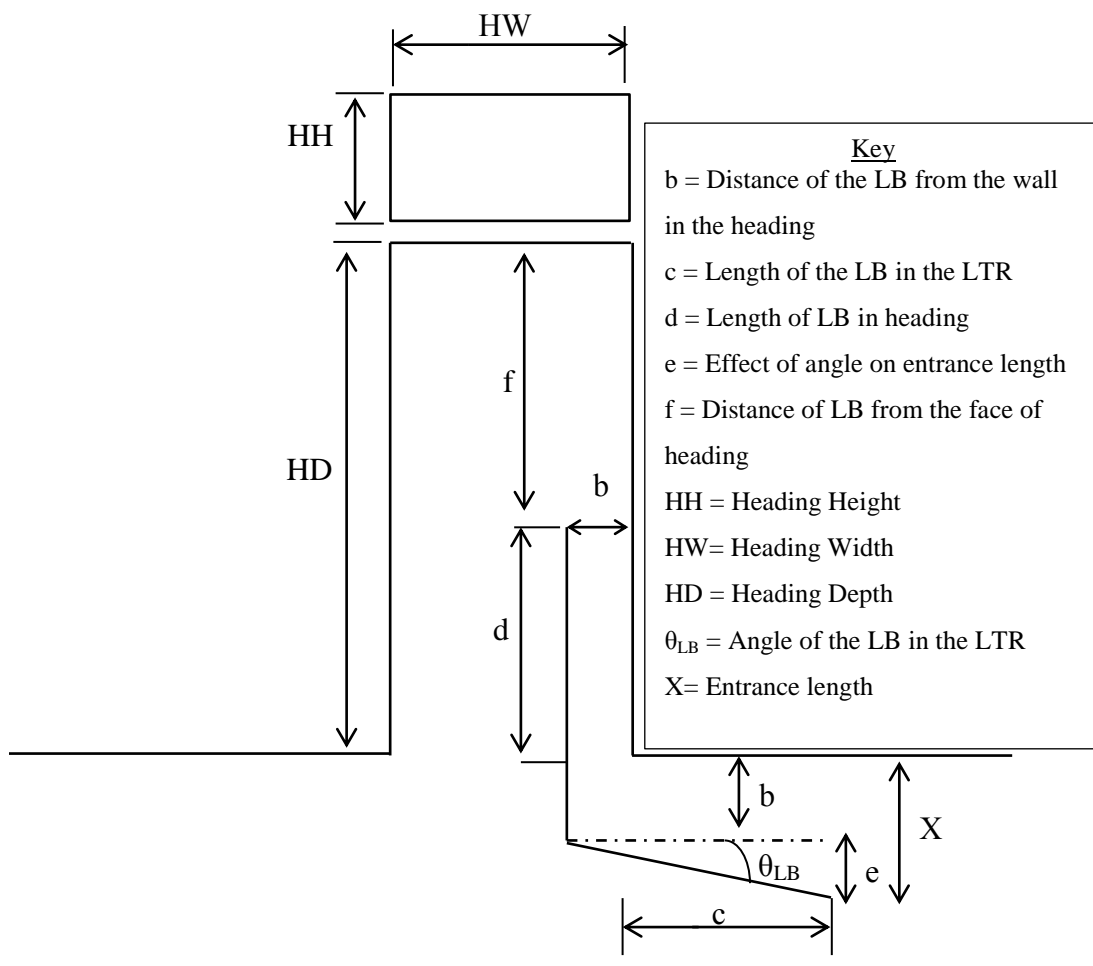


Figure 6.3 LB setting variables

Table 6.3 LB inlet areas for all heading dimensions

| LB inlet areas for heading height of 3m | | | | | | | | | | | |
|---|--------------|---------------|------------|----------------------|---------------|---------------|----------------|---------------------|----------------|---------------|----------------|
| (m ²) | | | | | | | | | | | |
| $\theta = 0^\circ$ | | | | $\theta = 7.5^\circ$ | | | | $\theta = 15^\circ$ | | | |
| b = 0.5 | | b = 1 | | b = 0.5 | | b = 1 | | b = 0.5 | | b = 1 | |
| (m) | | (m) | | (m) | | (m) | | (m) | | (m) | |
| c = 3 | c = 6 | $\frac{c}{3}$ | c = 6 | c = 3 | c = 6 | c = 3 | c = 6 | c = 3 | c = 6 | c = 3 | c = 6 |
| (m) | (m) | (m) | (m) | (m) | (m) | (m) | (m) | (m) | (m) | (m) | (m) |
| X=0.5 (m) | X=0.5 (m) | X=1 (m) | X=1 (m) | X=0.96 (m) | X=1.36 (m) | X=1.52 (m) | X=1.921 (m) | X=1.437 (m) | X=2.416 (m) | X=2.07 (m) | X=2.875 (m) |
| 1.5 | 1.5 | 3 | 3 | 2.88 | 4.07 | 4.58 | 5.76 | 4.31 | 6.73 | 6.22 | 8.63 |
| LB inlet areas for heading height of 4m | | | | | | | | | | | |
| (m ²) | | | | | | | | | | | |
| $\theta = 0^\circ$ | | | | $\theta = 7.5^\circ$ | | | | $\theta = 15^\circ$ | | | |
| b = 0.5 | | b = 1 | | b = 0.5 | | b = 1 | | b = 0.5 | | b = 1 | |
| (m) | | (m) | | (m) | | (m) | | (m) | | (m) | |
| c = 3 | c = 6 | c = 3 | c = 6 | c = 3 | c = 6 | c = 3 | c = 6 | c = 3 | c = 6 | c = 3 | c = 6 |
| (m) | (m) | (m) | (m) | (m) | (m) | (m) | (m) | (m) | (m) | (m) | (m) |
| 2 | 2 | 4 | 4 | 3.84 | 5.42 | 6.11 | 7.69 | 5.75 | 8.97 | 8.29 | 11.5 |

6.2.2 Flow rates at exit of LB in the headings

The flow rates measured at the exit of the LB for all the cases are given in Table B1. A number of factors besides the LTR velocity, and the height of the heading affected these flow rates by inducing the viscous affects which are given below:

- The length of the LB in the LTR and the heading.
- Angle of the LB in the LTR; the entrance length of the LB.
- Distance of the LB from the wall in the heading, dictates the reduction in area between the LB and the wall; bigger area at the entrance of the LB vs the area inside the heading when angled LB is used.

To develop an initial mathematical model, the flow rates measured for the first twelve cases (6.6 x 3 x 3m heading with 5m long LB in the heading) simulated with LTR velocity of 1m/s were analysed (for easy referencing called the standard cases in this research). This model was then refined by considering the effect of the system variables highlighted above on all the cases. In order to find how the flow rates at the exit of the LB changes with the change in the system variables of LB ventilation system, the air

flow rates measured at the exit of the LB for the standard cases were arranged in an ascending order, against different combinations of the involved parameters. After a lot of deliberation it was found that these flow rates are proportional, to the product of the entrance length, and the distance of the LB from the wall in the heading, as given in Table 6.4 and Figure 6.4. The product of entrance length and distance of the LB from the wall is the same for cases, where, LB was used with zero angles and same wall distance (same for Case 1 and 3 and 2 and 4). Therefore, out of the first four cases only Case 1 and 2 were used in the initial mathematical model.

The expression for this trend line is given in equation 6.3. This equation can only be used to estimate the flow rates at the exit of the LB for the 10 standard cases used to develop this equation. However, to use equation 6.3 for all other scenarios encompassed within the boundaries of this study, additional conditions were determined. This was done after deliberating upon the effects of the change in LTR velocity, height of the heading, length of the LB in the heading, and change in length of the LB in the LTR when it was used with zero angle.

Table 6.4 Flow rates at LB exit vs product of LB entrance length and distance from wall

| Cases | Entrance length (X) (m) | Distance from wall (b) (m) | X x b (m ²) | Flow rates (m ³ /s) |
|-------|-------------------------------|----------------------------------|----------------------------|-----------------------------------|
| 1 | 0.500 | 0.5 | 0.250 | 0.944 |
| 5 | 0.960 | 0.5 | 0.480 | 1.230 |
| 7 | 1.356 | 0.5 | 0.678 | 1.539 |
| 9 | 1.438 | 0.5 | 0.719 | 1.587 |
| 2 | 1.000 | 1 | 1.000 | 2.032 |
| 11 | 2.416 | 0.5 | 1.208 | 2.269 |
| 6 | 1.520 | 1 | 1.520 | 2.596 |
| 8 | 1.921 | 1 | 1.921 | 3.084 |
| 10 | 2.070 | 1 | 2.070 | 3.289 |
| 12 | 2.876 | 1 | 2.876 | 4.393 |

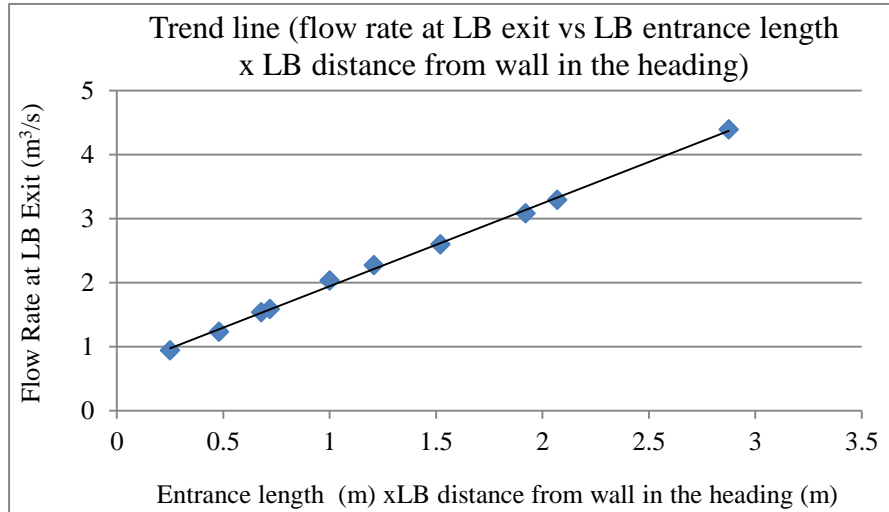


Figure 6.4 Trend line of flow rate at LB exit

$$\text{Flow rate at the exit of LB} = \text{FRE}_{\text{LB}} = 1.27 \times X \times b + 0.65 \quad (6.3)$$

6.2.2.1 Effect of the change in LTR velocity

The percentage increase in the flow rates at the exit of the LB with the increase in LTR velocity are given in Tables C1 through C4 for each heading dimension. The percentage differences in the LTR velocities are given in equations 6.4 through 6.6. The results showed that the average percentage increase in the flow rates at the exit of the LB with the increase in LTR velocity, for all the headings, was approximately equal to the corresponding percentage increase in the LTR velocities (maximum average difference of 1.2%).

$$\text{Percentage Increase 1-1.5 m/s} = ((1.5-1)/1) \times 100 = 50\% \quad (6.4)$$

$$\text{Percentage Increase 1-2 m/s} = ((2-1)/1) \times 100 = 100\% \quad (6.5)$$

$$\text{Percentage Increase 1.5-2 m/s} = ((2-1.5)/1.5) \times 100 = 33.33\% \quad (6.6)$$

6.2.2.2 Effect of the change in height of the heading

The percentage increase in the flow rates at exit of the LB, with the increase in the height of the heading, i.e. 6.6 x 3 x 10m vs 6.6 x 4 x 10m and 6.6 x 3 x 20m vs 6.6 x 4 x 20m are given in Tables D1 and D2. The percentage increase in the areas of the headings, with the change in the height of the heading from 3 - 4m is given in equation 6.7. The results showed that the average percentage increase in flow rates was

approximately equal to the corresponding percentage increase in the height of the heading (maximum average difference of 1.2%).

$$\text{Percentage Increase 3- 4 m} = ((4-3)/3) \times 100 = 33\% \quad (6.7)$$

6.2.2.3 Effect of the change in length of the LB in the LTR

The effect of the change in length of the LB in the LTR for LB used with an angle is already catered for in equation 6.3 by using the product of entrance length and distance of LB from the wall in the heading. However, when the LB was used without an angle, the product of entrance length and the distance of the LB from the wall stayed the same for cases with the same LB to wall distance, even with different LB lengths in the LTR. To cater for this, the percentage differences in flow rates at the exit of the LB for cases when the LB is used with zero angles were analysed. In the first twelve cases there are two cases each using 3m (Cases 1 and 2) and 6m (Cases 3 and 4) lengths of LB in the LTR. Two set of cases were formed from these four cases, Set 1 with Cases 1 and 3 and Set 2 with Cases 2 and 4. In the cases of both the sets, except for the length of LB in the heading, all the other settings are the same. The difference in flow rates for the cases in each set are given in Table 6.5. The results showed that with the increase in length of the LB in the LTR, the flow rate at the exit of the LB, decreased on average at the rate of approximately 1% per 2m increase in the length. Similarly, for all such sets of cases in the study, this difference on average was found to be around 1.5%.

Table 6.5 Percentage decrease in flow rate at the exit of LB for each LTR velocity with the increase in length of LB from 3 to 6m in the LTR for zero angled LB

| Cases | LTR velocity | | |
|------------------------------------|---|--------|-------------|
| | 1m/s | 1.5m/s | 2m/s |
| | Percentage decrease in flow rate at the exit of LB for each LTR velocity with the increase in length of LB from 3 to 6m in the LTR(%) | | |
| 1-3 | 1.43 | 1.49 | 1.36 |
| 2-4 | 1.48 | 1.5 | 1.59 |
| Average percentage decrease | | | 1.47 |

6.2.2.4 Effect of the change in length of the LB in the heading

Lengths of 5m and 7.5m were used in the 10m long heading and lengths of 10m and 15m were used in the 20m long heading. Equation 6.3 was developed for the standard cases (10m long heading with 5m long LB). The results showed that the flow rates at the exit of the LB changed with the change in the length of the LB in the heading. To quantify this change, cases with different lengths of LB in the heading and similar remaining configurations and dimensions were compared. The length of the LB inside the heading for the standard cases (1-12) is 5m and for the next twelve cases (13-24) in group 1 is 7.5m. The cases were grouped into twelve sets, where in each set all the configurations except for the length of the LB in the heading are the same (1-13, 2-14.....12-24). The percentage difference in flow rates at the exit of the LB between the cases in each set are given in Table 6.6. The results showed that with the increase in length of the LB, the flow rate at the exit of the LB decreased, on average, at the rate of approximately 1% per 2m increase in length of the LB. The average difference for all such sets of cases studied was also found to be equal to around 1% per 2m increase in length of the LB.

Table 6.6 Percentage decrease in flow rate at the exit of LB for each LTR velocity with the increase in length of LB from 5 to 7.5m for the 10m deep and 3m high heading

| Cases | LTR velocity | | |
|------------------------------------|---|-------------|-------------|
| | 1m/s | 1.5m/s | 2m/s |
| | Percentage decrease in flow rate for each LTR velocity with the increase in length of LB from 5 to 7.5m (%) | | |
| 1-13 | 1.31 | 1.23 | 1.45 |
| 2-14 | 1.31 | 1.51 | 1.67 |
| 3-15 | 1.29 | 1.47 | 1.34 |
| 4-16 | 1.58 | 1.48 | 1.43 |
| 5-17 | 1.3 | 1.35 | 1.41 |
| 6-18 | 1.39 | 1.38 | 1.38 |
| 7-19 | 1.2 | 1.33 | 1.18 |
| 8-20 | 1.36 | 1.22 | 1.31 |
| 9-21 | 1.29 | 1.33 | 1.3 |
| 10-22 | 1.28 | 1.35 | 1.3 |
| 11-23 | 1.29 | 1.31 | 1.3 |
| 12-24 | 1.29 | 1.29 | 1.28 |
| Average percentage decrease | 1.32 | 1.35 | 1.36 |

6.2.2.5 Conditions to use this equation for any heading dimension

Keeping in view the discussion given in section 6.2.2.1 to 6.2.2.4, the following conclusions can be drawn from the use of equation 6.3 to estimate the flow rate at the exit of the LB for the rest of the cases and for any other case falling within the boundaries of the studied cases.

- **Velocity**

Equation 6.3 is for LTR velocity of 1m/s: for higher or lower LTR velocities, increase/decrease the flow rate to the proportional increase or decrease in the LTR velocity.

- **Heading height**

Equation 6.3 is for heading height of 3m: increase/decreases the flow rate proportional to the percentage increase or decrease in height of the heading (compared to 3m).

- **Length of LB in LTR and distance from the wall in the heading**

- **LB at an angle in LTR**

The effect of the change in length of the LB in the LTR for angled LB is already catered for in equation 6.3 by using the product of the entrance length and distance from wall of the LB.

- **LB without an angle in LTR**

Equation 6.3 was designed for the LB length of 3m in the LTR. The viscous effect changes with the change in this length. Therefore, the estimated flow rate change is 1% increase/decrease per 2m decrease/increase in the length of the LB in the LTR respectively (using the reference length of 3m).

- **Length of LB in the heading**

Equation 6.3 is for LB length of 5m in the heading, for different lengths the estimated flow rate change is 1% increase/decrease per 2m decrease/increase in the length of the LB in the heading respectively (using the reference length of 5m).

6.2.2.6 Example case

Find flow rate for a case with LB angle of 6°, LB length in LTR of 6m, LB length in heading of 6m, LB distance from wall in the heading of 0.6m, LTR velocity of 1.4m/s and heading height of 3.5m.

Solution:

$$\text{Entrance length} = X = 0.6 + (\tan 6) \times (0.6+6) = 1.2936\text{m}$$

$$\text{Entrance length} \times \text{wall distance} = 1.2936 \times 0.6 = 0.7762$$

So flow rate = $(1.27 \times X) + 0.65 = 1.27 \times 0.7762 + 0.65 = 1.6357\text{m}^3/\text{s}$ (but this is for 3m high heading, with LB length of 5m in the heading and 1m/s LTR velocity)

$$\text{Heading height change} = ((3.5 - 3) / 3) \times 100 = 16.666\%$$

$$\text{Velocity change} = ((1.4 - 1)/1) \times 100 = 40\%$$

LB length in heading = $-(6 - 5) \times 1/2$ (1% reduction per 2m increase in length, negative sign since length has increased) = - 0.5%

$$\text{So net change is } 16.6666 + 40 - 0.5 = 56.16\%$$

$$\text{Flow rate at the exit of the LB is therefore} = 1.6357 + 1.6357 \times 0.5616 = 2.554\text{m}^3/\text{s}.$$

6.2.2.7 Generalised equation

Given the conditions above a generalised equation to estimate the flow rates at the exit of the LB was developed and can be written as equation 6.8. All the conditions given in section 6.2.2.5 were incorporated in this equation (6.8).

$$\text{Flow rate at the exit of the LB} = \text{FRE}_{\text{LB}} = [(1.27 \times (X \times b)) + 0.65] \times [1 + ((\text{LTR Vel} - 1)) + ((\text{HH} - 3)/3) - ((d - 5)/(2 \times 100)) - \underbrace{((c - 3)/(2 \times 100))}] \quad (6.8)$$

Use only when LB used
with zero degree in LTR

Where,

X = LB entrance length

b = Distance of the LB from the wall in the heading

c = Length of the LB in the LTR

d = Length of LB in the heading

HH = Heading height

LTR Vel = Velocity of air in the LTR

6.2.3 Conclusion

The effect of various system variables related to the installation of the LB, along with the effect of LTR velocity, and heading height and depth, on the flow rates at the exit of the LB, were estimated. These estimations have been represented in a user-friendly mathematical forms. A model to estimate the consolidated effect of all the studied system variables has also been formulated, by summing the individual effects. This was represented in equation 6.8 and could be used to estimate the flow rates at the exit of the LB for different, settings of the LB, LTR velocities and heading heights. The actual mining environment is not perfect so while using this estimation model a reduction factor may be used depending upon the quality of installed LB to cater for the leakage to get an acceptable estimation.

In the next section, the effect of change in LTR velocity on the flow rates inside the heading is analysed and discussed.

6.3 Comparison of Air Flows, with the Change in LTR Velocity

The effect of the LTR velocity on the flow rates inside the heading is discussed using the flow rate calculated at planes parallel to the face of the heading located at depths of 1m, 5m, 7.5 and 9.5m for the 10m deep heading and 1m, 10m, 15m, and 19.5m for the 20m deep headings. Special emphasis is given to flow rates close to the face of the heading (0.5m from the face).

Three LTR velocities i.e. 1m/s, 1.5m/s and 2m/s were used to simulate each of the 96 cases listed in Table A1 to visualize the effect of LTR velocities on the flow rates in the headings. The impact of these velocities on the flow rates, at the exit of the LB for all the cases has already been discussed. A comparison of the flow rates at the face of the heading and at the specified planes using these three LTR velocities, for each heading dimensions is given in this section.

6.3.1 Change of LTR velocity - 6.6 x 3 x 10m heading

The percentage increase in flow rates close to the face (0.5m from face) and the average increase, for all the cases, with the increase in LTR air velocity are shown in Table 6.7 and Figure 6.5. The percentage increase in flow rates with the increase in LTR air velocity at the depth planes of 1m, 5m, 7.5 and 9.5m respectively is given in Table E1. An increase in LTR velocity from 1 to 1.5, 1 to 2, and 1.5 to 2 m/s increase the flow rates at all the depth planes. The percentage difference between the LTR velocities of 1 to 1.5m/s is 50%, 1 to 2m/s is 100% and between 1.5 to 2m/s is 33%. The increase in flow rates with the increase in LTR velocity followed approximately the same percentage increase as is the difference between the LTR velocities. The average percentage variation was less than 1% (Table 6.7 and Figure 6.5) considering the flow rates at the 9.5m depth and less than 3% considering the flow rates at all the depth planes (Table E1).

Table 6.7 Percentage increase in flow rates at the 9.5m deep plane with the increase in LTR velocity

| Cases | LTR velocities | | | Percentage increase in flow rate with the increase in LTR velocity from 1 to 1.5, 1 to 2 and 1.5 to 2m/s | | |
|------------------------------------|--------------------------------|---------|---------|--|---------------|---------------|
| | 1m/s | 1.5m/s | 2m/s | 1-1.5 m/s (%) | 1-2 m/s (%) | 1.5-2 m/s (%) |
| | Flow rates (m ³ /s) | | | | | |
| 1 | 0.8698 | 1.32853 | 1.75826 | 52.74 | 102.15 | 32.35 |
| 2 | 1.2292 | 1.81762 | 2.41861 | 47.87 | 96.76 | 33.06 |
| 3 | 0.8502 | 1.302 | 1.73406 | 53.14 | 103.96 | 33.18 |
| 4 | 1.18929 | 1.76003 | 2.38526 | 47.99 | 100.56 | 35.52 |
| 5 | 1.12258 | 1.69541 | 2.26101 | 51.03 | 101.41 | 33.36 |
| 6 | 1.54101 | 2.30001 | 3.1098 | 49.25 | 101.8 | 35.21 |
| 7 | 1.4108 | 2.15337 | 2.89545 | 52.63 | 105.23 | 34.46 |
| 8 | 1.82831 | 2.7181 | 3.64927 | 48.67 | 99.6 | 34.26 |
| 9 | 1.46387 | 2.19548 | 2.93506 | 49.98 | 100.5 | 33.69 |
| 10 | 1.9587 | 2.89042 | 3.92107 | 47.57 | 100.19 | 35.66 |
| 11 | 2.08176 | 3.1401 | 4.20011 | 50.84 | 101.76 | 33.76 |
| 12 | 2.63228 | 3.94261 | 5.22523 | 49.78 | 98.51 | 32.53 |
| 13 | 0.89737 | 1.36675 | 1.81701 | 52.31 | 102.48 | 32.94 |
| 14 | 1.29384 | 1.9396 | 2.57561 | 49.91 | 99.07 | 32.79 |
| 15 | 0.8859 | 1.33652 | 1.79286 | 50.87 | 102.38 | 34.14 |
| 16 | 1.27301 | 1.91052 | 2.5586 | 50.08 | 100.99 | 33.92 |
| 17 | 1.18085 | 1.75338 | 2.33757 | 48.48 | 97.96 | 33.32 |
| 18 | 1.64005 | 2.4747 | 3.32073 | 50.89 | 102.48 | 34.19 |
| 19 | 1.47822 | 2.23081 | 3.0001 | 50.91 | 102.95 | 34.48 |
| 20 | 1.95503 | 2.9044 | 3.89801 | 48.56 | 99.38 | 34.21 |
| 21 | 1.51531 | 2.2858 | 3.0364 | 50.85 | 100.38 | 32.84 |
| 22 | 2.08793 | 3.10811 | 4.1423 | 48.86 | 98.39 | 33.27 |
| 23 | 2.1683 | 3.25079 | 4.3426 | 49.92 | 100.28 | 33.59 |
| 24 | 2.7873 | 4.23771 | 5.59221 | 52.04 | 100.63 | 31.96 |
| Average percentage increase | | | | 50.22 | 100.82 | 33.7 |

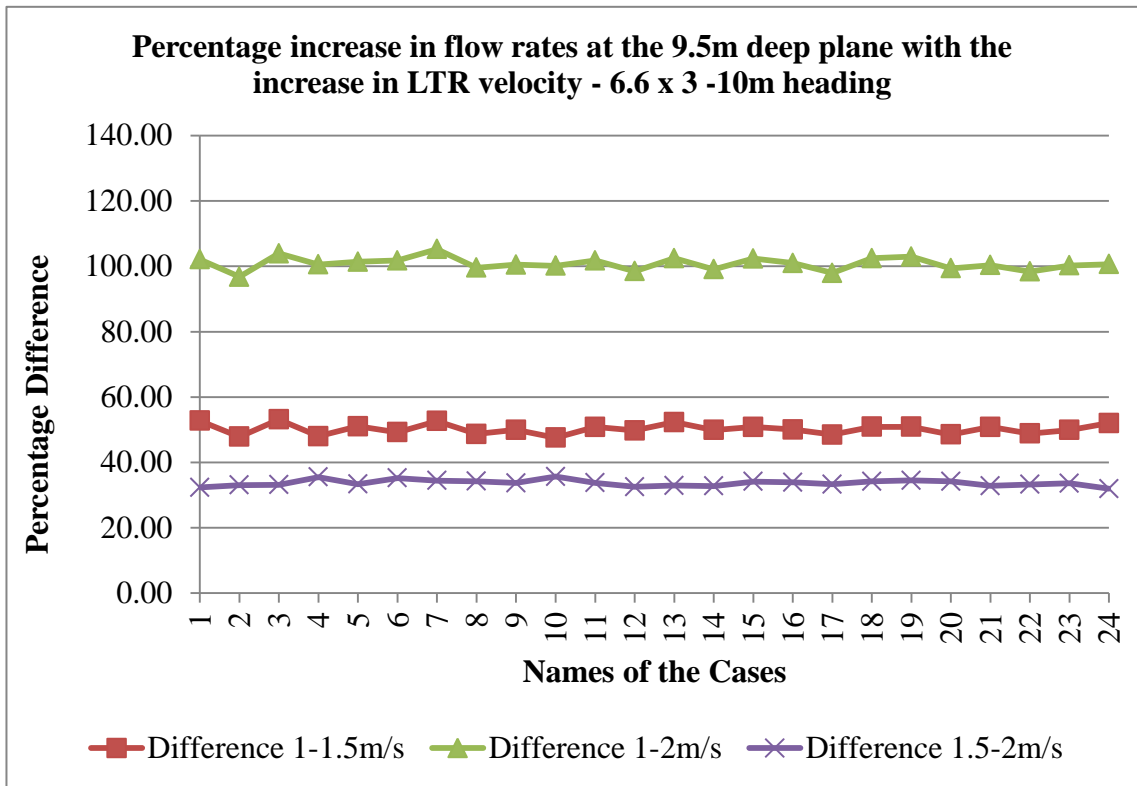


Figure 6.5 Percentage increase in flow rates at the 9.5m deep plane with the increase in LTR velocity for 6.6 x 3 x 10m heading

6.3.2 Change of LTR velocity - 6.6 x 4 x 10m heading

The percentage increase in flow rates close to the face and the average increase for all the cases with the increase in LTR air velocity are given in Table F1 and shown in Figure 6.6. The percentage increase in flow rates at all the depth planes with the increase in LTR velocity is given in Table E2. The difference between the average percentage increase in flow rates with the increase in LTR air velocity and the percentage increase in the LTR velocities, considering the flow rates at the 9.5m deep planes was less than 1% and for all the depth planes was less than 3%.

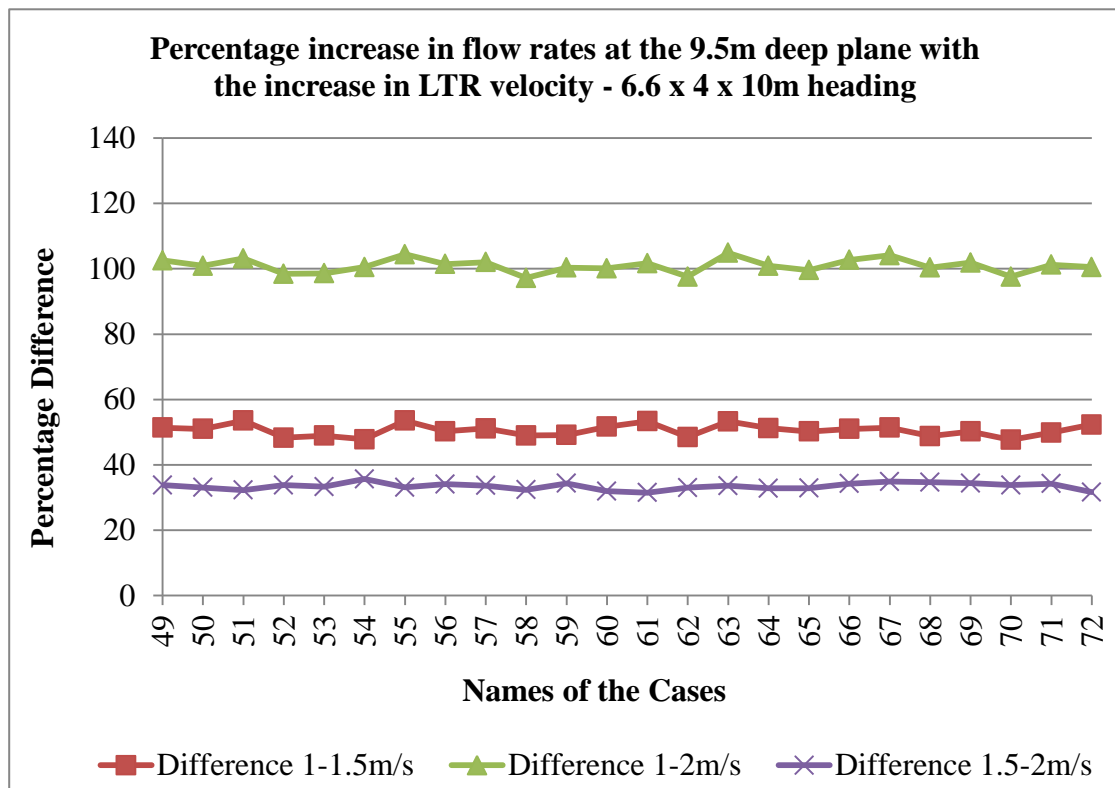


Figure 6.6 Percentage increase in flow rates at the 9.5m deep plane with the increase in LTR velocity for 6.6 x 4 x 10m heading

6.3.3 Change of LTR velocity - 6.6 x 3 x 20m heading

The percentage increase in flow rates close to the face and the average increase for all the cases with the increase in LTR air velocity are given in Table F2 and shown in Figure 6.7. The percentage increase in flow rates at all the depth planes with the increase in LTR velocity is given in Table E3. The effect of an increase in LTR velocity from 1 to 1.5, 1 to 2 and 1.5 to 2m/s showed behaviour similar to the 10m deep heading; the flow rates close to the face and at 1m, 10m, and 15m deep planes increased with the increase in the LTR velocity.

The increase in flow rates with the increase in LTR velocity followed approximately the same percentage increase as is the increase in the LTR velocities. The difference was less than 2% considering only the 19.5m deep planes and also when considering all the depth planes.

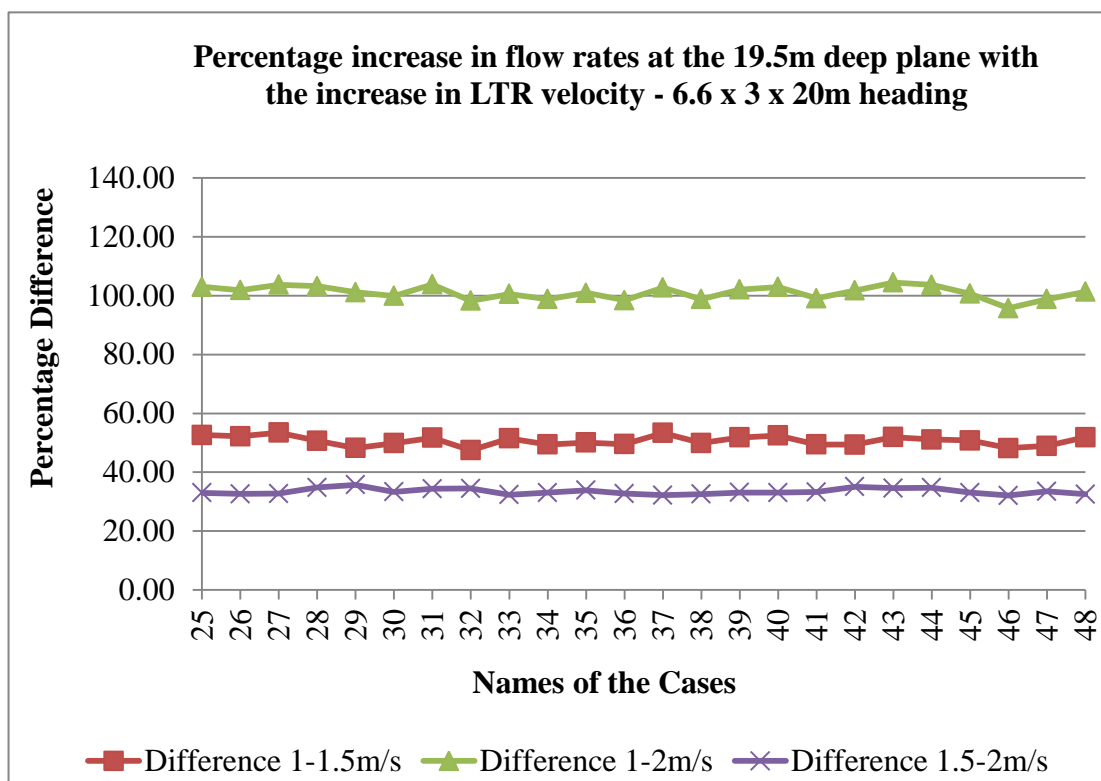


Figure 6.7 Percentage increase in flow rates at the 19.5m deep plane with the increase in LTR velocity for 6.6 x 3 x 20m heading

6.3.4 Change of LTR velocity - 6.6 x 4 x 20m heading

The percentage increase in flow rates with the increase in LTR air velocity close to the face and the average increase in flow rates for all the cases are given in Table F3 in Annex 'M' and shown in Figure 6.8. The percentage increase in flow rates with the increase in LTR air velocity at all the planes is given in Table E4. The effect of an increase in LTR velocity from 1 to 1.5, 1 to 2 and 1.5 to 2 m/s is similar to the 3m high heading. The difference between the average percentage increase in flow rates with the increase in LTR air velocity and the percentage difference between the LTR velocities, considering the flow rates at the 19.5m deep planes is less than 2% and for all the depth planes is less than 4%.

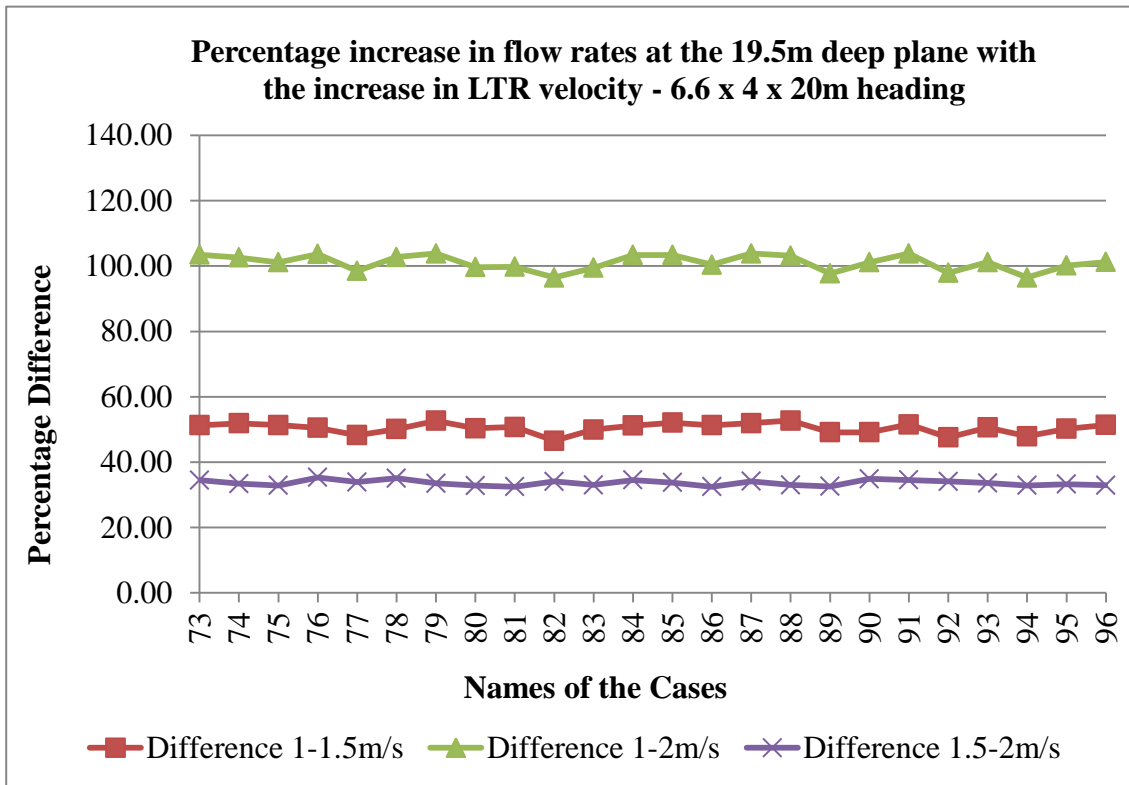


Figure 6.8 Percentage increase in flow rates at the 19.5m deep plane with the increase in LTR velocity for 6.6 x 4 x 20m heading

6.3.5 Conclusion

The flow rates at the face of the heading and at all depths inside the heading for all the headings dimensions and LB configurations increased proportionally to an increase in the LTR velocity. Therefore, flow rates inside a heading using any configuration of the LB can be varied by making a proportional change in the LTR velocity.

In the next section, the effect of first system variable related to the settings of the LB i.e. the change in LTR length of the LB inside the heading on the flow rates inside the heading is discussed and analysed.

6.4 Comparison of Air Flows with the Change in the Length of LB inside the Heading for Each LTR Velocity

The length of the LB inside the heading was varied to check its effect on the ventilation of the heading. The flow rate were calculated at planes parallel to the face of the heading located at depths of 1m, 5m, 7.5 and 9.5m respectively for the 10m deep heading and 1m, 10m, 15m, and 19.5m for the 20m deep headings.

As already discussed in Table 6.2, two lengths of the LB were used inside the heading; equal to half the length of heading and three by four the length of the heading. The half and three by four lengths for the 10m long heading are equal to 5m and 7.5m respectively, and for the 20m deep heading are 10 and 15m respectively. The first twelve cases for each dimension (each group of cases) of the heading were run using LB with smaller length (1-12, 25-36, 49-60, and 73-84) and the next 12 cases (13-24, 37-48, 60-72, and 85-96) were run with the longer LB as shown in Table A1. Therefore, for each heading dimension twelve sets of cases were simulated, where each set have two cases one with LB length equal to half the length of the heading and the other with three by four the length of the heading. The rest of the configurations for cases of a particular set are same.

A comparison of the flow rates for each set of cases for all the heading dimensions is discussed in this section, with emphasis on the flow rates close to the face of the heading. The percentage difference in flow rates was calculated to find out clearly how much the flow rate changed with an increase in the length of the LB.

6.4.1 Length of LB inside the heading - 6.6 x 3 x 10m heading

The percentage difference in flow rates, close to the face, at the 9.5m deep plane for each set of cases of group 1 (10m deep and 3m high heading using 5m and 7.5m LB) for all the LTR velocities is given in Table 6.8 and the flow rates at the 9.5m deep plane are shown in Figures 6.9 through 6.11. The air was delivered closer to the face with a longer LB. Therefore, flow rates close to the face; at the 9.5m deep plane were higher for all the cases with the LB closer to the face. The flow rates on average were

approximately 5% more with the 7.5m LB (3/4 the length of heading) for all LTR velocities considering all sets of cases.

Table 6.8 Percentage increase in flow rate for each LTR velocity with the increase in the length of LB in the heading from 5 to 7.5m

| Cases | Planes | LTR velocity | | |
|------------------------------------|--------|---|-------------|-------------|
| | | 1m/s | 1.5m/s | 2m/s |
| | | Percentage increase in flow rate for each LTR velocity with the increase in length of LB from 5 to 7.5m (%) | | |
| 1-13 | 9.5m | 3.17 | 2.88 | 3.34 |
| 2-14 | | 5.26 | 6.71 | 6.49 |
| 3-15 | | 4.2 | 2.65 | 3.39 |
| 4-16 | | 7.04 | 8.55 | 7.27 |
| 5-17 | | 5.19 | 3.42 | 3.39 |
| 6-18 | | 6.43 | 7.6 | 6.78 |
| 7-19 | | 4.78 | 3.6 | 3.61 |
| 8-20 | | 6.93 | 6.85 | 6.82 |
| 9-21 | | 3.51 | 4.11 | 3.45 |
| 10-22 | | 6.6 | 7.53 | 5.64 |
| 11-23 | | 4.16 | 3.53 | 3.39 |
| 12-24 | | 5.89 | 7.48 | 7.02 |
| Average percentage increase | | 5.26 | 5.41 | 5.05 |

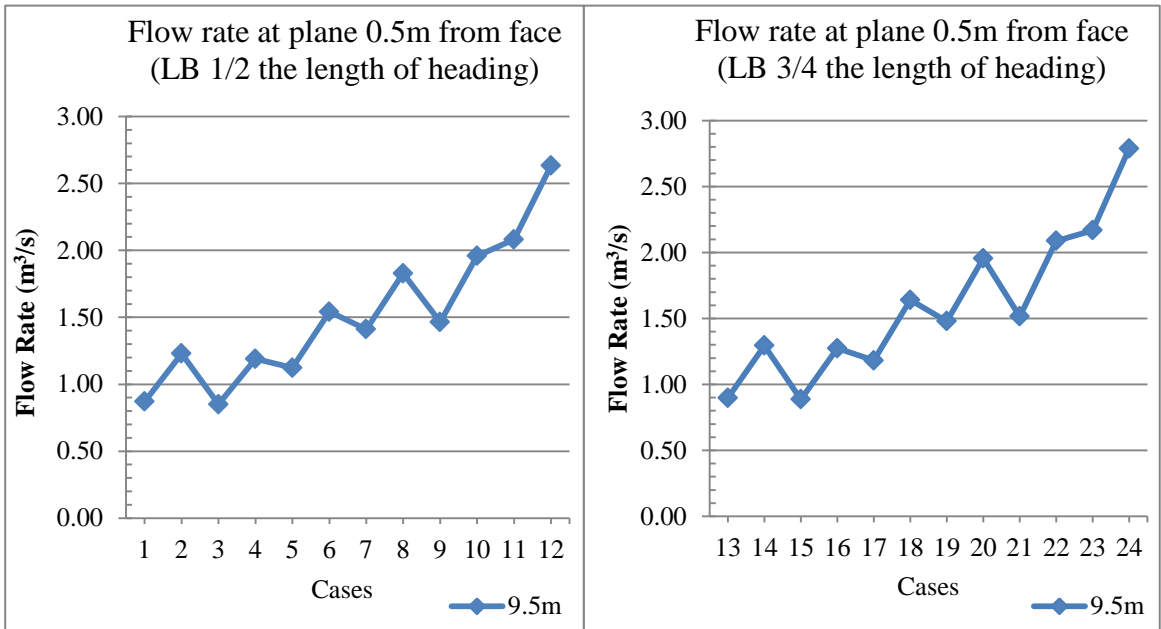


Figure 6.9 Flow rates at 9.5m deep planes using 5m and 7.5m LB inside the heading for LTR velocity of 1m/s

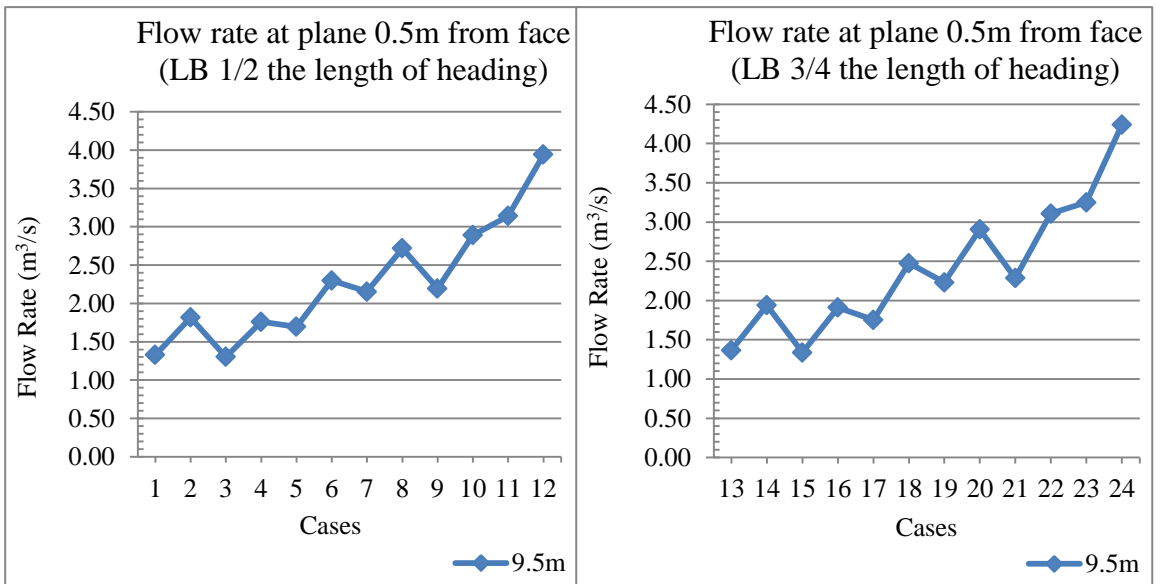


Figure 6.10 Flow rates at 9.5m deep planes using 5m and 7.5m LB inside the heading for LTR velocity of 1.5m/s

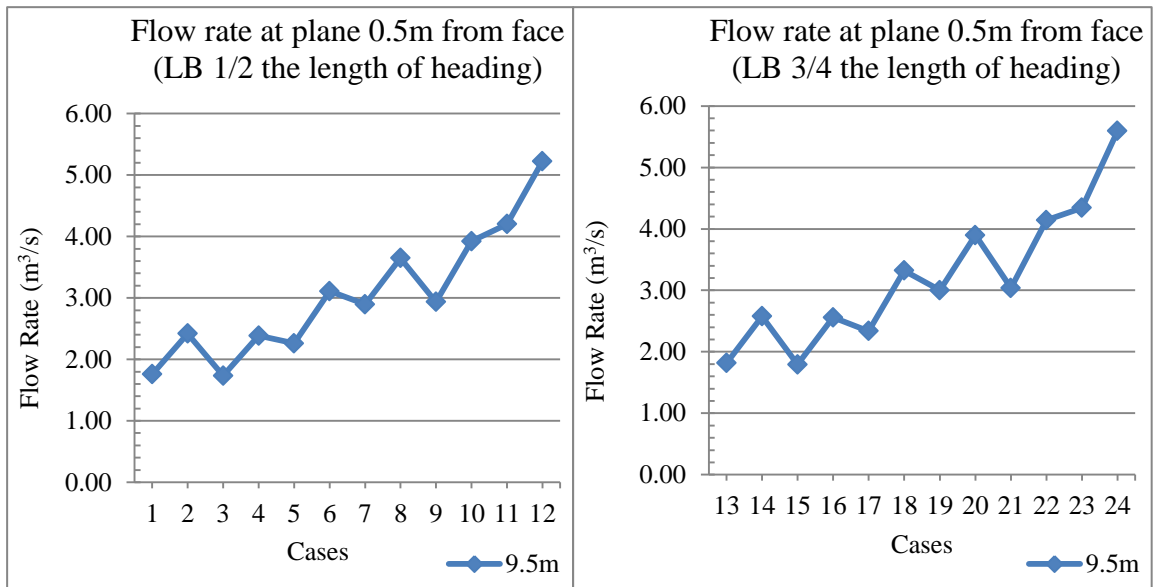


Figure 6.11 Flow rates at 9.5m deep planes using 5m and 7.5m LB inside the heading for LTR velocity of 2m/s

The flow rates at all the lower depth planes i.e. 1m, 5m and 7.5m deep however, were found to be higher with the 5m long LB for all the LTR velocities as shown in Figures 6.12 through 6.14. These flow rates are also given in Table G1. Since the quantity of air leaving the LB with a shorter length in the heading was slightly higher than with the longer LB due to lesser viscous effect, therefore, even though with the longer LB air was delivered close to the face, resulting in higher flow rates around the face area, but the flow rates in lower depth planes were higher with the shorter length of LB in the heading. Thus with a shorter LB part of the useful air did not even reach the face of the heading.

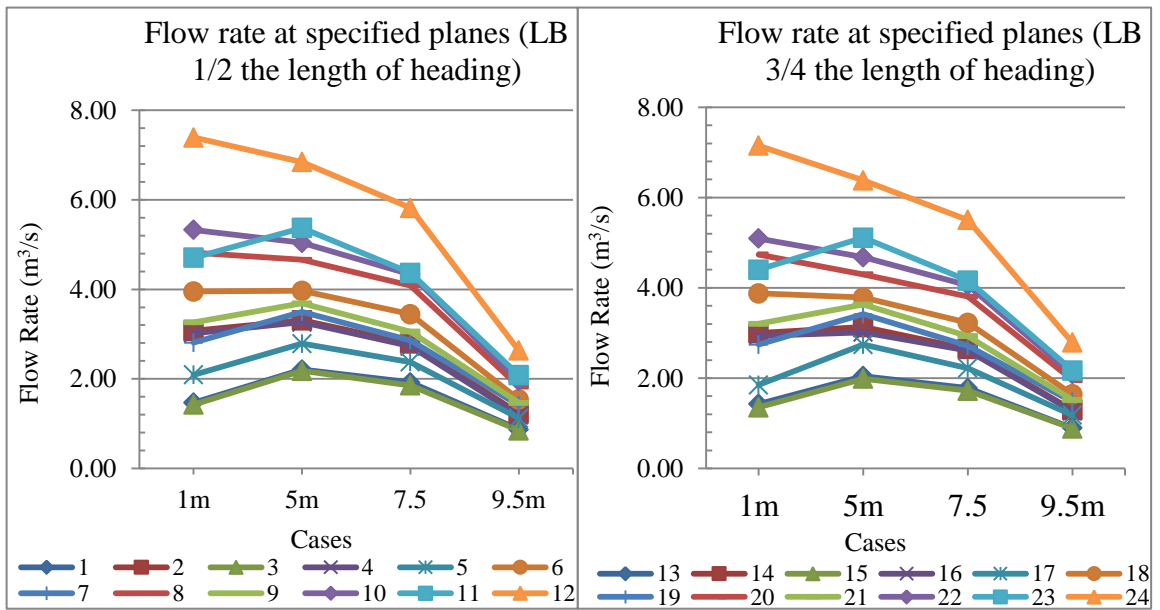


Figure 6.12 Flow rates at specified planes using 5m and 7.5m LB inside the heading for LTR velocity of 1m/s

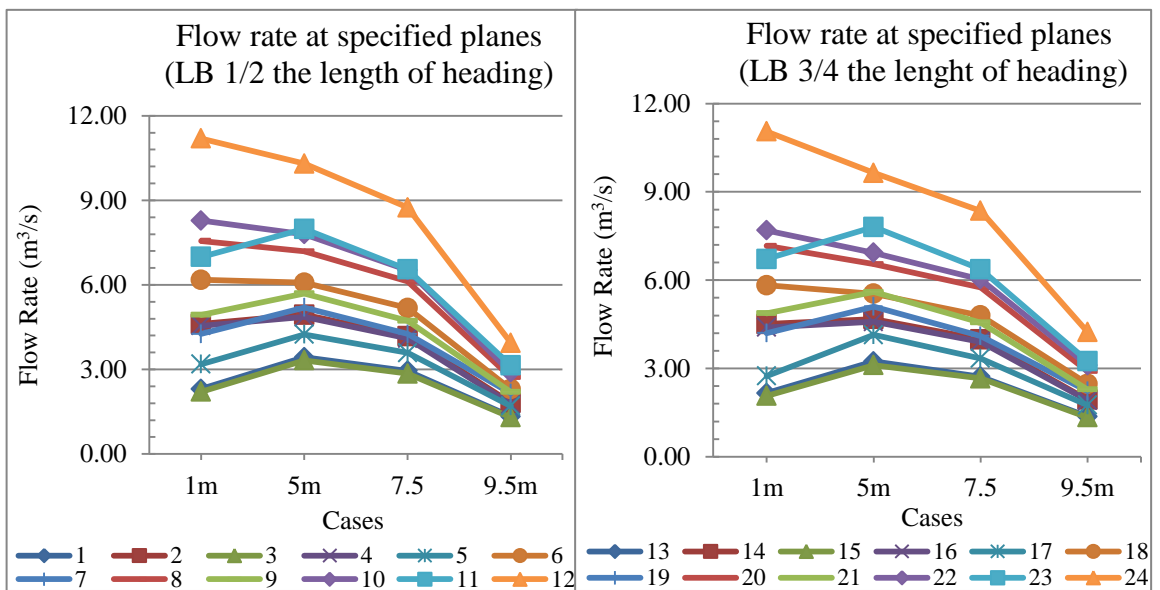


Figure 6.13 Flow rates at specified planes using 5m and 7.5m LB inside the heading for LTR velocity of 1.5m/s

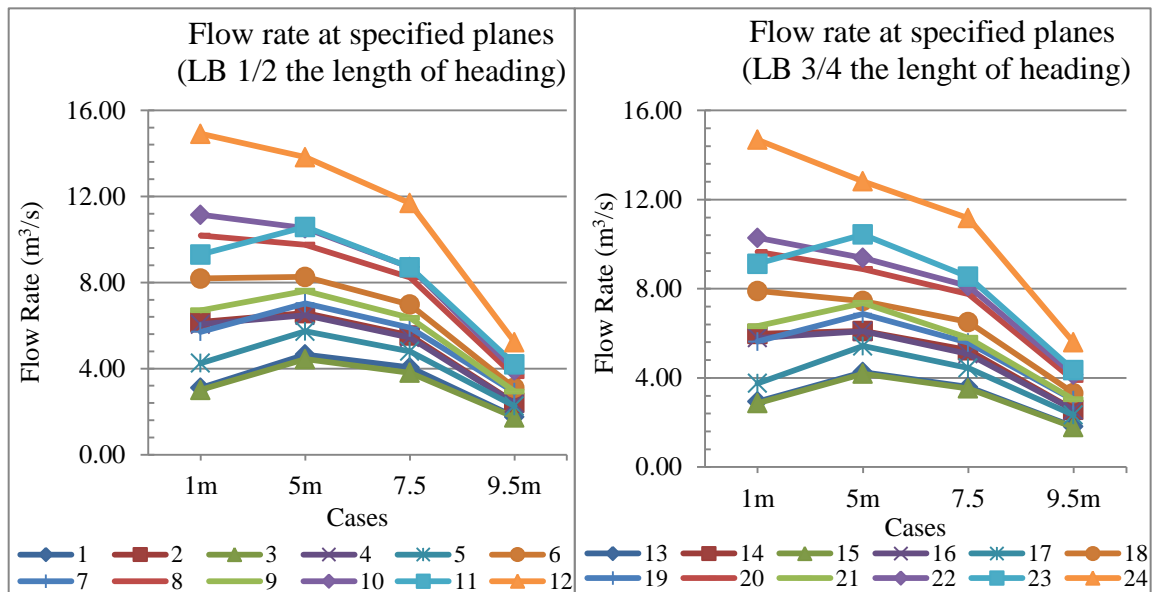


Figure 6.14 Flow rates at specified planes using 5m and 7.5m LB inside the heading for LTR velocity of 2m/s

A distinct trend was observed when the set of the cases as discussed above were separated for cases with 0.5m and 1m distance of the LB from the wall in the heading. The flow rate comparison at the 9.5m deep plane when seen separately for these sets of cases Table 6.9 showed that the increase is higher close to 7% when the LB distance from the wall was 1m, as compared to around 3.5% when the distance of the LB from the wall was 0.5m. This was found true for all the LTR velocities.

It was found that the air flowing through the channel between the LB and wall of heading was pushed away from the wall and closer to the LB due to centrifugal force, once it passed the bend and turned into the heading as shown in Figure 6.15. Resultantly, the air flow concentration at the exit of the LB was not uniform, and the air was more concentrated closer to the LB (higher air velocity). The variation in flow rate, anywhere inside the channel, between the wall of the heading and at the exit of LB was much more when the distance of the LB from the wall was 1m. Furthermore, air after leaving the LB, besides moving straight also turns inwards, towards the left wall of the heading, air close to the LB turned first and as the air moved farther away from the LB exit, more and more air starts turning. Therefore, when the variation in flow rate at the exit of the LB was high, the part of the air that turned before reaching the face contained more quantity of air. However, air flow in the channel became more and more uniform

with the increase in the length of the LB in the heading (similar to fluid flows in a pipe or channel). This reduction in variation with the increase in the length of this channel was also higher for longer distance of the LB from the wall in the heading (that is 1m) as shown in Figure 6.16. Where, the variation in the flow rate at the exit of the LB for Case 2 was more as compared to Case 14 with longer LB (both cases with 1m distance of LB from wall in heading). And the variation between Case 1 and Case 13 was lesser (cases with 0.5m LB distance from the wall of the heading). These are the reasons for a higher difference in flow rates between the cases with bigger LB to wall distance.

Table 6.9 Percentage increase in flow rate for each LTR velocity with the increase the length of LB in the heading from 5 to 7.5m separately for 0.5m and 1m distance of LB from wall in the heading

| Cases | Planes | LTR velocity | | | Cases | Planes | LTR velocity | | |
|------------------------------------|--------|---|-------------|-------------|------------------------------------|--------|---|-------------|-------------|
| | | 1m/s | 1.5m/s | 2m/s | | | 1m/s | 1.5m/s | 2m/s |
| | | Percentage increase in flow rate for each LTR velocity with the increase in length of LB from 5 to 7.5m (%) | | | | | Percentage increase in flow rate for each LTR velocity with the increase in length of LB from 5 to 7.5m (%) | | |
| 1-13 | 9.5m | 3.17 | 2.88 | 3.34 | 2-14 | 9.5m | 5.26 | 6.71 | 6.49 |
| 3-15 | | 4.2 | 2.65 | 3.39 | 4-16 | | 7.04 | 8.55 | 7.27 |
| 5-17 | | 5.19 | 3.42 | 3.39 | 6-18 | | 6.43 | 7.6 | 6.78 |
| 7-19 | | 4.78 | 3.6 | 3.61 | 8-20 | | 6.93 | 6.85 | 6.82 |
| 9-21 | | 3.51 | 4.11 | 3.45 | 10-22 | | 6.6 | 7.53 | 5.64 |
| 11-23 | | 4.16 | 3.53 | 3.39 | 12-24 | | 5.89 | 7.48 | 7.02 |
| Average percentage increase | | 4.17 | 3.36 | 3.43 | Average percentage increase | | 6.36 | 7.45 | 6.67 |

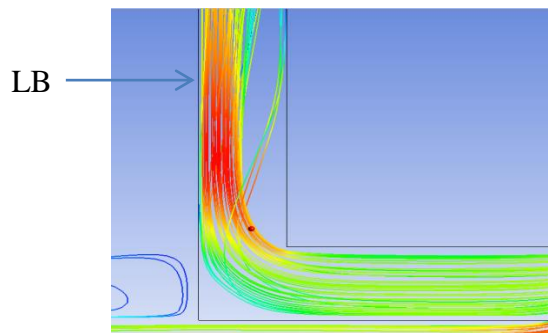


Figure 6.15 Air pushed away from the wall towards LB due to centrifugal force

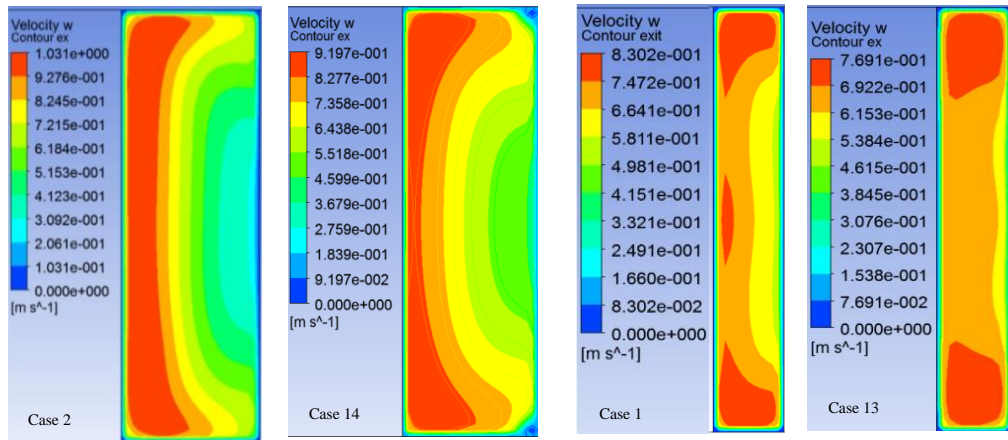


Figure 6.16 Flow rate variations at the exit of the LB for set of cases with 1m and 0.5m LB to wall distance (left to right)

6.4.2 Length of LB inside the heading - 6.6 x 4 x 10m heading

The flow rates close to the face; at the 9.5m deep plane similar to the 3m high heading were higher for all the cases with the LB closer to the face, as shown in Table H1 and Figures I1 through I3. The flow rates on average were approximately 5% more with the 7.5m LB (3/4 the length of heading) for all LTR velocities considering all sets of cases.

The flow rates at all the lower depth planes i.e. 1m, 5m and 7.5m deep (similar to the 3m high heading) were found to be higher with the 5m long LB for all the LTR velocities as shown in Figures J1 through J3 and Table G2.

The flow rate comparison at the 9.5m deep plane separately for the set of cases with 0.5m and 1m distance of LB from the wall in the heading showed a behavior similar to the 3m high heading. The difference (Table K1) was higher close to 7% when the distance of LB from the wall in the heading was 1m as compared to around 3.6% when the distance was 0.5m. This was found true for all the LTR velocities.

6.4.3 Length of LB inside the heading - 6.6 x 3 x 20m heading

The flow rate close to the face; at the 19.5m deep plane was higher for all the cases with the LB closer to the face, as shown in Table H2 and Figures I4 through I6. The flow rates on average were approximately 5% more with the 15m LB (3/4 the length of heading) for all LTR velocities considering all sets of cases.

The flow rates at all the lower depth planes i.e. 1m, 10m and 15m deep were higher with the 10m long LB for all the LTR velocities as shown in Figures J4 through J6 and Table G3.

The flow rate comparison at the 19.5m deep plane separately for the cases with 0.5m and 1m distance of LB from the wall in the heading showed (Table K2) that the difference was higher close to 5% when the distance of LB from the wall in the heading was 1m as compared to around 3.5% when the distance was 0.5m. This was true for all the LTR velocities.

6.4.4 Length of LB inside the heading - 6.6 x 4 x 20m heading

The flow rates close to the face; at the 19.5m deep plane similar to the 3m high heading were higher for all the cases with the LB closer to the face, as shown in Table H3 and Figures I7 through I9. The flow rates on average were about 4.5% more with the 15m LB (3/4 the length of heading) for all LTR velocities considering all sets of cases.

The flow rates at all the lower depth planes i.e. 1m, 10m and 15m deep (similar to the 3m high heading) showed higher flow rates with the 10m long LB for all the LTR velocities as shown in Figures J7 through J9 and Table G4.

The flow rate comparison at the 19.5m deep plane separately for the cases with 0.5m and 1m distance of LB from the wall in the heading showed (Table K3) that the difference was higher close to 5.5% when the distance of LB from the wall in the heading was 1m as compared to around 3.3% when the distance was 0.5m. This was found true for all the LTR velocities.

6.4.5 Conclusion

- The air was delivered close to the face with the longer LB resulting in more air flow at or near the face. This stood true for both the heights, so height has no effect on this phenomenon.
- The shorter the length of the LB in the heading the lesser is the viscous effect therefore, higher flow rates were available at the exit of the LB. Furthermore, with shorter LB less air reached the face of the heading. Therefore, higher flow rates were found at depths lower than the 9.5m and 19.5m depth for the short and

long heading respectively. This stood true for both the heights, so height has no effect on this phenomenon.

- The longer the distance of the LB from the wall in the heading, the bigger was the difference in flow rates close to the face of the heading between the short and long LB. Since, the increase in length of the LB improved the delivery of air close to the face of the heading more for higher distance of LB from the wall (by reducing the variation in flow rates in the channel between LB and wall of heading).

The next section, covers the effect of the second system variable related to the installation of the LB i.e. change in length of the LB inside the LTR on the flow rates inside the heading is analysed and discussed.

6.5 Comparison of Air Flows, with the Change in Length of LB Inside the LTR for Each LTR Velocity

The length of the LB inside the LTR was varied to check its effect on ventilation of the heading. The flow rate were calculated at planes parallel to the face of the heading located at depths of 1m, 5m, 7.5 and 9.5m for the 10m deep heading and 1m, 10m, 15m, and 19.5m for the 20m deep headings.

As already discussed in Table 6.2, two lengths of LB were used inside the LTR that is 3m and 6m. For each heading dimension (group) twelve sets of cases (1-3, 2-4 ...22-24) were simulated, where each set had a case with LB length equal to 3m and 6m each. The rest of the configurations were kept same for both the cases in a set. A comparison of the flow rates for each set of cases for all the heading dimensions is discussed in this section, with emphasis on the flow rates close to the face of the heading (0.5m from face). The percentage difference in flow rates was calculated to find out clearly how much the flow rate changes with an increase in the length of the LB in the LTR. LB inlet area with the 3m and 6m lengths stayed the same when the LB was used without an angle. However, when the LB was used with an angle the change in length of the LB in the LTR also changed the LB inlet area as shown in Table 6.2. Therefore, the set of cases using LB with zero angles and with angle (7.5° and 15°) have been discussed separately.

6.5.1 Length of LB inside the LTR - 6.6 x 3 x 10m heading

- **Zero degree LB- length of LB in LTR - 6.6 x 3 x 10m heading**

The percentage difference between the flow rates for each set of cases of group 1, at the 9.5m deep planes for LB with 3 and 6m length in the LTR is given in Table 6.10 (Case 1-3, 2-4, 13-15 and 14-16). The flow rates at these planes are shown in Figures 6.17 through 6.19 for each LTR velocity. When the LB was used with zero angles the increase in length of the LB in the LTR only increased the resistance, and thus a reduction in the flow rates at the exit of the LB, since, the increase in length in the LTR did not change the LB inlet area. The reduced flow rates at the exit of the LB resulted in lower flow rates at the face of the heading. The flow rates at the face decreased proportionally to the reduction in

the flow rates at the exit of the LB, for all the LTR velocities, as shown in Table 6.10.

- **Angled LB - Length of the LB in LTR - 6.6 x 3 x 10m heading**

The percentage difference in flow rates for each set of cases at the 9.5m deep planes for LB with 3m and 6m length in the LTR is given in Table 6.10 and the flow rates at these planes are shown in Figure 6.17 through Figure 6.19. The increase in length of the LB in the LTR, when it was used with an angle increased the LB inlet area. The increase in area allowed more air flow through the channel between the LB and the walls, resulting in more air at the exit of the LB. The flow rates at the face increased proportionally to the increase in flow rates at the exit of the LB, for all LTR velocities, as shown in Table 6.10.

Table 6.10 Percentage change in flow rate at the 9.5m deep plane and exit of the LB for each LTR velocity with the change in length of LB in the LTR from 3 to 6m

| Cases | LTR velocity | | | Cases | LTR velocity | | |
|-------|--|--------|-------|-------|--|--------|-------|
| | 1m/s | 1.5m/s | 2m/s | | 1m/s | 1.5m/s | 2m/s |
| | Percentage change in flow rate at the 9.5m deep planes for each LTR velocity with the change in length of LB in the LTR from 3 to 6m | | | | Percentage change in flow rate at the exit of LB for each LTR velocity with the change in length of LB in the LTR from 3 to 6m | | |
| 1-3 | -2.25 | -2 | -1.38 | 1-3 | -1.43 | -1.49 | -1.36 |
| 2-4 | -3.25 | -3.17 | -1.38 | 2-4 | -1.48 | -1.5 | -1.59 |
| 5-7 | 25.67 | 27.01 | 28.06 | 5-7 | 25.1 | 27.1 | 28.1 |
| 6-8 | 18.64 | 18.18 | 17.35 | 6-8 | 18.81 | 18.32 | 17.71 |
| 9-11 | 42.21 | 43.03 | 43.1 | 9-11 | 42.95 | 42.5 | 43.02 |
| 10-12 | 34.39 | 36.4 | 33.26 | 10-12 | 33.55 | 35.4 | 35.73 |
| 13-15 | -1.28 | -2.21 | -1.33 | 13-15 | -1.4 | -1.73 | -1.26 |
| 14-16 | -1.61 | -1.5 | -0.66 | 14-16 | -1.75 | -1.47 | -1.35 |
| 17-19 | 25.18 | 27.23 | 28.34 | 17-19 | 25.23 | 27.13 | 28.39 |
| 18-20 | 19.21 | 17.36 | 17.38 | 18-20 | 18.85 | 18.51 | 17.78 |
| 21-23 | 43.09 | 42.22 | 43.02 | 21-23 | 42.94 | 42.54 | 43.02 |
| 22-24 | 33.5 | 36.34 | 35 | 22-24 | 33.53 | 35.47 | 35.75 |

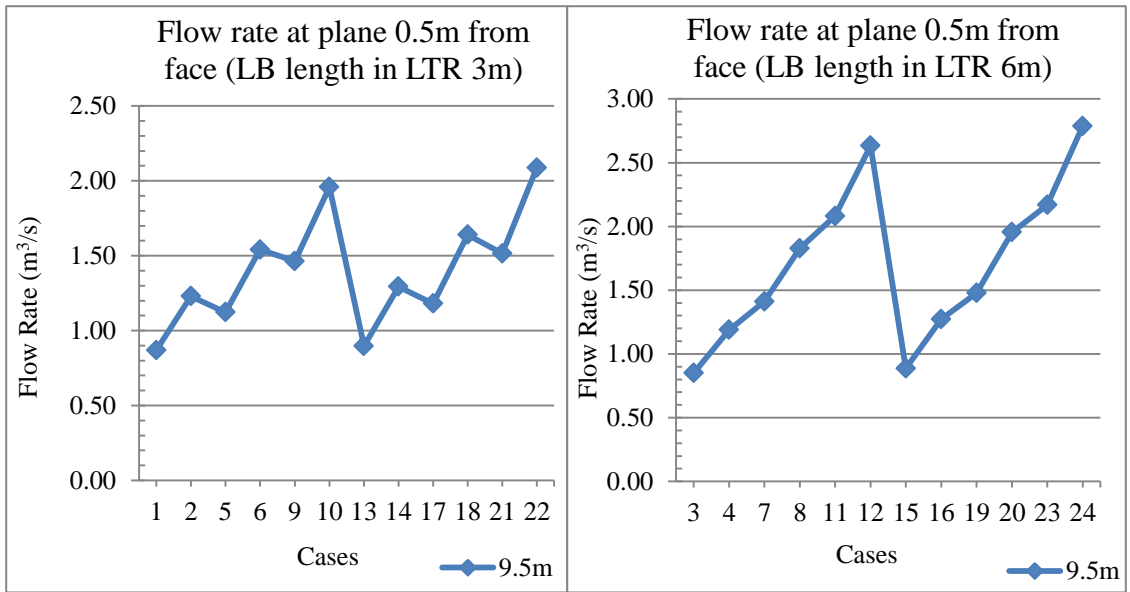


Figure 6.17 Flow rates at 9.5m deep planes using 3m and 6m LB inside the LTR for LTR velocity of 1m/s

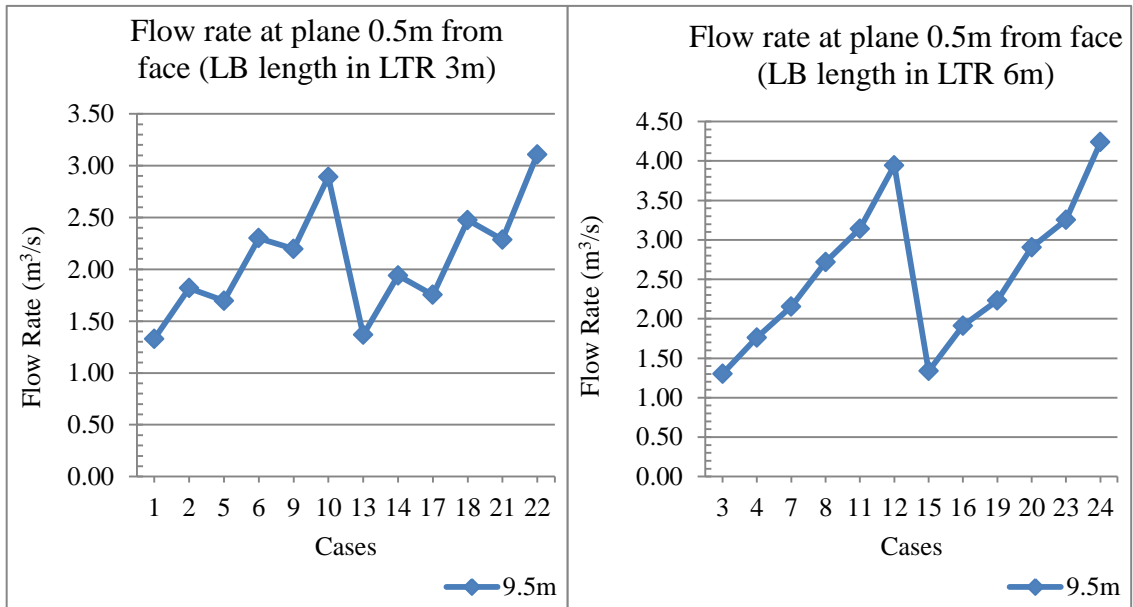


Figure 6.18 Flow rates at 9.5m deep planes using 3m and 6m LB inside the LTR for LTR velocity of 1.5m/s

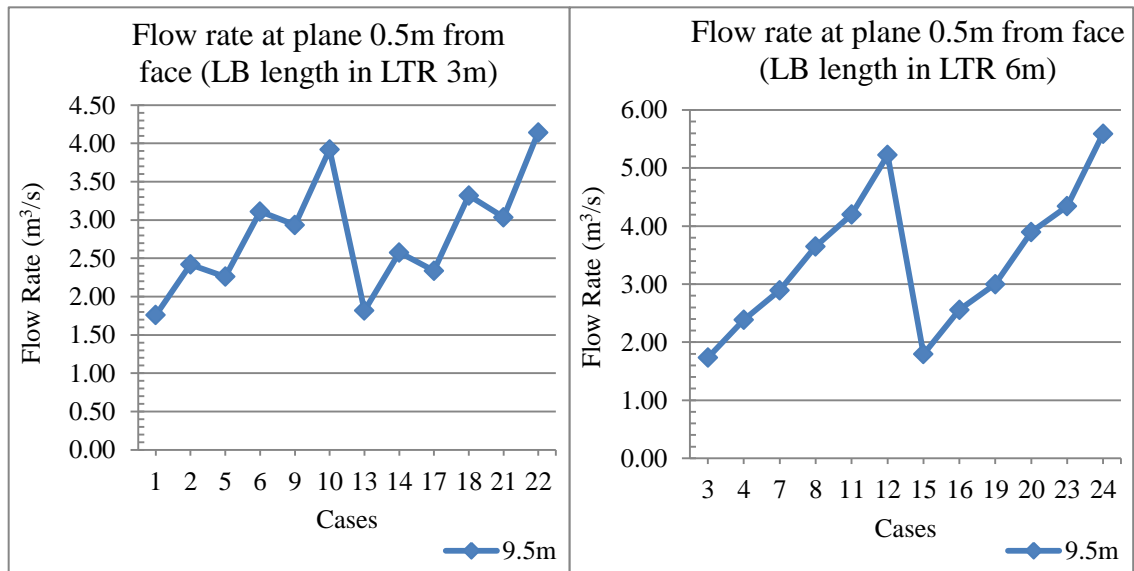


Figure 6.19 Flow rates at 9.5m deep planes using 3m and 6m LB inside the LTR for LTR velocity of 2m/s

The increase in length of the LB from 3 to 6m when the LB was used with zero angles reduced the flow rate at the exit of the LB and at all the planes in the heading as shown in Figures 6.20 through 6.22 and Table L1. The effect of this increase in length when the LB was installed with an angle increased the flows at the exit of the LB and at all planes in the heading also shown in Figures 6.20 through 6.22 and Table L1.

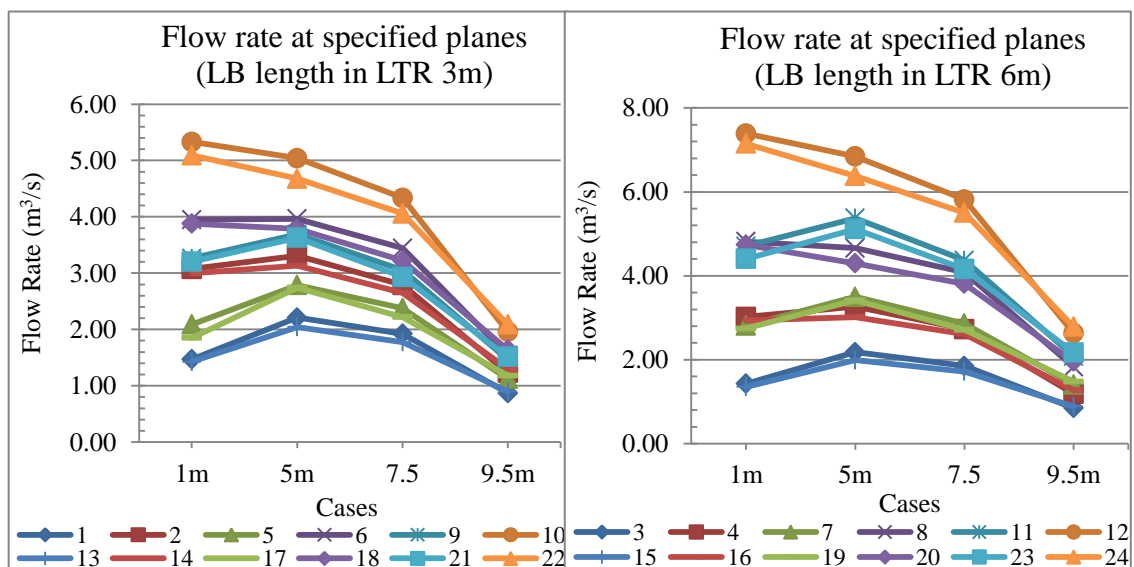


Figure 6.20 Flow rates at specified planes using 3m and 6m LB inside the LTR for LTR velocity of 1m/s

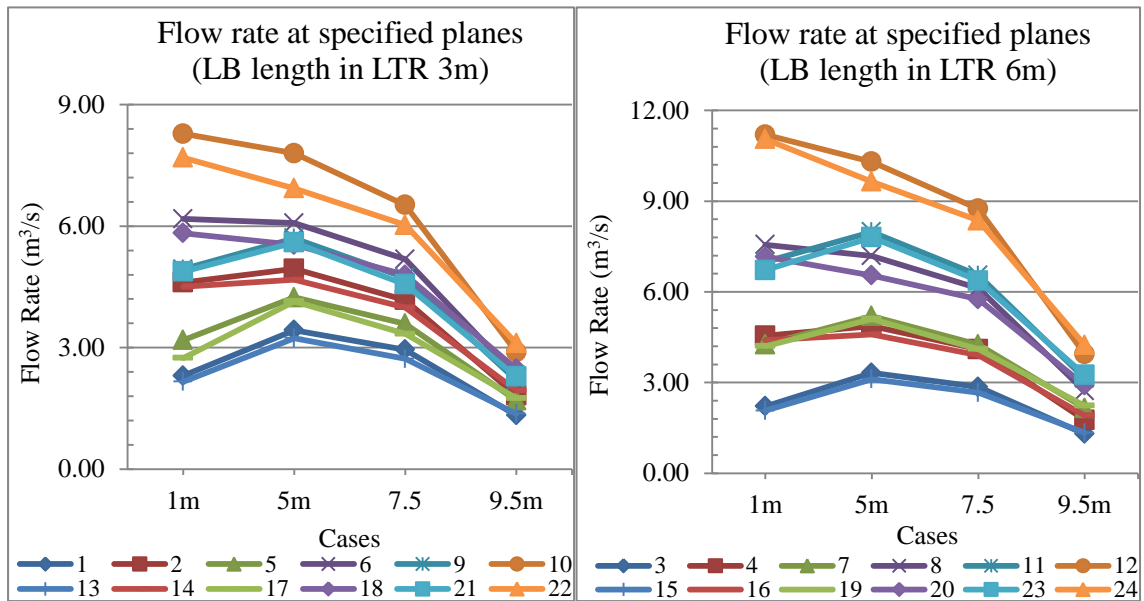


Figure 6.21 Flow rates at specified planes using 3m and 6m LB inside the LTR for LTR velocity of 1.5m/s

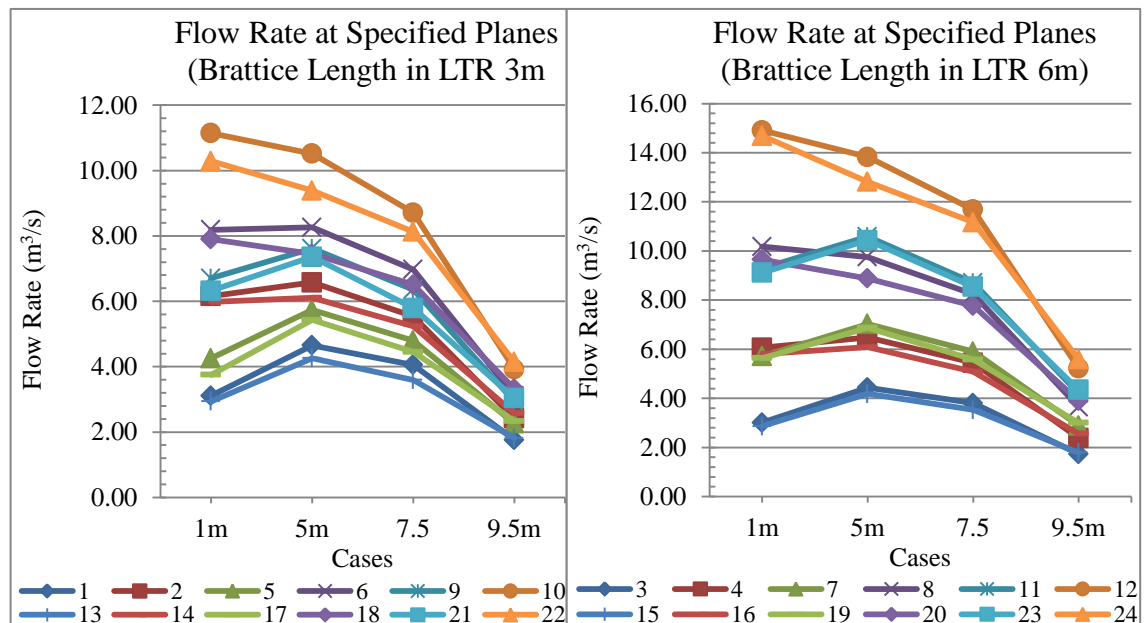


Figure 6.22 Flow rates at specified planes using 3m and 6m LB inside the LTR for LTR velocity of 2m/s

6.5.2 Length of LB inside the LTR - 6.6 x 4 x 10m heading

- **Zero degree LB - length of LB in LTR - 6.6 x 4 x 10m heading**

Similar to the 3m high heading, the increase in length of the LB for each set of cases from 3m to 6m in the LTR, reduced the flow rates at the exit of the LB and

thus resulted in lower flow rates at the face of the heading as shown in Table M1 and Figures N1 through N3 for all LTR velocities. The flow rates at the face decreased proportionally to the reduction in the flow rates at the exit of the LB, for all the LTR velocities, as shown in Table M1.

- **Angled LB - Length of the LB in LTR - 6.6 x 3 x 10m heading**

The increase in length of the LB in the LTR for each set of cases from 3m to 6m in the LTR increased the air flow at the exit of the LB and at the face, similar to the 3m high heading, as shown in Table M1 and Figures N1 through N3. The flow rates increased at the face proportionally to the increase in the flow rate at the exit of the LB for all LTR velocities as shown in Table M1.

- The increase in length of the LB from 3 to 6m when the LB was used with zero angles, reduced the flow rate, similar to the 3m high heading at the exit of the LB, and at all the planes in the heading as shown in Figures O1 through O3 and Table L2. The effect of this increase in length when the LB is installed with an angle increased the flows at the exit of the LB and at all planes in the heading also shown in Figures O1 through O3 and Table L2.

6.5.3 Length of LB inside the LTR- 6.6 x 3 x 20m heading

- **Zero degree LB - length of LB in LTR - 6.6 x 3 x 20m heading**

Similar to the 10m long heading, due to the longer LB in the LTR (used with zero angle) the flow rates at the exit of the LB reduced, which resulted in lower flow rates at the face of the heading for each set of the cases as shown in Table M2 and Figures N4 through N6 for all LTR velocities, and the reduction was proportional to the reduction of flow rates at the exit of the LB (Table M2).

- **Angled LB - Length of the LB in LTR - 6.6 x 3 x 20m heading**

The increase in length of the LB in the LTR increased the air flow at the exit of the LB, and at the face of the heading for each set of the cases as shown in Table M2 and Figures N4 through N7. This was found true for all the LTR velocities and the increase was proportional to the increase in flow rates at the exit of the LB.

- The increase in the length of the LB from 3 to 6m when the LB was used with zero angles reduced the flow rates at the exit of the LB and at all the planes in

the heading as shown in Figures O4 through O6 and Table L3. The effect of this increase in length, when the LB was installed with an angle, increased the flows at the exit of the LB and at all planes in the heading also shown in Figures O4 through O6 and Table L3.

6.5.4 Length of LB inside the LTR - 6.6 x 4 x 20m heading

- **Length of the LB in LTR - Zero Angle of the LB – 6.6 x 4 x 20m heading**

Similar to the 3m high heading, longer LB resulted in lower flow rates at the face of the heading as shown in Table M3 and Figures N7 through N9 for all LTR velocities, and the reduction was found proportional to the reduction of flow rates at the exit of the LB.

- **Angled LB - Length of the LB in LTR - 6.6 x 4 x 20m heading**

The increase in length of the LB in the LTR increased the flow rate at the exit of the LB and at the face of the heading as shown in Table L4 and Figures N7 through N9 for all LTR velocities, and the increase was found proportional to the increase in flow rates at the exit of the LB.

- The increase in length of the LB from 3 to 6m when the LB was used with zero angles reduced the flow rate at the exit of the LB and at all depth planes inside the heading as shown in Figures O7 through O9 and Table L4. The effect of this increase in length when the LB was installed with an angle increased the flows at the exit of the LB and at all planes in the heading also shown in O7 through O9 and Table L4.

6.5.5 Conclusion

The increase in length of the LB in the LTR affected the cases where the LB was used with and without an angle in the LTR differently. When the LB was used without an angle in the LTR, the increase in length only increased the resistance offered to the flow and thus reduced the flow rate at the exit of the LB, and proportionally at the face of the heading. The increase in length, when the LB was used with an angle, increased the inlet area and thus increased the flow rate at the exit and proportional to that increase an increase in flow rate at the face of the heading as well. Therefore, an increase in length

of the LB beyond 3m in the LTR, when it is used without an angle does not improve the air flow rates in the heading.

The next section, covers the effects of the third system variable related to the installation of the LB i.e. change in distance of the LB from the wall on the flow rates inside the heading is analysed and discussed.

6.6 Comparison of Air Flows, with the Change in the Distance of LB from the Wall inside the Heading for Each LTR Velocity

The distance of the LB from the walls in the LTR and heading was varied to find the impact of this distance on the air flows. Two distances equal to 0.5m and 1m were used, to find the variation of flows rates within this range. The distance of the LB from the wall in the LTR is not discussed here, since it changed with the change in angle of the LB in the LTR, therefore, its impact is discussed in section 6.7- “Change of angle of the LB in the LTR”.

For each heading dimension twelve sets of cases (1-2, 3-4 ...23-24) were simulated as already discussed in Table 6.2, where every set had a case, each, with distance of the LB from the wall in the heading equal to 0.5m and 1m. The rest of the configurations are same for both the cases in a set. The two consecutive cases, odd followed by even had same configurations except for the distance of the LB from the wall; for the odd cases the distance is 0.5m and for the even it is 1m. The flow rate were calculated at planes parallel to the face of the heading located at depths of 1m, 5m, 7.5 and 9.5m for the 10m deep heading and 1m, 10m, 15m, and 19.5m for the 20m deep headings. A comparison of the flow rates for each set of cases for all the heading dimensions (all groups) is discussed in this section, with emphasis on the flow rates close to the face of the heading (0.5m from face). The percentage difference in flow rates for each set and LTR velocity was calculated, to clearly find, how much the flow rate changes with an increase in the distance of the LB from the wall in the heading.

6.6.1 Distance of LB from the wall inside the heading - 6.6 x 3 x 10m heading

The percentage difference in the flow rates for each set of cases using LB distance of 0.5m and 1m from the wall in the heading, close to the face at the 9.5m deep plane, for all the LTR velocities is given in Table 6.11 and shown in Figures 6.23 through 6.25.

The flow rates close to the face; at the 9.5m deep plane were found to be higher for all the cases when the distance of the LB from the wall in the heading was 1m, since the flow rates at the exit of the LB were higher for cases with 1m distance of the LB from the wall in the heading (due to bigger inlet area).

Table 6.11 Percentage increase in flow rate at 9.5m deep plane for each LTR velocity with the increase in the distance of the LB from 0.5 to 1m from the wall in the heading

| Cases | LTR velocity | | |
|-------|---|--------|-------|
| | 1m/s | 1.5m/s | 2m/s |
| | Percentage increase in flow rate for each LTR velocity with the increase in wall distance of the LB from wall of the heading from 0.5 to 1m at the 9.5m depth plane (%) | | |
| 1-2 | 41.32 | 36.81 | 37.56 |
| 3-4 | 39.88 | 35.18 | 37.55 |
| 5-6 | 37.27 | 35.66 | 37.54 |
| 7-8 | 29.59 | 26.23 | 26.03 |
| 9-10 | 33.8 | 31.65 | 33.59 |
| 11-12 | 26.44 | 25.56 | 24.41 |
| 13-14 | 44.18 | 41.91 | 41.75 |
| 15-16 | 43.7 | 42.95 | 42.71 |
| 17-18 | 38.89 | 41.14 | 42.06 |
| 19-20 | 32.26 | 30.19 | 29.93 |
| 21-22 | 37.79 | 35.97 | 36.42 |
| 23-24 | 28.55 | 30.36 | 28.78 |

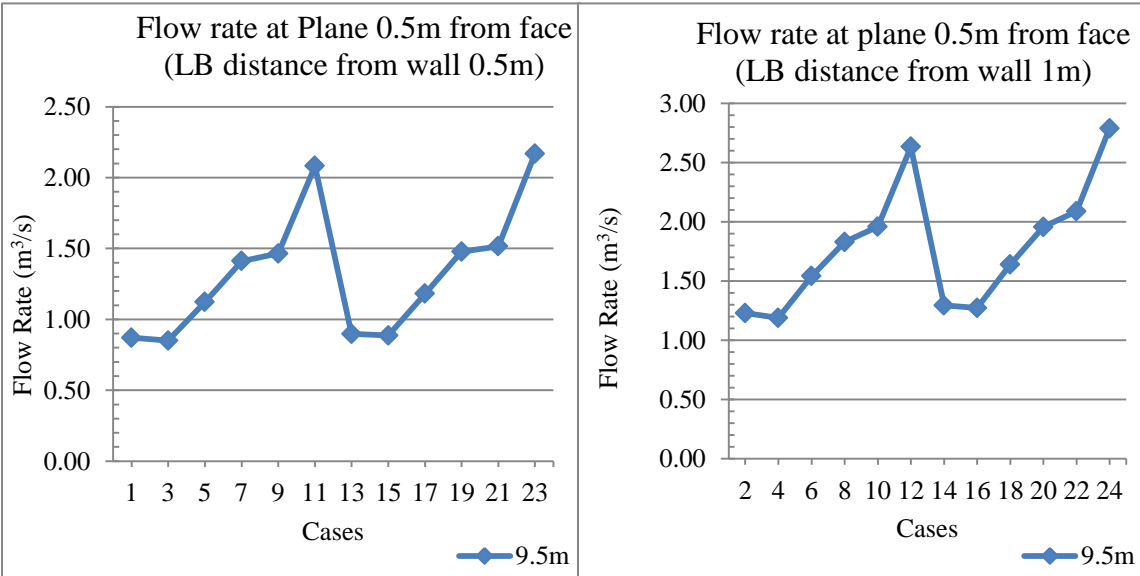


Figure 6.23 Flow rates at 9.5m deep planes using 0.5m and 1m distance of LB from wall for LTR velocity of 1m/s

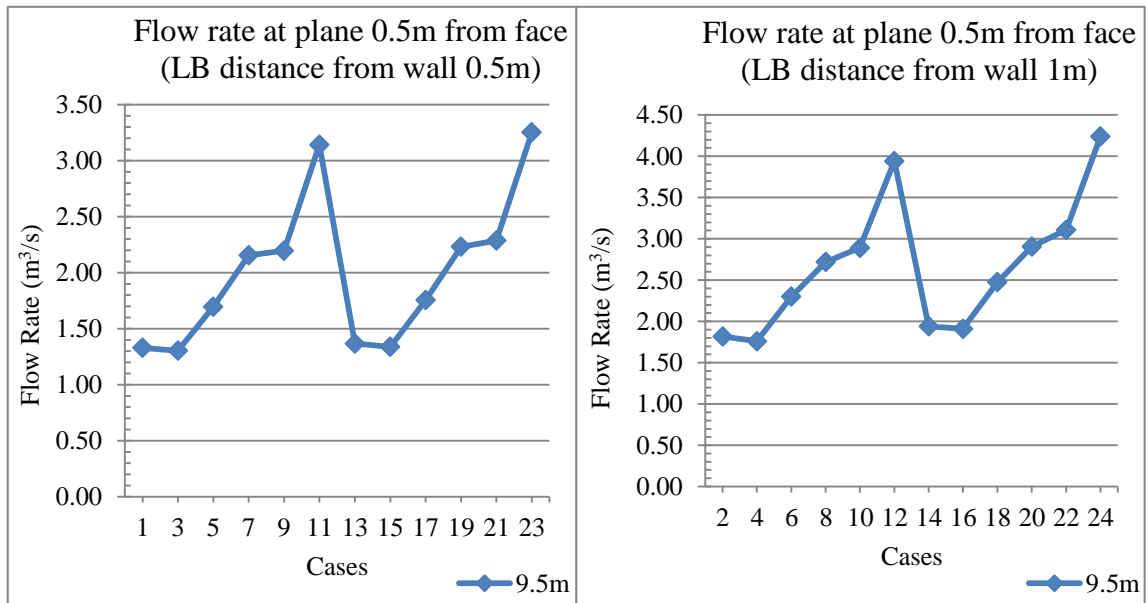


Figure 6.24 Flow rates at 9.5m deep planes using 0.5m and 1m distance of LB from wall for LTR velocity of 1.5m/s

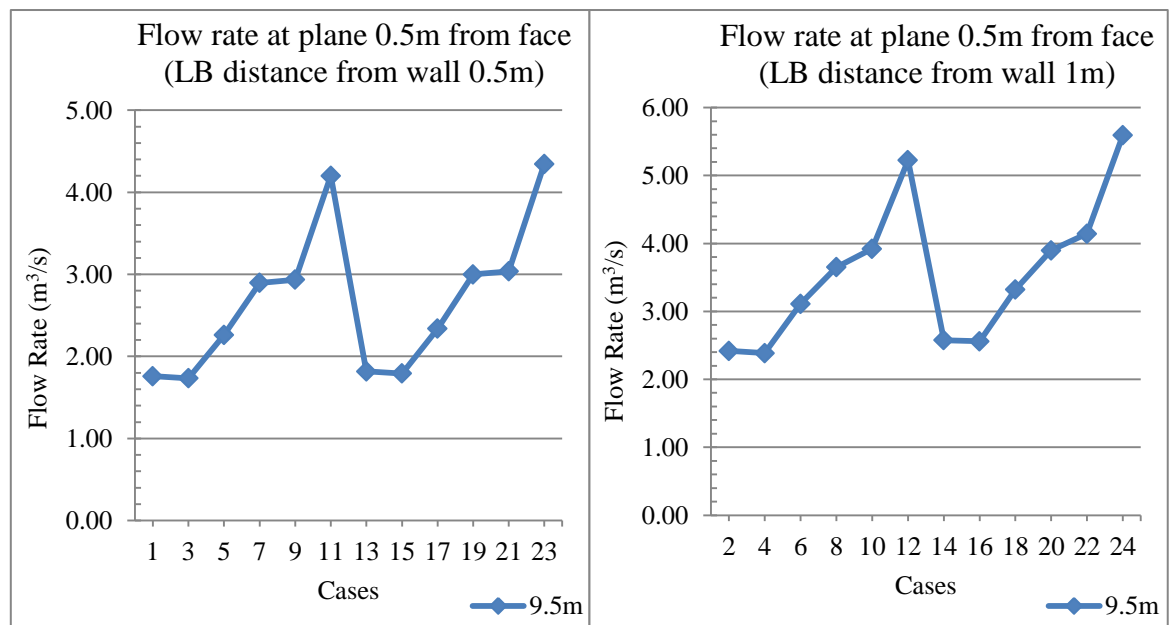


Figure 6.25 Flow rates at 9.5m deep planes using 0.5m and 1m distance of LB from wall for LTR velocity of 2m/s

The flow rates at all the lower depth planes i.e. 1m, 5m and 7.5m deep in each set of cases as expected, were also found to be higher with the 1m distance of the LB from the wall in the heading, for all the LTR velocities as shown in Figures 6.26 through 6.28 and Table P1.

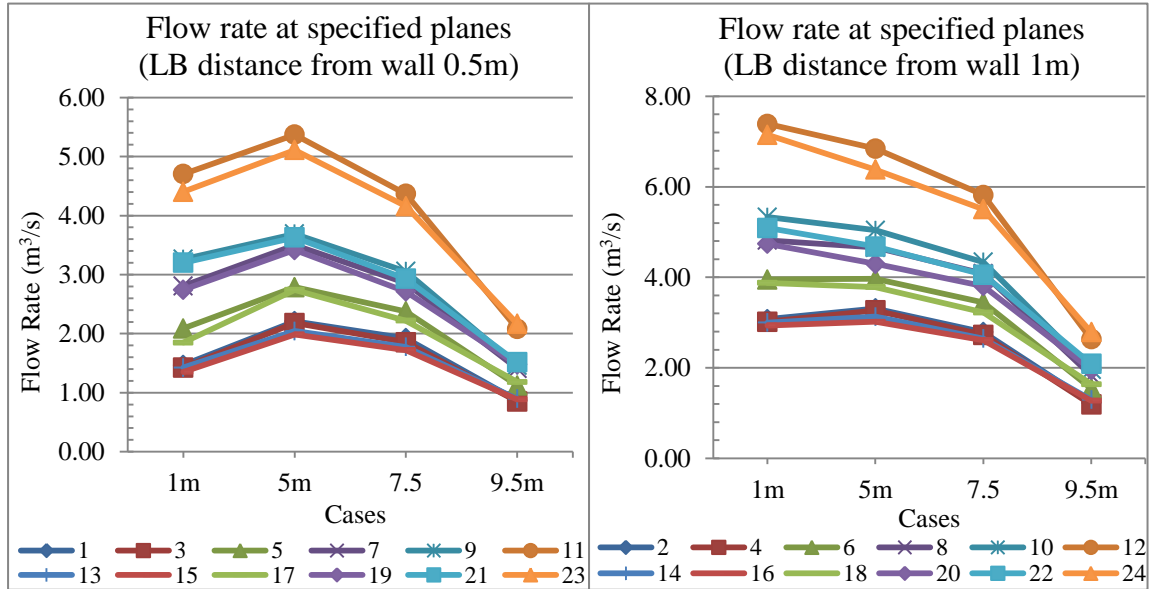


Figure 6.26 Flow rates at specified planes using 5m and 7.5m LB inside the heading for LTR velocity of 1m/s

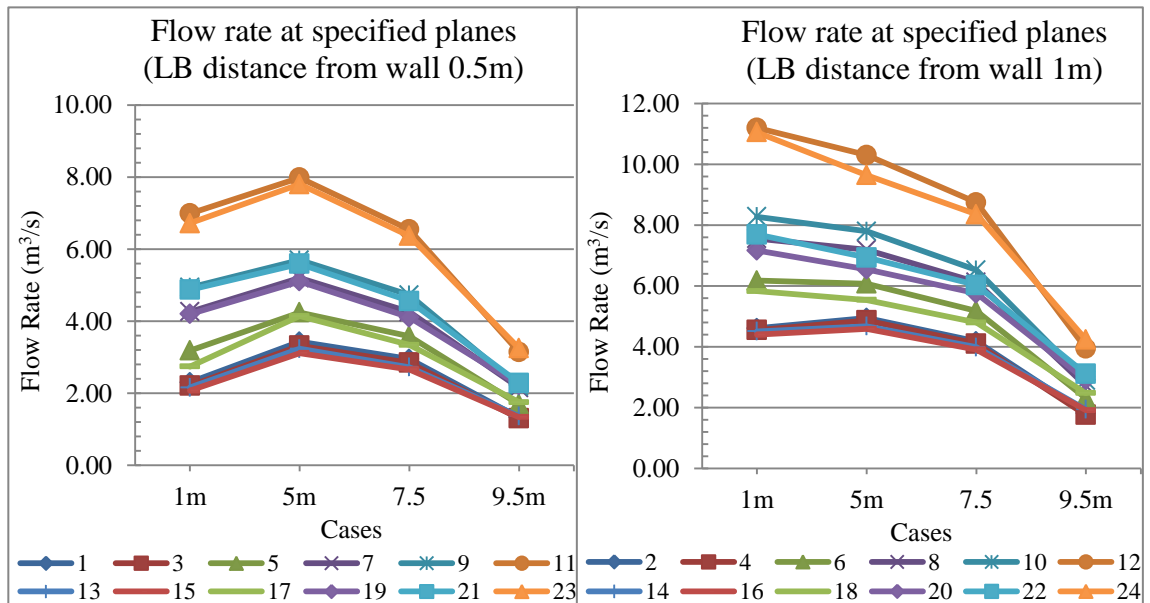


Figure 6.27 Flow rates at specified planes using 5m and 7.5m LB inside the heading for LTR velocity of 1.5m/s

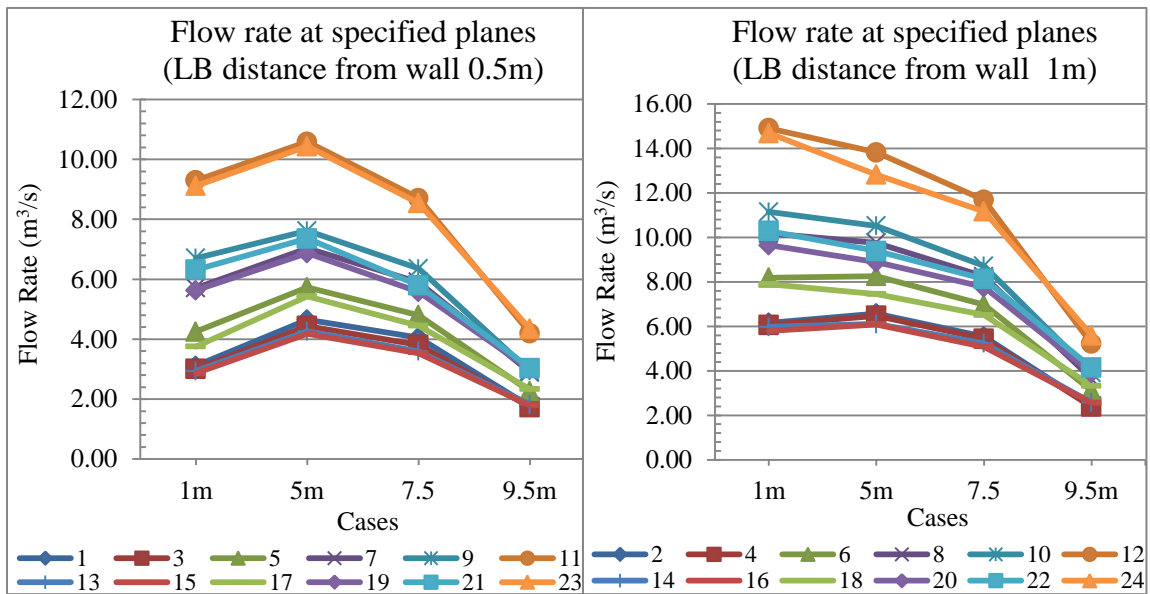


Figure 6.28 Flow rates at specified planes using 5m and 7.5m LB inside the heading for LTR velocity of 2m/s

A comparison of the percentage difference in flow rates at the face of the heading for each set of cases with the difference of the flow rates at the exit of the LB for the same sets is given in Table 6.12. The percentage differences in flow rates at the exit of the LB were found to be much higher than the ones close to the face of the heading for each set.

The reason for this reduction in difference is that, when the air turned into the narrow channel between the LB and the wall of the heading from the similar channel in the LTR, most of the air gets concentrated close to the LB. When the air exited the LB, air beside moving straight also started turning inwards (towards the left wall of the heading), the air close to the LB turned first, and as the air moved farther away from the ‘LB exit’, more and more air started turning. Therefore, when the variation in flow rate at the exit was higher, the part of the air that turned before reaching the face contained more quantity of air. Furthermore, this turning of the air with 0.5m LB to wall distance, only takes place closer to the face of the heading as compared to the 1m distance, because when the air exits a narrower channel the throw is higher. Therefore, the proportion of the air exiting the LB and delivered close to the face of the heading was found to be much higher (discussed in more detail in section 6.8) when the distance of the LB from the wall was 0.5m, than, when the distance was 1m as shown in Figures 6.29 and 6.30.

Table 6.12 Percentage increase in flow rate at 9.5m deep plane and at the exit of the LB for each LTR velocity with the increase in the distance of the LB from 0.5 to 1m from the wall in the heading

| Cases | LTR velocity | | | LTR velocity | | |
|-------|---|--------|-------|--|--------|--------|
| | 1m/s | 1.5m/s | 2m/s | 1m/s | 1.5m/s | 2m/s |
| | Percentage increase in flow rate for each LTR velocity with the increase in wall distance of the LB from wall of the heading from 0.5 to 1m at the 9.5m depth plane (%) | | | Percentage increase in flow rate for each LTR velocity with the increase in distance of the LB from wall of the heading from 0.5 to 1m at the exit of LB (%) | | |
| 1-2 | 41.32 | 36.81 | 37.56 | 115.3 | 113.4 | 113.33 |
| 3-4 | 39.88 | 35.18 | 37.55 | 115.18 | 113.39 | 112.85 |
| 5-6 | 37.27 | 35.66 | 37.54 | 111.04 | 110.25 | 112.7 |
| 7-8 | 29.59 | 26.23 | 26.03 | 100.43 | 95.71 | 95.45 |
| 9-10 | 33.8 | 31.65 | 33.59 | 107.2 | 103.53 | 103.82 |
| 11-12 | 26.44 | 25.56 | 24.41 | 93.58 | 93.38 | 93.44 |
| 13-14 | 44.18 | 41.91 | 41.75 | 115.3 | 112.79 | 112.86 |
| 15-16 | 43.7 | 42.95 | 42.71 | 114.55 | 113.35 | 112.66 |
| 17-18 | 38.89 | 41.14 | 42.06 | 110.86 | 110.19 | 112.77 |
| 19-20 | 32.26 | 30.19 | 29.93 | 100.11 | 95.94 | 95.19 |
| 21-22 | 37.79 | 35.97 | 36.42 | 107.23 | 103.5 | 103.84 |
| 23-24 | 28.55 | 30.36 | 28.78 | 93.58 | 93.41 | 93.48 |

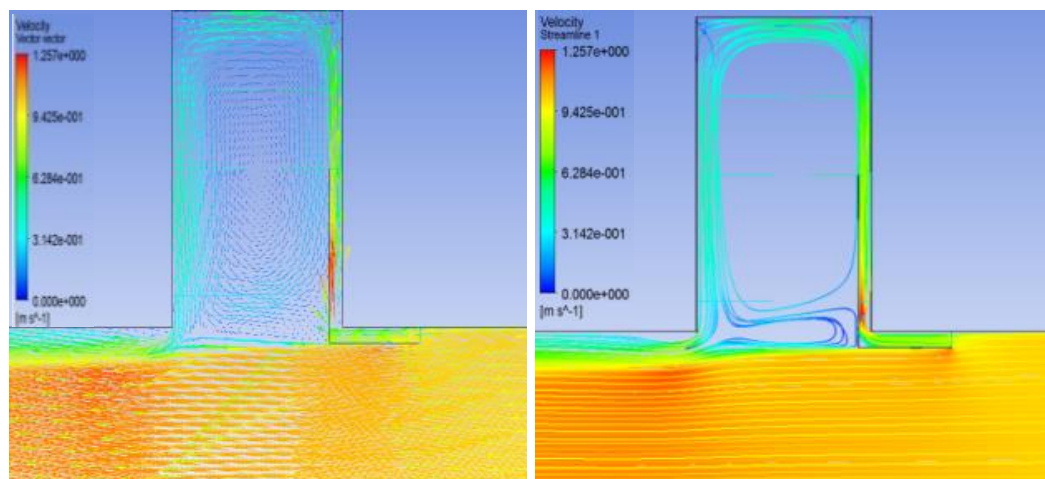


Figure 6.29 Velocity vectors and velocity stream lines (left to right) - Case 1 for 1m/s LTR velocity (0.5m distance of LB from the wall in the heading)

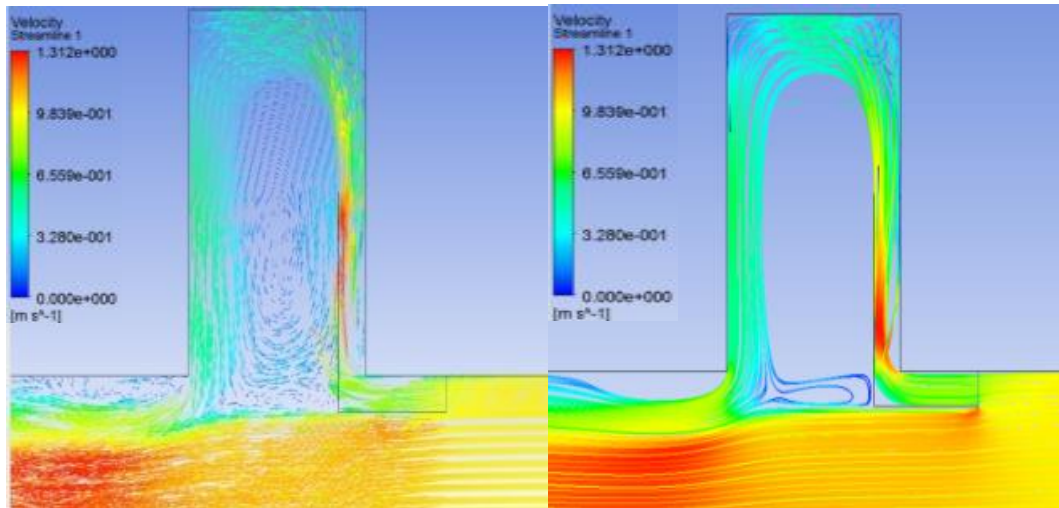


Figure 6.30 Velocity vectors and velocity stream lines (left to right) - Case 2 for 1m/s LTR velocity (1m distance of LB from the wall in the heading)

Another important observation is that, the increase in the length of LB in the heading reduced the flow rate variations at the LB exits. This reduction was found to be higher for cases with 1m distance than with 0.5m distance of the LB from the wall (minimum length is required to make this flow uniform, see section 6.8.1). The twelve sets of cases (each set has two cases with all similar conditions except for the distance of the LB from the wall in the heading of 0.5 and 1m) used for this section, were further segregated into two groups of six sets each; one with the sets of cases using longer LB in the heading (three by four the length of the heading) and the other with shorter LB (half the length of the heading) as shown in Table 6.13. A comparison of these two groups of sets showed that the percentage increase in flow rates for the set of cases with 1m and 0.5m distance from the wall in the heading was higher when a longer LB was used, (Table 6.13 and 6.14), since the impact of increase in length was more when the distance of the LB from the wall was 1m.

Table 6.13 Percentage increase in flow rate at 9.5m deep plane, for each set of cases, for each LTR velocity, with the increase in the distance of the LB from 0.5 to 1m from the wall in the heading, separately for cases using 5m long LB and 7.5m long LB

| Cases | LTR Velocity | | | Cases | LTR Velocity | | |
|-------|---|--------|-------|-------|---|--------|-------|
| | 1m/s | 1.5m/s | 2m/s | | 1m/s | 1.5m/s | 2m/s |
| | Percentage increase in flow rate for each LTR velocity with the increase in wall distance of the LB from wall of the heading from 0.5 to 1m at the 9.5m depth plane (%) | | | | Percentage increase in flow rate for each LTR velocity with the increase in wall distance of the LB from wall of the heading from 0.5 to 1m at the 9.5m depth plane (%) | | |
| 1-2 | 41.32 | 36.81 | 37.56 | 13-14 | 44.18 | 41.91 | 41.75 |
| 3-4 | 39.88 | 35.18 | 37.55 | 15-16 | 43.7 | 42.95 | 42.71 |
| 5-6 | 37.27 | 35.66 | 37.54 | 17-18 | 38.89 | 41.14 | 42.06 |
| 7-8 | 29.59 | 26.23 | 26.03 | 19-20 | 32.26 | 30.19 | 29.93 |
| 9-10 | 33.8 | 31.65 | 33.59 | 21-22 | 37.79 | 35.97 | 36.42 |
| 11-12 | 26.44 | 25.56 | 24.41 | 23-24 | 28.55 | 30.36 | 28.78 |

Table 6.14 Difference of the percentage increase in flow rates for the set of cases with 1m and 0.5m distance from the wall in the heading, between the sets with long (7.5m) and short (5m) LB

| Cases | LTR Velocity | | |
|-------------------|--|--------|------|
| | 1m/s | 1.5m/s | 2m/s |
| | Difference, first six differences with shorter LB vs next six differences with longer LB (3m high heading) (%) | | |
| %(13-14)-%(1-2) | 2.86 | 5.1 | 4.19 |
| %(15-16)-%(3-4) | 3.81 | 7.77 | 5.16 |
| %(17-18)-%(5-6) | 1.61 | 5.48 | 4.52 |
| %(19-20)-%(7-8) | 2.66 | 3.97 | 3.9 |
| %(21-22)-%(9-10) | 3.99 | 4.32 | 2.83 |
| %(23-24)-%(11-12) | 2.1 | 4.8 | 4.37 |

6.6.2 Distance of LB from the wall inside the heading - 6.6 x 4 x 10m heading

The percentage differences in the flow rates, close to the face, and at the exit of the LB, for each set of cases using LB distance of 0.5m and 1m from the wall of the heading, are given in Table Q1 and the flow rates close to the face are shown in Figure R1 through R3. The flow rates followed trends similar to the 3m high heading.

The flow rates at all the lower depth planes i.e. 1m, 5m and 7.5m in each set of case were also found higher, similar to the 3m high heading with the 1m distance of the LB from the wall in the heading for all the LTR velocities as shown in Figures S1 through S3 and Table P2.

6.6.3 Distance of LB from the wall inside the heading - 6.6 x 3 x 20m heading

The percentage differences in the flow rates, close to the face, and at the exit of the LB, for each set of cases using LB distance of 0.5m and 1m from the wall of the heading, are given in Table Q2 and the flow rates close to the face are shown in Figures R4 through R6. The flow rates followed the same trend as was for the 10m deep headings.

The flow rates at all the lower depth planes i.e. 1m, 10m and 15m in each set of case were also found higher, similar to the 10m deep headings with the 1m distance of the LB from the wall in the heading for all the LTR velocities as shown in Figures S4 through S6 and Table P3.

6.6.4 Distance of LB from the wall inside the heading - 6.6 x 4 x 20m heading

The percentage differences of the flow rates, close to the face, and at the exit of the LB, for each set of cases using LB distance of 0.5m and 1m from the wall of the heading, are given in Table Q3 and the flow rates close to the face are shown in Figures R7 through R9. The flow rates followed the same trend as was for the 3m high heading.

The flow rates at all the lower depth planes i.e. 1m, 10m and 15m in each set of case were also found higher, similar to the 3m high heading with the 1m distance of the LB from the wall for all the LTR velocities as shown in Figures S7 through S9 and Table P4.

6.6.5 Conclusion

- Bigger distance of the LB from the wall produced higher flow rates inside the heading for same LTR velocities. The flow rates changed proportionally to the change in the height of the heading and velocity of air in the LTR.
- When the air moved through the channel between the wall of the heading and the LB, the flow rate were found to be higher closer to the LB then the wall of the heading. This variation was more for bigger distance of the LB from the wall

and it decreased with the increase in the length of the LB. The effect of the increase in the length of the LB to reduce this variation was also found to be higher for bigger distance of the LB from the wall in the heading.

In the next section, the effect of the fourth system variable related to the installation of the LB i.e. change in angle of the LB in the LTR on the flow rates inside the heading is analysed and discussed.

6.7 Comparison of Air Flows, with the Change in Angle of LB in the LTR for Each LTR Velocity

The angle of the LB inside the LTR was varied to check its influence on the ventilation of the heading. LB was tested with three angles 0° , 7.5° and 15° inside the LTR to find the impact of angle within this range. For each heading dimension eight sets of cases (1-5-9, 2-6-10, 3-7-11, 4-8-12, 13-17-21...16-20-24) were simulated, where each set has a case with angle of the LB in the LTR equal to 0° , 7.5° and 15° each. The rest of the configurations are same for the three cases in a set. The introduction of the angle varied the LB inlet area; comparison of the inlet areas is already given in Table 6.3. The increase in area increased the flow rates at the exit of the LB, dictated by the factors (entrance length x distance of the LB from the wall in the heading) given in section 6.2.2.

A comparison of the flow rates close to the face of the heading and at depth planes inside the heading for each set of cases and for all the heading dimensions is discussed in this section, with emphasis, on the flow rates close to the face of the heading. The percentage difference in flow rates were calculated, to find how the flow rates changed with an increase in the angle of the LB in the LTR.

6.7.1 Angle of LB in the LTR - 6.6 x 3 x 10m heading

The percentage increase in flow rates with the increase in the angle of the LB in the LTR from 0° to 7.5° , 0° to 15° , and 7.5° to 15° , close to the face and at the exit of the LB for each set of the cases are given in Table 6.15 and Table 6.16 respectively. The comparison of flow rates for each set at the 9.5m deep plane is shown in Figures 6.31 through 6.33.

The flow rates close to the face; at the 9.5m deep increased with the increase in angle of LB in the LTR. The flow rate increased almost at similar proportions to the increase in flow rates at the exit of the LB, due to the increase in angle of the LB in the LTR for each LTR air velocity.

Table 6.15 Percentage increase in flow rates at the 9.5m deep plane with the increase in LB angle in the LTR from 0° to 7.5°, 0° to 15°, and 7.5° to 15°

| Percentage increase in flow rate at the 9.5m deep plane with the increase in LB angle in the LTR from 0° to 7.5°, 0° to 15°, and 7.5° - 15° | | | | | | | | | |
|---|---|--------|-------|--|--------|-------|--|--------|-------|
| Cases | LTR velocity | | | | | | | | |
| | 1m/s | 1.5m/s | 2m/s | 1m/s | 1.5m/s | 2m/s | 1m/s | 1.5m/s | 2m/s |
| | Percentage increase in flow rate with LB angle increase from 0° to 7.5° (%) | | | Percentage increase in flow rate with LB angle increase from 0° to 15° (%) | | | Percentage increase in flow rate with LB angle increase from 7.5° to 15° (%) | | |
| 1-5,1-9,5-9 | 29.06 | 27.62 | 28.59 | 68.3 | 65.26 | 66.93 | 30.4 | 29.5 | 29.81 |
| 2-6,2-10,6-10 | 25.37 | 26.54 | 28.58 | 59.35 | 59.02 | 62.12 | 27.1 | 25.67 | 26.09 |
| 3-7,3-11,7-11 | 65.94 | 65.39 | 66.98 | 144.9 | 141.2 | 142.2 | 47.56 | 45.82 | 45.06 |
| 4-8,4-12,8-12 | 53.73 | 54.43 | 52.99 | 121.3 | 124 | 119.1 | 43.97 | 45.05 | 43.19 |
| 13-17,13-21,17-21 | 31.59 | 28.29 | 28.65 | 68.86 | 67.24 | 67.11 | 28.32 | 30.37 | 29.9 |
| 14-18,14-22,18-22 | 26.76 | 27.59 | 28.93 | 61.37 | 60.24 | 60.83 | 27.31 | 25.6 | 24.74 |
| 15-19,15-23,19-23 | 66.86 | 66.91 | 67.33 | 144.8 | 143.2 | 142.2 | 46.68 | 45.72 | 44.75 |
| 16-20,16-24,20-24 | 53.58 | 52.02 | 52.35 | 119 | 121.8 | 118.6 | 42.57 | 45.91 | 43.46 |

Table 6.16 Percentage increase in flow rates at the exit of LB with the increase in LB angle in the LTR from 0° to 7.5°, 0° to 15°, and 7.5° to 15°

| Percentage increase in flow rate at the exit of LB with the increase in LB angle in the LTR from 0° to 7.5°, 0° to 15°, and 7.5° - 15° | | | | | | | | | |
|--|---|--------|-------|--|--------|-------|--|--------|-------|
| Cases | LTR velocity | | | | | | | | |
| | 1m/s | 1.5m/s | 2m/s | 1m/s | 1.5m/s | 2m/s | 1m/s | 1.5m/s | 2m/s |
| | Percentage increase in flow rate with LB angle increase from 0° to 7.5° (%) | | | Percentage increase in flow rate with LB angle increase from 0° to 15° (%) | | | Percentage increase in flow rate with LB angle increase from 7.5° to 15° (%) | | |
| 1-5,1-9,5-9 | 30.35 | 28.4 | 28.68 | 68.22 | 67.15 | 67.05 | 29.06 | 30.18 | 29.81 |
| 2-6,2-10,6-10 | 27.77 | 26.51 | 28.31 | 61.9 | 59.42 | 59.61 | 26.71 | 26.01 | 24.39 |
| 3-7,3-11,7-11 | 65.42 | 65.68 | 67.12 | 144 | 141.8 | 142.2 | 47.48 | 45.95 | 44.93 |
| 4-8,4-12,8-12 | 54.08 | 51.96 | 53.46 | 119.5 | 119.1 | 120.1 | 42.44 | 44.21 | 43.44 |
| 13-17,13-21,17-21 | 30.35 | 28.23 | 28.74 | 68.26 | 66.97 | 67.3 | 29.08 | 30.2 | 29.95 |
| 14-18,14-22,18-22 | 27.66 | 26.67 | 28.69 | 61.95 | 59.68 | 60.21 | 26.86 | 26.06 | 24.49 |
| 15-19,15-23,19-23 | 65.56 | 65.9 | 67.39 | 143.9 | 142.2 | 142.3 | 47.34 | 45.98 | 44.76 |
| 16-20,16-24,20-24 | 54.42 | 52.36 | 53.65 | 120.1 | 119.6 | 120.5 | 42.53 | 44.1 | 43.48 |

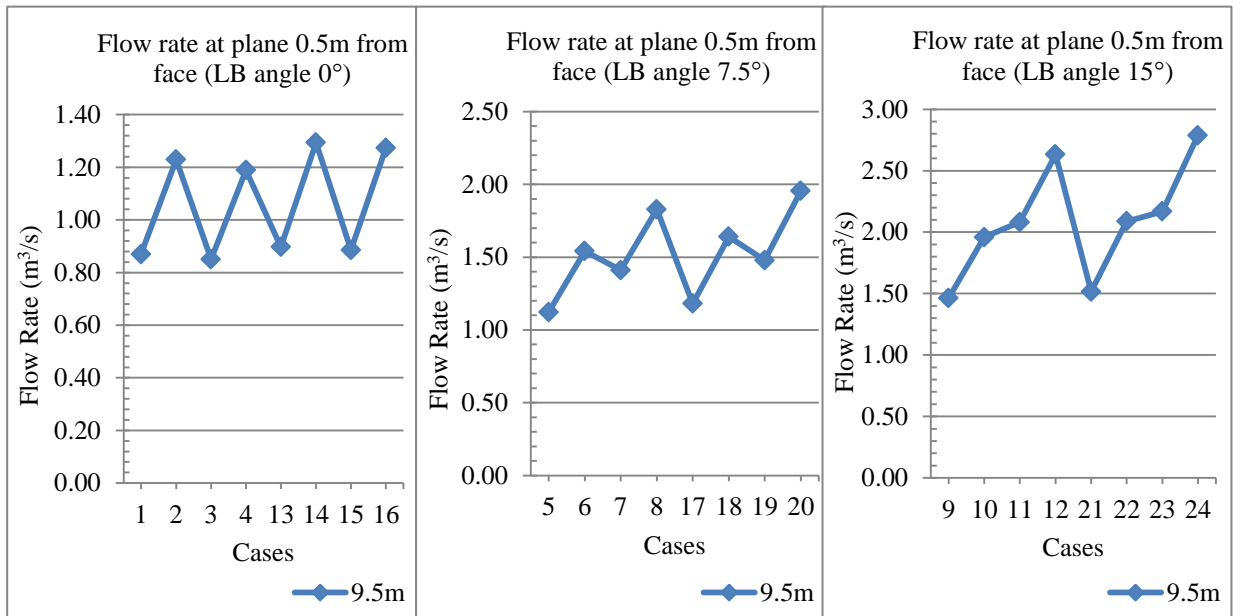


Figure 6.31 Flow rates at 9.5m deep plane using 0°, 7.5° and 15° LB inside the LTR for LTR velocity of 1m/s

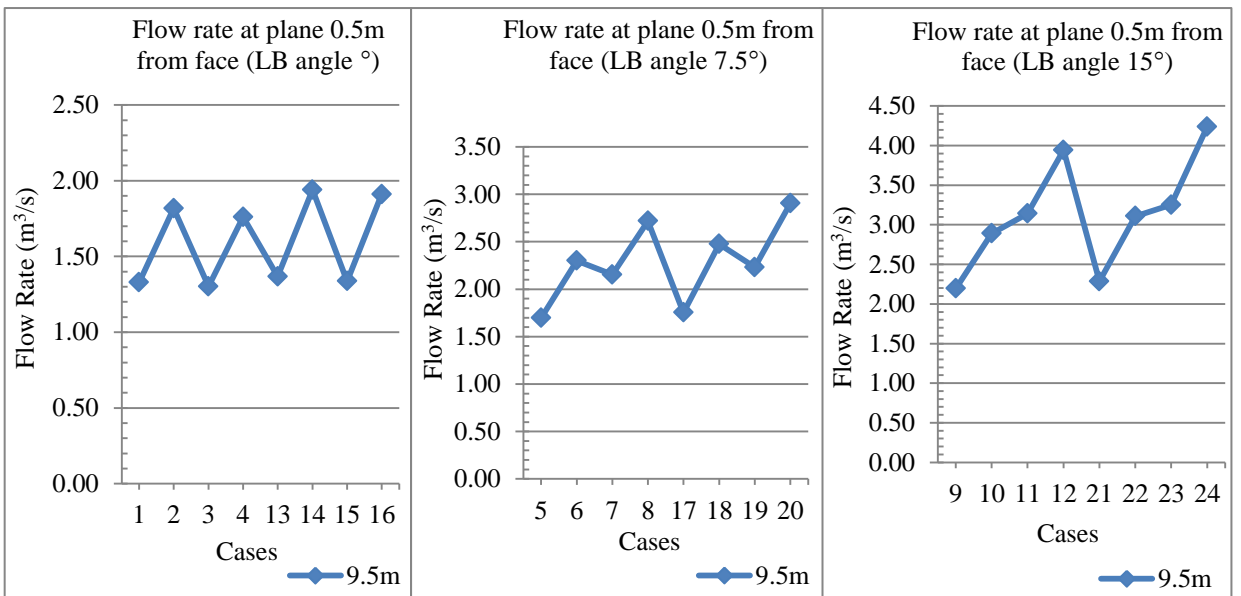


Figure 6.32 Flow rates at 9.5m deep plane using 0°, 7.5° and 15° LB inside the LTR for LTR velocity of 1.5m/s

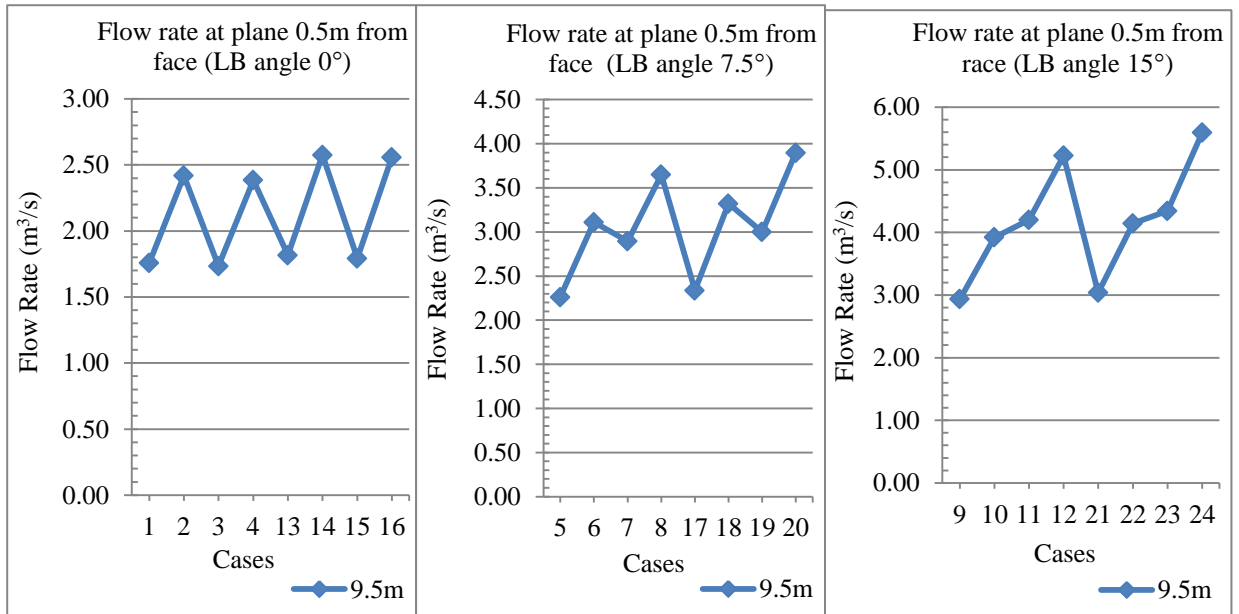


Figure 6.33 Flow rates at 9.5m deep plane using 0°, 7.5° and 15° LB inside the LTR for LTR velocity of 2m/s

The flow rates at all the lower depth planes i.e. 1m, 5m and 7.5m deep were also found to be higher for each set of cases with a higher angle of the LB in the LTR, and for all LTR velocities as shown in Figures 6.34 through 6.36 and Table T1.

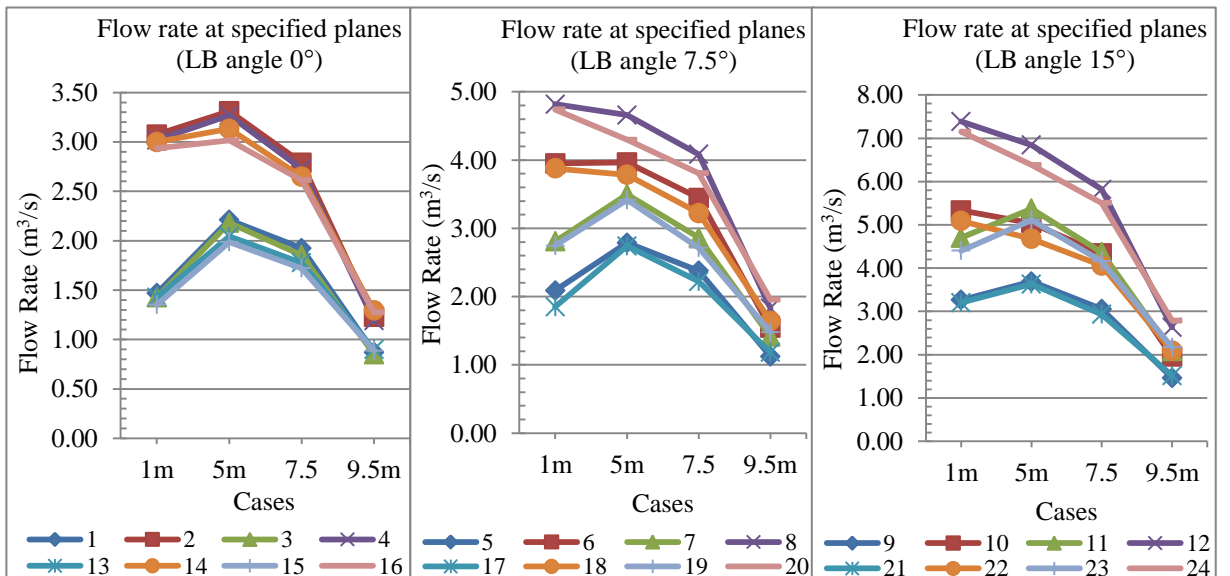


Figure 6.34 Flow rates at specified planes using 0°, 7.5° and 15° LB inside the LTR for LTR velocity of 1m/s

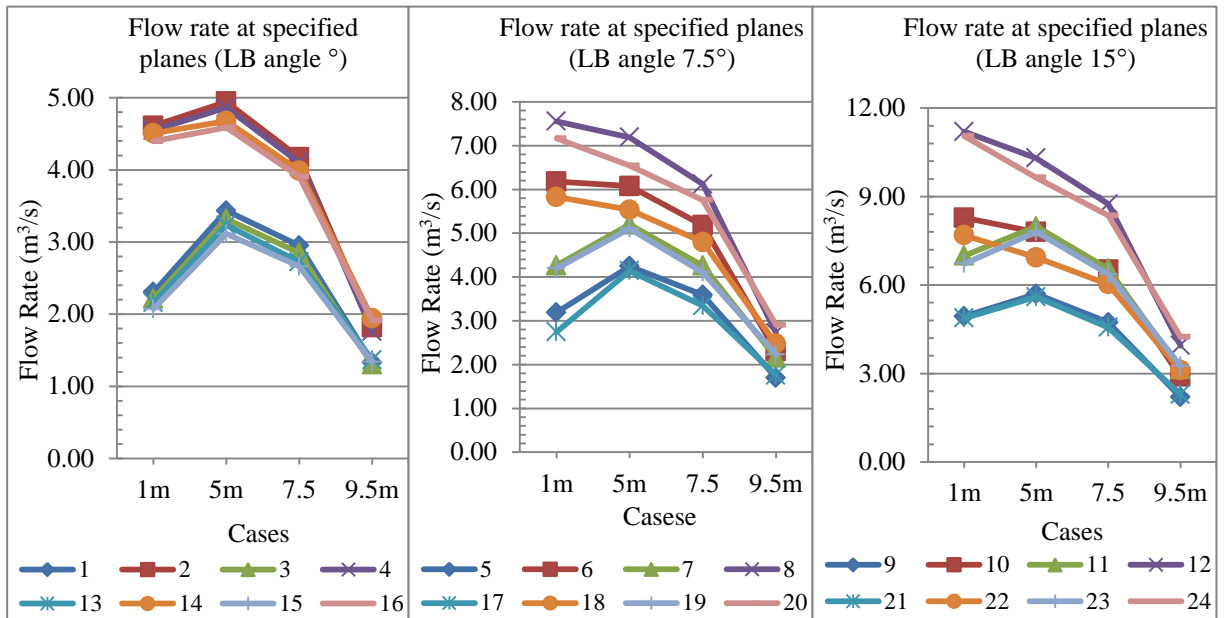


Figure 6.35 Flow rates at specified planes using 0°, 7.5° and 15° LB inside the LTR for LTR velocity of 1.5m/s

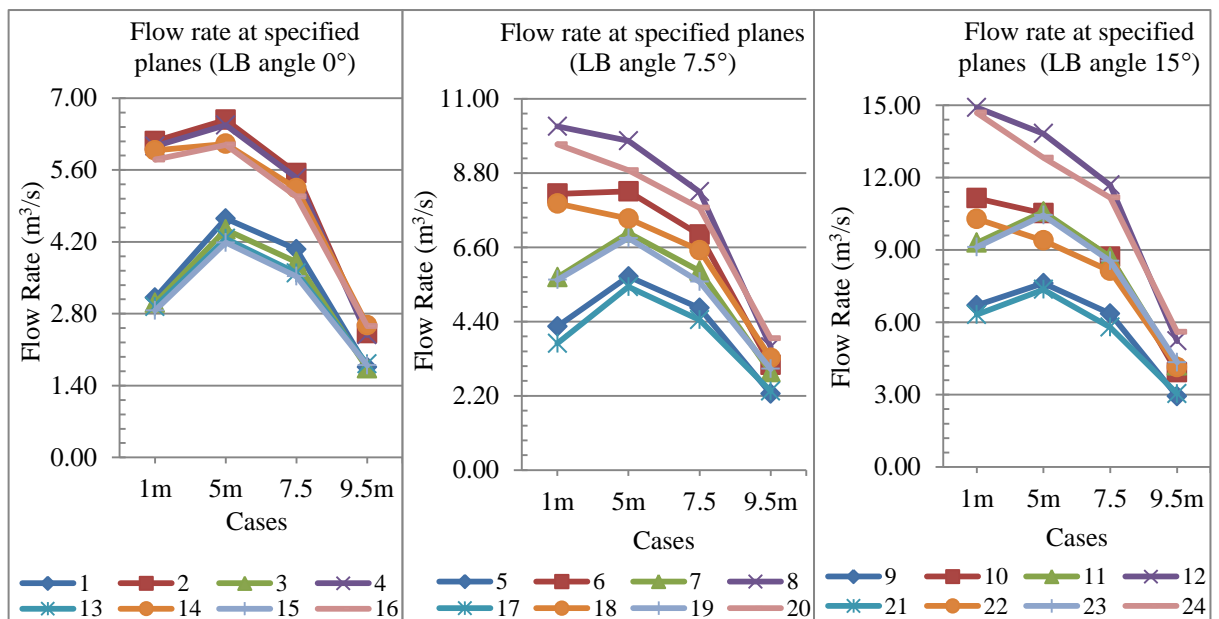


Figure 6.36 Flow rates at specified planes using 0°, 7.5° and 15° LB inside the LTR for LTR velocity of 2m/s

6.7.2 Angle of LB in the LTR - 6.6 x 4 x 10m heading

The percentage difference in the flow rates close to the face and at the exit of the LB between the cases using LB with 0°, 7.5° and 15° for each set of this heading dimension are given in Tables U1 and U2. The comparison of flow rates at the 9.5m deep plane is shown in Figures V1 through V3. The comparison of flow rates at all the specified planes are given in Figures W1 through W3 and Table T2. The flow trends were found similar to the 3m high heading.

6.7.3 Angle of LB in the LTR - 6.6 x 3 x 20m heading

The percentage difference of the flow rates close to the face and at the exit of the LB between the cases using LB with 0°, 7.5° and 15° for each set of this heading dimension are given in Tables U3 and U4. The comparison of flow rates at the 19.5m deep plane is shown in Figures V4 through V6. The comparison of flow rates at all the specified planes are given in Figures W4 through W6 and Table T3. The flow trends were found similar to the 10m deep headings.

6.7.4 Angle of LB in the LTR - 6.6 x 4 x 20m heading

The percentage difference of the flow rates close to the face and at the exit of the LB between the cases using LB with 0°, 7.5° and 15° for each set of this heading dimension are given in Tables U5 and U6. The comparison of flow rates at the 19.5m deep plane are shown in Figures V7 through V9. The comparison of flow rates at all the specified planes are given in Figures W7 through W9 and Table T4. The flow trends were found similar to the 3m high headings.

6.7.5 Conclusion

The flow rates close to face, and at all the depth planes inside the heading, increased with the increase in the angle of the LB in the LTR. The increase in flow rates at the face of the heading was proportional to the increase in flow rates at the exit of the LB for all the heading dimensions and LTR velocities. To increase flow rates close to the face of the heading, LB with an appropriate angle can be a better solution than using LB with LB to wall distance higher than 1m (unless it is supplemented with additional engineering solutions). The narrow LB to wall distance in the heading will ensure that

most of the air exiting the LB reaches the face. Further discussion on the impact of angle on the flow rates close to the face of the heading is covered in the next section (6.8).

In the next section, a mathematical model is presented to estimate the flow rates close to the face of the heading. This is done using the findings of the discussion and analysis given above and after further deliberation, on the effect of the system variables associated with the LB ventilation system, in particular on the flow rates close to the face of the heading.

6.8 Flow Rate Estimation at the Face of the Heading

A number of factors besides the LTR velocity, height of the heading affect the flow rates close to the face of the heading (0.5m away from face), which are given below:

- The length of the LB in the LTR and the heading.
- Angle of the LB in the LTR, the inlet length at the entrance of the LB.
- Distance of the LB from the wall in the heading. (Dictates the amount of reduction in area of the channel between the LB and the wall, at the entrance of the heading from a bigger area at the inlet, when LB is used with an angle).
- Distance of the LB from the face of the heading.

In the formulation of a mathematical model for the estimation of flow rates at the exit of the LB (section 6.2), it was seen that the product of the entrance length and the distance of the LB from the wall in the heading was proportional to the flow rates at the exit of the LB (for the 10 cases that were used). However, the flow rates close to the face of the heading for those standard cases did not show this proportionality. Therefore, a comparison of the flow rates at the exit of the LB and the face of the heading for the standard cases was carried out as shown in Table 6.17. The comparison showed that the difference in the flow rates for cases (2, 4, 6, 8, 10, and 12) with 1m distance of the LB from the wall is around 67% and 9% for cases (1, 3, 5, 7, 9, and 11) with 0.5m distance. To cater for this, and to keep the calculations simple, a factor equivalent to 1 with 0.5m distance of the LB from the wall in the heading and 0.55 for 1m distance was used to develop the initial mathematical model. This resulted in a linear relation between the two plotted parameters (flow rates of these ten cases, and the product of entrance of the LB (X), distance of the LB from the wall in the heading (b) and a factor F_{LB} = Factor for LB ventilation system) as shown in Table 6.18 and Figure 6.37. The product of the X and b addressed the flow rate at the exit of the LB and the factor addressed the effects of variation in flow rate concentration at the exit of LB. The expression of the trend line for this linear relation is given in equation 6.9.

Table 6.17 Percentage difference in flow rate at the exit of the LB and close to the face of the heading

| Case | LB exit flow rate | Flow rate at 0.5m from face | Percentage difference in flow rate at the exit of the LB and 0.5m from face with respect to flow rate at 0.5m from face |
|------|---------------------|-----------------------------|---|
| | (m ³ /s) | (m ³ /s) | (%) |
| 1 | 0.944 | 0.870 | 8.48 |
| 2 | 2.032 | 1.229 | 65.27 |
| 3 | 0.930 | 0.850 | 9.40 |
| 4 | 2.002 | 1.189 | 68.29 |
| 5 | 1.230 | 1.123 | 9.57 |
| 6 | 2.596 | 1.541 | 68.44 |
| 7 | 1.539 | 1.411 | 9.06 |
| 8 | 3.084 | 1.828 | 68.67 |
| 9 | 1.587 | 1.464 | 8.44 |
| 10 | 3.289 | 1.959 | 67.92 |
| 11 | 2.269 | 2.082 | 9.00 |
| 12 | 4.393 | 2.632 | 66.87 |

Table 6.18 Flow rate at the face of the heading (0.5m from face) vs product of factor, X and b

| Case | Entrance length of LB (X) | LB distance from wall in heading (b) | X x b | F _{LB} | F _{LB} x X x b | Flow rate at face (FRF _{LB}) |
|------|---------------------------|--------------------------------------|-------------------|-----------------|-------------------------|--|
| | (m) | (m) | (m ²) | - | (m ²) | (m ³ /s) |
| 1 | 0.5 | 0.5 | 0.25 | 1 | 0.25 | 0.87 |
| 5 | 0.96 | 0.5 | 0.48 | 1 | 0.48 | 1.12 |
| 2 | 1 | 1 | 1 | 0.55 | 0.55 | 1.23 |
| 7 | 1.36 | 0.5 | 0.68 | 1 | 0.688 | 1.41 |
| 9 | 1.44 | 0.5 | 0.72 | 1 | 0.72 | 1.46 |
| 6 | 1.52 | 1 | 1.52 | 0.55 | 0.84 | 1.54 |
| 8 | 1.92 | 1 | 1.92 | 0.55 | 1.056 | 1.83 |
| 10 | 2.07 | 1 | 2.07 | 0.55 | 1.14 | 1.96 |
| 11 | 2.42 | 0.5 | 1.21 | 1 | 1.21 | 2.08 |
| 12 | 2.87 | 1 | 2.87 | 0.55 | 1.58 | 2.63 |

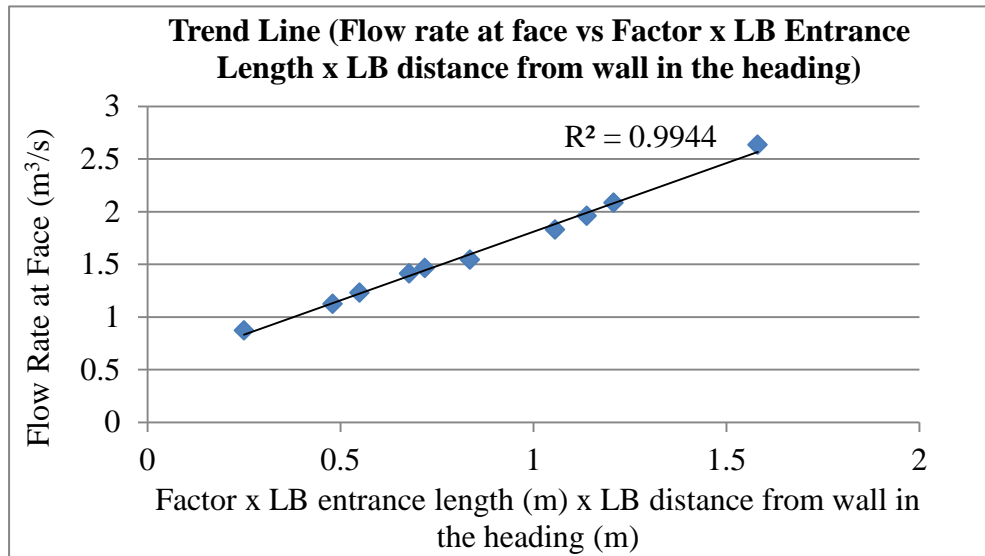


Figure 6.37 Trend line of air flow rate at the face of the heading (0.5m distance from face)

$$\text{Flow rate close to the face} = \text{FRF}_{\text{LB}} = 1.30 \times F_{\text{LB}} \times X \times b + 0.51 \quad (6.9)$$

However, equation 6.9 can only be used to estimate the flow rate close to the face of the heading for the ten cases given used to develop this preliminary model. To find an expression that could be used for any heading height, LTR velocity and a range of LB settings encompassed with the boundaries of this study, further deliberation upon the effects of the following factors on the flow rates close to the face of the heading was carried out. This is discussed in the ensuing paragraphs of this section.

- Change in the LTR velocity
- Change in the height of the heading
- Change in the length and angle of LB in the LTR.
- Length of the LB in the heading distance from the face

6.8.1 Effect of the change in velocity

As already discussed in section 6.3, the average percentage increase in the flow rates close to the face with the increase in LTR velocity for all the heading dimensions was approximately equal to the corresponding percentage increase in the LTR velocities (maximum deviation in the average difference of less than 2%).

6.8.2 Effect of the change in heading height

The percentage increase in the flow rates close to the face with the increase in height of the heading that is 6.6 x 3 x 10m vs 6.6 x 4 x 10m and 6.6 x 3 x 20m vs 6.6 x 4 x 20m are given in Figures 6.38 and 6.39 respectively. The results showed that the average percentage increase in flow rates was approximately equal to the corresponding percentage increase in the height of the heading (maximum average difference of less than 1%).

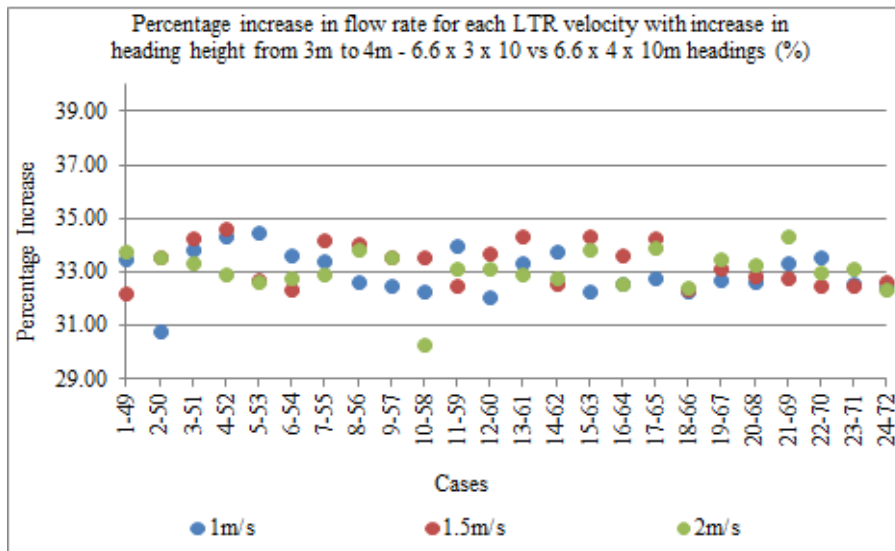


Figure 6.38 Percentage increase in flow rates close to the face for each LTR velocity with the increase in heading height from 3m to 4m - 6.6 x 3 x 10m vs 6.6 x 4 x 10m headings

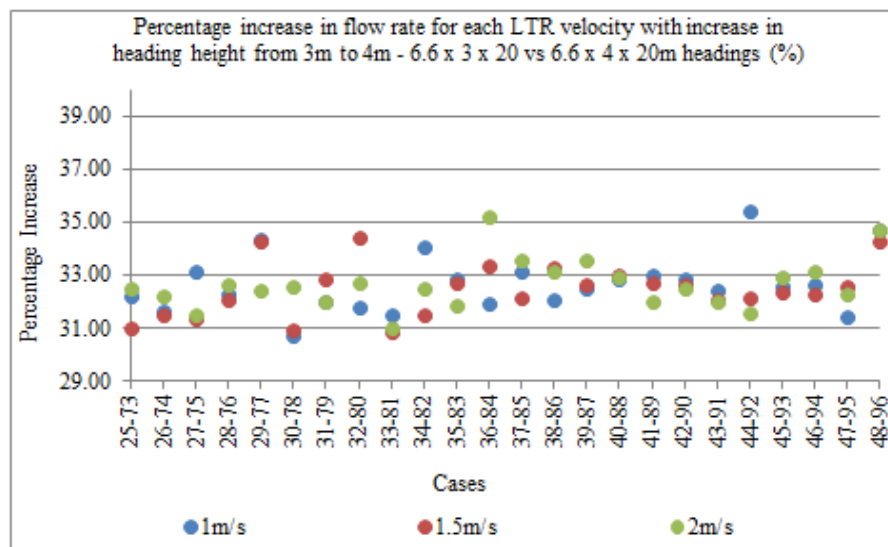


Figure 6.39 Percentage increase in flow rates close to the face for each LTR velocity with the increase in heading height from 3m to 4m - 6.6 x 3 x 20m vs 6.6 x 4 x 20m headings

6.8.3 Effect of the length and angle of LB in the LTR

The effect of the change in length and angle of the LB in the LTR for LB used with an angle is already catered for in equation 6.9 by using the product of the entrance length and distance of the LB from the wall in the heading. The viscous effect due to the increase in length of LB in the LTR when used with zero angles was calculated by comparing the flow rates of the set of cases with different LB lengths in LTR and similar remaining settings as shown in Table 6.19. It was found that the flow rate on average decreased at the rate of 0.61% per 1m increase in length of LB. This was approximated as “1% decrease per 2m increase in the length of LB” for simplicity of calculations.

Table 6.19 Percentage decrease in flow rate close to face with the increase in length of LB from 3 to 6m in the LTR for zero angled LB

| Cases | LTR velocity | | |
|------------------------------------|--|--------|-------------|
| | 1m/s | 1.5m/s | 2m/s |
| | Percentage decrease in flow rate at the exit of LB for each LTR velocity with the increase in length of LB from 3 to 6m in the LTR (%) | | |
| 1-3 | 2.25 | 2.00 | 1.38 |
| 2-4 | 3.25 | 3.17 | 1.38 |
| 25-27 | 2.10 | 1.60 | 1.78 |
| 26-28 | 1.96 | 2.84 | 1.24 |
| 49-51 | 1.98 | 0.51 | 1.70 |
| 50-52 | 0.62 | 2.43 | 1.89 |
| 73-75 | 1.41 | 1.34 | 2.51 |
| 74-76 | 1.49 | 2.39 | 0.94 |
| Percentage average decrease | | | 1.84 |

6.8.4 Effect of the length of LB in heading and distance from face

The length of LB inside the heading used in the standard cases was 5m with 4.5m distance of the LB exit from close to face (0.5m away from face) of heading. The effect of change in this length of LB and distance from the face was ascertained by comparing the standard cases with the cases of the 20m deep heading (group 2 with similar heading height of 3m, for details of group refer to Table 6.2). A comparison of the lengths and distances from face of LB, between the standard and cases from group 2, is given in

Table 6.20. In the cases of group 2 when a 15m long LB was used the distance of the LB from the face was 4.5m similar to the standard cases. Therefore, a comparison between these cases of group 2 and the standard cases was done to capture the effect of the change in length of the LB. This was then used to find the effect of the distance of the LB from the face by comparing the standard cases with the cases of group 2 where a 10m long LB was used.

Table 6.20 Difference of LB lengths and distances from the face for the 10m long heading with 5m LB and the 20m long heading

| Cases | Length of LB in heading (m) | Distance of LB 0.5m short from the face (m) | Difference-Length of LB in heading with Case 1-12 (m) | Difference-Distance of LB 0.5m short from the face with Case 1-12 (m) |
|----------|-----------------------------|---|---|---|
| 37 to 48 | 15 | 4.5 | 10 | 0 |
| 25to 36 | 10 | 9.5 | 5 | 5 |

As already seen in sections 6.4 and 6.6 that the air flow concentration at the exit of the LB is not uniform, and the air is more concentrated close to the LB. It has also been seen that the air at the exit of the LB was more evenly dispersed when its distance from the wall was less, as this distance increased the concentration of air close to the LB increased. However, as the length of the LB increased in the heading the air flow in the channel between the LB and the heading wall became more uniform. In order to find this length it was important to calculate the effect of increase in the length of the LB in the heading. Therefore, before finding the effects of the change in length and distance of the LB from the face, the minimum length of LB required to achieve an evenly distributed air flow at the exit of the LB was found for each distance of the LB from the wall of the heading as given below:

Minimum length of LB to neutralize the variation in flow rates at the exit of LB

To find these lengths, and to quantify the effect of the increase in length of the LB in the heading on this flow rate reduction, cases with 0.5m and 1m wall distance from the long heading with 15m long LB (maximum for this study) were analysed. This was done by constructing equally spaced eleven vertical planes inside the channel between the LB and the wall of the heading. The first plane was constructed at a depth of 5m. These

vertical planes were split into two halves equal to 0.25m and 0.5m each for the 0.5m and 1m wall distances respectively, and flow rate through these halves at each depth was calculated. Approximately, similar results were found for each category (0.5m wall distance and 1m wall distance) of cases from group 2. Therefore, only one case from each category is presented here i.e. Case 37 with 0.5m wall distance and Case 38 with 1m distance. The rest of the configurations are the same for both the cases. The detailed results are given in Tables 6.21 and 6.22. For Case 38 (1m wall distance), it was found that the difference in flow rates was around 50% at the 6m depth, this reduced to approximately 5% at the depth of 15m. The difference in flow rates between the two halves of the planes constructed for Case 37 (0.5m wall distance) was very low around 5% even at the 6m depth, and it almost became zero at the depth of 10m (or LB length of 10m). To visualize the impact of length on the air flow variations, the velocity vectors at depths of 5 to 15m are shown in Figures 6.40 and 6.41 for both the cases. It can be seen that the increase in length of LB had a bigger effect when the distance of the LB from the wall was 1m (since the flow rate were already very uniform with 0.5m distance).

Table 6.21 Comparison of the flow rate between two halves of the “LB-wall channel” in the heading - Case 38 with 1m/s LTR velocity

| Planes | Half close to wall | Half close to LB | Percentage difference between two halves | Percentage difference of the two immediate percentage differences at column 4 |
|---------------------------|--------------------|------------------|--|---|
| | | | (%) | |
| 6m | 0.784 | 1.159 | 47.83 | - |
| 7m | 0.825 | 1.119 | 35.64 | 25.50 |
| 8m | 0.855 | 1.089 | 27.37 | 23.20 |
| 9m | 0.881 | 1.064 | 20.77 | 24.10 |
| 10m | 0.9 | 1.045 | 16.11 | 22.44 |
| 11m | 0.916 | 1.031 | 12.55 | 22.07 |
| 12m | 0.928 | 1.02 | 9.91 | 21.03 |
| 13m | 0.937 | 1.011 | 7.90 | 20.34 |
| 14m | 0.945 | 1.005 | 6.35 | 19.61 |
| 15m | 0.947 | 1.003 | 5.91 | 6.86 |
| Average Difference | | | | 20.57 |

Table 6.22 Comparison of the flow rate between two halves of the “LB - wall channel” in the heading - Case 37 with 1m/s LTR velocity

| Planes | Half close to wall | Half close to LB | Percentage difference between two halves | Percentage difference of the two immediate percentage differences at column 4 |
|---------------------------|--------------------|------------------|--|---|
| 6m | 0.421 | 0.446 | 5.89 | |
| 7m | 0.428 | 0.442 | 3.18 | 46.1 |
| 8m | 0.432 | 0.439 | 1.66 | 47.65 |
| 9m | 0.435 | 0.438 | 0.71 | 57.38 |
| 10m | 0.437 | 0.438 | 0.15 | 78.37 |
| Average Difference | | | | 57.38 |

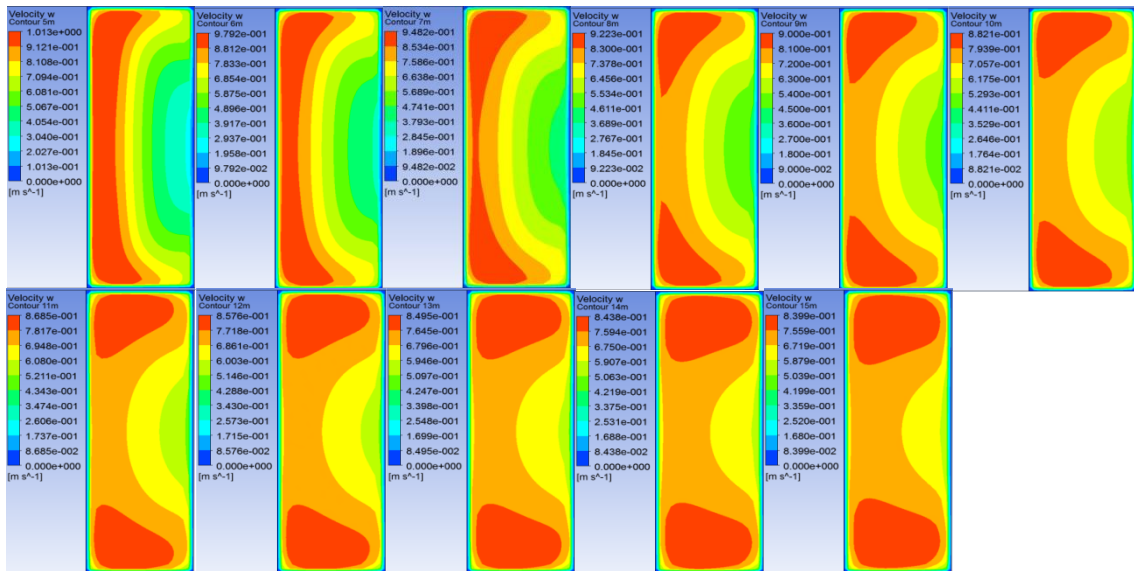


Figure 6.40 Axial velocity contours at 5 to 15m length of the LB for Case 38 (1 m LB wall distance)

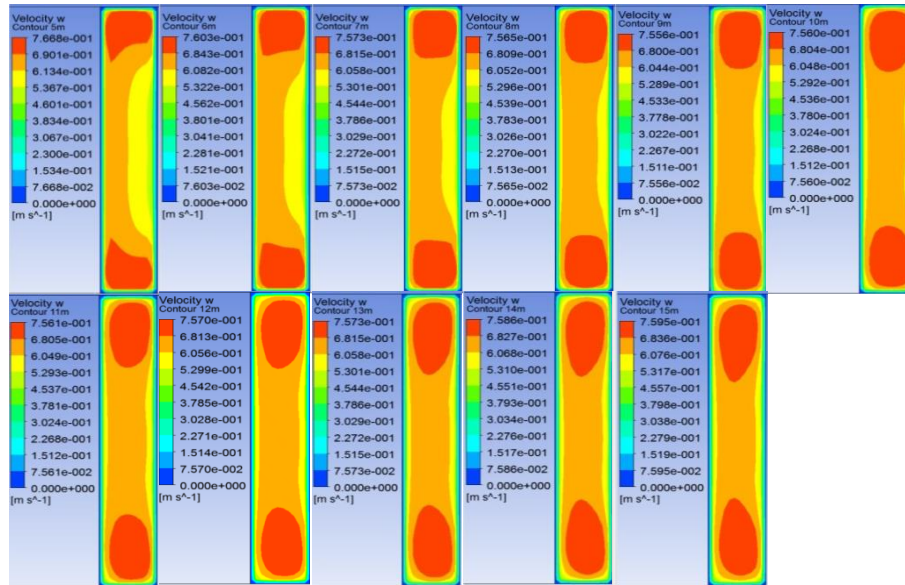


Figure 6.41 Axial velocity contours at 5 to 15m length of the LB for Case 37 (0.5m LB wall distance)

Therefore, it was concluded/assumed that for air flow in the channel between the LB and wall of the heading to become uniform (negligible difference in the flow rates between the two halves at LB exit), a minimum lengths of LB is required. This length was found to vary with the distance of the LB from the wall in the heading, and was found to be “15m and 10m for the 1m and 0.5m distance of LB from the wall of heading respectively”. “So an increase of 0.1m LB wall distance from 0.5m requires an additional length of 1m over the 10m length of LB to evenly disperse the air flow at the exit of the LB”.

In Tables 6.21 and 6.22 the percentage decrease rate, i.e. how the difference was decreasing with each metre increase in length of the LB is also given (percentage difference of the two immediate percentage differences). The average decrease rate for Case 38 was approximately 20% and for Case 37 was approximately 57%. The decrease rate for the case with 0.5m wall distance although were higher, but the overall effect on the difference in magnitude of the flow rates of the two halves of the planes (constructed in the channel between the LB and wall of the heading) were much higher for the 1m wall distance.

- **Factor for length of LB in heading**

The distance of LB from the face of the heading is same equal to 4.5m for the standard case and the Cases 37 to 48 of group 2 (15m long LB) (Table 6.20). Therefore, a comparison of these cases was used to calculate the effect of the length of LB. The percentage difference, between the flow rates at the face of the heading, for these set of cases was calculated and is given in Table 6.23. The average differences between the set of cases with 5m LB and 15m LB (from 10m and 20m headings) and other similar configurations was found approximately equal to 2.25% when the distance of the LB from the wall in the heading was 0.5m and 9.16% for 1m distance.

Table 6.23 Percentage difference in flow rate (0.5m from the face) 10m heading vs 20m heading with 5 and 15 m LB in heading, separately for LB wall distance of 0.5m and 1m - 1m/s LTR velocity

| Cases | Flow rate (0.5m from face) | Cases | Flow rate (0.5m from face) | Percentage difference of flow rate (0.5m from the face) 10m heading vs 20m heading with 5 and 15 m LB in heading (%) | |
|---------------------------|----------------------------------|-------|----------------------------------|---|-------------------------------------|
| | (m ³ /s) | | (m ³ /s) | LB distance from heading wall 0.5m | LB distance from heading wall 1m |
| 37 | 0.880 | 1 | 0.880 | 1.240 | |
| 38 | 1.355 | 2 | 1.229 | | 9.270 |
| 39 | 0.870 | 3 | 0.850 | 2.314 | |
| 40 | 1.312 | 4 | 1.1893 | | 9.350 |
| 41 | 1.155 | 5 | 1.123 | 2.800 | |
| 42 | 1.721 | 6 | 1.541 | | 10.400 |
| 43 | 1.444 | 7 | 1.411 | 2.270 | |
| 44 | 2.003 | 8 | 1.828 | | 8.740 |
| 45 | 1.489 | 9 | 1.464 | 1.690 | |
| 46 | 2.187 | 10 | 1.959 | | 10.440 |
| 47 | 2.150 | 11 | 2.082 | 3.160 | |
| 48 | 2.822 | 12 | 2.632 | | 6.720 |
| Average difference | | | | 2.250 | 9.160 |

This increase in flow rate was only caused by the difference in the length of the LB. As already seen in Tables 6.21 and 6.22 that the average decrease rate per metre increase in the length of LB; between the percentages differences of the

halves of the LB exit were equal to 20% and 57% for case with LB wall distance of 1m and 0.5m respectively. Therefore, it was concluded that the effect of increase in length of the LB from the standard 5m length should be an incremental factor, changing at the rates given above. These incremental factors for each metre increase in length of LB from the 5m length were calculated in Tables 6.24 and 6.25 for cases with 1m and 0.5m distance of the LB from the wall of the heading. Where, the average percentage difference in flow rates close to the face of the heading with 5m and 15m long LB's were equated using the incremental factors. The incremental factor was calculated up to a difference of 10m (15m length of LB) for 1m distance of LB from the wall of the heading and 5m (10m length of LB) for 0.5m distance (to cater for the effect of flow rate variations at the exit of the LB, see Tables 6.21 and 6.22). The increment was found equal to 2% for the 1st metre increase in length of the LB in the heading (from 5m of standard cases) for 1m LB to wall distance and 1% for the 0.5m distance. For further increase in length this percentage was incremented at rate of 80% and 43% of the previous increment for the 1m and 0.5m wall distances respectively. The summarized instructions to use this incremental factor to cater for the length of the LB in the heading are given in section 6.8.3.

Table 6.24 Incremental percentage increase in flow rate due to the increase in length of the LB from 5m (wall distance 1m)

| Case 1-12 vs Cases 37-48 with LB distance of 1m from wall of heading | | | |
|--|--|---|--|
| Increase in LB length from 5m | Percentage incremental effect with each metre increase in length | Cumulative percentage increase for corresponding increase in the length of LB from 5m | Remarks |
| 1 | 2.000 | 2.000 | The effect is decreasing at the rate of 20% from the previous metre increase in length |
| 2 | 1.600 | 3.600 | |
| 3 | 1.280 | 4.880 | |
| 4 | 1.020 | 5.904 | |
| 5 | 0.820 | 6.723 | |
| 6 | 0.655 | 7.378 | |
| 7 | 0.524 | 7.903 | |
| 8 | 0.419 | 8.322 | |
| 9 | 0.335 | 8.659 | |
| 10 | 0.268 | 8.926 | |
| Total increase | 8.926 | | |

Table 6.25 Incremental percentage increase in flow rate due to the increase in length of the LB from 5m (wall distance 0.5m)

| Case 1-12 vs Cases 37-48 with LB distance of 0.5m from wall of heading | | | |
|--|--|---|---|
| Increase in LB length from 5m | Percentage incremental effect with each metre increase in length | Cumulative percentage increase for corresponding increase in the length of LB from 5m | Remarks |
| 1 | 1.000 | 1.000 | The effect is decreasing at the rate of 57% from the previous metre increase in length. |
| 2 | 0.430 | 1.430 | |
| 3 | 0.185 | 1.615 | |
| 4 | 0.079 | 1.694 | |
| 5 | 0.034 | 1.729 | |
| Total increase | 1.7286 | | |

- **Distance of LB from face**

As discussed in Table 6.20 both the length of the LB and the distance from the face of the heading are different for the standard cases and the cases of group 2 using 10m long (cases 25-36) headings. Therefore, these cases were used to estimate the effect of the distance of the LB from the face of the heading. The difference in flow rate close to the face between these twelve set of cases is given in Table 6.26. The average difference was approximately -1% when distance of the LB from the wall in the heading was 0.5m and 5% for 1m distance.

Table 6.26 Percentage difference in flow rate (0.5m from the face) 10m heading vs 20m heading with 5m and 10 m LB in heading, separately for LB wall distance of 0.5m and 1m - 1m/s LTR velocity

| Cases | Flow rate (0.5m from face) | Cases | Flow rate (0.5m from face) | Percentage difference in flow rates (0.5m from the face) 10m heading vs 20m heading with 5 and 10 m LB in heading (%) | |
|---------------------------|----------------------------------|-------|----------------------------------|--|-------------------------------------|
| | (m ³ /s) | | (m ³ /s) | LB distance from heading wall 0.5m | LB distance from heading wall 1m |
| 25 | 0.859 | 1 | 0.870 | -1.278 | |
| 26 | 1.275 | 2 | 1.229 | | 3.572 |
| 27 | 0.841 | 3 | 0.850 | -1.127 | |
| 28 | 1.250 | 4 | 1.189 | | 4.888 |
| 29 | 1.110 | 5 | 1.123 | -1.104 | |
| 30 | 1.646 | 6 | 1.541 | | 6.366 |
| 31 | 1.405 | 7 | 1.411 | -0.420 | |
| 32 | 1.951 | 8 | 1.828 | | 6.311 |
| 33 | 1.451 | 9 | 1.464 | -0.896 | |
| 34 | 2.061 | 10 | 1.959 | | 4.959 |
| 35 | 2.059 | 11 | 2.082 | -1.105 | |
| 36 | 2.747 | 12 | 2.632 | | 4.194 |
| Average difference | | | | -0.988 | 5.048 |

When, the distance from the exit of the LB to the face increased beyond 4.5m (standard case distance), the increase in travelling distance added additional frictional effect (between air and wall of the heading), reducing the quantity of air reaching the face. A percentage reduction of 1% in flow rate per 2m increase in this distance was assumed. Using this consideration along with the previous considerations for length of the LB the estimated flow rates were calculated for the set of cases with LB distance of 1m from the wall of heading and with 0.5m distance as shown in Tables 6.27 and 6.28 respectively.

Table 6.26 Incremental percentage increase /decrease in flow rate due to the difference in the length of the LB and LB exit distance from the face from the standard cases (1st 12 cases) - 1m wall distance

| Case 1-12 vs Cases 25-36 with LB distance of 1m from wall of heading | | | | | |
|--|--|--|---|--------------|--|
| Increase in LB length from 5m | Percentage incremental effect with each metre increase in length | Increase in LB face distance from 4.5m | Percentage incremental effect with each metre increase distance from face | Net increase | Remarks |
| 1 | 2.00 | 1 | 5/2 | 4.22% | Net increase include the effect of increase in length of LB and increase in distance from the face |
| 2 | 1.60 | 2 | | | |
| 3 | 1.28 | 3 | | | |
| 4 | 1.02 | 4 | | | |
| 5 | 0.82 | 4.5 | | | |
| Total increase | 6.72% | Total decrease | -2.50% | | |

Note: - The average net increase as shown in Table 6.25 should be around 5%, and the net increase with the approximations used in the mathematical model is about 4.22%.

Table 6.27 Incremental percentage increase /decrease in flow rate due to the difference in the length of the LB and LB exit distance from the face from the standard cases (1st 12 cases)- 0.5 wall distance

| Case 1-12 vs Cases 25-36 with LB distance of 0.5m from wall of heading | | | | | |
|--|--|--------------------------------------|---|--------------|--|
| Increase in LB length from 5m | Percentage incremental effect with each metre increase in length | Increase in LB face distance from 5m | Percentage incremental effect with each metre increase distance from face | Net increase | Remarks |
| 1 | 1.00 | 1 | 5/2 | -0.77% | Net increase include the effect of increase in length of LB and increase in distance from the face |
| 2 | 0.43 | 2 | | | |
| 3 | 0.19 | 3 | | | |
| 4 | 0.08 | 4 | | | |
| 5 | 0.03 | 4.5 | | | |
| Total increase | 1.73% | Total decrease | -2.50% | | |

Note: - The average net increase as shown in Table 6.25 should be around -0.99%, and the net increase with the approximations used in the mathematical model is -0.772%.

6.8.5 Summary of the rules to use equation 6.9 for any heading dimension

Keeping in view the discussion given above, equation 6.9 could be used to estimate the flow rate for rest of the studied cases, and for any other case falling within the boundaries of the studied cases abiding to the following conditions.

1) Factor (F_{LB})

The factor used in equation 6.9 can be interpolated for any other distance between 0.5 and 1m (between 1 and 0.55).

2) Velocity

For LTR velocity greater than or less than 1m/s, increase or decrease the flow rate calculated using equation 6.9, to the proportional increase or decrease in velocity.

3) Heading height

Increase or decrease the flow rate calculated using equation 6.9 proportional to the percentage increase or decrease in height of the heading (as compared to 3m).

4) Factor for the length of LB in the heading (FL_{LB})

• 1m distance of LB from wall

Use a factor of 2% for the 1st metre increase in length from the 5m length. For further increase in the length LB increase 80% of the previous metre increase in length up to a maximum of 10m difference. Add the cumulative effect and increase the percentage amount calculated using equation 6.9.

• 0.5 m distance of LB from wall

Use a factor of 1% for the 1st metre increase in length from the 5m length. For further increase in the length in the length of the LB increase 43% of the previous metre increase in length up to a maximum of 5m difference. Add the cumulative effect and increase the percentage amount calculated using equation 6.9.

• Any other distance of the LB from wall

Interpolate to find the percentage for the first metre increase in length, the reduction factor and the number of metres to calculate the cumulative effect.

5) Distance of the LB from the face

Use a factor of 1% for every 2m increase/decrease in distance from the 4.5m distance (distance from face). Add the cumulative effect and decrease / increase the same percent amount of flow as calculated using equation 6.9.

6) Length of LB in the LTR

The effect of the change in length of the LB in the LTR for LB used with an angle is already catered for in the expression by using the product of the entrance length and distance of the LB from the wall in the heading. However, for the LB with zero angles in the LTR, the viscous effect for increase in length of the LB more than 3m is estimated at the rate of 1% decrease in flow rate per 2m increase in the length of the LB.

Note: - The first step is to find the flow rates for the new configuration in the standard 10m heading with 5m long LB and 1m/s LTR velocity. This should be followed by the above adjustments to find the flow rate for the exact LTR velocity and length of the LB and heading.

6.8.6 Generalised equation

Given the conditions above a generalised equation to estimate the flow rates at the exit of the LB was developed to simplify the solution procedure. All the conditions given in section 6.8.3 were incorporated in the formulation of this equation (6.10).

$$\text{Flow rate close to the face of the heading (0.5m from the face)} = \text{FRF}_{\text{LB}} = [(1.30 \times \text{F}_{\text{LB}} \times (\text{X} \times \text{b})) + 0.51] \times [1 + ((\text{LTR Vel} - 1)) + ((\text{HH} - 3)/3) - ((\text{f} - 4.5) / (2 \times 100)) + (((\text{F}_{\text{LB}} \text{ First metre}) + (\sum_{i=2}^n \text{F}_{\text{LB}} \text{ First metre} \times \text{RF}_{\text{LB}}^{(i-1)})) / 100) - \underbrace{((\text{c} - 3) / (2 \times 100))}_{\text{Only for LB used with zero degree in LTR}}] \quad (6.10)$$

Where,

X = LB entrance length

b = Distance of the LB from the wall in the heading

c = Length of the LB in the LTR

d = Length of LB in the heading

f = Distance of LB from the face of the heading

HH = Heading height

LTR Vel = Velocity of air in the LTR

First metre factor = 2 (only to be used when LB length more than 5m) for 1m distance of LB from the wall and 1 for 0.5m distance, for other distances it can be interpolated.

n = 10 for 1m distance of LB from the wall and 5 for 0.5m distance, for other distances it can be interpolated.

Reduction Factor = $RF_{LB} = 0.8$ for 1m distance of LB from the wall and 0.43 for 0.5m distance, for other distances it can be interpolated.

6.8.5 Conclusion

The effect of various system variables related to the installation of the LB, along with the effect of LTR velocity, and heading height and depth on the flow rates close to the face of the heading (0.5m from the face) were estimated. These estimations were represented in user friendly mathematical forms. A model to estimate the consolidated effect of all the studied system variables of LB ventilation system was also formulated by summing the individual effects. This was represented in equation 6.10 and could be used to estimate the flow rates close to the face of the heading for different configurations of the LB, LTR velocities and heading dimensions, falling within the boundaries of the study. The actual mining environment is not perfect so while using this estimation model a reduction factor may be used depending upon the quality of installed LB to cater for the leakage to get an acceptable estimation.

The next section, gives a very brief description of the distinct air flow pattern inside the heading ventilated using the LB ventilation system, emphasising the location of the low air flow and dead zones.

6.9 Dead Zones/Low Flow Rate Regions

The air flow in the heading followed a similar trend for all the cases as far as the low flow rate/recirculation regions are concerned, in all cases low velocity regions were formed at the corners, centre of the heading and behind the angled LB. Seven most prominent low flow rate/recirculation regions were formed as shown in Figure 6.42. These regions can become potential zones of methane accumulation in the LB ventilation system. The extent of these regions changed with the variation in the settings of the LB, i.e. the distance from the wall, the length of the LB, and the angle of the LB. The variation of the size of these regions with the change in these settings is briefly discussed here. It is important to highlight here that streamlines have been used in most of the Figures of this section to clearly show the general trends of the airflow. The areas of low velocity and recirculation may appear blank, but airflows do exist in these regions and can be seen more clearly by representing these airflows using velocity vectors (as was shown in Figure 6.29 and 6.30 earlier).

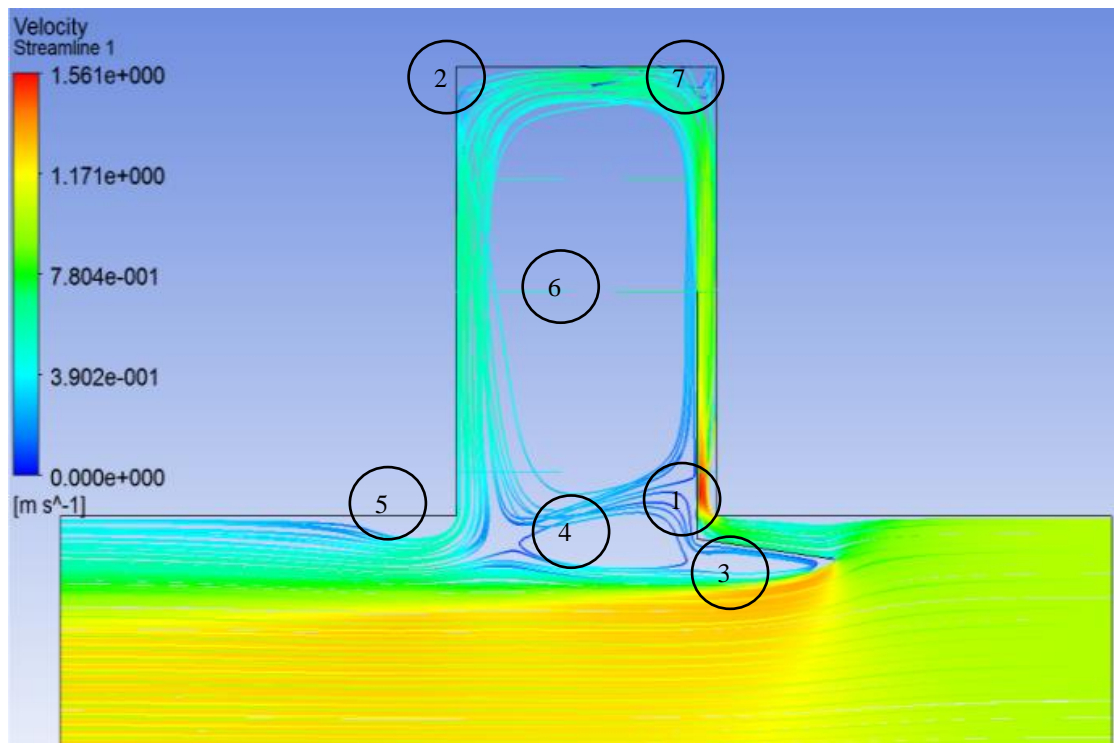


Figure 6.42 Typical low flow rate and recirculation zones - Ventilation of a heading using LB

- **Region 1**

This region of low flow rate is shown in Figure 6.43. It was caused due to the presence of LB turn and was found in all the settings of the LB. It has already been discussed in the previous sections.

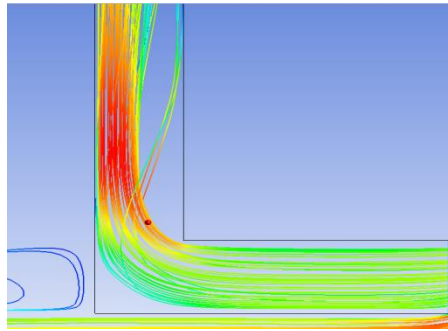


Figure 6.43 Typical low flow rate zone 1 - Ventilation of a heading using LB

- **Region 2**

This region was formed due to the corner at the left face of the heading and remained almost the same for all cases. This region for different cases can be seen in Figures 6.44 through 6.48.

- **Region 3**

A cavity was created behind the LB when it was used with an angle, the size of the region increased with the increase in the size of the LB inlet, either due to the increase in the length of the LB in the LTR (when LB was used with an angle) or due to the increase in angle of the LB as shown in Figures 6.46 through 6.48.

- **Region 4**

The air after moving along the face of the heading turned, and moved parallel and close to the side wall (left) of the heading to join the main stream of air in the LTR. At the entrance of the heading, this air divided into three parts, the air close to the wall (which joined the air in the LTR), the air farthest from the wall (which turned counter clock wise to create recirculation), and the layer of air at the middle of these two streams. This region of recirculation was created by this middle stream of air, which failed to move straight or turn completely into the heading and slowed down creating this low flow region. This zone joins zone 3 creating a bigger zone

in the cases where the LB was used with an angle as shown in Figures 6.46 through 6.48.

- **Region 5**

The air after moving along the face of the heading turned down to join the air in the LTR moving downstream. The airflow of the main air stream in the LTR was very less behind the LB for all the cases and was not sufficient to turn the returning air downstream. The returning air therefore, continued its downward movement until it met the high velocity main stream, resulting in the formation of this zone (the presence of the sharp corner also contributed to this separation). When the LB was used with 1m distance from the face or used with an angle the region behind the LB got bigger, the main air stream in the LTR thus got shorter (in width) increasing the distance for the return air to join with it. Therefore, this zone got bigger and bigger with the increase in the entrance length of the LB as shown in Figures 6.44 through 6.48.

- **Region 6**

The most prominent feature of the heading ventilation using LB was the presence of a low flow region (region 6) in the centre of the heading. The air after ventilating the face turned in the opposite direction to join the main stream in the LTR. It travelled along the wall, and a very little portion of this air farthest from the wall turned counter clock wise and moved up. This air flow was very low as and not even visible in streamlines view of the velocity vectors as shown in Figures 6.44 through 6.48 and may allow layering of tenacious gases. The low air flow can only be seen once the velocity vectors are used to see the air flows as seen in earlier Figures (Figure 6.29 and 6.30).

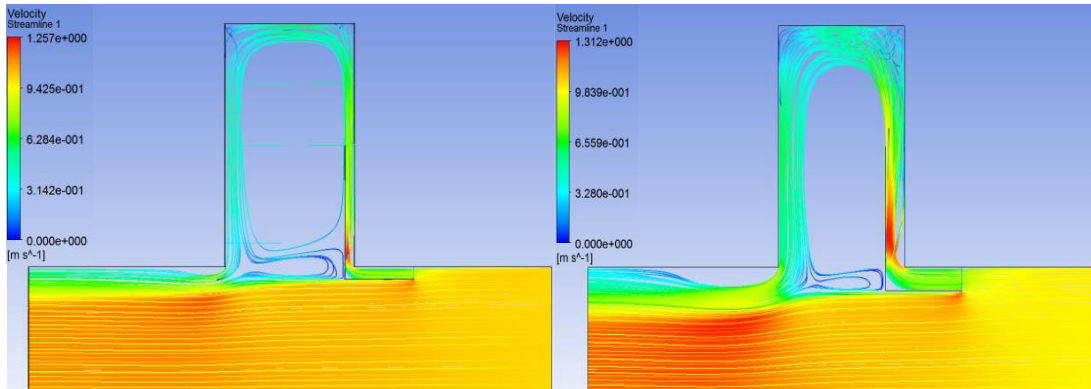


Figure 6.44 10m long headings using LB settings of; 0° angle, 5m length of LB in heading, 3m length in LTR, 0.5m and 1m distance from face (left to right)

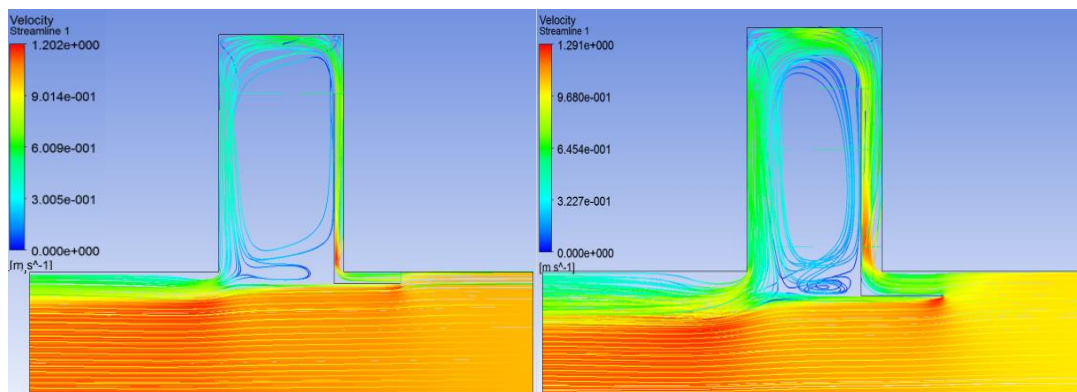


Figure 6.45 10m long headings using LB settings of; 0° angle, 7.5m length of LB in heading, 3m length in LTR, 0.5m and 1m distance from face (left to right)

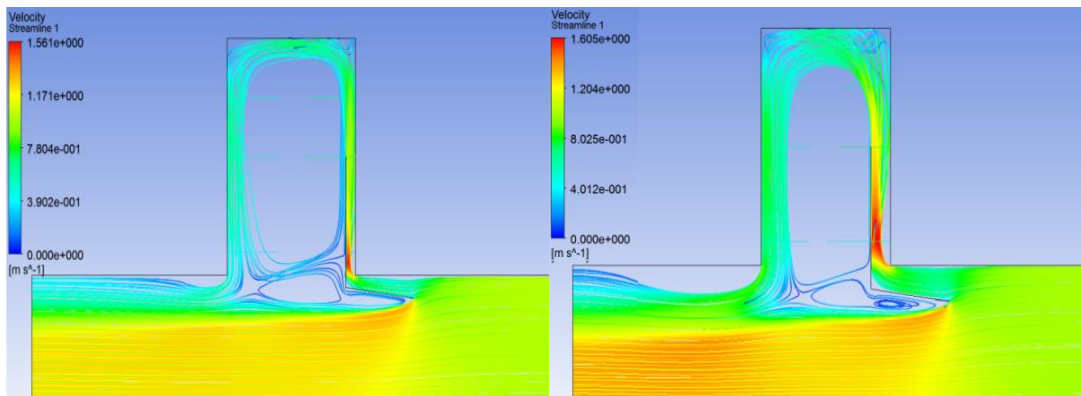


Figure 6.46 10m long headings using LB settings of; 7.5° angle, 5m length of LB in heading, 3m length in LTR, 0.5m and 1m distance from face (left to right)

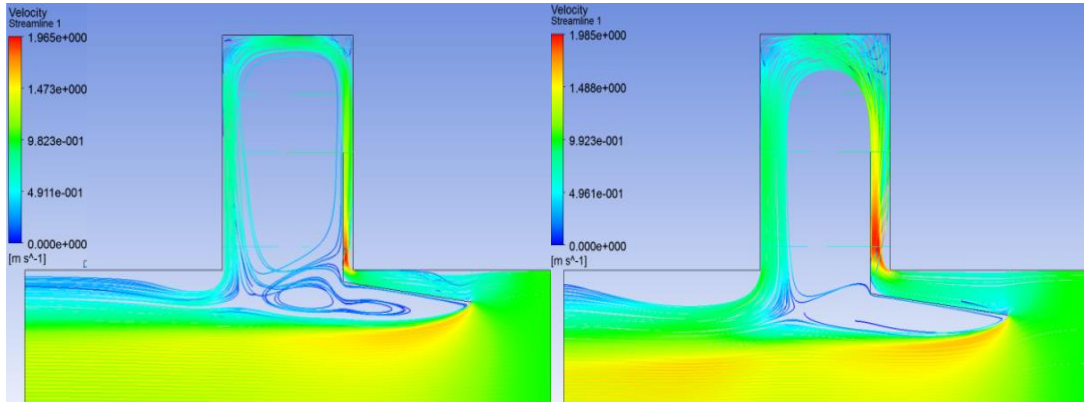


Figure 6.47 10m long headings using LB settings of; 7.5° angle, 5m length of LB in heading, 6m length in LTR, 0.5m and 1m distance from face (left to right)

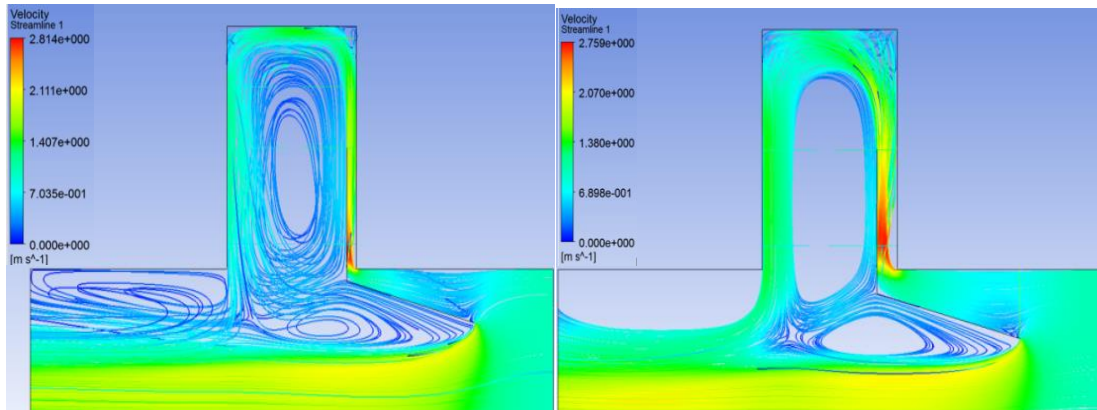


Figure 6.48 10m long headings using LB settings of; 15° angle, 7.5m length of LB in heading, 6m length in LTR, 0.5m and 1m distance from face (left to right)

- **Region 7**

Another recirculation region, although visible from the top view and appears similar to Region 2, but, is actually different, and the difference could be seen from the side view of the heading by plotting the air flow velocity vectors on the vertical planes drawn at different distances from the right wall. The air exiting the LB hit the face, turned left on reaching the face, swept the face and moved (returns) parallel to the side wall of the heading, towards the LTR. However, a part of this air, close to the right wall, created recirculation zones as shown in Figure 6.49. The figure only shows a part of the plane after the exit of the LB. The air at the bottom of the heading rose and formed a counter clockwise recirculation zone close to the face, and the air at the top turned downward and formed a clockwise recirculation zone. The extent (length and width) of this

region varied with the distance of the LB from the right wall and the distance of the LB exit from the face of the heading.

The more the distance of the LB from the wall of the heading and the distance of the LB exit from the face of the heading the longer this zone became as shown in Figure 6.49.

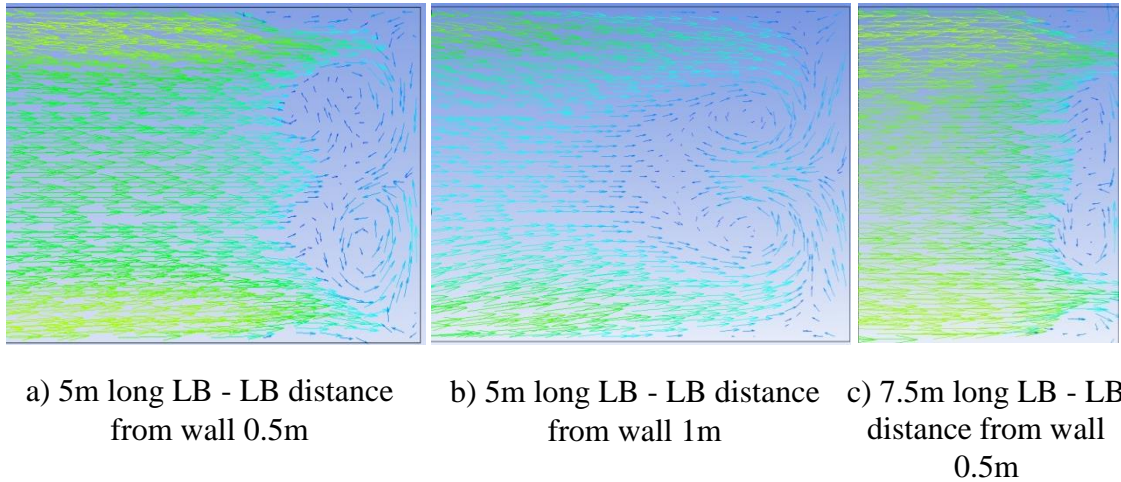


Figure 6.49 Air flow vectors on a vertical plane drawn at a distance of 0.1m from the right wall for 10m long heading

The zone became smaller and disappeared, going away from the right wall of the heading (stayed approximately up till the extent of the LB), where all the air turned left, and swept the face of the heading as shown in Figure 6.50. Therefore, shorter the distance of the LB from the wall, and the shorter the distance of the LB exit from the face, the shorter is the length and width of this region.

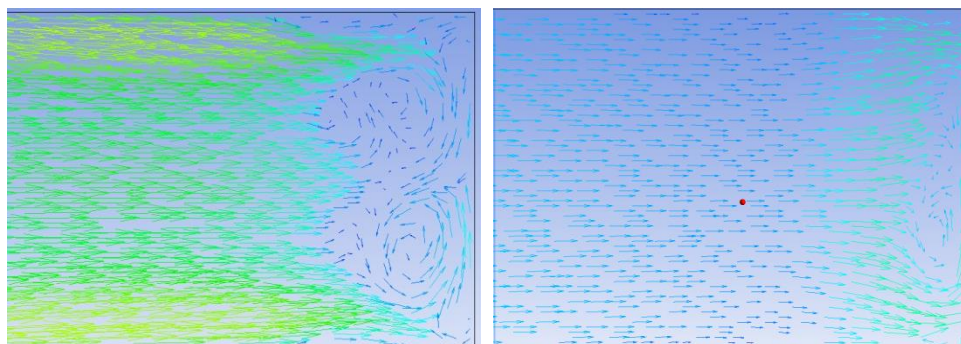


Figure 6.50 Air flow vectors on a vertical plane drawn at a distance of 0.1m and 0.4m from the right wall for 10m long heading using a 5m long LB having a wall distance of 0.5m

6.10 Conclusion

- The effect of variables related to the installation of the LB along with the effect of LTR velocity, and heading height and depth on the flow rates at the exit of the LB and face of the heading were studied, estimated and represented in easy to use mathematical forms. These estimation models may be used with a reduction factor depending on the quality of the installed LB to cater for the leakage to get an acceptable estimation.
- The increase in the flow rates at the exit of the LB and the face of the heading was found to be proportional to the increase in the LTR velocity and the height of the heading.
- It was found that the increase in length of the LB increased the flow rates at the face of the heading. But the effect was more prominent with 1m distance of the LB from the wall of the heading than 0.5m. Since the throw of air with a narrow channel was already higher than the bigger channel as expected.
- The increase in length of the LB in the LTR increased the flow rates at the exit of the LB and the face of the heading when the LB was used with an angle in the LTR, however, when the LB was installed with zero angles, the increase in the viscous effect due to the increase in length of LB reduced the flow rates at the exit of the LB and thus close to the face of the heading.
- When the air moved through the channel between the wall of the heading and the LB, the flow rate was found to be higher closer to the LB than the wall of the heading. This variation was more for bigger distance of the LB from the wall and it decreased with the increase in the length of the LB. The effect of the increase in the length of the LB to reduce this variation was found to be higher for bigger distance of the LB from the wall in the heading.
- The increase in distance of the LB from the wall increased the flow rates at the exit of the LB and close to the face of the heading. However, with bigger LB to wall distance most of the air exiting the LB did not even reach the face of the heading. Therefore, to increase flow rates close to the face of the heading, instead of using LB to wall distance higher than 1m, LB with an appropriate angle can be a better solution (unless additional engineering solutions are used).

The narrow LB to wall distance in the heading will ensure that most of the air exiting the LB reaches the face.

- The distinct low flow rate and recirculation zones were also identified.

In the next chapter, ventilation of a heading using LB in the presence of a CM making a straight cut is presented. The most effective scenarios from the current Chapter (Chapter 6) (and are discussed in the next chapter), which gave maximum air flows at the face of the heading for each angle of the LB in the LTR, were used. This was done to find the effectiveness of the ventilation of a heading in the presence of a CM and identify the recirculation and the low velocity zones which could affect the dilution and removal of undesired gases and dust. This information should aid in the design of possible ventilation solutions on the CM.

7 ANALYSIS AND DISCUSSION - VENTILATION OF HEADINGS WITH CONTINUOUS MINER USING LINE BRATTICE

7.1 General

The variation in flow rates and air flow patterns in an empty heading with the changes in the settings of the control variables related to LB ventilation system have been discussed in detail in Chapter 6. In this chapter, the ventilation of a heading using LB in the presence of a CM making a straight cut is discussed to develop a better understanding of the face ventilation process. A simplified model of the CM without the drum and scrubber with the dimensions of 3.3 m x 1.5m x 10.5 m (W x H x L) was used for this case. The CM was placed in the left top corner of the heading. The most effective scenarios from Chapter 6 (Case B), which gave maximum air flows at the face of the heading for each angle of the LB in the LTR, were used for this case. This was done to find the effectiveness of the ventilation of a heading in the presence of a CM and identify the recirculation and the low velocity zones which could affect the dilution and removal of undesired gases and dust. This basic knowledge may help the designing and installation of possible solutions on the CM to improve ventilation.

As already discussed, the flow rates increase with the increase in the distance of the LB from the wall in the heading (Chapter 6, Section 6.6) and the increase in entrance length at the LB inlet (Chapter 6, Section 6.7). The settings of the LB used for this Case are given below.

- Length of LB in the Heading = 15m (three by four the length of the heading), as already seen (Chapter 6, section 6.4), longer LB gave high flow rate close to the face of the heading.
- Angle of LB = 0°, 7.5°, and 15°.
- Distance from the wall in the heading = 1m.
- Length of LB in LTR = 6m, for each angles of the LB, although as seen before (Chapter 6, Section 6.5.3), for LB with zero angle in the LTR, longer the LB, lesser is the air flow at the exit of the LB and close to the face, but the percentage difference was small, so for standardization purpose the same length was used for the zero angle as well.

The scenarios resulted from these settings were simulated for each LTR velocity of 1m/s, 1.5m/s, and 2m/s and heading dimension of 6.6m x 3m x 20m and 6.6m x 4m x 20m. A total of 18 scenarios were therefore, simulated for this case. The schematic view of the model simulated is given in Figures 7.1.

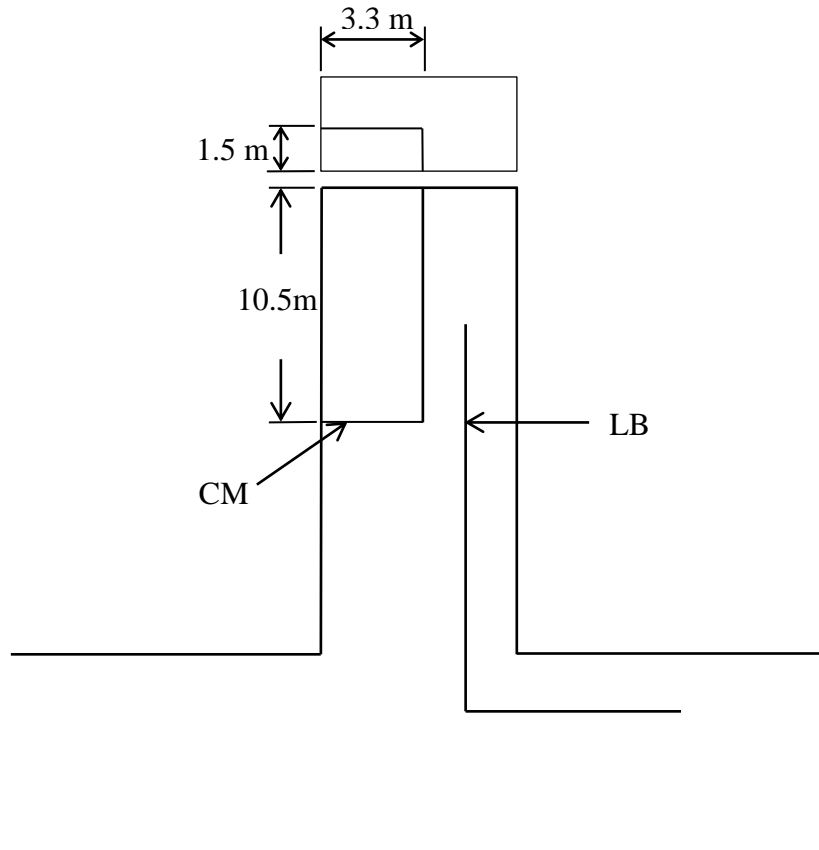


Figure 7.1 Schematic of the CM in the heading

The flow rates at the exit of the LB and the face of the heading were discussed in Chapter 6, therefore, in this Chapter only the effects of the CM on the air flow patterns / velocity vectors have been discussed, with specific emphasis on the air flows close to the face.

The airflows for all the simulated scenarios, with each LTR velocity, resulted in a distinct but, similar pattern (although the flow rates varied). Therefore, only the impact of the CM on the air flow patterns in general has been discussed here without any emphasis on a particular scenario or going into each case separately.

7.2 CM in 6.6 x 3 x 20m Heading

The presence of the CM divided the heading and thus the air flows delivered by the LB into two halves, the bottom half of the heading with a reduced width, and the top half with the complete width of the heading. The airflows therefore, behaved differently in both the halves, and the overall flow was affected by the combination of air flow of both the halves.

To understand these two behaviours, air flows were, visualized and analysed on horizontal planes and vertical planes, constructed at different heights and distances from the right wall and face of the heading respectively.

7.2.1 Airflows on a horizontal plane and vertical plane constructed at a distance of 0.7m from right wall

The velocity vectors of the air, on the horizontal plane at the height of 0.5m and on the vertical plane at a distance of 0.7m from the right wall are shown in Figure 7.3. The velocity vectors on the vertical plane followed the similar flow pattern as discussed in Chapter 6, Section 6.9; formation of two recirculation zones are clear which were formed by the turning of the air from the top and bottom of the heading. However, the air flows on the horizontal plane behaved differently from the cases without the CM, due to availability of restricted width at the bottom of the heading. The air on reaching close to face, divided into three streams, the outer most stream of the air (1), i.e. the air close to the LB (taking air stream exiting the LB as reference), the middle stream of air (2) and the inner stream of air (3) (closest to the right wall of the heading) as shown in Figure 7.2.

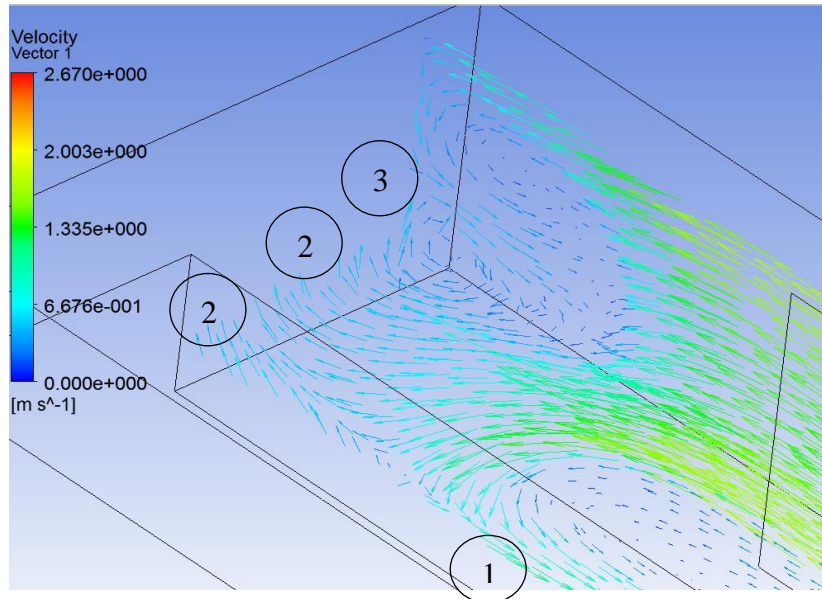


Figure 7.2 Velocity vectors on the 0.5m high horizontal plane and vertical plane at 0.7m from the right wall of the heading

The outer stream of air (1) exited the LB, turned left and followed the return path (counter clock wise) parallel to the CM boundary to meet the main air stream in the LTR, as shown in Figure 7.2. The middle stream of air (2) after exiting the LB moved towards the face of heading and the CM, hit them, and changed direction to rise up as shown and labelled in Figure 7.2 and shown in Figure 7.3. The inner stream of air (3), i.e. the air close to the right wall of the heading after exiting the LB hit the face and started turning clockwise and upward, creating a recirculation zone in vertical plane.

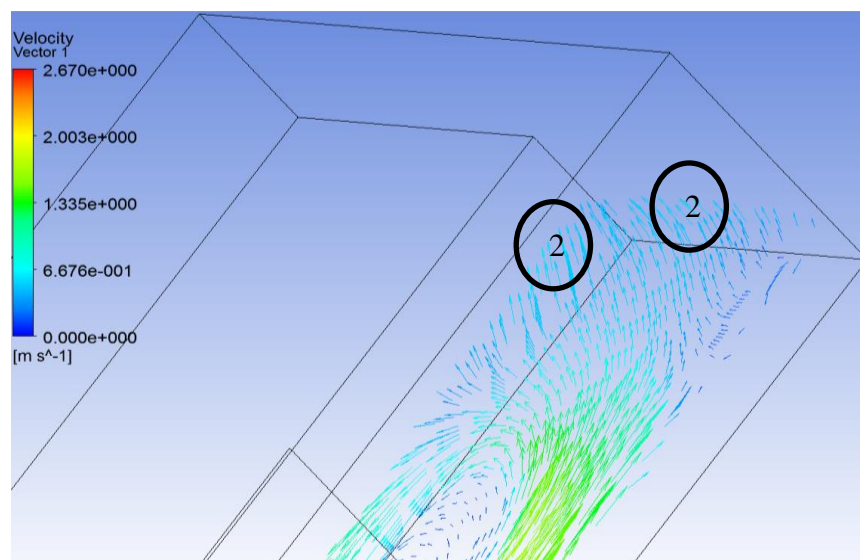


Figure 7.3 Velocity vectors on the 0.5m high horizontal plane showing middle stream of air rising up

7.2.2 Airflows on a horizontal plane constructed at a height of 2.9m and a vertical plane constructed at a distance of 0.7m from right wall

The air flow at the upper half of the heading is different from the lower half of the heading, but the stream of air can still be divided into three streams, the inner stream (closest to the LB), outer stream (closest to the right wall of the heading) and the middle stream (between the inner and outer stream). The inner stream of air as discussed earlier, after exiting the LB hit the face and turned down to form a clock wise recirculation zone on the vertical plane as shown in Figure 7.4.

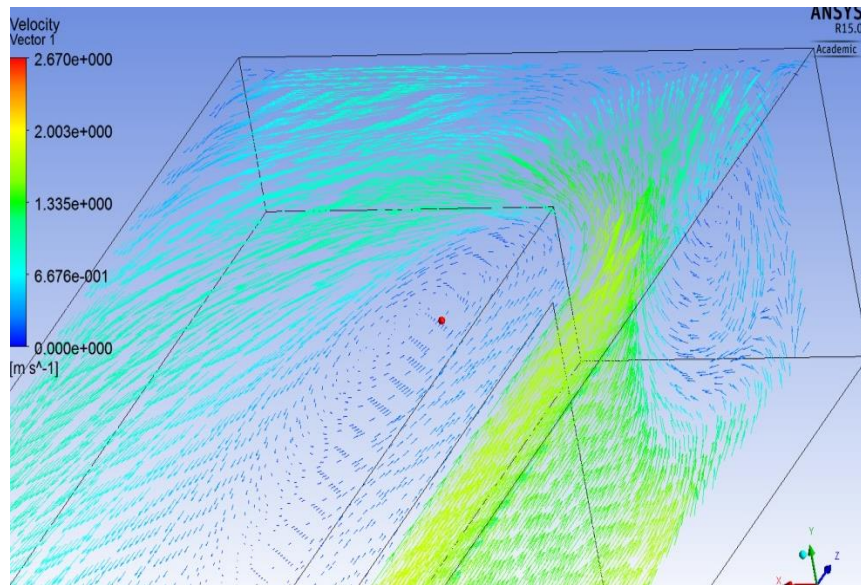


Figure 7.4 Velocity vectors on the 2.9 m high horizontal plane and vertical plane at 0.7m from the right wall of the heading

The middle stream of air after exiting the LB moved towards the face of the heading and on hitting the face started moving down. The rising air from the middle stream of air from the bottom half of the heading meets the middle stream of air from the top half of the heading approximately at the vertical centre of the heading as shown in Figure 7.5.

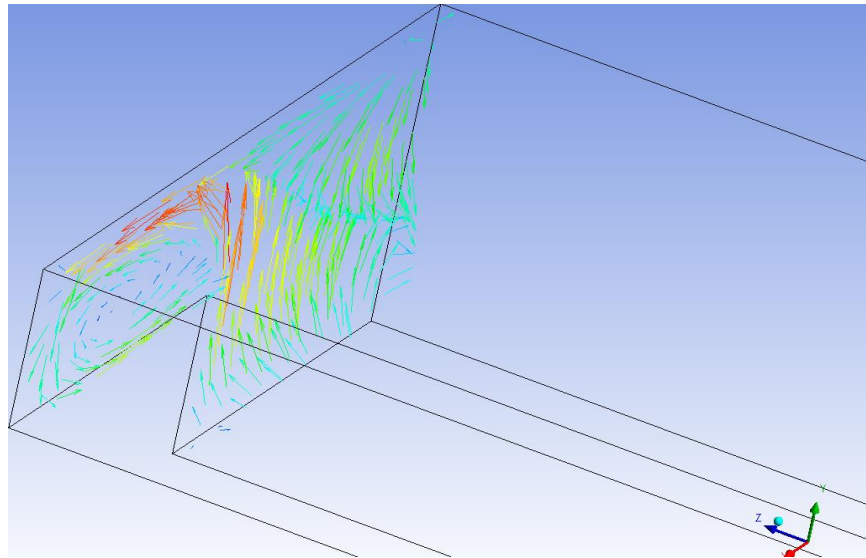


Figure 7.5 Three dimensional view of the velocity vectors on the 19.9 m deep vertical plane (perpendicular to the LB)

The outer stream of air, after exiting the LB moved towards the face of the heading and also started turning towards the left wall of the heading. The outer stream of air has two prominent features, first, at the middle of the heading over the top right corner of the CM the stream of air got slower, marked as (region 4), and shown in Figure 7.6. Second, a small part of the outer stream on reaching the left wall of the heading, close to the face started curling down, marked as (region 5), and shown in Figure 7.7. The main portion of the air after moving along the face travelled along the left face of the heading (on the return way) and joined the air in the LTR.

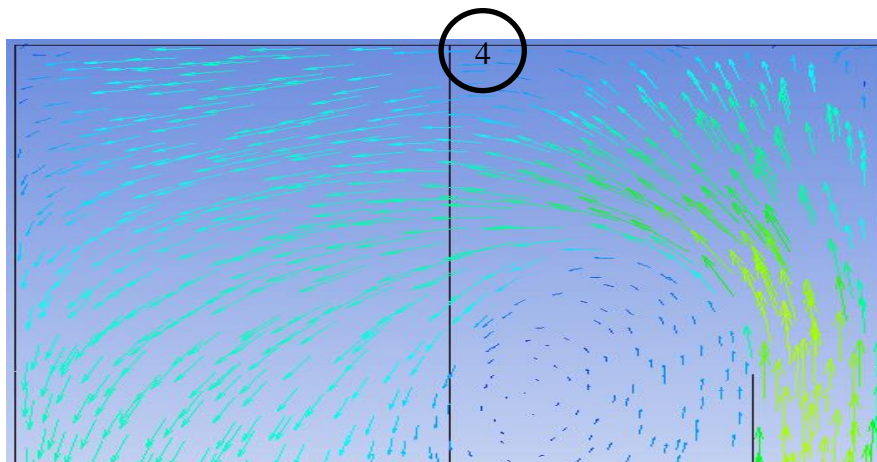


Figure 7.6 Velocity vectors on the 2.9m high plane; slower air in region 4

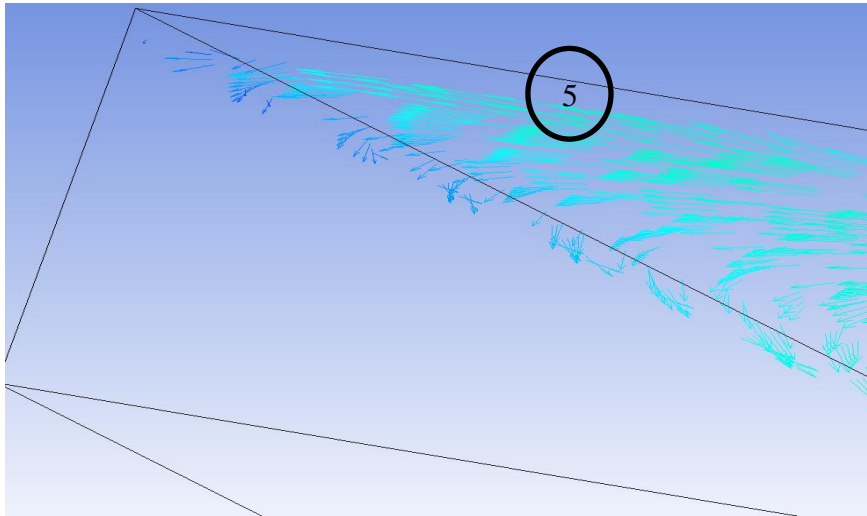


Figure 7.7 Velocity vectors on the 2.9m high plane; curling down of outer air stream from the left side wall of the heading (region 5)

The outer stream of air from the bottom half of the heading after striking the face of the heading rose to the top of the heading as shown in Figure 7.5. This air slowed down the outer stream of air of the top half of the heading in the area close to the top right corner of the CM shown as region 4. The downward curling of air in region 5 continued till the top of the CM (this can be seen in the following section).

7.2.3 Airflows on a horizontal plane constructed at a height of 1.6m and vertical plane constructed at a distance of 0.7m from right wall

A horizontal plane at a height of 1.6m (almost the mid height) and a vertical plane at a distance of 0.7m from the right wall of the heading were constructed to visualise the behaviour of air. The mid height lies at 1.5m, which coincides with the height of the CM (horizontal plane constructed at a height of 1.5m did not have any flows to show over the CM), therefore, to visualise the air flow on the complete horizontal plane it was constructed at a height of 1.6m instead of 1.5m.

The air flows on this horizontal plane were found to be entirely different from the air flows of the horizontal planes in the top and bottom half of the heading as shown in Figure 7.8. The prominent features of this plane are:

- The two recirculation zones of the vertical plane met approximately at this (middle) horizontal plane.
- Similarly, the middle streams of air moving up from the bottom half of the heading, met the middle stream of air moving down from the top half of the heading.

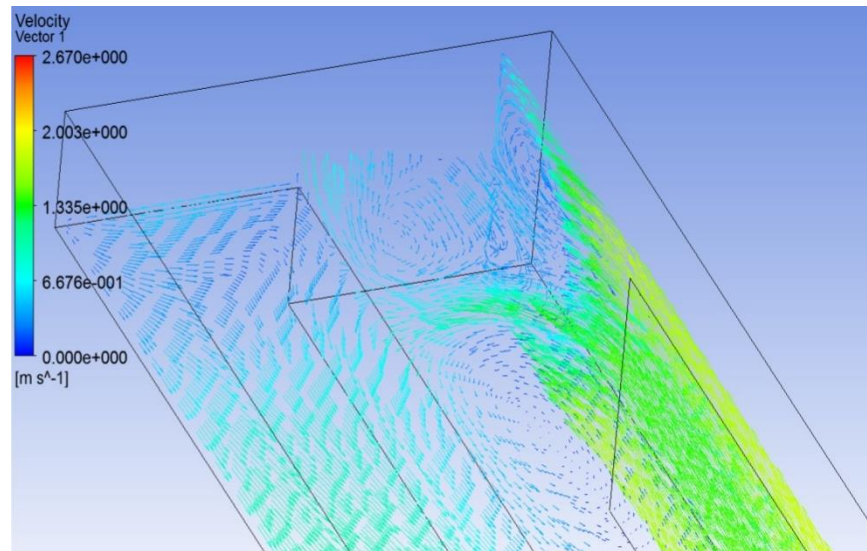


Figure 7.8 Velocity vectors on the 1.6 m high horizontal plane and vertical plane at 0.7m from the right wall of the heading

- The top view of the air flow patterns (velocity vectors) on the horizontal plane constructed at the height of 1.6m is shown in Figures 7.9 and 7.10. The presence of two distinct airflows close to the face of the heading, in the left and right half of the heading could be seen.

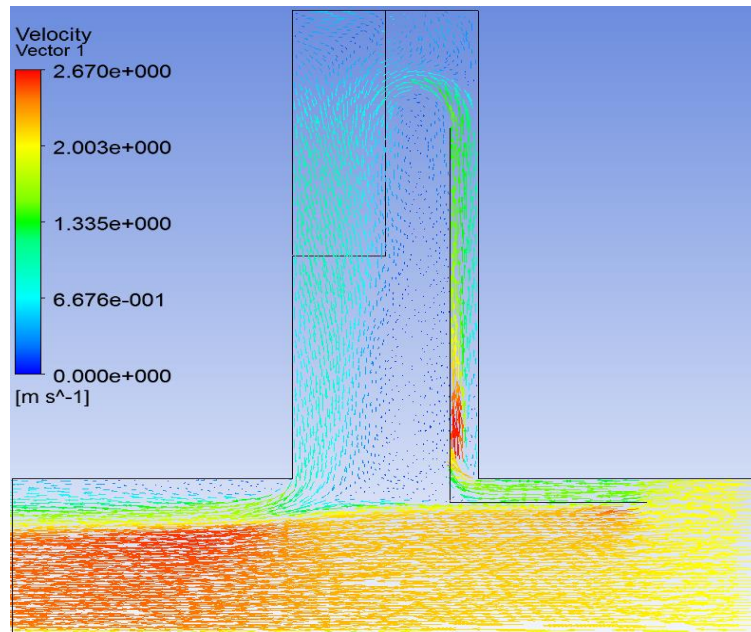


Figure 7.9 Velocity vectors on the 1.6m high horizontal plane

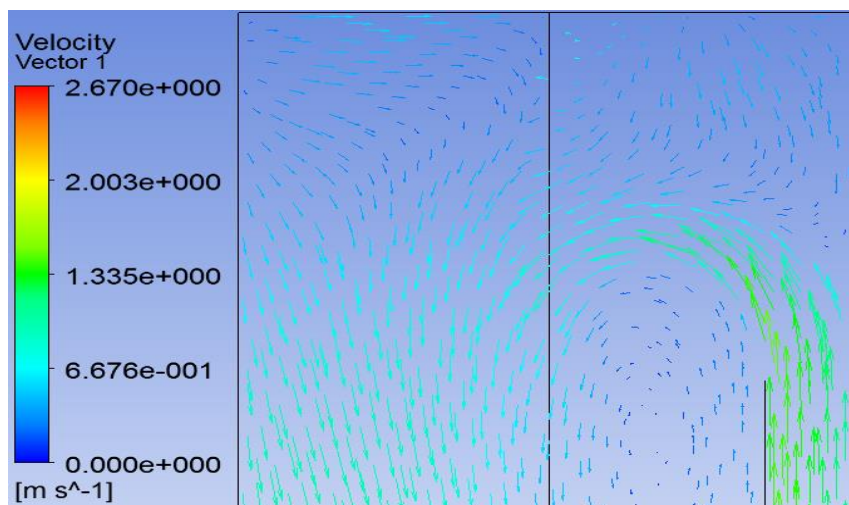


Figure 7.10 Velocity vectors on the 1.6m high horizontal plane close to the face

- The middle streams of air from the top and bottom halves of the heading met at the middle of the heading and started moving on the horizontal plane away from the face of the heading as shown by the air flows in the right half of the heading in these two figures. This air joined the main air stream to return to the LTR.
- The air in the left half is that part of the air from the inner stream of air of the top half of the heading which on striking the left wall of the heading started

moving down. This air after hitting the top of the CM also joined the main return air stream.

- Both the airflows are joining the main air stream which is critical to ensure that these zones do not become recirculation zones. Only at the centre of these two regions, very small amount of air can be seen rising up (more prominent in Figure 7.11).
- The presence of these two distinct airflows prevents the air stream exiting the LB from reaching close to the face of the heading at mid height of the heading. The outer stream of air unlike the bottom half of the heading, due to availability of more width followed a bigger return path by moving over the CM and followed a return path parallel to the left wall of the heading.

7.3 CM in 6.6 x 4 x 20m Heading

A similar behaviour of air flow was observed in the 4m high heading a view of the velocity vectors on the horizontal plane (on close to the face of the heading) constructed at the height of 2m is shown in Figure 7.11, which resembles the similar plane constructed for the 3m high heading.

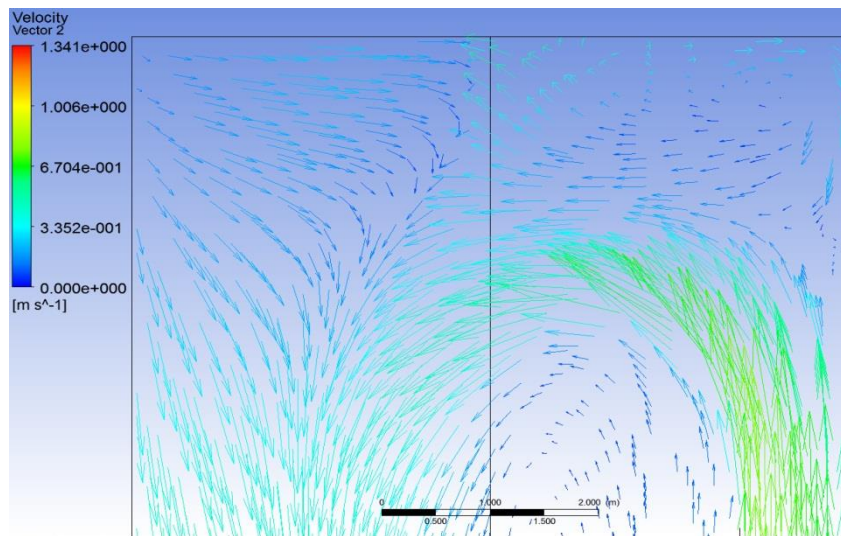


Figure 7.11 Velocity vectors on the 2m high horizontal plane close to the face for 4m high heading

7.4 Conclusion

The distinct air flow patterns in the top, bottom and middle regions of the heading using different horizontal and vertical planes were identified and shown. It was found that recirculation zones are formed on the vertical plane at the right side of the heading due to the downward and upward movement of air from the top and bottom of the heading. These zones were similar to the zones formed when the CM was not used in the heading.

It was found that the air in general swept the face and rose to the upper half of the heading, most of air from the upper half of the heading returned to join the LTR air. The velocity vectors on the top planes were reasonably flat with very little movement of air in the downward direction (even that is limited to the top of the CM). Therefore, methane which is naturally buoyant (Specific Gravity 0.55), and tends to concentrate in roof cavities and layer along the roof of airways or working faces, should be swept effectively using this ventilation scheme.

This basic knowledge may help the designing and installation of possible solutions on the CM to improve ventilation of the heading.

In the next chapter the effects of various system variables related to the ducted fan system on the flow rates close to the face of the heading, along with mathematical models to estimate the flow rates are also presented.

8 VENTILATION OF A HEADING USING FAN AND DUCT SYSTEM

8.1 General

It is a common practice to carry out the ventilation of a long heading using the ducted fan systems in underground coal mining. This is typically carried out using a force or an exhaust fan duct ventilation system, which is hung from the roadway roof. The effectiveness of the ventilation, using the ducted fan system, typically depends on a number of factors/parameters such as, the diameter of the duct, the length of the duct, distance of the duct mouth to face, the power of the fan (quantity delivered by the fan), the orientation of the duct (distance from the sidewall and the roof), the airflows in the LTR etc. However, these factors are not always given much deliberation and the standard routines are followed during the installation of a system. If the air flows are low at the face, the fan is replaced by a more powerful one, not realizing how it is affecting the airflows inside the heading. The understanding of the airflow pattern inside the heading, with the change in the settings of the ducted system is however, of significant importance and should be kept in mind when choosing a ducted system.

A mathematical model is therefore, presented here to understand /estimate the effect of the change of each of the fan and ducted system variables (considered for this study) on the airflow going into the heading, and thus the ventilation of the heading. This can help in choosing the more appropriate fan and duct system, and thus improve health and safety conditions. Both the force and exhaust fan duct systems were simulated under various settings as given in section 3.6, Tables 3.8 through 3.11, which are summarized below:

- Duct Size (570mm and 760mm).
- Fan design flow rates ($2.97\text{m}^3/\text{s}$ @ $0.15\text{m}^3/\text{s}/\text{m}^2$ and $3.71\text{m}^3/\text{s}$ @ $0.15\text{m}^3/\text{s}/\text{m}^2$).
- Distance of the duct mouth to face of the heading, 8m and 10m for force fan system and 2m and 4m for exhaust fan duct system.
- LTR velocity of 2m/s and distance of the duct from side wall and roof, 1m and 0.5m respectively were kept constant for all the case.

The air flow patterns and flow rates close to the face for both the systems are presented separately, clearly identifying the recirculation zones at various locations using horizontal and vertical planes constructed inside the heading. This information could also prove important to design and introduce supplementary engineering solutions for the overall improvement of ventilation.

8.2 Force Fan Duct System

8.2.1 Flow rates

A total of eight cases as summarized in Table 8.1, plus an additional case using a bent duct were simulated. The variation of the fan design flow rates (maintained at the exit of the duct), diameter and length of the duct, changed the volume flow rates inside the heading at similar locations. The air flow rates (going into the heading) delivered by the force fan duct system close to the face of the heading, have been calculated for each case and tabulated in Table 8.2. These flow rates were calculated using the positive axial velocities going into the planes constructed parallel to the face of the heading at the distances of 0.5m, 0.4m, and 0.3m from the face. The percentage of fresh air at these distances have also been calculated, using the quantity of air delivered by the fan and the quantity of air actually present at these distances (assuming the quantity of air delivered by the fan is reaching the face of the heading). This has helped to calculate the maximum percentage of fresh air reaching the face and thus the minimum amount of recirculation (100 - % of fresh air) taking place near the face of the heading for each case. The percentage of fresh air reaching the face may always be less than this percentage.

Keeping in view the tabulated data given in Table 8.2, the following was found about the total flow rates and the amount of fresh air close to the face of the heading using a force fan duct system:

Table 8.1 Details of force fan duct cases

| Names (Heading Width-Heading Height-Heading Length-Duct Diameter- Duct Mouth To Face Distance-Air Flow) |
|---|
| 6.6-3-20-0.57-8m-2.97 |
| 6.6-3-20-0.57-8m-3.71 |
| 6.6-3-20-0.57-10m-2.97 |
| 6.6-3-20-0.57-10m-3.71 |
| 6.6-3-20-0.76-8m-2.97 |
| 6.6-3-20-0.76-8m-3.71 |
| 6.6-3-20-0.76-10m-2.97 |
| 6.6-3-20-0.76-10m-3.71 |

Table 8.2 Flow rates and percentage of fresh air flow rates on planes at specified distances from the face

| Names (Heading Width-Heading Height-Heading Length-Duct Diameter- Duct Mouth To Face Distance-Air Flow) | Distance from the face of the heading | | | | | |
|---|---------------------------------------|---------------|--------------------------------|---------------|--------------------------------|---------------|
| | 0.5m | | 0.4m | | 0.3m | |
| | Flow rates (m ³ /s) | Fresh air (%) | Flow rates (m ³ /s) | Fresh air (%) | Flow rates (m ³ /s) | Fresh air (%) |
| 6.6-3-20-0.57-8m-2.97 | 7.55 | 39.33 | 6.49 | 45.75 | 5.20 | 57.09 |
| 6.6-3-20-0.57-8m-3.7125 | 9.53 | 38.95 | 8.13 | 45.66 | 6.57 | 56.50 |
| 6.6-3-20-0.57-10m-2.97 | 6.56 | 45.30 | 5.51 | 53.88 | 4.32 | 68.73 |
| 6.6-3-20-0.57-10m-3.7125 | 8.25 | 44.99 | 6.96 | 53.35 | 5.48 | 67.75 |
| 6.6-3-20-0.76-8m-2.97 | 6.34 | 46.85 | 5.60 | 53.05 | 4.65 | 63.83 |
| 6.6-3-20-0.76-8m-3.7125 | 7.94 | 46.76 | 7.01 | 52.99 | 5.82 | 63.77 |
| 6.6-3-20-0.76-10m-2.97 | 5.02 | 59.16 | 4.24 | 70.06 | 3.34 | 88.89 |
| 6.6-3-20-0.76-10m-3.7125 | 6.30 | 58.94 | 5.33 | 69.65 | 4.21 | 88.10 |

Volume flow rates close to the face of the heading

- When the diameter of the duct, and the duct exit flow rate were kept constant, the flow rate close to the face of the heading increased with the decrease in duct mouth to face distance.
- When the diameter of duct and duct mouth to face distance were kept constant, the flow rate close to the face of the heading increased with the increase in the air flow exiting from the duct.

- When the duct mouth to face distance and the duct exit flow rate were kept constant, the flow rate close to the face of the heading increased with the decrease in duct diameter as expected.

Volume flow rate of fresh air close to the face of the heading

- When the diameter of the duct and the duct exit flow rate were kept constant, the percentage of the fresh air close to the face of the heading decreased with the decrease in the distance of the duct mouth to the face.
- When the diameter of duct and the distance of the duct mouth to face were kept constant, the percentage of fresh air close to the face of the heading remained constant with the increase in the air flow exiting from the duct (it is the percentage of fresh air in the total air reaching the face).
- When the distance of the duct mouth to the face and the duct exit flow rate were kept constant, the percentage of fresh air close to the face of the heading increased with the increase in duct diameter as expected.

8.2.2 Mathematical formulation to estimate air flows for force fan duct system

In order to find a relationship to estimate the flow rates reaching the face (0.5m from face) of the heading using a force fan duct system, the flow rates close to the face of the heading for all the cases were plotted against the summation of the system factors as given in Table 8.3 and shown in Figure 8.1. These factors were calculated to cater for the effects of change in diameter, change in the duct mouth to face distance and the change in flow rate exiting the duct (fan design flow rate). A linear relation (equation 8.1) was found between the summation of these factors and the corresponding flow rates close to the face of the heading. The factors for each system variable were calculated based on the reasoning given below:

Table 8.3 Flow rate close to the face and different factors for force fan duct system

| Names (Heading Width- Heading Height-Heading Length-Duct Diameter- Duct Mouth To Face Distance-Air Flow) | Distance from the face | | | | |
|--|---|-----------------------------------|--|--|--------------------|
| | 0.5m | | | | |
| | Flow rates (FR _F) (m ³ /s) | Face factor (FF _F) | Diameter factor (FD _F) | Flow rate factor (FFR _F) | ΣSystem factors |
| 6.6-3-20-0.57-8m-2.97 | 7.55 | 1.15 | 1.2 | 1 | 3.35 |
| 6.6-3-20-0.57-8m-3.7125 | 9.53 | 1.15 | 1.2 | 1.25 | 3.60 |
| 6.6-3-20-0.57-10m-2.97 | 6.56 | 1 | 1.31 | 1 | 3.31 |
| 6.6-3-20-0.57-10m-3.7125 | 8.25 | 1 | 1.31 | 1.25 | 3.56 |
| 6.6-3-20-0.76-8m-2.97 | 6.34 | 1.26 | 1 | 1 | 3.26 |
| 6.6-3-20-0.76-8m-3.7125 | 7.94 | 1.26 | 1 | 1.25 | 3.51 |
| 6.6-3-20-0.76-10m-2.97 | 5.02 | 1 | 1 | 1 | 3.00 |
| 6.6-3-20-0.76-10m-3.7125 | 6.30 | 1 | 1 | 1.25 | 3.25 |

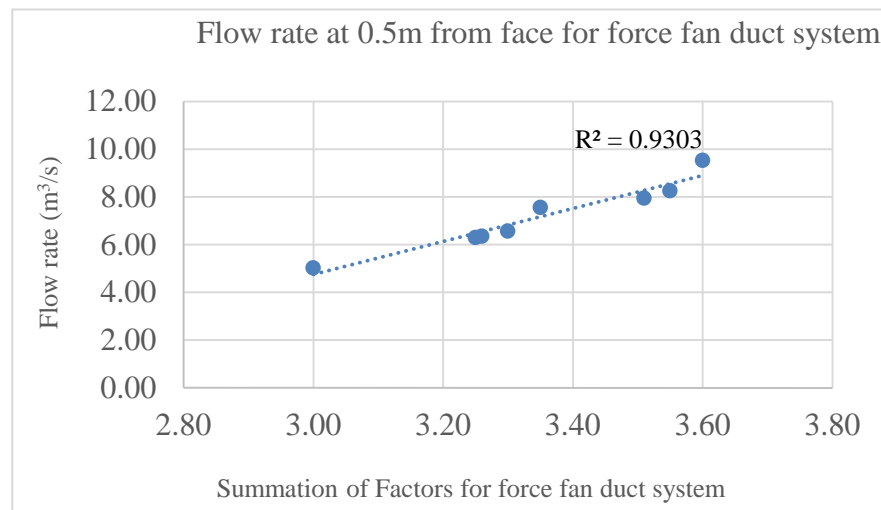


Figure 8.1 Flow rate close to the face of the heading vs Factors for force fan duct system

$$\text{Flow rate at the face of the heading} = \text{FRF}_F = 6.91 \times \sum \text{System factors} - 15.98 \quad (8.1)$$

- **Factor for flow rate for force duct fan system (FFR_F)**

All the cases in this study were simulated with two flow rates at the exit of the duct (fan design flow rates); 2.97m³/s and 3.971m³/s. The percentage difference between these two flow rates is equal to 25%. A comparison of flow rates at the face of the heading for each set of cases run with these flow rates and similar

remaining settings is given in Table 8.4. It was found that an increase in design flow rate exiting the force fan duct system resulted in a proportional (approximate) increase in the flow rate close to the face of the heading. Therefore, a flow rate factor equal to 1 was assumed for cases using 2.971m³/s of flow rate at the exit of the duct and hence a flow rate factor of 1.25 (25% more flow rate as compared to 2.971m³/s) was used for the cases using 3.7125m³/s of fan design flow rate.

Table 8.4 Percentage increase in flow rate at the face of the heading with the increase in fan design flow rate from 2.971-3.7125 m³/s

| Names (Heading Width- Heading Height-Heading Length-Duct Diameter- Duct Mouth To Face Distance-Air Flow) | Percentage increase in flow rate at the face of the heading with the increase in fan design flow rate from 2.971-3.7125 m ³ /s | |
|--|---|---|
| | Flow rates (m ³ /s) | Percentage increase in flow rate (%) |
| 6.6-3-20-0.57-8m-2.97 | 7.55 | 26.19 |
| 6.6-3-20-0.57-8m-3.7125 | 9.53 | |
| 6.6-3-20-0.57-10m-2.97 | 6.56 | 25.86 |
| 6.6-3-20-0.57-10m-3.7125 | 8.25 | |
| 6.6-3-20-0.76-8m-2.97 | 6.34 | 25.23 |
| 6.6-3-20-0.76-8m-3.7125 | 7.94 | |
| 6.6-3-20-0.76-10m-2.97 | 5.02 | 25.46 |
| 6.6-3-20-0.76-10m-3.7125 | 6.30 | |

- **Factor diameter for force fan duct system (FD_F)**

To find this factor, cases with different duct diameters and similar remaining settings were grouped together. As expected, it was found that the change in diameter changed the flow rates close to the face of the heading for each set. The percentage change in the flow rate close to the face of the heading with the reduction in diameter from 0.76m to 0.57m varied with the duct mouth to face distance as given in Table 8.5.

Table 8.5 Percentage increase in flow rate at the face of the heading with the decrease in duct diameter from 0.76 - 0.57m

| Names (Heading Width-Heading Height-Heading Length-Duct Diameter-Duct Mouth To Face Distance-Air Flow) | Percentage increase in flow rate at the face of the heading with the decrease in duct diameter from 0.76 - 0.57m | | Approximated difference to keep the calculations simple |
|--|--|--------------------------------------|---|
| | Flow rates (m ³ /s) | Percentage increase in flow rate (%) | |
| 6.6-3-20-0.76-8m-2.97 | 6.34 | 19.13 | 20 |
| 6.6-3-20-0.57-8m-2.97 | 7.55 | | |
| 6.6-3-20-0.76-8m-3.7125 | 7.94 | 20.04 | |
| 6.6-3-20-0.57-8m-3.7125 | 9.53 | | |
| 6.6-3-20-0.76-10m-2.97 | 5.02 | 30.59 | 30 |
| 6.6-3-20-0.57-10m-2.97 | 6.56 | | |
| 6.6-3-20-0.76-10m-3.7125 | 6.30 | 31.01 | |
| 6.6-3-20-0.57-10m-3.7125 | 8.25 | | |

When this distance was 8m, the flow rate increased approximately by 20% with the reduction in diameter from 0.76m to 0.57m. For the distance of 10m the increase was approximately 30%. A diameter factor of 1 was assumed for a 0.76m diameter for all duct mouth to face distances. Therefore, the diameter factors for the 0.57m diameter duct with 8m distance became 1.2 and for 10m the distance became 1.30. The factors for the intermediate diameters and duct mouth face distances can be interpolated. For example, for the 0.6m diameter duct with 9m duct mouth to face distance, this factor can be calculated as below using equation 8.2 (the formula for interpolation) :

$$Y = Y_1 + (Y_2 - Y_1) \times [(X - X_1) / (X_2 - X_1)] \quad (8.2)$$

Where (X₁, Y₁), (X, Y), ((X₂, Y₂)) are three points of a linear relation, X, Y lies between the other two points and all the points except Y are known:

$$\text{Factor at 8m distance} = 1.2 + [(1 - 1.2) \times ((0.6 - 0.57) / (0.76 - 0.57))] = 1.168$$

$$\text{Factor at 10m distance} = 1.3 + [(1 - 1.3) \times ((0.6 - 0.57) / (0.76 - 0.57))] = 1.2526$$

$$\text{Factor at 9m distance} = 1.168 + [(1.2526 - 1.168) \times ((9 - 8) / (10 - 8))] = 1.2103$$

- **Factor duct mouth to face distance for force fan duct system (FF_F)**

To find this factor cases with different duct mouth to face distance, and similar remaining settings were grouped together. It was found, that the change in this distance changed the flow rates close to the face of the heading for each set. The

percentage change in flow rate close to the face of the heading with the reduction in duct mouth to face distance from 10m to 8m varied with the duct diameter as given in Table 8.6.

Table 8.6 Percentage increase in flow rate at the face of the heading with the reduction in distance of the duct mouth to face of the heading from 10m - 8m

| Names (Heading Width- Heading Height-Heading Length-Duct Diameter- Duct Mouth to Face Distance-Air Flow) | Percentage increase in flow rate at the face of the heading with the reduction in distance of the duct mouth to face of the heading from 10m - 8m | | Approximated difference to keep the calculations simple |
|--|---|--|---|
| | Flow rates (m ³ /s) | Percentage increase in flow rate (%) | |
| 6.6-3-20-0.57-10m-2.97 | 6.56 | 15.19 | 15 |
| 6.6-3-20-0.57-8m-2.97 | 7.55 | | |
| 6.6-3-20-0.57-10m-3.7125 | 8.25 | 15.49 | |
| 6.6-3-20-0.57-8m-3.7125 | 9.53 | | |
| 6.6-3-20-0.76-10m-2.97 | 5.02 | 26.27 | 26 |
| 6.6-3-20-0.76-8m-2.97 | 6.34 | | |
| 6.6-3-20-0.76-10m-3.7125 | 6.30 | 26.05 | |
| 6.6-3-20-0.76-8m-3.7125 | 7.94 | | |

When the duct diameter was 0.57m the flow rates increased approximately by 15% with the reduction in the duct mouth to face distance from 10m to 8m. For the duct diameter of 0.76m, this increase was approximately equal to 26%. A face factor equal to 1 was assumed for 10m duct mouth to face distance for all the duct diameters. Therefore, the face factor for 8m duct mouth to face distance with 0.76m duct diameter became equal to 1.26 (26% increase in flow rate compared to 10m distance) and for 0.57m duct diameter became 1.15.

The factors for the intermediate diameters and duct mouth distances from the face of the heading can be interpolated using equation 8.2. For example for a 0.6m diameter duct with 9m distance of the duct mouth to face this factor can be calculated as below:

Factor at 10m = 1 (as per rule)

Factor at 8m = $1.15 + [(1.26 - 1.15) \times ((0.6 - 0.57) / (0.76 - 0.57))] = 1.1673$

Factor at 9m = $1.1673 + [(1 - 1.1673) \times ((9 - 8) / (10 - 8))] = 1.08365$

- **Error - Mathematical model**

The maximum error of the mathematical model to estimate the flow rates close to the face of the heading used to estimate the flow rates for all the cases simulated in this study was found to be less than 7% as shown in Table 8.7.

Table 8.7 Percentage error of the mathematical model for force fan duct system

| Names (Heading Width- Heading Height-Heading Length-Duct Diameter- Duct Mouth To Face Distance-Air Flow) | Σ System factors | Simulated flow rate (m ³ /s) | $y = 6.911 \times \Sigma \text{Factors} - 15.983$ | Error (%) |
|--|-------------------------|---|---|--------------|
| 6.6-3-20-0.57-10m-2.97 | 3.35 | 7.55 | 7.17 | 5.08 |
| 6.6-3-20-0.57-8m-2.97 | 3.60 | 9.53 | 8.90 | 6.65 |
| 6.6-3-20-0.57-10m-3.7125 | 3.30 | 6.56 | 6.82 | -4.07 |
| 6.6-3-20-0.57-8m-3.7125 | 3.55 | 8.25 | 8.55 | -3.63 |
| 6.6-3-20-0.76-10m-2.97 | 3.26 | 6.34 | 6.55 | -3.27 |
| 6.6-3-20-0.76-8m-2.97 | 3.51 | 7.94 | 8.27 | -4.22 |
| 6.6-3-20-0.76-10m-3.7125 | 3.00 | 5.02 | 4.75 | 5.39 |
| 6.6-3-20-0.76-8m-3.7125 | 3.25 | 6.30 | 6.48 | -2.84 |

8.2.3 Flow definition

The variation of the fan design flow rates (maintained at the exit of the duct), diameter and length of the duct, changed the volume flow rates inside the heading at similar locations, but the air flow pattern inside the heading remained approximately similar. The high velocity stream of air after leaving the duct, hit the face of the heading and spread in all directions. The air flow close to the face of the heading, on a plane parallel to the face of the heading at a distance of 0.01m from the face can be divided into three regions as shown in Figure 8.2. The air flow pattern on this plane is shown in Figure 8.3.

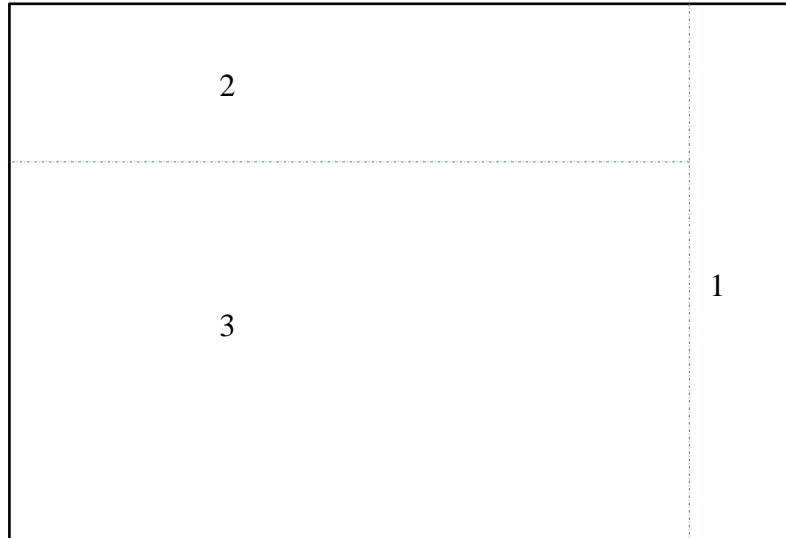


Figure 8.2 Regions of air flow on a plane parallel to the face at 0.01m distance from the face

The layer of air very close to the face (0.1m from face) in region 2 and 3 turned left swept the face of the heading and hit the left face of the heading. The air in the region 2 moved parallel to the face of the heading, hit the left face of the heading, turned in the negative direction, and moved parallel to the left face of the heading towards LTR. The air in the region 3 moved at a slightly downward angle towards the left wall and floor of the heading, but on hitting the left wall of the heading it rose up. Most of the air after moving along the face moved to the top of the heading as shown in Figure 8.4.

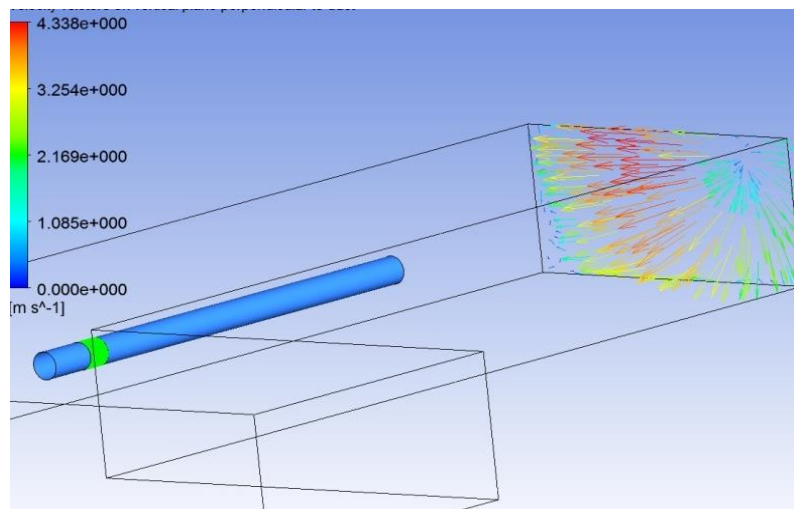


Figure 8.3 Air flows on a plane parallel to the face at 0.01m distance from the face

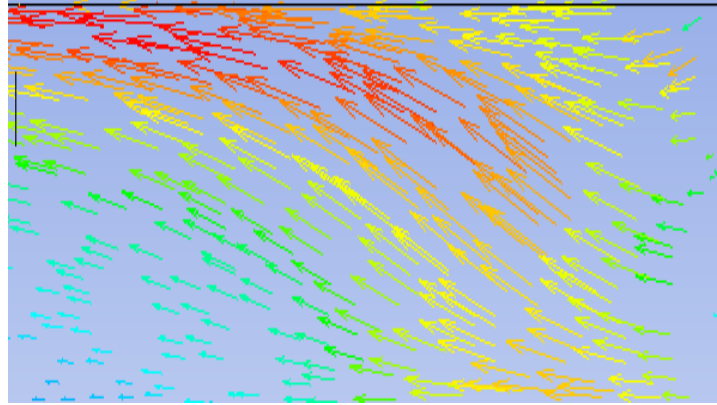


Figure 8.4 Air flows on a plane parallel to the left side wall of the heading at a distance of 0.6m from the left wall (showing the section after the duct exit)

The inner layers of air in the region 2 and 3 away from the face (0.3m to 1m) on hitting the face turned counter clockwise creating a lot of recirculation in the centre of the heading. This recirculation increased the flow rate close to the face and is prominent only in the upper half of the heading as shown in Figure 8.5. The airflows on horizontal planes constructed at the heights of 0.1m and 2.9m from the bottom of the heading are shown in Figure 8.5. Looking at the bottom plane, the air from region 3 which was moving down at an angle, biased towards the left wall of the heading reached the floor of the heading and continued moving towards the left wall of the heading. The outer most layers (left) of this air moved parallel to the left wall of the heading towards the LTR, a part of this air, however, turned counter clockwise back towards the face of the heading. The inner portion of the air on the horizontal plane moving at an angle towards the LTR and the left wall of the heading is pushed towards the left wall of the heading by the counter clock wise movement of this returning air.

The airflows at the top of the heading on a horizontal plane constructed at a height of 2.9m from the floor of the heading are shown in Figure 8.5. Most of the air after hitting the face of the heading (after exiting from the duct) swept the face and starting rising (to the top of the heading). A part of this air curled back towards the face creating a lot of recirculation close to the face in the central and upper half of the heading (as shown in Figure 8.5b). The rest of the air on reaching the ceiling of the heading spread out and continued moving towards the LTR and also towards the inlet of the duct, since the duct inlet was placed at the entrance of the heading; the fan therefore pulled this air causing

recirculation. This recirculation, at the inlet of the duct, could be avoided by keeping the opening of the duct inside the LTR using a duct with a bend. The difference between the airflows with these two systems of ducts is given in section 8.2.4.

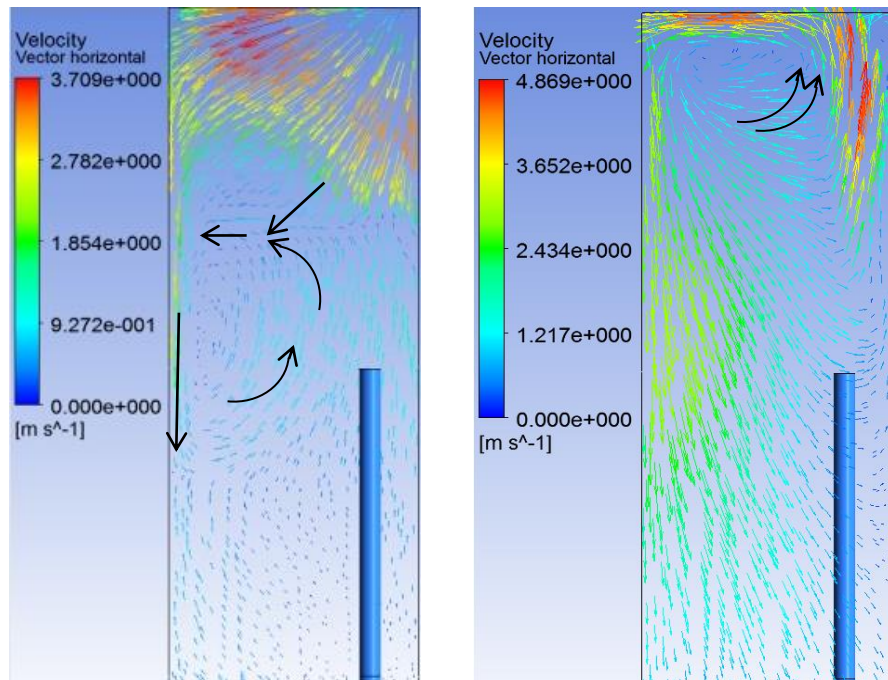


Figure 8.5 Airflows on horizontal planes constructed at height of 0.1m and 2.9m from the bottom of the heading

The movement of the air from region 1 (ref Figure 8.2) is shown in Figure 8.6 on a plane constructed at a distance of 0.1m and parallel to the right face. The air in this region moved down, hit the bottom face of the heading, and started moving in the negative direction (towards the LTR). The air coming from the opposite side (as shown in Figure 8.5a) stopped the movement of this air and forced it to turn clock wise creating a recirculation zone on the vertical plane as shown in Figure 8.6.

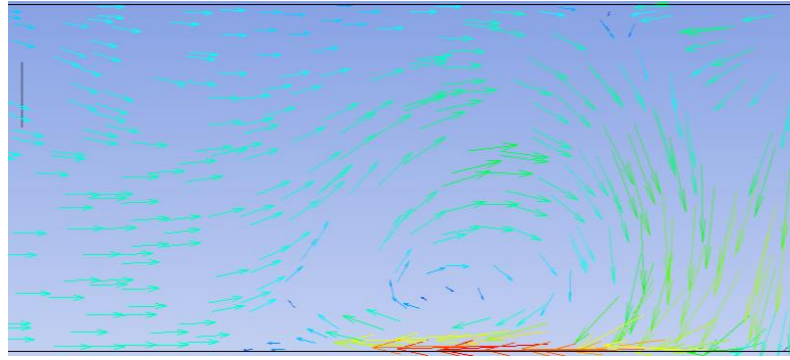
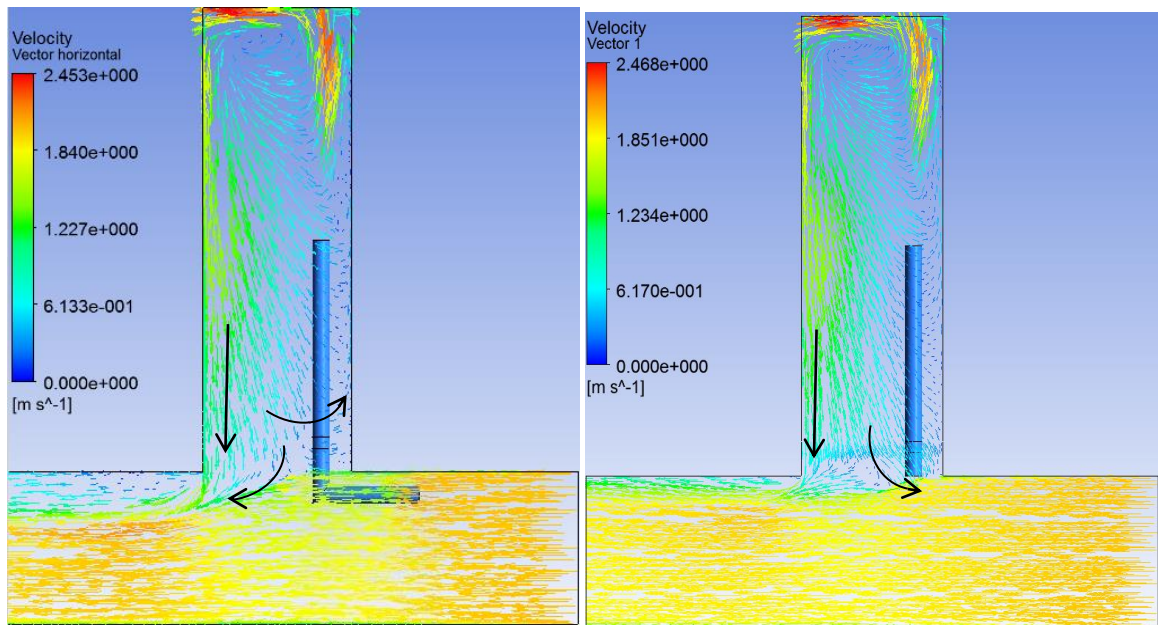


Figure 8.6 Air flows on a plane parallel to the right face of the heading at a distance of 0.1m from the right face (showing the section after the duct exit)

8.2.4 Force fan duct system - Duct inlet at entrance of heading vs duct inlet 3m inside LTR

The analysis of the force fan duct system with the duct inlet at the entrance of the heading showed the movement of the return air (at the top of the heading) inclined towards the inlet of the duct. The resulting recirculation reduced the amount of fresh air delivered by the fan to the face of the heading. A case using the 0.76m diameter duct with 10m distance from the face having a duct inlet 3m into the LTR as shown in Figure 8.7a was simulated. This was done to check the change in the air flow pattern on the top of the heading (horizontal plane constructed at a height of 2.9m from the floor of the heading). The fan design flow rate equal to $2.97\text{m}^3/\text{s}$ was used.

The system was compared with a system using similar settings except for the inlet position of the duct. The airflow rates close to the face remained similar. However, the air flow pattern on the top plane showed considerable change. The returning air still spread on the top plane to some extent, but as seen from the velocity vectors, a much higher concentration of the returning air joined the air in the LTR, and no returning air entered into the duct. As opposed to this system, a much higher concentration of returning air could be seen entering the duct again when the duct inlet was placed at the entrance of the heading as shown in Figure 8.7b. Therefore, with a force fan duct system the duct inlet should be placed inside the LTR using a duct with a bend (which will though need a more powerful fan to keep the same flow rate at the exit of the duct, but the recirculation will be reduced significantly).



a) Duct inlet inside the LTR

b) Duct inlet at the entrance of heading

Figure 8.7 Airflows on horizontal planes constructed at a heights 2.9m from the floor of the heading

8.2.5 Conclusion

The quantity of air that reached the face of the heading, with both the 0.57m and 0.76m diameter ducts, and duct mouth to face distances of 8m and 10m was found to be higher than the fan exit flow rate. Due to recirculation, the amount of fresh air that reached the face was at least, less than 50% of the total air that actually reached the face for all the cases. The amount of recirculation, increased with the reduction in diameter and duct mouth to face distance. Therefore, duct mouth to face distance should not be less than 10m, and the biggest possible/permissible diameter should be used to reduce the recirculation. The inlet of the force fan duct should not be placed inside, or at the entrance of the heading. It should be placed inside the LTR, using a bend in the duct to avoid recirculation of the air.

8.3 Exhaust Fan Duct System

8.3.1 Flow rates

A total of eight cases as summarized in Table 8.8 were simulated using exhaust duct fan systems. Similar to the force fan duct system, the variation of fan design flow rates, diameter and length of the duct changed the volume flow rates calculated inside the heading at similar locations. The air flows delivered by the exhaust fan duct system close to the face of the heading have been calculated for each case and tabulated in Table 8.9. These flow rates were calculated using the positive axial velocities going into the planes, which are constructed parallel to the face of the heading at the distances of 0.5m, 0.4m, and 0.3m. The flow rates decreased closer to the face.

Table 8.8 Details of Exhaust fan duct system cases

| Names (Heading Width-Heading Height-Heading Length-Duct Diameter-Duct Mouth To Face Distance-Air Flow) |
|--|
| 6.6-3-20-0.57-2m-2.97 |
| 6.6-3-20-0.57-2m-3.7125 |
| 6.6-3-20-0.57-4m-2.97 |
| 6.6-3-20-0.57-4m-3.7125 |
| 6.6-3-20-0.76-2m-2.97 |
| 6.6-3-20-0.76-2m-3.7125 |
| 6.6-3-20-0.76-4m-2.97 |
| 6.6-3-20-0.76-4m-3.7125 |

Table 8.9 Flow rates at specified distances from the face of the heading for exhaust fan duct system

| Names (Heading Width- Heading Height-Heading Length-Duct Diameter- Duct Mouth To Face Distance-Air Flow) | Distance from the face | | |
|--|-----------------------------------|-----------------------------------|--------------------------------|
| | 0.5m | 0.4m | 0.3m |
| | Flow rates (m ³ /s) | Flow rates (m ³ /s) | Flow rates (m ³ /s) |
| 6.6-3-20-0.57-2m-2.97 | 1.968 | 1.64 | 1.29 |
| 6.6-3-20-0.57-2m-3.7125 | 2.155 | 1.79 | 1.42 |
| 6.6-3-20-0.57-4m-2.97 | 1.931 | 1.59 | 1.24 |
| 6.6-3-20-0.57-4m-3.7125 | 2.120 | 1.76 | 1.39 |
| 6.6-3-20-0.76-2m-2.97 | 2.365 | 1.98 | 1.59 |
| 6.6-3-20-0.76-2m-3.7125 | 2.603 | 2.15 | 1.71 |
| 6.6-3-20-0.76-4m-2.97 | 2.240 | 1.88 | 1.46 |
| 6.6-3-20-0.76-4m-3.7125 | 2.464 | 2.04 | 1.62 |

Volume flow rates close to the face of the heading

Keeping in view the tabulated data given in Table 8.9, the following was found about the flow rates close to the face of the heading (0.5m from the face), ventilated using a force fan duct system:

- When the diameter of the duct and the duct design flow (fan design flow rate) rate were kept constant, the flow rate close to the face of the heading increased with the decrease in the distance of the duct mouth to face.
- When the diameter of duct and the distance of the duct mouth to face were kept constant, the flow rate close to the face of the heading increased with the increase in the duct design flow rate.
- When the distance of the duct mouth to face and the duct design flow rate were kept constant, the flow rate close to the face of the heading increased with the increase in the duct diameter.

8.3.2 Mathematical formulation to estimate air flows for exhaust duct system

In order to find a relationship to estimate the flow rates reaching the face (0.5m from face) of the heading, using a exhaust fan duct system, the flow rates close to the face of the heading for all the cases were plotted against the summation of the system factors as

given in Table 8.10 and shown in Figure 8.8. These factors were calculated to cater for the effects of change in diameter, change in the distance of the duct mouth to face (Face factors) and the change in fan design flow rate. A best fit linear relation was found between the two quantities and is given in equation 8.3. The factors were calculated based on the reasoning given below:

Table 8.10 Flow rate close to the face and different factors for Exhaust fan duct system

| Names (Heading Width- Heading Height-Heading Length-Duct Diameter- Duct Mouth to Face Distance-Air Flow) | Distance from the face | | | | |
|--|--|--|---|-------------------------|--------------------|
| | 0.5m | | | | |
| | Flow rates (FRF _E) (m ³ /s) | Flow rate factor (FFR _E) | Diameter factor (FDE _E) | Face factor (FFE) | ΣSystem factors |
| 6.6-3-20-0.57-2m-2.97 | 1.968 | 1 | 0.83 | 1 | 2.83 |
| 6.6-3-20-0.57-2m-3.7125 | 2.155 | 1.1 | 0.83 | 1 | 2.93 |
| 6.6-3-20-0.57-4m-2.97 | 1.931 | 1 | 0.86 | 0.98 | 2.84 |
| 6.6-3-20-0.57-4m-3.7125 | 2.120 | 1.1 | 0.86 | 0.98 | 2.94 |
| 6.6-3-20-0.76-2m-2.97 | 2.365 | 1 | 1 | 1 | 3 |
| 6.6-3-20-0.76-2m-3.7125 | 2.603 | 1.1 | 1 | 1 | 3.1 |
| 6.6-3-20-0.76-4m-2.97 | 2.240 | 1 | 1 | 0.95 | 2.95 |
| 6.6-3-20-0.76-4m-3.7125 | 2.464 | 1.1 | 1 | 0.95 | 3.05 |

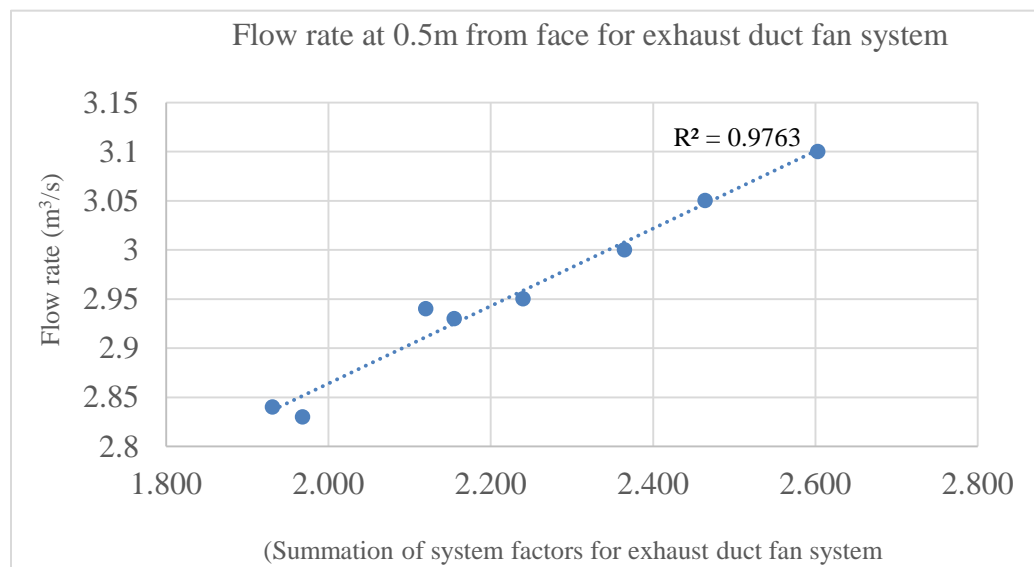


Figure 8.8 Flow rate close to the face of the heading vs Factors for exhaust fan duct system

$$\text{Flow rate} = \text{FRF}_E = (0.39 \times \sum \text{System Factors}) + 2.07 \quad (8.3)$$

- **Factor flow rate for exhaust fan duct system (FFRE)**

All the cases in this study were simulated with two fan design flow rates; $2.97\text{m}^3/\text{s}$ and $3.971\text{m}^3/\text{s}$. The difference between these two flow rates is equal to 25%. A comparison of flow rates at the face of the heading for each set of cases run with these flow rates and the same remaining settings is given in Table 8.11. It was found that an increase in the fan design flow rate by 25%, increased the flow rate at the face of the heading approximately by 10% for all duct diameters and all duct mouth to face distances. A flow rate factor equal to 1 was assumed for $2.971\text{m}^3/\text{s}$ duct design flow rate. The flow rate factor for fan design flow rate of $3.7125\text{m}^3/\text{s}$, therefore, becomes equal to 1.10 (10% more flow rate as compared to $2.971\text{m}^3/\text{s}$). The factors for other duct design flow rates can be interpolated using methods discussed for the force fan duct system.

Table 8.11 Percentage increase in flow rate at the face of the heading with the increase in fan design flow rate from $2.971\text{m}^3/\text{s}$ to $3.7125\text{m}^3/\text{s}$

| Names (Heading Width-Heading Height-Heading Length-Duct Diameter- Duct Mouth To Face Distance-Air Flow) | Percentage increase in flow rate at the face of the heading with the increase in fan/duct design flow rate from $2.971\text{m}^3/\text{s}$ to $3.7125\text{m}^3/\text{s}$ | |
|---|---|--------------------------------------|
| | Flow rates (m^3/s) | Percentage increase in flow rate (%) |
| 6.6-3-20-0.57-2m-2.97 | 1.968 | 9.50 |
| 6.6-3-20-0.57-2m-3.7125 | 2.155 | |
| 6.6-3-20-0.57-4m-2.97 | 1.931 | 9.79 |
| 6.6-3-20-0.57-4m-3.7125 | 2.120 | |
| 6.6-3-20-0.76-2m-2.97 | 2.365 | 10.06 |
| 6.6-3-20-0.76-2m-3.7125 | 2.603 | |
| 6.6-3-20-0.76-4m-2.97 | 2.240 | 10.01 |
| 6.6-3-20-0.76-4m-3.7125 | 2.464 | |

- **Factor diameter for exhaust fan duct system (FDE_E)**

To find this factor, cases with different duct diameters and similar remaining settings were grouped together. It was found that the change in diameter changed the flow rates close to the face of the heading for each set. The percentage change in the flow rate close to the face of the heading with the

reduction in diameter from 0.76m to 0.57m varied with the duct mouth to face distance as given in Table 8.12.

When this distance was 2m the flow rate decreased approximately by 17% with the reduction in diameter from 0.76m to 0.57m. For the distance of 4m the decrease was approximately 14%. A diameter factor of 1 was assumed for 0.76m duct diameter for all duct mouth to face distances. Therefore, the diameter factors for the 0.57m diameter duct with 2m distance became 0.83 and for 4m distance became 0.86. The factors for the intermediate diameters and duct mouth face distances can be interpolated using methods discussed for the force fan duct system.

Table 8.12 Percentage increase in flow rate at the face of the heading with the decrease in duct diameter from 0.76 - 0.57m

| Names (Heading Width-Heading Height-Heading Length-Duct Diameter-Duct Mouth To Face Distance-Air Flow) | Percentage decrease in flow rate at the face of the heading with the decrease in duct diameter from 0.76 - 0.57m | | Approximated difference to keep the calculations simple |
|--|--|--------------------------------------|---|
| | Flow rates (m ³ /s) | Percentage decrease in flow rate (%) | |
| 6.6-3-20-0.76-2m-2.97 | 2.365 | 16.79 | 17 |
| 6.6-3-20-0.57-2m-2.97 | 1.968 | | |
| 6.6-3-20-0.76-2m-3.7125 | 2.603 | 17.21 | |
| 6.6-3-20-0.57-2m-3.7125 | 2.155 | | |
| 6.6-3-20-0.76-4m-2.97 | 2.240 | 13.79 | 14 |
| 6.6-3-20-0.57-4m-2.97 | 1.931 | | |
| 6.6-3-20-0.76-4m-3.7125 | 2.474 | 14.32 | |
| 6.6-3-20-0.57-4m-3.7125 | 2.120 | | |

- **Factor duct mouth to face distance for exhaust fan duct system (FF_E)**

To find this factor, cases with different duct mouth to face distance similar remaining settings were grouped together. It was found that the change in this distance changed the flow rates close to the face of the heading for each set. The percentage change in flow rate close to the face of the heading with the increase in duct mouth to face distance from 2m to 4m varied with the duct diameter as given in Table 8.13.

When the duct diameter was 0.57m the flow rates decreased approximately by 2%, and for the duct diameter of 0.76m this decrease was approximately equal to

5%. A factor equal to 1 was assumed for the 2m duct mouth to face distance for all duct diameters. Therefore, the face factor for 4m duct mouth to face distance with 0.76m duct diameter became equal to 0.95 (5% reduction in flow rate compared to 2m distance) and for 0.57m diameter duct it became equal to 0.98.

Table 8.13 Percentage reduction in flow rate at the face of the heading with the increase in distance of the duct mouth to face of the heading from 2m - 4m

| Names (Heading Width-Heading Height-Heading Length-Duct Diameter-Duct Mouth To Face Distance-Air Flow) | Percentage decrease in flow rate at the face of the heading with the increase in duct mouth distance to face of the heading from 2m - 4m | | Approximated difference to keep the calculations simple |
|--|--|--------------------------------------|---|
| | Flow rates (m ³ /s) | Percentage increase in flow rate (%) | |
| 6.6-3-20-0.57-4m-2.97 | 1.931 | 1.880081301 | 2 |
| 6.6-3-20-0.57-2m-2.97 | 1.968 | | |
| 6.6-3-20-0.57-4m-3.7125 | 2.120 | 1.62412993 | |
| 6.6-3-20-0.57-2m-3.7125 | 2.155 | | |
| 6.6-3-20-0.76-4m-2.97 | 2.240 | 5.285412262 | 5 |
| 6.6-3-20-0.76-2m-2.97 | 2.365 | | |
| 6.6-3-20-0.76-4m-3.7125 | 2.464 | 5.332308874 | |
| 6.6-3-20-0.76-2m-3.7125 | 2.603 | | |

- **Error of the mathematical model**

The maximum error of the mathematical model for exhaust fan duct system, used to estimate the flow rates for the simulated cases of this study was found to be less than 1% as shown in Table 8.14.

Table 8.14 Percentage error of the mathematical model for exhaust fan duct system

| Names (Heading Width-Heading Height-Heading Length-Duct Diameter- Duct Mouth To Face Distance-Air Flow) | Σ System factors | Simulated flow rate (m ³ /s) | $y = y = 0.3943 \times \Sigma \text{Factors} + 2.0754$ | Error (%) |
|---|-------------------------|---|--|-----------|
| 6.6-3-20-0.57-2m-2.97 | 2.83 | 1.97 | 2.85 | -0.76 |
| 6.6-3-20-0.57-2m-3.7125 | 2.93 | 2.16 | 2.93 | 0.17 |
| 6.6-3-20-0.57-4m-2.97 | 2.84 | 1.93 | 2.84 | 0.11 |
| 6.6-3-20-0.57-4m-3.7125 | 2.94 | 2.12 | 2.91 | 0.98 |
| 6.6-3-20-0.76-2m-2.97 | 3 | 2.37 | 3.01 | -0.26 |
| 6.6-3-20-0.76-2m-3.7125 | 3.1 | 2.60 | 3.10 | -0.06 |
| 6.6-3-20-0.76-4m-2.97 | 2.95 | 2.24 | 2.96 | -0.29 |
| 6.6-3-20-0.76-4m-3.7125 | 3.05 | 2.46 | 3.05 | 0.10 |

8.3.3 Flow definition

Similar to the force fan duct system, the variation of the fan design flow rates, diameter and length of the duct, changed the volume flow rates calculated inside the heading at similar locations, but the air flow pattern inside the heading remained similar. These air flow patterns are expected to change with the change in the positioning of the duct and LTR velocity. For the studied cases, air entered from the downstream side of the heading, ventilated the face in a clock wise direction, and entered the exhaust duct as shown in Figure 8.9. The air pulled by the fan from the LTR did not enter the duct immediately; it continued moving towards the face due to the momentum of the air, hit the face, turned clockwise and swept the face of the heading before entering into the duct. The airflow pattern on a vertical plane constructed parallel to the left wall of the heading at a distance of 0.6m from the face is shown in Figure 8.10. The air turning

towards the right wall (clock wise movement of air) can be clearly seen in the inset view (showing the same parallel plane as seen from the top of the heading).

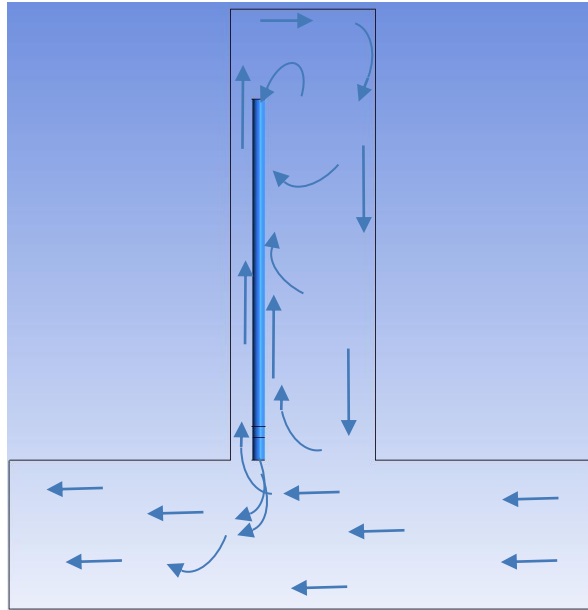


Figure 8.9 Air flow path of exhaust duct ventilation system

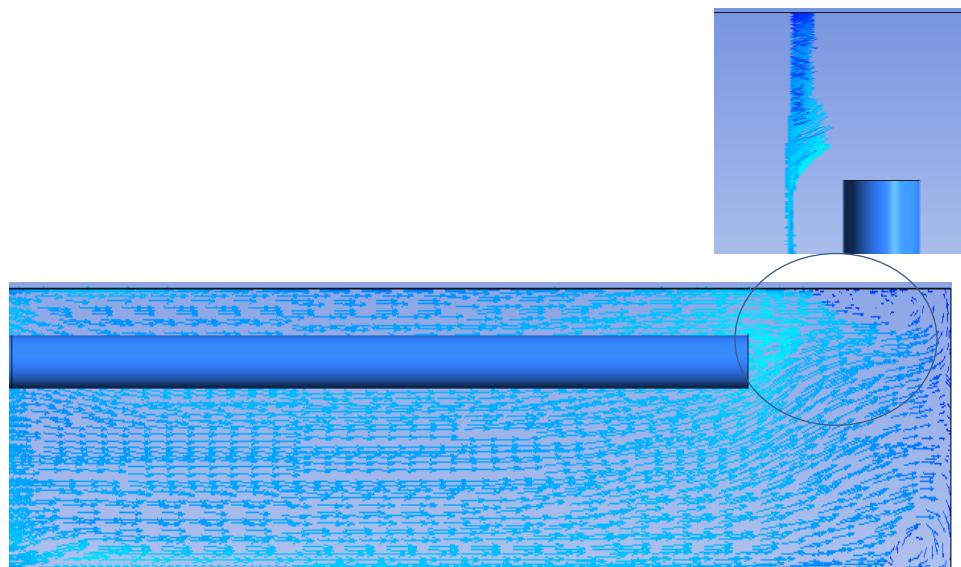


Figure 8.10 Air flows on a plane parallel to the left wall of the heading at a distance of 0.6m (air moving parallel to the duct), inset; air turning clock wise on reaching close to the face

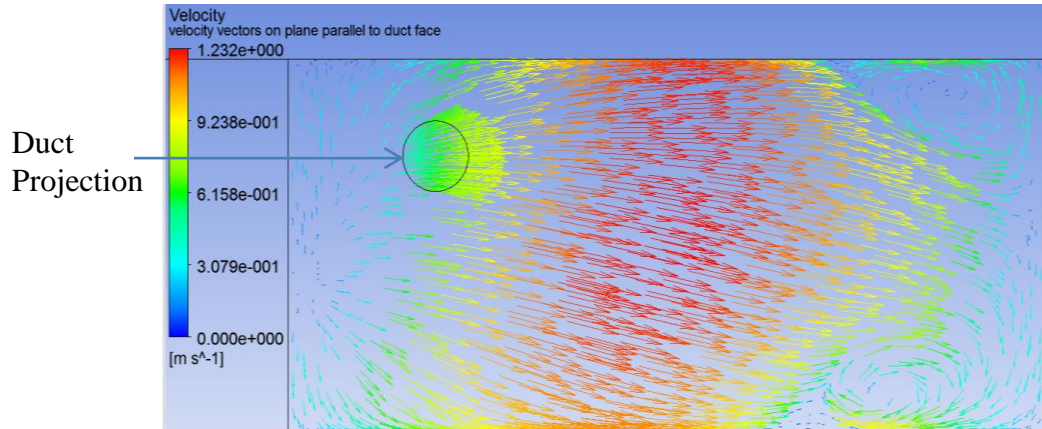


Figure 8.11 Air flow on a plane parallel to the face at 0.01m distance from the face

The air flow pattern on a plane constructed parallel to the face of the heading, at a distance of 0.01m from it is shown in Figure 8.11. The air movement close to the face can be seen very clearly, air on reaching the face turned clock wise towards the right face of the heading. The two recirculation zones were formed in the top and bottom right corners of the heading. Air after moving along the face, turned clock wise (on the horizontal plane) and entered the exhaust duct as shown in Figure 8.12.

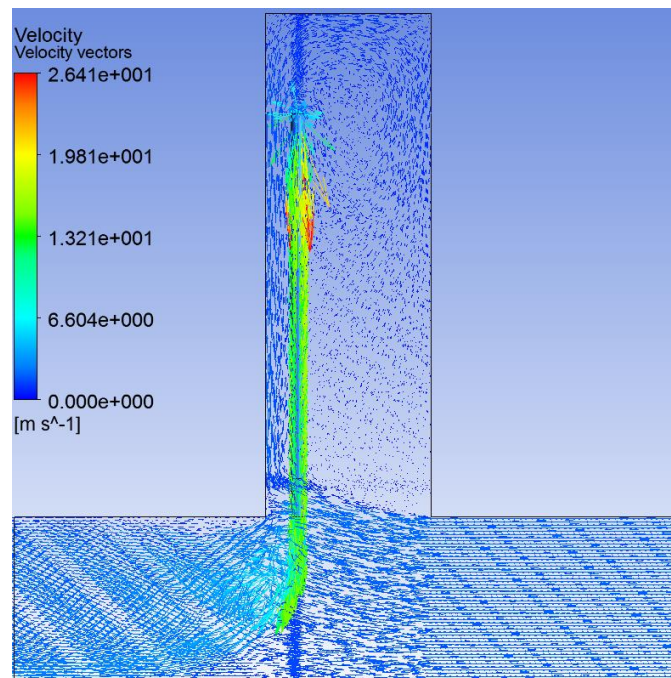


Figure 8.12 Air flow on a horizontal plane, exhaust fan duct ventilation system

8.3.4 Conclusion

The flow rates close to the face of the heading with both the 0.57m and 0.76m diameter ducts for the exhaust duct system were much lower than the force fan duct system. The air velocities as seen from the velocity vectors were also low. The flow rate increased with, the increase in the diameter of the duct, increase in fan/duct design flow rate, and the reduction in the duct mouth to face distance. Therefore, when using an exhaust duct ventilation system, duct mouth to face distance should not be more than 4m, and the biggest possible/permissible diameter should be used to maximize flow rate close to the face of the heading.

It was found that the force fan duct system produced a lot of recirculation and the exhaust fan duct system produced lower air flow rates close to the face. It is expected that the air flow patterns should change considerably with the change in the orientations of the duct for both the systems, but still the limitations of both the systems should remain. An overlap system using both the force and exhaust systems, which is seldom used in the South African mining industry, is expected to overcome the limitations of both the systems.

In the next chapter, the key findings, key contributions, and limitations of the research, along with the recommendations for future work are given.

9 CONCLUSIONS AND RECOMMENDATIONS

9.1 Introduction

The research was carried out to evaluate the ventilation of a heading connected to the LTR in a Room and Pillar coal mine using CFD analysis. ANSYS Fluent numerical code was used to simulate various design alternatives that may be encountered in an actual underground mine. The influence of various system drivers used for each ventilation design on the flow rates were evaluated and calculated. Mathematical models were developed using the cumulative effect of all the studied system variables to calculate flow rates close to the face of the heading and also at the exit of the LB, for the LB and fan with duct ventilation systems.

The research showed that it is possible to develop fluid dynamic models, at acceptable confidence levels, in ANSYS Fluent, for various ventilation layouts and operating conditions and demonstrated that it can be an attractive approach to evaluate face ventilation systems with and without the use of auxiliary ventilation devices. This approach gave a better understanding of the flow behaviour, through detailed information on airflow patterns and flow rates.

9.2 Key Findings of the Research

Key findings of this thesis are summarized as below:

- The results of the validation studies carried out in the actual mining environment showed that CFD numerical code ANSYS Fluent was an appropriate tool to study the face ventilation of a heading in a three dimensional environment using full scale models.
- The evaluation of the ventilation of a heading connected to the LTR, ventilated without the use of any auxiliary equipment, showed that the air entered from the downstream side and joined the LTR air from the upstream side, and the overall flow rate was minimal as compared to the flow rate in the main stream.
 - The flow rates and the maximum axial velocities increased with the increase in the LTR velocity to the depth of 10m (maximum flow rate of $1.26\text{m}^3/\text{s}$ and

1.58m³/s going into the heading, were found for the 3m and 4m high heading using LTR velocity of 2m/s).

- The maximum axial velocities and air flow rates and were found to be maximum at the depth of 5m where the maximum recirculation occurred, after which there was a sharp decrease in both the quantities as shown in Figures 4.3 and 4.8 respectively.
- At depths deeper than 10m both the maximum axial velocities and the flow rates were very low. Maximum air penetration depths were found with the LTR velocity of 1.35m/s and the penetration decreased with the increase or decrease in velocity from the 1.35m/s velocity. A similar trend was followed by the flow rates as well, although they become too low to be meaningful as far as the ventilation of the heading is concerned after the 10m depth.
- The ventilation of a heading with the use of LB, showed that the flow rates at the exit of the LB and close to the face of the heading were dependent on the system variables associated with this ventilation system, i.e. LTR velocity, heading dimension and settings of the LB (distance of the LB from the wall in the LTR and heading, the length of the LB in the LTR and the heading, the angle of the LB in the LTR).
 - In the case of a short 10m deep heading, higher air flow rate were observed close to the face of the heading with the use of the LB as compared to the heading ventilated without LB. The flow rates close to the face of the heading almost doubled with the introduction of a LB even with a 0.5m distance from the wall in the LTR and the heading. The increase was more prominent with the bigger distance of the LB from the wall.

The flow rate close to the face of a 20m long heading were almost non-existent when it was ventilated without the LB; with the use of the LB the flow rates were found almost equivalent to the flow rates of the short heading ventilated with a LB.
 - The flow rates at the exit of the LB, the face of the heading, and at all depths inside the heading increased proportionally to the increase in the LTR velocity.

- The flow rates at the exit of the LB, the face of the heading and at all depths inside the heading increased proportionally to the increase in the height of the heading. However, the height of the heading did not affect the per square meter flow rate for any configuration of the LB and LTR velocity.
- The flow rates at the exit of the LB were found proportional to the product of the entrance length and the distance of the LB from the wall in the heading. Just increasing the inlet length by increasing the angle (opening) of the LB will not increase the flow rate at the exit of the LB; the distance of the LB from the wall in the heading should also be increased. If this distance is not increased, the viscous effect caused due to the reduction of the area reduces the entrance of air in the channel between the LB and the wall, see Table 6.3. Furthermore, the flow rates increased proportionally to the increase in LTR velocity and the height of the heading.
- When the LB was used without an angle in the LTR, the increase in its length beyond 3m reduced the flow rate at the exit of the LB at the rate of 1% per 2m increase in length. Therefore, a LB longer than 3m should not be used in the LTR when it is used without an angle.
- The flow rate at the exit of the LB could be estimated using equation 6.8 given below:

$$\text{Flow rate at the exit of the LB} = \text{FRE}_{\text{LB}} = [(1.27 \times (X \times b)) + 0.65] \times [1 + ((\text{LTR Vel} - 1)) + ((\text{HH} - 3)/3) - \underbrace{((d - 5)/(2 \times 100)) - ((c - 3)/(2 \times 100))}_{\text{Only when LB used with zero degree in LTR}}]$$

Where,

X = LB entrance length

b = Distance of the LB from the wall in the heading

c = Length of the LB in the LTR

d = Length of LB in the heading

HH = Heading height

LTR Vel = Velocity of air in the LTR

- The air was delivered closer to the face of the heading with a longer LB resulting in higher flow rates. A minimum distance of 5m of the LB exit from the face of a heading for a heading equal to or longer than 20m should be used.
- The increase in length of the LB in the LTR when the LB was used without an angle, increased the resistance offered to the air and thus reduced the flow rate at the exit of the LB and proportionally at the face of the heading. The increase in length when the LB was used with an angle, increased the inlet area and thus increased the air flow at the exit of the LB and a proportional increase at the face of the heading as well. A LB longer than 3m should not be used in the LTR when it is used without an angle.
- An increase in distance of the LB from the wall in the heading increased the flow rates at the exit of the LB and close to the face of the heading. But this distance was found to affect the distribution of air inside the channel (wall of the heading and LB). This was caused by the pushing of air due to centrifugal force close to the LB when it turned into the heading.
 The flow however, became uniform as the air travelled through this channel. It was found that a minimum length equal to 10m and 15m were required to achieve an evenly distributed flow at the exit of the LB for the 0.5m and 1m distance of the LB from the wall respectively. When the minimum lengths were not used more and more of the useful air leaving the LB returned without reaching the face of the heading, since the air closer to the LB after leaving the LB turned first. Therefore, longer LB to wall distance is suited for long headings, where a LB of at least 15m is required, if installed in shorter headings the distance from the face should be kept to the minimum. A LB with a wall distance greater than 1m will not ensure provision of sufficient flow rate close to the face, unless used very close to the face or coupled with additional engineering solutions. Therefore, to increase flow rates close to the face of the heading, instead of using LB to wall distance higher than 1m, LB with an appropriate angle can be a better solution. The narrow LB to wall distance in the heading will ensure that most of the air exiting the LB reaches the face.

- The flow rates close to the face of the heading and at all depth planes inside the heading increased due to the increase in the angle of LB in the LTR. This increase was proportional to the increase in the flow rates at the exit of the LB. Therefore, the flow rates close to the face can be increased by increasing the angle of the LB in the LTR.
- The flow rates close to the face of the heading could be estimated for the cases falling with the boundary of the study using equation 6.10 given below:

$$\text{Flow rate close to the face of the heading (0.5m from the face)} = \text{FRF}_{\text{LB}} = [(1.30 \times \text{F}_{\text{LB}} \times (\text{X} \times \text{b})) + 0.51] \times [1 + ((\text{LTR Vel} - 1)) + ((\text{HH} - 3)/3) - ((\text{f} - 4.5) / (2 \times 100)) + (((\text{FL}_{\text{LB}} \text{ First metre}) + (\sum_{i=2}^n \text{FL}_{\text{LB}} \text{ First metre} \times \text{RF}_{\text{LB}}^{(i-1)})) / 100) - ((\text{c} - 3) / (2 \times 100))]]$$

Only for LB used with zero degree in LTR

Where,

F_{LB} = Factor LB ventilation system

X = LB entrance length

b = Distance of the LB from the wall in the heading

c = Length of the LB in the LTR

d = Length of LB in the heading

f = Distance of LB from the face of the heading

HH = Heading height

LTR Vel = Velocity of air in the LTR

First metre factor = 2 (only to be used when LB length more than 5m) for 1m distance of LB from the wall and 1 for 0.5m distance, for other distances it can be interpolated.

n = 10 for 1m distance of LB from the wall and 5 for 0.5m distance, for other distances it can be interpolated.

Reduction Factor = RF_{LB} = 0.8 for 1m distance of LB from the wall and 0.43 for 0.5m distance, for other distances it can be interpolated.

- CFD numerical code ANSYS Fluent was found very useful to identify the low flow and recirculation zones in the heading ventilated using LB. Various results were presented graphically to clearly show these zones.
- A heading in the presence of a CM once ventilated using LB showed that the presence of the CM divided the air flows into two halves, the bottom half with reduced width due to the presence of the CM and the top half (where the methane accumulates) with the full width. Distinct airflows were observed in the top, bottom and middle of the heading, with most of the air after moving along the face rose to the top of the heading and returned to the LTR. The air flow pattern remained the same for the 3m and 4m high heading. This knowledge may help in designing and installation of possible ventilation solutions on the CM to improve ventilation of the heading.
- The ventilation of a heading using a force fan duct system showed that the air on reaching the face swept it and rose to the upper half of the heading. A lot of this air in the centre and upper half of the heading recirculate close to the face of the heading.

Furthermore, it was found that:

- The duct should not be placed at the entrance of the heading, as part of the returning air entered the duct. The duct entrance should be kept inside the LTR using a bended duct.
- Using the assumption, that all the air exiting the duct was reaching the face, it was found that:
 - The percentage of fresh air was less than 50% of the total air that was actually present close to the face of the heading.
 - The less the distance of the duct mouth to the face the more was the percentage of recirculation (the flow rate with 8m distance was more than 10m distance, due to the increase in recirculation).
 - An increase in the fan design flow rate did not change the percentage of fresh air reaching the face of the heading (however, the amount of fresh air increased at the same proportion as was the increase in the design flow rate, but the amount of recirculation also increased).

- The bigger the diameter of the duct (0.76m), the more was the percentage of fresh air that reached the face of the heading (although with a smaller diameter duct more air (20 to 30%) reached close to the face of the heading, but it happened because of the increase in recirculation).
- Keeping in view the above, the distance of the duct mouth to face of the heading for a force fan duct ventilation system should not be less than 10m, and the biggest possible diameter should be used to reduce recirculation.
- The flow rates close to the face of the heading using a force fan duct ventilation system was found to be dependent on the diameter of duct, the distance of the duct mouth to face and the fan design flow rate (flow rate exiting from the duct). The flow rates close to the face of the heading could be estimated using equation 8.1 given below with an error of less than 7% :

$$FRF_F = (6.91 \times \sum \text{System Factors}) - 15.98$$

Where,

Summation of system factors = flow rate factor (FFR_F) + duct diameter factor (FD_F) + face factor (FF_F) (to cater for the distance of duct mouth to the face).

- The ventilation of a heading using an exhaust duct ventilation system showed that higher velocity of air entered the heading from the downstream side ventilated the face (turned clock wise) and entered the exhaust duct. The flow rates close to the face of the heading were much lower than the ones achieved using the force fan duct ventilation system.
 - The flow rates close to the face of the heading were affected by the distance of the duct mouth to face, the fan design flow rate and the diameter of the duct. Higher flow rates were achieved for, shorter duct mouth to face distance (very small difference of 2-5% per 2m reduction in distance), higher fan design flow rate (10% increase per 25% increase in design flow rate), and bigger duct diameter (14-17% reduction in flow rate with the reduction in diameter from 0.76m to 0.57m). Therefore, to increase the flow rates close to the face of the heading, the distance of the duct mouth to face should

be reduced (close to 3m), a more powerful fan (having higher design flow rate) should be used, and a bigger duct diameter should be used. The flow rates close to the face of the heading could be estimated within an accuracy of 1% using the equation 8.3 given below:

$$FRF_E = (0.39 \times \sum \text{System Factors}) + 2.07$$

Where,

Summation of system factors = system design flow rate (FFR)+ duct diameter factor (FDE_E)+ face factor (FF_E)(to cater for the distance of duct mouth to the face).

- The validation studies have shown that if the auxiliary devices are installed correctly the numerical results can be in-line with the experimental results. However, a tolerance factor of 5-10% may be used while using the estimation models given in the study.

9.3 Research Contribution

- The research has demonstrated the capabilities of CFD to evaluate the performance of face ventilation systems. This could encourage the mining industry to use CFD during the interactive design process to modify/improve ventilation systems, and improve health conditions and productivity.
- The air flow patterns and the flow rates close to the face of the heading with the use of the auxiliary ventilation systems were made clear. This could also help mine ventilation engineers to improve their ventilation designs.
- The influence of the system variables of the auxiliary ventilation systems were made clear which could be beneficial to optimise the use of these systems and during the designing/addition of supplementary engineering solutions if required.
- Demonstrated how to develop estimation models using comparative analyses.
- The estimation models presented have not been related to the Codes of practice which may vary from country to country. The models however, can be used anywhere, and may help to estimate airflows and make changes to meet country

specific regulations. The mine managers can use the mathematical models presented in the study to provide quick reference charts/spread sheets to the supervisory staff to correctly install the auxiliary devices during the different phases of the mining and ensure sufficient ventilation.

- The practicing mining engineers can also benefit from this research, use the approach followed/results in their research and play with design alternatives to explore more solutions for the mining industry.
- The work can also serve Academia as part of the curriculum to teach future mining engineers how the different variables associated face ventilation system affect the ventilation in a heading.

9.4 Research Limitations

- The ANSYS Fluent software licence (life time) costs approximately 6000 U.S Dollars, and an additional annual technical enhancement and customer support fee of approximately 1000 U.S Dollars. This is a disadvantage, although its results are extremely important and of great value.
- Intel (R) Xeon(R) CPU E5-2687W v2 @ 3.40GHz 3.40 GHz with 16 GB RAM using 8 core parallel processing was the computational system that was primarily used in this research. Besides that, one machine (AMD Opteron (TM) Processor 6276) running on a shared server was also used. Electricity interruptions and the limited number of cores available to carry out parallel processing increased the time to complete the work. Higher computational powers could have reduced the computational time and allowed the study of additional cases and scenarios, but it requires additional cost.
- The accuracy of the results is highly dependent on the mesh size and thus the available computational resources. The solution should be mesh size independent; any further reduction in the mesh size used should not affect the results. This was ensured in the study, and a very fine mesh size was used, but since it increased the convergence time for each simulation, a limited number of cases for the fan with duct ventilation system were simulated and studied.
- Due to computational constraints, the maximum heading depth of 20m and only one width of the heading (6.6m) was used.

- The modelling and meshing of the problem domain is generally carried out using separate software and then the meshed model is imported into ANSYS. Therefore, the initial practice and learning of the meshing and modelling techniques was carried out using GAMBIT software. However, the actual work was carried out completely using the ANSYS software, since the service provider stopped the upgrading and issuing of new licences for GAMBIT.

9.5 Recommendations for the Future Research Work

- The major emphasis/idea of this research was to highlight as to how the subject should be addressed in a sequential and detailed manner. Further research in the following sequence should now be carried out to build on this research:
 - The effect of the change in width of the heading.
 - The effects of leaky LB and ducts.
 - The effect of changing the position of the duct and velocity of air in the LTR.
 - Overlap fan duct system to find if it can overcome the limitations of the force and exhaust duct ventilation systems.
 - The effect of the liberation of methane gas at different rates inside the heading.
 - The effect of the introduction of an actual CM along with methane gas and coal dust.
 - The effect of the introduction of other engineering solutions on the CM along with methane gas and coal dust.
 - Similarly presence of a roof bolter and so on.
- Provision of mathematical models for these scenarios through further research can not only improve health and safety conditions, make planning and implementation easier, but will also ease the formulation and improvement of the instructions and regulations related to the installation of auxiliary ventilation equipment.
- The individual mining companies are using numerical modelling techniques during the interactive design process to optimally use the ventilation devices. But generally this work is not being shared with the academic institutes which can provide an ideal platform to integrate a systematic research in this field. The

major benefit of the involvement of the academic institutes is that the outcome of the research would be available to everyone. High performance computational facilities should therefore, be made available in the universities to carry out in depth studies in this field using numerical modelling.

REFERENCES

- AMC Consultants Pty Ltd. (2005). *Basic Mine Ventilation, Revision 5*. [Online] <http://wenku.baidu.com/view/3a566fb769dc5022aaea00b6.html>. [Accessed: 2 July 2014].
- Aminossadati, S. M., and Hooman, K. (2008). Numerical Simulation of Ventilation Air Flow in Underground Mine Workings. *12th U.S./North American Mine Ventilation Symposium*. Reno, Nevada, 9-12 June. pp. 253-259.
- Amyotte, P. R., and Pegg, M. J. (1993). Explosion Hazards in Underground Coal Mines, *International Journal of Toxicological and Environmental Chemistry*. Vol. 40. pp. 189-199.
- Anderson, J. D., Jr. (1995). *Computational Fluid Dynamics the Basics with Applications*. New York : Mcgraw-Hill.
- ANSYS® Academic Research (2015). Release 15.0, Help System, ANSYS Design Modeler User's Guide, ANSYS, Inc. (Introduction Chapter).
- ANSYS® Academic Research (2015). Release 15.0, Help System, ANSYS Fluent Getting Started Guide, ANSYS, Inc. (Chapter 2).
- ANSYS® Academic Research (2015). Release 15.0, Help System, ANSYS Fluent Meshing User's Guide, ANSYS, Inc. (Chapter 2).
- ANSYS® Academic Research (2015). Release 15.0, Help System, ANSYS Fluent Theory Guide, ANSYS, Inc. (Chapter 4).
- Bates, P. D., Lane, S. N., and Ferguson, R. I. (eds) (2005). *Computational Fluid Dynamics: Applications in Environmental Hydraulics*. West Sussex: John Wiley and sons.
- Campbell, J. A. L. (1987). The Recirculation Hoax. *Proceedings of Third U.S. Mine Ventilation Symposium*. Pennsylvania State University, Pennsylvania, 12-14 October. pp. 24-29.

- Candra, K.J., Sasmito, A.P., and Sadashiv, M. A. (2014). Dust dispersion and management in underground mining faces. *International Journal of Mining Science and Technology*. Volume 24(1), pp. 39-44.
- Candra, K.J., Sasmito, A.P., and Sadashiv, M. A. (2015). Introduction and evaluation of a novel hybrid brattice for improved dust control in underground mining faces: A computational study. *International Journal of Mining Science and Technology*. Volume 24(1), pp 537-543.
- Chabedi, K. (2015). Surface and Underground Mining, [Lecture], MINN 3013 Course, University of the Witwatersrand. School of Mining Engineering.
- Chapra, C. C., and Canale, R. P. (2010). *Numerical Methods for Engineers*. Sixth Edition. New York: Mcgraw Hill.
- Collins, G. W. II. (2003). *Fundamental Numerical Methods and Data Analysis*. NASA Astrophysics Data System (ADS).
- Conglu, W., Guomin, W. U., and Gen, W. (2012). Study on Parametric and Numerical Simulation of Local Forced Ventilation. *8th International Symposium on Safety Science and Technology (ISSST)*. Nanjing, 23-26 October. pp. 786-792.
- Creedy, D. P. (1996). Methane Prediction in Collieries: Safety in Mines Research Advisory Committee (SIMRAC) Report COL 303, June 1996.
- Department of Mineral Resources (DMR) Republic of South Africa. *Mine Health and Safety Act No 29 of 1996*. [Online]. Available from <http://www.dmr.gov.za/mine-health-a-safety.html>. [Accessed: 13 August 2014].
- Diego, I., Torno, S., Torano, J., Menedez, M., and Gent, M. (2011). A Practical use of CFD for Ventilation of Underground Works. *Tunnelling and Underground Space Technology*. Vol. 26 (1). pp.189-200.
- Dougall, A. W. (2010). *Review of Current and Expected Underground Coal Mining Methods and an Evaluation of the Best Practices Associated with These*. A Thesis

Submitted in Partial Fulfilment of University of the Witwatersrand for the Degree of Masters in Engineering. University of the Witwatersrand, Republic of South Africa.

Dubinski, J., Krause, E., Skiba, J. (2011). Global Technical and Environmental Problems Connected with the Coal Mine Methane. *Proceedings of the 22nd World Mining Congress and Expo 2011*. Istanbul, Turkey, 11-16 September.

Feroze, T., and Phillips, H. W. (2015). An Initial Investigation of Room and Pillar Ventilation Using CFD to Investigate the Effects of Last Through Road Velocity. *24th International Mining Congress and Exhibition of Turkey (IMCET 15)*. Antalya, Turkey, 14-17 April. pp. 970-977.

GAMBIT ® Academic Research (2007). Release 2.4, Help System, Gambit User Manual, Fluent, Inc. (Chapter 3.86).

Goodman, G. V. R., and Pollock, D. E. (2004). Use of a Directional Spray System Design to Control Respirable Dust and Face Gas Concentrations Around a Continuous Mining Machine. *Journal of Occupational and Environmental Hygiene*. Vol. 1(12). pp. 806-815.

Haghgoo, M. R. (2013). CMPT 898(02) Progress Report - A comparison of CFD Software Packages to find the Suitable One for Numerical Modeling of Gasification Process. University of Saskatchewan. [Online]. Available from <http://www.cs.usask.ca/faculty/spiteri/students/rhaghgoo.pdf> [Accessed: 1 July 2014].

Hartman, H. L., Mutmanský, J. M., Ramani, R. V., Wang, Y. J. (2012). *Mine Ventilation and Air Conditioning*. Third Edition. Wiley-Interscience Publication John Wiley and Sons, Inc.

Hoffmann, K. A. and Chaing, S. T. (2000). *Computational Fluid Dynamics Volume I*. Fourth Edition. Wichita, Kansas: Engineering Education System.

Holding, W. (1982). Explosive Dust. In: Burrows, J. (ed). *Environmental Engineering in South African Mines*. Cape Town: Cape and Transvaal Printers (Pty) Ltd.

- Jamil, N. (2012). A Comparison of Direct and Indirect Solvers for Linear Systems of Equations. *International Journal of Emerging Sciences*. Vol. 2(2). pp. 310-321.
- Kissell, F.N. (2003). Handbook for Methane Control in Mining. U.S. Department of Health and Human Services. Public Health Service. Centres for Disease Control and Prevention. National Institute for Occupational Safety and Health. Pittsburgh Research Laboratory.
- Lauder, B. E. (1991). *An Introduction to the Modeling of Turbulence*. VKI Lecture Series 1991-02, March 18-21, 1991. From Nichols, R. H. *Turbulence Models and Their Application to Complex Flows*. University of Alabama at Birmingham. [Online]. Available from: <http://people.nas.nasa.gov/~pulliam/Turbulence>. [Accessed: 1 February 2014].
- Lihong, Z., Christopher, P., Yi, Z. (2015). CFD Modeling of Methane Distribution at a Continuous Miner Face with Various Curtain Setback Distances. *International Journal of Mining Science and Technology*. Volume 25(4). pp. 635-640.
- Li, N. (2015). *Comparison between Three Different CFD Software and Numerical Simulation of an Ambulance Hall*. A Thesis Submitted in Partial Fulfilment of KTH School of Industrial Engineering and Management Energy Technology Stockholm. [ONLINE] Available from: www.diva-portal.org/smash/get/diva2:792705/FULLTEXT01.pdf [Accessed: 10 September 2015].
- Luxner, J. V. (1969). Face ventilation in underground bituminous coal mines. Airflow and methane distribution patterns in immediate face area - line brattice, Report of investigations 7223, US Department of Interior, Bureau of Mines.
- Mcperson, M. J. (1993). *Subsurface Ventilation and Environmental Engineering*. New York: Champan & Hall.
- Meyer, C.F, 1989. The Effect of Last Through Road Air Velocities on Unventilated Headings, Chamber of Mines Research Organisation (COMRO) Project CC8E10, 28 April 1989.

- Meyer, C. F. (1993). Improving Underground Ventilation Conditions in Coal Mines: Safety in Mines Research Advisory Committee (SIMRAC) Final Project Report COL 029a, November 1993.
- Meyer, C. F., and Vanzyl, F. J. (1999). Reduce Explosion Risks and Improve Safety and Health Conditions by Better Ventilation Practices in Mechanical Miner Headings: Safety in Mines Research Advisory Committee (SIMRAC) Final Project Report COL 205, April 1999.
- Meyer, J. P., Le Grange, L. A., and Meyer, C. (1991). The Utilisation of Air Scoops for the Improvement of Ventilation in a Coal Mine Heading. *Mining Science and Technology*, Vol. 13(1). pp. 17-24.
- Pawinski, J., and Roszkowski, J. (1985). Emission of Methane into Mine Galleries Driven in Coal by Means of Combined Cutter-Loaders. *Archives of Mining Science*, Vol. 30 (2). pp.207-213.
- Peng, S. S., and Chiang, H. S. (1984). *Longwall Mining*. New York: John Wiley & Sons.
- Phillips, H. R., and Brandt, M.P. (1995). Coal Mine Explosions - Risk and Remedy. *Proceedings of SIMRAC Symposium, SAIMM*, Johannesburg, 1st September 1995. pps. 15.
- Phillips, H. R. (2015). Lessons Learnt from Mine Explosions. *The Australian Mine ventilation Conference*. Sydney, NSW, 31 August - 2 September 2015. pp.19-28.
- Purushotham, T. and Bandopadhyay, S. (2010). Analyzing Shock Losses at Air-Crossings in a Mine Ventilation Network using CFD Simulations. *Proceedings of the 13th U.S./North American Mine Ventilation Symposium*, Sudbury, Ontario, Canada, 13-16 June. pp. 463-468.
- Reed, W., and Taylor, C. (2007). Factors Affecting the Development of Mine Face Ventilation Systems in the 20th Century, *Presented at the Society for Mining*,

Metallurgy and Exploration (SME) Annual Meeting and Exhibit. Denver, Colorado, 25 - 28 February 2007.

Ren, T., and Balusu, R. (2010). The Use of CFD Modelling as a Tool for Solving Mining Health and Safety Problems. *10th Underground Coal Operators' Conference*. University of Wollongong and the Australasian Institute of Mining and Metallurgy. Wollongong, 11-12 February 2010. pp. 339-349.

Sasmito, A.P., Birgersson, E. Ly. H., and Mujumdar, A.S. (2013). Some approaches to improve ventilation system in underground coal mines environment - A computational fluid dynamic study. *Tunneling and Underground Space Technology*. Volume 34. pp. 82–95.

Schultz, M.J., Beiter, D.A., Watkins, T.R., Baran, J.N. (1993). Face Ventilation Investigation: Clark Elkorn Coal Company. Pittsburgh Safety and Health Technology Centre, Ventilation Division. Investigative Report No. P385-V286.

Siddique, H., Tuck, M., and Naser, J. (2005). A Three-Dimensional Simulation of Mine Ventilation Using Computational Fluid Dynamics. *Eighth International Mine Ventilation Congress*, Brisbane, 6 - 8 July. pp. 489-492.

Silvester, S. A. (2002). *The integration of CFD and VR methods to assist auxiliary ventilation practice*. A Thesis Submitted in Partial Fulfilment of the University of Nottingham for the Degree of P.hD. University of Nottingham.

Stanton, W. D., Belle, W. K. B., Dekker, K. J. J., and Du Plesis, J. L. (2006), *South African Mining Industry Best Practice on the Prevention of Silicosis*. Braamfontein South Africa: Mine Health and Safety Council Safety in Mines Research Advisory Committee.

Strang, G. (2009), *Introduction to Linear Algebra*. Fourth Edition. Wellesley: Wellesley-Cambridge Press.

Suglo, R. S., and Frimpong, S. (2002a). Accuracy of Tracer Gas Surveys in Auxiliary Ventilation Systems in Coal Mines. *Proceedings of the North American/Ninth US*

- Mine Ventilation Symposium*. Kingston, Ontario, Canada, 8-12 June 2002. pp.169-177.
- Suglo, R. S., and Frimpong, S. (2002b). Performance of Auxiliary Ventilation Systems in Development Headings in Coal Mines. *Proceedings of the North American/Ninth US Mine Ventilation Symposium*. Kingston, Ontario, Canada, 8-12 June 2002. pp.177-182.
- Szlazak, N., Szlazak, J., Tor, A., Obracaj, A., and Borowski, M. (2003). Ventilation Systems in Dead End Headings with Coal Dust and Methane Hazard. *30th International Conference of Safety in Mines Research Institutes*, South African Institute of Mining and Metallurgy (SAIMM). Johannesburg, 5-9 October. pp. 673 - 688.
- Taylor, C. D., Goodman, G.V.R., and Vincze, T. (1992). Extended Cut Face Ventilation for Remotely Controlled and Automated Mining Systems. *Proceedings of the Symposium, New Technology in Mine Health and Safety*. Phoenix, Arizona, 24-27 February. pp. 3-11.
- Taylor, C. D., Rider, J. P., and Thimons, E. D. (1997). Impact of Unbalanced Intake and Scrubber Flow on Face Methane Concentrations. *Proceedings of the 6th International Mine Ventilation Congress*. Pittsburgh, Pennsylvania, 17-22 May. pp 169-172.
- Taylor, C. D., Timko, R. J., Thimons, E. D., and Mal, T. (2005). Using Ultrasonic Anemometers to Evaluate Factors Affecting Face Ventilation Effectiveness. *Presented at the 2005 Society for Mining, Metallurgy and Exploration (SME) Annual Meeting*. Salt Lake City, Utah. 28th February to 2nd March. pps. 7.
- Thimons, E.D., Taylor, C.D., and Zimmer, J. A. (1999). Ventilating the box cut of a two-pass 40ft extended cut. *Journal of the Mine Ventilation Society of South Africa*, Vol 59(3). 108-115.

- Thorp, N. (1982), Auxiliary Ventilation Practice. In: Burrows, J. (ed). *Environmental Engineering in South African Mines*. Cape Town: Cape and Transvaal Printers (Pty) Ltd.
- Tien, J. C. (1988). Face ventilation during cross-cut development in a room and pillar operation. Proceedings of the 4th U.S Mine Ventilation Symposium. Berkeley, USA, 20-22 June. pp.202-208.
- Tkachuk, S. P., Bobrov, A. I., Ivanov, Y. A., and Busygin, K. K. (1997). Trends of Aerogas Control Efficiency Improvement in Coal Mines of Ukraine. *Proceedings of the 27th International Conference of Safety in Mines Research Institutes, ICS-MRI 97*. New Delhi, 20-22 February 1997. pp. 463-466.
- Torano, J., Torno, S., Menendez, M., Gent, M., and Velasco, J. (2009). Models of Methane Behaviour in Auxiliary Ventilation of Underground Coal Mining. *International Journal of Coal Geology*. Vol. 80(1), pp. 35-43.
- United States Environmental Protection Agency (U.S. EPA) (2010). *U.S. Underground Coal Mine Ventilation Air Methane Exhaust Characterization*. [Online] July 2010. Available from: <http://www3.epa.gov>. [Accessed: 29 January 2014].
- Van Heerden, J., and Sullivan, P. (1993). The Application of CFD for Evaluation of Dust Suppression and Auxiliary Ventilation Systems Used with Continuous Miners. *Proceedings of the 6th US Mine Ventilation Symposium, Society for Mining, Metallurgy and Exploration (SME)*. Salt Lake City, Utah, 21-23 June. pp. 293–297.
- Wala, A.M., Jacob, J., Huang, P.G., and Brown, J.T. (2003). A New Approach to Evaluate Mine Face Ventilation. *Mining Engineering, Society for Mining, Metallurgy and Exploration (SME)*. Vol. 55(3). pp.25-30.
- Wala, A.M. Vytla, S., Taylor, C.D., and Huang, G. (2007). Mine Face Ventilation: A Comparison of CFD Results Against Benchmark Experiments for the CFD Code Validation. *Mining Engineering, Society for Mining, Metallurgy and Exploration (SME)*. Vol. 59(10). pp. 49-55.

- Wang, P. F., Feng, T., Ronghua, L. (2011). Numerical simulation of dust distribution at a fully mechanized face under the isolation effect of air curtain. *Mining Science and Technology*. Volume 21(1). pp. 65–69.
- Wu, H. W., and Gillies, A. D. S. (2005). Real-Time Airflow Monitoring and Control within the Mine Production System. *Eighth International Mine Ventilation Congress*. Brisbane, 6-8 July 2005. pp. 383-389.
- Xu, G., Luxbacher, K. D., Ragab, S., Xu, J., and Ding, X. (2016). Computational Fluid Dynamics Applied to Mining Engineering: A Review. *International Journal of Mining, Reclamation and Environment*. DOI:10.1080/17480930.2016.1138570. pps. 26.
- Yuan, L., and Smith, A. C. (2008). Numerical Study on Effects of Coal Properties on Spontaneous Heating in Longwall Gob Areas. *Fuel*. Vol. 87(15-16). pp. 3409–3419.
- Zhang, X., Zhang, Y., and Tien, J. C. (2011). The Efficiency Study of the Push-Pull Ventilation System in Underground Mines. *11th Underground Coal Operators' Conference*. University of Wollongong & Australasian Institute of Mining and Metallurgy, NSW, 10-11 February. pp. 225-230.
- Zheng, Y., and Tien, J. C. (2008). DPM Dispersion Study using CFD for Underground Metal/Nonmetal Mines. *Proceedings of the 12th North American Mine Ventilation Symposium*. Reno, Nevada, 9-12 June. pp. 487-493.

APPENDIX A

COMPLETE AND NUMERICAL NAMES

Table A1 Complete and numerical names of all the cases of Case B

| Complete names | Numerical names | Complete names | Numerical names |
|-----------------------------------|-----------------|-----------------------------------|-----------------|
| 1-6.6-3-10-Half-3-0.5-0 | 1 | 49-6.6-4-10-Half-3-0.5-0 | 49 |
| 2-6.6-3-10-Half-3-1-0 | 2 | 50-6.6-4-10-Half-3-1-0 | 50 |
| 3-6.6-3-10-Half-6-0.5-0 | 3 | 51-6.6-4-10-Half-6-0.5-0 | 51 |
| 4-6.6-3-10-Half-6-1-0 | 4 | 52-6.6-3-10-Half-6-1-0-1 | 52 |
| 5-6.6-3-10-Half-3-0.5-7.5 | 5 | 53-6.6-4-10-Half-3-0.5-7.5 | 53 |
| 6-6.6-3-10-Half-3-1-7.5 | 6 | 54-6.6-4-10-Half-3-1-7.5 | 54 |
| 7-6.6-3-10-Half-6-0.5-7.5 | 7 | 55-6.6-4-10-Half-6-0.5-7.5 | 55 |
| 8-6.6-3-10-Half-6-1-7.5 | 8 | 56-6.6-4-10-Half-6-1-7.5 | 56 |
| 9-6.6-3-10-Half-3-0.5-15 | 9 | 57-6.6-4-10-Half-3-0.5-15 | 57 |
| 10-6.6-3-10-Half-3-1-15 | 10 | 58-6.6-4-10-Half-3-1-15 | 58 |
| 11-6.6-3-10-Half-6-0.5-15 | 11 | 59-6.6-4-10-Half-6-0.5-15 | 59 |
| 12-6.6-3-10-Half-6-1-15 | 12 | 60-6.6-4-10-Half-6-1-15 | 60 |
| 13-6.6-3-10-threebyfour-3-0.5-0 | 13 | 61-6.6-4-10-threebyfour-3-0.5-0 | 61 |
| 14-6.6-3-10-threebyfour-3-1-0 | 14 | 62-6.6-4-10-threebyfour-3-1-0 | 62 |
| 15-6.6-3-10-threebyfour-6-0.5-0 | 15 | 63-6.6-4-10-threebyfour-6-0.5-0 | 63 |
| 16-6.6-3-10-threebyfour-6-1-0 | 16 | 64-6.6-4-10-threebyfour-6-1-0 | 64 |
| 17-6.6-3-10-threebyfour-3-0.5-7.5 | 17 | 65-6.6-4-10-threebyfour-3-0.5-7.5 | 65 |
| 18-6.6-3-10-threebyfour-3-1-7.5 | 18 | 66-6.6-4-10-threebyfour-3-1-7.5 | 66 |
| 19-6.6-3-10-threebyfour-6-0.5-7.5 | 19 | 67-6.6-4-10-threebyfour-6-0.5-7.5 | 67 |
| 20-6.6-3-10-threebyfour-6-1-7.5 | 20 | 68-6.6-4-10-threebyfour-6-1-7.5 | 68 |
| 21-6.6-3-10-threebyfour-3-0.5-15 | 21 | 69-6.6-4-10-threebyfour-3-0.5-15 | 69 |
| 22-6.6-3-10-threebyfour-3-1-15 | 22 | 70-6.6-4-10-threebyfour-3-1-15 | 70 |
| 23-6.6-3-10-threebyfour-6-0.5-15 | 23 | 71-6.6-4-10-threebyfour-6-0.5-15 | 71 |
| 24-6.6-3-10-threebyfour-6-1-15 | 24 | 72-6.6-4-10-threebyfour-6-1-15 | 72 |
| 25-6.6-3-20-Half-3-0.5-0 | 25 | 73-6.6-4-20-Half-3-0.5-0 | 73 |
| 26-6.6-3-20-Half-3-1-0 | 26 | 74-6.6-4-20-Half-3-1-0 | 74 |
| 27-6.6-3-20-Half-6-0.5-0 | 27 | 75-6.6-4-20-Half-6-0.5-0 | 75 |
| 28-6.6-3-20-Half-6-1-0 | 28 | 76-6.6-4-20-Half-6-1-0 | 76 |
| 29-6.6-3-20-Half-3-0.5-7.5 | 29 | 77-6.6-4-20-Half-3-0.5-7.5 | 77 |
| 30-6.6-3-20-Half-3-1-7.5 | 30 | 78-6.6-4-20-Half-3-1-7.5 | 78 |
| 31-6.6-3-20-Half-6-0.5-7.5 | 31 | 79-6.6-4-20-Half-6-0.5-7.5 | 79 |
| 32-6.6-3-20-Half-6-1-7.5 | 32 | 80-6.6-4-20-Half-6-1-7.5 | 80 |
| 33-6.6-3-20-Half-3-0.5-15 | 33 | 81-6.6-4-20-Half-3-0.5-15 | 81 |

| Complete names | Numerical names | Complete names | Numerical names |
|-----------------------------------|-----------------|-----------------------------------|-----------------|
| 34-6.6-3-20-Half-3-1-15 | 34 | 82-6.6-4-20-Half-3-1-15 | 82 |
| 35-6.6-3-20-Half-6-0.5-15 | 35 | 83-6.6-4-20-Half-6-0.5-15 | 83 |
| 36-6.6-3-20-Half-6-1-15 | 36 | 84-6.6-4-20-Half-6-1-15 | 84 |
| 37-6.6-3-20-threebyfour-3-0.5-0 | 37 | 85-6.6-4-20-threebyfour-3-0.5-0 | 85 |
| 38-6.6-3-20-threebyfour-3-1-0 | 38 | 86-6.6-4-20-threebyfour-3-1-0 | 86 |
| 39-6.6-3-20-threebyfour-6-0.5-0 | 39 | 87-6.6-4-20-threebyfour-6-0.5-0 | 87 |
| 40-6.6-3-20-threebyfour-6-1-0 | 40 | 88-6.6-4-20-threebyfour-6-1-0 | 88 |
| 41-6.6-3-20-threebyfour-3-0.5-7.5 | 41 | 89-6.6-4-20-threebyfour-3-0.5-7.5 | 89 |
| 42-6.6-3-20-threebyfour-3-1-7.5 | 42 | 90-6.6-4-20-threebyfour-3-1-7.5 | 90 |
| 43-6.6-3-20-threebyfour-6-0.5-7.5 | 43 | 91-6.6-4-20-threebyfour-6-0.5-7.5 | 91 |
| 44-6.6-3-20-threebyfour-6-1-7.5 | 44 | 92-6.6-4-20-threebyfour-6-1-7.5 | 92 |
| 45-6.6-3-20-threebyfour-3-0.5-15 | 45 | 93-6.6-4-20-threebyfour-3-0.5-15 | 93 |
| 46-6.6-3-20-threebyfour-3-1-15 | 46 | 94-6.6-4-20-threebyfour-3-1-15 | 94 |
| 47-6.6-3-20-threebyfour-6-0.5-15 | 47 | 95-6.6-4-20-threebyfour-6-0.5-15 | 95 |
| 48-6.6-3-20-threebyfour-6-1-15 | 48 | 96-6.6-4-20-threebyfour-6-1-15 | 96 |

APPENDIX B

FLOW RATES AT THE EXIT OF LB FOR EACH LTR VELOCITY

Table B1 Flow rates at the exit of the LB for all heading dimensions with each LTR velocity

| Cases | LTR velocity | | | Cases | LTR velocity | | |
|-------|--|--------|-------|-------|--------------|--------|--------|
| | 1m/s | 1.5m/s | 2m/s | | 1m/s | 1.5m/s | 2m/s |
| | Flow rates at the exit of LB (m ³ /s) | | | | | | |
| 1 | 0.944 | 1.433 | 1.907 | 49 | 1.253 | 1.904 | 2.558 |
| 2 | 2.032 | 3.058 | 4.069 | 50 | 2.718 | 4.080 | 5.433 |
| 3 | 0.930 | 1.412 | 1.881 | 51 | 1.234 | 1.878 | 2.521 |
| 4 | 2.002 | 3.012 | 4.004 | 52 | 2.676 | 4.011 | 5.357 |
| 5 | 1.230 | 1.840 | 2.455 | 53 | 1.633 | 2.441 | 3.279 |
| 6 | 2.596 | 3.869 | 5.221 | 54 | 3.456 | 5.196 | 6.952 |
| 7 | 1.539 | 2.339 | 3.144 | 55 | 2.046 | 3.136 | 4.186 |
| 8 | 3.084 | 4.577 | 6.145 | 56 | 4.097 | 6.153 | 8.255 |
| 9 | 1.587 | 2.395 | 3.186 | 57 | 2.117 | 3.180 | 4.232 |
| 10 | 3.289 | 4.875 | 6.495 | 58 | 4.378 | 6.540 | 8.744 |
| 11 | 2.269 | 3.413 | 4.557 | 59 | 3.013 | 4.570 | 6.108 |
| 12 | 4.393 | 6.601 | 8.815 | 60 | 5.870 | 8.796 | 11.737 |
| 13 | 0.931 | 1.416 | 1.880 | 61 | 1.237 | 1.880 | 2.523 |
| 14 | 2.005 | 3.012 | 4.001 | 62 | 2.680 | 4.020 | 5.358 |
| 15 | 0.918 | 1.391 | 1.856 | 63 | 1.218 | 1.852 | 2.491 |
| 16 | 1.970 | 2.968 | 3.947 | 64 | 2.640 | 3.951 | 5.287 |
| 17 | 1.214 | 1.815 | 2.420 | 65 | 1.610 | 2.408 | 3.207 |
| 18 | 2.560 | 3.815 | 5.149 | 66 | 3.406 | 5.096 | 6.811 |
| 19 | 1.520 | 2.308 | 3.107 | 67 | 2.019 | 3.069 | 4.140 |
| 20 | 3.042 | 4.521 | 6.065 | 68 | 4.057 | 6.018 | 8.066 |
| 21 | 1.567 | 2.363 | 3.145 | 69 | 2.085 | 3.158 | 4.173 |
| 22 | 3.247 | 4.809 | 6.410 | 70 | 4.323 | 6.409 | 8.411 |
| 23 | 2.240 | 3.369 | 4.498 | 71 | 2.961 | 4.470 | 5.960 |
| 24 | 4.336 | 6.515 | 8.702 | 72 | 5.709 | 8.552 | 11.535 |
| 25 | 0.919 | 1.397 | 1.862 | 73 | 1.210 | 1.840 | 2.471 |
| 26 | 1.980 | 2.988 | 3.977 | 74 | 2.620 | 3.933 | 5.238 |
| 27 | 0.910 | 1.380 | 1.840 | 75 | 1.196 | 1.807 | 2.432 |
| 28 | 1.951 | 2.936 | 3.922 | 76 | 2.582 | 3.857 | 5.170 |
| 29 | 1.202 | 1.798 | 2.399 | 77 | 1.578 | 2.353 | 3.159 |

| Cases | LTR velocity | | | Cases | LTR velocity | | |
|-------|--|--------|-------|-------|--------------|--------|--------|
| | 1m/s | 1.5m/s | 2m/s | | 1m/s | 1.5m/s | 2m/s |
| | Flow rates at the exit of LB (m ³ /s) | | | | | | |
| 30 | 2.532 | 3.777 | 5.109 | 78 | 3.324 | 5.020 | 6.724 |
| 31 | 1.506 | 2.286 | 3.070 | 79 | 1.977 | 3.021 | 4.048 |
| 32 | 3.002 | 4.475 | 5.988 | 80 | 3.972 | 5.937 | 7.953 |
| 33 | 1.549 | 2.337 | 3.119 | 81 | 2.037 | 3.070 | 4.078 |
| 34 | 3.219 | 4.768 | 6.350 | 82 | 4.221 | 6.304 | 8.455 |
| 35 | 2.209 | 3.334 | 4.438 | 83 | 2.909 | 4.415 | 5.905 |
| 36 | 4.288 | 6.446 | 8.608 | 84 | 5.648 | 8.512 | 11.321 |
| 37 | 0.905 | 1.373 | 1.833 | 85 | 1.192 | 1.811 | 2.430 |
| 38 | 1.950 | 2.939 | 3.899 | 86 | 2.580 | 3.875 | 5.180 |
| 39 | 0.897 | 1.356 | 1.812 | 87 | 1.173 | 1.788 | 2.408 |
| 40 | 1.920 | 2.896 | 3.851 | 88 | 2.541 | 3.807 | 5.100 |
| 41 | 1.185 | 1.770 | 2.360 | 89 | 1.575 | 2.347 | 3.102 |
| 42 | 2.500 | 3.719 | 5.019 | 90 | 3.276 | 4.899 | 6.589 |
| 43 | 1.482 | 2.250 | 3.030 | 91 | 1.980 | 2.960 | 4.000 |
| 44 | 2.969 | 4.407 | 5.922 | 92 | 3.904 | 5.802 | 7.771 |
| 45 | 1.529 | 2.305 | 3.067 | 93 | 2.042 | 3.046 | 4.021 |
| 46 | 3.165 | 4.688 | 6.250 | 94 | 4.177 | 6.266 | 8.158 |
| 47 | 2.185 | 3.286 | 4.389 | 95 | 2.881 | 4.306 | 5.716 |
| 48 | 4.229 | 6.358 | 8.494 | 96 | 5.500 | 8.324 | 11.228 |

APPENDIX C

EFFECT OF LTR VELOCITY ON THE FLOW RATE AT EXIT OF LB

Table C1 Percentage increase in flow rates at the exit of the LB with the increase in LTR velocity - 6.6 x 3 x 10m heading

| Cases | LTR velocity | | | Percentage increase in flow rate with the increase in LTR velocity from 1 to 1.5, 1 to 2 and 1.5 to 2m/s | | |
|------------------------------------|--|--------|-------|--|---------------|---------------|
| | 1m/s | 1.5m/s | 2m/s | 1-1.5 m/s (%) | 1-2 m/s (%) | 1.5-2 m/s (%) |
| | Flow rates at the exit of LB (m ³ /s) | | | | | |
| 1 | 0.944 | 1.433 | 1.907 | 51.87 | 102.14 | 33.10 |
| 2 | 2.032 | 3.058 | 4.069 | 50.53 | 100.29 | 33.06 |
| 3 | 0.930 | 1.412 | 1.881 | 51.76 | 102.27 | 33.28 |
| 4 | 2.001 | 3.012 | 4.004 | 50.50 | 100.07 | 32.94 |
| 5 | 1.230 | 1.840 | 2.455 | 49.60 | 99.56 | 33.40 |
| 6 | 2.596 | 3.869 | 5.221 | 49.04 | 101.14 | 34.96 |
| 7 | 1.539 | 2.339 | 3.144 | 52.00 | 104.35 | 34.44 |
| 8 | 3.084 | 4.577 | 6.145 | 48.42 | 99.28 | 34.26 |
| 9 | 1.587 | 2.395 | 3.186 | 50.90 | 100.73 | 33.03 |
| 10 | 3.289 | 4.875 | 6.494 | 48.22 | 97.46 | 33.22 |
| 11 | 2.269 | 3.413 | 4.557 | 50.42 | 100.82 | 33.51 |
| 12 | 4.393 | 6.601 | 8.815 | 50.27 | 100.68 | 33.55 |
| 13 | 0.931 | 1.415 | 1.880 | 52.00 | 101.85 | 32.80 |
| 14 | 2.005 | 3.012 | 4.001 | 50.22 | 99.56 | 32.84 |
| 15 | 0.918 | 1.391 | 1.856 | 51.49 | 102.15 | 33.45 |
| 16 | 1.970 | 2.968 | 3.947 | 50.64 | 100.37 | 33.01 |
| 17 | 1.214 | 1.815 | 2.420 | 49.53 | 99.36 | 33.33 |
| 18 | 2.560 | 3.815 | 5.149 | 49.05 | 101.16 | 34.96 |
| 19 | 1.520 | 2.308 | 3.107 | 51.80 | 104.39 | 34.65 |
| 20 | 3.042 | 4.521 | 6.065 | 48.63 | 99.37 | 34.13 |
| 21 | 1.567 | 2.363 | 3.145 | 50.83 | 100.70 | 33.07 |
| 22 | 3.247 | 4.809 | 6.410 | 48.11 | 97.42 | 33.29 |
| 23 | 2.240 | 3.369 | 4.498 | 50.40 | 100.80 | 33.51 |
| 24 | 4.336 | 6.515 | 8.702 | 50.27 | 100.70 | 33.56 |
| Average percentage increase | | | | 50.27 | 100.69 | 33.56 |

Table C2 Percentage increase in flow rates at the exit of the LB with the increase in LTR velocity - 6.6 x 3 x 20m heading

| Cases | LTR velocity | | | Percentage increase in flow rate with the increase in LTR velocity from 1 to 1.5, 1 to 2 and 1.5 to 2m/s | | |
|------------------------------------|--|--------|-------|--|---------------|---------------|
| | 1m/s | 1.5m/s | 2m/s | 1-1.5 m/s (%) | 1-2 m/s (%) | 1.5-2 m/s (%) |
| | Flow rates at the exit of LB (m ³ /s) | | | | | |
| 25 | 0.919 | 1.397 | 1.862 | 52.05 | 102.69 | 33.31 |
| 26 | 1.980 | 2.988 | 3.977 | 50.92 | 100.85 | 33.09 |
| 27 | 0.910 | 1.380 | 1.840 | 51.65 | 102.18 | 33.32 |
| 28 | 1.951 | 2.936 | 3.922 | 50.50 | 101.03 | 33.57 |
| 29 | 1.202 | 1.798 | 2.399 | 49.55 | 99.50 | 33.41 |
| 30 | 2.532 | 3.777 | 5.109 | 49.15 | 101.75 | 35.27 |
| 31 | 1.506 | 2.286 | 3.070 | 51.76 | 103.85 | 34.32 |
| 32 | 3.002 | 4.475 | 5.988 | 49.04 | 99.43 | 33.81 |
| 33 | 1.549 | 2.337 | 3.119 | 50.91 | 101.39 | 33.45 |
| 34 | 3.219 | 4.768 | 6.350 | 48.15 | 97.30 | 33.18 |
| 35 | 2.209 | 3.334 | 4.438 | 50.90 | 100.87 | 33.12 |
| 36 | 4.288 | 6.446 | 8.608 | 50.34 | 100.77 | 33.54 |
| 37 | 0.905 | 1.373 | 1.833 | 51.76 | 102.62 | 33.51 |
| 38 | 1.950 | 2.939 | 3.899 | 50.72 | 99.97 | 32.67 |
| 39 | 0.897 | 1.356 | 1.812 | 51.24 | 102.06 | 33.60 |
| 40 | 1.920 | 2.896 | 3.851 | 50.87 | 100.60 | 32.97 |
| 41 | 1.185 | 1.770 | 2.360 | 49.42 | 99.23 | 33.34 |
| 42 | 2.500 | 3.719 | 5.019 | 48.75 | 100.77 | 34.97 |
| 43 | 1.482 | 2.250 | 3.030 | 51.82 | 104.46 | 34.68 |
| 44 | 2.969 | 4.407 | 5.922 | 48.43 | 99.47 | 34.39 |
| 45 | 1.529 | 2.305 | 3.067 | 50.80 | 100.64 | 33.04 |
| 46 | 3.165 | 4.688 | 6.250 | 48.12 | 97.49 | 33.33 |
| 47 | 2.185 | 3.286 | 4.389 | 50.41 | 100.88 | 33.55 |
| 48 | 4.229 | 6.358 | 8.494 | 50.35 | 100.87 | 33.60 |
| Average percentage increase | | | | 50.32 | 100.86 | 33.63 |

Table C 3 Percentage increase in flow rates at the exit of the LB with the increase in LTR velocity - 6.6 x 4 x 10m heading

| Cases | LTR velocity | | | Percentage increase in flow rate with the increase in LTR velocity from 1 to 1.5, 1 to 2 and 1.5 to 2m/s | | |
|------------------------------------|--|--------|--------|--|--------------|---------------|
| | 1m/s | 1.5m/s | 2m/s | 1-1.5 m/s (%) | 1-2 m/s (%) | 1.5-2 m/s (%) |
| | Flow rates at the exit of LB (m ³ /s) | | | | | |
| 49 | 1.253 | 1.904 | 2.558 | 51.91 | 104.14 | 34.38 |
| 50 | 2.718 | 4.080 | 5.433 | 50.12 | 99.88 | 33.15 |
| 51 | 1.234 | 1.877 | 2.521 | 52.18 | 104.35 | 34.28 |
| 52 | 2.676 | 4.011 | 5.357 | 49.91 | 100.22 | 33.56 |
| 53 | 1.633 | 2.441 | 3.279 | 49.49 | 100.83 | 34.34 |
| 54 | 3.456 | 5.196 | 6.952 | 50.36 | 101.18 | 33.8 |
| 55 | 2.045 | 3.136 | 4.185 | 53.32 | 104.62 | 33.46 |
| 56 | 4.097 | 6.153 | 8.255 | 50.18 | 101.49 | 34.17 |
| 57 | 2.116 | 3.180 | 4.231 | 50.27 | 99.93 | 33.05 |
| 58 | 4.378 | 6.540 | 8.744 | 49.37 | 99.71 | 33.7 |
| 59 | 3.013 | 4.570 | 6.108 | 51.69 | 102.75 | 33.66 |
| 60 | 5.870 | 8.796 | 11.737 | 49.84 | 99.95 | 33.44 |
| 61 | 1.237 | 1.880 | 2.522 | 52 | 103.95 | 34.18 |
| 62 | 2.680 | 4.020 | 5.358 | 49.99 | 99.94 | 33.3 |
| 63 | 1.218 | 1.852 | 2.491 | 52.02 | 104.46 | 34.5 |
| 64 | 2.640 | 3.951 | 5.287 | 49.66 | 100.28 | 33.82 |
| 65 | 1.610 | 2.408 | 3.207 | 49.62 | 99.25 | 33.18 |
| 66 | 3.406 | 5.096 | 6.811 | 49.62 | 100 | 33.67 |
| 67 | 2.019 | 3.069 | 4.140 | 51.98 | 105.02 | 34.9 |
| 68 | 4.057 | 6.018 | 8.066 | 48.34 | 98.82 | 34.03 |
| 69 | 2.085 | 3.158 | 4.173 | 51.47 | 100.15 | 32.14 |
| 70 | 4.323 | 6.409 | 8.411 | 48.26 | 94.56 | 31.23 |
| 71 | 2.961 | 4.470 | 5.960 | 50.94 | 101.25 | 33.33 |
| 72 | 5.709 | 8.552 | 11.535 | 49.79 | 102.04 | 34.88 |
| Average percentage increase | | | | 50.51 | 101.2 | 33.67 |

Table C4 Percentage increase in flow rates at the exit of the LB with the increase in LTR velocity - 6.6 x 4 x 20m heading

| Cases | LTR velocity | | | Percentage increase in flow rate with the increase in LTR velocity from 1 to 1.5, 1 to 2 and 1.5 to 2m/s | | |
|------------------------------------|--|--------|--------|--|---------------|---------------|
| | 1m/s | 1.5m/s | 2m/s | 1-1.5 m/s (%) | 1-2 m/s (%) | 1.5-2 m/s (%) |
| | Flow rates at the exit of LB (m ³ /s) | | | | | |
| 73 | 1.210 | 1.840 | 2.471 | 52.10 | 104.21 | 34.27 |
| 74 | 2.620 | 3.933 | 5.238 | 50.13 | 99.95 | 33.18 |
| 75 | 1.196 | 1.807 | 2.432 | 51.13 | 103.44 | 34.61 |
| 76 | 2.582 | 3.857 | 5.170 | 49.35 | 100.20 | 34.04 |
| 77 | 1.578 | 2.353 | 3.159 | 49.11 | 100.17 | 34.24 |
| 78 | 3.324 | 5.020 | 6.724 | 51.01 | 102.28 | 33.96 |
| 79 | 1.977 | 3.021 | 4.048 | 52.79 | 104.72 | 33.99 |
| 80 | 3.972 | 5.937 | 7.953 | 49.45 | 100.19 | 33.95 |
| 81 | 2.037 | 3.070 | 4.078 | 50.71 | 100.20 | 32.84 |
| 82 | 4.221 | 6.304 | 8.455 | 49.36 | 100.32 | 34.12 |
| 83 | 2.909 | 4.415 | 5.905 | 51.79 | 103.01 | 33.75 |
| 84 | 5.648 | 8.512 | 11.321 | 50.71 | 100.45 | 33.00 |
| 85 | 1.192 | 1.811 | 2.430 | 51.92 | 103.87 | 34.19 |
| 86 | 2.580 | 3.875 | 5.180 | 50.19 | 100.76 | 33.67 |
| 87 | 1.173 | 1.788 | 2.408 | 52.42 | 105.27 | 34.67 |
| 88 | 2.541 | 3.807 | 5.100 | 49.82 | 100.69 | 33.96 |
| 89 | 1.575 | 2.347 | 3.102 | 49.02 | 96.92 | 32.14 |
| 90 | 3.276 | 4.899 | 6.589 | 49.54 | 101.12 | 34.49 |
| 91 | 1.980 | 2.960 | 4.000 | 49.54 | 102.04 | 35.11 |
| 92 | 3.904 | 5.802 | 7.771 | 48.62 | 99.05 | 33.94 |
| 93 | 2.042 | 3.046 | 4.021 | 49.19 | 96.96 | 32.02 |
| 94 | 4.177 | 6.266 | 8.158 | 50.01 | 95.31 | 30.20 |
| 95 | 2.881 | 4.306 | 5.716 | 49.44 | 98.40 | 32.77 |
| 96 | 5.500 | 8.324 | 11.228 | 51.36 | 104.15 | 34.88 |
| Average percentage increase | | | | 50.36 | 100.99 | 33.67 |

APPENDIX D

EFFECT OF HEADING HEIGHT ON AIR FLOW AT THE EXIT OF LB

Table D1 Percentage increase in flow rates at the exit of the LB for each LTR velocity with the increase in heading height; 6.6 x 3 x 10m vs 6.6 x 4 x 10m headings

| Cases | LTR velocity | | |
|------------------------------------|---|--------------|--------------|
| | 1m/s | 1.5m/s | 2m/s |
| | Percentage increase in flow rate for each LTR velocity with increase in heading height from 3m to 4m - 6.6 x 3 x 10 vs 6.6 x 4 x 10m headings (%) | | |
| 1-49 | 32.79 | 32.83 | 34.11 |
| 2-50 | 33.79 | 33.42 | 33.51 |
| 3-51 | 32.63 | 33.00 | 34.00 |
| 4-52 | 33.69 | 33.16 | 33.78 |
| 5-53 | 32.76 | 32.66 | 33.60 |
| 6-54 | 33.13 | 34.31 | 33.15 |
| 7-55 | 32.94 | 34.09 | 33.12 |
| 8-56 | 32.85 | 34.42 | 34.33 |
| 9-57 | 33.33 | 32.78 | 32.80 |
| 10-58 | 33.12 | 34.15 | 34.63 |
| 11-59 | 32.76 | 33.88 | 34.04 |
| 12-60 | 33.64 | 33.26 | 33.15 |
| 13-61 | 32.81 | 32.81 | 34.20 |
| 14-62 | 33.66 | 33.46 | 33.92 |
| 15-63 | 32.67 | 33.14 | 34.19 |
| 16-64 | 34.01 | 33.14 | 33.95 |
| 17-65 | 32.60 | 32.68 | 32.53 |
| 18-66 | 33.05 | 33.56 | 32.28 |
| 19-67 | 32.84 | 32.99 | 33.24 |
| 20-68 | 33.36 | 33.10 | 33.00 |
| 21-69 | 33.05 | 33.62 | 32.69 |
| 22-70 | 33.14 | 33.27 | 31.21 |
| 23-71 | 32.21 | 32.69 | 32.50 |
| 24-72 | 31.68 | 31.26 | 32.56 |
| Average percentage increase | 33.02 | 33.24 | 33.35 |

Table D2 Percentage increase in flow rates at the exit of the LB for each LTR velocity with the increase in heading height; 6.6 x 3 x 20m vs 6.6 x 4 x 20m headings

| Cases | LTR velocity | | |
|------------------------------------|--|--------------|--------------|
| | 1m/s | 1.5m/s | 2m/s |
| | Percentage increase in flow rate for each LTR velocity with the increase in heading height from 3m to 4m- 6.6 x 3 x 20 vs 6.6 x 4 x 20m headings (%) | | |
| 25-73 | 31.73 | 31.77 | 32.72 |
| 26-74 | 32.31 | 31.62 | 31.71 |
| 27-75 | 31.36 | 30.91 | 32.18 |
| 28-76 | 32.38 | 31.37 | 31.83 |
| 29-77 | 31.27 | 30.89 | 31.71 |
| 30-78 | 31.27 | 32.91 | 31.62 |
| 31-79 | 31.29 | 32.18 | 31.84 |
| 32-80 | 32.31 | 32.68 | 32.82 |
| 33-81 | 31.50 | 31.33 | 30.73 |
| 34-82 | 31.14 | 32.21 | 33.15 |
| 35-83 | 31.67 | 32.45 | 33.07 |
| 36-84 | 31.72 | 32.04 | 31.51 |
| 37-85 | 31.73 | 31.87 | 32.55 |
| 38-86 | 32.32 | 31.85 | 32.85 |
| 39-87 | 30.81 | 31.83 | 32.90 |
| 40-88 | 32.36 | 31.44 | 32.42 |
| 41-89 | 32.97 | 32.61 | 31.42 |
| 42-90 | 31.04 | 31.75 | 31.27 |
| 43-91 | 33.58 | 31.58 | 32.00 |
| 44-92 | 31.49 | 31.65 | 31.21 |
| 45-93 | 33.54 | 32.11 | 31.09 |
| 46-94 | 31.98 | 33.67 | 30.53 |
| 47-95 | 31.88 | 31.03 | 30.25 |
| 48-96 | 30.07 | 30.94 | 32.19 |
| Average percentage increase | 31.82 | 31.86 | 31.90 |

APPENDIX E

EFFECT OF LTR VELOCITY ON FLOW RATES

Table E1 Percentage increase in flow rates at the specified planes with the increase in LTR velocity from 1-1.5, 1-2 and 1.5-2m/s - 6.6 x 3 x 10 m heading

| Case | Planes | LTR velocities | | | Percentage increase in flow rate with the increase in LTR velocity from 1 to 1.5, 1 to 2 and 1.5 to 2m/s | | |
|------|-------------|--------------------------------|--------------|--------------|--|---------------|---------------|
| | | 1m/s | 1.5m/s | 2m/s | 1-1.5 m/s (%) | 1-2 m/s (%) | 1.5-2 m/s (%) |
| | | Flow rates (m ³ /s) | | | | | |
| 1 | 1m | 1.469 | 2.304 | 3.108 | 56.89 | 111.61 | 34.87 |
| | 5m | 2.210 | 3.433 | 4.654 | 55.37 | 110.63 | 35.57 |
| | 7.5 | 1.923 | 2.950 | 4.054 | 53.39 | 110.78 | 37.41 |
| | 9.5m | 0.870 | 1.329 | 1.758 | 52.74 | 102.15 | 32.35 |
| 2 | 1m | 3.073 | 4.609 | 6.160 | 49.97 | 100.46 | 33.67 |
| | 5m | 3.310 | 4.944 | 6.577 | 49.33 | 98.69 | 33.05 |
| | 7.5 | 2.789 | 4.173 | 5.538 | 49.63 | 98.56 | 32.7 |
| | 9.5m | 1.229 | 1.818 | 2.419 | 47.87 | 96.76 | 33.06 |
| 3 | 1m | 1.427 | 2.210 | 3.008 | 54.92 | 110.83 | 36.09 |
| | 5m | 2.181 | 3.320 | 4.438 | 52.28 | 103.54 | 33.66 |
| | 7.5 | 1.853 | 2.851 | 3.807 | 53.8 | 105.41 | 33.56 |
| | 9.5m | 0.850 | 1.302 | 1.734 | 53.14 | 103.96 | 33.18 |
| 4 | 1m | 3.019 | 4.546 | 6.062 | 50.59 | 100.81 | 33.34 |
| | 5m | 3.268 | 4.863 | 6.474 | 48.82 | 98.11 | 33.12 |
| | 7.5 | 2.728 | 4.102 | 5.445 | 50.37 | 99.6 | 32.74 |
| | 9.5m | 1.189 | 1.760 | 2.385 | 47.99 | 100.56 | 35.52 |
| 5 | 1m | 2.088 | 3.187 | 4.254 | 52.61 | 103.7 | 33.48 |
| | 5m | 2.786 | 4.242 | 5.734 | 52.27 | 105.81 | 35.16 |
| | 7.5 | 2.378 | 3.588 | 4.802 | 50.92 | 101.94 | 33.81 |
| | 9.5m | 1.123 | 1.695 | 2.261 | 51.03 | 101.41 | 33.36 |
| 6 | 1m | 3.951 | 6.176 | 8.186 | 56.32 | 107.2 | 32.54 |
| | 5m | 3.965 | 6.074 | 8.259 | 53.18 | 108.28 | 35.97 |
| | 7.5 | 3.443 | 5.181 | 6.971 | 50.46 | 102.47 | 34.56 |
| | 9.5m | 1.541 | 2.300 | 3.110 | 49.25 | 101.8 | 35.21 |
| 7 | 1m | 2.808 | 4.261 | 5.713 | 51.73 | 103.42 | 34.07 |
| | 5m | 3.499 | 5.198 | 7.030 | 48.58 | 100.93 | 35.23 |
| | 7.5 | 2.862 | 4.257 | 5.902 | 48.76 | 106.26 | 38.65 |
| | 9.5m | 1.411 | 2.153 | 2.895 | 52.63 | 105.23 | 34.46 |

| Case | Planes | LTR velocities | | | Percentage increase in flow rate with the increase in LTR velocity from 1 to 1.5, 1 to 2 and 1.5 to 2m/s | | |
|------|-------------|--------------------------------|--------------|--------------|--|---------------|---------------|
| | | 1m/s | 1.5m/s | 2m/s | 1-1.5 m/s (%) | 1-2 m/s (%) | 1.5-2 m/s (%) |
| | | Flow rates (m ³ /s) | | | | | |
| 8 | 1m | 4.818 | 7.557 | 10.181 | 56.87 | 111.33 | 34.72 |
| | 5m | 4.659 | 7.190 | 9.756 | 54.33 | 109.4 | 35.69 |
| | 7.5 | 4.084 | 6.121 | 8.242 | 49.87 | 101.81 | 34.66 |
| | 9.5m | 1.828 | 2.718 | 3.649 | 48.67 | 99.6 | 34.26 |
| 9 | 1m | 3.263 | 4.936 | 6.706 | 51.27 | 105.52 | 35.86 |
| | 5m | 3.689 | 5.698 | 7.617 | 54.44 | 106.45 | 33.68 |
| | 7.5 | 3.055 | 4.728 | 6.355 | 54.76 | 108.02 | 34.42 |
| | 9.5m | 1.464 | 2.195 | 2.935 | 49.98 | 100.5 | 33.69 |
| 10 | 1m | 5.330 | 8.278 | 11.145 | 55.32 | 109.1 | 34.63 |
| | 5m | 5.040 | 7.798 | 10.518 | 54.72 | 108.69 | 34.88 |
| | 7.5 | 4.336 | 6.522 | 8.713 | 50.42 | 100.95 | 33.59 |
| | 9.5m | 1.959 | 2.890 | 3.921 | 47.57 | 100.19 | 35.66 |
| 11 | 1m | 4.705 | 6.992 | 9.299 | 48.62 | 97.66 | 33 |
| | 5m | 5.371 | 7.984 | 10.585 | 48.65 | 97.07 | 32.58 |
| | 7.5 | 4.368 | 6.547 | 8.705 | 49.89 | 99.3 | 32.96 |
| | 9.5m | 2.082 | 3.140 | 4.200 | 50.84 | 101.76 | 33.76 |
| 12 | 1m | 7.389 | 11.196 | 14.907 | 51.53 | 101.75 | 33.14 |
| | 5m | 6.844 | 10.304 | 13.825 | 50.56 | 102 | 34.17 |
| | 7.5 | 5.819 | 8.743 | 11.686 | 50.25 | 100.82 | 33.66 |
| | 9.5m | 2.632 | 3.943 | 5.225 | 49.78 | 98.51 | 32.53 |
| 13 | 1m | 1.426 | 2.159 | 2.937 | 51.4 | 106 | 36.06 |
| | 5m | 2.043 | 3.235 | 4.262 | 58.3 | 108.59 | 31.77 |
| | 7.5 | 1.777 | 2.723 | 3.594 | 53.28 | 102.27 | 31.97 |
| | 9.5m | 0.897 | 1.367 | 1.817 | 52.31 | 102.48 | 32.94 |
| 14 | 1m | 2.999 | 4.508 | 5.980 | 50.31 | 99.39 | 32.65 |
| | 5m | 3.132 | 4.677 | 6.108 | 49.3 | 94.98 | 30.6 |
| | 7.5 | 2.647 | 3.987 | 5.241 | 50.62 | 97.97 | 31.43 |
| | 9.5m | 1.294 | 1.940 | 2.576 | 49.91 | 99.07 | 32.79 |
| 15 | 1m | 1.352 | 2.071 | 2.864 | 53.12 | 111.77 | 38.3 |
| | 5m | 1.987 | 3.114 | 4.185 | 56.68 | 110.58 | 34.4 |
| | 7.5 | 1.720 | 2.661 | 3.529 | 54.68 | 105.1 | 32.59 |
| | 9.5m | 0.886 | 1.337 | 1.793 | 50.87 | 102.38 | 34.14 |
| 16 | 1m | 2.936 | 4.397 | 5.800 | 49.77 | 97.54 | 31.9 |
| | 5m | 3.016 | 4.588 | 6.089 | 52.11 | 101.87 | 32.71 |

| Case | Planes | LTR velocities | | | Percentage increase in flow rate with the increase in LTR velocity from 1 to 1.5, 1 to 2 and 1.5 to 2m/s | | |
|------------------------------------|-------------|--------------------------------|--------------|--------------|--|---------------|---------------|
| | | 1m/s | 1.5m/s | 2m/s | 1-1.5 m/s (%) | 1-2 m/s (%) | 1.5-2 m/s (%) |
| | | Flow rates (m ³ /s) | | | | | |
| | 7.5 | 2.612 | 3.904 | 5.081 | 49.47 | 94.52 | 30.14 |
| | 9.5m | 1.273 | 1.911 | 2.559 | 50.08 | 100.99 | 33.92 |
| 17 | 1m | 1.850 | 2.744 | 3.754 | 48.31 | 102.9 | 36.81 |
| | 5m | 2.741 | 4.141 | 5.432 | 51.08 | 98.18 | 31.18 |
| | 7.5 | 2.220 | 3.340 | 4.450 | 50.45 | 100.41 | 33.21 |
| | 9.5m | 1.181 | 1.753 | 2.338 | 48.48 | 97.96 | 33.32 |
| 18 | 1m | 3.877 | 5.827 | 7.899 | 50.29 | 103.73 | 35.55 |
| | 5m | 3.785 | 5.536 | 7.451 | 46.27 | 96.87 | 34.59 |
| | 7.5 | 3.224 | 4.796 | 6.511 | 48.79 | 101.97 | 35.75 |
| | 9.5m | 1.640 | 2.475 | 3.321 | 50.89 | 102.48 | 34.19 |
| 19 | 1m | 2.744 | 4.201 | 5.633 | 53.1 | 105.3 | 34.09 |
| | 5m | 3.416 | 5.105 | 6.872 | 49.46 | 101.19 | 34.61 |
| | 7.5 | 2.715 | 4.105 | 5.579 | 51.18 | 105.49 | 35.92 |
| | 9.5m | 1.478 | 2.231 | 3.000 | 50.91 | 102.95 | 34.48 |
| 20 | 1m | 4.740 | 7.163 | 9.653 | 51.14 | 103.66 | 34.75 |
| | 5m | 4.298 | 6.542 | 8.883 | 52.23 | 106.69 | 35.78 |
| | 7.5 | 3.807 | 5.756 | 7.767 | 51.18 | 104 | 34.94 |
| | 9.5m | 1.955 | 2.904 | 3.898 | 48.56 | 99.38 | 34.21 |
| 21 | 1m | 3.203 | 4.876 | 6.320 | 52.25 | 97.34 | 29.62 |
| | 5m | 3.630 | 5.595 | 7.360 | 54.15 | 102.77 | 31.54 |
| | 7.5 | 2.931 | 4.561 | 5.794 | 55.59 | 97.65 | 27.03 |
| | 9.5m | 1.515 | 2.286 | 3.036 | 50.85 | 100.38 | 32.84 |
| 22 | 1m | 5.091 | 7.690 | 10.287 | 51.03 | 102.05 | 33.78 |
| | 5m | 4.679 | 6.931 | 9.387 | 48.14 | 100.64 | 35.44 |
| | 7.5 | 4.058 | 6.026 | 8.127 | 48.5 | 100.26 | 34.86 |
| | 9.5m | 2.088 | 3.108 | 4.142 | 48.86 | 98.39 | 33.27 |
| 23 | 1m | 4.402 | 6.719 | 9.119 | 52.62 | 107.13 | 35.71 |
| | 5m | 5.112 | 7.805 | 10.439 | 52.68 | 104.2 | 33.74 |
| | 7.5 | 4.159 | 6.370 | 8.540 | 53.16 | 105.34 | 34.07 |
| | 9.5m | 2.168 | 3.251 | 4.343 | 49.92 | 100.28 | 33.59 |
| 24 | 1m | 7.149 | 11.054 | 14.689 | 54.61 | 105.46 | 32.89 |
| | 5m | 6.381 | 9.643 | 12.820 | 51.12 | 100.93 | 32.95 |
| | 7.5 | 5.504 | 8.356 | 11.170 | 51.82 | 102.95 | 33.67 |
| | 9.5m | 2.787 | 4.238 | 5.592 | 52.04 | 100.63 | 31.96 |
| Average percentage increase | | | | | 51.41 | 102.67 | 33.86 |

Table E2 Percentage increase in flow rates at the specified planes with the increase in LTR velocity from 1-1.5, 1-2 and 1.5-2m/s - 6.6 x 4 x 10 m heading

| Case | Planes | LTR velocities | | | Percentage increase in flow rate with the increase in LTR velocity from 1 to 1.5, 1 to 2 and 1.5 to 2m/s | | |
|------|-------------|--------------------------------|--------------|--------------|--|---------------|---------------|
| | | 1m/s | 1.5m/s | 2m/s | 1-1.5 m/s (%) | 1-2 m/s (%) | 1.5-2 m/s (%) |
| | | Flow rates (m ³ /s) | | | | | |
| 49 | 1m | 2.000 | 3.094 | 4.209 | 54.75 | 110.51 | 36.03 |
| | 5m | 2.885 | 4.484 | 6.113 | 55.41 | 111.89 | 36.35 |
| | 7.5 | 2.531 | 3.885 | 5.288 | 53.5 | 108.94 | 36.11 |
| | 9.5m | 1.161 | 1.757 | 2.352 | 51.38 | 102.58 | 33.83 |
| 50 | 1m | 4.067 | 6.128 | 8.225 | 50.67 | 102.25 | 34.23 |
| | 5m | 4.293 | 6.544 | 8.764 | 52.43 | 104.13 | 33.92 |
| | 7.5 | 3.683 | 5.584 | 7.386 | 51.63 | 100.57 | 32.27 |
| | 9.5m | 1.608 | 2.428 | 3.231 | 50.97 | 100.88 | 33.06 |
| 51 | 1m | 1.958 | 3.015 | 4.156 | 53.96 | 112.21 | 37.83 |
| | 5m | 2.826 | 4.412 | 6.026 | 56.11 | 113.26 | 36.61 |
| | 7.5 | 2.493 | 3.822 | 5.226 | 53.28 | 109.64 | 36.76 |
| | 9.5m | 1.138 | 1.748 | 2.312 | 53.53 | 103.13 | 32.31 |
| 52 | 1m | 4.001 | 6.061 | 8.131 | 51.48 | 103.23 | 34.16 |
| | 5m | 4.247 | 6.462 | 8.644 | 52.16 | 103.54 | 33.77 |
| | 7.5 | 3.631 | 5.516 | 7.309 | 51.94 | 101.31 | 32.5 |
| | 9.5m | 1.598 | 2.369 | 3.170 | 48.3 | 98.43 | 33.8 |
| 53 | 1m | 2.764 | 4.170 | 5.528 | 50.86 | 100.01 | 32.58 |
| | 5m | 3.629 | 5.610 | 7.531 | 54.58 | 107.51 | 34.24 |
| | 7.5 | 3.129 | 4.712 | 6.379 | 50.58 | 103.84 | 35.37 |
| | 9.5m | 1.510 | 2.250 | 2.999 | 48.94 | 98.57 | 33.33 |
| 54 | 1m | 5.228 | 8.016 | 10.836 | 53.35 | 107.29 | 35.18 |
| | 5m | 5.235 | 8.021 | 10.857 | 53.2 | 107.39 | 35.37 |
| | 7.5 | 4.584 | 6.928 | 9.297 | 51.14 | 102.8 | 34.19 |
| | 9.5m | 2.059 | 3.044 | 4.129 | 47.83 | 100.53 | 35.65 |
| 55 | 1m | 3.610 | 5.533 | 7.611 | 53.26 | 110.84 | 37.57 |
| | 5m | 4.565 | 6.996 | 9.224 | 53.26 | 102.09 | 31.86 |
| | 7.5 | 3.779 | 5.751 | 7.967 | 52.17 | 110.83 | 38.54 |
| | 9.5m | 1.882 | 2.890 | 3.848 | 53.55 | 104.44 | 33.14 |
| 56 | 1m | 6.404 | 9.820 | 13.202 | 53.34 | 106.15 | 34.44 |
| | 5m | 6.114 | 9.441 | 12.684 | 54.41 | 107.45 | 34.35 |

| Case | Planes | LTR velocities | | | Percentage increase in flow rate with the increase in LTR velocity from 1 to 1.5, 1 to 2 and 1.5 to 2m/s | | |
|------|-------------|--------------------------------|--------------|--------------|--|---------------|---------------|
| | | 1m/s | 1.5m/s | 2m/s | 1-1.5 m/s (%) | 1-2 m/s (%) | 1.5-2 m/s (%) |
| | | Flow rates (m ³ /s) | | | | | |
| | 7.5 | 5.414 | 8.206 | 11.007 | 51.58 | 103.32 | 34.13 |
| | 9.5m | 2.425 | 3.644 | 4.885 | 50.24 | 101.44 | 34.07 |
| | 1m | 4.331 | 6.576 | 8.883 | 51.84 | 105.11 | 35.09 |
| | 5m | 4.871 | 7.481 | 9.887 | 53.58 | 102.96 | 32.15 |
| 57 | 7.5 | 4.000 | 6.201 | 8.137 | 55.02 | 103.4 | 31.21 |
| | 9.5m | 1.940 | 2.932 | 3.920 | 51.12 | 102.02 | 33.68 |
| | 1m | 7.113 | 10.895 | 14.406 | 53.16 | 102.52 | 32.23 |
| | 5m | 6.636 | 10.168 | 13.570 | 53.23 | 104.49 | 33.45 |
| 58 | 7.5 | 5.793 | 8.773 | 11.663 | 51.44 | 101.31 | 32.93 |
| | 9.5m | 2.591 | 3.860 | 5.110 | 48.98 | 97.18 | 32.36 |
| | 1m | 6.094 | 9.143 | 11.980 | 50.04 | 96.6 | 31.03 |
| | 5m | 6.764 | 10.199 | 13.758 | 50.78 | 103.39 | 34.89 |
| 59 | 7.5 | 5.636 | 8.606 | 11.539 | 52.69 | 104.74 | 34.08 |
| | 9.5m | 2.790 | 4.161 | 5.591 | 49.12 | 100.36 | 34.36 |
| | 1m | 9.784 | 14.623 | 19.549 | 49.45 | 99.8 | 33.69 |
| | 5m | 8.927 | 13.457 | 18.056 | 50.74 | 102.25 | 34.18 |
| 60 | 7.5 | 7.747 | 11.621 | 15.538 | 50 | 100.55 | 33.71 |
| | 9.5m | 3.476 | 5.272 | 6.957 | 51.66 | 100.13 | 31.96 |
| | 1m | 1.858 | 2.863 | 3.959 | 54.13 | 113.11 | 38.27 |
| | 5m | 2.682 | 4.176 | 5.544 | 55.68 | 106.69 | 32.76 |
| 61 | 7.5 | 2.404 | 3.549 | 4.857 | 47.65 | 102.07 | 36.86 |
| | 9.5m | 1.197 | 1.836 | 2.415 | 53.36 | 101.7 | 31.52 |
| | 1m | 3.977 | 5.983 | 7.851 | 50.45 | 97.42 | 31.22 |
| | 5m | 4.042 | 6.023 | 7.955 | 49.02 | 96.8 | 32.07 |
| 62 | 7.5 | 3.452 | 5.180 | 6.927 | 50.06 | 100.67 | 33.72 |
| | 9.5m | 1.731 | 2.571 | 3.420 | 48.49 | 97.55 | 33.04 |
| | 1m | 1.813 | 2.814 | 3.803 | 55.14 | 109.68 | 35.15 |
| | 5m | 2.580 | 4.024 | 5.404 | 55.99 | 109.49 | 34.3 |
| 63 | 7.5 | 2.197 | 3.375 | 4.576 | 53.57 | 108.24 | 35.6 |
| | 9.5m | 1.172 | 1.796 | 2.400 | 53.31 | 104.84 | 33.62 |
| | 1m | 3.894 | 5.776 | 7.700 | 48.32 | 97.72 | 33.3 |
| | 5m | 3.978 | 5.864 | 7.790 | 47.41 | 95.81 | 32.84 |
| 64 | 7.5 | 3.411 | 5.066 | 6.762 | 48.52 | 98.25 | 33.48 |

| Case | Planes | LTR velocities | | | Percentage increase in flow rate with the increase in LTR velocity from 1 to 1.5, 1 to 2 and 1.5 to 2m/s | | |
|------------------------------------|-------------|--------------------------------|--------------|--------------|--|---------------|---------------|
| | | 1m/s | 1.5m/s | 2m/s | 1-1.5 m/s (%) | 1-2 m/s (%) | 1.5-2 m/s (%) |
| | | Flow rates (m ³ /s) | | | | | |
| | 9.5m | 1.688 | 2.553 | 3.392 | 51.25 | 100.91 | 32.83 |
| 65 | 1m | 2.467 | 3.627 | 4.914 | 47.01 | 99.19 | 35.49 |
| | 5m | 3.527 | 5.298 | 6.981 | 50.2 | 97.9 | 31.75 |
| | 7.5 | 2.925 | 4.321 | 5.718 | 47.71 | 95.47 | 32.33 |
| | 9.5m | 1.568 | 2.355 | 3.130 | 50.19 | 99.58 | 32.89 |
| 66 | 1m | 5.058 | 7.610 | 10.311 | 50.45 | 103.84 | 35.49 |
| | 5m | 4.817 | 7.200 | 9.600 | 49.48 | 99.3 | 33.34 |
| | 7.5 | 4.208 | 6.319 | 8.538 | 50.17 | 102.92 | 35.13 |
| | 9.5m | 2.170 | 3.276 | 4.398 | 51 | 102.7 | 34.24 |
| 67 | 1m | 3.521 | 5.418 | 7.398 | 53.89 | 110.12 | 36.54 |
| | 5m | 4.440 | 6.862 | 8.868 | 54.57 | 99.74 | 29.22 |
| | 7.5 | 3.639 | 5.598 | 7.261 | 53.84 | 99.54 | 29.71 |
| | 9.5m | 1.962 | 2.970 | 4.006 | 51.37 | 104.15 | 34.86 |
| 68 | 1m | 6.108 | 9.301 | 12.588 | 52.28 | 106.1 | 35.35 |
| | 5m | 5.492 | 8.415 | 11.402 | 53.23 | 107.62 | 35.5 |
| | 7.5 | 4.970 | 7.549 | 10.164 | 51.9 | 104.5 | 34.63 |
| | 9.5m | 2.593 | 3.858 | 5.195 | 48.77 | 100.35 | 34.66 |
| 69 | 1m | 4.154 | 6.210 | 8.214 | 49.49 | 97.73 | 32.28 |
| | 5m | 4.790 | 7.189 | 9.533 | 50.08 | 99.02 | 32.61 |
| | 7.5 | 3.806 | 5.599 | 7.669 | 47.12 | 101.52 | 36.98 |
| | 9.5m | 2.021 | 3.036 | 4.080 | 50.23 | 101.88 | 34.38 |
| 70 | 1m | 6.643 | 10.032 | 13.508 | 51 | 103.33 | 34.66 |
| | 5m | 5.999 | 8.931 | 12.020 | 48.88 | 100.37 | 34.58 |
| | 7.5 | 5.231 | 7.912 | 10.638 | 51.24 | 103.35 | 34.45 |
| | 9.5m | 2.789 | 4.119 | 5.510 | 47.68 | 97.59 | 33.8 |
| 71 | 1m | 5.666 | 8.653 | 11.780 | 52.72 | 107.9 | 36.13 |
| | 5m | 6.537 | 10.004 | 13.602 | 53.05 | 108.1 | 35.97 |
| | 7.5 | 5.511 | 8.421 | 11.368 | 52.81 | 106.28 | 34.99 |
| | 9.5m | 2.874 | 4.307 | 5.782 | 49.87 | 101.22 | 34.26 |
| 72 | 1m | 9.389 | 14.129 | 18.869 | 50.48 | 100.96 | 33.55 |
| | 5m | 8.158 | 12.295 | 16.467 | 50.7 | 101.84 | 33.93 |
| | 7.5 | 7.140 | 10.737 | 14.396 | 50.38 | 101.63 | 34.08 |
| | 9.5m | 3.691 | 5.622 | 7.401 | 52.31 | 100.5 | 31.64 |
| Average percentage increase | | | | | 51.49 | 103.07 | 34.05 |

Table E3 Percentage increase in flow rates at the specified planes with the increase in LTR velocity from 1-1.5, 1-2 and 1.5-2m/s - 6.6 x 3 x 20 m heading

| Case | Planes | LTR Velocities | | | Percentage increase in flow rate with the increase in LTR velocity from 1 to 1.5, 1 to 2 and 1.5 to 2m/s | | |
|------|--------------|--------------------------------|--------------|--------------|--|---------------|---------------|
| | | 1m/s | 1.5m/s | 2m/s | 1-1.5 m/s (%) | 1-2 m/s (%) | 1.5-2 m/s (%) |
| | | Flow Rates (m ³ /s) | | | | | |
| 25 | 1m | 1.323 | 1.998 | 2.727 | 50.99 | 106.09 | 36.49 |
| | 10m | 1.989 | 2.974 | 3.971 | 49.53 | 99.68 | 33.54 |
| | 15m | 1.828 | 2.759 | 3.710 | 50.94 | 102.97 | 34.47 |
| | 19.5m | 0.859 | 1.311 | 1.744 | 52.64 | 103.03 | 33.01 |
| 26 | 1m | 2.594 | 3.967 | 5.344 | 52.92 | 106.02 | 34.72 |
| | 10m | 3.128 | 4.722 | 6.404 | 50.95 | 104.74 | 35.64 |
| | 15m | 3.083 | 4.668 | 6.299 | 51.4 | 104.29 | 34.93 |
| | 19.5m | 1.275 | 1.940 | 2.573 | 52.2 | 101.86 | 32.63 |
| 27 | 1m | 1.275 | 1.953 | 2.628 | 53.18 | 106.1 | 34.55 |
| | 10m | 1.958 | 2.927 | 3.906 | 49.47 | 99.48 | 33.46 |
| | 15m | 1.797 | 2.698 | 3.652 | 50.14 | 103.26 | 35.38 |
| | 19.5m | 0.841 | 1.290 | 1.713 | 53.44 | 103.72 | 32.76 |
| 28 | 1m | 2.560 | 3.926 | 5.277 | 53.37 | 106.12 | 34.39 |
| | 10m | 3.080 | 4.664 | 6.291 | 51.44 | 104.28 | 34.89 |
| | 15m | 3.038 | 4.608 | 6.191 | 51.67 | 103.75 | 34.34 |
| | 19.5m | 1.250 | 1.885 | 2.541 | 50.71 | 103.19 | 34.82 |
| 29 | 1m | 1.739 | 2.551 | 3.439 | 46.72 | 97.8 | 34.81 |
| | 10m | 2.505 | 3.742 | 5.138 | 49.41 | 105.14 | 37.3 |
| | 15m | 2.203 | 3.374 | 4.530 | 53.13 | 105.61 | 34.27 |
| | 19.5m | 1.110 | 1.646 | 2.234 | 48.22 | 101.16 | 35.72 |
| 30 | 1m | 3.396 | 5.234 | 6.843 | 54.12 | 101.5 | 30.74 |
| | 10m | 3.802 | 5.809 | 7.683 | 52.8 | 102.08 | 32.26 |
| | 15m | 3.875 | 5.899 | 7.900 | 52.24 | 103.86 | 33.91 |
| | 19.5m | 1.646 | 2.467 | 3.290 | 49.89 | 99.89 | 33.36 |
| 31 | 1m | 2.394 | 3.734 | 5.005 | 55.96 | 109.04 | 34.03 |
| | 10m | 3.146 | 4.722 | 6.449 | 50.1 | 105 | 36.57 |
| | 15m | 2.679 | 4.036 | 5.535 | 50.67 | 106.59 | 37.12 |
| | 19.5m | 1.405 | 2.131 | 2.864 | 51.71 | 103.82 | 34.35 |
| 32 | 1m | 4.027 | 6.296 | 8.352 | 56.35 | 107.39 | 32.64 |
| | 10m | 4.405 | 6.885 | 9.086 | 56.31 | 106.27 | 31.96 |

| Case | Planes | LTR Velocities | | | Percentage increase in flow rate with the increase in LTR velocity from 1 to 1.5, 1 to 2 and 1.5 to 2m/s | | |
|------|--------------|--------------------------------|--------------|--------------|--|---------------|---------------|
| | | 1m/s | 1.5m/s | 2m/s | 1-1.5 m/s (%) | 1-2 m/s (%) | 1.5-2 m/s (%) |
| | | Flow Rates (m ³ /s) | | | | | |
| | 15m | 4.489 | 6.906 | 9.234 | 53.85 | 105.73 | 33.72 |
| | 19.5m | 1.952 | 2.878 | 3.870 | 47.46 | 98.29 | 34.48 |
| | 1m | 2.731 | 4.107 | 5.491 | 50.42 | 101.1 | 33.69 |
| | 10m | 3.187 | 5.029 | 6.662 | 57.77 | 109.03 | 32.49 |
| 33 | 15m | 2.830 | 4.368 | 5.807 | 54.38 | 105.23 | 32.94 |
| | 19.5m | 1.451 | 2.198 | 2.910 | 51.5 | 100.55 | 32.37 |
| | 1m | 4.506 | 6.849 | 9.226 | 51.99 | 104.75 | 34.71 |
| | 10m | 4.848 | 7.452 | 9.997 | 53.7 | 106.19 | 34.15 |
| 34 | 15m | 4.700 | 7.245 | 9.780 | 54.17 | 108.1 | 34.98 |
| | 19.5m | 2.061 | 3.079 | 4.098 | 49.42 | 98.83 | 33.07 |
| | 1m | 3.899 | 5.811 | 7.714 | 49.04 | 97.86 | 32.76 |
| | 10m | 4.635 | 7.051 | 9.258 | 52.12 | 99.74 | 31.3 |
| 35 | 15m | 4.044 | 6.034 | 7.990 | 49.19 | 97.55 | 32.42 |
| | 19.5m | 2.059 | 3.090 | 4.138 | 50.08 | 100.96 | 33.9 |
| | 1m | 6.406 | 9.723 | 12.628 | 51.79 | 97.13 | 29.87 |
| | 10m | 6.502 | 9.812 | 12.988 | 50.9 | 99.74 | 32.36 |
| 36 | 15m | 6.193 | 9.502 | 12.436 | 53.42 | 100.8 | 30.88 |
| | 19.5m | 2.748 | 4.109 | 5.453 | 49.54 | 98.46 | 32.72 |
| | 1m | 1.235 | 1.900 | 2.527 | 53.85 | 104.6 | 32.98 |
| | 10m | 1.948 | 2.908 | 3.868 | 49.24 | 98.56 | 33.05 |
| 37 | 15m | 1.732 | 2.659 | 3.563 | 53.55 | 105.75 | 34 |
| | 19.5m | 0.881 | 1.350 | 1.786 | 53.33 | 102.73 | 32.22 |
| | 1m | 2.483 | 3.820 | 5.219 | 53.86 | 110.21 | 36.62 |
| | 10m | 2.912 | 4.452 | 6.121 | 52.88 | 110.2 | 37.5 |
| 38 | 15m | 2.890 | 4.388 | 5.757 | 51.82 | 99.19 | 31.2 |
| | 19.5m | 1.355 | 2.032 | 2.694 | 49.95 | 98.82 | 32.59 |
| | 1m | 1.172 | 1.794 | 2.439 | 53.02 | 108.02 | 35.94 |
| | 10m | 1.879 | 2.767 | 3.794 | 47.2 | 101.85 | 37.13 |
| 39 | 15m | 1.706 | 2.560 | 3.463 | 50.05 | 102.95 | 35.25 |
| | 19.5m | 0.870 | 1.321 | 1.759 | 51.83 | 102.08 | 33.1 |
| | 1m | 2.420 | 3.716 | 5.075 | 53.54 | 109.68 | 36.57 |
| | 10m | 2.865 | 4.388 | 5.933 | 53.18 | 107.1 | 35.2 |
| 40 | 15m | 2.781 | 4.252 | 5.565 | 52.89 | 100.11 | 30.88 |

| Case | Planes | LTR Velocities | | | Percentage increase in flow rate with the increase in LTR velocity from 1 to 1.5, 1 to 2 and 1.5 to 2m/s | | |
|------------------------------------|--------------|--------------------------------|--------------|--------------|--|---------------|---------------|
| | | 1m/s | 1.5m/s | 2m/s | 1-1.5 m/s (%) | 1-2 m/s (%) | 1.5-2 m/s (%) |
| | | Flow Rates (m ³ /s) | | | | | |
| | 19.5m | 1.312 | 2.001 | 2.663 | 52.51 | 102.94 | 33.07 |
| 41 | 1m | 1.539 | 2.344 | 3.158 | 52.34 | 105.23 | 34.72 |
| | 10m | 2.382 | 3.602 | 5.014 | 51.2 | 110.48 | 39.2 |
| | 15m | 2.148 | 3.219 | 4.391 | 49.85 | 104.44 | 36.43 |
| | 19.5m | 1.155 | 1.726 | 2.300 | 49.42 | 99.11 | 33.26 |
| 42 | 1m | 3.230 | 4.894 | 6.543 | 51.53 | 102.55 | 33.67 |
| | 10m | 3.707 | 5.619 | 7.393 | 51.56 | 99.42 | 31.58 |
| | 15m | 3.591 | 5.573 | 7.386 | 55.19 | 105.67 | 32.53 |
| | 19.5m | 1.721 | 2.570 | 3.472 | 49.37 | 101.76 | 35.08 |
| 43 | 1m | 2.225 | 3.508 | 4.762 | 57.68 | 114.04 | 35.74 |
| | 10m | 2.988 | 4.509 | 6.172 | 50.9 | 106.59 | 36.91 |
| | 15m | 2.509 | 3.853 | 5.277 | 53.58 | 110.37 | 36.98 |
| | 19.5m | 1.444 | 2.193 | 2.952 | 51.93 | 104.49 | 34.6 |
| 44 | 1m | 3.946 | 6.099 | 8.148 | 54.58 | 106.5 | 33.59 |
| | 10m | 4.232 | 6.645 | 8.796 | 57.02 | 107.87 | 32.38 |
| | 15m | 4.140 | 6.353 | 8.585 | 53.46 | 107.4 | 35.14 |
| | 19.5m | 2.003 | 3.028 | 4.080 | 51.14 | 103.66 | 34.74 |
| 45 | 1m | 2.655 | 3.967 | 5.352 | 49.4 | 101.6 | 34.94 |
| | 10m | 2.965 | 4.667 | 6.261 | 57.41 | 111.18 | 34.16 |
| | 15m | 2.736 | 4.127 | 5.545 | 50.82 | 102.67 | 34.38 |
| | 19.5m | 1.489 | 2.246 | 2.988 | 50.79 | 100.65 | 33.06 |
| 46 | 1m | 4.360 | 6.548 | 8.803 | 50.21 | 101.93 | 34.43 |
| | 10m | 4.581 | 6.997 | 9.400 | 52.72 | 105.18 | 34.35 |
| | 15m | 4.431 | 6.858 | 9.118 | 54.75 | 105.77 | 32.96 |
| | 19.5m | 2.187 | 3.242 | 4.281 | 48.21 | 95.74 | 32.07 |
| 47 | 1m | 3.754 | 5.547 | 7.411 | 47.77 | 97.43 | 33.6 |
| | 10m | 4.375 | 6.683 | 8.871 | 52.76 | 102.79 | 32.75 |
| | 15m | 3.861 | 5.776 | 7.594 | 49.61 | 96.68 | 31.47 |
| | 19.5m | 2.150 | 3.202 | 4.275 | 48.95 | 98.84 | 33.49 |
| 48 | 1m | 6.248 | 9.327 | 12.366 | 49.29 | 97.92 | 32.58 |
| | 10m | 6.205 | 9.546 | 12.456 | 53.85 | 100.75 | 30.48 |
| | 15m | 5.821 | 8.903 | 11.887 | 52.94 | 104.2 | 33.52 |
| | 19.5m | 2.822 | 4.287 | 5.680 | 51.91 | 101.29 | 32.51 |
| Average percentage increase | | | | | 51.86 | 103.36 | 33.92 |

Table E4 Percentage increase in flow rates at the specified planes with the increase in LTR velocity from 1-1.5, 1-2 and 1.5-2m/s - 6.6 x 4 x 20 m heading

| Case | Planes | LTR Velocities | | | Percentage increase in flow rate with the increase in LTR velocity change from 1 to 1.5, 1 to 2 and 1.5 to 2m/s | | |
|------|--------------|--------------------------------|--------------|--------------|---|---------------|---------------|
| | | 1m/s | 1.5m/s | 2m/s | 1-1.5 m/s (%) | 1-2 m/s (%) | 1.5-2 m/s (%) |
| | | Flow Rates (m ³ /s) | | | | | |
| 73 | 1m | 1.778 | 2.661 | 3.610 | 49.65 | 103.05 | 35.68 |
| | 10m | 2.683 | 3.977 | 5.372 | 48.21 | 100.21 | 35.09 |
| | 15m | 2.424 | 3.661 | 4.946 | 51.06 | 104.06 | 35.09 |
| | 19.5m | 1.136 | 1.718 | 2.311 | 51.3 | 103.51 | 34.51 |
| 74 | 1m | 3.508 | 5.347 | 7.162 | 52.41 | 104.16 | 33.95 |
| | 10m | 4.175 | 6.276 | 8.590 | 50.3 | 105.72 | 36.87 |
| | 15m | 4.112 | 6.321 | 8.492 | 53.72 | 106.51 | 34.34 |
| | 19.5m | 1.679 | 2.551 | 3.402 | 51.89 | 102.62 | 33.39 |
| 75 | 1m | 1.691 | 2.589 | 3.532 | 53.11 | 108.9 | 36.44 |
| | 10m | 2.604 | 3.915 | 5.291 | 50.37 | 103.24 | 35.15 |
| | 15m | 2.371 | 3.603 | 4.851 | 51.93 | 104.58 | 34.65 |
| | 19.5m | 1.120 | 1.695 | 2.253 | 51.36 | 101.14 | 32.89 |
| 76 | 1m | 3.454 | 5.257 | 7.053 | 52.19 | 104.2 | 34.18 |
| | 10m | 4.101 | 6.198 | 8.453 | 51.12 | 106.1 | 36.38 |
| | 15m | 4.007 | 6.152 | 8.321 | 53.54 | 107.68 | 35.26 |
| | 19.5m | 1.654 | 2.490 | 3.370 | 50.51 | 103.7 | 35.34 |
| 77 | 1m | 2.303 | 3.450 | 4.568 | 49.84 | 98.37 | 32.39 |
| | 10m | 3.340 | 5.006 | 6.956 | 49.86 | 108.23 | 38.95 |
| | 15m | 2.955 | 4.498 | 6.113 | 52.19 | 106.84 | 35.91 |
| | 19.5m | 1.491 | 2.210 | 2.959 | 48.23 | 98.48 | 33.9 |
| 78 | 1m | 4.520 | 6.989 | 9.299 | 54.62 | 105.72 | 33.05 |
| | 10m | 5.109 | 7.736 | 10.305 | 51.41 | 101.69 | 33.2 |
| | 15m | 5.291 | 8.021 | 10.793 | 51.61 | 103.99 | 34.55 |
| | 19.5m | 2.152 | 3.230 | 4.363 | 50.12 | 102.78 | 35.08 |
| 79 | 1m | 3.228 | 4.925 | 6.656 | 52.59 | 106.22 | 35.15 |
| | 10m | 4.271 | 6.411 | 8.769 | 50.1 | 105.31 | 36.78 |
| | 15m | 3.585 | 5.485 | 7.426 | 53.01 | 107.15 | 35.38 |
| | 19.5m | 1.855 | 2.832 | 3.781 | 52.68 | 103.84 | 33.51 |
| 80 | 1m | 5.393 | 8.342 | 11.200 | 54.68 | 107.69 | 34.27 |
| | 10m | 5.957 | 9.140 | 12.021 | 53.45 | 101.81 | 31.51 |

| Case | Planes | LTR Velocities | | | Percentage increase in flow rate with the increase in LTR velocity change from 1 to 1.5, 1 to 2 and 1.5 to 2m/s | | |
|------|--------------|--------------------------------|--------------|--------------|---|---------------|---------------|
| | | 1m/s | 1.5m/s | 2m/s | 1-1.5 m/s (%) | 1-2 m/s (%) | 1.5-2 m/s (%) |
| | | Flow Rates (m ³ /s) | | | | | |
| | 15m | 5.986 | 9.317 | 12.208 | 55.65 | 103.96 | 31.04 |
| | 19.5m | 2.573 | 3.868 | 5.137 | 50.34 | 99.66 | 32.81 |
| 81 | 1m | 3.559 | 5.352 | 7.125 | 50.4 | 100.23 | 33.13 |
| | 10m | 4.217 | 6.555 | 8.838 | 55.45 | 109.59 | 34.83 |
| | 15m | 3.768 | 5.885 | 7.850 | 56.19 | 108.36 | 33.4 |
| | 19.5m | 1.908 | 2.877 | 3.812 | 50.77 | 99.76 | 32.49 |
| 82 | 1m | 5.983 | 9.017 | 12.233 | 50.72 | 104.47 | 35.66 |
| | 10m | 6.526 | 10.051 | 13.337 | 54.02 | 104.37 | 32.69 |
| | 15m | 6.362 | 9.820 | 12.990 | 54.37 | 104.20 | 32.27 |
| | 19.5m | 2.764 | 4.050 | 5.430 | 46.52 | 96.48 | 34.10 |
| 83 | 1m | 5.230 | 7.853 | 10.511 | 50.15 | 100.98 | 33.86 |
| | 10m | 6.171 | 9.471 | 12.526 | 53.47 | 102.98 | 32.26 |
| | 15m | 5.342 | 8.044 | 10.735 | 50.57 | 100.94 | 33.45 |
| | 19.5m | 2.735 | 4.102 | 5.457 | 49.95 | 99.49 | 33.04 |
| 84 | 1m | 8.512 | 12.844 | 16.991 | 50.9 | 99.62 | 32.29 |
| | 10m | 8.856 | 13.200 | 17.536 | 49.05 | 98.02 | 32.85 |
| | 15m | 8.250 | 12.583 | 16.654 | 52.51 | 101.85 | 32.35 |
| | 19.5m | 3.625 | 5.480 | 7.373 | 51.17 | 103.38 | 34.54 |
| 85 | 1m | 1.630 | 2.484 | 3.351 | 52.4 | 105.55 | 34.87 |
| | 10m | 2.571 | 3.912 | 5.211 | 52.17 | 102.7 | 33.21 |
| | 15m | 2.320 | 3.521 | 4.756 | 51.78 | 105.04 | 35.09 |
| | 19.5m | 1.173 | 1.784 | 2.386 | 52.08 | 103.39 | 33.74 |
| 86 | 1m | 3.334 | 5.063 | 6.909 | 51.87 | 107.22 | 36.44 |
| | 10m | 3.902 | 5.950 | 8.126 | 52.49 | 108.24 | 36.56 |
| | 15m | 3.829 | 5.796 | 7.728 | 51.38 | 101.85 | 33.34 |
| | 19.5m | 1.790 | 2.709 | 3.588 | 51.31 | 100.43 | 32.46 |
| 87 | 1m | 1.561 | 2.385 | 3.195 | 52.74 | 104.63 | 33.97 |
| | 10m | 2.490 | 3.723 | 4.989 | 49.54 | 100.39 | 34 |
| | 15m | 2.252 | 3.381 | 4.574 | 50.17 | 103.15 | 35.29 |
| | 19.5m | 1.153 | 1.752 | 2.350 | 51.93 | 103.82 | 34.16 |
| 88 | 1m | 3.281 | 5.122 | 6.806 | 56.12 | 107.44 | 32.87 |
| | 10m | 3.842 | 5.849 | 7.914 | 52.25 | 106.01 | 35.31 |
| | 15m | 3.697 | 5.628 | 7.500 | 52.23 | 102.87 | 33.27 |

| Case | Planes | LTR Velocities | | | Percentage increase in flow rate with the increase in LTR velocity change from 1 to 1.5, 1 to 2 and 1.5 to 2m/s | | |
|------------------------------------|--------------|--------------------------------|--------------|--------------|---|---------------|---------------|
| | | 1m/s | 1.5m/s | 2m/s | 1-1.5 m/s (%) | 1-2 m/s (%) | 1.5-2 m/s (%) |
| | | Flow Rates (m ³ /s) | | | | | |
| | 19.5m | 1.743 | 2.662 | 3.540 | 52.72 | 103.13 | 33.01 |
| 89 | 1m | 2.049 | 3.040 | 4.110 | 48.36 | 100.61 | 35.22 |
| | 10m | 3.177 | 4.829 | 6.523 | 51.97 | 105.27 | 35.08 |
| | 15m | 2.896 | 4.255 | 5.793 | 46.94 | 100.05 | 36.15 |
| | 19.5m | 1.536 | 2.291 | 3.037 | 49.13 | 97.73 | 32.59 |
| 90 | 1m | 4.350 | 6.823 | 8.990 | 56.83 | 106.67 | 31.78 |
| | 10m | 4.953 | 7.478 | 9.880 | 51 | 99.49 | 32.12 |
| | 15m | 4.724 | 7.379 | 9.782 | 56.22 | 107.09 | 32.57 |
| | 19.5m | 2.287 | 3.410 | 4.601 | 49.11 | 101.16 | 34.9 |
| 91 | 1m | 2.943 | 4.658 | 6.267 | 58.25 | 112.91 | 34.53 |
| | 10m | 3.964 | 6.014 | 8.241 | 51.7 | 107.88 | 37.04 |
| | 15m | 3.495 | 5.366 | 7.345 | 53.52 | 110.15 | 36.89 |
| | 19.5m | 1.912 | 2.897 | 3.898 | 51.51 | 103.83 | 34.53 |
| 92 | 1m | 5.229 | 8.218 | 10.903 | 57.18 | 108.54 | 32.67 |
| | 10m | 5.601 | 8.857 | 11.752 | 58.13 | 109.82 | 32.69 |
| | 15m | 5.501 | 8.435 | 11.360 | 53.33 | 106.5 | 34.68 |
| | 19.5m | 2.712 | 4.002 | 5.368 | 47.58 | 97.92 | 34.11 |
| 93 | 1m | 3.233 | 4.889 | 6.595 | 51.19 | 103.96 | 34.9 |
| | 10m | 3.995 | 6.195 | 8.343 | 55.08 | 108.84 | 34.66 |
| | 15m | 3.670 | 5.472 | 7.390 | 49.1 | 101.37 | 35.06 |
| | 19.5m | 1.974 | 2.973 | 3.972 | 50.59 | 101.21 | 33.61 |
| 94 | 1m | 5.855 | 8.746 | 11.771 | 49.3697 | 101.02 | 34.58 |
| | 10m | 6.102 | 9.322 | 12.330 | 52.7681 | 102.06 | 32.27 |
| | 15m | 5.957 | 9.074 | 12.098 | 52.3214 | 103.09 | 33.33 |
| | 19.5m | 2.901 | 4.290 | 5.700 | 47.8913 | 96.49 | 32.86 |
| 95 | 1m | 4.984 | 7.453 | 9.902 | 49.54 | 98.69 | 32.87 |
| | 10m | 5.832 | 8.904 | 11.895 | 52.67 | 103.97 | 33.6 |
| | 15m | 5.198 | 7.678 | 10.131 | 47.71 | 94.91 | 31.95 |
| | 19.5m | 2.826 | 4.245 | 5.657 | 50.23 | 100.17 | 33.25 |
| 96 | 1m | 8.082 | 12.135 | 16.032 | 50.15 | 98.38 | 32.12 |
| | 10m | 8.634 | 12.876 | 16.975 | 49.14 | 96.62 | 31.84 |
| | 15m | 7.753 | 11.865 | 15.485 | 53.04 | 99.73 | 30.51 |
| | 19.5m | 3.802 | 5.756 | 7.652 | 51.39 | 101.26 | 32.94 |
| Average percentage increase | | | | | 51.72 | 103.32 | 34.01 |

APPENDIX F

EFFECT OF LTR VELOCITY ON FLOW RATE CLOSE TO FACE

Table F1 Percentage increase in flow rates at the 9.5m deep plane with the increase in LTR velocity from 1 to 1.5, 1 to 2 and 1.5 to 2m/s - 6.6 x 4 x 10 m heading

| Case | LTR velocities | | | Percentage increase in flow rate for increase in LTR velocity from 1 to 1.5, 1 to 2 and 1.5 to 2m/s | | |
|------------------------------------|--------------------------------|--------|-------|---|---------------|---------------|
| | 1m/s | 1.5m/s | 2m/s | 1-1.5 m/s (%) | 1-2 m/s (%) | 1.5-2 m/s (%) |
| | Flow rates (m ³ /s) | | | | | |
| 49 | 1.161 | 1.757 | 2.352 | 51.38 | 102.58 | 33.83 |
| 50 | 1.608 | 2.428 | 3.231 | 50.97 | 100.88 | 33.06 |
| 51 | 1.138 | 1.748 | 2.312 | 53.53 | 103.13 | 32.31 |
| 52 | 1.598 | 2.369 | 3.170 | 48.3 | 98.43 | 33.8 |
| 53 | 1.510 | 2.250 | 2.999 | 48.94 | 98.57 | 33.33 |
| 54 | 2.059 | 3.044 | 4.129 | 47.83 | 100.53 | 35.65 |
| 55 | 1.882 | 2.890 | 3.848 | 53.55 | 104.44 | 33.14 |
| 56 | 2.425 | 3.644 | 4.885 | 50.24 | 101.44 | 34.07 |
| 57 | 1.940 | 2.932 | 3.920 | 51.12 | 102.02 | 33.68 |
| 58 | 2.591 | 3.860 | 5.110 | 48.98 | 97.18 | 32.36 |
| 59 | 2.790 | 4.161 | 5.591 | 49.12 | 100.36 | 34.36 |
| 60 | 3.476 | 5.272 | 6.957 | 51.66 | 100.13 | 31.96 |
| 61 | 1.197 | 1.836 | 2.415 | 53.36 | 101.7 | 31.52 |
| 62 | 1.731 | 2.571 | 3.420 | 48.49 | 97.55 | 33.04 |
| 63 | 1.172 | 1.796 | 2.400 | 53.31 | 104.84 | 33.62 |
| 64 | 1.688 | 2.553 | 3.392 | 51.25 | 100.91 | 32.83 |
| 65 | 1.568 | 2.355 | 3.130 | 50.19 | 99.58 | 32.89 |
| 66 | 2.170 | 3.276 | 4.398 | 51 | 102.7 | 34.24 |
| 67 | 1.962 | 2.970 | 4.006 | 51.37 | 104.15 | 34.86 |
| 68 | 2.593 | 3.858 | 5.195 | 48.77 | 100.35 | 34.66 |
| 69 | 2.021 | 3.036 | 4.080 | 50.23 | 101.88 | 34.38 |
| 70 | 2.789 | 4.119 | 5.510 | 47.68 | 97.59 | 33.8 |
| 71 | 2.874 | 4.307 | 5.782 | 49.87 | 101.22 | 34.26 |
| 72 | 3.691 | 5.622 | 7.401 | 52.31 | 100.5 | 31.64 |
| Average percentage increase | | | | 50.56 | 100.94 | 33.47 |

Table F2 Percentage increase in flow rates at the 19.5m deep plane with the increase in LTR velocity from 1 to 1.5, 1 to 2 and 1.5 to 2m/s - 6.6 x 3 x 20 m heading

| Case | LTR velocities | | | Percentage increase in flow rate for increase in LTR velocity from 1 to 1.5, 1 to 2 and 1.5 to 2m/s | | |
|------------------------------------|--------------------------------|--------|-------|---|---------------|---------------|
| | 1m/s | 1.5m/s | 2m/s | 1-1.5 m/s (%) | 1-2 m/s (%) | 1.5-2 m/s (%) |
| | Flow Rates (m ³ /s) | | | | | |
| 25 | 0.859 | 1.311 | 1.744 | 52.64 | 103.03 | 33.01 |
| 26 | 1.275 | 1.940 | 2.573 | 52.2 | 101.86 | 32.63 |
| 27 | 0.841 | 1.290 | 1.713 | 53.44 | 103.72 | 32.76 |
| 28 | 1.250 | 1.885 | 2.541 | 50.71 | 103.19 | 34.82 |
| 29 | 1.110 | 1.646 | 2.234 | 48.22 | 101.16 | 35.72 |
| 30 | 1.646 | 2.467 | 3.290 | 49.89 | 99.89 | 33.36 |
| 31 | 1.405 | 2.131 | 2.864 | 51.71 | 103.82 | 34.35 |
| 32 | 1.952 | 2.878 | 3.870 | 47.46 | 98.29 | 34.48 |
| 33 | 1.451 | 2.198 | 2.910 | 51.5 | 100.55 | 32.37 |
| 34 | 2.061 | 3.079 | 4.098 | 49.42 | 98.83 | 33.07 |
| 35 | 2.059 | 3.090 | 4.138 | 50.08 | 100.96 | 33.9 |
| 36 | 2.748 | 4.109 | 5.453 | 49.54 | 98.46 | 32.72 |
| 37 | 0.881 | 1.350 | 1.786 | 53.33 | 102.73 | 32.22 |
| 38 | 1.355 | 2.032 | 2.694 | 49.95 | 98.82 | 32.59 |
| 39 | 0.870 | 1.321 | 1.759 | 51.83 | 102.08 | 33.1 |
| 40 | 1.312 | 2.001 | 2.663 | 52.51 | 102.94 | 33.07 |
| 41 | 1.155 | 1.726 | 2.300 | 49.42 | 99.11 | 33.26 |
| 42 | 1.721 | 2.570 | 3.472 | 49.37 | 101.76 | 35.08 |
| 43 | 1.444 | 2.193 | 2.952 | 51.93 | 104.49 | 34.6 |
| 44 | 2.003 | 3.028 | 4.080 | 51.14 | 103.66 | 34.74 |
| 45 | 1.489 | 2.246 | 2.988 | 50.79 | 100.65 | 33.06 |
| 46 | 2.187 | 3.242 | 4.281 | 48.21 | 95.74 | 32.07 |
| 47 | 2.150 | 3.202 | 4.275 | 48.95 | 98.84 | 33.49 |
| 48 | 2.822 | 4.287 | 5.680 | 51.91 | 101.29 | 32.51 |
| Average percentage increase | | | | 50.67 | 101.08 | 33.46 |

Table F3 Percentage increase in flow rates at the 19.5m deep plane with the increase in LTR velocity from 1 to 1.5, 1 to 2 and 1.5 to 2m/s - 6.6 x 4 x 20 m heading

| Names | LTR Velocities | | | Percentage increase in flow rate for increase in LTR velocity change from 1 to 1.5, 1 to 2 and 1.5 to 2m/s | | |
|------------------------------------|--------------------------------|--------|-------|--|---------------|---------------|
| | 1m/s | 1.5m/s | 2m/s | 1-1.5 m/s (%) | 1-2 m/s (%) | 1.5-2 m/s (%) |
| | Flow Rates (m ³ /s) | | | | | |
| 73 | 1.136 | 1.718 | 2.311 | 51.3 | 103.51 | 34.51 |
| 74 | 1.679 | 2.551 | 3.402 | 51.89 | 102.62 | 33.39 |
| 75 | 1.120 | 1.695 | 2.253 | 51.36 | 101.14 | 32.89 |
| 76 | 1.654 | 2.490 | 3.370 | 50.51 | 103.7 | 35.34 |
| 77 | 1.491 | 2.210 | 2.959 | 48.23 | 98.48 | 33.9 |
| 78 | 2.152 | 3.230 | 4.363 | 50.12 | 102.78 | 35.08 |
| 79 | 1.855 | 2.832 | 3.781 | 52.68 | 103.84 | 33.51 |
| 80 | 2.573 | 3.868 | 5.137 | 50.34 | 99.66 | 32.81 |
| 81 | 1.908 | 2.877 | 3.812 | 50.77 | 99.76 | 32.49 |
| 82 | 2.764 | 4.050 | 5.430 | 46.52 | 96.48 | 34.1 |
| 83 | 2.735 | 4.102 | 5.457 | 49.95 | 99.49 | 33.04 |
| 84 | 3.625 | 5.480 | 7.373 | 51.17 | 103.38 | 34.54 |
| 85 | 1.173 | 1.784 | 2.386 | 52.08 | 103.39 | 33.74 |
| 86 | 1.790 | 2.709 | 3.588 | 51.31 | 100.43 | 32.46 |
| 87 | 1.153 | 1.752 | 2.350 | 51.93 | 103.82 | 34.16 |
| 88 | 1.743 | 2.662 | 3.540 | 52.72 | 103.13 | 33.01 |
| 89 | 1.536 | 2.291 | 3.037 | 49.13 | 97.73 | 32.59 |
| 90 | 2.287 | 3.410 | 4.601 | 49.11 | 101.16 | 34.9 |
| 91 | 1.912 | 2.897 | 3.898 | 51.51 | 103.83 | 34.53 |
| 92 | 2.712 | 4.002 | 5.368 | 47.58 | 97.92 | 34.11 |
| 93 | 1.974 | 2.973 | 3.972 | 50.59 | 101.21 | 33.61 |
| 94 | 2.901 | 4.290 | 5.700 | 47.89 | 96.49 | 32.86 |
| 95 | 2.826 | 4.245 | 5.657 | 50.23 | 100.17 | 33.25 |
| 96 | 3.802 | 5.756 | 7.652 | 51.39 | 101.26 | 32.94 |
| Average percentage increase | | | | 50.43 | 101.06 | 33.66 |

APPENDIX G

EFFECT OF LENGTH OF LB INSIDE HEADING ON FLOW RATES

Table G1 Percentage change in flow rate for each LTR velocity with the change in the length of LB inside the heading from 5 to 7.5m (1/2 to 3/4 the length of the heading) - 6.6 x 3 x 10m heading

| Cases | Planes | LTR velocity | | |
|-------|-------------|---|-------------|-------------|
| | | 1m/s | 1.5m/s | 2m/s |
| | | Percentage change in flow rate for each LTR velocity with the change in length of LB from 5 to 7.5m (%) | | |
| 1-13 | 1m | -2.94 | -6.33 | -5.51 |
| | 5m | -7.52 | -5.78 | -8.42 |
| | 7.5 | -7.63 | -7.70 | -11.36 |
| | 9.5m | 3.17 | 2.88 | 3.34 |
| 2-14 | 1m | -2.41 | -2.19 | -2.93 |
| | 5m | -5.38 | -5.40 | -7.14 |
| | 7.5 | -5.09 | -4.46 | -5.36 |
| | 9.5m | 5.26 | 6.71 | 6.49 |
| 3-15 | 1m | -5.22 | -6.32 | -4.80 |
| | 5m | -8.85 | -6.22 | -5.70 |
| | 7.5 | -7.18 | -6.64 | -7.31 |
| | 9.5m | 4.20 | 2.65 | 3.39 |
| 4-16 | 1m | -2.75 | -3.28 | -4.33 |
| | 5m | -7.69 | -5.66 | -5.94 |
| | 7.5 | -4.25 | -4.82 | -6.69 |
| | 9.5m | 7.04 | 8.55 | 7.27 |
| 5-17 | 1m | -11.41 | -13.90 | -11.75 |
| | 5m | -1.61 | -2.38 | -5.26 |
| | 7.5 | -6.62 | -6.91 | -7.33 |
| | 9.5m | 5.19 | 3.42 | 3.39 |
| 6-18 | 1m | -1.86 | -5.65 | -3.51 |
| | 5m | -4.56 | -8.86 | -9.79 |
| | 7.5 | -6.38 | -7.42 | -6.61 |
| | 9.5m | 6.43 | 7.60 | 6.78 |
| 7-19 | 1m | -2.30 | -1.41 | -1.40 |

| Cases | Planes | LTR velocity | | |
|-------|-------------|---|-------------|-------------|
| | | 1m/s | 1.5m/s | 2m/s |
| | | Percentage change in flow rate for each LTR velocity with the change in length of LB from 5 to 7.5m (%) | | |
| | 5m | -2.38 | -1.80 | -2.25 |
| | 7.5 | -5.11 | -3.57 | -5.47 |
| | 9.5m | 4.78 | 3.60 | 3.61 |
| | | | | |
| 8-20 | 1m | -1.62 | -5.21 | -5.19 |
| | 5m | -7.75 | -9.01 | -8.95 |
| | 7.5 | -6.77 | -5.96 | -5.76 |
| | 9.5m | 6.93 | 6.85 | 6.82 |
| 9-21 | 1m | -1.85 | -1.21 | -5.75 |
| | 5m | -1.62 | -1.80 | -3.37 |
| | 7.5 | -4.05 | -3.53 | -8.83 |
| | 9.5m | 3.51 | 4.11 | 3.45 |
| 10-22 | 1m | -4.48 | -7.11 | -7.70 |
| | 5m | -7.17 | -11.12 | -10.75 |
| | 7.5 | -6.40 | -7.60 | -6.72 |
| | 9.5m | 6.60 | 7.53 | 5.64 |
| 11-23 | 1m | -6.42 | -3.91 | -1.94 |
| | 5m | -4.82 | -2.24 | -1.38 |
| | 7.5 | -4.78 | -2.70 | -1.90 |
| | 9.5m | 4.16 | 3.53 | 3.39 |
| 12-24 | 1m | -3.24 | -1.27 | -1.46 |
| | 5m | -6.77 | -6.42 | -7.27 |
| | 7.5 | -5.42 | -4.43 | -4.41 |
| | 9.5m | 5.89 | 7.48 | 7.02 |

Table G2 Percentage change in flow rate for each LTR velocity with the change in the length of LB in the heading from 5 to 7.5m (1/2 to 3/4 the length of the heading) - 6.6 x 4 x 10m heading

| Cases | Planes | LTR velocity | | |
|-------|-------------|---|-------------|-------------|
| | | 1m/s | 1.5m/s | 2m/s |
| | | Percentage change in flow rate for each LTR velocity with the change in length of LB from 5 to 7.5m (%) | | |
| 49-61 | 1m | -7.10 | -7.47 | -5.95 |
| | 5m | -7.04 | -6.87 | -9.32 |
| | 7.5 | -5.03 | -8.65 | -8.15 |
| | 9.5m | 3.15 | 4.50 | 2.70 |
| 50-62 | 1m | -2.21 | -2.36 | -4.55 |
| | 5m | -5.85 | -7.96 | -9.23 |
| | 7.5 | -6.26 | -7.23 | -6.22 |
| | 9.5m | 7.66 | 5.88 | 5.87 |
| 51-63 | 1m | -7.39 | -6.68 | -8.49 |
| | 5m | -8.71 | -8.78 | -10.32 |
| | 7.5 | -11.86 | -11.69 | -12.45 |
| | 9.5m | 2.93 | 2.79 | 3.80 |
| 52-64 | 1m | -2.66 | -4.69 | -5.30 |
| | 5m | -6.33 | -9.25 | -9.88 |
| | 7.5 | -6.05 | -8.16 | -7.48 |
| | 9.5m | 5.67 | 7.77 | 6.99 |
| 53-65 | 1m | -10.74 | -13.02 | -11.11 |
| | 5m | -2.81 | -5.56 | -7.31 |
| | 7.5 | -6.52 | -8.31 | -10.36 |
| | 9.5m | 3.84 | 4.71 | 4.37 |
| 54-66 | 1m | -3.24 | -5.07 | -4.85 |
| | 5m | -7.99 | -10.23 | -11.58 |
| | 7.5 | -8.21 | -8.80 | -8.16 |
| | 9.5m | 5.37 | 7.63 | 6.51 |
| 55-67 | 1m | -2.47 | -2.07 | -2.80 |
| | 5m | -2.74 | -1.91 | -3.87 |
| | 7.5 | -3.71 | -2.65 | -8.86 |

| Cases | Planes | LTR velocity | | |
|-------|-------------|---|-------------|-------------|
| | | 1m/s | 1.5m/s | 2m/s |
| | | Percentage change in flow rate for each LTR velocity with the change in length of LB from 5 to 7.5m (%) | | |
| | 9.5m | 4.25 | 2.77 | 4.10 |
| 56-68 | 1m | -4.63 | -5.29 | -4.65 |
| | 5m | -10.18 | -10.87 | -10.11 |
| | 7.5 | -8.20 | -8.00 | -7.67 |
| | 9.5m | 6.93 | 5.89 | 6.35 |
| 57-69 | 1m | -4.09 | -5.57 | -7.54 |
| | 5m | -1.67 | -3.91 | -3.58 |
| | 7.5 | -4.87 | -9.72 | -5.75 |
| | 9.5m | 4.15 | 3.54 | 4.08 |
| 58-70 | 1m | -6.60 | -7.93 | -6.23 |
| | 5m | -9.60 | -12.17 | -11.42 |
| | 7.5 | -9.70 | -9.82 | -8.78 |
| | 9.5m | 7.62 | 6.69 | 7.84 |
| 59-71 | 1m | -7.01 | -5.35 | -1.67 |
| | 5m | -3.36 | -1.91 | -1.13 |
| | 7.5 | -2.22 | -2.14 | -1.48 |
| | 9.5m | 2.98 | 3.50 | 3.43 |
| 60-72 | 1m | -4.04 | -3.38 | -3.48 |
| | 5m | -8.61 | -8.64 | -8.80 |
| | 7.5 | -7.84 | -7.60 | -7.34 |
| | 9.5m | 6.18 | 6.64 | 6.38 |

Table G3 Percentage change in flow rate for each LTR velocity with the change in the length of LB in the heading from 10 to 15m (1/2 to 3/4 the length of the heading) - 6.6 x 3 x 20m heading

| Cases | Planes | LTR velocity | | |
|-------|--------------|---|-------------|-------------|
| | | 1m/s | 1.5m/s | 2m/s |
| | | Percentage change in flow rate for each LTR velocity with the change in length of LB from 10 to 15m (%) | | |
| 25-37 | 1m | -6.66 | -4.89 | -7.34 |
| | 10m | -2.04 | -2.23 | -2.58 |
| | 15m | -5.27 | -3.63 | -3.97 |
| | 19.5m | 2.55 | 3.01 | 2.40 |
| 26-38 | 1m | -4.29 | -3.71 | -2.35 |
| | 10m | -6.91 | -5.72 | -4.42 |
| | 15m | -6.25 | -5.99 | -8.59 |
| | 19.5m | 6.28 | 4.71 | 4.68 |
| 27-39 | 1m | -8.06 | -8.15 | -7.20 |
| | 10m | -4.02 | -5.47 | -2.87 |
| | 15m | -5.05 | -5.10 | -5.19 |
| | 19.5m | 3.52 | 2.43 | 2.69 |
| 28-40 | 1m | -5.46 | -5.36 | -3.83 |
| | 10m | -6.98 | -5.91 | -5.70 |
| | 15m | -8.46 | -7.73 | -10.10 |
| | 19.5m | 4.92 | 6.17 | 4.79 |
| 29-41 | 1m | -11.49 | -8.11 | -8.17 |
| | 10m | -4.90 | -3.76 | -2.43 |
| | 15m | -2.51 | -4.60 | -3.06 |
| | 19.5m | 4.02 | 4.86 | 2.95 |
| 30-42 | 1m | -4.88 | -6.48 | -4.39 |
| | 10m | -2.49 | -3.28 | -3.78 |
| | 15m | -7.33 | -5.54 | -6.51 |
| | 19.5m | 4.55 | 4.18 | 5.52 |
| 31-43 | 1m | -7.08 | -6.05 | -4.85 |
| | 10m | -5.03 | -4.53 | -4.29 |
| | 15m | -6.36 | -4.55 | -4.65 |
| | 19.5m | 2.75 | 2.90 | 3.09 |
| 32-44 | 1m | -2.02 | -3.13 | -2.44 |
| | 10m | -3.94 | -3.50 | -3.20 |
| | 15m | -7.78 | -8.01 | -7.03 |
| | 19.5m | 2.66 | 5.23 | 5.44 |

| Cases | Planes | LTR velocity | | |
|-------|--------------|---|-------------|-------------|
| | | 1m/s | 1.5m/s | 2m/s |
| | | Percentage change in flow rate for each LTR velocity with the change in length of LB from 10 to 15m (%) | | |
| 33-45 | 1m | -2.77 | -3.42 | -2.53 |
| | 10m | -6.97 | -7.19 | -6.02 |
| | 15m | -3.30 | -5.53 | -4.51 |
| | 19.5m | 2.63 | 2.15 | 2.69 |
| 34-46 | 1m | -3.25 | -4.39 | -4.58 |
| | 10m | -5.51 | -6.11 | -5.97 |
| | 15m | -5.71 | -5.35 | -6.76 |
| | 19.5m | 6.12 | 5.27 | 4.48 |
| 35-47 | 1m | -3.73 | -4.54 | -3.93 |
| | 10m | -5.62 | -5.22 | -4.18 |
| | 15m | -4.53 | -4.27 | -4.95 |
| | 19.5m | 4.41 | 3.62 | 3.31 |
| 36-48 | 1m | -2.47 | -4.07 | -2.07 |
| | 10m | -4.58 | -2.71 | -4.09 |
| | 15m | -6.01 | -6.30 | -4.41 |
| | 19.5m | 2.71 | 4.34 | 4.18 |

Table G4 Percentage flow rate change for each LTR velocity with the change in the length of LB in the heading from 10 to 15m (1/2 to 3/4 the length of the heading) - 6.6 x 4 x 20m heading

| Cases | Planes | LTR velocity | | |
|-------|--------------|--|-------------|-------------|
| | | 1m/s | 1.5m/s | 2m/s |
| | | Percentage flow rate change for each LTR velocity with the change in length of LB from 10 to 15m (%) | | |
| 73-85 | 1m | -8.32 | -6.64 | -7.19 |
| | 10m | -4.20 | -1.64 | -3.01 |
| | 15m | -4.29 | -3.83 | -3.83 |
| | 19.5m | 3.29 | 3.82 | 3.23 |
| 74-86 | 1m | -4.96 | -5.30 | -3.54 |
| | 10m | -6.55 | -5.19 | -5.40 |
| | 15m | -6.89 | -8.31 | -9.00 |
| | 19.5m | 6.61 | 6.20 | 5.46 |
| 75-87 | 1m | -7.68 | -7.90 | -9.56 |
| | 10m | -4.38 | -4.90 | -5.72 |
| | 15m | -5.06 | -6.16 | -5.72 |
| | 19.5m | 2.96 | 3.35 | 4.33 |
| 76-88 | 1m | -5.01 | -2.56 | -3.51 |
| | 10m | -6.33 | -5.63 | -6.37 |
| | 15m | -7.73 | -8.52 | -9.86 |
| | 19.5m | 5.34 | 6.88 | 5.04 |
| 77-89 | 1m | -11.02 | -11.90 | -10.02 |
| | 10m | -4.88 | -3.54 | -6.23 |
| | 15m | -2.03 | -5.41 | -5.24 |
| | 19.5m | 3.03 | 3.65 | 2.64 |
| 78-90 | 1m | -3.76 | -2.39 | -3.32 |
| | 10m | -3.07 | -3.33 | -4.12 |
| | 15m | -10.72 | -8.00 | -9.36 |
| | 19.5m | 6.29 | 5.58 | 5.44 |
| 79-91 | 1m | -8.81 | -5.42 | -5.86 |
| | 10m | -7.19 | -6.20 | -6.02 |
| | 15m | -2.50 | -2.18 | -1.09 |
| | 19.5m | 3.09 | 2.30 | 3.09 |
| 80-92 | 1m | -3.05 | -1.48 | -2.65 |
| | 10m | -5.97 | -3.10 | -2.24 |
| | 15m | -8.10 | -9.47 | -6.95 |
| | 19.5m | 5.41 | 3.47 | 4.49 |

| Cases | Planes | LTR velocity | | |
|-------|--------------|---|-------------|-------------|
| | | 1m/s | 1.5m/s | 2m/s |
| | | Percentage flow rate change for each LTR velocity with the change in length of LB from 10 to15m (%) | | |
| 81-93 | 1m | -9.14 | -8.66 | -7.45 |
| | 10m | -5.26 | -5.48 | -5.60 |
| | 15m | -2.59 | -7.01 | -5.86 |
| | 19.5m | 3.45 | 3.33 | 4.20 |
| 82-94 | 1m | -2.13 | -3.00 | -3.78 |
| | 10m | -6.49 | -7.25 | -7.55 |
| | 15m | -6.36 | -7.61 | -6.87 |
| | 19.5m | 4.96 | 5.94 | 4.96 |
| 83-95 | 1m | -4.71 | -5.09 | -5.79 |
| | 10m | -5.49 | -5.99 | -5.04 |
| | 15m | -2.71 | -4.55 | -5.62 |
| | 19.5m | 3.31 | 3.50 | 3.66 |
| 84-96 | 1m | -5.06 | -5.53 | -5.65 |
| | 10m | -2.51 | -2.45 | -3.20 |
| | 15m | -6.03 | -5.70 | -7.01 |
| | 19.5m | 4.88 | 5.04 | 3.79 |

APPENDIX H

**EFFECT OF LENGTH OF LB INSIDE HEADING ON FLOW RATE CLOSE TO
FACE**

Table H1 Percentage increase in flow rate for each LTR velocity with the increase in the length of LB in the heading from 5 to 7.5m - 6.6 x 4 x 10m heading

| Cases | Planes | LTR velocity | | |
|----------------|--------|---|-------------|-------------|
| | | 1m/s | 1.5m/s | 2m/s |
| | | Percentage increase in flow rate for each LTR velocity with the increase in length of LB from 5 to 7.5m (%) | | |
| 49-61 | 9.5m | 3.15 | 4.50 | 2.70 |
| 50-62 | | 7.66 | 5.88 | 5.87 |
| 51-63 | | 2.93 | 2.79 | 3.80 |
| 52-64 | | 5.67 | 7.77 | 6.99 |
| 53-65 | | 3.84 | 4.71 | 4.37 |
| 54-66 | | 5.37 | 7.63 | 6.51 |
| 55-67 | | 4.25 | 2.77 | 4.10 |
| 56-68 | | 6.93 | 5.89 | 6.35 |
| 57-69 | | 4.15 | 3.54 | 4.08 |
| 58-70 | | 7.62 | 6.69 | 7.84 |
| 59-71 | | 2.98 | 3.50 | 3.43 |
| 60-72 | | 6.18 | 6.64 | 6.38 |
| Average | | 5.06 | 5.19 | 5.20 |

Table H2 Percentage increase in flow rate for each LTR velocity with the increase in the length of LB in the heading from 10 to 15m - 6.6 x 3 x 20m heading

| Cases | Planes | LTR velocity | | |
|----------------|--------|--|-------------|-------------|
| | | 1m/s | 1.5m/s | 2m/s |
| | | Percentage increase flow rate for each LTR velocity with the increase in length of LB from 10 to 15m (%) | | |
| 25-37 | 19.5m | 2.55 | 3.01 | 2.40 |
| 26-38 | | 6.28 | 4.71 | 4.68 |
| 27-39 | | 3.52 | 2.43 | 2.69 |
| 28-40 | | 4.92 | 6.17 | 4.79 |
| 29-41 | | 4.02 | 4.86 | 2.95 |
| 30-42 | | 4.55 | 4.18 | 5.52 |
| 31-43 | | 2.75 | 2.90 | 3.09 |
| 32-44 | | 2.66 | 5.23 | 5.44 |
| 33-45 | | 2.63 | 2.15 | 2.69 |
| 34-46 | | 6.12 | 5.27 | 4.48 |
| 35-47 | | 4.41 | 3.62 | 3.31 |
| 36-48 | | 2.71 | 4.34 | 4.18 |
| Average | | | 3.93 | 4.07 |

Table H3 Percentage increase in flow rate for each LTR velocity with the increase in the length of LB in the heading from 10 to 15m - 6.6 x 4 x 20m heading

| Cases | Planes | LTR velocity | | |
|----------------|--------|--|-------------|-------------|
| | | 1m/s | 1.5m/s | 2m/s |
| | | Percentage increase flow rate for each LTR velocity with the increase in length of LB from 10 to 15m (%) | | |
| 73-85 | 19.5m | 3.29 | 3.82 | 3.23 |
| 74-86 | | 6.61 | 6.20 | 5.46 |
| 75-87 | | 2.96 | 3.35 | 4.33 |
| 76-88 | | 5.34 | 6.88 | 5.04 |
| 77-89 | | 3.03 | 3.65 | 2.64 |
| 78-90 | | 6.29 | 5.58 | 5.44 |
| 79-91 | | 3.09 | 2.30 | 3.09 |
| 80-92 | | 5.41 | 3.47 | 4.49 |
| 81-93 | | 3.45 | 3.33 | 4.20 |
| 82-94 | | 4.96 | 5.94 | 4.96 |
| 83-95 | | 3.31 | 3.50 | 3.66 |
| 84-96 | | 4.88 | 5.04 | 3.79 |
| Average | | | 4.38 | 4.42 |

EFFECT OF LENGTH OF LB INSIDE HEADING ON FLOW RATE CLOSE TO FACE

- Flow rates at 9.5m deep planes using 5m and 7.5m LB inside the heading for LTR velocities of 1m/s, 1.5m/s, 2m/s - 6.6 x 4 x 10m heading

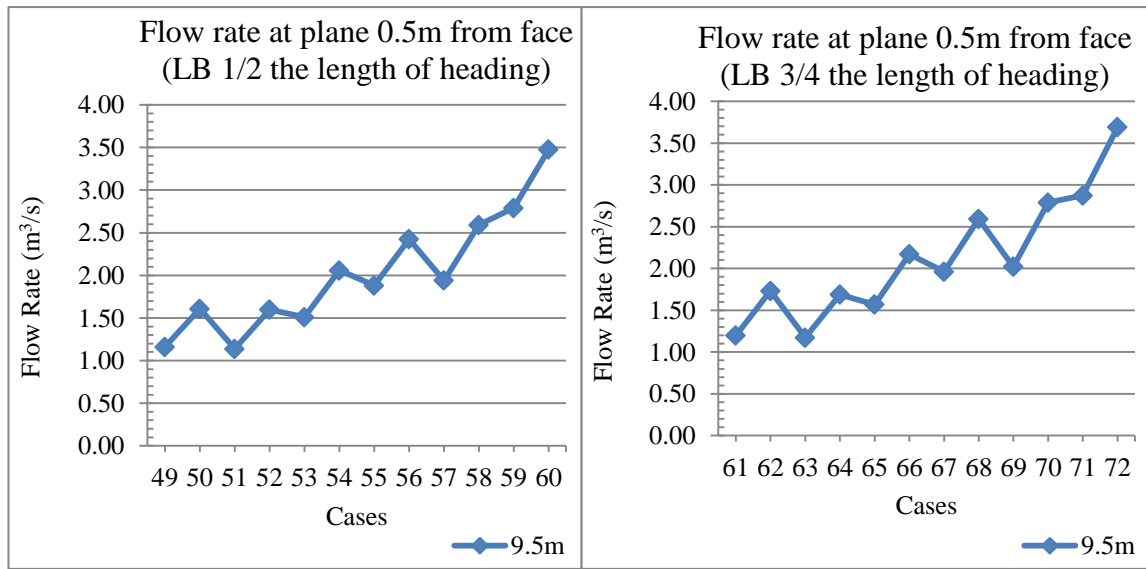


Figure I1 Flow rates at 9.5m deep planes using 5m and 7.5m LB inside the heading for LTR velocity of 1m/s

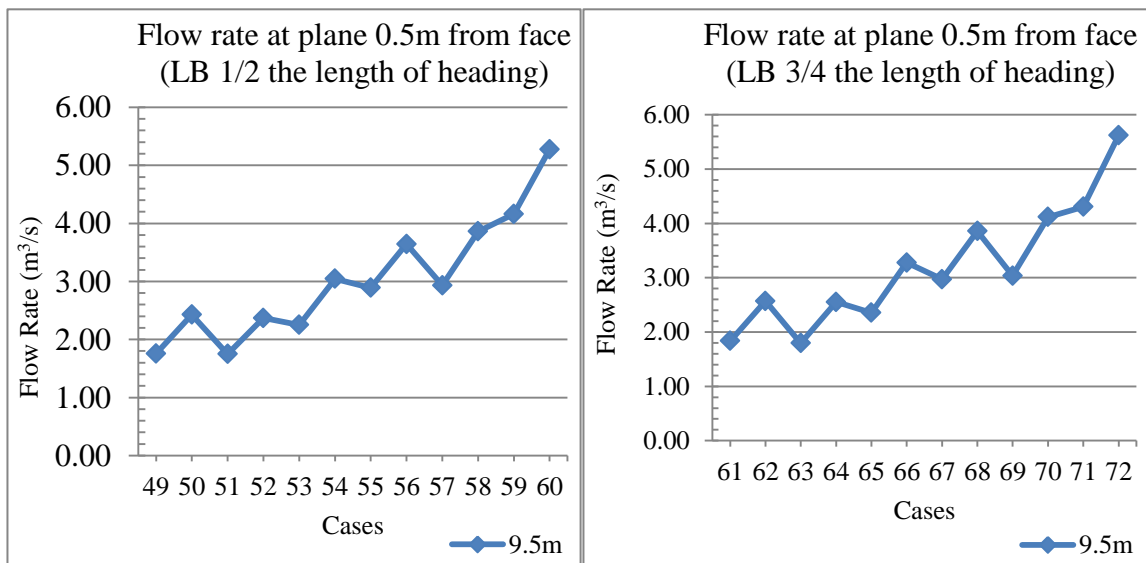


Figure I2 Flow rates at 9.5m deep planes using 5m and 7.5m LB inside the heading for LTR velocity of 1.5m/s

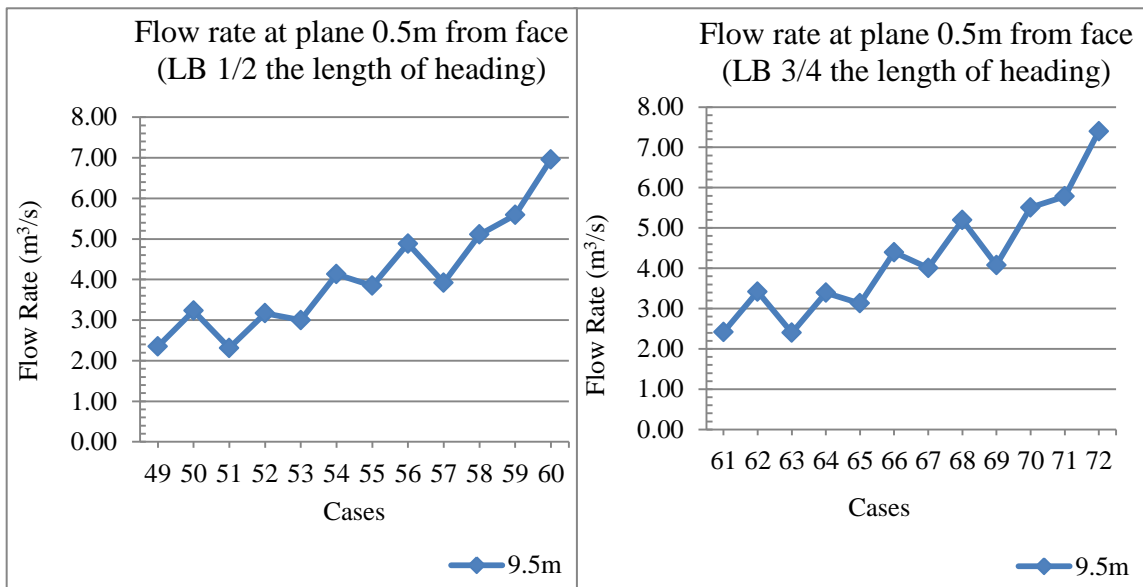


Figure I3 Flow rates at 9.5m deep planes using 5m and 7.5m LB inside the heading for LTR velocity of 2m/s

- Flow rates at 19.5m deep planes using 10m and 15m LB inside the heading for LTR velocities of 1m/s, 1.5m/s, 2m/s - 6.6 x 3 x 20m heading

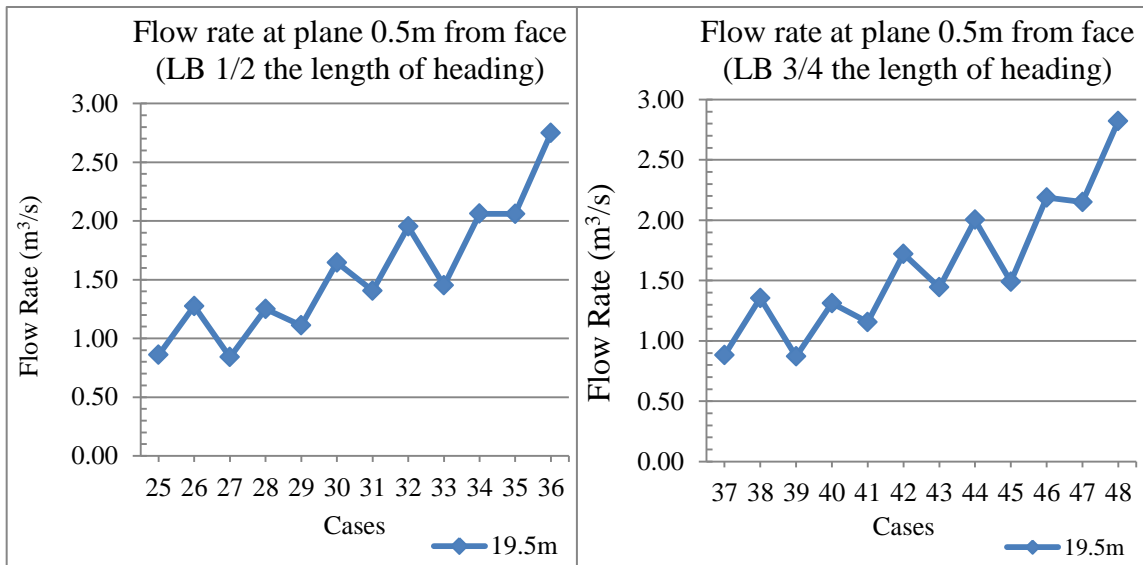


Figure I4 Flow rates at 19.5m deep planes using 10m and 15m LB inside the heading for LTR velocity of 1m/s

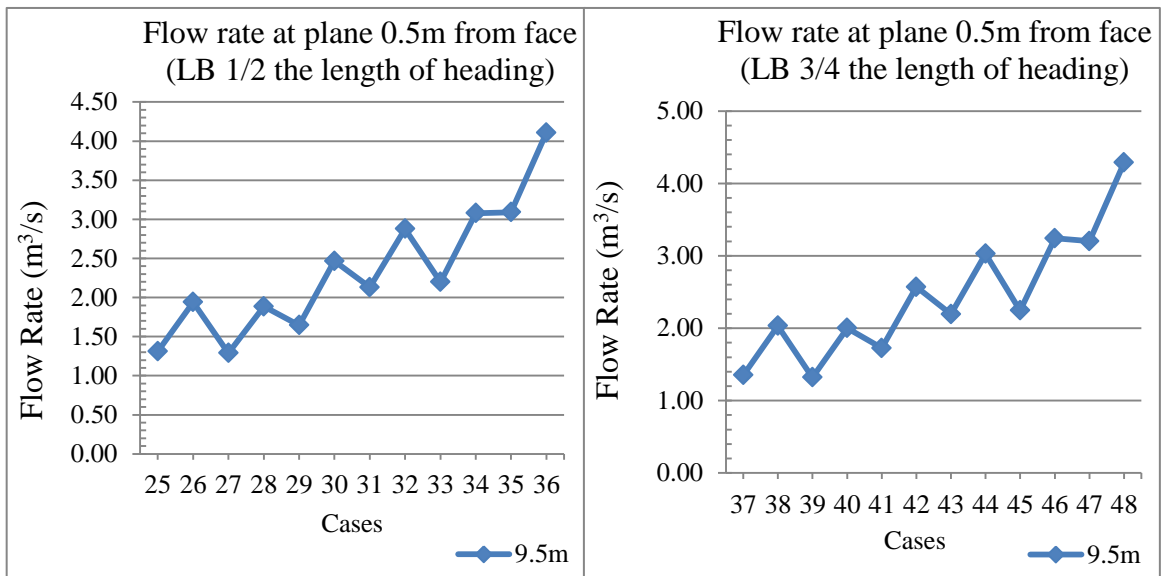


Figure I5 Flow rates at 19.5m deep planes using 10m and 15m LB inside the heading for LTR velocity of 1.5m/s

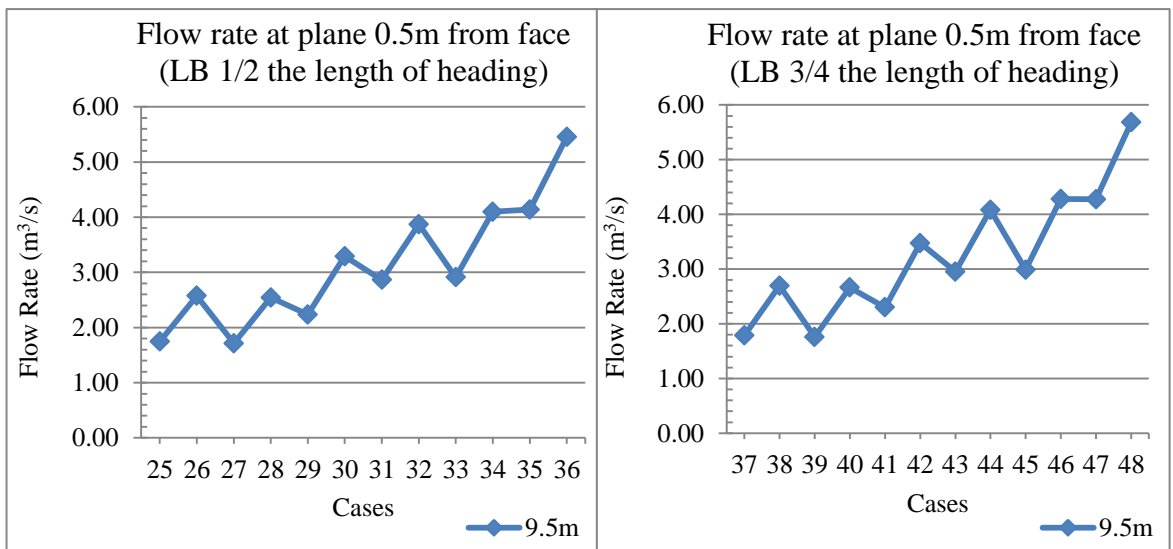


Figure I6 Flow rates at 19.5m deep planes using 10m and 15m LB inside the heading for LTR velocity of 2m/s

- Flow rates at 19.5m deep planes using 10m and 15m LB inside the heading for LTR velocities of 1m/s, 1.5m/s, 2m/s - 6.6 x 4 x 20m heading

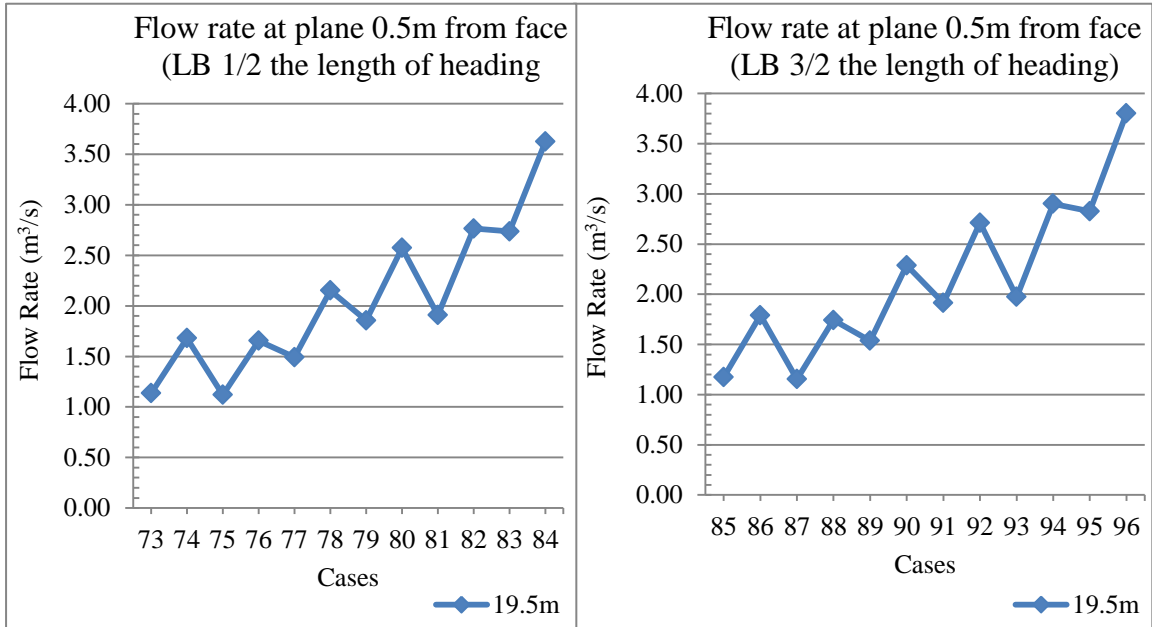


Figure I7 Flow rates at 19.5m deep planes using 10m and 15m LB inside the heading for LTR velocity of 1m/s

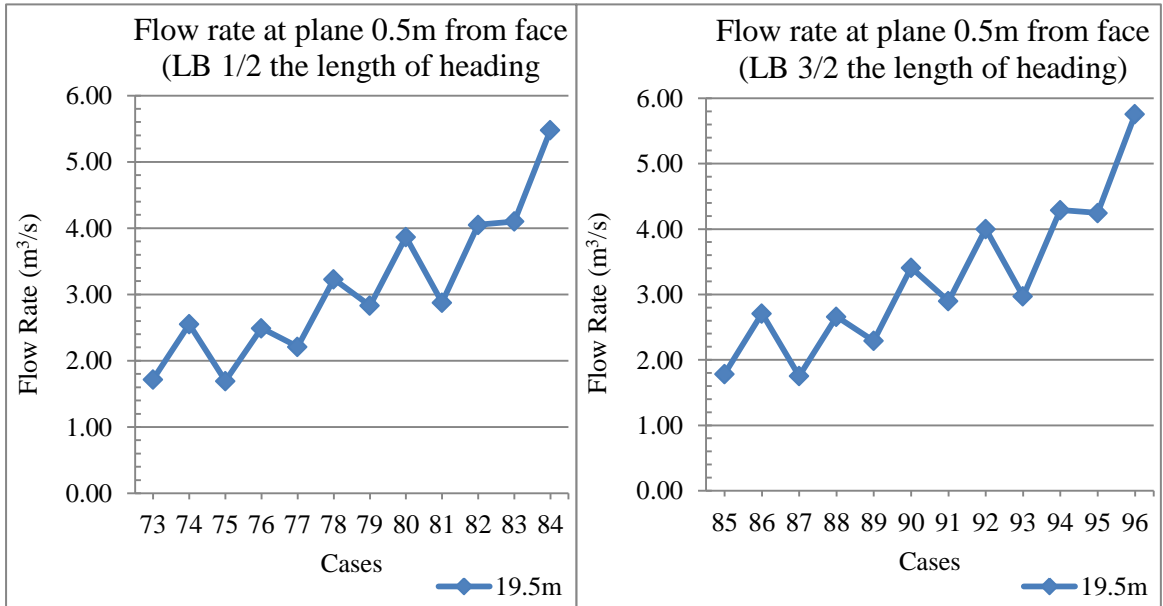


Figure I8 Flow rates at 19.5m deep planes using 10m and 15m LB inside the heading for LTR velocity of 1.5m/s

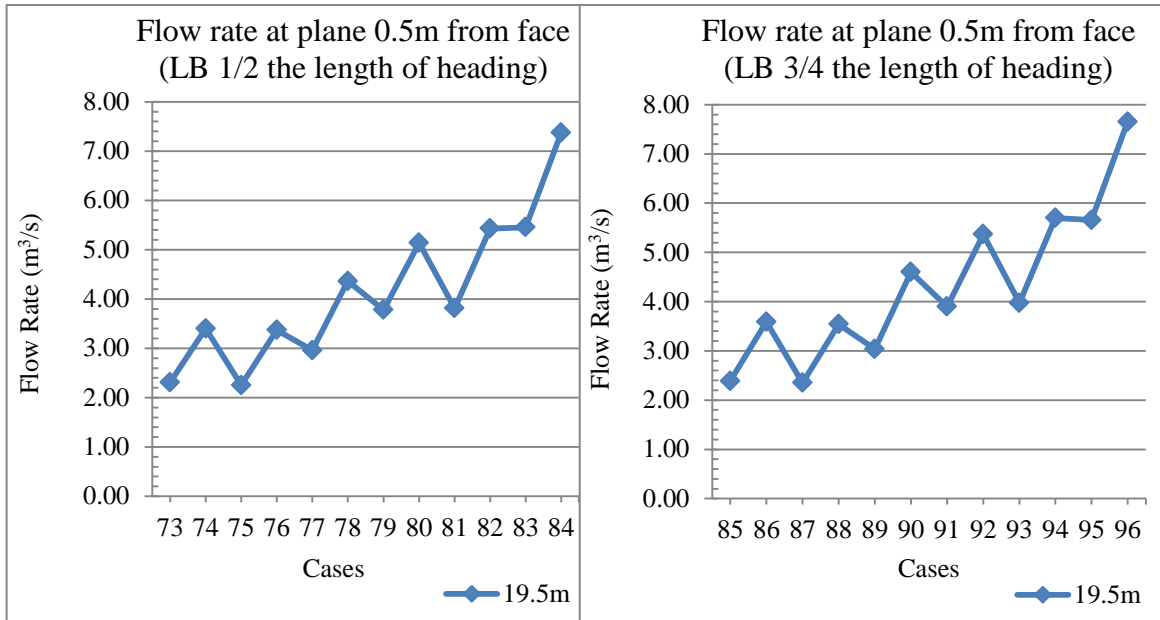


Figure I9 Figure I9 Flow rates at 19.5m deep planes using 10m and 15m LB inside the heading for LTR velocity of 2m/s

EFFECT OF LENGTH OF LB INSIDE HEADING ON FLOW RATES

- Flow rates at specified planes using 5m and 7.5m LB inside the heading for LTR velocities of 1m/s, 1.5m/s, 2m/s - 6.6 x 4 x 10m heading

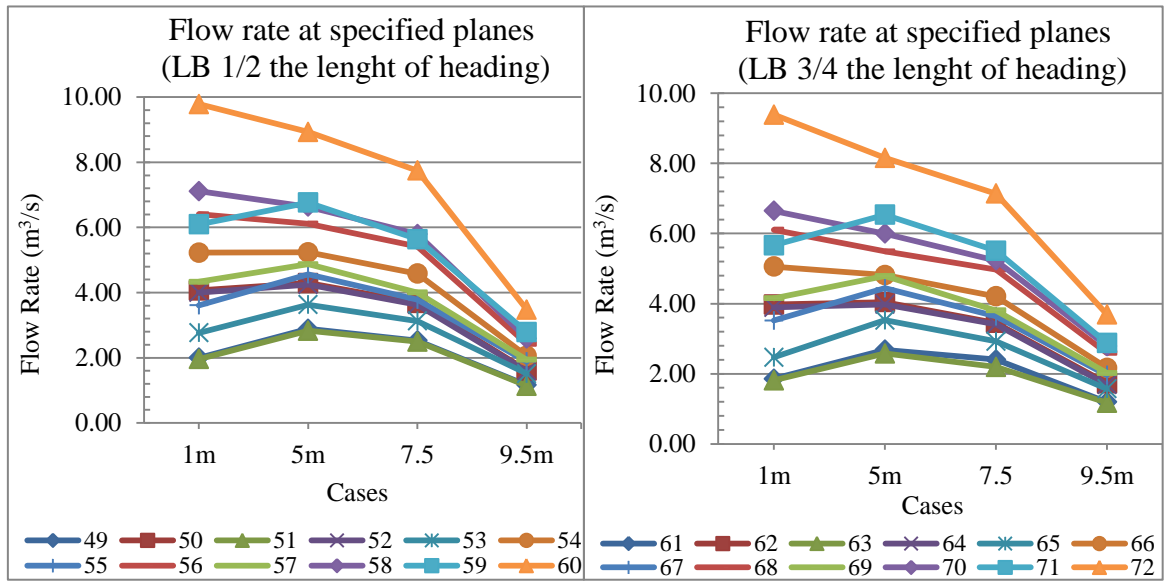


Figure J1 Flow rates at specified planes using 5m and 7.5m LB inside the heading for LTR velocity of 1m/s

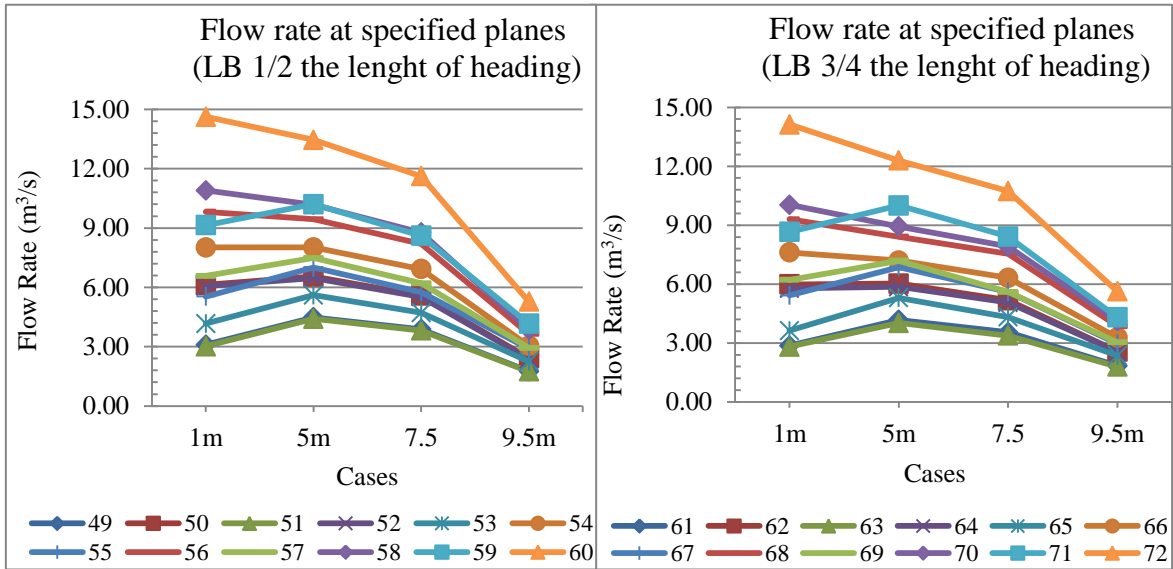


Figure J2 Flow rates at specified planes using 5m and 7.5m LB inside the heading for LTR velocity of 1.5m/s

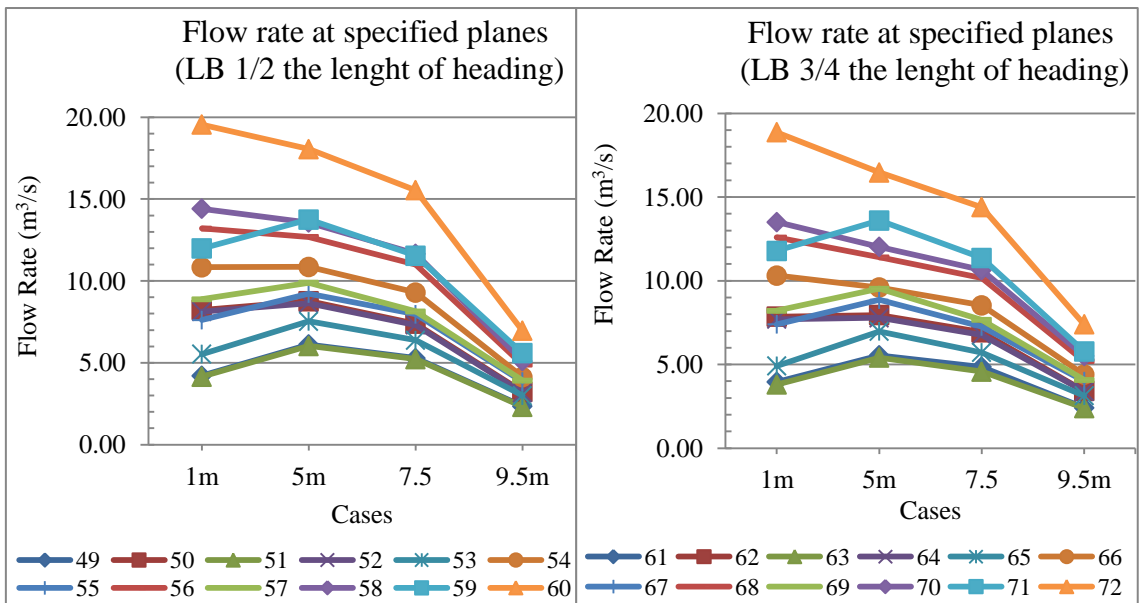


Figure J3 Flow rates at specified planes using 5m and 7.5m LB inside the heading for LTR velocity of 2m/s

- Flow rates at specified planes using 10m and 15m LB inside the heading for LTR velocities of 1m/s, 1.5m/s, 2m/s - 6.6 x 3 x 20m heading

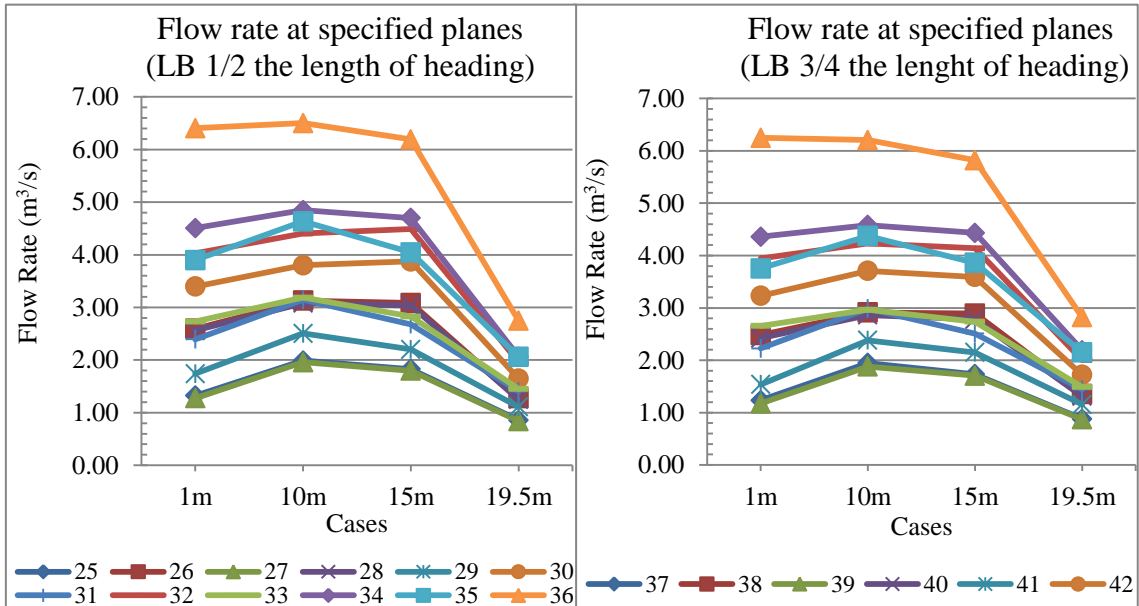


Figure J4 Flow rates at specified planes using 10m and 15m LB inside the heading for LTR velocity of 1m/s

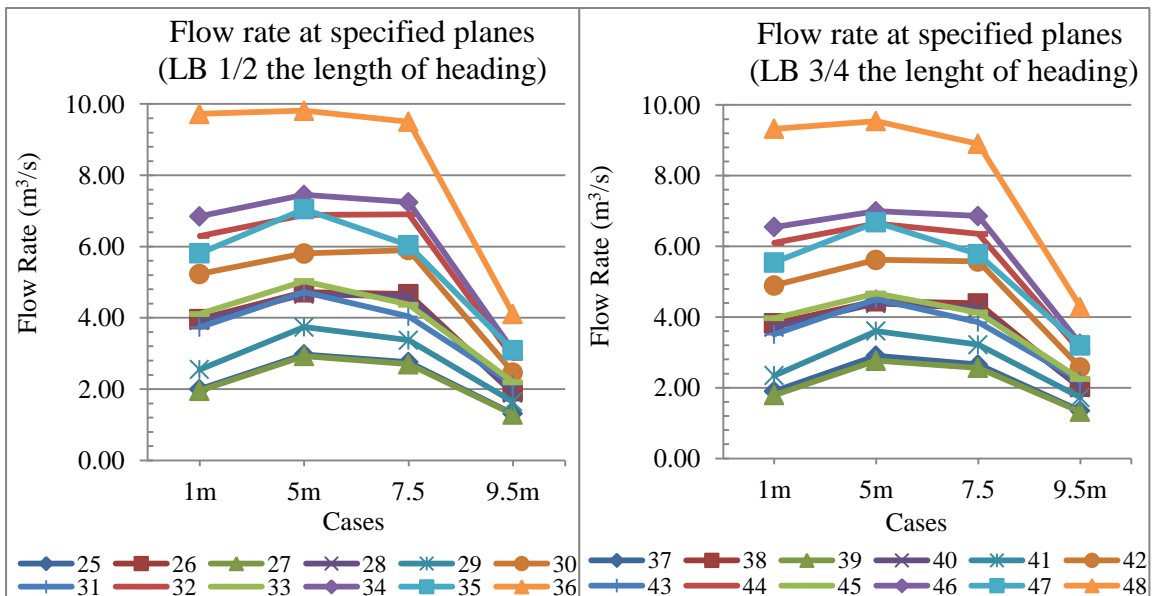


Figure J5 Flow rates at specified planes using 10m and 15m LB inside the heading for LTR velocity of 1.5m/s

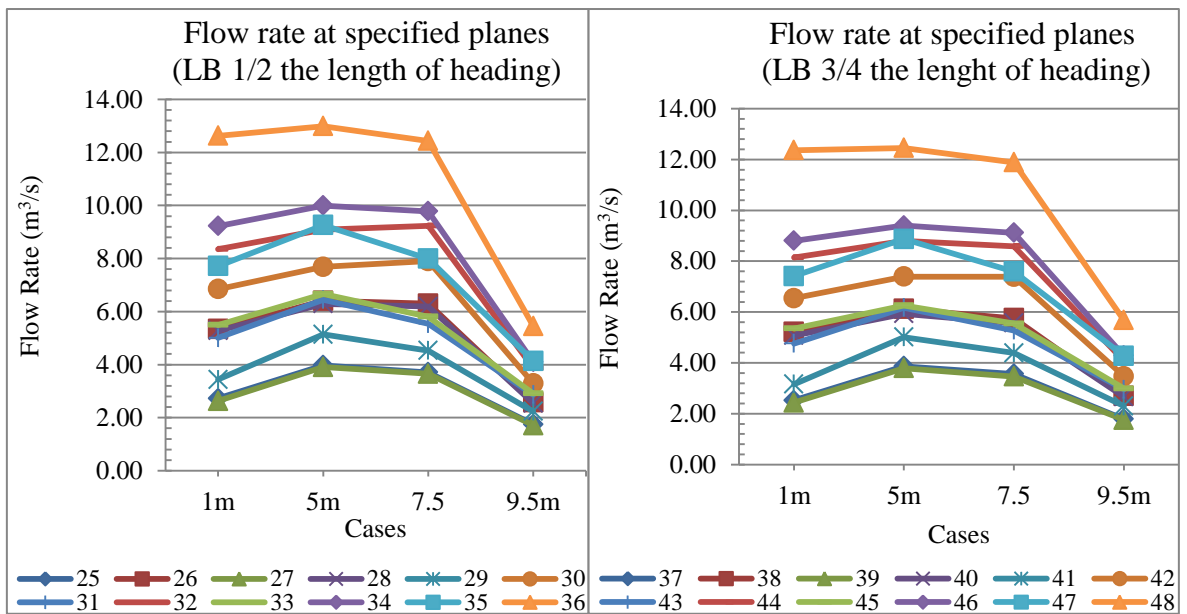


Figure J6 Flow rates at specified planes using 10m and 15m LB inside the heading for LTR velocity of 2m/s

- Flow rates at specified planes using 10m and 15m LB inside the heading for LTR velocities of 1m/s, 1.5m/s, 2m/s - 6.6 x 4 x 20m heading

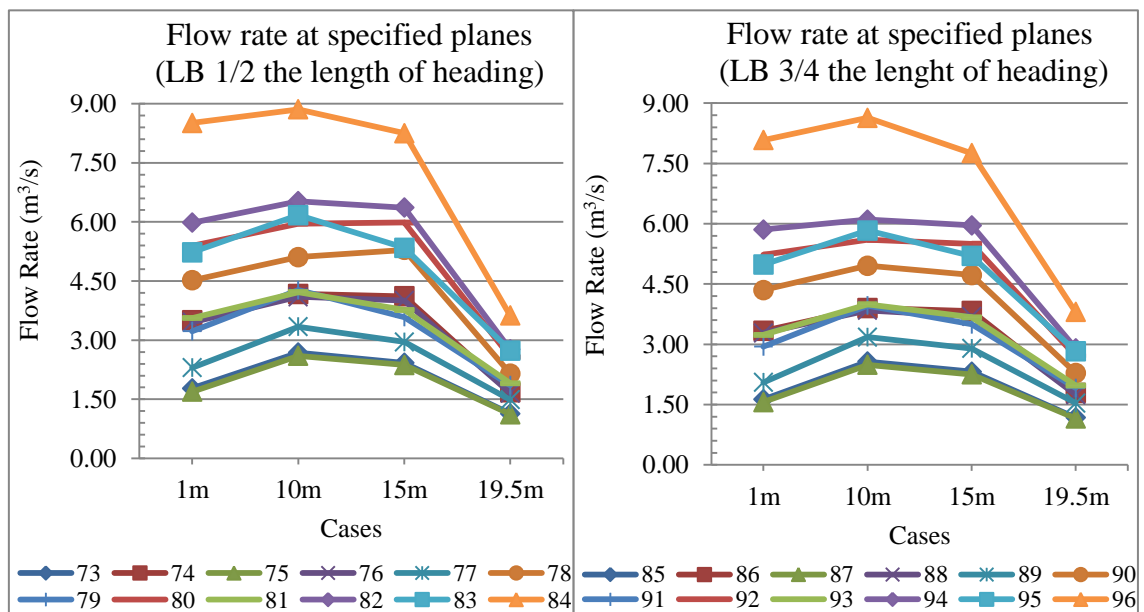


Figure J7 Flow rates at specified planes using 10m and 15m LB inside the heading for LTR velocity of 1m/s

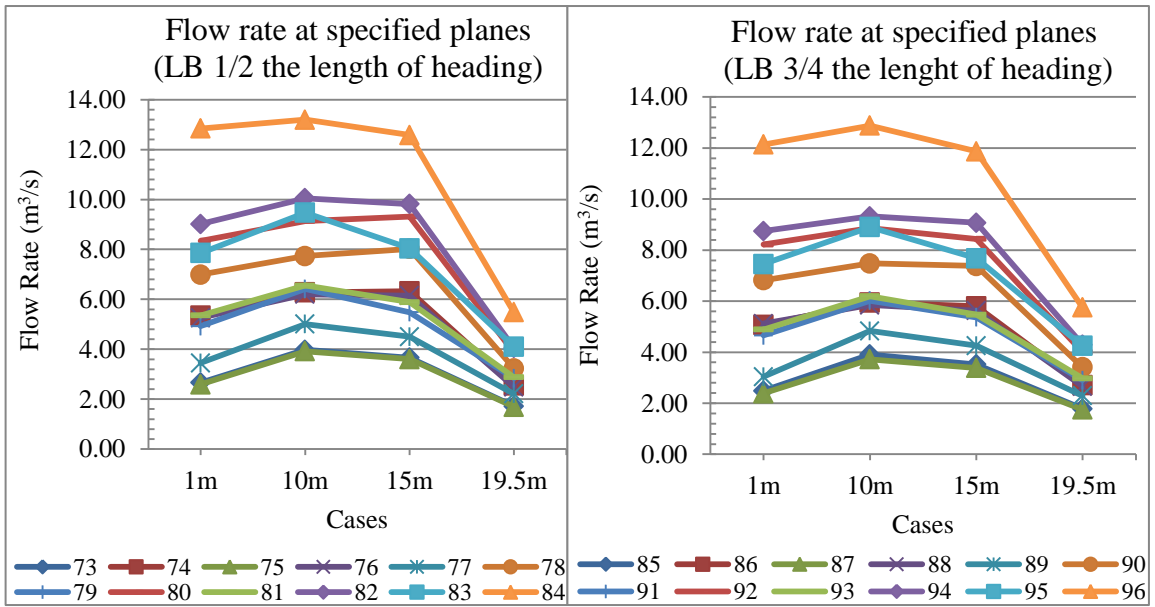


Figure J8 Flow rates at specified planes using 10m and 15m LB inside the heading for LTR velocity of 1.5m/s

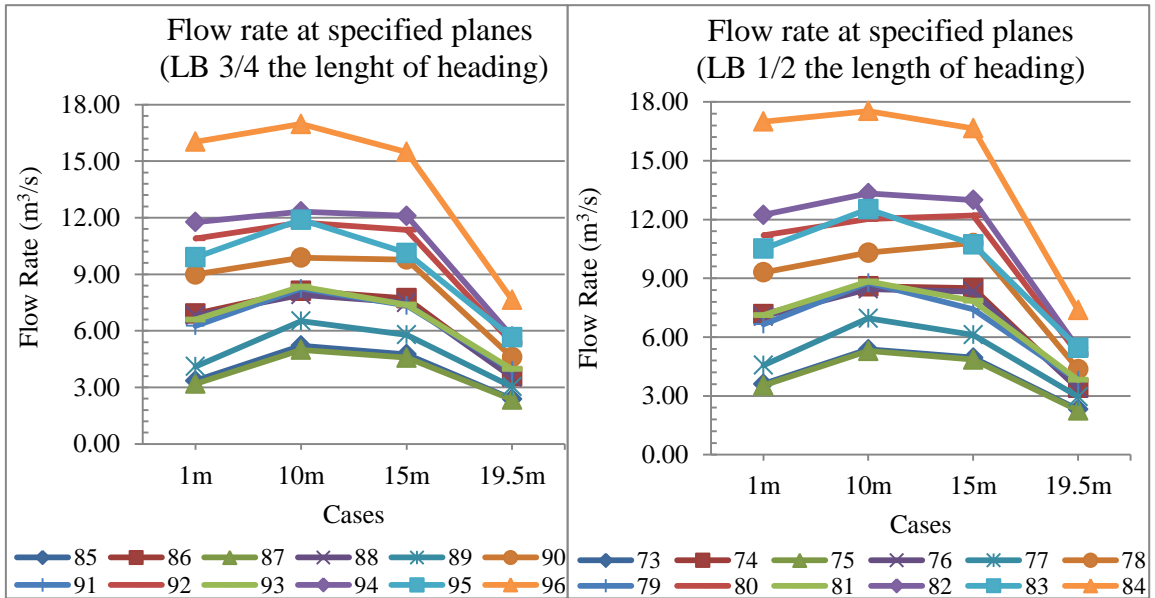


Figure J9 Flow rates at specified planes using 10m and 15m LB inside the heading for LTR velocity of 2m/s

APPENDIX K

**EFFECT OF LB LENGTH INSIDE HEADING FOR EACH WALL DISTANCE
ON FLOW RATES CLOSE TO FACE**

Table K1 Percentage increase in flow rate for each LTR velocity with the increase in length of LB in the heading from 5 to 7.5m, separately for 0.5 and 1m distance of the LB from wall in the heading - 6.6 x 4 x 10m heading

| Cases | Planes | LTR Velocity | | | Cases | Planes | LTR Velocity | | |
|------------------------------------|--------|---|-------------|-------------|------------------------------------|--------|---|-------------|-------------|
| | | 1m/s | 1.5m/s | 2m/s | | | 1m/s | 1.5m/s | 2m/s |
| | | Percentage increase in flow rate for each LTR velocity with the increase in length of LB from 5 to 7.5m (%) | | | | | Percentage increase in flow rate for each LTR velocity with the increase in length of LB from 5 to 7.5m (%) | | |
| 49-61 | 9.5m | 3.15 | 4.50 | 2.70 | 50-62 | 9.5m | 7.66 | 5.88 | 5.87 |
| 51-63 | | 2.93 | 2.79 | 3.80 | 52-64 | | 5.67 | 7.77 | 6.99 |
| 53-65 | | 3.84 | 4.71 | 4.37 | 54-66 | | 5.37 | 7.63 | 6.51 |
| 55-67 | | 4.25 | 2.77 | 4.10 | 56-68 | | 6.93 | 5.89 | 6.35 |
| 57-69 | | 4.15 | 3.54 | 4.08 | 58-70 | | 7.62 | 6.69 | 7.84 |
| 59-71 | | 2.98 | 3.50 | 3.43 | 60-72 | | 6.18 | 6.64 | 6.38 |
| Average percentage increase | | 3.55 | 3.63 | 3.74 | Average percentage increase | | 6.57 | 6.75 | 6.66 |

Table K2 Percentage increase in flow rate for each LTR velocity with the increase in length of LB in the heading from 10 to 15m, separately for 0.5 and 1m distance of the LB from wall in the heading - 6.6 x 3 x 20m heading

| Cases | Planes | LTR Velocity | | | Cases | Planes | LTR Velocity | | |
|------------------------------------|--------|---|-------------|-------------|------------------------------------|--------|---|-------------|-------------|
| | | 1m/s | 1.5m/s | 2m/s | | | 1m/s | 1.5m/s | 2m/s |
| | | Percentage increase in flow rate for each LTR velocity with the increase in length of LB from 10 to 15m (%) | | | | | Percentage increase in flow rate for each LTR velocity with the increase in length of LB from 10 to 15m (%) | | |
| 25-37 | 19.5m | 2.55 | 3.01 | 2.40 | 26-38 | 19.5m | 6.28 | 4.71 | 4.68 |
| 27-39 | | 3.52 | 2.43 | 2.69 | 28-40 | | 4.92 | 6.17 | 4.79 |
| 29-41 | | 4.02 | 4.86 | 2.95 | 30-42 | | 4.55 | 4.18 | 5.52 |
| 31-43 | | 2.75 | 2.90 | 3.09 | 32-44 | | 2.66 | 5.23 | 5.44 |
| 33-45 | | 2.63 | 2.15 | 2.69 | 34-46 | | 6.12 | 5.27 | 4.48 |
| 35-47 | | 4.41 | 3.62 | 3.31 | 36-48 | | 2.71 | 4.34 | 4.18 |
| Average percentage increase | | 4.17 | 3.36 | 3.43 | Average percentage increase | | 4.54 | 4.98 | 4.85 |

Table K3 Percentage increase in flow rate for each LTR velocity with the increase in length of LB in the heading from 10 to 15m, separately for 0.5 and 1m distance of the LB from wall in the heading - 6.6 x 4 x 20m heading

| Cases | Planes | LTR Velocity | | | Cases | Planes | LTR Velocity | | |
|------------------------------------|--------|---|-------------|-------------|------------------------------------|--------|---|-------------|-------------|
| | | 1m/s | 1.5m/s | 2m/s | | | 1m/s | 1.5m/s | 2m/s |
| | | Percentage increase in flow rate for each LTR velocity with the increase in length of LB from 10 to 15m (%) | | | | | Percentage increase in flow rate for each LTR velocity with the increase in length of LB from 10 to 15m (%) | | |
| 73-85 | 19.5m | 3.29 | 3.82 | 3.23 | 74-86 | 19.5m | 6.61 | 6.20 | 5.46 |
| 75-87 | | 2.96 | 3.35 | 4.33 | 76-88 | | 5.34 | 6.88 | 5.04 |
| 77-89 | | 3.03 | 3.65 | 2.64 | 78-90 | | 6.29 | 5.58 | 5.44 |
| 79-91 | | 3.09 | 2.30 | 3.09 | 80-92 | | 5.41 | 3.47 | 4.49 |
| 81-93 | | 3.45 | 3.33 | 4.20 | 82-94 | | 4.96 | 5.94 | 4.96 |
| 83-95 | | 3.31 | 3.50 | 3.66 | 84-96 | | 4.88 | 5.04 | 3.79 |
| Average percentage increase | | 3.19 | 3.32 | 3.52 | Average percentage increase | | 5.58 | 5.52 | 4.87 |

APPENDIX L

EFFECT OF THE LENGTH OF LB INSIDE THE LTR ON FLOW RATES

Table L1 Percentage change in flow rate for each LTR velocity with the change in the length of LB in the LTR from 3 to 6m - 6.6 x 3 x 10m heading

| Cases | Planes | LTR velocity | | |
|-------|-------------|--|--------------|--------------|
| | | 1m/s | 1.5m/s | 2m/s |
| | | Percentage change in flow rate for each LTR velocity with the change in length of LB in the LTR from 3 to 6m (%) | | |
| 1-3 | 1m | -2.86 | -4.08 | -3.22 |
| | 5m | -1.32 | -3.28 | -4.64 |
| | 7.5 | -3.63 | -3.38 | -6.09 |
| | 9.5m | -2.25 | -2.00 | -1.38 |
| 2-4 | 1m | -1.76 | -1.35 | -1.59 |
| | 5m | -1.29 | -1.63 | -1.58 |
| | 7.5 | -2.19 | -1.71 | -1.67 |
| | 9.5m | -3.25 | -3.17 | -1.38 |
| 5-7 | 1m | 34.48 | 33.70 | 34.29 |
| | 5m | 25.58 | 22.53 | 22.60 |
| | 7.5 | 20.35 | 18.63 | 22.92 |
| | 9.5m | 25.67 | 27.01 | 28.06 |
| 6-8 | 1m | 21.93 | 22.36 | 24.37 |
| | 5m | 17.49 | 18.37 | 18.13 |
| | 7.5 | 18.60 | 18.14 | 18.22 |
| | 9.5m | 18.64 | 18.18 | 17.35 |
| 9-11 | 1m | 44.19 | 41.67 | 38.68 |
| | 5m | 45.58 | 40.12 | 38.97 |
| | 7.5 | 42.99 | 38.49 | 36.99 |
| | 9.5m | 42.21 | 43.03 | 43.10 |
| 10-12 | 1m | 38.63 | 35.25 | 33.76 |
| | 5m | 35.79 | 32.14 | 31.44 |
| | 7.5 | 34.21 | 34.05 | 34.12 |
| | 9.5m | 34.39 | 36.40 | 33.26 |
| 13-15 | 1m | -5.15 | -4.07 | -2.49 |
| | 5m | -2.74 | -3.73 | -1.81 |
| | 7.5 | -3.16 | -2.28 | -1.81 |
| | 9.5m | -1.28 | -2.21 | -1.33 |
| 14-16 | 1m | -2.10 | -2.45 | -3.01 |

| Cases | Planes | LTR velocity | | |
|-------|-------------|--|--------------|--------------|
| | | 1m/s | 1.5m/s | 2m/s |
| | | Percentage change in flow rate for each LTR velocity with the change in length of LB in the LTR from 3 to 6m (%) | | |
| | 5m | -3.71 | -1.90 | -0.31 |
| | 7.5 | -1.33 | -2.08 | -3.05 |
| | 9.5m | -1.61 | -1.50 | -0.66 |
| | | | | |
| 17-19 | 1m | 48.30 | 53.10 | 50.06 |
| | 5m | 24.60 | 23.27 | 26.49 |
| | 7.5 | 22.29 | 22.88 | 25.38 |
| | 9.5m | 25.18 | 27.23 | 28.34 |
| 18-20 | 1m | 22.24 | 22.93 | 22.20 |
| | 5m | 13.56 | 18.18 | 19.22 |
| | 7.5 | 18.10 | 20.00 | 19.29 |
| | 9.5m | 19.21 | 17.36 | 17.38 |
| 21-23 | 1m | 37.46 | 37.80 | 44.28 |
| | 5m | 40.84 | 39.49 | 41.83 |
| | 7.5 | 41.89 | 39.68 | 47.41 |
| | 9.5m | 43.09 | 42.22 | 43.02 |
| 22-24 | 1m | 40.42 | 43.75 | 42.79 |
| | 5m | 36.38 | 39.13 | 36.57 |
| | 7.5 | 35.62 | 38.66 | 37.44 |
| | 9.5m | 33.50 | 36.34 | 35.00 |

Table L2 Percentage change in flow rate for each LTR velocity with the change in the length of LB in the LTR from 3 to 6m - 6.6 x 4 x 10m heading

| Cases | Planes | LTR velocity | | |
|-------|-------------|--|--------------|--------------|
| | | 1m/s | 1.5m/s | 2m/s |
| | | Percentage change in flow rate for each LTR velocity with the change in length of LB in the LTR from 3 to 6m (%) | | |
| 49-51 | 1m | -2.07 | -2.57 | -1.28 |
| | 5m | -2.05 | -1.61 | -1.42 |
| | 7.5 | -1.50 | -1.64 | -1.17 |
| | 9.5m | -1.93 | -0.54 | -1.67 |
| 50-52 | 1m | -1.62 | -1.09 | -1.14 |
| | 5m | -1.08 | -1.26 | -1.37 |
| | 7.5 | -1.41 | -1.21 | -1.05 |
| | 9.5m | -0.66 | -2.42 | -1.87 |
| 53-55 | 1m | 30.60 | 32.68 | 37.67 |
| | 5m | 25.77 | 24.69 | 22.48 |
| | 7.5 | 20.76 | 22.04 | 24.90 |
| | 9.5m | 24.62 | 28.48 | 28.30 |
| 54-56 | 1m | 22.50 | 22.50 | 21.83 |
| | 5m | 16.79 | 17.71 | 16.82 |
| | 7.5 | 18.10 | 18.45 | 18.40 |
| | 9.5m | 17.77 | 19.69 | 18.30 |
| 57-59 | 1m | 40.70 | 39.04 | 34.86 |
| | 5m | 38.86 | 36.33 | 39.16 |
| | 7.5 | 40.89 | 38.77 | 41.81 |
| | 9.5m | 43.80 | 41.89 | 42.61 |
| 58-60 | 1m | 37.55 | 34.21 | 35.70 |
| | 5m | 34.53 | 32.34 | 33.06 |
| | 7.5 | 33.73 | 32.45 | 33.23 |
| | 9.5m | 34.15 | 36.57 | 36.16 |
| 61-63 | 1m | -2.38 | -1.73 | -3.95 |
| | 5m | -3.82 | -3.63 | -2.51 |
| | 7.5 | -8.58 | -4.91 | -5.79 |
| | 9.5m | -2.13 | -2.17 | -0.61 |
| 62-64 | 1m | -2.07 | -3.46 | -1.93 |
| | 5m | -1.58 | -2.65 | -2.08 |
| | 7.5 | -1.19 | -2.20 | -2.38 |
| | 9.5m | -2.49 | -0.68 | -0.84 |
| 65-67 | 1m | 42.70 | 49.39 | 50.54 |

| Cases | Planes | LTR velocity | | |
|-------|-------------|--|--------------|--------------|
| | | 1m/s | 1.5m/s | 2m/s |
| | | Percentage change in flow rate for each LTR velocity with the change in length of LB in the LTR from 3 to 6m (%) | | |
| | 5m | 25.86 | 29.52 | 27.03 |
| | 7.5 | 24.40 | 29.56 | 26.99 |
| | 9.5m | 25.11 | 26.09 | 27.97 |
| | 1m | 20.75 | 22.22 | 22.09 |
| 66-68 | 5m | 14.02 | 16.88 | 18.77 |
| | 7.5 | 18.11 | 19.48 | 19.03 |
| | 9.5m | 19.52 | 17.75 | 18.13 |
| 69-71 | 1m | 36.41 | 39.36 | 43.42 |
| | 5m | 36.46 | 39.16 | 42.69 |
| | 7.5 | 44.81 | 50.42 | 48.23 |
| | 9.5m | 42.18 | 41.84 | 41.71 |
| 70-72 | 1m | 41.33 | 40.85 | 39.68 |
| | 5m | 36.00 | 37.66 | 36.99 |
| | 7.5 | 36.48 | 35.71 | 35.33 |
| | 9.5m | 32.36 | 36.50 | 34.30 |

Table L3 Percentage change in flow rate for each LTR velocity with the change in the length of LB in the LTR from 3 to 6m - 6.6 x 3 x 20m heading

| Cases | Planes | LTR velocity | | |
|-------|--------------|--|--------------|--------------|
| | | 1m/s | 1.5m/s | 2m/s |
| | | Percentage change in flow rate for each LTR velocity with the change in the length of LB in the LTR from 3 to 6m (%) | | |
| 25-27 | 1m | -3.62 | -2.22 | -3.62 |
| | 10m | -1.54 | -1.58 | -1.64 |
| | 15m | -1.70 | -2.22 | -1.56 |
| | 19.5m | -2.11 | -1.59 | -1.77 |
| 26-28 | 1m | -1.32 | -1.03 | -1.27 |
| | 10m | -1.55 | -1.22 | -1.77 |
| | 15m | -1.45 | -1.28 | -1.71 |
| | 19.5m | -1.91 | -2.87 | -1.26 |
| 29-31 | 1m | 37.72 | 46.39 | 45.55 |
| | 10m | 25.60 | 26.18 | 25.51 |
| | 15m | 21.60 | 19.65 | 22.18 |
| | 19.5m | 26.53 | 29.52 | 28.20 |
| 30-32 | 1m | 18.59 | 20.30 | 22.05 |
| | 10m | 15.86 | 18.53 | 18.27 |
| | 15m | 15.83 | 17.06 | 16.90 |
| | 19.5m | 18.57 | 16.65 | 17.62 |
| 33-35 | 1m | 42.79 | 41.48 | 40.49 |
| | 10m | 45.43 | 40.22 | 38.97 |
| | 15m | 42.94 | 38.14 | 37.59 |
| | 19.5m | 41.91 | 40.58 | 42.20 |
| 34-36 | 1m | 42.17 | 41.97 | 36.88 |
| | 10m | 34.12 | 31.68 | 29.92 |
| | 15m | 31.78 | 31.14 | 27.16 |
| | 19.5m | 33.32 | 33.42 | 33.07 |
| 37-39 | 1m | -5.06 | -5.57 | -3.47 |
| | 10m | -3.53 | -4.85 | -1.93 |
| | 15m | -1.47 | -3.72 | -2.82 |
| | 19.5m | -1.18 | -2.15 | -1.50 |
| 38-40 | 1m | -2.52 | -2.73 | -2.77 |
| | 10m | -1.62 | -1.42 | -3.07 |
| | 15m | -3.78 | -3.10 | -3.33 |
| | 19.5m | -3.17 | -1.51 | -1.16 |
| 41-43 | 1m | 44.60 | 49.67 | 50.80 |

| Cases | Planes | LTR velocity | | |
|-------|--------------|--|--------------|--------------|
| | | 1m/s | 1.5m/s | 2m/s |
| | | Percentage change in flow rate for each LTR velocity with the change in the length of LB in the LTR from 3 to 6m (%) | | |
| | 10m | 25.43 | 25.17 | 23.11 |
| | 15m | 16.80 | 19.70 | 20.18 |
| | 19.5m | 25.00 | 27.10 | 28.38 |
| | | | | |
| 42-44 | 1m | 22.15 | 24.62 | 24.54 |
| | 10m | 14.15 | 18.26 | 18.99 |
| | 15m | 15.27 | 14.00 | 16.24 |
| | 19.5m | 16.44 | 17.82 | 17.53 |
| 45-47 | 1m | 41.38 | 39.84 | 38.46 |
| | 10m | 47.55 | 43.19 | 41.69 |
| | 15m | 41.12 | 39.98 | 36.95 |
| | 19.5m | 44.37 | 42.60 | 43.06 |
| 46-48 | 1m | 43.32 | 42.44 | 40.47 |
| | 10m | 35.44 | 36.44 | 32.51 |
| | 15m | 31.36 | 29.82 | 30.37 |
| | 19.5m | 29.03 | 32.25 | 32.69 |

Table L4 Percentage change in flow rate for each LTR velocity with the change in length of LB in the LTR from 3 to 6m - 6.6 x 4 x 20m heading

| Cases | Planes | LTR velocity | | |
|-------|--------------|--|--------------|--------------|
| | | 1m/s | 1.5m/s | 2m/s |
| | | Percentage change in flow rate for each LTR velocity with the change in the length of LB in the LTR from 3 to 6m (%) | | |
| 73-75 | 1m | -4.90 | -2.70 | -2.16 |
| | 10m | -2.97 | -1.55 | -1.50 |
| | 15m | -2.15 | -1.58 | -1.90 |
| | 19.5m | -1.38 | -1.35 | -2.53 |
| 74-76 | 1m | -1.53 | -1.68 | -1.51 |
| | 10m | -1.78 | -1.24 | -1.60 |
| | 15m | -2.56 | -2.68 | -2.01 |
| | 19.5m | -1.47 | -2.37 | -0.94 |
| 77-79 | 1m | 40.16 | 42.74 | 45.71 |
| | 10m | 27.87 | 28.07 | 26.07 |
| | 15m | 21.30 | 21.94 | 21.47 |
| | 19.5m | 24.42 | 28.15 | 27.78 |
| 78-80 | 1m | 19.30 | 19.35 | 20.44 |
| | 10m | 16.58 | 18.15 | 16.65 |
| | 15m | 13.13 | 16.15 | 13.12 |
| | 19.5m | 19.58 | 19.75 | 17.74 |
| 81-83 | 1m | 46.97 | 46.72 | 47.52 |
| | 10m | 46.34 | 44.48 | 41.73 |
| | 15m | 41.79 | 36.70 | 36.74 |
| | 19.5m | 43.36 | 42.58 | 43.17 |
| 82-84 | 1m | 42.27 | 42.44 | 38.90 |
| | 10m | 35.71 | 31.33 | 31.49 |
| | 15m | 29.69 | 28.13 | 28.20 |
| | 19.5m | 31.16 | 35.32 | 35.77 |
| 85-87 | 1m | -4.23 | -4.02 | -4.66 |
| | 10m | -3.15 | -4.82 | -4.25 |
| | 15m | -2.93 | -3.97 | -3.83 |
| | 19.5m | -1.70 | -1.80 | -1.49 |
| 86-88 | 1m | -1.59 | 1.17 | -1.48 |
| | 10m | -1.55 | -1.70 | -2.60 |
| | 15m | -3.44 | -2.90 | -2.95 |
| | 19.5m | -2.65 | -1.74 | -1.33 |
| 89-91 | 1m | 43.65 | 53.23 | 52.45 |

| Cases | Planes | LTR velocity | | |
|-------|--------------|--|--------------|--------------|
| | | 1m/s | 1.5m/s | 2m/s |
| | | Percentage change in flow rate for each LTR velocity with the change in the length of LB in the LTR from 3 to 6m (%) | | |
| | 10m | 24.76 | 24.54 | 26.35 |
| | 15m | 20.71 | 26.11 | 26.80 |
| | 19.5m | 24.50 | 26.49 | 28.34 |
| | | | | |
| 90-92 | 1m | 20.19 | 20.46 | 21.28 |
| | 10m | 13.09 | 18.43 | 18.94 |
| | 15m | 16.46 | 14.30 | 16.12 |
| | 19.5m | 18.58 | 17.36 | 16.67 |
| 93-95 | 1m | 54.13 | 52.45 | 50.15 |
| | 10m | 45.98 | 43.71 | 42.57 |
| | 15m | 41.63 | 40.31 | 37.09 |
| | 19.5m | 43.16 | 42.81 | 42.42 |
| 94-96 | 1m | 38.02 | 38.74 | 36.20 |
| | 10m | 41.49 | 38.13 | 37.68 |
| | 15m | 30.15 | 30.77 | 28.00 |
| | 19.5m | 31.07 | 34.17 | 34.25 |

APPENDIX M

**EFFECT OF LENGTH OF LB IN LTR ON FLOW RATES AT EXIT OF LB
AND FACE OF HEADING**

Table M1 Percentage change in flow rate at the 9.5m deep plane and exit of the LB for each LTR velocity with the increase in length of LB in the LTR from 3 to 6m - 6.6 x 4 x 10m heading

| Cases | LTR velocity | | | Cases | LTR Velocity | | |
|-------|---|--------|-------|-------|--|--------|-------|
| | 1m/s | 1.5m/s | 2m/s | | 1m/s | 1.5m/s | 2m/s |
| | Percentage change in flow rate at the 9.5m deep plane for each LTR velocity with the increase in the length of LB in the LTR from 3 to 6m (%) | | | | Percentage change in flow rate at the exit of LB for each LTR velocity with the increase in length of LB in the LTR from 3 to 6m (%) | | |
| 49-51 | -1.93 | -0.54 | -1.67 | 49-51 | -1.54 | -1.37 | -1.44 |
| 50-52 | -0.66 | -2.42 | -1.87 | 50-52 | -1.55 | -1.69 | -1.39 |
| 53-55 | 24.62 | 28.48 | 28.30 | 53-55 | 25.27 | 28.47 | 27.63 |
| 54-56 | 17.77 | 19.69 | 18.30 | 54-56 | 18.56 | 18.42 | 18.75 |
| 57-59 | 43.80 | 41.89 | 42.61 | 57-59 | 42.34 | 43.68 | 44.35 |
| 58-60 | 34.15 | 36.57 | 36.16 | 58-60 | 34.07 | 34.50 | 34.24 |
| 61-63 | -2.13 | -2.17 | -0.61 | 61-63 | -1.51 | -1.49 | -1.26 |
| 62-64 | -2.49 | -0.68 | -0.84 | 62-64 | -1.49 | -1.71 | -1.33 |
| 65-67 | 25.11 | 26.09 | 27.97 | 65-67 | 25.45 | 27.43 | 29.08 |
| 66-68 | 19.52 | 17.75 | 18.13 | 66-68 | 19.12 | 18.11 | 18.42 |
| 69-71 | 42.18 | 41.84 | 41.71 | 69-71 | 42.04 | 41.54 | 42.82 |
| 70-72 | 32.36 | 36.50 | 34.30 | 70-72 | 32.07 | 33.43 | 37.14 |

Table M2 Percentage change in flow rate at the 19.5m deep plane and exit of the LB for each LTR velocity with the increase in the length of LB in the LTR from 3 to 6m - 6.6 x 3 x 20m heading

| Cases | LTR velocity | | | Cases | LTR Velocity | | |
|-------|--|--------|-------|-------|--|--------|-------|
| | 1m/s | 1.5m/s | 2m/s | | 1m/s | 1.5m/s | 2m/s |
| | Percentage change in flow rate at the 19.5m deep plane for each LTR velocity with the increase in the length of LB in the LTR from 3 to 6m (%) | | | | Percentage change in flow rate at the exit of LB for each LTR velocity with the increase in the length of LB in the LTR from 3 to 6m (%) | | |
| 25-27 | -2.11 | -1.59 | -1.77 | 25-27 | -0.91 | -1.17 | -1.17 |
| 26-28 | -1.91 | -2.87 | -1.26 | 26-28 | -1.47 | -1.74 | -1.38 |
| 29-31 | 26.53 | 29.52 | 28.20 | 29-31 | 25.27 | 27.13 | 28.00 |
| 30-32 | 18.57 | 16.65 | 17.62 | 30-32 | 18.56 | 18.47 | 17.20 |
| 33-35 | 41.91 | 40.58 | 42.20 | 33-35 | 42.63 | 42.63 | 42.27 |
| 34-36 | 33.32 | 33.42 | 33.07 | 34-36 | 33.21 | 35.19 | 35.56 |
| 37-39 | -1.18 | -2.15 | -1.50 | 37-39 | -0.90 | -1.23 | -1.17 |
| 38-40 | -3.17 | -1.51 | -1.16 | 38-40 | -1.54 | -1.45 | -1.22 |
| 41-43 | 25.00 | 27.10 | 28.38 | 41-43 | 25.10 | 27.11 | 28.39 |
| 42-44 | 16.44 | 17.82 | 17.53 | 42-44 | 18.76 | 18.51 | 18.00 |
| 45-47 | 44.37 | 42.60 | 43.06 | 45-47 | 42.91 | 42.54 | 43.08 |
| 46-48 | 29.03 | 32.25 | 32.69 | 46-48 | 33.61 | 35.62 | 35.90 |

Table M3 Percentage change in flow rate at the 19.5m deep plane and exit of the LB for each LTR velocity with the increase in length of LB in the LTR from 3 to 6m - 6.6 x 4 x 20m heading

| Cases | LTR velocity | | | Cases | LTR velocity | | |
|-------|--|--------|-------|-------|--|--------|-------|
| | 1m/s | 1.5m/s | 2m/s | | 1m/s | 1.5m/s | 2m/s |
| | Percentage change in flow rate at the 19.5m deep plane for each LTR velocity with the increase in the length of LB in the LTR from 3 to 6m (%) | | | | Percentage change in flow rate at the 19.5m deep plane for each LTR velocity with the increase in the length of LB in the LTR from 3 to 6m (%) | | |
| 73-75 | -1.38 | -1.35 | -2.53 | 73-75 | -1.19 | -1.82 | -1.56 |
| 74-76 | -1.47 | -2.37 | -0.94 | 74-76 | -1.42 | -1.93 | -1.30 |
| 77-79 | 24.42 | 28.15 | 27.78 | 77-79 | 25.29 | 28.38 | 28.13 |
| 78-80 | 19.58 | 19.75 | 17.74 | 78-80 | 19.50 | 18.27 | 18.27 |
| 81-83 | 43.36 | 42.58 | 43.17 | 81-83 | 42.82 | 43.84 | 44.82 |
| 82-84 | 31.16 | 35.32 | 35.77 | 82-84 | 33.80 | 35.02 | 33.89 |
| 85-87 | -1.70 | -1.80 | -1.49 | 85-87 | -1.59 | -1.26 | -0.91 |
| 86-88 | -2.65 | -1.74 | -1.33 | 86-88 | -1.50 | -1.75 | -1.54 |
| 89-91 | 24.50 | 26.49 | 28.34 | 89-91 | 25.68 | 26.12 | 28.95 |
| 90-92 | 18.58 | 17.36 | 16.67 | 90-92 | 19.17 | 18.43 | 17.94 |
| 93-95 | 43.16 | 42.81 | 42.42 | 93-95 | 41.13 | 41.37 | 42.17 |
| 94-96 | 31.07 | 34.17 | 34.25 | 94-96 | 31.67 | 32.85 | 37.63 |

EFFECT OF LB LENGTH IN LTR ON FLOW RATES CLOSE TO FACE

- Flow rates at 9.5m deep planes using 3m and 6m LB inside the LTR for LTR velocities of 1m/s, 1.5m/s, 2m/s - 6.6 x 4 x 10m heading

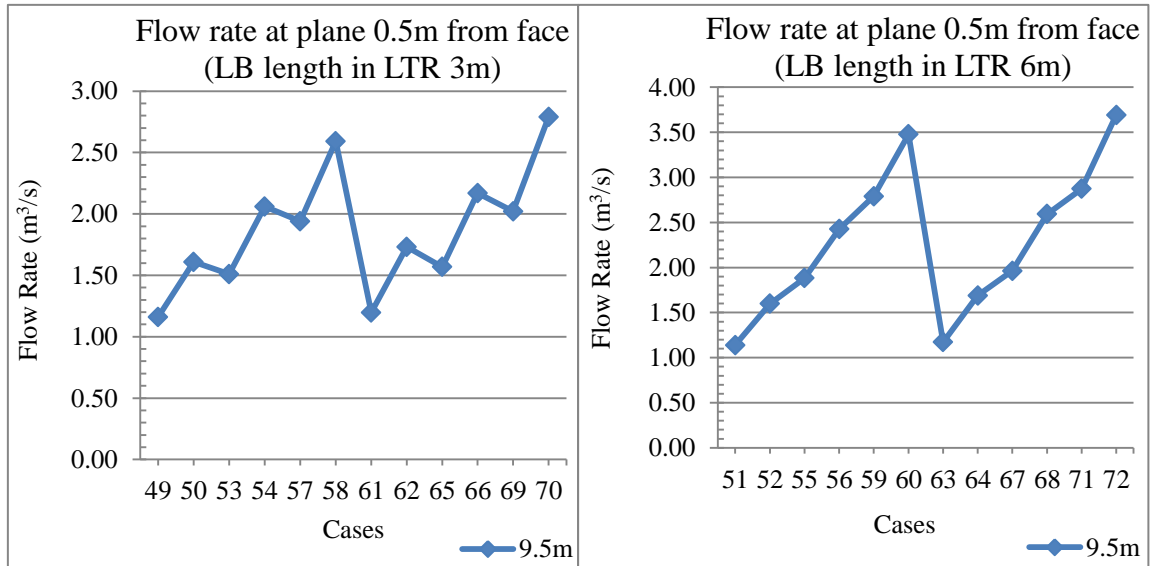


Figure N1 Flow rates at 9.5m deep planes using 3m and 6m LB inside the LTR for LTR velocity of 1m/s

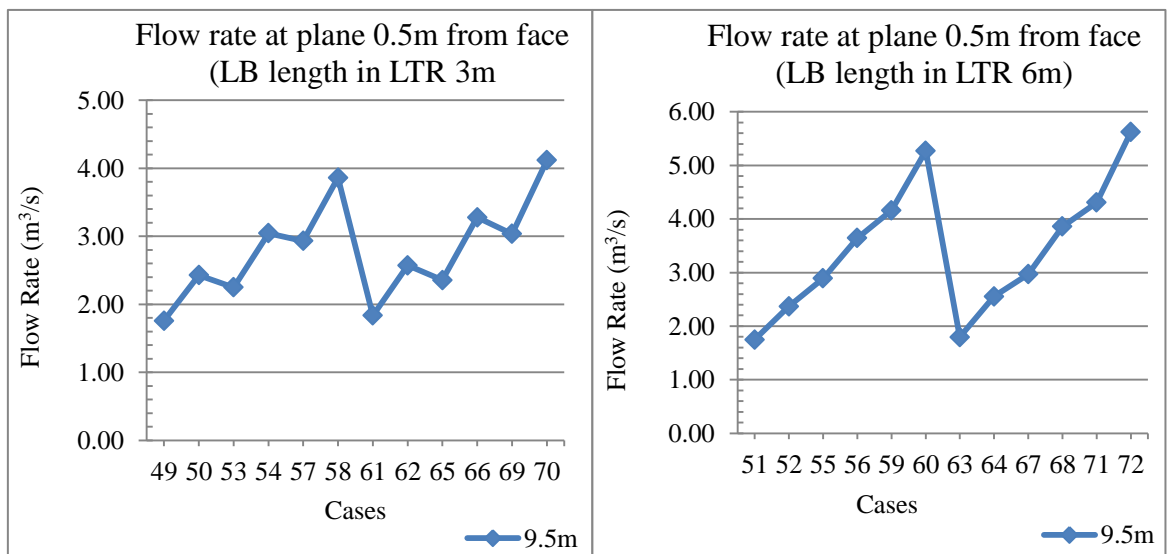


Figure N2 Flow rates at 9.5m deep planes using 3m and 6m LB inside the LTR for LTR velocity of 1.5m/s

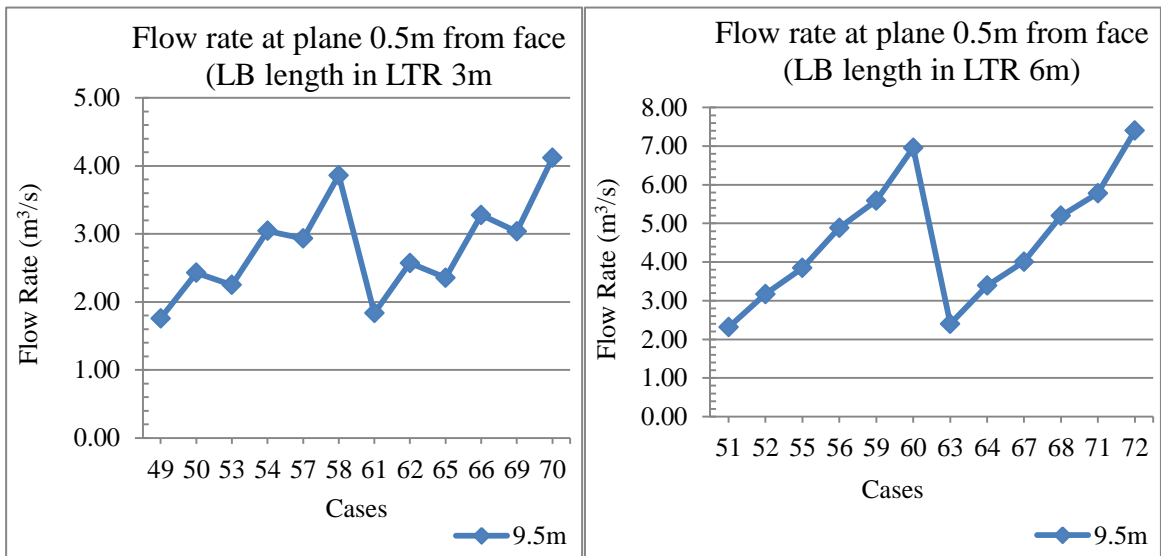


Figure N3 Flow rates at 9.5m deep planes using 3m and 6m LB inside the LTR for LTR velocity of 2m/s

- Flow rates at 19.5m deep planes using 3m and 6m LB inside the LTR for LTR velocities of 1m/s, 1.5m/s, 2m/s - 6.6 x 3 x 20m heading

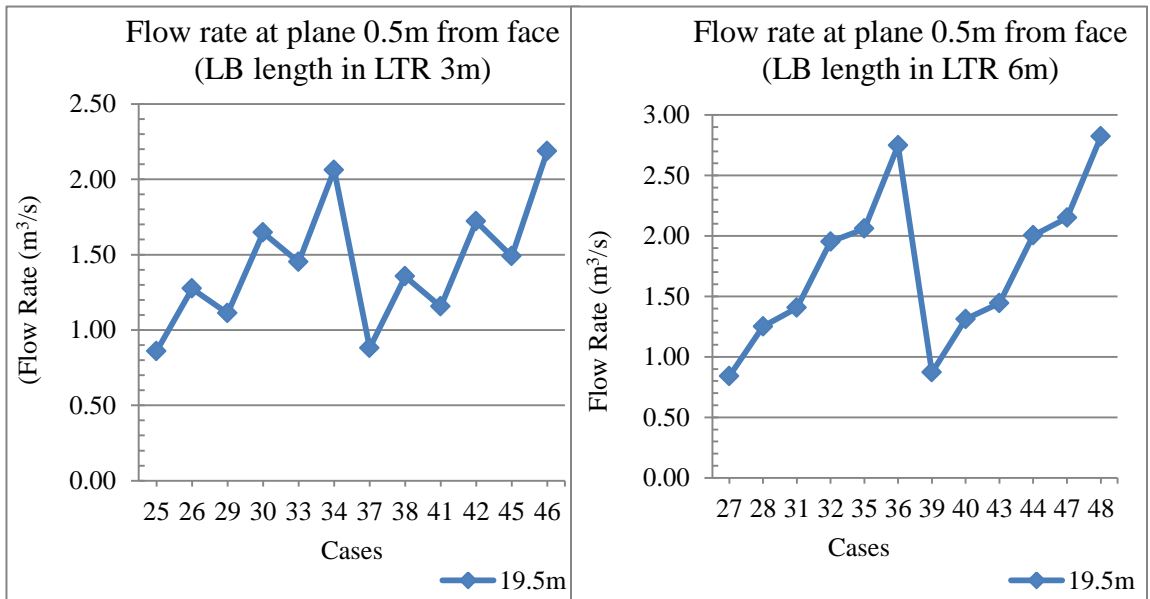


Figure N4 Flow rates at 19.5m deep planes using 3m and 6m LB inside the LTR for LTR velocity of 1m/s

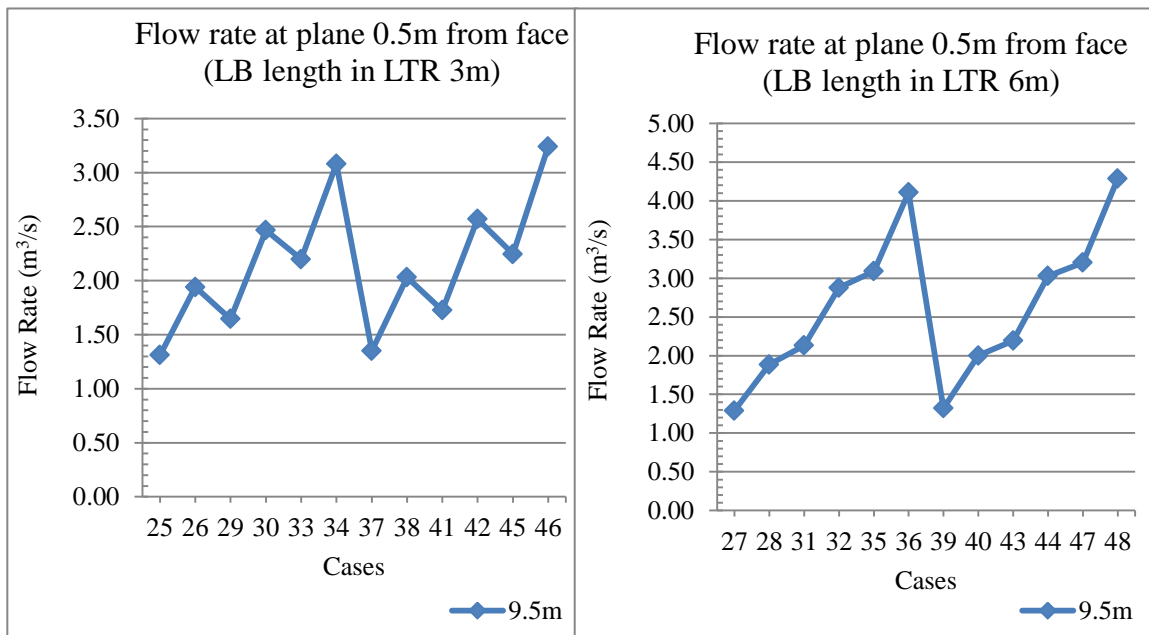


Figure N5 Flow rates at 19.5m deep planes using 3m and 6m LB inside the LTR for LTR velocity of 1.5m/s

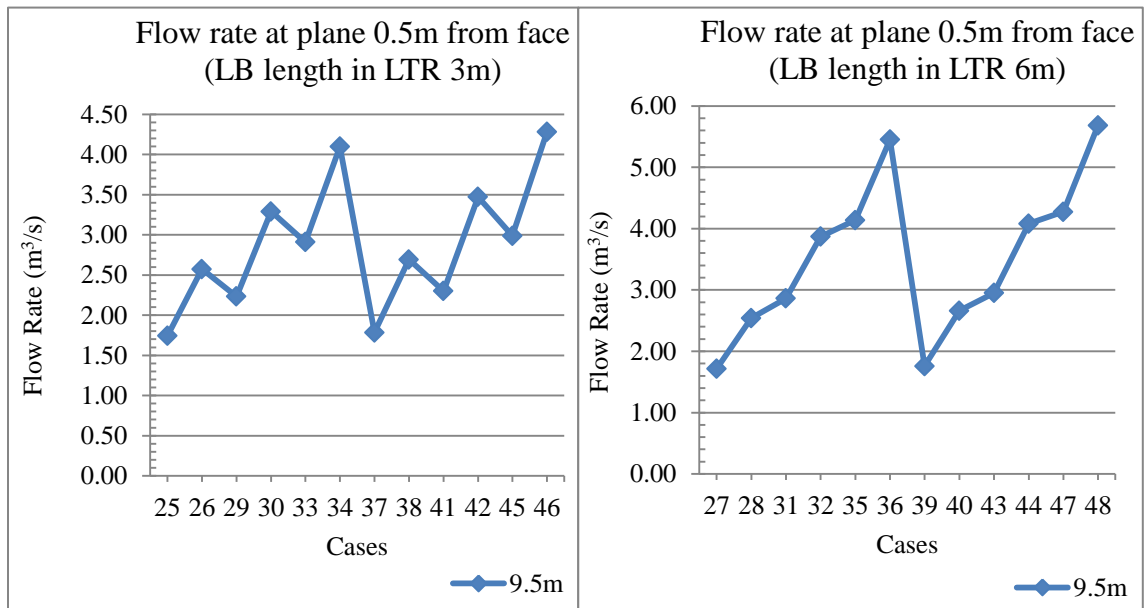


Figure N6 Flow rates at 19.5m deep planes using 3m and 6m LB inside the LTR for LTR velocity of 2m/s

- Flow rates at 19.5m deep planes using 3m and 6m LB inside the LTR for LTR velocities of 1m/s, 1.5m/s, 2m/s - 6.6 x 4 x 20m heading

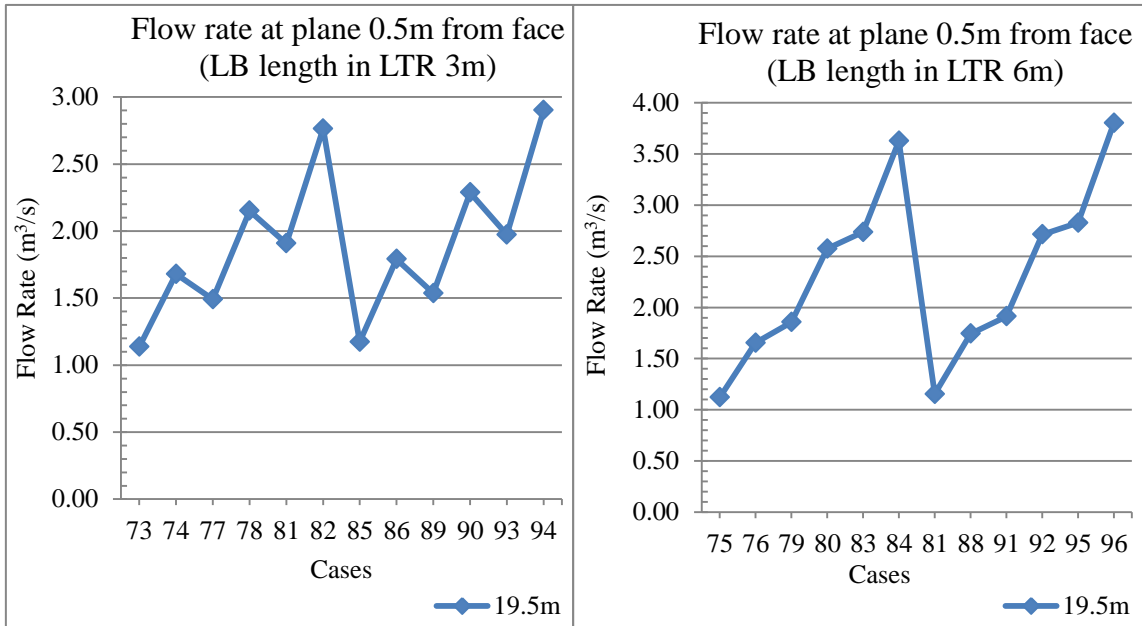


Figure N7 Flow rates at 19.5m deep planes using 3m and 6m LB inside the LTR for LTR velocity of 1m/s

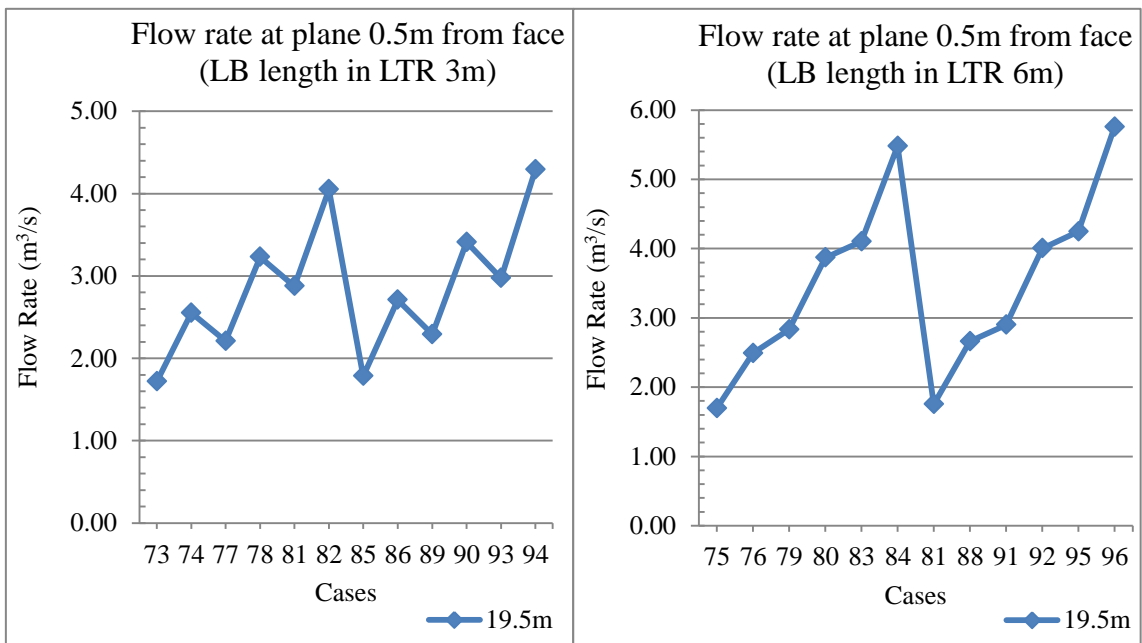


Figure N8 Flow rates at 19.5m deep planes using 3m and 6m LB inside the LTR for LTR velocity of 1.5m/s

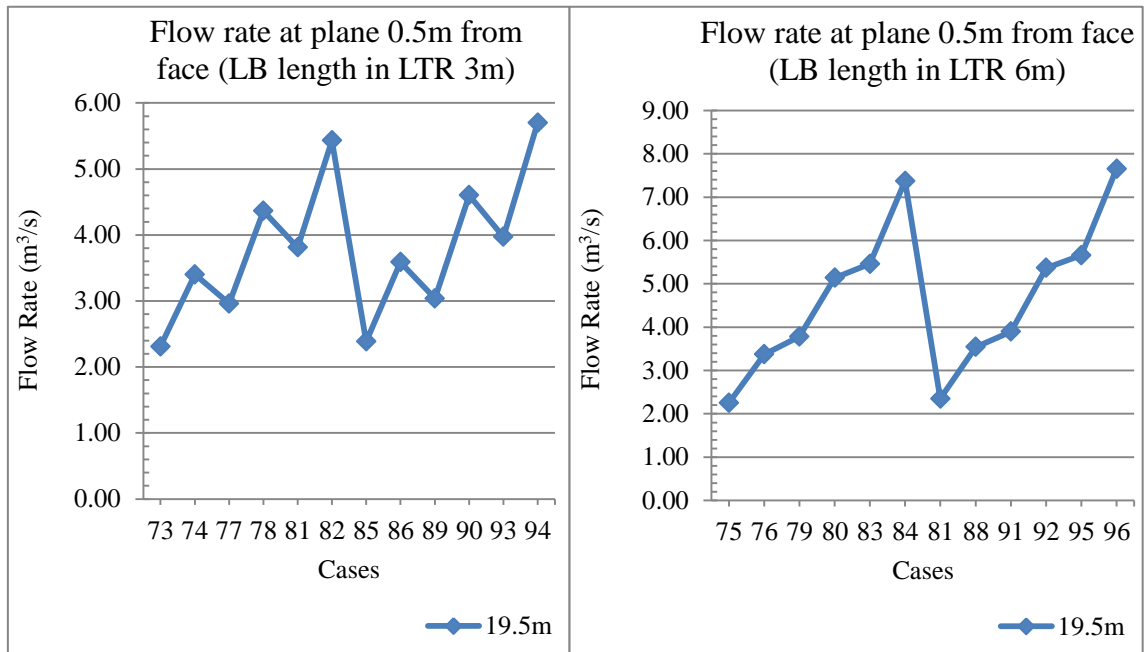


Figure N9 Flow rates at 19.5m deep planes using 3m and 6m LB inside the LTR for LTR velocity of 2m/s

EFFECT OF LB LENGTH IN LTR ON FLOW RATE AT ALL DEPTH PLANES

- Flow rates at specified planes using 3m and 6m LB inside the LTR for LTR velocities of 1m/s, 1.5m/s, 2m/s - 6.6 x 4 x 10m heading

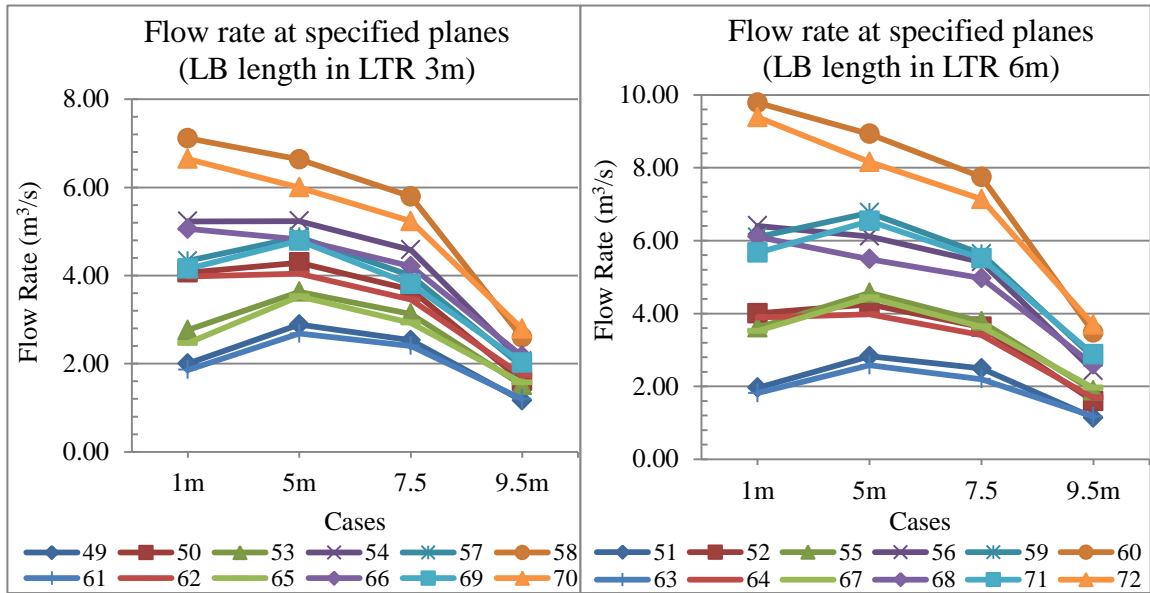


Figure O1 Flow rates at specified planes using 3m and 6m LB inside the LTR for LTR velocity of 1m/s

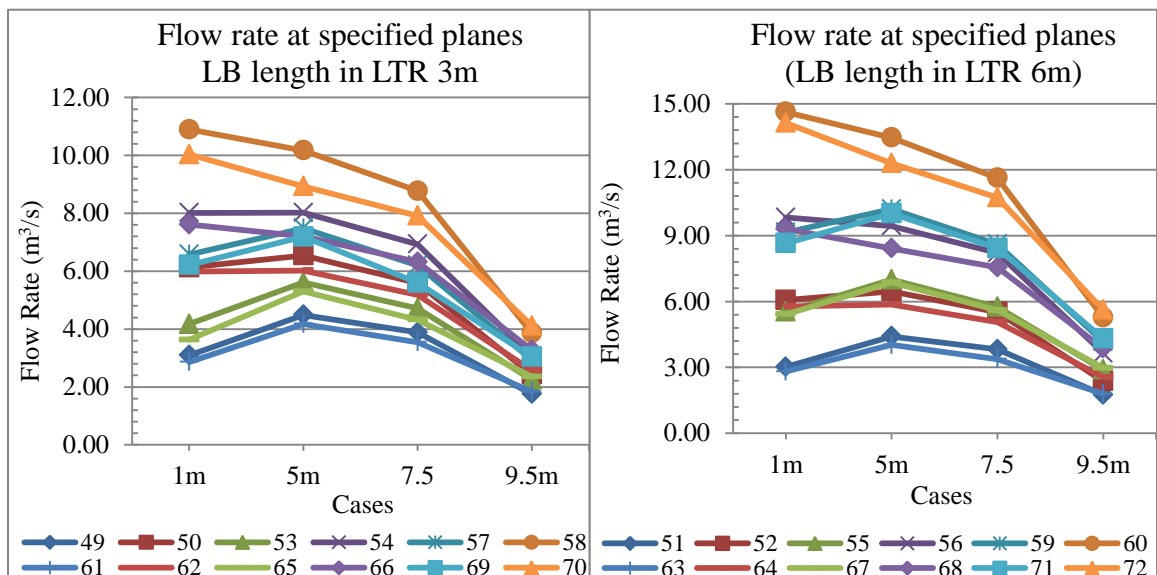


Figure O2 Flow rates at specified planes using 3m and 6m LB inside the LTR for LTR velocity of 1.5m/s

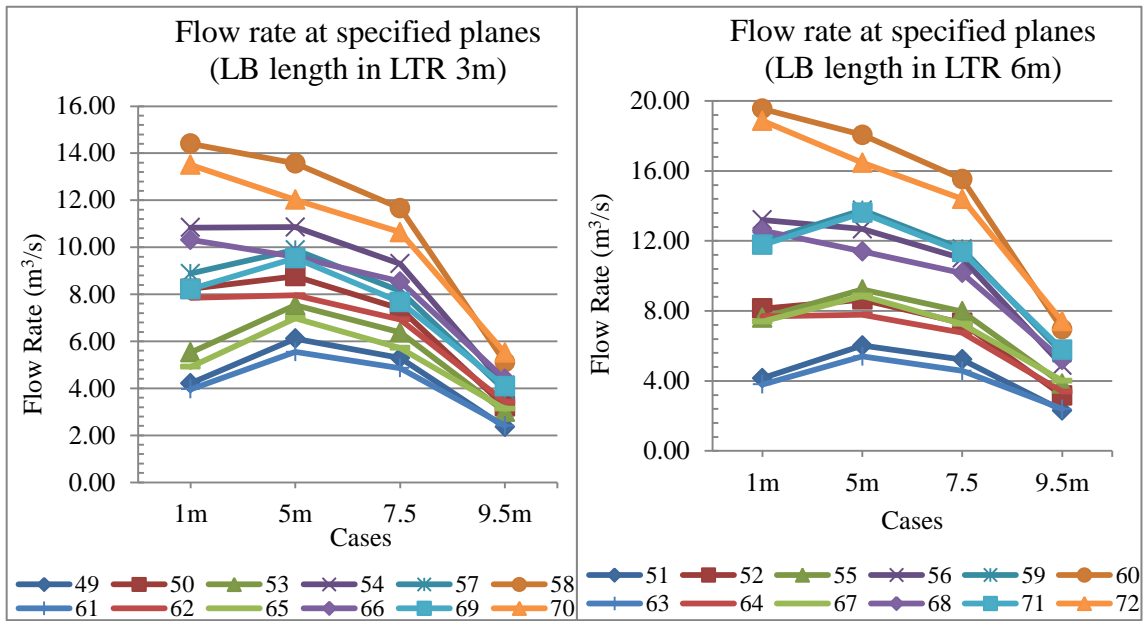


Figure O3 Flow rates at specified planes using 3m and 6m LB inside the LTR for LTR velocity of 2m/s

- Flow rates at specified planes using 3m and 6m LB inside the LTR for LTR velocities of 1m/s, 1.5m/s, 2m/s - 6.6 x 3 x 20m heading

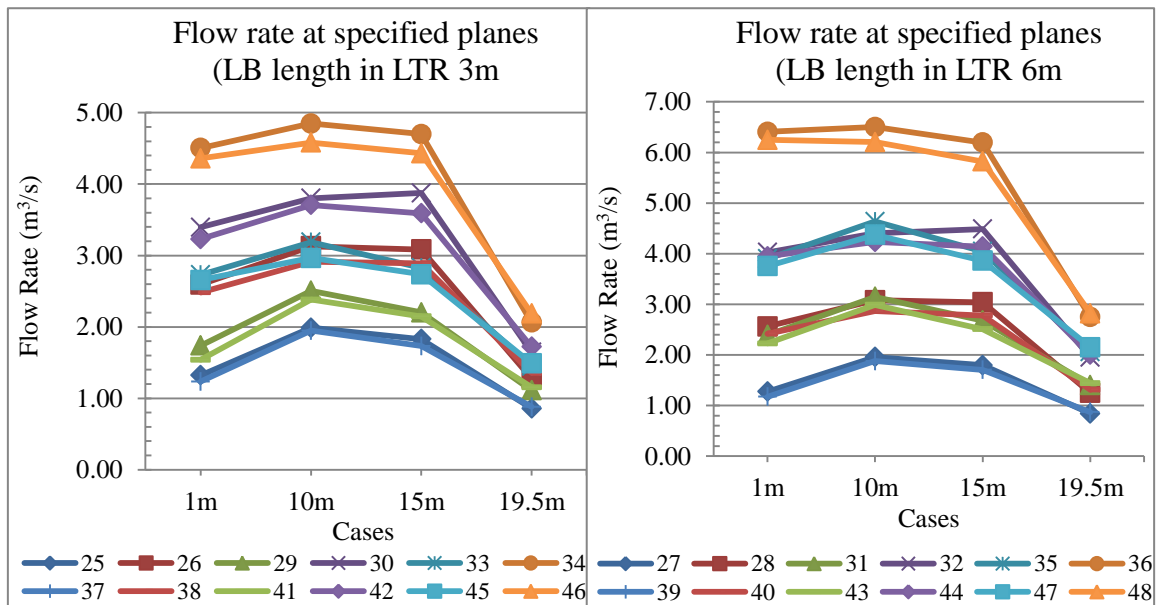


Figure O4 Flow rates at specified planes using 3m and 6m LB inside the LTR for LTR velocity of 1m/s

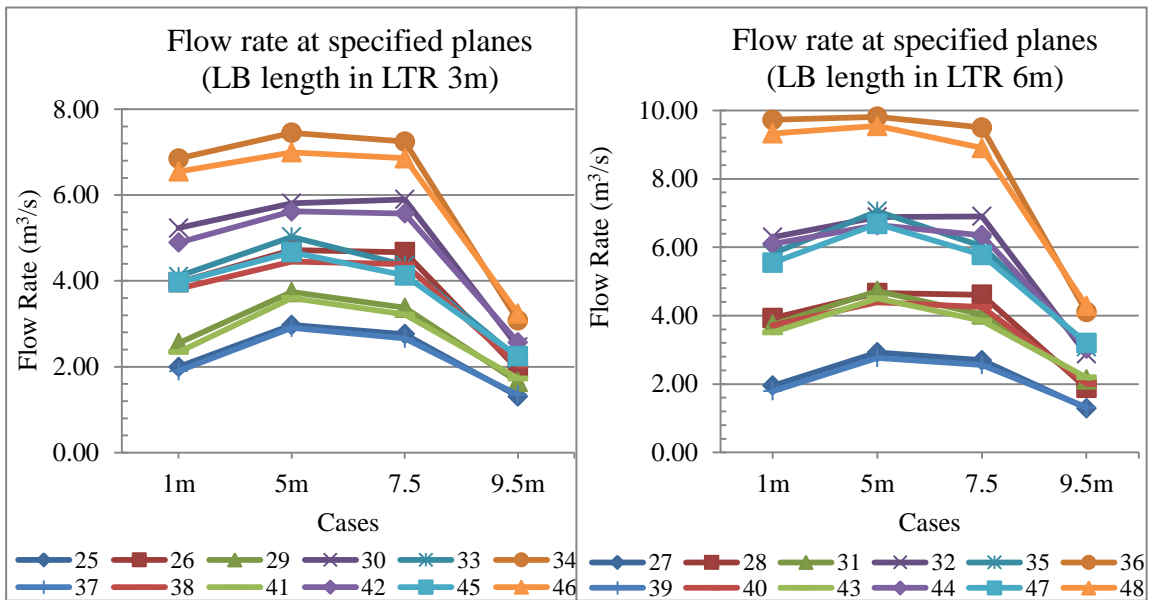


Figure O5 Flow rates at specified planes using 3m and 6m LB inside the LTR for LTR velocity of 1.5m/s

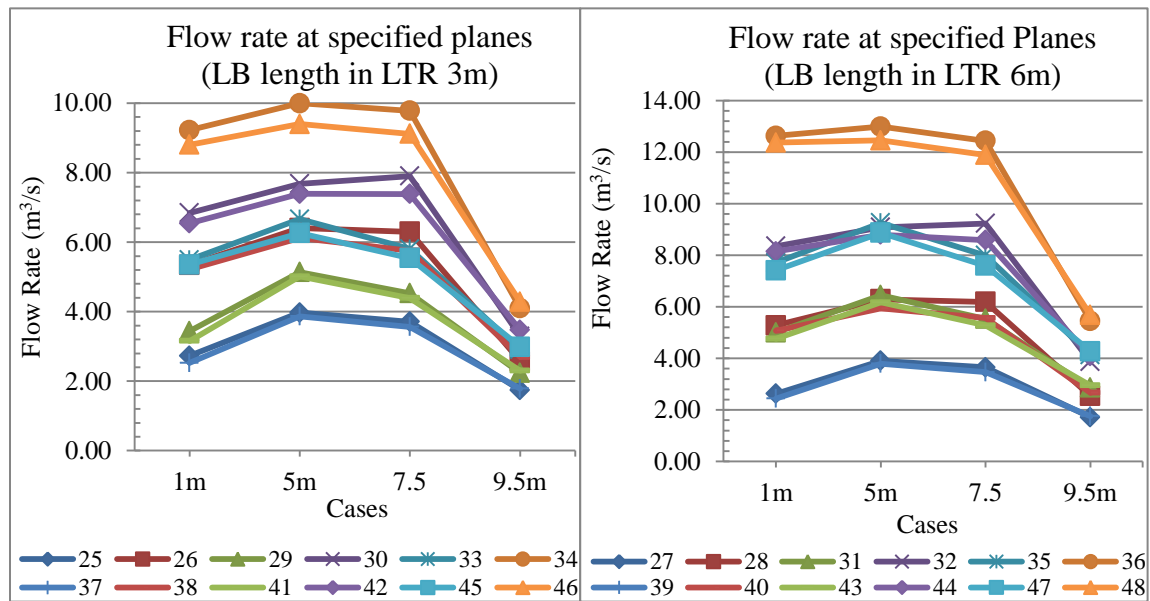


Figure O6 Flow rates at specified planes using 3m and 6m LB inside the LTR for LTR velocity of 2m/s

- Flow rates at specified planes using 3m and 6m LB inside the LTR for LTR velocities of 1m/s, 1.5m/s, 2m/s - 6.6 x 4 x 20m heading

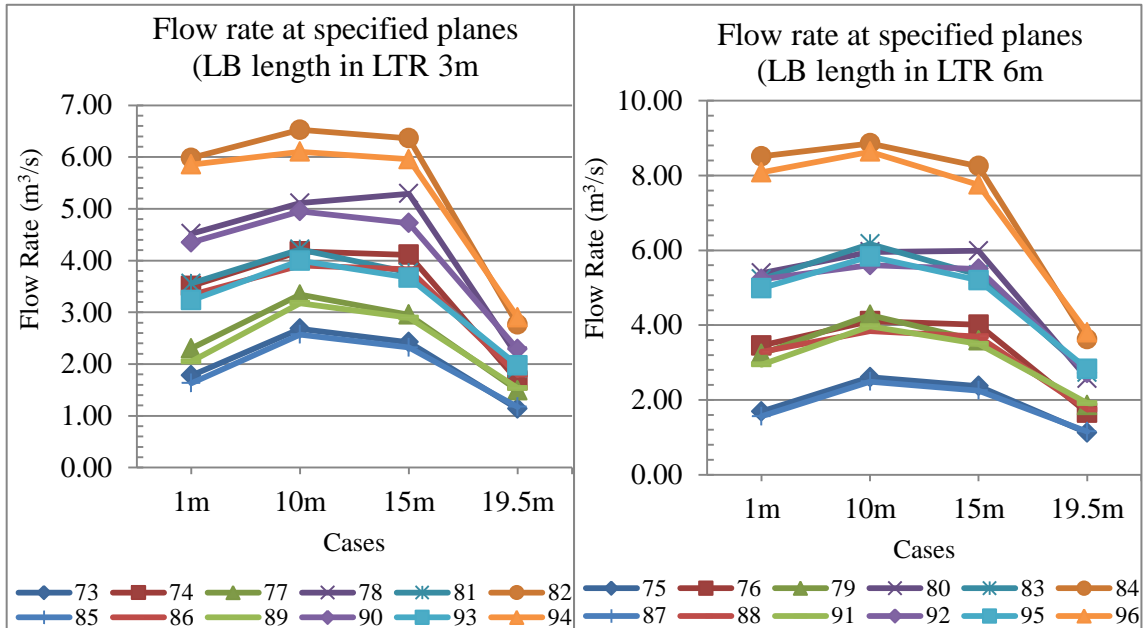


Figure O7 Flow rates at specified planes using 3m and 6m LB inside the LTR for LTR velocity of 1m/s

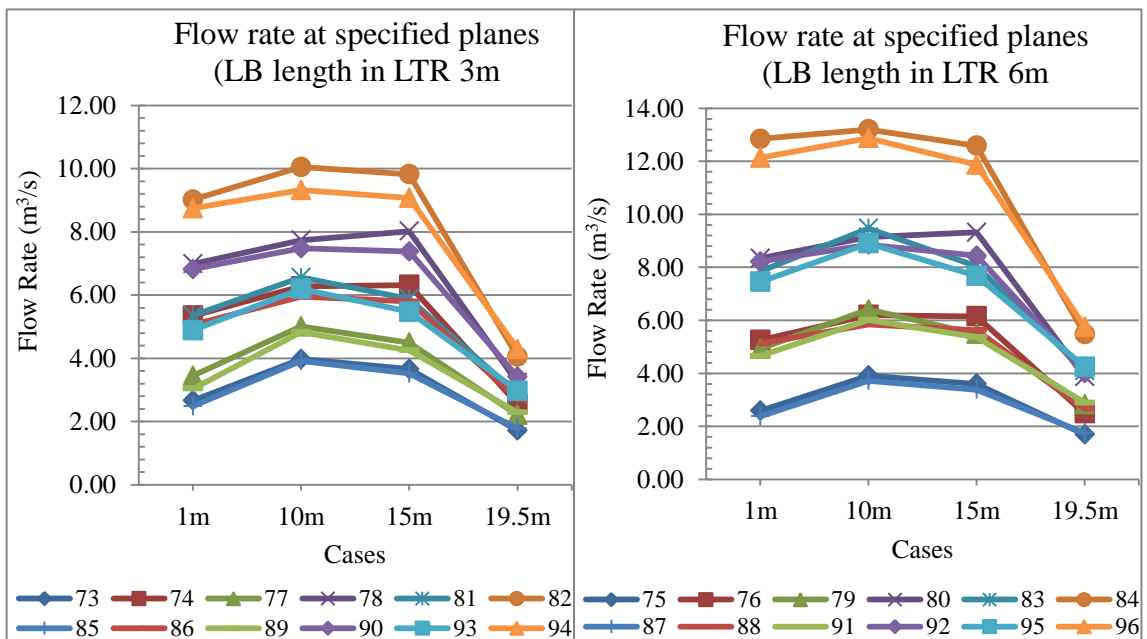


Figure O8 Flow rates at specified planes using 3m and 6m LB inside the LTR for LTR velocity of 1.5m/s

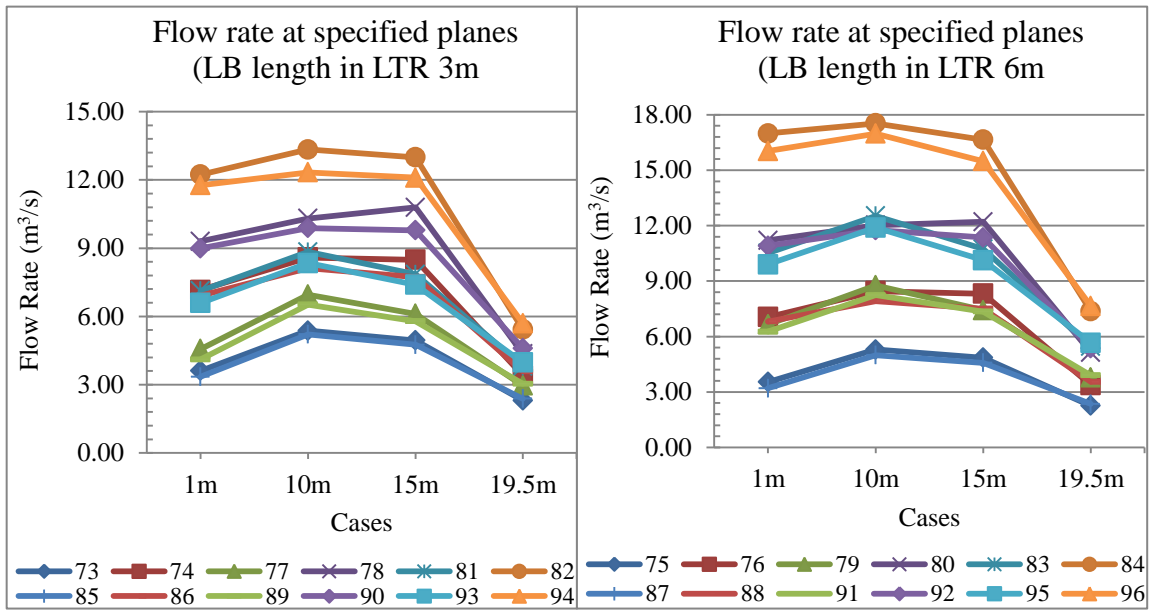


Figure O9 Flow rates at specified planes using 3m and 6m LB inside the LTR for LTR velocity of 2m/s

APPENDIX P

EFFECT OF DISTANCE OF LB FROM WALL IN HEADING ON FLOW RATE

Table P1 Percentage increase in flow rate at specified planes for each LTR velocity with the increase in the distance of the LB from 0.5 to 1m from the wall in the heading - 6.6 x 3 x10m heading

| Cases | Planes | LTR velocity | | |
|-------|-------------|--|--------------|--------------|
| | | 1m/s | 1.5m/s | 2m/s |
| | | Percentage increase in flow rate for each LTR velocity with the increase in distance of LB from 0.5 to 1m from the wall in the heading (%) | | |
| 1-2 | 1m | 109.22 | 99.99 | 98.20 |
| | 5m | 49.82 | 44.00 | 41.32 |
| | 7.5 | 45.02 | 41.46 | 36.60 |
| | 9.5m | 41.32 | 36.81 | 37.56 |
| 3-4 | 1m | 111.60 | 105.69 | 101.54 |
| | 5m | 49.85 | 46.46 | 45.86 |
| | 7.5 | 47.19 | 43.91 | 43.03 |
| | 9.5m | 39.88 | 35.18 | 37.55 |
| 5-6 | 1m | 89.19 | 93.79 | 92.44 |
| | 5m | 42.33 | 43.18 | 44.04 |
| | 7.5 | 44.82 | 44.37 | 45.19 |
| | 9.5m | 37.27 | 35.66 | 37.54 |
| 7-8 | 1m | 71.55 | 77.35 | 78.22 |
| | 5m | 33.16 | 38.31 | 38.78 |
| | 7.5 | 42.71 | 43.78 | 39.64 |
| | 9.5m | 29.59 | 26.23 | 26.03 |
| 9-10 | 1m | 63.35 | 67.73 | 66.20 |
| | 5m | 36.61 | 36.86 | 38.09 |
| | 7.5 | 41.93 | 37.95 | 37.10 |
| | 9.5m | 33.80 | 31.65 | 33.59 |
| 11-12 | 1m | 57.06 | 60.12 | 60.30 |
| | 5m | 27.43 | 29.06 | 30.61 |
| | 7.5 | 33.22 | 33.53 | 34.23 |
| | 9.5m | 26.44 | 25.56 | 24.41 |
| 13-14 | 1m | 110.35 | 108.84 | 103.60 |
| | 5m | 53.30 | 44.59 | 43.30 |
| | 7.5 | 49.01 | 46.43 | 45.84 |

| Cases | Planes | LTR velocity | | |
|-------|-------------|--|--------------|--------------|
| | | 1m/s | 1.5m/s | 2m/s |
| | | Percentage increase in flow rate for each LTR velocity with the increase in distance of LB from 0.5 to 1m from the wall in the heading (%) | | |
| | 9.5m | 44.18 | 41.91 | 41.75 |
| 15-16 | 1m | 117.11 | 112.36 | 102.53 |
| | 5m | 51.76 | 47.34 | 45.49 |
| | 7.5 | 51.83 | 46.71 | 44.00 |
| | 9.5m | 43.70 | 42.95 | 42.71 |
| 17-18 | 1m | 109.58 | 112.37 | 110.43 |
| | 5m | 38.07 | 33.67 | 37.15 |
| | 7.5 | 45.19 | 43.58 | 46.31 |
| | 9.5m | 38.89 | 41.14 | 42.06 |
| 19-20 | 1m | 72.74 | 70.52 | 71.36 |
| | 5m | 25.83 | 28.16 | 29.27 |
| | 7.5 | 40.22 | 40.22 | 39.21 |
| | 9.5m | 32.26 | 30.19 | 29.93 |
| 21-22 | 1m | 58.98 | 57.71 | 62.77 |
| | 5m | 28.90 | 23.87 | 27.55 |
| | 7.5 | 38.45 | 32.13 | 40.28 |
| | 9.5m | 37.79 | 35.97 | 36.42 |
| 23-24 | 1m | 62.40 | 64.51 | 61.09 |
| | 5m | 24.82 | 23.54 | 22.82 |
| | 7.5 | 32.33 | 31.17 | 30.79 |
| | 9.5m | 28.55 | 30.36 | 28.78 |

Table P2 Percentage increase in flow rate at specified planes for each LTR velocity with the increase in the distance of the LB from 0.5 to 1m from the wall in the heading - 6.6 x 4 x 10m heading

| Cases | Planes | LTR velocity | | |
|-------|-------------|--|--------------|--------------|
| | | 1m/s | 1.5m/s | 2m/s |
| | | Percentage increase in flow rate for each LTR velocity with the increase in distance of LB from 0.5 to 1m from the wall in the heading (%) | | |
| 49-50 | 1m | 103.38 | 98.03 | 95.40 |
| | 5m | 48.80 | 45.95 | 43.35 |
| | 7.5 | 45.50 | 43.73 | 39.67 |
| | 9.5m | 38.55 | 38.18 | 37.38 |
| 51-52 | 1m | 104.32 | 101.03 | 95.67 |
| | 5m | 50.28 | 46.48 | 43.43 |
| | 7.5 | 45.63 | 44.35 | 39.85 |
| | 9.5m | 40.34 | 35.57 | 37.10 |
| 53-54 | 1m | 89.13 | 92.25 | 96.01 |
| | 5m | 44.25 | 42.97 | 44.17 |
| | 7.5 | 46.49 | 47.03 | 45.74 |
| | 9.5m | 36.34 | 35.32 | 37.68 |
| 55-56 | 1m | 77.40 | 77.49 | 73.46 |
| | 5m | 33.95 | 34.95 | 37.50 |
| | 7.5 | 43.26 | 42.70 | 38.16 |
| | 9.5m | 28.85 | 26.07 | 26.95 |
| 57-58 | 1m | 64.24 | 65.68 | 62.17 |
| | 5m | 36.23 | 35.92 | 37.25 |
| | 7.5 | 44.82 | 41.48 | 43.33 |
| | 9.5m | 33.54 | 31.64 | 30.34 |
| 59-60 | 1m | 51.88 | 50.30 | 52.54 |
| | 5m | 32.60 | 32.04 | 31.67 |
| | 7.5 | 36.44 | 34.36 | 34.29 |
| | 9.5m | 26.47 | 28.78 | 26.74 |
| 61-62 | 1m | 114.08 | 108.97 | 98.32 |
| | 5m | 50.70 | 44.25 | 43.50 |
| | 7.5 | 43.62 | 45.97 | 42.62 |
| | 9.5m | 44.61 | 40.01 | 41.63 |
| 63-64 | 1m | 114.75 | 105.31 | 102.50 |
| | 5m | 54.21 | 45.72 | 44.14 |
| | 7.5 | 55.23 | 50.12 | 47.78 |

| Cases | Planes | LTR velocity | | |
|-------|-------------|--|--------------|--------------|
| | | 1m/s | 1.5m/s | 2m/s |
| | | Percentage increase in flow rate for each LTR velocity with the increase in distance of LB from 0.5 to 1m from the wall in the heading (%) | | |
| | 9.5m | 44.08 | 42.14 | 41.31 |
| 65-66 | 1m | 105.03 | 109.82 | 109.81 |
| | 5m | 36.55 | 35.89 | 37.52 |
| | 7.5 | 43.85 | 46.24 | 49.33 |
| | 9.5m | 38.35 | 39.09 | 40.51 |
| 67-68 | 1m | 73.48 | 71.65 | 70.16 |
| | 5m | 23.70 | 22.63 | 28.58 |
| | 7.5 | 36.57 | 34.85 | 39.97 |
| | 9.5m | 32.16 | 29.89 | 29.70 |
| 69-70 | 1m | 59.93 | 61.55 | 64.46 |
| | 5m | 25.24 | 24.24 | 26.09 |
| | 7.5 | 37.47 | 41.32 | 38.72 |
| | 9.5m | 37.99 | 35.65 | 35.05 |
| 71-72 | 1m | 65.70 | 63.27 | 60.17 |
| | 5m | 24.81 | 22.90 | 21.06 |
| | 7.5 | 29.56 | 27.50 | 26.64 |
| | 9.5m | 28.45 | 30.54 | 27.99 |

Table P3 Percentage increase in flow rate at specified planes for each LTR velocity with the increase in the distance of the LB from 0.5 to 1m from the wall in the heading - 6.6 x 3 x 20m heading

| Cases | Planes | LTR velocity | | |
|-------|--------------|--|--------------|--------------|
| | | 1m/s | 1.5m/s | 2m/s |
| | | Percentage increase in flow rate for each LTR velocity with the increase in distance of LB from 0.5 to 1m from the wall in the heading (%) | | |
| 25-26 | 1m | 96.07 | 98.59 | 96.01 |
| | 10m | 57.29 | 58.78 | 61.27 |
| | 15m | 68.67 | 69.18 | 69.76 |
| | 19.5m | 48.43 | 48.00 | 47.58 |
| 27-28 | 1m | 100.77 | 101.02 | 100.78 |
| | 10m | 57.28 | 59.35 | 61.06 |
| | 15m | 69.09 | 70.81 | 69.50 |
| | 19.5m | 48.73 | 46.08 | 48.35 |
| 29-30 | 1m | 95.32 | 105.17 | 98.98 |
| | 10m | 51.78 | 55.22 | 49.52 |
| | 15m | 75.89 | 74.87 | 74.39 |
| | 19.5m | 48.23 | 49.90 | 47.29 |
| 31-32 | 1m | 68.19 | 68.62 | 66.87 |
| | 10m | 40.02 | 45.81 | 40.89 |
| | 15m | 67.54 | 71.08 | 66.85 |
| | 19.5m | 38.90 | 35.01 | 35.13 |
| 33-34 | 1m | 65.01 | 66.74 | 68.01 |
| | 10m | 52.12 | 48.19 | 50.05 |
| | 15m | 66.09 | 65.87 | 68.41 |
| | 19.5m | 42.05 | 40.09 | 40.83 |
| 35-36 | 1m | 64.30 | 67.33 | 63.69 |
| | 10m | 40.28 | 39.16 | 40.28 |
| | 15m | 53.13 | 57.47 | 55.65 |
| | 19.5m | 33.44 | 32.95 | 31.78 |
| 37-38 | 1m | 101.05 | 101.06 | 106.57 |
| | 10m | 49.47 | 53.11 | 58.23 |
| | 15m | 66.91 | 65.03 | 61.59 |
| | 19.5m | 53.84 | 50.44 | 50.87 |
| 39-40 | 1m | 106.44 | 107.13 | 108.08 |
| | 10m | 52.42 | 58.62 | 56.38 |
| | 15m | 63.00 | 66.09 | 60.73 |
| | 19.5m | 50.74 | 51.42 | 51.39 |

| Cases | Planes | LTR velocity | | |
|-------|--------------|--|--------------|--------------|
| | | 1m/s | 1.5m/s | 2m/s |
| | | Percentage increase in flow rate for each LTR velocity with the increase in distance of LB from 0.5 to 1m from the wall in the heading (%) | | |
| 41-42 | 1m | 109.92 | 108.80 | 107.18 |
| | 10m | 55.62 | 55.99 | 47.44 |
| | 15m | 67.19 | 73.14 | 68.20 |
| | 19.5m | 48.98 | 48.93 | 50.97 |
| 43-44 | 1m | 77.34 | 73.85 | 71.09 |
| | 10m | 41.63 | 47.38 | 42.51 |
| | 15m | 65.01 | 64.89 | 62.68 |
| | 19.5m | 38.78 | 38.07 | 38.22 |
| 45-46 | 1m | 64.20 | 65.08 | 64.47 |
| | 10m | 54.51 | 49.91 | 50.13 |
| | 15m | 61.96 | 66.18 | 64.44 |
| | 19.5m | 46.87 | 44.36 | 43.28 |
| 47-48 | 1m | 66.45 | 68.15 | 66.86 |
| | 10m | 41.83 | 42.85 | 40.41 |
| | 15m | 50.77 | 54.12 | 56.53 |
| | 19.5m | 31.27 | 33.87 | 32.89 |

Table P4 Percentage increase in flow rate at specified planes for each LTR velocity with the increase in the distance of the LB from 0.5 to 1m from the wall in the heading - 6.6 x 4 x 20m heading

| Cases | Planes | LTR velocity | | |
|-------|--------------|--|--------------|--------------|
| | | 1m/s | 1.5m/s | 2m/s |
| | | Percentage increase in flow rate for each LTR velocity with the increase in distance of LB from 0.5 to 1m from the wall in the heading (%) | | |
| 73-74 | 1m | 97.29 | 100.93 | 98.38 |
| | 10m | 55.61 | 57.81 | 59.90 |
| | 15m | 69.67 | 72.66 | 71.70 |
| | 19.5m | 47.86 | 48.45 | 47.22 |
| 75-76 | 1m | 104.27 | 103.05 | 99.68 |
| | 10m | 57.53 | 58.31 | 59.74 |
| | 15m | 68.95 | 70.74 | 71.51 |
| | 19.5m | 47.73 | 46.91 | 49.61 |
| 77-78 | 1m | 96.30 | 102.56 | 103.57 |
| | 10m | 52.96 | 54.54 | 48.15 |
| | 15m | 79.01 | 78.33 | 76.55 |
| | 19.5m | 44.32 | 46.16 | 47.44 |
| 79-80 | 1m | 67.08 | 69.37 | 68.27 |
| | 10m | 39.46 | 42.57 | 37.08 |
| | 15m | 66.97 | 69.86 | 64.40 |
| | 19.5m | 38.70 | 36.57 | 35.86 |
| 81-82 | 1m | 68.12 | 68.48 | 71.68 |
| | 10m | 54.76 | 53.34 | 50.90 |
| | 15m | 68.85 | 66.89 | 65.47 |
| | 19.5m | 44.85 | 40.76 | 42.47 |
| 83-84 | 1m | 54.86 | 55.36 | 52.97 |
| | 10m | 41.15 | 37.10 | 37.57 |
| | 15m | 45.71 | 46.22 | 45.57 |
| | 19.5m | 32.19 | 34.03 | 35.28 |
| 85-86 | 1m | 104.53 | 103.81 | 106.19 |
| | 10m | 51.80 | 52.11 | 55.95 |
| | 15m | 65.05 | 64.61 | 62.48 |
| | 19.5m | 52.62 | 51.84 | 50.39 |
| 87-88 | 1m | 110.17 | 114.82 | 113.05 |
| | 10m | 54.31 | 57.11 | 58.64 |
| | 15m | 64.20 | 66.45 | 63.97 |

| Cases | Planes | LTR velocity | | |
|-------|--------------|--|--------------|--------------|
| | | 1m/s | 1.5m/s | 2m/s |
| | | Percentage increase in flow rate for each LTR velocity with the increase in distance of LB from 0.5 to 1m from the wall in the heading (%) | | |
| | 19.5m | 51.15 | 51.93 | 50.64 |
| 89-90 | 1m | 112.31 | 124.44 | 118.72 |
| | 10m | 55.87 | 54.87 | 51.48 |
| | 15m | 63.14 | 73.44 | 68.88 |
| | 19.5m | 48.89 | 48.88 | 51.47 |
| 91-92 | 1m | 77.64 | 76.44 | 74.00 |
| | 10m | 41.29 | 47.28 | 42.60 |
| | 15m | 57.39 | 57.20 | 54.66 |
| | 19.5m | 41.81 | 38.13 | 37.70 |
| 93-94 | 1m | 81.10 | 78.91 | 78.49 |
| | 10m | 52.74 | 50.46 | 47.79 |
| | 15m | 62.31 | 65.82 | 63.71 |
| | 19.5m | 46.96 | 44.32 | 43.52 |
| 95-96 | 1m | 62.16 | 62.83 | 61.90 |
| | 10m | 48.05 | 44.62 | 42.71 |
| | 15m | 49.16 | 54.55 | 52.85 |
| | 19.5m | 34.54 | 35.59 | 35.28 |

APPENDIX Q

**EFFECT OF DISTANCE OF LB FROM WALL IN HEADING ON FLOW RATE
CLOSE TO THE FACE AND AT THE EXIT OF LB**

Table Q1 Percentage increase in flow rate at 9.5m deep plane and at the exit of the LB for each LTR velocity with the increase in the distance of the LB from 0.5 to 1m from the wall in the heading - 6.6 x 4 x 10m heading

| Cases | LTR velocity | | | LTR velocity | | |
|-------|--|--------|-------|--|--------|--------|
| | 1m/s | 1.5m/s | 2m/s | 1m/s | 1.5m/s | 2m/s |
| | Percentage increase in flow rate for each LTR velocity with the increase in wall distance of the LB from 0.5 to 1m at the depth of 9.5m in the heading (%) | | | Percentage increase in flow rate for each LTR velocity with the increase in wall distance of the LB from 0.5 to 1m at the exit of LB (%) | | |
| 49-50 | 38.55 | 38.18 | 37.38 | 116.91 | 114.35 | 112.38 |
| 51-52 | 40.34 | 35.57 | 37.1 | 116.88 | 113.64 | 112.5 |
| 53-54 | 36.34 | 35.32 | 37.68 | 111.63 | 112.85 | 111.99 |
| 55-56 | 28.85 | 26.07 | 26.95 | 100.3 | 96.2 | 97.23 |
| 57-58 | 33.54 | 31.64 | 30.34 | 106.87 | 105.63 | 106.64 |
| 59-60 | 26.47 | 28.78 | 26.74 | 94.86 | 92.48 | 92.16 |
| 61-62 | 44.61 | 40.01 | 41.63 | 116.69 | 113.82 | 112.42 |
| 63-64 | 44.08 | 42.14 | 41.31 | 116.72 | 113.35 | 112.28 |
| 65-66 | 38.35 | 39.09 | 40.51 | 111.58 | 111.59 | 112.38 |
| 67-68 | 32.16 | 29.89 | 29.7 | 100.91 | 96.1 | 94.83 |
| 69-70 | 37.99 | 35.65 | 35.05 | 107.36 | 102.96 | 101.57 |
| 71-72 | 28.45 | 30.54 | 27.99 | 92.8 | 91.33 | 93.56 |

Table Q2 Percentage increase in flow rate at 19.5m deep plane and at the exit of the LB for each LTR velocity with the increase in the distance of the LB from 0.5 to 1m from the wall in the heading - 6.6 x 3 x 20m heading

| Cases | LTR velocity | | | LTR velocity | | |
|-------|---|--------|-------|--|--------|--------|
| | 1m/s | 1.5m/s | 2m/s | 1m/s | 1.5m/s | 2m/s |
| | Percentage increase in flow rate for each LTR velocity with the increase in wall distance of the LB from 0.5 to 1m at the depth of 19.5m in the heading (%) | | | Percentage increase in flow rate for each LTR velocity with the increase in wall distance of the LB from 0.5 to 1m at the exit of LB (%) | | |
| 25-26 | 48.43 | 48 | 47.58 | 115.3 | 113.4 | 113.33 |
| 27-28 | 48.73 | 46.08 | 48.35 | 115.18 | 113.39 | 112.85 |
| 29-30 | 48.23 | 49.9 | 47.29 | 111.04 | 110.25 | 112.7 |
| 31-32 | 38.9 | 35.01 | 35.13 | 100.43 | 95.71 | 95.45 |
| 33-34 | 42.05 | 40.09 | 40.83 | 107.2 | 103.53 | 103.82 |
| 35-36 | 33.44 | 32.95 | 31.78 | 93.58 | 93.38 | 93.44 |
| 37-38 | 53.84 | 50.44 | 50.87 | 115.3 | 112.79 | 112.86 |
| 39-40 | 50.74 | 51.42 | 51.39 | 114.55 | 113.35 | 112.66 |
| 41-42 | 48.98 | 48.93 | 50.97 | 110.86 | 110.19 | 112.77 |
| 43-44 | 38.78 | 38.07 | 38.22 | 100.11 | 95.94 | 95.19 |
| 45-46 | 46.87 | 44.36 | 43.28 | 107.23 | 103.5 | 103.84 |
| 47-48 | 31.27 | 33.87 | 32.89 | 93.58 | 93.41 | 93.48 |

Table Q3 Percentage increase in flow rate at 19.5m deep plane and at the exit of the LB for each LTR velocity with the increase in the distance of the LB from 0.5 to 1m from the wall in the heading - 6.6 x 4 x 20m heading

| Cases | LTR velocity | | | LTR velocity | | |
|-------|---|--------|-------|--|--------|--------|
| | 1m/s | 1.5m/s | 2m/s | 1m/s | 1.5m/s | 2m/s |
| | Percentage increase in flow rate for each LTR velocity with the increase in wall distance of the LB from 0.5 to 1m at the depth of 19.5m in the heading (%) | | | Percentage increase in flow rate for each LTR velocity with the increase in wall distance of the LB from 0.5 to 1m at the exit of LB (%) | | |
| 73-74 | 47.86 | 48.45 | 47.22 | 116.49 | 113.7 | 111.97 |
| 75-76 | 47.73 | 46.91 | 49.61 | 115.99 | 113.45 | 112.54 |
| 77-78 | 44.32 | 46.16 | 47.44 | 110.62 | 113.3 | 112.85 |
| 79-80 | 38.7 | 36.57 | 35.86 | 100.9 | 96.51 | 96.46 |
| 81-82 | 44.85 | 40.76 | 42.47 | 107.23 | 105.38 | 107.36 |
| 83-84 | 32.19 | 34.03 | 35.28 | 94.15 | 92.78 | 91.7 |
| 85-86 | 52.62 | 51.84 | 50.39 | 116.45 | 113.98 | 113.15 |
| 87-88 | 51.15 | 51.93 | 50.64 | 116.63 | 112.93 | 111.8 |
| 89-90 | 48.89 | 48.88 | 51.47 | 107.99 | 108.72 | 112.43 |
| 91-92 | 41.81 | 38.13 | 37.7 | 97.21 | 95.99 | 94.29 |
| 93-94 | 46.96 | 44.32 | 43.52 | 104.6 | 105.73 | 102.89 |
| 95-96 | 34.54 | 35.59 | 35.28 | 90.89 | 93.34 | 96.42 |

EFFECT OF LB DISTANCE FROM WALL IN HEADING ON FLOW RATE AT FACE

- Flow rates at 9.5m deep planes using LB with distance with 0.5m and 1m from the wall in the heading for LTR velocities of 1m/s, 1.5m/s, 2m/s - 6.6 x 4 x 10m heading

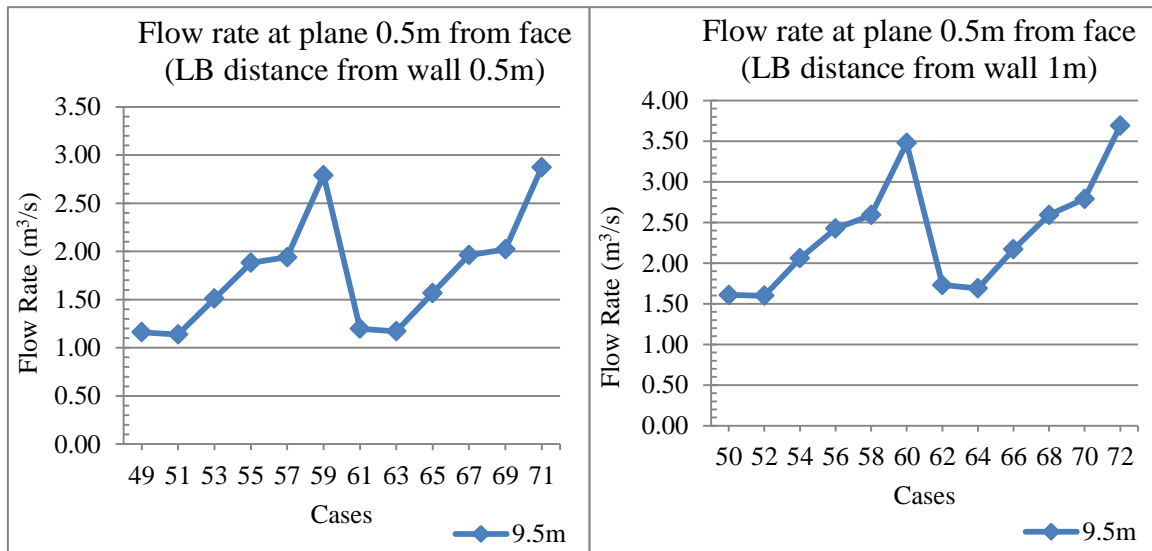


Figure R1 Flow rates at 9.5m deep planes using 0.5m and 1m distance of LB from wall for LTR velocity of 1m/s

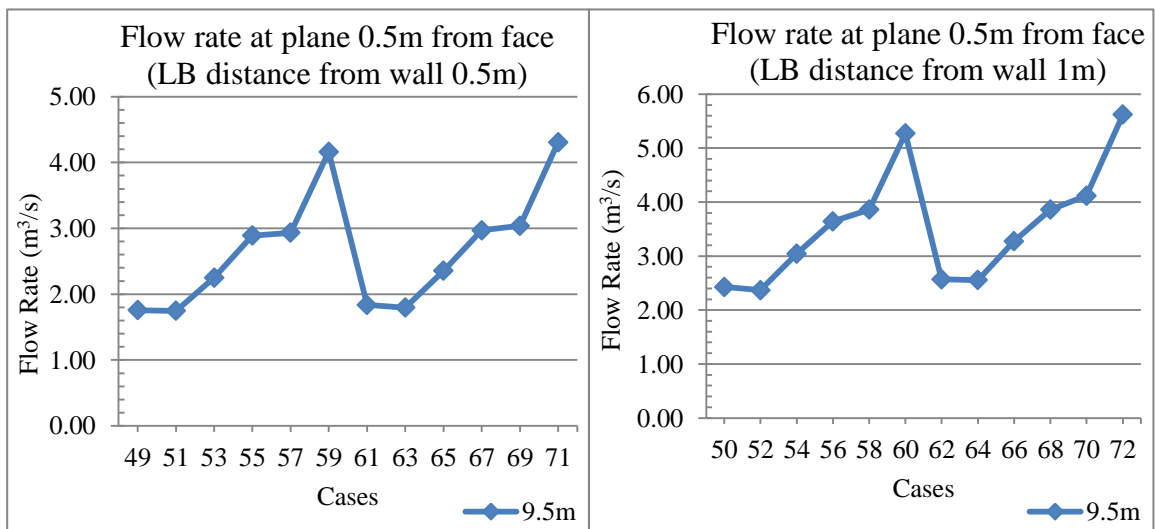


Figure R2 Flow rates at 9.5m deep planes using 0.5m and 1m distance of LB from wall for LTR velocity of 1.5m/s

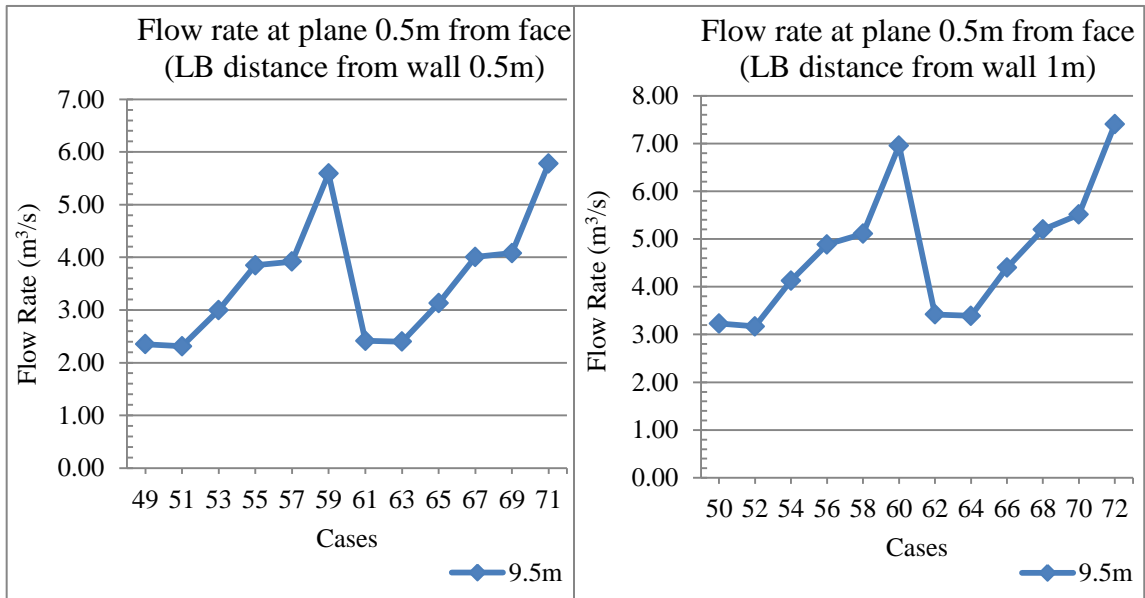


Figure R3 Flow rates at 9.5m deep planes using 0.5m and 1m distance of LB from wall for LTR velocity of 2m/s

- Flow rates at 19.5m deep planes using LB with distance with 0.5m and 1m from the wall in the heading for LTR velocities of 1m/s, 1.5m/s, 2m/s - 6.6 x 3 x 20m heading

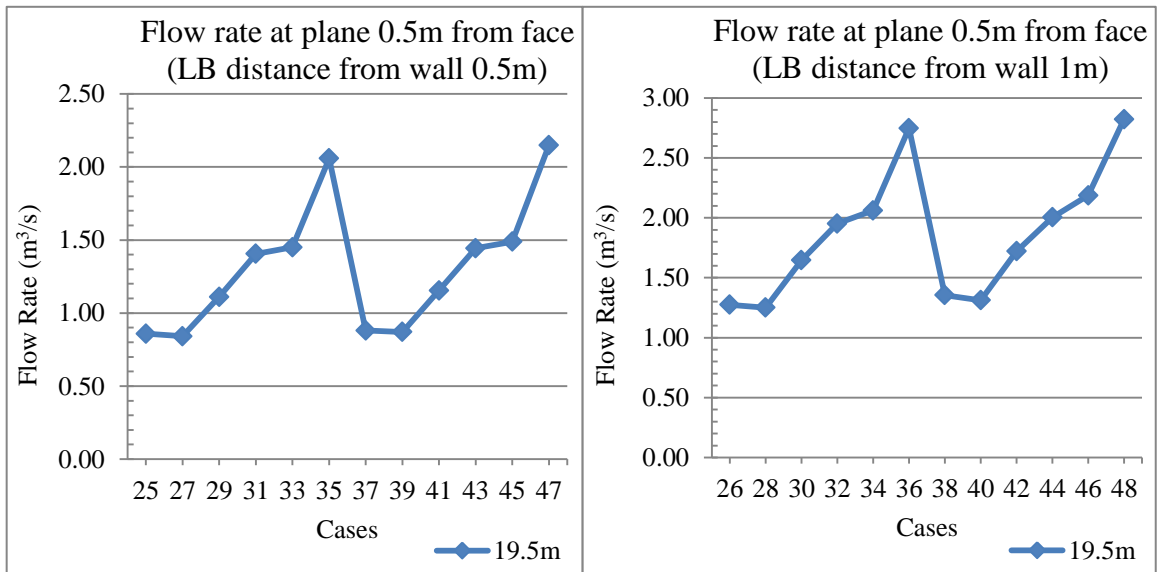


Figure R4 Flow rates at 19.5m deep planes using 0.5m and 1m distance of LB from wall for LTR velocity of 1m/s

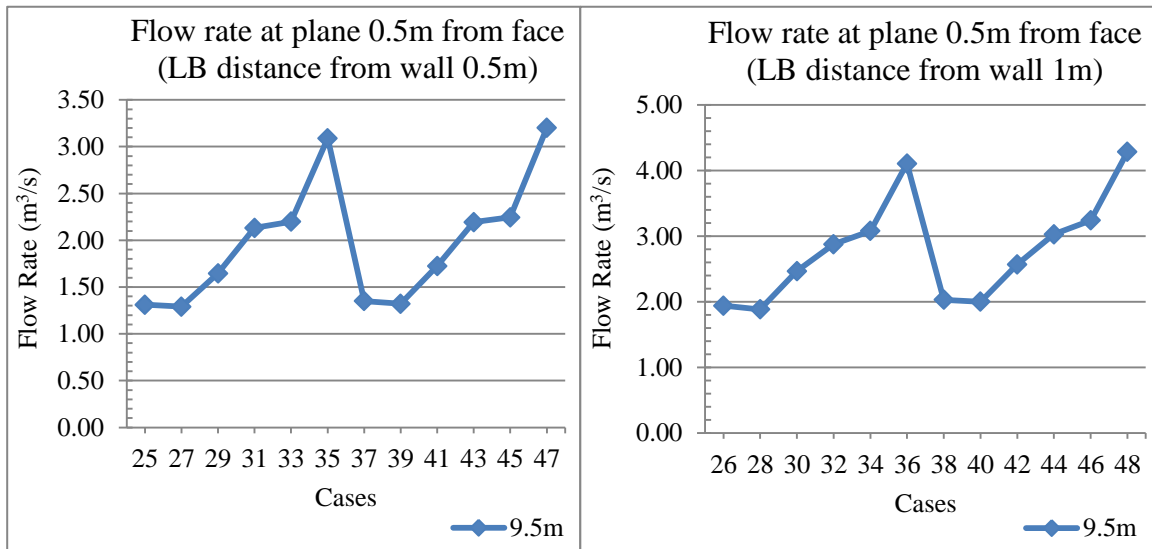


Figure R5 Flow rates at 19.5m deep planes using 0.5m and 1m distance of LB from wall for LTR velocity of 1.5m/s

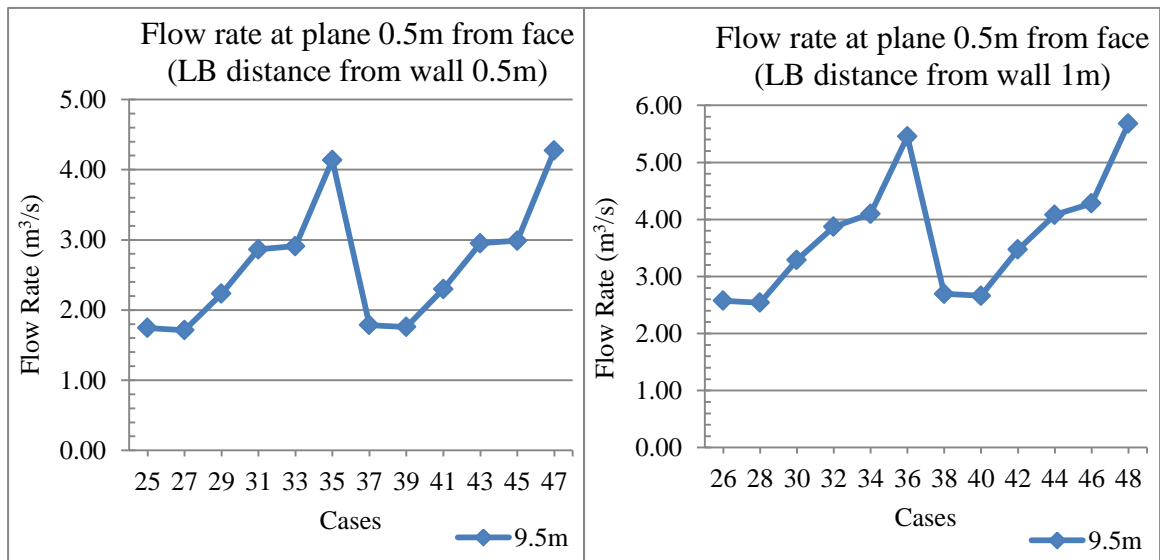


Figure R6 Flow rates at 19.5m deep planes using 0.5m and 1m distance of LB from wall for LTR velocity of 2m/s

- Flow rates at 19.5m deep planes using LB with distance with 0.5m and 1m from the wall in the heading for LTR velocities of 1m/s, 1.5m/s, 2m/s - 6.6 x 4 x 20m heading

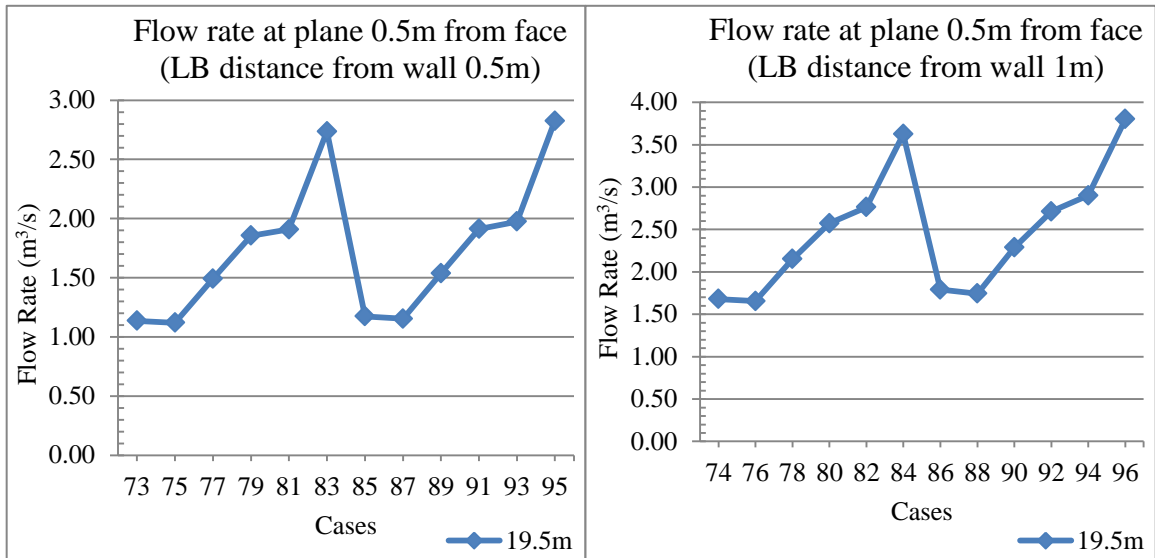


Figure R7 Flow rates at 19.5m deep planes using 0.5m and 1m distance of LB from wall for LTR velocity of 1m/s

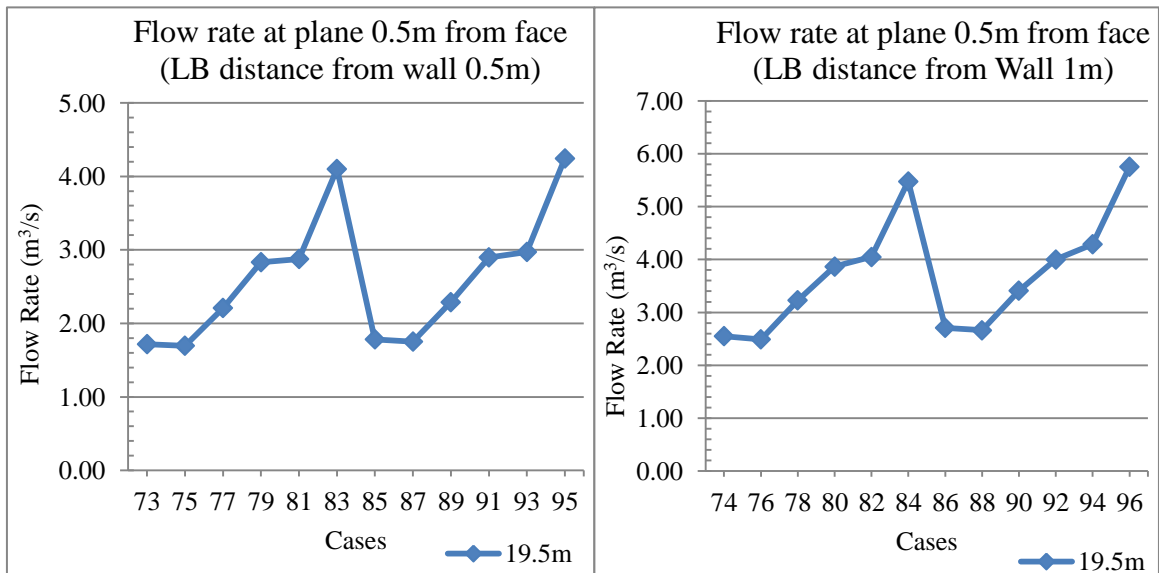


Figure R8 Flow rates at 19.5m deep planes using 0.5m and 1m distance of LB from wall for LTR velocity of 1.5m/s

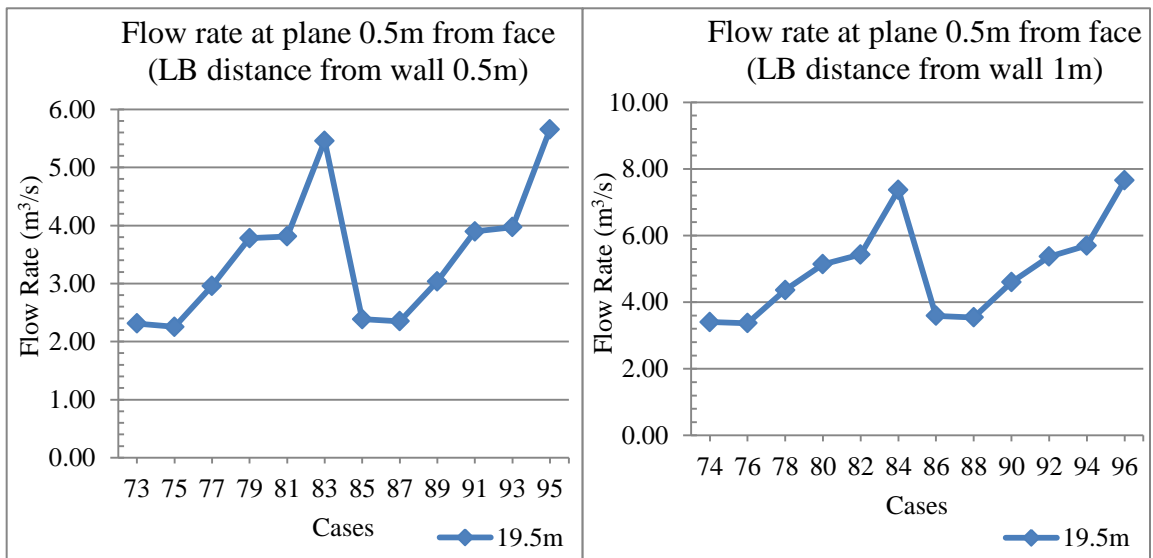


Figure R9 Flow rates at 19.5m deep plane using 0.5m and 1m distance of LB from wall for LTR velocity of 2m/s

EFFECT OF LB DISTANCE FROM WALL IN HEADING ON FLOW RATE AT ALL DEPTH PLANES

- Flow rates at specified depth planes using LB with 0.5m and 1m distance from the wall in the heading for LTR velocities of 1m/s, 1.5m/s, 2m/s - 6.6 x 4 x 10m heading

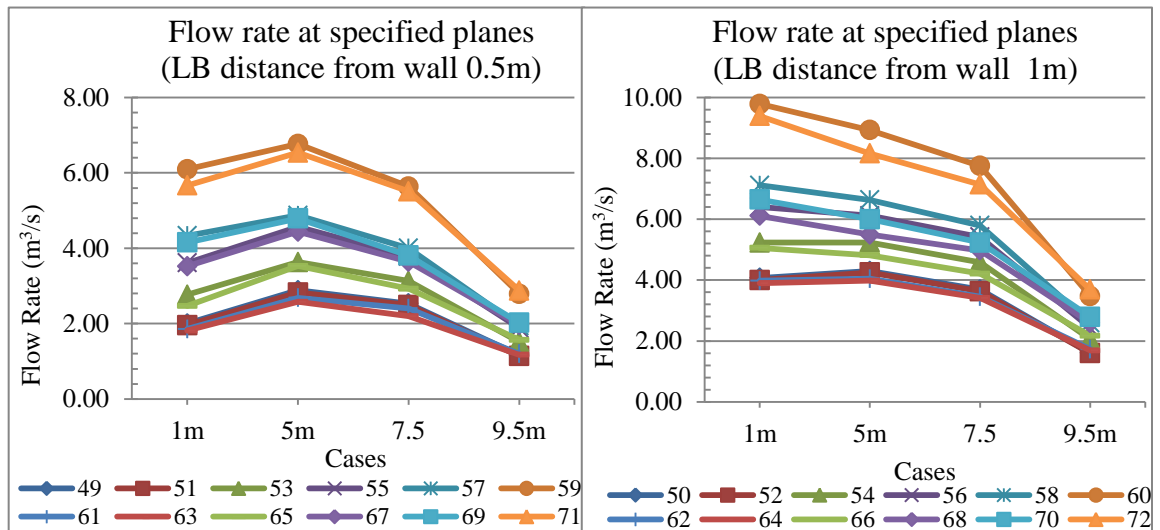


Figure S1 Flow rates at specified planes using 5m and 7.5m LB inside the heading for LTR velocity of 1m/s

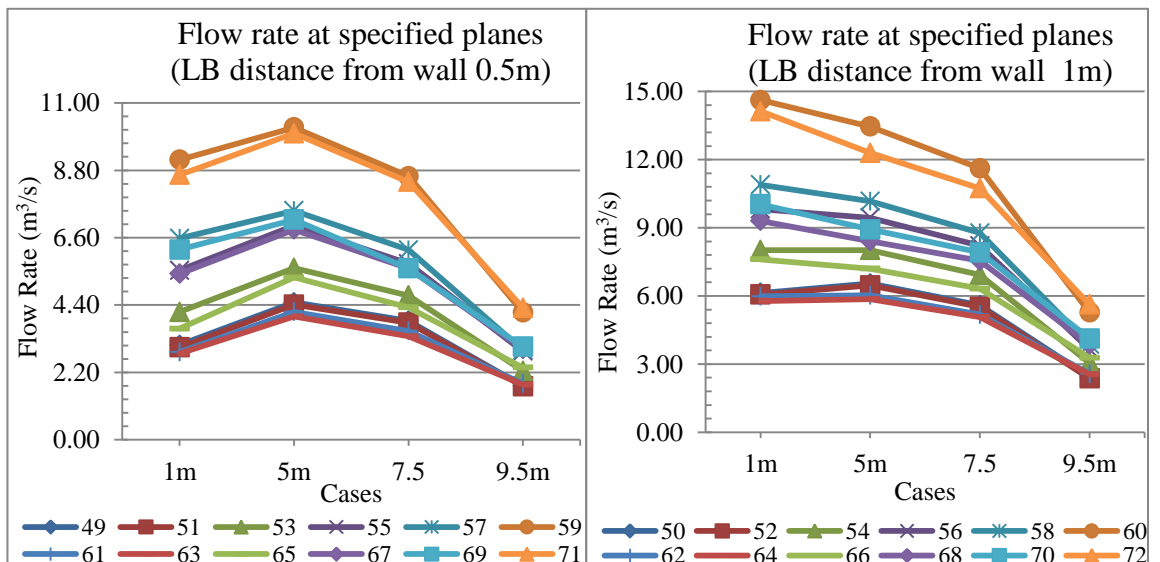


Figure S2 Flow rates at specified planes using 5m and 7.5m LB inside the heading for LTR velocity of 1.5m/s

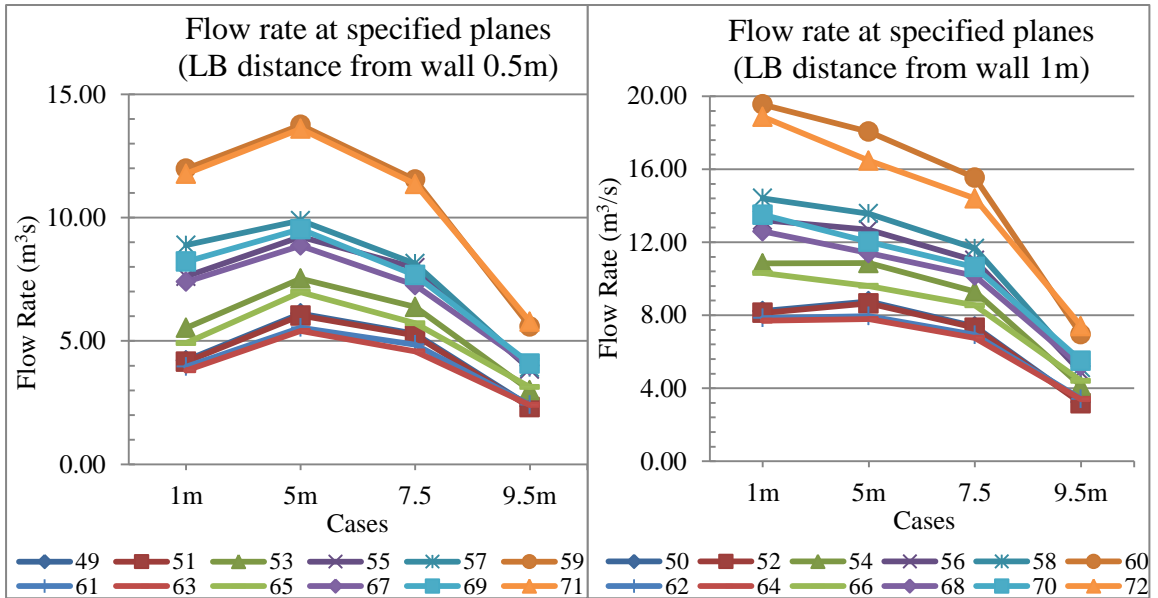


Figure S3 Flow rates at specified planes using 5m and 7.5m LB inside the heading for LTR velocity of 2m/s

- Flow rates at specified depth planes using LB with 0.5m and 1m distance from the wall in the heading for LTR velocities of 1m/s, 1.5m/s, 2m/s - 6.6 x 3 x 20m heading

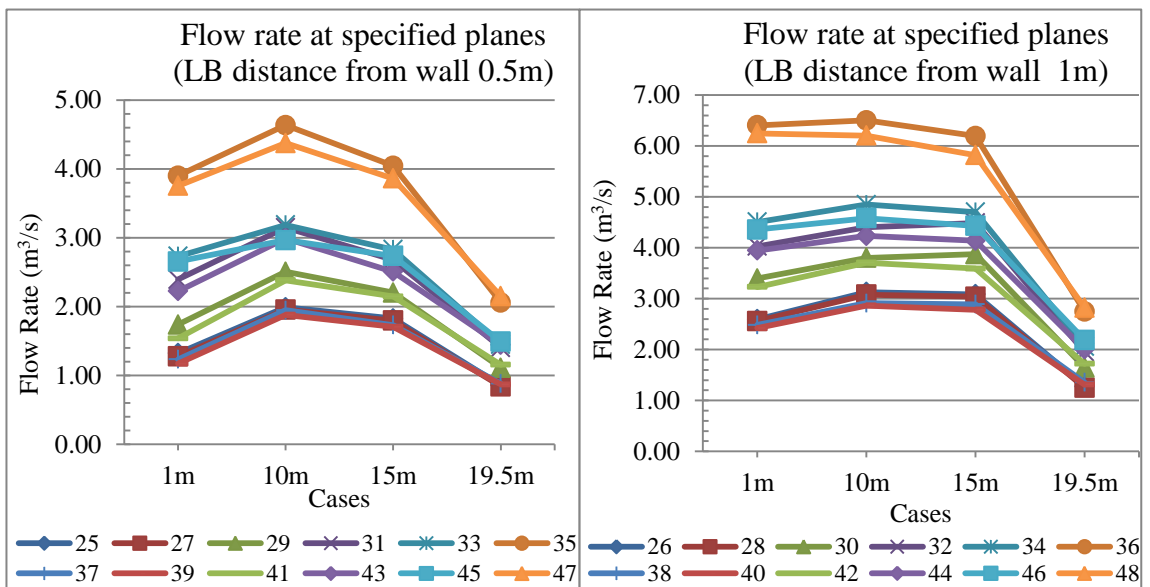


Figure S4 Flow rates at specified planes using 10m and 15m LB inside the heading for LTR velocity of 1m/s

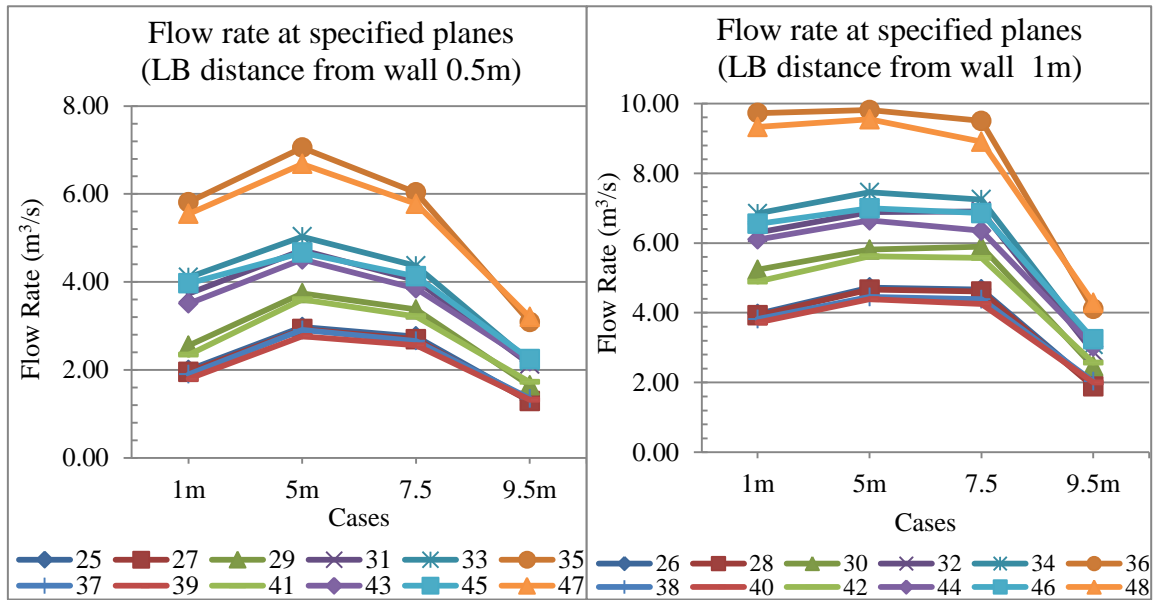


Figure S5 Flow rates at specified planes using 10m and 15m LB inside the heading for LTR velocity of 1.5m/s

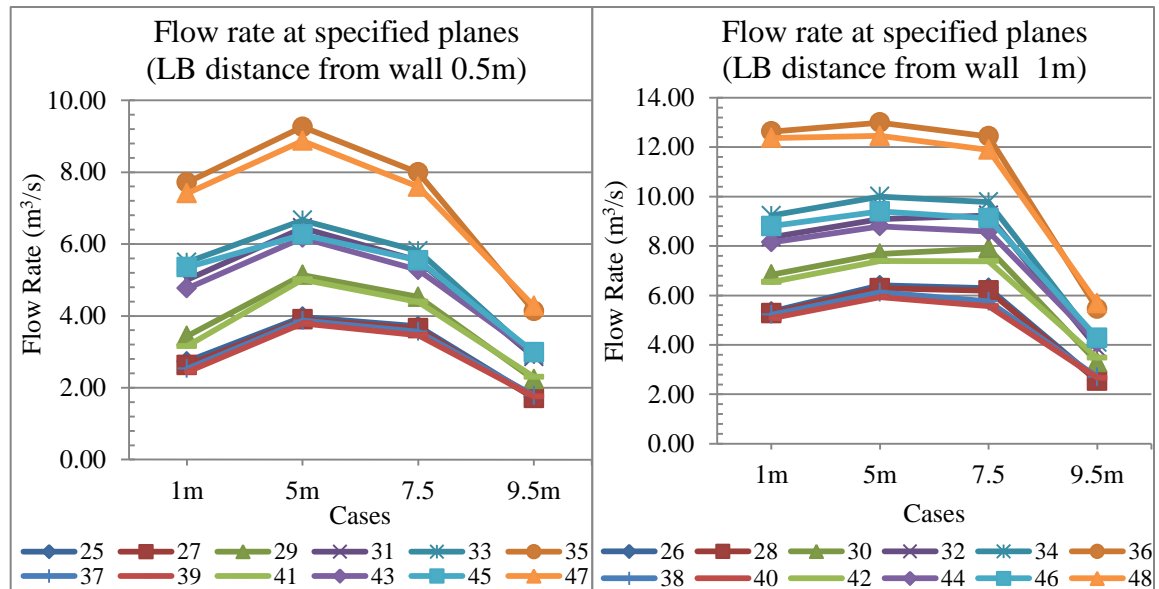


Figure S6 Flow rates at specified planes using 10m and 15m LB inside the heading for LTR velocity of 2m/s

- Flow rates at specified depth planes using LB with 0.5m and 1m distance from the wall in the heading for LTR velocities of 1m/s, 1.5m/s, 2m/s - 6.6 x 4 x 20m heading

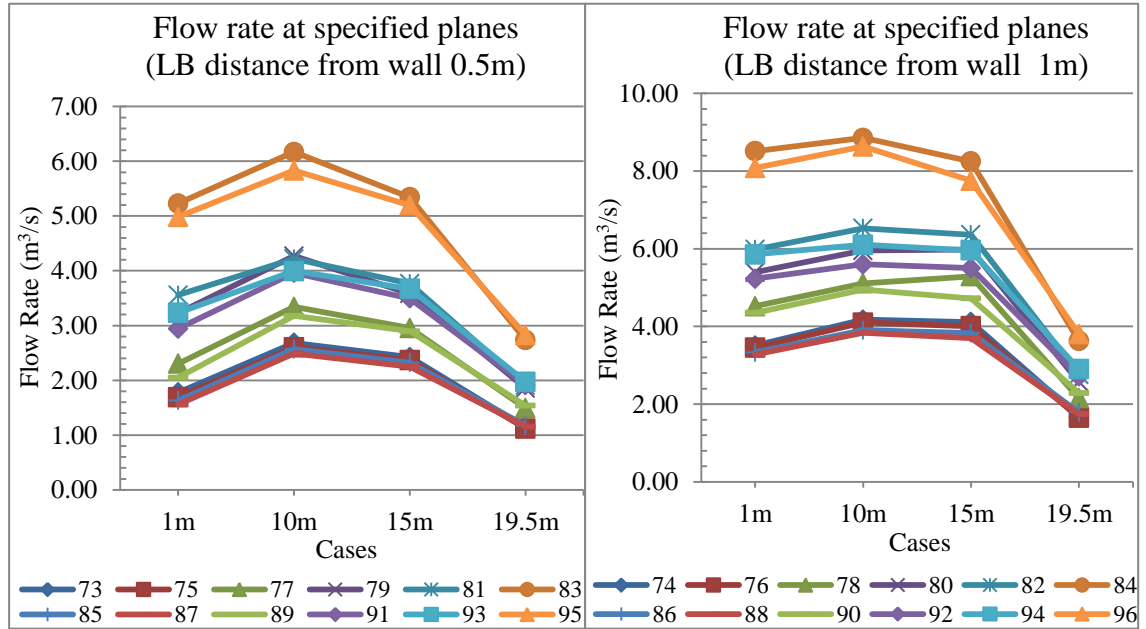


Figure S7 Flow rates at specified planes using 10m and 15m LB inside the heading for LTR velocity of 1m/s

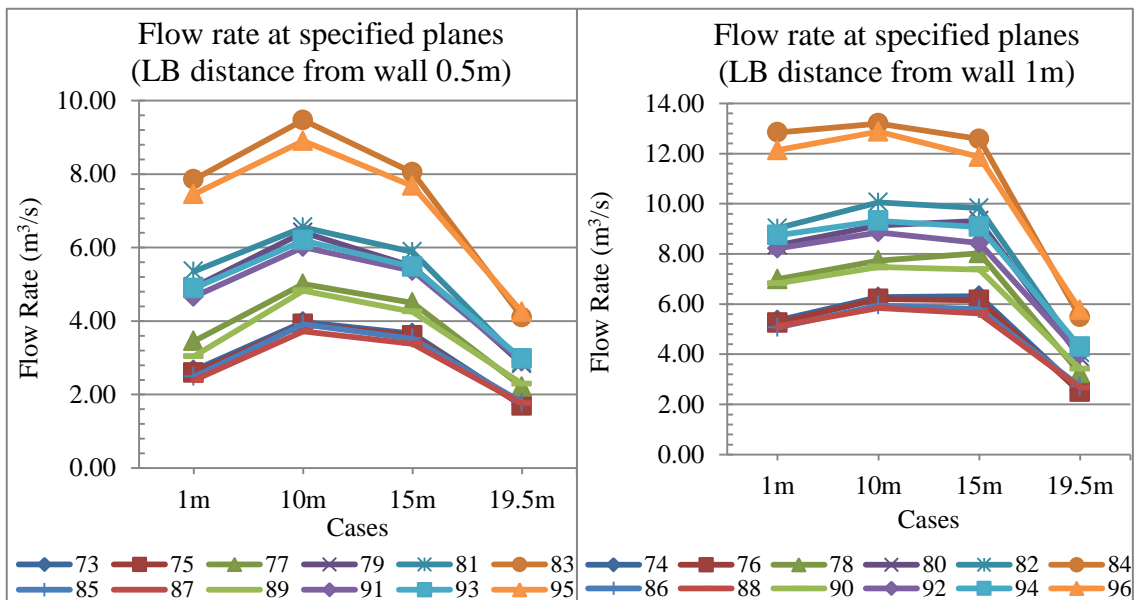


Figure S8 Flow rates at specified planes using 10m and 15m LB inside the heading for LTR velocity of 1m/s

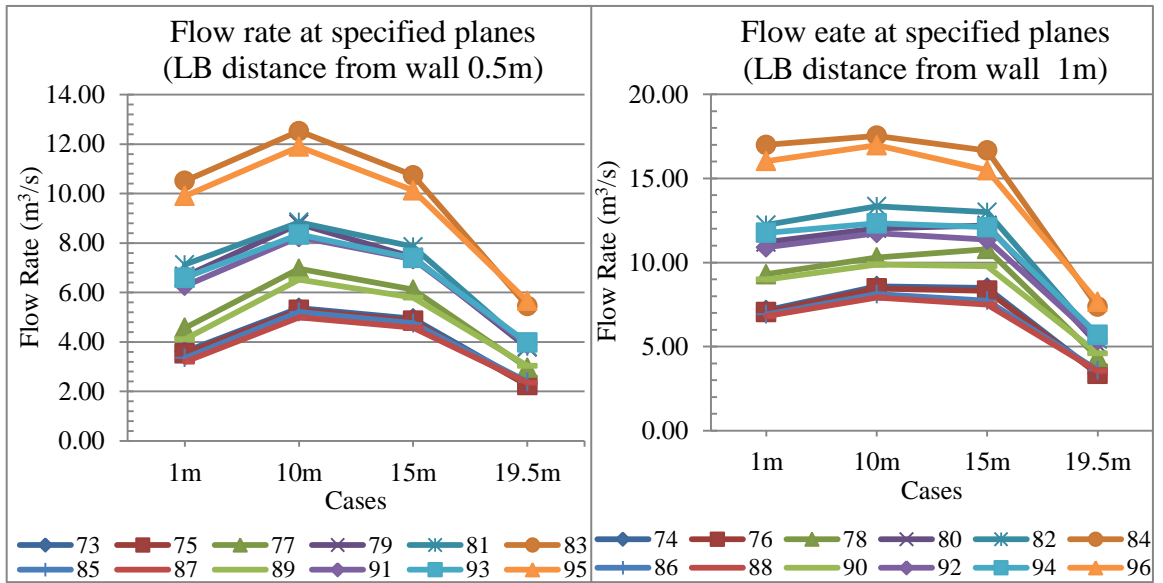


Figure S9 Flow rates at specified planes using 10m and 15m LB inside the heading for LTR velocity of 2m/s

APPENDIX T

EFFECT OF CHANGE IN ANGLE OF LB IN LTR ON FLOW RATES AT ALL DEPTH PLANES INSIDE THE HEADING

Table T1 Percentage increase in flow rates at the specified planes with the increase in angle (0°, 7.5° and 15°) of LB in the LTR – 6.6 x 3 x 10m heading

| Percentage increase in flow rates at the specified planes with the increase in angle of the LB in the LTR (between the cases with LB at 0°, 7.5° and 15°) | | | | | | | | | | |
|---|--------|--|--------|-------|---|--------|--------|---|--------|-------|
| Cases | Planes | LTR velocity | | | | | | | | |
| | | 1m/s | 1.5m/s | 2m/s | 1m/s | 1.5m/s | 2m/s | 1m/s | 1.5m/s | 2m/s |
| | | Percentage increase in flow rate with the increase in LB angle from 0° to 7.5° (%) | | | Percentage increase in flow rate with the increase in LB angle from 0° to 15° (%) | | | Percentage increase in flow rate with the increase in LB angle from 7.5° to 15° (%) | | |
| 1-5, 1-9, 5-9 | 1m | 42.18 | 38.30 | 36.86 | 122.13 | 114.17 | 115.74 | 56.24 | 54.86 | 57.64 |
| | 5m | 26.09 | 23.57 | 23.20 | 66.96 | 65.97 | 63.65 | 32.42 | 34.30 | 32.83 |
| | 7.5m | 23.62 | 21.63 | 18.44 | 58.83 | 60.25 | 56.75 | 28.48 | 31.75 | 32.35 |
| | 9.5m | 29.06 | 27.62 | 28.59 | 68.30 | 65.26 | 66.93 | 30.40 | 29.50 | 29.81 |
| 2-6, 2-10, 6-10 | 1m | 28.56 | 34.01 | 32.88 | 73.43 | 79.63 | 80.91 | 34.90 | 34.04 | 36.14 |
| | 5m | 19.79 | 22.87 | 25.57 | 52.24 | 57.74 | 59.91 | 27.10 | 28.38 | 27.35 |
| | 7.5m | 23.45 | 24.14 | 25.88 | 55.45 | 56.27 | 57.33 | 25.92 | 25.89 | 24.98 |
| | 9.5m | 25.37 | 26.54 | 28.58 | 59.35 | 59.02 | 62.12 | 27.10 | 25.67 | 26.09 |
| 3-7, 3-11, 7-11 | 1m | 96.83 | 92.78 | 89.92 | 229.74 | 216.34 | 209.15 | 67.52 | 64.10 | 62.78 |
| | 5m | 60.45 | 56.56 | 58.39 | 146.31 | 140.44 | 138.48 | 53.51 | 53.58 | 50.56 |
| | 7.5m | 54.39 | 49.33 | 55.03 | 135.67 | 129.69 | 128.67 | 52.65 | 53.81 | 47.50 |
| | 9.5m | 65.94 | 65.39 | 66.98 | 144.85 | 141.18 | 142.21 | 47.56 | 45.82 | 45.06 |
| 4-8, 4-12, 8-12 | 1m | 59.57 | 66.22 | 67.94 | 144.75 | 146.26 | 145.90 | 53.38 | 48.15 | 46.42 |
| | 5m | 42.58 | 47.85 | 50.71 | 109.45 | 111.88 | 113.56 | 46.90 | 43.31 | 41.70 |
| | 7.5m | 49.69 | 49.20 | 51.35 | 113.30 | 113.13 | 114.60 | 42.49 | 42.85 | 41.79 |
| | 9.5m | 53.73 | 54.43 | 52.99 | 121.33 | 124.01 | 119.06 | 43.97 | 45.05 | 43.19 |
| 13-17, 13-21, 17-21 | 1m | 29.77 | 27.12 | 27.81 | 124.63 | 125.88 | 115.19 | 73.10 | 77.69 | 68.36 |
| | 5m | 34.15 | 28.03 | 27.45 | 77.63 | 72.98 | 72.67 | 32.41 | 35.11 | 35.48 |
| | 7.5m | 24.97 | 22.67 | 23.82 | 64.99 | 67.48 | 61.22 | 32.02 | 36.54 | 30.20 |
| | 9.5m | 31.59 | 28.29 | 28.65 | 68.86 | 67.24 | 67.11 | 28.32 | 30.37 | 29.90 |
| 14-18, 14-22, 18-22 | 1m | 29.29 | 29.27 | 32.10 | 69.77 | 70.58 | 72.03 | 31.31 | 31.96 | 30.23 |
| | 5m | 20.82 | 18.37 | 21.99 | 49.36 | 48.20 | 53.70 | 23.63 | 25.20 | 25.99 |
| | 7.5m | 21.77 | 20.28 | 24.23 | 53.30 | 51.14 | 55.07 | 25.89 | 25.65 | 24.83 |
| | 9.5m | 26.76 | 27.59 | 28.93 | 61.37 | 60.24 | 60.83 | 27.31 | 25.60 | 24.74 |
| 15-19, 15-23, 19-23 | 1m | 102.90 | 102.88 | 96.70 | 225.55 | 224.49 | 218.42 | 60.45 | 59.95 | 61.88 |
| | 5m | 71.86 | 63.94 | 64.19 | 157.21 | 150.65 | 149.42 | 49.67 | 52.89 | 51.91 |
| | 7.5m | 57.82 | 54.24 | 58.12 | 141.75 | 139.38 | 142.03 | 53.18 | 55.19 | 53.07 |
| | 9.5m | 66.86 | 66.91 | 67.33 | 144.76 | 143.23 | 142.22 | 46.68 | 45.72 | 44.75 |
| 16-20, 16-24, 20-24 | 1m | 61.43 | 62.90 | 66.43 | 143.51 | 151.37 | 153.27 | 50.84 | 54.31 | 52.18 |
| | 5m | 42.49 | 42.60 | 45.89 | 111.55 | 110.18 | 110.56 | 48.47 | 47.39 | 44.32 |
| | 7.5m | 45.75 | 47.41 | 52.85 | 110.70 | 114.02 | 119.83 | 44.56 | 45.18 | 43.82 |
| | 9.5m | 53.58 | 52.02 | 52.35 | 118.95 | 121.81 | 118.57 | 42.57 | 45.91 | 43.46 |

Table T2 Percentage increase in flow rates at the specified planes with the increase in angle (0°, 7.5° and 15°) of LB in the LTR – 6.6 x 4 x 10m heading

| Percentage increase in flow rates at the specified planes with the increase in angle of the LB in the LTR (between the cases with LB at 0°,7.5° and 15°) | | | | | | | | | | |
|--|--------|--|--------|-------|---|--------|--------|---|--------|-------|
| Cases | Planes | LTR velocity | | | | | | | | |
| | | 1m/s | 1.5m/s | 2m/s | 1m/s | 1.5m/s | 2m/s | 1m/s | 1.5m/s | 2m/s |
| | | Percentage increase in flow rate with the increase in LB angle from 0° to 7.5° (%) | | | Percentage increase in flow rate with the increase in LB angle from 0° to 15° (%) | | | Percentage increase in flow rate with the increase in LB angle from 7.5° to 15° (%) | | |
| 49-53, 49-57, 53-57 | 1m | 38.23 | 34.76 | 31.34 | 116.59 | 112.51 | 111.04 | 56.69 | 57.70 | 60.69 |
| | 5m | 25.79 | 25.12 | 23.19 | 68.84 | 66.86 | 61.72 | 34.22 | 33.35 | 31.28 |
| | 7.5m | 23.64 | 21.29 | 20.62 | 58.05 | 59.62 | 53.86 | 27.83 | 31.60 | 27.56 |
| | 9.5m | 30.12 | 28.02 | 27.54 | 67.17 | 66.89 | 66.70 | 28.48 | 30.36 | 30.71 |
| 50-54, 50-58, 54-58 | 1m | 28.55 | 30.83 | 31.75 | 74.91 | 77.80 | 75.15 | 36.07 | 35.91 | 32.94 |
| | 5m | 21.94 | 22.56 | 23.89 | 54.57 | 55.38 | 54.84 | 26.75 | 26.78 | 24.98 |
| | 7.5m | 24.48 | 24.07 | 25.86 | 57.31 | 57.11 | 57.89 | 26.38 | 26.63 | 25.45 |
| | 9.5m | 28.04 | 25.37 | 27.81 | 61.13 | 58.99 | 58.16 | 25.84 | 26.82 | 23.74 |
| 51-55, 51-59, 55-59 | 1m | 84.35 | 83.50 | 83.16 | 211.18 | 203.25 | 188.29 | 68.80 | 65.26 | 57.40 |
| | 5m | 61.52 | 58.57 | 53.06 | 139.36 | 131.20 | 128.29 | 48.19 | 45.80 | 49.15 |
| | 7.5m | 51.58 | 50.48 | 52.44 | 126.06 | 125.19 | 120.78 | 49.14 | 49.65 | 44.83 |
| | 9.5m | 65.34 | 65.37 | 66.41 | 145.12 | 138.09 | 141.78 | 48.25 | 43.97 | 45.29 |
| 52-56, 52-60, 56-60 | 1m | 60.06 | 62.02 | 62.37 | 144.54 | 141.27 | 140.41 | 52.78 | 48.91 | 48.07 |
| | 5m | 43.98 | 46.10 | 46.74 | 110.22 | 108.25 | 108.89 | 46.01 | 42.54 | 42.35 |
| | 7.5m | 49.11 | 48.77 | 50.60 | 113.39 | 110.66 | 112.58 | 43.10 | 41.61 | 41.16 |
| | 9.5m | 51.80 | 53.78 | 54.10 | 117.59 | 122.52 | 119.46 | 43.34 | 44.70 | 42.42 |
| 61-65, 61-69, 69-65 | 1m | 32.81 | 26.68 | 24.13 | 123.61 | 116.88 | 107.48 | 68.37 | 71.21 | 67.14 |
| | 5m | 31.52 | 26.89 | 25.92 | 78.59 | 72.16 | 71.96 | 35.79 | 35.68 | 36.56 |
| | 7.5m | 21.70 | 21.75 | 17.73 | 58.33 | 57.75 | 57.89 | 30.10 | 29.57 | 34.12 |
| | 9.5m | 30.99 | 28.28 | 29.61 | 68.80 | 65.36 | 68.95 | 28.87 | 28.90 | 30.35 |
| 62-66, 62-70, 70-66 | 1m | 27.19 | 27.19 | 31.33 | 67.05 | 67.66 | 72.05 | 31.34 | 31.82 | 31.01 |
| | 5m | 19.17 | 19.53 | 20.68 | 48.41 | 48.28 | 51.10 | 24.54 | 24.05 | 25.21 |
| | 7.5m | 21.89 | 21.98 | 23.26 | 51.54 | 52.74 | 53.57 | 24.33 | 25.22 | 24.59 |
| | 9.5m | 25.32 | 27.44 | 28.59 | 61.07 | 60.20 | 61.11 | 28.53 | 25.70 | 25.29 |
| 63-67, 63-71, 67-71 | 1m | 94.14 | 92.58 | 94.55 | 212.45 | 207.57 | 209.79 | 60.94 | 59.71 | 59.24 |
| | 5m | 72.10 | 70.53 | 64.09 | 153.39 | 148.61 | 151.70 | 47.24 | 45.79 | 53.39 |
| | 7.5m | 65.60 | 65.89 | 58.68 | 150.78 | 149.55 | 148.42 | 51.44 | 50.43 | 56.55 |
| | 9.5m | 67.45 | 65.34 | 66.88 | 145.24 | 139.74 | 140.90 | 46.45 | 45.00 | 44.35 |
| 64-68, 64-72, 68-72 | 1m | 56.83 | 61.02 | 63.48 | 141.09 | 144.60 | 145.05 | 53.73 | 51.91 | 49.89 |
| | 5m | 38.05 | 43.50 | 46.38 | 105.08 | 109.67 | 111.40 | 48.55 | 46.11 | 44.42 |
| | 7.5m | 45.70 | 49.02 | 50.30 | 109.32 | 111.94 | 112.89 | 43.66 | 42.23 | 41.65 |
| | 9.5m | 53.61 | 51.10 | 53.18 | 118.64 | 120.18 | 118.20 | 42.34 | 45.72 | 42.45 |

Table T3 Percentage increase in flow rates at the specified planes with the increase in angle (0°, 7.5° and 15°) of LB in the LTR - 6.6 x 3 x 20m heading

| Percentage increase in flow rates at the specified planes with the increase in angle of the LB in the LTR (between the cases with LB at 0°,7.5° and 15°) | | | | | | | | | | |
|--|--------|--|--------|-------|---|--------|--------|---|--------|-------|
| Cases | Planes | LTR velocity | | | | | | | | |
| | | 1m/s | 1.5m/s | 2m/s | 1m/s | 1.5m/s | 2m/s | 1m/s | 1.5m/s | 2m/s |
| | | Percentage increase in flow rate with the increase in LB angle from 0° to 7.5° (%) | | | Percentage increase in flow rate with the increase in LB angle from 0° to 15° (%) | | | Percentage increase in flow rate with the increase in LB angle from 7.5° to 15° (%) | | |
| 25-29, 25-33, 29-33 | 1m | 31.40 | 27.69 | 26.12 | 106.39 | 105.61 | 101.39 | 57.06 | 61.02 | 59.68 |
| | 10m | 25.95 | 25.85 | 29.40 | 60.27 | 69.10 | 67.77 | 27.24 | 34.37 | 29.66 |
| | 15m | 20.52 | 22.27 | 22.09 | 54.79 | 58.32 | 56.51 | 28.43 | 29.48 | 28.19 |
| | 19.5m | 29.28 | 25.54 | 28.10 | 68.94 | 67.68 | 66.88 | 30.67 | 33.57 | 30.27 |
| 26-30, 26-34, 30-34 | 1m | 30.90 | 31.93 | 28.03 | 73.69 | 72.64 | 72.62 | 32.69 | 30.86 | 34.83 |
| | 10m | 21.54 | 23.03 | 19.97 | 55.00 | 57.82 | 56.09 | 27.52 | 28.28 | 30.11 |
| | 15m | 25.69 | 26.38 | 25.42 | 52.43 | 55.22 | 55.27 | 21.28 | 22.82 | 23.80 |
| | 19.5m | 29.11 | 27.15 | 27.85 | 61.67 | 58.72 | 59.24 | 25.22 | 24.83 | 24.55 |
| 27-31, 27-35, 31-35 | 1m | 87.78 | 91.18 | 90.45 | 205.77 | 197.51 | 193.55 | 62.84 | 55.62 | 54.13 |
| | 10m | 60.67 | 61.35 | 65.11 | 136.73 | 140.93 | 137.03 | 47.34 | 49.32 | 43.56 |
| | 15m | 49.09 | 49.62 | 51.54 | 125.08 | 123.66 | 118.76 | 50.97 | 49.49 | 44.36 |
| | 19.5m | 67.11 | 65.22 | 67.19 | 144.91 | 139.54 | 141.59 | 46.56 | 44.98 | 44.50 |
| 28-32, 28-36, 32-36 | 1m | 57.31 | 60.37 | 58.28 | 150.23 | 147.64 | 139.32 | 59.07 | 54.43 | 51.20 |
| | 10m | 43.04 | 47.64 | 44.43 | 111.14 | 110.40 | 106.45 | 47.61 | 42.51 | 42.94 |
| | 15m | 47.73 | 49.85 | 49.17 | 103.83 | 106.19 | 100.89 | 37.98 | 37.59 | 34.67 |
| | 19.5m | 57.31 | 52.70 | 52.30 | 119.73 | 118.02 | 114.61 | 40.79 | 42.78 | 40.91 |
| 37-41, 37-45, 41-45 | 1m | 24.60 | 23.38 | 24.99 | 115.00 | 108.78 | 111.84 | 72.55 | 69.22 | 69.49 |
| | 10m | 22.27 | 23.88 | 29.61 | 52.19 | 60.52 | 61.86 | 24.47 | 29.58 | 24.88 |
| | 15m | 24.03 | 21.04 | 23.24 | 58.00 | 55.19 | 55.63 | 27.39 | 28.21 | 26.28 |
| | 19.5m | 31.13 | 27.78 | 28.79 | 69.08 | 66.28 | 67.34 | 28.94 | 30.13 | 29.94 |
| 38-42, 38-46, 42-46 | 1m | 30.10 | 28.12 | 25.36 | 75.59 | 71.42 | 68.67 | 34.97 | 33.79 | 34.55 |
| | 10m | 27.31 | 26.21 | 20.78 | 57.33 | 57.17 | 53.57 | 23.58 | 24.53 | 27.15 |
| | 15m | 24.24 | 26.99 | 28.28 | 53.31 | 56.28 | 58.38 | 23.40 | 23.06 | 23.46 |
| | 19.5m | 27.00 | 26.50 | 28.88 | 61.43 | 59.55 | 58.93 | 27.11 | 26.13 | 23.32 |
| 39-43, 39-47, 43-47 | 1m | 89.78 | 95.56 | 95.27 | 220.18 | 209.20 | 203.87 | 68.71 | 58.11 | 55.62 |
| | 10m | 58.97 | 62.96 | 62.70 | 132.78 | 141.56 | 133.85 | 46.43 | 48.23 | 43.73 |
| | 15m | 47.03 | 50.49 | 52.41 | 126.30 | 125.63 | 119.31 | 53.91 | 49.93 | 43.90 |
| | 19.5m | 65.87 | 65.98 | 67.85 | 147.01 | 142.33 | 143.05 | 48.92 | 46.00 | 44.81 |
| 40-44, 40-48, 44-48 | 1m | 63.03 | 64.14 | 60.56 | 158.16 | 151.01 | 143.68 | 58.35 | 52.93 | 51.77 |
| | 10m | 47.72 | 51.42 | 48.26 | 116.60 | 117.54 | 109.96 | 46.63 | 43.67 | 41.61 |
| | 15m | 48.84 | 49.40 | 54.26 | 109.31 | 109.37 | 113.59 | 40.63 | 40.14 | 38.46 |
| | 19.5m | 52.71 | 51.34 | 53.24 | 115.10 | 114.25 | 113.35 | 40.86 | 41.57 | 39.22 |

Table T4 Percentage increase in flow rates at the specified planes with the increase in angle (0°, 7.5° and 15°) of LB in the LTR - 6.6 x 4 x 20m heading

| Percentage increase in flow rates at the specified planes with the increase in angle of the LB in the LTR (between the cases with LB at 0°, 7.5° and 15°) | | | | | | | | | | |
|---|--------|--|--------|-------|---|--------|--------|---|--------|-------|
| Cases | Planes | LTR velocity | | | | | | | | |
| | | 1m/s | 1.5m/s | 2m/s | 1m/s | 1.5m/s | 2m/s | 1m/s | 1.5m/s | 2m/s |
| | | Percentage increase in flow rate with the increase in LB angle from 0° to 7.5° (%) | | | Percentage increase in flow rate with the increase in LB angle from 0° to 15° (%) | | | Percentage increase in flow rate with the increase in LB angle from 7.5° to 15° (%) | | |
| 73-77, 73-81, 77-81 | 1m | 29.51 | 29.67 | 26.53 | 100.14 | 101.15 | 97.37 | 54.53 | 55.12 | 55.98 |
| | 10m | 24.49 | 25.88 | 29.48 | 57.15 | 64.83 | 64.51 | 26.23 | 30.94 | 27.06 |
| | 15m | 21.95 | 22.87 | 23.61 | 55.46 | 60.74 | 58.73 | 27.48 | 30.83 | 28.42 |
| | 19.5m | 31.29 | 28.63 | 28.04 | 68.02 | 67.44 | 64.93 | 27.98 | 30.18 | 28.81 |
| 74-78, 74-82, 78-82 | 1m | 28.86 | 30.73 | 29.84 | 70.55 | 68.66 | 70.81 | 32.35 | 29.01 | 31.55 |
| | 10m | 22.37 | 23.27 | 19.97 | 56.29 | 60.15 | 55.26 | 27.72 | 29.92 | 29.42 |
| | 15m | 28.67 | 26.90 | 27.10 | 54.71 | 55.37 | 52.98 | 20.24 | 22.43 | 20.36 |
| | 19.5m | 28.14 | 26.64 | 28.24 | 64.60 | 58.77 | 59.61 | 28.45 | 25.37 | 24.46 |
| 75-79, 75-83, 79-83 | 1m | 90.88 | 90.24 | 88.44 | 209.29 | 203.31 | 197.57 | 62.03 | 59.44 | 57.92 |
| | 10m | 64.05 | 63.76 | 65.73 | 137.02 | 141.90 | 136.72 | 44.47 | 47.72 | 42.84 |
| | 15m | 51.17 | 52.24 | 53.07 | 125.28 | 123.26 | 121.27 | 49.02 | 46.65 | 44.56 |
| | 19.5m | 65.64 | 67.09 | 67.86 | 144.25 | 141.99 | 142.26 | 47.46 | 44.83 | 44.32 |
| 76-80, 76-84, 80-84 | 1m | 56.13 | 58.68 | 58.79 | 146.43 | 144.34 | 140.89 | 57.84 | 53.98 | 51.70 |
| | 10m | 45.24 | 47.48 | 42.21 | 115.93 | 112.98 | 107.47 | 48.67 | 44.41 | 45.88 |
| | 15m | 49.40 | 51.45 | 46.72 | 105.92 | 104.54 | 100.15 | 37.84 | 35.06 | 36.41 |
| | 19.5m | 55.51 | 55.34 | 52.43 | 119.11 | 120.07 | 118.76 | 40.90 | 41.67 | 43.52 |
| 85-89, 85-93, 89-93 | 1m | 25.70 | 22.36 | 22.68 | 98.36 | 96.78 | 96.82 | 57.81 | 60.82 | 60.44 |
| | 10m | 23.61 | 23.44 | 25.18 | 55.41 | 58.38 | 60.12 | 25.73 | 28.30 | 27.91 |
| | 15m | 24.83 | 20.85 | 21.79 | 58.22 | 55.42 | 55.38 | 26.75 | 28.61 | 27.58 |
| | 19.5m | 30.95 | 28.41 | 27.31 | 68.28 | 66.64 | 66.48 | 28.51 | 29.77 | 30.77 |
| 86-90, 86-94, 90-94 | 1m | 30.48 | 34.75 | 30.13 | 75.63 | 72.74 | 70.38 | 34.60 | 28.20 | 30.93 |
| | 10m | 26.93 | 25.68 | 21.59 | 56.38 | 56.66 | 51.74 | 23.20 | 24.65 | 24.79 |
| | 15m | 23.38 | 27.33 | 26.59 | 55.59 | 56.56 | 56.55 | 26.11 | 22.96 | 23.67 |
| | 19.5m | 27.76 | 25.90 | 28.22 | 62.04 | 58.38 | 58.86 | 26.84 | 25.80 | 23.90 |
| 87-91, 87-95, 91-95 | 1m | 88.53 | 95.34 | 96.16 | 219.24 | 212.54 | 209.97 | 69.32 | 60.00 | 58.02 |
| | 10m | 59.23 | 61.53 | 65.18 | 134.25 | 139.15 | 138.43 | 47.11 | 48.05 | 44.34 |
| | 15m | 55.23 | 58.70 | 60.57 | 130.85 | 127.08 | 121.49 | 48.72 | 43.09 | 37.93 |
| | 19.5m | 65.86 | 65.40 | 65.87 | 145.08 | 142.34 | 140.70 | 47.77 | 46.52 | 45.12 |
| 88-92, 88-96, 92-96 | 1m | 59.36 | 60.44 | 60.20 | 146.31 | 136.89 | 135.56 | 54.57 | 47.65 | 47.04 |
| | 10m | 45.79 | 51.42 | 48.49 | 124.74 | 120.14 | 114.49 | 54.15 | 45.38 | 44.45 |
| | 15m | 48.80 | 49.88 | 51.46 | 109.71 | 110.84 | 106.47 | 40.94 | 40.68 | 36.32 |
| | 19.5m | 55.62 | 50.38 | 51.62 | 118.16 | 116.27 | 116.15 | 40.19 | 43.82 | 42.56 |

APPENDIX U

**EFFECT OF CHANGE IN ANGLE OF LB IN LTR ON FLOW RATES CLOSE TO
FACE AND EXIT OF LB**

Table U1 Percentage increase in flow rates at the 9.5m deep plane with the increase in LB angle in the LTR from 0° to 7.5°, 0° to 15°, and 7.5° to 15°- 6.6 x 4 x 10m heading

| Percentage increase in flow rates at the 9.5m deep plane with the increase in LB angle in the LTR from 0° to 7.5°, 0° to 15°, and 7.5° to 15° | | | | | | | | | |
|---|---|--------|-------|--|--------|--------|--|--------|-------|
| Cases | LTR velocity | | | | | | | | |
| | 1m/s | 1.5m/s | 2m/s | 1m/s | 1.5m/s | 2m/s | 1m/s | 1.5m/s | 2m/s |
| | Percentage increase in flow rate with LB angle increase from 0° to 7.5° (%) | | | Percentage increase in flow rate with LB angle increase from 0° to 15° (%) | | | Percentage increase in flow rate with LB angle increase from 7.5° to 15° (%) | | |
| 49-53,49-57,53-57 | 30.12 | 28.02 | 27.54 | 67.17 | 66.89 | 66.70 | 28.48 | 30.36 | 30.71 |
| 50-54,50-58,54-58 | 28.04 | 25.37 | 27.81 | 61.13 | 58.99 | 58.16 | 25.84 | 26.82 | 23.74 |
| 51-55,51-59,55-59 | 65.34 | 65.37 | 66.41 | 145.12 | 138.09 | 141.78 | 48.25 | 43.97 | 45.29 |
| 52-56,52-60,56-60 | 51.80 | 53.78 | 54.10 | 117.59 | 122.52 | 119.46 | 43.34 | 44.70 | 42.42 |
| 61-65,61-69,65-69 | 30.99 | 28.28 | 29.61 | 68.80 | 65.36 | 68.95 | 28.87 | 28.90 | 30.35 |
| 62-66,62-70,66-70 | 25.32 | 27.44 | 28.59 | 61.07 | 60.20 | 61.11 | 28.53 | 25.70 | 25.29 |
| 63-67,63-71,67-71 | 67.45 | 65.34 | 66.88 | 145.24 | 139.74 | 140.90 | 46.45 | 45.00 | 44.35 |
| 64-68,64-72,68-72 | 53.61 | 51.10 | 53.18 | 118.64 | 120.18 | 118.20 | 42.34 | 45.72 | 42.45 |

Table U2 Percentage increase in flow rates at the exit of the LB with the increase in LB angle in the LTR from 0° to 7.5°, 0° to 15°, and 7.5° to 15°- 6.6 x 4 x 10m heading

| Percentage increase in flow rates at the exit of the LB with the increase in LB angle in the LTR from 0° to 7.5°, 0° to 15°, and 7.5° to 15° | | | | | | | | | |
|--|---|--------|-------|--|--------|--------|--|--------|-------|
| Cases | LTR velocity | | | | | | | | |
| | 1m/s | 1.5m/s | 2m/s | 1m/s | 1.5m/s | 2m/s | 1m/s | 1.5m/s | 2m/s |
| | Percentage increase in flow rate with LB angle increase from 0° to 7.5° (%) | | | Percentage increase in flow rate with LB angle increase from 0° to 15° (%) | | | Percentage increase in flow rate with LB angle increase from 7.5° to 15° (%) | | |
| 49-53,49-57,53-57 | 30.31 | 28.24 | 28.20 | 68.91 | 67.08 | 65.42 | 29.62 | 30.29 | 29.04 |
| 50-54,50-58,54-58 | 27.14 | 27.34 | 27.97 | 61.09 | 60.29 | 60.95 | 26.70 | 25.87 | 25.78 |
| 51-55,51-59,55-59 | 65.80 | 67.03 | 66.02 | 144.19 | 143.40 | 142.28 | 47.28 | 45.72 | 45.93 |
| 52-56,52-60,56-60 | 53.12 | 53.40 | 54.09 | 119.39 | 119.30 | 119.09 | 43.28 | 42.96 | 42.18 |
| 61-65,61-69,65-69 | 30.14 | 28.10 | 27.15 | 68.57 | 67.98 | 65.42 | 29.52 | 31.13 | 30.11 |
| 62-66,62-70,66-70 | 27.08 | 26.77 | 27.12 | 61.31 | 59.45 | 56.97 | 26.94 | 25.78 | 23.49 |
| 63-67,63-71,67-71 | 65.77 | 65.72 | 66.22 | 143.10 | 141.37 | 139.28 | 46.65 | 45.65 | 43.95 |
| 64-68,64-72,68-72 | 53.68 | 52.32 | 52.56 | 116.27 | 116.46 | 118.17 | 40.73 | 42.10 | 43.01 |

Table U3 Percentage increase in flow rates at the 19.5m deep plane with the increase in LB angle in the LTR from 0° to 7.5°, 0° to 15°, and 7.5° to 15° - 6.6 x 3 x 20m heading

| Percentage increase in flow rates at the 9.5m deep plane with the increase in LB angle in the LTR from 0° to 7.5°, 0° to 15°, and 7.5° to 15° | | | | | | | | | |
|---|---|--------|-------|--|--------|--------|--|--------|-------|
| Cases | LTR velocity | | | | | | | | |
| | 1m/s | 1.5m/s | 2m/s | 1m/s | 1.5m/s | 2m/s | 1m/s | 1.5m/s | 2m/s |
| | Percentage increase in flow rate with LB angle increase from 0° to 7.5° (%) | | | Percentage increase in flow rate with LB angle increase from 0° to 15° (%) | | | Percentage increase in flow rate with LB angle increase from 7.5° to 15° (%) | | |
| 25-29,25-33,29-33 | 29.28 | 25.54 | 28.10 | 68.94 | 67.68 | 66.88 | 30.67 | 33.57 | 30.27 |
| 26-30,26-34,30-34 | 29.11 | 27.15 | 27.85 | 61.67 | 58.72 | 59.24 | 25.22 | 24.83 | 24.55 |
| 27-31,27-35,31-35 | 67.11 | 65.22 | 67.19 | 144.91 | 139.54 | 141.59 | 46.56 | 44.98 | 44.50 |
| 28-32,28-36,32-36 | 57.31 | 52.70 | 52.30 | 119.73 | 118.02 | 114.61 | 40.79 | 42.78 | 40.91 |
| 37-41,37-45,41-45 | 31.13 | 27.78 | 28.79 | 69.08 | 66.28 | 67.34 | 28.94 | 30.13 | 29.94 |
| 38-42,38-46,42-46 | 27.00 | 26.50 | 28.88 | 61.43 | 59.55 | 58.93 | 27.11 | 26.13 | 23.32 |
| 39-43,39-47,43-47 | 65.87 | 65.98 | 67.85 | 147.01 | 142.33 | 143.05 | 48.92 | 46.00 | 44.81 |
| 40-44,40-48,44-48 | 52.71 | 51.34 | 53.24 | 115.10 | 114.25 | 113.35 | 40.86 | 41.57 | 39.22 |

Table U4 Percentage increase in flow rates at the exit of the LB with the increase in LB angle in the LTR from 0° to 7.5°, 0° to 15°, and 7.5° to 15° - 6.6 x 3 x 20m heading

| Percentage increase in flow rates at the exit of the LB with the increase in LB angle in the LTR from 0° to 7.5°, 0° to 15°, and 7.5° to 15° | | | | | | | | | |
|--|---|--------|-------|--|--------|--------|--|--------|-------|
| Cases | LTR velocity | | | | | | | | |
| | 1m/s | 1.5m/s | 2m/s | 1m/s | 1.5m/s | 2m/s | 1m/s | 1.5m/s | 2m/s |
| | Percentage increase in flow rate with LB angle increase from 0° to 7.5° (%) | | | Percentage increase in flow rate with LB angle increase from 0° to 15° (%) | | | Percentage increase in flow rate with LB angle increase from 7.5° to 15° (%) | | |
| 25-29,25-33,29-33 | 30.89 | 28.73 | 28.82 | 68.62 | 67.35 | 67.53 | 28.83 | 30.00 | 30.04 |
| 26-30,26-34,30-34 | 27.90 | 26.40 | 28.47 | 62.56 | 59.58 | 59.69 | 27.10 | 26.25 | 24.30 |
| 27-31,27-35,31-35 | 65.48 | 65.60 | 66.85 | 142.72 | 141.52 | 141.15 | 46.68 | 45.85 | 44.54 |
| 28-32,28-36,32-36 | 53.90 | 52.40 | 52.68 | 119.78 | 119.55 | 119.51 | 42.81 | 44.06 | 43.77 |
| 37-41,37-45,41-45 | 30.92 | 28.90 | 28.73 | 68.95 | 67.89 | 67.30 | 29.05 | 30.25 | 29.97 |
| 38-42,38-46,42-46 | 28.21 | 26.53 | 28.73 | 62.31 | 59.51 | 60.30 | 26.60 | 26.07 | 24.53 |
| 39-43,39-47,43-47 | 65.26 | 65.89 | 67.23 | 143.64 | 142.30 | 142.22 | 47.42 | 46.06 | 44.84 |
| 40-44,40-48,44-48 | 54.65 | 52.15 | 53.77 | 120.26 | 119.50 | 120.55 | 42.42 | 44.26 | 43.42 |

Table U5 Percentage increase in flow rates at the 19.5m deep plane with the increase in LB angle in the LTR from 0° to 7.5°, 0° to 15°, and 7.5° to 15° - 6.6 x 4 x 20m heading

| Percentage increase in flow rates at the 9.5m deep plane with the increase in LB angle in the LTR from 0° to 7.5°, 0° to 15°, and 7.5° to 15° | | | | | | | | | |
|---|---|--------|-------|--|--------|--------|--|--------|-------|
| Cases | LTR velocity | | | | | | | | |
| | 1m/s | 1.5m/s | 2m/s | 1m/s | 1.5m/s | 2m/s | 1m/s | 1.5m/s | 2m/s |
| | Percentage increase in flow rate with LB angle increase from 0° to 7.5° (%) | | | Percentage increase in flow rate with angle LB increase from 0° to 15° (%) | | | Percentage increase in flow rate with LB angle increase from 7.5° to 15° (%) | | |
| 73-77,73-81,77-81 | 31.29 | 28.63 | 28.04 | 68.02 | 67.44 | 64.93 | 27.98 | 30.18 | 28.81 |
| 74-78,74-82,78-82 | 28.14 | 26.64 | 28.24 | 64.60 | 58.77 | 59.61 | 28.45 | 25.37 | 24.46 |
| 75-79,75-83,79-83 | 65.64 | 67.09 | 67.86 | 144.25 | 141.99 | 142.26 | 47.46 | 44.83 | 44.32 |
| 76-80,76-84,80-84 | 55.51 | 55.34 | 52.43 | 119.11 | 120.07 | 118.76 | 40.90 | 41.67 | 43.52 |
| 85-89,85-93,89-93 | 30.95 | 28.41 | 27.31 | 68.28 | 66.64 | 66.48 | 28.51 | 29.77 | 30.77 |
| 86-90,86-94,90-94 | 27.76 | 25.90 | 28.22 | 62.04 | 58.38 | 58.86 | 26.84 | 25.80 | 23.90 |
| 87-91,87-95,91-95 | 65.86 | 65.40 | 65.87 | 145.08 | 142.34 | 140.70 | 47.77 | 46.52 | 45.12 |
| 88-92,88-96,92-96 | 55.62 | 50.38 | 51.62 | 118.16 | 116.27 | 116.15 | 40.19 | 43.82 | 42.56 |

Table U6 Percentage increase in flow rates at the exit of the LB with the increase in LB angle in the LTR from 0° to 7.5°, 0° to 15°, and 7.5° to 15° - 6.6 x 4 x 20m heading

| Percentage increase in flow rates at the exit of the LB with the increase in LB angle in the LTR from 0° to 7.5°, 0° to 15°, and 7.5° to 15° | | | | | | | | | |
|--|---|--------|-------|--|--------|--------|--|--------|-------|
| Cases | LTR velocity | | | | | | | | |
| | 1m/s | 1.5m/s | 2m/s | 1m/s | 1.5m/s | 2m/s | 1m/s | 1.5m/s | 2m/s |
| | Percentage increase in flow rate with LB angle increase from 0° to 7.5° (%) | | | Percentage increase in flow rate with LB angle increase from 0° to 15° (%) | | | Percentage increase in flow rate with LB angle increase from 7.5° to 15° (%) | | |
| 73-77,73-81,77-81 | 30.43 | 27.87 | 27.85 | 68.33 | 66.79 | 65.02 | 29.05 | 30.43 | 29.07 |
| 74-78,74-82,78-82 | 26.90 | 27.63 | 28.38 | 61.13 | 60.29 | 61.43 | 26.98 | 25.59 | 25.75 |
| 75-79,75-83,79-83 | 65.38 | 67.19 | 66.42 | 143.29 | 144.34 | 142.78 | 47.11 | 46.14 | 45.88 |
| 76-80,76-84,80-84 | 53.83 | 53.93 | 53.82 | 118.70 | 120.68 | 118.97 | 42.17 | 43.37 | 42.35 |
| 85-89,85-93,89-93 | 32.14 | 29.62 | 27.63 | 71.27 | 68.19 | 65.47 | 29.61 | 29.76 | 29.64 |
| 86-90,86-94,90-94 | 26.98 | 26.43 | 27.20 | 61.90 | 61.71 | 57.50 | 27.50 | 27.90 | 23.82 |
| 87-91,87-95,91-95 | 68.76 | 65.57 | 66.10 | 145.62 | 140.82 | 137.41 | 45.55 | 45.45 | 42.93 |
| 88-92,88-96,92-96 | 53.63 | 52.40 | 52.37 | 116.43 | 118.66 | 120.16 | 40.88 | 43.48 | 44.49 |

APPENDIX V

EFFECT OF LB ANGLE IN LTR ON FLOW RATE CLOSE TO FACE

- Flow rates at 9.5m deep planes using 0°, 7.5° and 15° LB inside the LTR for LTR velocities of 1m/s, 1.5m/s, 2m/s - 6.6 x 4 x 10m heading

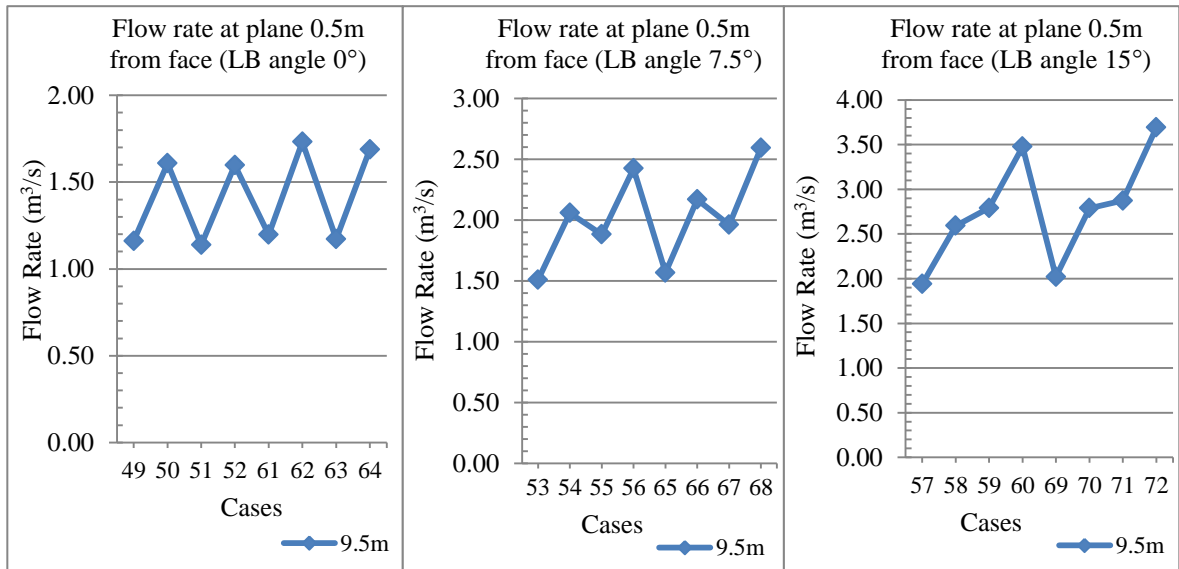


Figure V1 Flow rates at 9.5m deep planes using 0°, 7.5° and 15° LB inside the LTR for LTR velocity of 1m/s

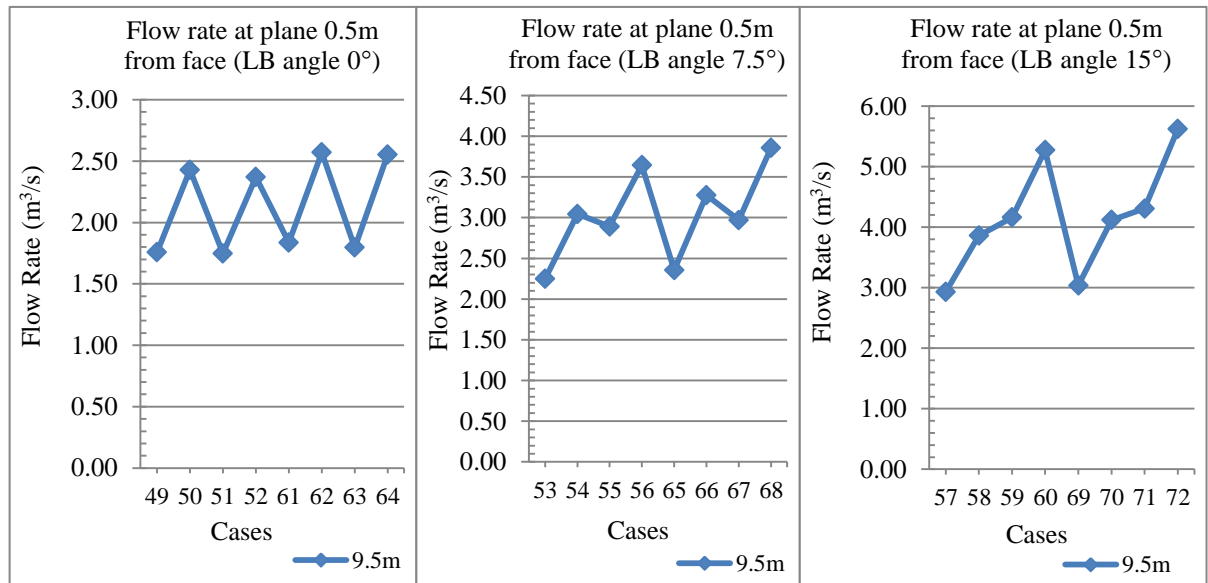


Figure V2 Flow rates at 9.5m deep planes using 0°, 7.5° and 15° LB inside the LTR for LTR velocity of 1.5m/s

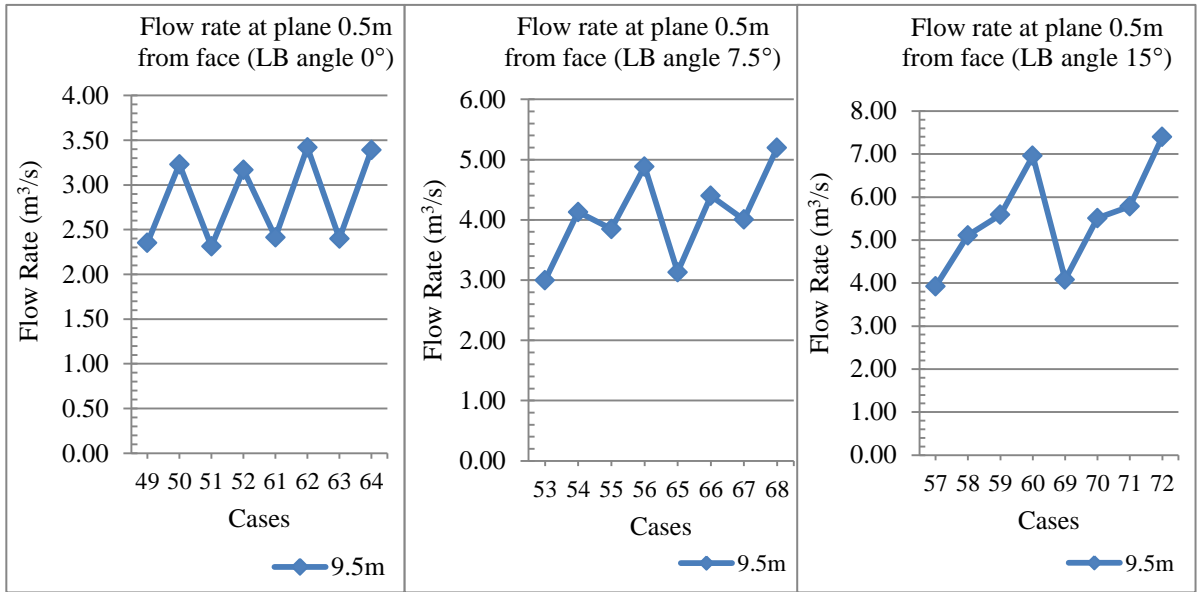


Figure V3 Flow rates at 9.5m deep planes using 0°, 7.5° and 15° LB inside the LTR for LTR velocity of 2m/s

- Flow rates at 19.5m deep planes using 0°, 7.5° and 15° LB inside the LTR for LTR velocities of 1m/s, 1.5m/s, 2m/s - 6.6 x 3 x 20m heading

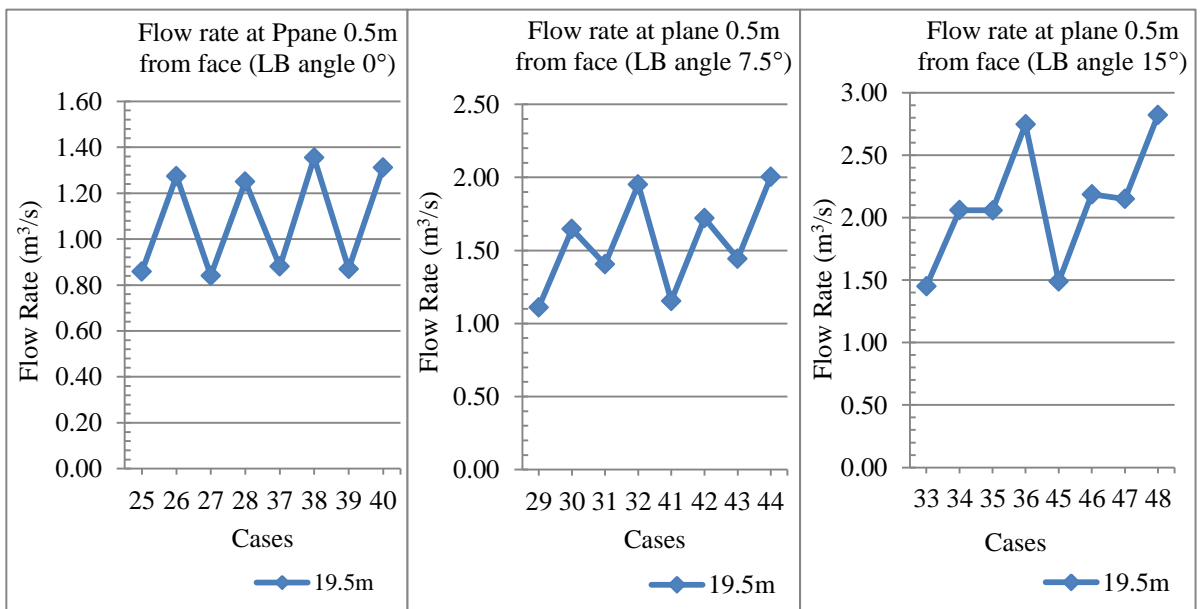


Figure V4 Flow rates at 19.5m deep planes using 0°, 7.5° and 15° LB inside the LTR for LTR velocity of 1m/s

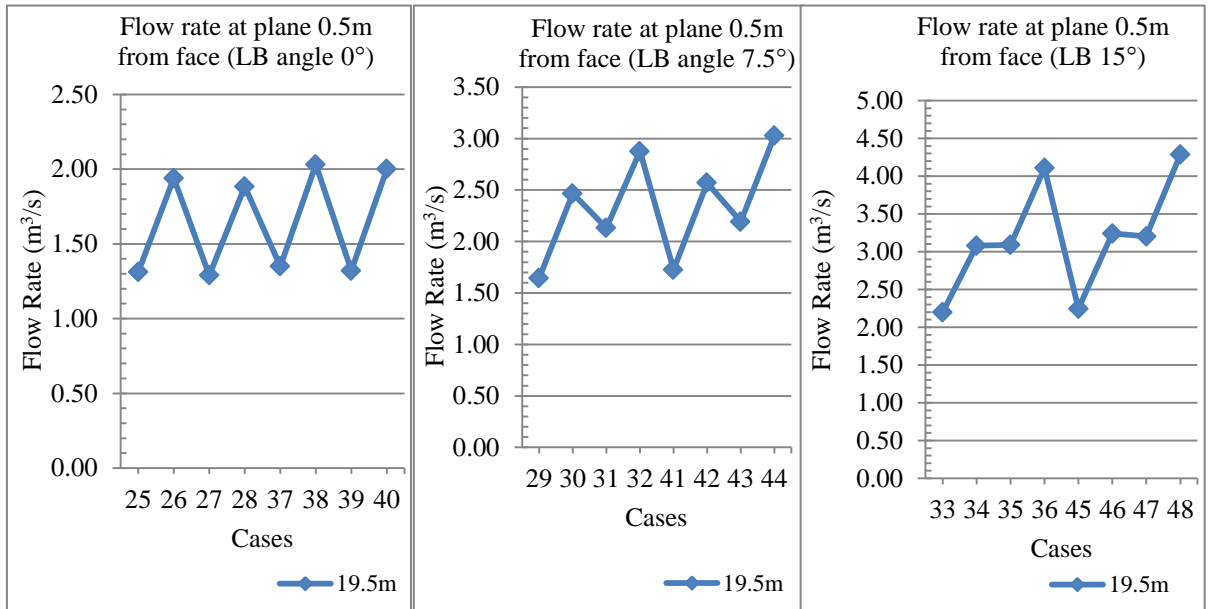


Figure V5 Flow rates at 19.5m deep planes using 0°, 7.5° and 15° LB inside the LTR for LTR velocity of 1.5m/s

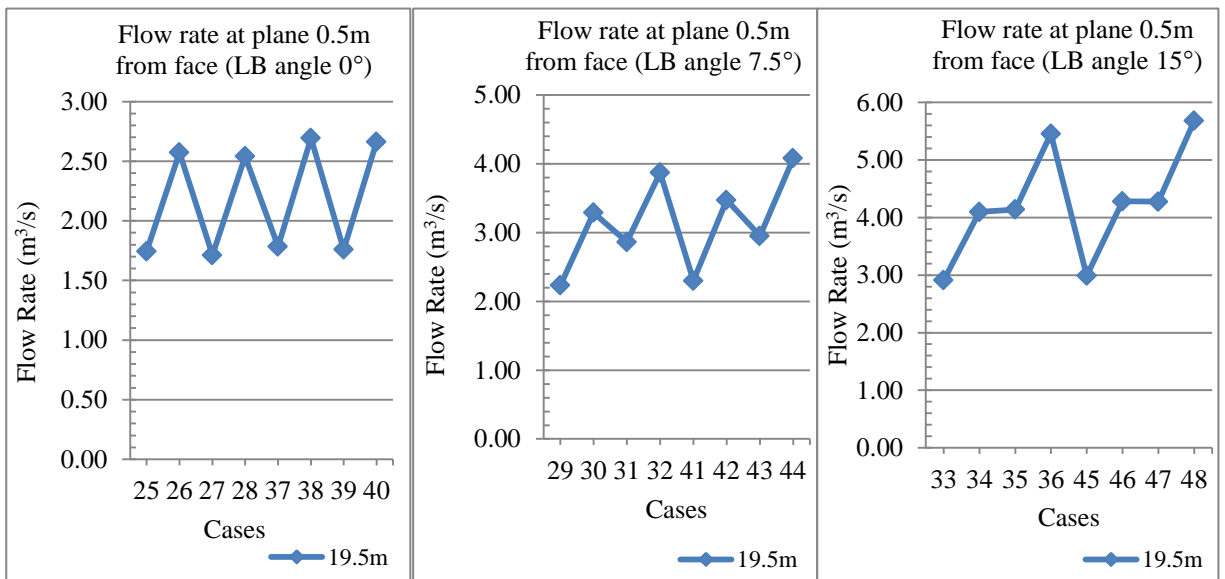


Figure V6 Flow rates at 19.5m deep planes using 0°, 7.5° and 15° LB inside the LTR for LTR velocity of 2m/s

- Flow rates at 19.5m deep planes using 0°, 7.5° and 15° LB inside the LTR for LTR velocities of 1m/s, 1.5m/s, 2m/s - 6.6 x 4 x 20m heading

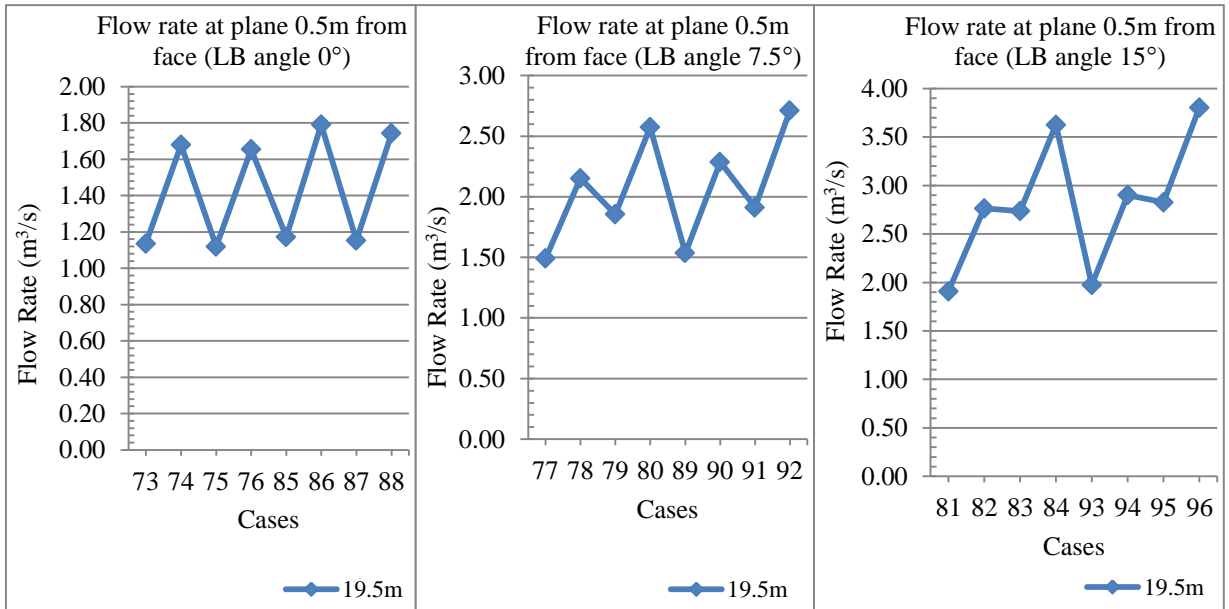


Figure V7 Flow rates at 19.5m deep planes using 0°, 7.5° and 15° LB inside the LTR for LTR velocity of 1m/s

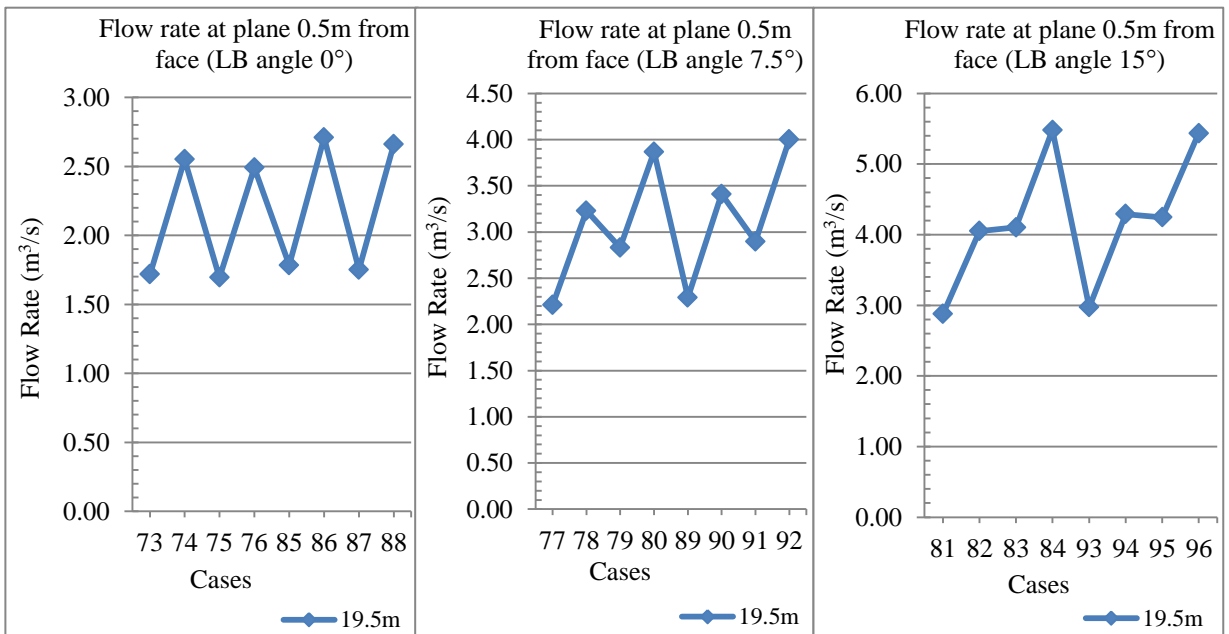


Figure V8 Flow rates at 19.5m deep planes using 0°, 7.5° and 15° LB inside the LTR for LTR velocity of 1.5m/s

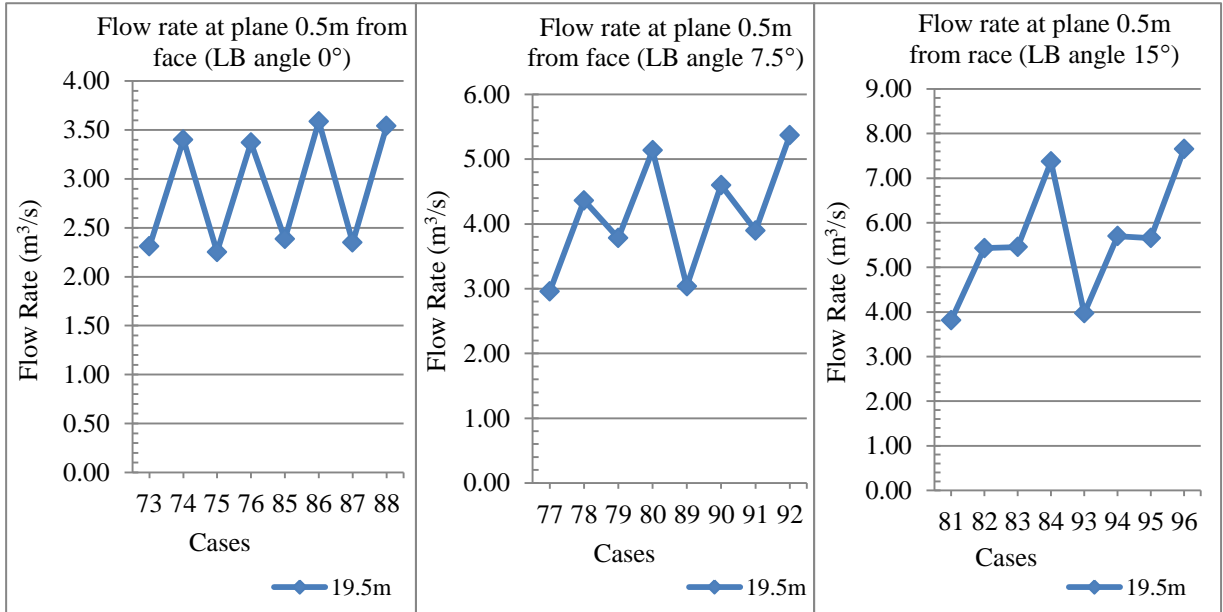


Figure V9 Flow rates at 19.5m deep planes using 0°, 7.5° and 15° LB inside the LTR for LTR velocity of 2m/s

EFFECT OF LB ANGLE IN LTR ON FLOW RATE

- Flow rates at specified planes using 0°, 7.5° and 15° LB inside the LTR for LTR velocities of 1m/s, 1.5m/s, 2m/s - 6.6 x 4 x 10m heading

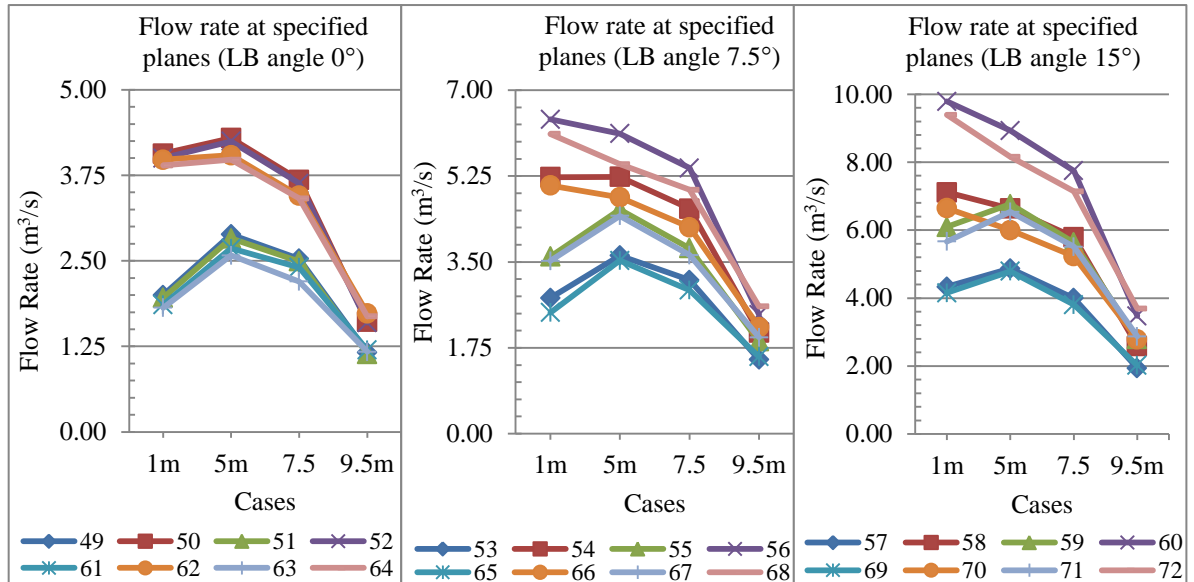


Figure W1 Flow rates at specified planes using 0°, 7.5° and 15° LB inside the LTR for LTR velocity of 1m/s

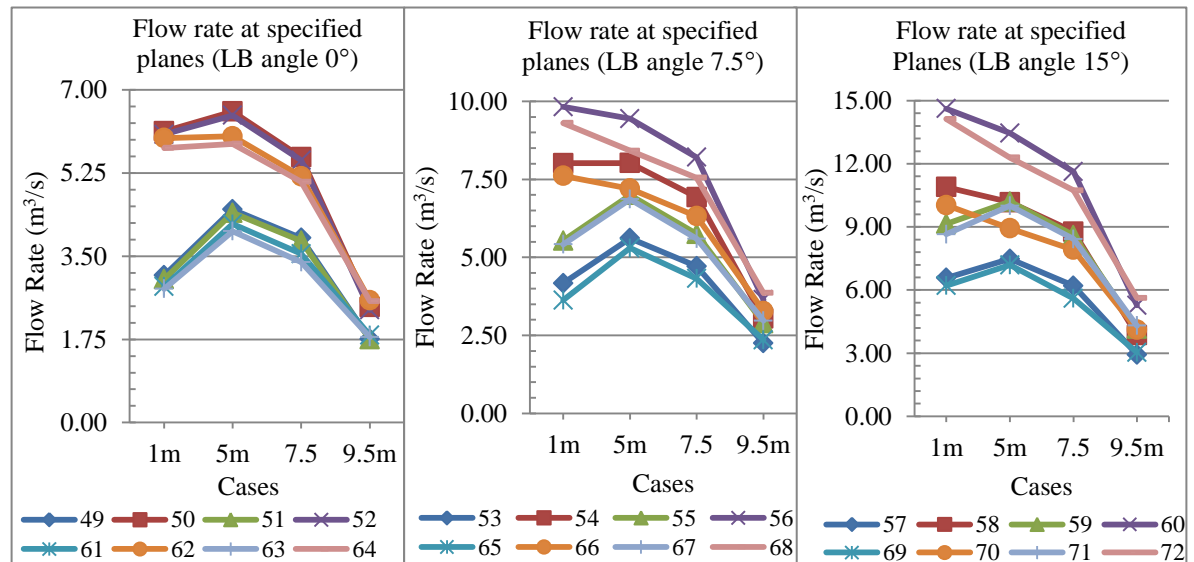


Figure W2 Flow rates at specified planes using 0°, 7.5° and 15° LB inside the LTR for LTR velocity of 1.5m/s

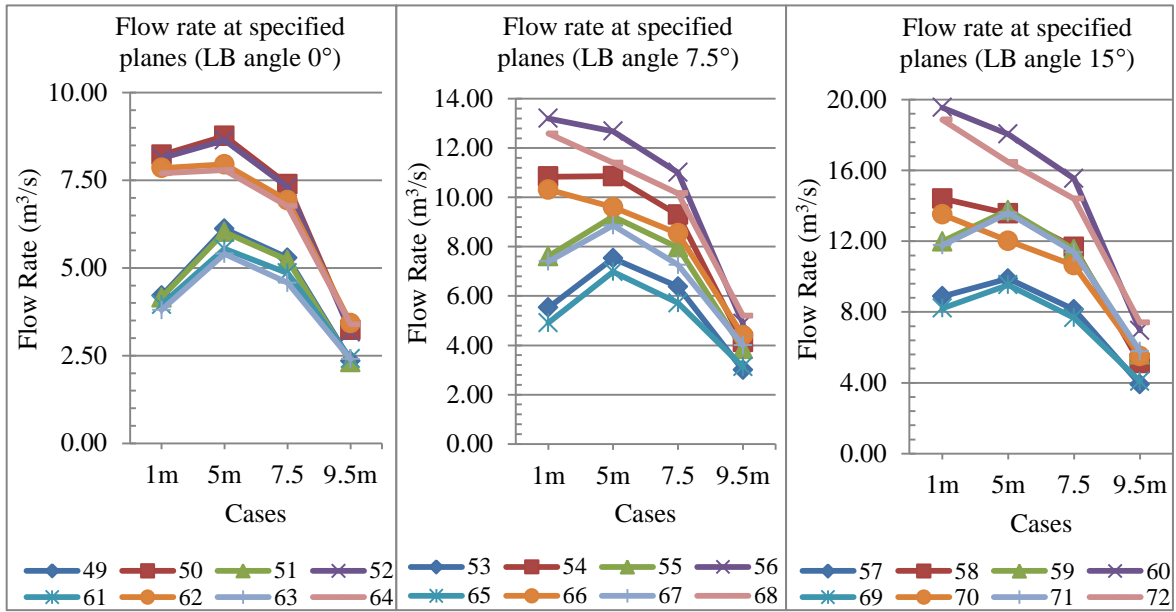


Figure W3 Flow rates at specified planes using 0°, 7.5° and 15° LB inside the LTR for LTR velocity of 2m/s

- Flow rates at specified planes using 0°, 7.5° and 15° LB inside the LTR for LTR velocities of 1m/s, 1.5m/s, 2m/s - 6.6 x 3 x 20m heading

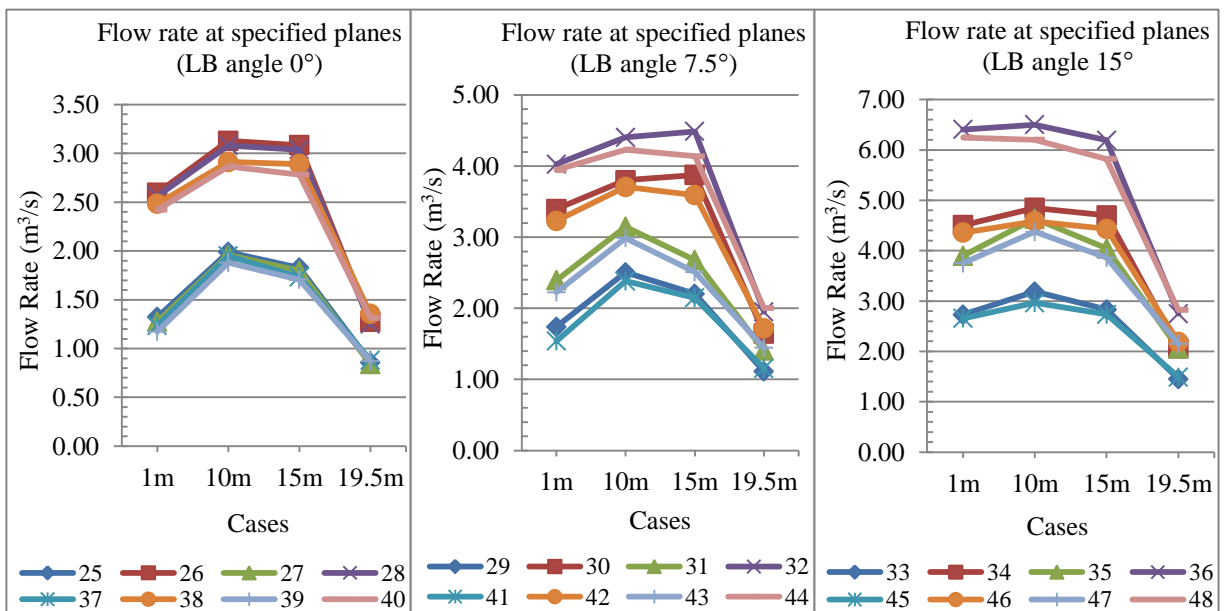


Figure W4 Flow rates at specified planes using 0°, 7.5° and 15° LB inside the LTR for LTR velocity of 1m/s

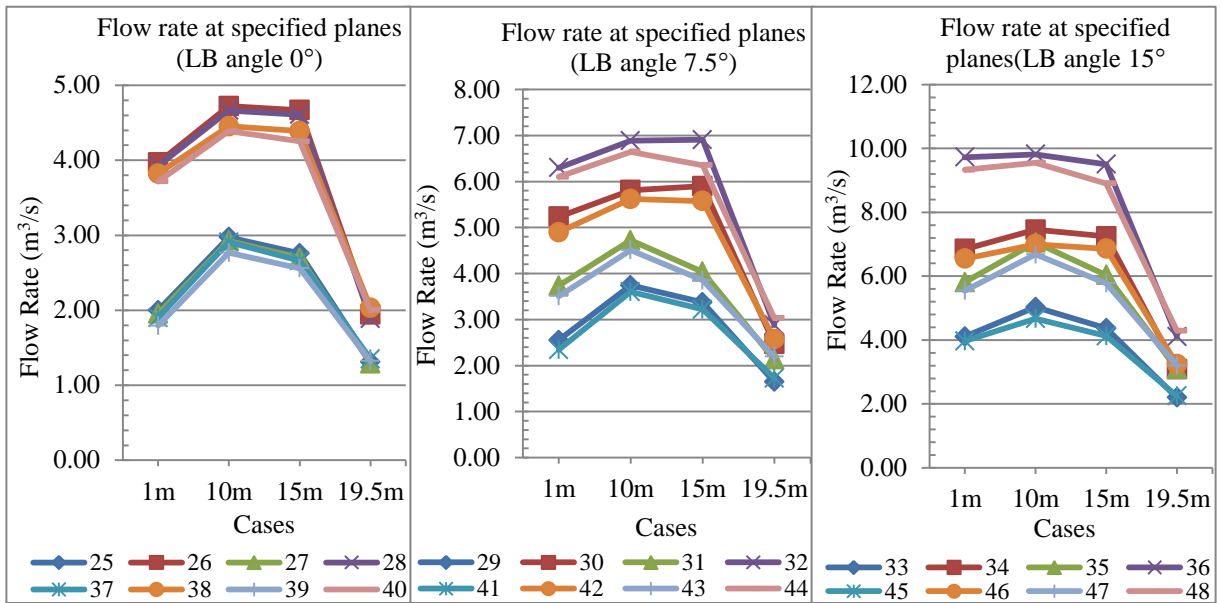


Figure W5 Flow rates at specified planes using 0°, 7.5° and 15° LB inside the LTR for LTR velocity of 1.5m/s

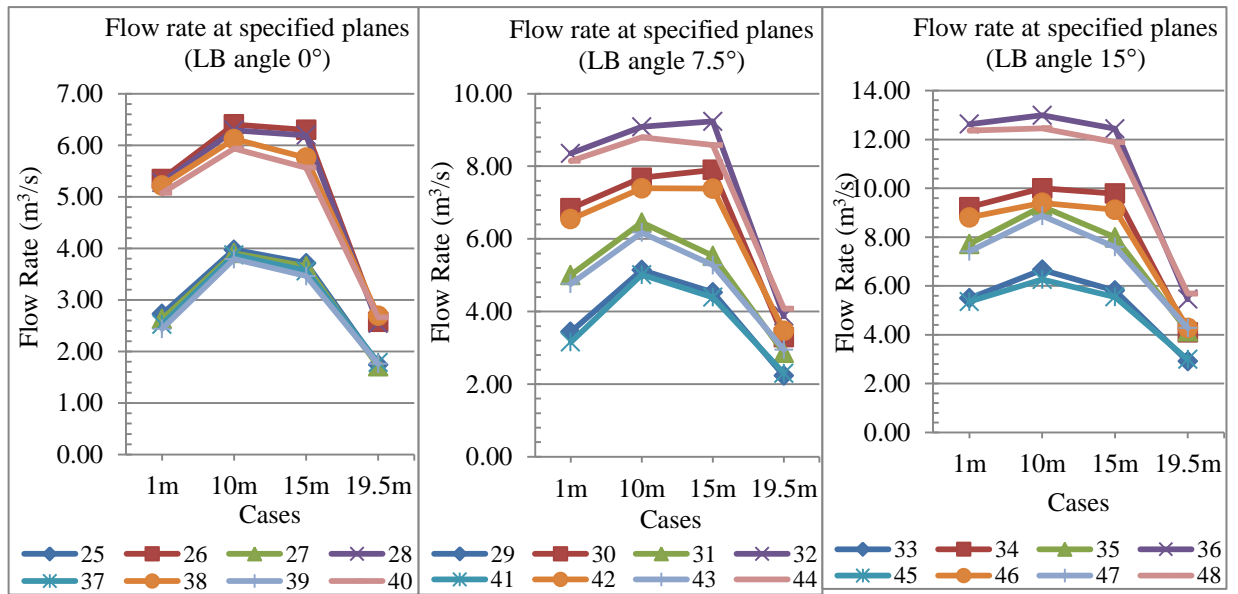


Figure W6 Flow rates at specified planes using 0°, 7.5° and 15° LB inside the LTR for LTR velocity of 2m/s

- Flow rates at specified using 0°, 7.5° and 15° LB inside the LTR for LTR velocities of 1m/s, 1.5m/s, 2m/s - 6.6 x 4 x 20m heading

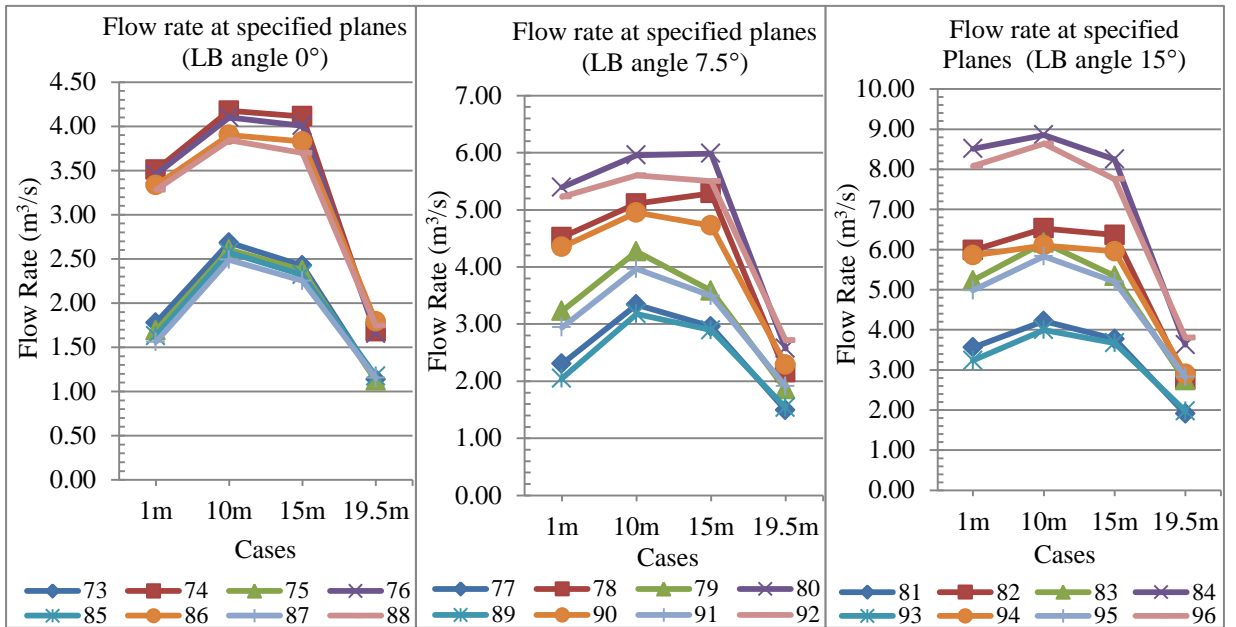


Figure W7 Flow rates at specified planes using 0°, 7.5° and 15° LB inside the LTR for LTR velocity of 1m/s

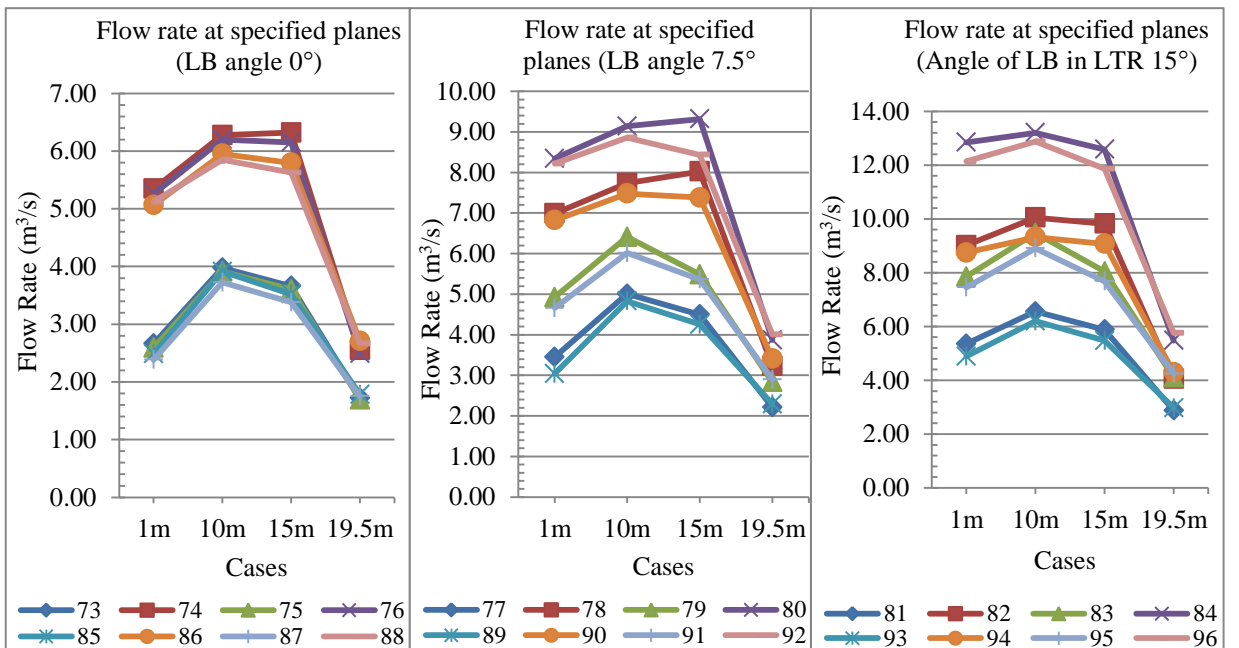


Figure W8 Flow rates at specified planes using 0°, 7.5° and 15° LB inside the LTR for LTR velocity of 1.5m/s

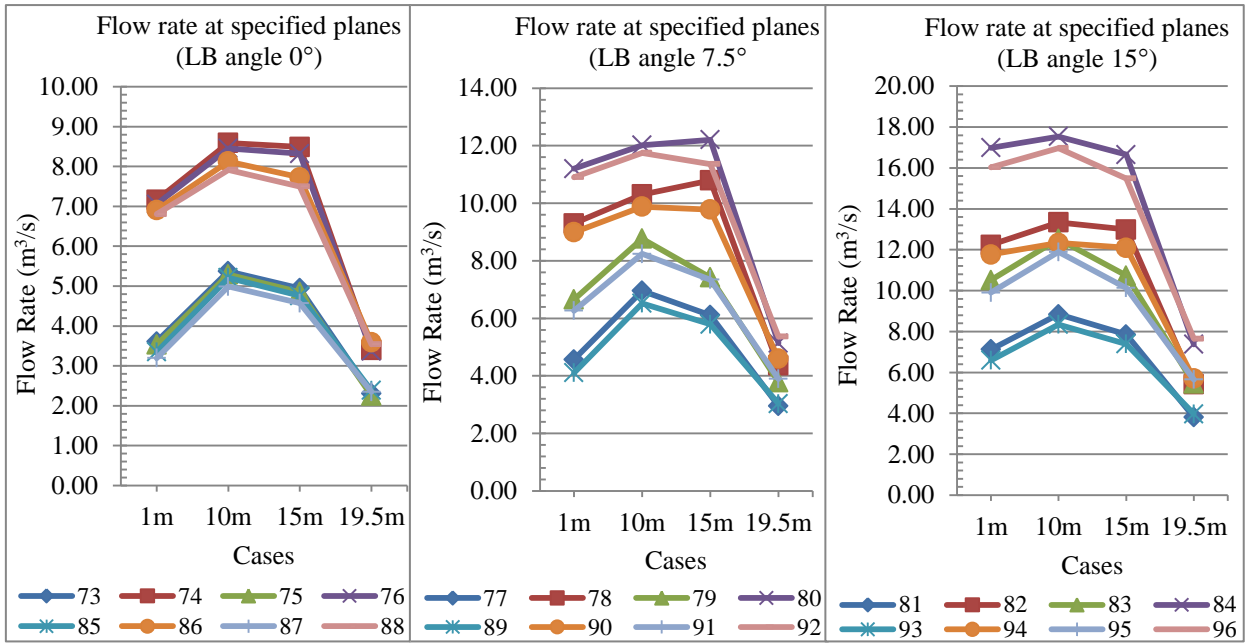


Figure W9 Flow rates at specified planes using 0°, 7.5° and 15° LB inside the LTR for LTR velocity of 2m/s

SUMMARY OF PAPER ABSTRACT ON THE RESEARCH

The publications listed below have originated from this thesis so far:

Paper 1

Part of Chapter 4 were compiled and published as the paper: **Feroze, T.,** and Phillips, H. R. (2015). An initial investigation of room and pillar ventilation using CFD to investigate the effects of last through road velocity. *24th International Mining Congress and Exhibition of Turkey (IMCET 15)*. Antalya, Turkey, 14-17 April. pp. 970-977. The following is an extract of the paper abstract:

Abstract

Computational Fluid Dynamics (CFD) has often been used to analyse the air flows in underground mines. In this paper the results of a base-line investigation conducted using a three dimensional CFD analysis to find the depth of air flow in empty headings without any auxiliary devices are presented. The model dimensions are kept constant and air penetration into the heading for four last through road (LTR) velocities is compared. Determination of penetration of air is based on the maximum axial velocity and flow rates are calculated using absolute axial velocity at different depth planes. The results have been compared with experimental results of another researcher published 25 years ago, Meyer (1989).

Further research is continuing to determine the effects of different auxiliary ventilation devices using this CFD methodology, as well as obtaining empirical data in an experimental tunnel established at the University of the Witwatersrand.

Keywords: Ventilation, room and pillar, Computational Fluid Dynamics (CFD), Last Through Road (LTR) Velocity

Paper 2

Parts of Chapter 4 and 6 were compiled, and accepted as the paper: **Feroze, T., and Genc, B. (2016)**. Estimating effects of line brattice ventilation system variables using CFD in the empty heading in room and pillar mining. *Journal of the Southern African Institute of Mining and Metallurgy*. The following is an extract of the paper abstract:

Abstract

The ventilation of underground coal mines plays an important role when it comes to minimizing the risk of methane and coal dust explosions. The ability of ventilation, with the use of line brattice (LB), to take away methane and coal dust in empty heading is dependent on the amount of air leaving the LB and entering the heading. The quantity of this air depends on the associated system variables namely heading dimension, settings of the LB and velocity of air in the Last Through Road (LTR). However, the exact effect of these system variables on the flow rate at the exit of the LB in empty heading is not known. The installation of LBs in South African coal mines are generally carried out based on experience. This can result in over or under ventilation and may increase the cost of providing ventilation or cause accidents, respectively. In this paper, using Computational Fluid Dynamics (CFD), the air flow rate at the exit of the LB in empty heading was estimated using full scale three dimensional models. The CFD model used was validated using experimental results. As part of the procedure firstly, the settings of these three system variables were varied, the flow rates at the exit of the LB were measured and finally the results were used to calculate the effect of each system variable. The final outcome of the paper is a mathematical formula which can be used to estimate airflow rate at the exit of the LB in empty headings for any practical scenario.

The outcome of this paper will help coal mining sector in South Africa by providing estimation models based on scientific reasoning for the installation of LB, and it will also serve academia as part of curriculum towards educating future mining engineers. The work presented in this paper is part of a Ph.D. research study in the School of Mining Engineering at the University of the Witwatersrand.

Keywords: *Ventilation, room and pillar, Line Brattice, Computational Fluid Dynamics (CFD), Air flow estimation at LB exit*

Paper 3

Parts of Chapter 4 and 6 were compiled and accepted as the paper: **Feroze, T., and Genc, B.**(2016). Evaluation of line brattice length in an empty heading to improve air flow rate at the face using CFD. *International Journal of Mining Science and Technology*. The following is an extract of the paper abstract:

Abstract

The effectiveness of line brattice (LB) ventilation system depends on the associated system variables. However, the effect of these variables on the air flow rates close to the face of the heading is not extensively studied. In this paper, the effect of the LB length in relation to the LB-wall distance, on the air flow rate reaching the face is analysed. Scenarios were developed using four LB lengths, two LB-wall distances and two heading depths. These scenarios were simulated with a validated CFD model. The air flow rates and patterns at various locations inside the heading were analysed. This helped to find the minimum LB-face distance that should be maintained for each LB-wall distance to maximise the air flow rate at the face. The minimum length when used will improve ventilation and reduce energy cost.

Keywords

Coal mine ventilation; Auxiliary ventilation; Line brattice ventilation system; Computational Fluid Dynamics

Paper 4

Parts of Chapter 4 and 8 were compiled and accepted as the paper: **Feroze, T., and Genc, B. (2016).** Analysis of ducted fan system variables on ventilation in an empty heading using CFD. *Journal of the Southern African Institute of Mining and Metallurgy*. The following is an extract of the paper abstract:

Abstract

This paper discusses the ducted fan system variables on ventilation in an empty heading. It demonstrates the use of CFD and comparative analyses to estimate the effect of some of the system variables associated with the forcing and exhausting ducted fan systems on the ventilation of empty headings. The diameter of the duct, duct mouth to face distance, and the power of the fan (quantity delivered by the fan) were varied and their effect on ventilation was determined. This was done through a comparative analysis of the flow rates calculated close to the face of the heading. Estimation models were developed, which can be used to calculate the flow rate close to the face of the empty heading for different settings of the studied system variables.

The study showed that recirculation for a forcing ducted fan system can be reduced by increasing the duct diameter and by increasing the duct mouth to face distance. Increasing the duct diameter, from 0.57m to 0.76m, and duct mouth to face distance, from 8m to 10m respectively, reduced recirculation by approximately 20%. For the exhausting ducted fan system, the higher flow rates were achieved with the reduction in the duct mouth to face distance, increase in fan design flow rate and duct diameter.

The outcome of this paper will help ventilation engineers in deciding the optimum duct fan system, required for sufficient ventilation.

Keywords: Ducted fan, ventilation, CFD

Paper 5

Parts of Chapter 4 and 6 were compiled and submitted as the paper: **Feroze, T., and Genc, B. (2016).** A CFD model to evaluate variables of the line brattice ventilation system in an empty heading. *Journal of the Southern African Institute of Mining and Metallurgy*. The following is an extract of the paper abstract:

Abstract

Blind headings are an integral part of the room and pillar coal mines. These headings are also the major source of methane and coal dust. Most of the methane and coal dust explosions therefore, occur in the blind headings. The primary cause of these explosions is the disruption of the local ventilation system employed in these headings. Line Brattice (LB) ventilation system is of great utility when it comes to the ventilation of blind headings by directing the air from the Last Through Road (LTR) into the heading. The amount of air that becomes available to ventilate the face of the empty heading depends on the associated system variables. These variables are heading dimension, settings of the LB and velocity of air in the LTR. The installation of LB is commonly carried out by the supervisory staff working underground based on work experience which may lead to improper ventilation. Therefore, the correct installation of the LB still remains a challenge.

In this study, a validated model of Computational Fluid Dynamics (CFD) has been used to analyse the effect of the LB ventilation system variables on the air flow rates close to the face of the empty heading (0.5m from face). Full scale three dimensional models with two heading heights equal to 3m and 4m, two heading depths equal to 10m and 20m, various settings of LB and three LTR velocities equal to 1m/s, 1.5m/s and 2m/s were simulated. The air flow rates and patterns, at various locations inside the heading and close to the face of the empty heading were analysed. A comparative study was carried out to assess and calculate the effect of each of these system variables on the flow rates close to the face of the heading. Based on the findings, a user-friendly numerical model was formulated which can be used to estimate the flow rate close to the face of an empty heading for different practical settings of the system variables. This new easy-to-use model can specifically help the supervisory staff working underground to swiftly implement the ventilation plan abiding to the regulation and the mine

standards. The model can also serve academia as part of the curriculum towards educating future mining engineers. The work presented in this paper is part of a PhD research study in the School of Mining Engineering at the University of the Witwatersrand.

Keywords: Line brattice ventilation system, empty heading, CFD

Paper 6

Parts of Chapter 2, 3 and 4 were compiled and submitted as the paper: **Feroze, T., and Genc, B. (2016).** Ventilation of underground coal mines – A Computational Fluid Dynamics study. Submitted for the *Mine ventilation society of South Africa (MVSSA) Conference 2016*. The following is an extract of the paper abstract:

Abstract

The auxiliary ventilation systems used to ventilate the development headings has conventionally been studied by conducting experiments. Since the efficiency of any auxiliary ventilation system is dependent on a number of system variables, conducting such experiments on a large scale become a challenging exercise. With the advancement in computer systems and numerical codes, an alternate solution becoming popular in the mining industry is the use of Computational Fluid Dynamics (CFD). Although a number of researchers are using such software in the mining industry, the accuracy of the results is still questioned by the conservatives. This paper outlines not only the steps to be followed for conducting a CFD study in general, but also provides the results of three validation studies relating to auxiliary ventilation. This was done to emphasis how CFD can be used with confidence to study ventilation in underground mines. The work presented in this paper is part of a Ph.D. research study in the School of Mining Engineering at the University of the Witwatersrand.

Keywords: *Ventilation, underground coal mines, CFD, auxiliary ventilation systems*